

AD-A223 282

UNITED STATES AIR FORCE  
HIGH SCHOOL APPRENTICESHIP PROGRAM

1989

PROGRAM MANAGEMENT REPORT

VOLUME II OF III

UNIVERSAL ENERGY SYSTEMS, INC.

DTIC  
ELECTE  
JUN 26 1990  
S D  
Co

Program Director, UES  
Rodney C. Darrah

Program Manager, AFOSR  
Lt. Col. Claude Cavender

Program Administrator, UES  
Susan K. Espy

Submitted to  
Air Force Office of Scientific Research  
Bolling Air Force Base  
Washington, DC

December 1989

**DISTRIBUTION STATEMENT A**  
Approved for public release;  
Distribution Unlimited

**BEST  
AVAILABLE COPY**

## RESEARCH REPORTS

### 1989 HIGH SCHOOL APPRENTICESHIP PROGRAM

Technical  
Report

Number  
VOLUME I

Title

Participant

#### Aero Propulsion Laboratory

|   |  |                       |
|---|--|-----------------------|
| 1 | Flat Plate Heat Pipe   | Matthew Bold          |
| 2 | High Power Sources   | Robert Bradford       |
| 3 | Oils Change with Friction  | Roxanne Fischer       |
| 4 | Liquid Chromatography  | Terence Hill          |
| 5 | Laser Doppler Velocimeter Testing  | Alisha Hix            |
| 6 | LIPS-III Satellite Program   | Christopher Miller    |
| 7 | Aircraft Engine Axial-Flow Compressors<br>and Mathematical Modeling of<br>Compressor Performance | Bradley Reigelsperger |

#### Armament Laboratory

|    |   |                 |
|----|---|-----------------|
| 8  | Operation & Protocol Manual   | Jules Bergmann  |
| 9  | Fuzes and Guns  | Steven Bryan    |
| 10 | Adaptions of Existing Star Catalogs for<br>Space-Based Interceptor Applications | Tonya Cook      |
| 11 | Differences in the Activation Energy of<br>Nitroguanidines                      | Kathryn Deibler |
| 12 | Comparison of Average vs. Spectral<br>LOWTRAN in Calculating Exitance           | Chris Ellis     |
| 13 | The Creation and Installation of Z-248<br>Help Menus                            | Dana Farver     |
| 14 | File Size Analysis and Transfer Program   | Kenneth Gage    |
| 15 | Design of In-House Radar Control System   | Reid Harrison   |
| 16 | HSAP Event Summary  | Derek Holland   |

**BEST  
AVAILABLE COPY**

|    |  |                 |
|----|--|-----------------|
| 17 | Pulse Doppler Radar  | Jeffrey Leong   |
| 18 | Enhancement of Input and Output for the Epic-2 Hydrocode                             | Bryan McGraw    |
| 19 | Enhancement of Input and Output for Epic3 Hydrocode Calculations                     | Neil Overholtz  |
| 20 | An Analysis of the Offset Fin Configuration using Computational Fluid Dynamics (CFD) | Shan-ni Perry   |
| 21 | Interfacing the Tektronix Workstation with the RTD 710A Digitizer                    | Lisa Schmidt    |
| 22 | The Operation and Reliability of a 5MJ Pulse Power System                            | Patricia Tu     |
| 23 | Infrared Laser Polarimetry   | Danielle Walker |

#### Armstrong Aerospace Medical Research Laboratory

|    |   |                  |
|----|---|------------------|
| 24 | An Alternate Analysis of the Peripheral Vision Horizon Device Flight Data | Michael Chabinyo |
| 25 | Workload and Ergonomics   | Ann Hartung      |
| 26 | Cockpit Accommodation   | Keisha Hayes     |
| 27 | Experiencing a Research Environment                                       | Angela Karter    |
| 28 | The Effect of CTFE on the Liver   | Douglas Marshak  |
| 29 | The Summer Work Experience at The Harry G. Armstrong Research Laboratory  | Carolyn Mellott  |
| 30 | Bioengineering and Biodynamics  | Britt Peschke    |
| 31 | Toxicology  | Jennifer Walker  |

#### VOLUME II

#### Astronautics Laboratory

|    |  |               |
|----|--|---------------|
| 32 | Hover Testing of Kinetic Kill Vehicles in a Controlled Environment | Ross Benedict |
| 33 | Filament Winding Project   | Peter George  |
| 34 | Solid Rocket Propellants   | Sharron Groom |

|                                |  |                  |
|--------------------------------|--|------------------|
| 35                             | Computer Support for the Minuteman III<br>Demonstration Motor Test and the Advanced<br>Solid Axial Stage | Lloyd Neurauter  |
| 36                             | Thermoplastic Binders  | Sandi Novak      |
| 37                             | Pyrolytic Carbon on Carbon Fibers  | Sonya Park       |
| 38                             | Engineering Design Evaluation  | Alexander Sagers |
| 39                             | Carbon-Carbon  | Richard Sims     |
| 40                             | Create a Database on the VAX network   | Benjamin Sommers |
| 41                             | Space Structure  | Shirley Williams |
| Avionics Laboratory            |  |                  |
| 42                             | Model of a Lambertian Surface  | Matthew Brewer   |
| 43                             | F-15 Radar Simulation  | Sook Hee Choung  |
| 44                             | Analyzing Electro-Optic Sensors  | Sheri Cody       |
| 45                             | Computer Circuitry   | Christine Garcia |
| 46                             | Rotate Image   | Lori Harris      |
| 47                             | Ada Programming  | Amy Listerman    |
| 48                             | An Investigation of the GaAs Mesfet  | Joan McManamon   |
| 49                             | The Optical Spectroscopy of Ti <sup>3+</sup> doped<br>YA10   | Allison Potter   |
| 50                             | The Research and Development Division  | Julie Roesner    |
| 51                             | Evaluating Ada Compilers   | Jerard Wilson    |
| Engineering and Service Center |  |                  |
| 52                             | Theorized Effects of Simulated Aircraft<br>Loading on the Density of Asphalt<br>Concrete Pavements       | Gregory Dixon    |
| 53                             | Environmental Simulation Chamber<br>Studies of the Atmospheric Chemistry<br>of Hydrazine                 | Dorothy Iffrig   |
| 54                             | HQAFESC Technical Information Center   | Byron Kuhn       |



|    |                                     |                 |
|----|-------------------------------------|-----------------|
| 55 | Gas Chromatographic Investigation   | Scott Lamb      |
| 56 | Piping Code and FEA Program Reviews | Keith Levesque  |
| 57 | 9700-Area Centrifuge                | Cyrus Riley     |
| 58 | Material Testing System (MTS)       | Robin Woodworth |

#### Flight Dynamics Laboratory

|    |   |                   |
|----|---|-------------------|
| 59 | Creation of a F-15/F-16 Aircraft Data Bank  | Tremayne Andreson |
| 60 | Evaluation of Several Methods for Predicting Surface Pressures in the Shadow Regions of Aerospace Vehicles                      | Eric Bailey       |
| 61 | An Introduction to Agility Research   | Mark Boeke        |
| 62 | Instrumentation of Aerospace Structural Integrity Tests   | Wendy Choate      |
| 63 | No Report Submitted   | William Davenport |
| 64 | No Report Submitted   | Andrea Dean       |
| 65 | Working on the Z-248 14 inch Color Monitor  | Cedric McGhee     |
| 66 | Aircraft Transparency Durability: Analysis of the F-111 and a Study of the Application of Combat Missions to Durability Testing | David Merritt     |
| 67 | Testing the Environment's Effects on Equipment  | Valerie Petry     |
| 68 | Working with Antonio Ayala  | Kimberly Schock   |
| 69 | No Report Submitted   | Mark Screven      |
| 70 | High Speed Performance Computer Resources Team  | James Wilkinson   |

#### VOLUME III Geophysics Laboratory

|    |  |                 |
|----|--|-----------------|
| 71 | Determining Typhoon Wind Intensity Using SSM/I Brightness Temperature Data | Stephen Britten |
| 72 | Artificial Intelligence and Lightning Prediction                           | Brian Burke     |



|                          |                          |
|--------------------------|--------------------------|
| A                        |                          |
| <input type="checkbox"/> | <input type="checkbox"/> |
| Codes                    |                          |
| Refer                    |                          |
| Cial                     |                          |
| A-1                      |                          |

|  |   |                    |
|--|---|--------------------|
| 73   | The Aurora: A comparative Study of the Correlation Between Kp and Bz Values and Oval Diameter | Eric Eisenberg     |
| 74   | Apprenticeship Report; Optical Physics Laboratory   | Christopher Guild  |
| 75   | Ionosphere - Total Electron Content   | Maki Inada         |
| 76   | Space Particles Environment   | Susan Jacavanco    |
| 77   | Assembly of a Radio Wave Scintillations Amplifier   | David Kelleher     |
| 78   | Displaying Tektronix Files on a Zenith PC   | John Walker        |
| Occupational and Environment Health Laboratory |   |                    |
| 79   | Using Soil and Aquatic Bioassays to Assess the Toxicity of Contaminated Soil and Wastewater   | Jonathan Jarrell   |
| 80   | Fate and Transport of JP-4 Constituents   | Andrea Perez       |
| 81   | Final Job Report  | Alan Thomason      |
| Rome Air Development Center                    |   |                    |
| 82   | A Spectrum of Scientific Analysis: A Final Report   | Daniel Abbis       |
| 83   | Software Q & A: A Study in Computer Testing   | Matthew Anderson   |
| 84   | Neural Computing  | Carolynn Bruce     |
| 85   | The Effects of Aperture Weighting on Far-Field Radiation Patterns                             | Katherine DeBruin  |
| 86   | No Report Submitted   | Benjamin Dreidel   |
| 87   | Subiminal Communication   | Stephanie Hurlburt |
| 88   | No Report Submitted   | Michael Marko      |
| 89   | Probability and Random Test Length  | Karen Panek        |
| 90   | Program Acquisition and Management  | Thomas Potter      |

|    |   |                  |
|----|---|------------------|
| 91 | Error Injector Unit Project Testing Programs  | Richmond Reai    |
| 92 | Test Plan for the Evaluation of Advanced Sector Operations Control Center (SOCC) Workstations (PRDA 89-4) | Eric Shaw        |
| 93 | Analog Optical Processing Experiments   | Shane Stanek     |
| 94 | Cartographic Applications for Tactical and Strategic Systems  | Juliet Vescio    |
| 95 | Infrared Camera User's Manual   | Katie Ward       |
| 96 | A Study of Optic Turbulence   | Barbara Westfall |

#### School of Aerospace Medicine

|     |  |                  |
|-----|--|------------------|
| 97  | The Influence of Broad Spectrum Light on Neuroendocrine Responses and Performance  | Jeanne Barton    |
| 98  | CorTemp Disposable Temperature Sensor  | Whitney Brandt   |
| 99  | Electrically and Chemically Induced Release of L-Glutamate from Hippocampal Mossy Fiber Synaptosomes                             | Christina Cheney |
| 100 | Determination of Restriction Enzyme Patterns of Raw DNA with Biotinylated Probes to Heat Shock Protein and Tumor Necrosis Factor | Brian McBurnett  |
| 101 | The Influence of Broad Spectrum Illumination on Circadian Neuroendocrine Responses and Performance                               | Lori Olenick     |
| 102 | Neurochemistry of Photic Entrainment of the Circadian Activity Rhythm in the Syrian Hamster                                      | Joanna Saucedo   |
| 103 | Developing a Fast Circuit to Integrate the Signal in a Video Frame   | John Taboada     |

Form Approved  
OMB No. 0704-0188

|  |  |   |  |   |  |
|--|--|---|--|---|--|
| 1. AGENCY USE ONLY (Leave blank)   |  | 2. REPORT DATE  |  | 3. REPORT TYPE AND DATES COVERED<br>Annual                              |  |
| 4. TITLE AND SUBTITLE<br>United States Air Force<br>High School Apprenticeship Program<br>1987 JULY              |  |   |  | 5. FUNDING NUMBERS<br>61102F<br>2305/D5                                 |  |
| 6. AUTHOR(S)<br>Dr. Darrah, Lt. Col Claude Cavender  |  |   |  |   |  |
| 7. PERFORMING ORGANIZATION NAME(S) AND ADDRESS(ES)<br>Universal Energy Systems, Inc                              |  |   |  | 8. PERFORMING ORGANIZATION<br>REPORT NUMBER<br>AFOSR-TR. 88-00000       |  |
| 9. SPONSORING / MONITORING AGENCY NAME(S) AND ADDRESS(ES)<br>AFOSR/XOT<br>Bld 410<br>Bolling AFB D.C. 20332-6448 |  |   |  | 10. SPONSORING / MONITORING<br>AGENCY REPORT NUMBER<br>F49620-88-C-0053 |  |
| 11. SUPPLEMENTARY NOTES  |  |   |  |   |  |
| 12a. DISTRIBUTION / AVAILABILITY STATEMENT<br>Approved For Public Release  |  |   |  | 12b. DISTRIBUTION CODE  |  |
| 13. ABSTRACT (Maximum of 200 words)<br>See Attached  |  |   |  |   |  |
| 14. SUBJECT TERMS  |  |   |  | 15. NUMBER OF PAGES   |  |
|  |  |   |  | 16. PRICE CODE  |  |
| 17. SECURITY CLASSIFICATION<br>OF REPORT<br>Unclassified   |  | 18. SECURITY CLASSIFICATION<br>OF THIS PAGE<br>Unclassified |  | 19. SECURITY CLASSIFICATION<br>OF ABSTRACT<br>Unclassified              |  |
|  |  |   |  | 20. LIMITATION OF ABSTRACT<br>N/A                                       |  |

## INTRODUCTION

AFOSR-TR- 90 0660

In the near future the United States may face shortages of scientists and engineers in fields such as physics, electronic engineering, computer science and aeronautical engineering. High School students are currently not selecting to prepare for careers in these areas in numbers large enough to match the projected needs in the United States.

The Air Force faces "a formidable challenge - the acquisition and retention of the technological competence needed to ensure a strong national security, both in-house and in the industrial and academic base which supports defense preparedness." The Director of the Office and Science of Technology Policy in the Executive Office of the President in 1979 responded to this need by requesting the federal agencies to incorporate in their contract research programs the mechanisms to stimulate career interests in science and technology in high school students showing promise in these areas. The Air Force High School Apprenticeship Program is an example of the response to this. (JF) E

Under the Special Studies section of the Summer Faculty Research Program an Air Force High School Apprenticeship was initiated. This program's purpose is to place outstanding high school students whose interests are in the areas of engineering and science to work in a laboratory environment. The students who were selected to participate worked in one of the Air Force Laboratories for a duration of 8 weeks during their summer vacation.

The Air Force High School Apprenticeship Program was modeled after the Army's High School Program, which is very successful.

The following time schedule was used in order to accomplish this effort.

ASTRONAUTICS LABORATORY

# FINAL REPORT

Student: Ross Benedict

Mentor: David Ductor

August 11, 1989

Astronautics Laboratory  
Air Force Systems Command

### Acknowledgements:

I am grateful to my mentor, David Ductor, for his patient instruction and willingness to answer my many questions. I also appreciate the help and association of the rest of my section members, notably; Cade Coombs and Chris Zarobsky, co-op students from Purdue University. I was happy to be of service to everyone in the Vehicle Systems Analysis and Integration Section.



## Final Report

During the summer of 1989 I worked at the Astronautics Laboratory (Air Force Systems Command) as part of the Vehicle Systems Analysis and Integration (VSAA) Section. The VSAA section provides analysis for the rest of the lab while also running the National Hover Test Facility.

The National Hover Test Facility is a unique facility for the hover testing of kinetic kill vehicles in a controlled environment. During the Kinetic Kill Vehicle Hovered Interceptor Test (KHIT) the facility had seven successful tests including four free-flight tests. KHIT was a test of a Kinetic Kill Vehicle propulsion system in a dynamic situation. On the 1st of August 1989 the Onboard Navigation Target Acquisition and Real Time Guidance Experimental Test (ONTARGET) had its first successful test. The ONTARGET test tested a seeker during flight conditions and also successfully used the aim-point-shift algorithms. The aim-point-shift algorithms are used to change the IR seeker's lock-on from a missiles plume to the missiles hard-body thus allowing an intercept.

KHIT and ONTARGET are both SDI programs dealing with Kinetic Energy Weapons, specifically Kinetic Kill Vehicles (KKV). A KKV uses its own kinetic energy or momentum to disable or destroy its intended target. Ground-based testing is used instead of space-based testing to reduce costs and risks.

KHIT was a series of three static tests and four free-flight tests. The three static tests were done to test the vehicle's propulsion system and onboard equipment. The free-flight tests proved that a KKV could be hover tested by having the vehicle hover without having safety cables or other instrumentation attached.

ONTARGET is a series of three tests in which the vehicle uses an IR seeker to locate a Bates solid rocket motor, to simulate an Inter-Continental Ballistic Missile, while the vehicle is in flight. This was done to see how the seeker would react in a flight situation and to test the aim-point-shift algorithms.

I was assigned by my mentor to assist Chris Zarobsky, a co-op student from Purdue University, in writing the facility description document for the National Hover Test Facility. This document will be made available to companies that are interested in hover testing their own KKV's. My input to this project included producing numerous illustrations and assisting in editing the document. I also was involved in a meeting with personnel from Vandenburg Air Force Base to discuss the document and the use of the Universal Documentation System. Once Zarobsky and my work is completed the document will be passed on to senior section members for approval before it is released for publication. I have attached a copy of the National Hover Test Facility Description Document.

While working on the Facility Document I used various Macintosh computer systems and software. For the illustrations I used MacDraw II. Normally I would have a picture of the item to be drawn, however, several of the drawings required me to work from memory. While editing the document I used Word 3.01, the program the document was written with.

I also assisted co-op Cade Coombs in doing an analysis of Pulse and Boost-sustained motors in tactical air-to-air missiles. My work with Cade consisted of aiding him in data reduction and the production of graphs and charts to facilitate the presentation of his findings. I used the Cricket Graph program for data reduction and graphing. I was required to place the data that

Cade generated into Cricket Graph, another program for the Macintosh computer system, and then used the built-in graphing function to make the graphs.

National Hover Test Facility  
Description Document

Astronautics Laboratory  
Edwards Air Force Base, CA

C. Zarobsky  
R. Benedict

## SECTION I

### TEST FACILITY OVERVIEW

#### 1-1. TEST FACILITY

The SDIO National Flight Test Facility is a uniquely qualified facility for the purpose of static and flight testing Kinetic Kill Vehicles (KKVs). Some of the features which make the facility unique are its independent propellant storage and propellant handling capability, several independent data acquisition systems, off-board tracking and measurement capability, and various stand alone telemetry and range safety systems. To date, the facility has provided support for both the KKV Hovered Interceptor Test (KHIT) and the Onboard Navigation Target Acquisition and Real-time Guidance Experimental Test (ONTARGET) program. A detailed facility legacy is discussed in Section 7.

The Flight Test Facility is located on Leuhman Ridge in the Mojave desert at the Astronautics Laboratory, Edwards AFB, CA. Historically, the ridge operated as the Rocket Propulsion Laboratory and has supported propulsion testing for all major US Booster systems. The facility is operated by the Analysis and Integration branch of Vehicle Systems. An overview of the facility is shown in Figure 1.

The primary objective of the facility is to support ground based, reduced risk, flight and static testing of KKV's by providing a complete test facility and engineering team.

#### 1-2. HIGH BAY TEST AREA

The high bay building contains both facility hardware and specialized instrumentation and test hardware to accomplish ground based testing. The facility characteristics include a 110% spill containment berm, an overhead crane for lifting and moving objects inside the high bay, and a blast resistant observation bay window between the control room and the high bay for direct observation. The flight volume is encompassed by a nylon net which serves as both a capture medium after the vehicle completes its maneuvers in the flight volume and a safety net for the facility should the maneuvers become erratic before flight shut-down occurs. Also available in the high bay is a complete set of film and video cameras for historical reference and post-flight analysis.

Specialized instruments include: two contrast video tracking cameras to provide real-time trajectory information, a unique telemetry configuration using a combination of anechoic material and directional antennas to reduce multipath interference and maintain a clean signal, a precision external position and velocity identification system using laser interferometers for flight profile trajectory reconstruction, a high accuracy center-of-gravity and moment-of-inertia (C.G./M.O.I.) measurement device to provide data for C.G. migration and mass properties time history trace of the test article before and after flight, and a launch cradle and scissor jack stand that can be easily modified for different vehicle configurations.

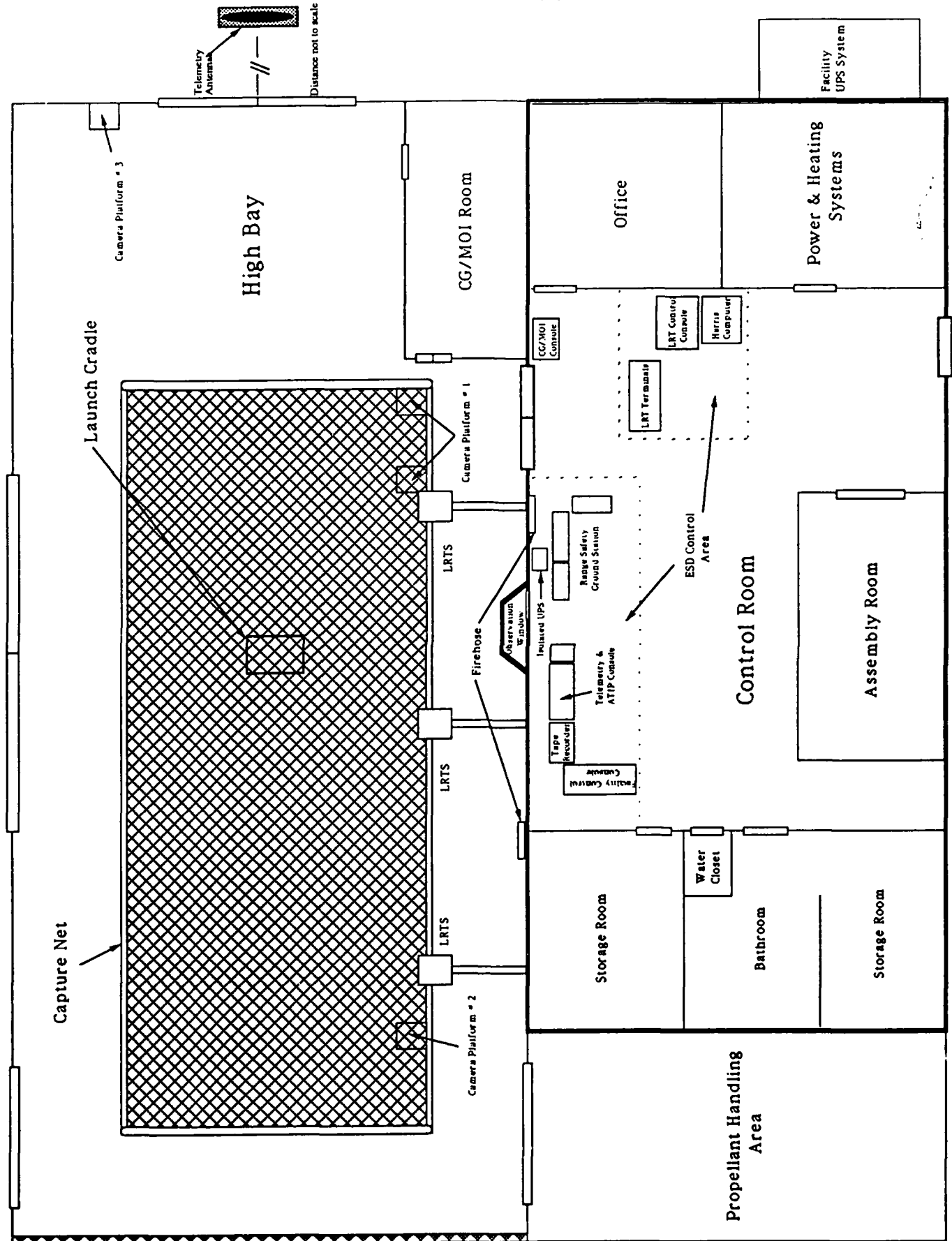


Figure 1. Facility Overview

### 1-3. CONTROL ROOM

The control room which adjoins the high bay is the primary operations center. It is constructed of twelve inch thick concrete, with a seven p.s.i. overpressure blast resistance rating. It contains a dust controlled vehicle assembly room with laminar flow bench for pre- and post-flight cleaning and purging of the test article, a large centralized area for ground support equipment, and necessary rooms for storage and office space. The entire control room can be sealed internally and the air conditioning system put into a recirculation mode to prevent any hazardous vapors in the high bay from migrating into the control room. Instrumentation and control equipment includes a stand alone telemetry ground station, four data acquisition microcomputers, a VAX workstation, a laser tracker control and data acquisition station, a ground control station for use in a flight avionics package or as the primary range safety system, video monitors for real-time observation, and a complete communications link between AL safety operations and all the operational buildings at the site. The capacity to interface special ground test equipment with standard facility equipment also exists.

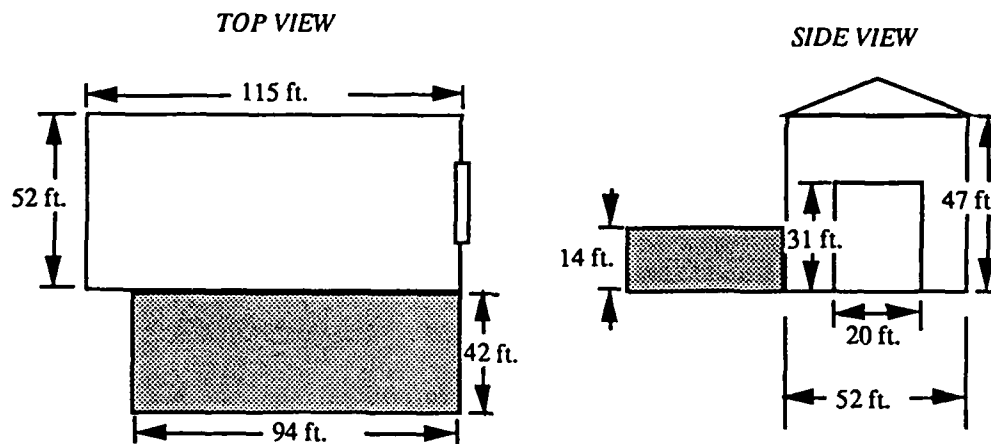


Figure 2. Facility Dimensions

### 1-4. PRIMARY OPERATIONS CENTER

In addition to the test facility high bay and control room, another building is dedicated to KKV testing. This primary operations center is located approximately 600 feet from the high bay and control room, and serves to support the test facility and personnel. This building contains a large amount of office space and a conference room which has a direct video and audio link with the high bay. Figure 3 shows the area layout with the test facility, the

primary operations center, the propellant storage locations, and the IR Target Simulator.

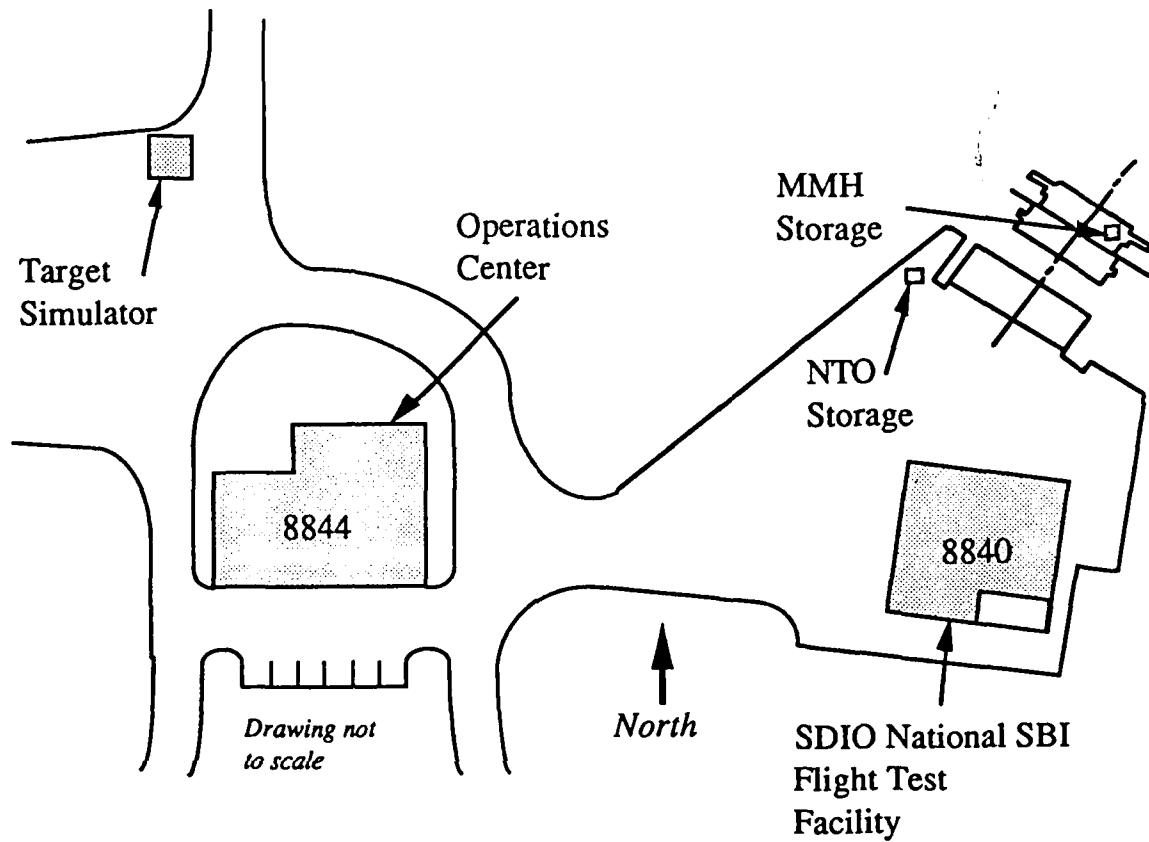


Figure 3. Test Area Overview



## SECTION 2

## FACILITY SUPPORT SYSTEMS

## 2-1. CONTRAST TRACKING

An important consideration in flight testing is the ability to collect and distribute real-time and post-test trajectory information. The real-time position information of the vehicle in three axes is provided by the facility ground control console which utilizes a contrast camera tracking system located in the high bay. The contrast tracking camera system consists of two black to white image CCD video cameras and tracking software which tracks the contrast of a white area painted on the vehicle against the dark background of the high bay. One camera is mounted on the ceiling and one camera is mounted on the east side wall in order to provide the required three dimensional coordinate information. Figure 4 depicts the 87° field of view volume constraint which is based on pixel size and screen display. The current configuration permits an accuracy of approximately  $\pm 0.5$  feet.

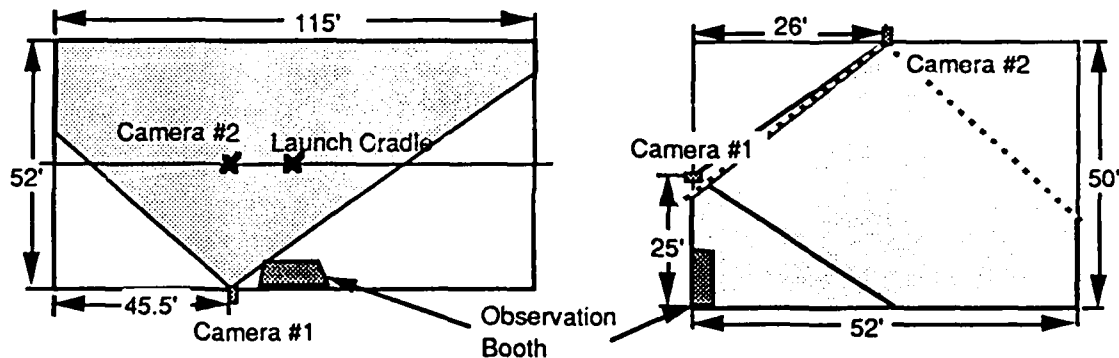


Figure 4. Contrast Tracking Camera FOV

The tracking system is an integral part of the facility range safety system. Real-time vehicle trajectory information is provided to the facility ground computer for range safety shut-down evaluation. The range safety shut-down system is detailed in Section 4. The same real-time trajectory information is also available at 60 Hz for use in control system navigation updates.

## 2-2. LASER TRACKING

An external non-intrusive tracking system obtaining vehicle attitude and position measurements with a higher degree of accuracy than either the onboard vehicle instrumentation or the contrast video tracker, is currently under development at the Astronautics Laboratory. This system, the Laser Ranger Tracking System (LRTS), is a non-contact system that provides the

high accuracy information necessary to determine thruster characteristics and vehicle dynamics during post-test analysis.

The LRTS provides range information by laser interferometry. The current system uses three laser tracking units (LTUs) mounted approximately twenty-two feet apart on the high bay wall and three 6.5 oz. retroreflectors mounted on the vehicle. Each LTU consists of a 0.4 milliwatt output Helium/Neon laser controlled by an IBM AT microcomputer. All laser operations are performed remotely from the control room. Figure 5 shows the LRTS orientation in the facility.

Each LTU tracks a single retroreflector. After an extensive calibration sequence, the trackers are locked on to the vehicle retroreflectors and retain lock-on throughout flight using a combination of two angular motors and their respective controllers. As the object is moved, each LTU maintains its beam centered upon the retro and provides change in range information at 100 KHz. Angular hub encoders are used to determine laser azimuth and elevation. The IBM microcomputer controller is responsible for retaining lock on and relaying the range and angle information to the LRTS system computer. The system computer, a Harris MCX-5, is used to record the change in range and angular encoder information while a separate processor is used to calculate a set of three dimensional coordinates relative to the stationary facility reference frame.

The existing system can provide position and attitude information with accurate to within 100 microns. The expansion capability of the LRTS includes installation of three additional LTUs to provide increased accuracy and software modifications to provide 100 Hz real-time attitude and position information via a standard computer interface. Also available are extremely lightweight retroreflectors for use on future flight vehicles.

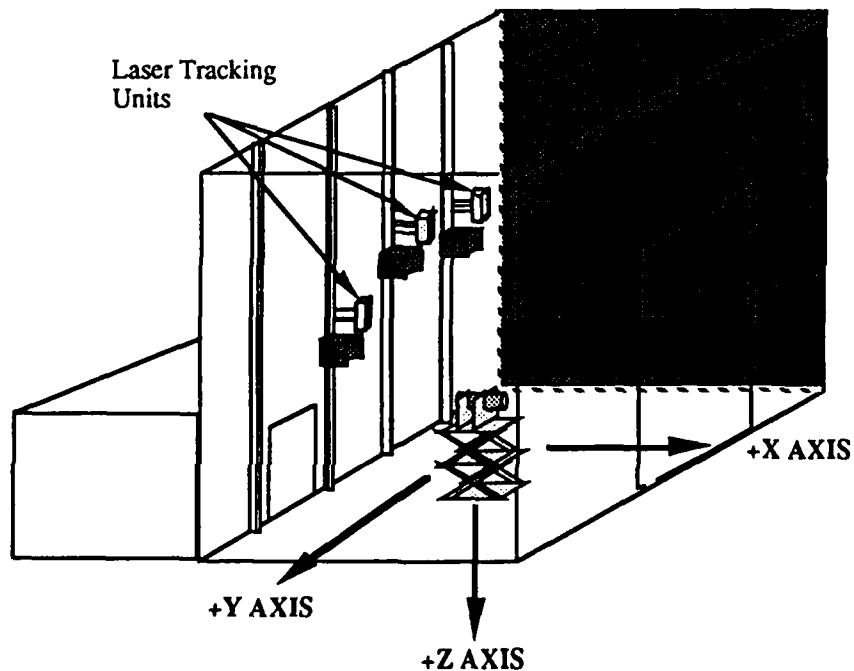


Figure 5. LRTS Layout

## 2-3. DATA ACQUISITION AND INSTRUMENTATION

Data acquisition is accomplished during static tests using hardwire links or through a telemetry link. Flight data acquisition uses an S-band telemetry link. Available data acquisition computers include: a DEC Micro Vax 3200 computer and work station, two Aydin Vector Model 1249 telemetry test sets, two Macintosh II microcomputers, two IBM compatible microcomputers, and an HP 3572A DAS. Table 1 lists the DAS capability. Existing software and hardware data links can be easily configured to meet most data acquisition needs. Post-test data is available in engineering units in Macintosh, IBM, and Vax ASCII format.

Table 1. Data Acquisition Capability

The table of data acquisition capability has not yet been completed.

Telemetry signals are recorded using two Bell & Howell Model 3728E DataTape Magnetic Tape Drives. The Model 3728E has 6 direct channels and 1 FM channel. Analog recording capacity is 6 megabits per second. Five direct channels have a digital capacity of 2 megabits per second. One direct channel has been upgraded to handle 3.5 megabits per second. A time code generator is used to record a reference for later playback.

For non-flight operations the range safety ground console can act as the primary data acquisition system for checkout and fault diagnostics. An umbilical hardwire link specific to the vehicle will be designed to provide vehicle health information to the ground control station for pre-test operations. Pre-flight preparations which can be performed via this umbilical include commanded valve vs received valve data, squib checks, pre-flight ordnance, power checkout, battery charging circuit, and helium load monitoring. The umbilical will have the ability to release remotely via a command actuated solenoid directed from inside the control room. Another umbilical is available to establish a GN2, or other coolant, flow to cool the avionics housing during non-flight operation.

A variety of vehicle instrumentation is available for use during free flight and static tests. Available transducers and accompanying signal conditioning units include light-weight thermocouples, pressure sensors, and tri-axial accelerometers. Table 2 lists the base-line instrumentation.

Table 2. Baseline Instrumentation

The table of available baseline instrumentation has not yet been completed.

#### 2-4. ATIP

An Airborne Telemetry and Instrumentation Package (ATIP) has been developed here at the AL by test engineers to provide a light-weight telemetered data acquisition system for use in free flight tests. The ATIP system's primary purpose is to provide an instrumentation package capable of data acquisition independent of the flight control system. This includes maintaining a data link to the vehicle after the flight termination system has been activated, providing critical post-test safety information. In addition, real-time and post-test fault diagnostic information is available for flight performance analysis. By providing its own transmitting and receiving link, ATIP is completely autonomous of the test vehicle's avionics.

In its current configuration ATIP weighs approximately 11 lbs. Thirteen channels of data are provided for at 3900 Hz. ATIP data recording is synced with IRIG-B 10 msec interrupt signal. Data capacity, currently 80 megabytes, is limited only by disk space which is easily expanded. An operational schematic detailing the proven KHIT ATIP instrumentation configuration is shown in Figure 6.

#### 2-5. CG/MOI MEASUREMENT

The location of the center of gravity and the moments of inertia (CG/MOI) of the test article are measured directly at the facility using a Space Electronics KGR-300S mass properties instrument. This instrument can accurately measure the center of gravity in three axes to within 0.001 inches.

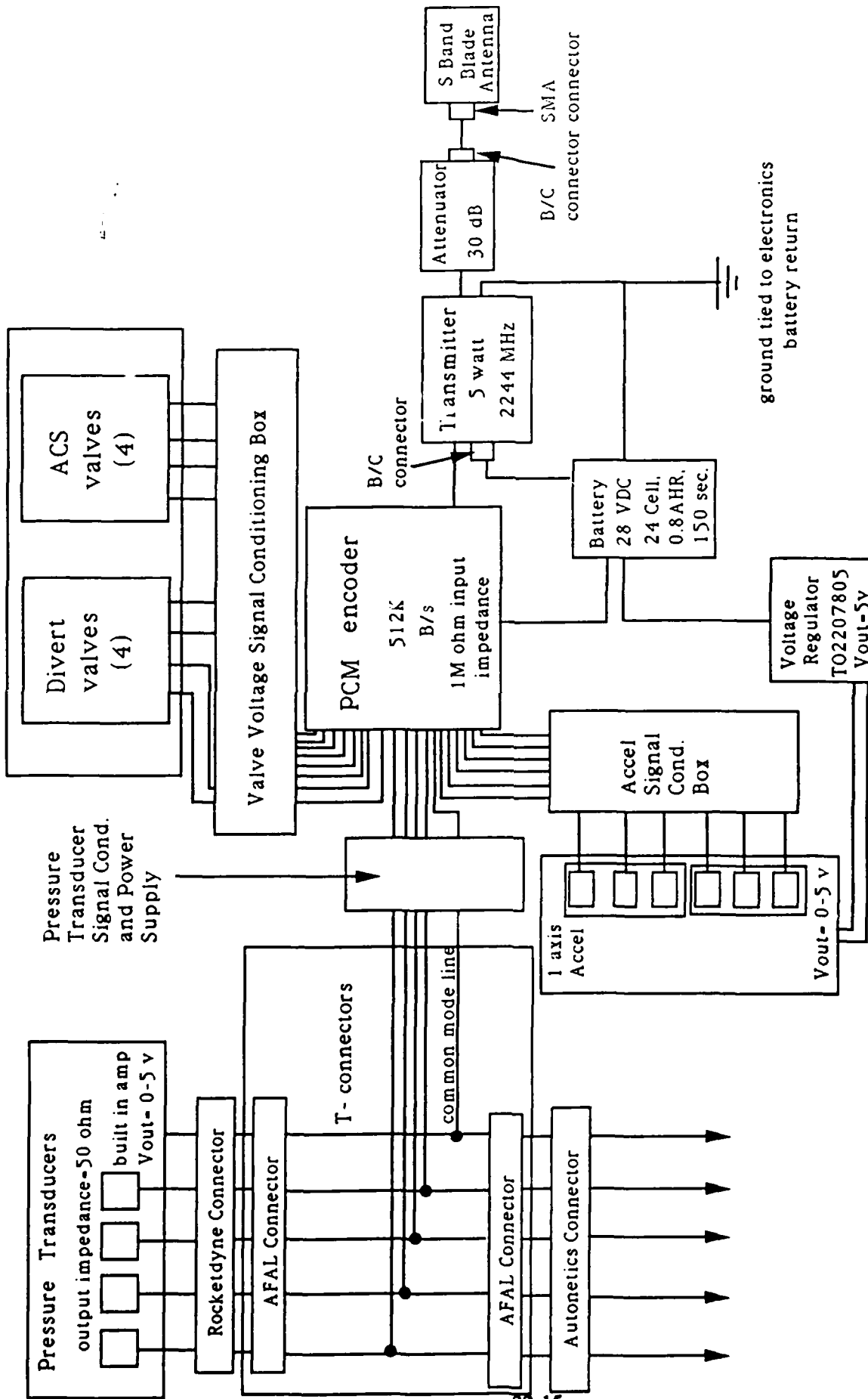


Figure 6. ATIP Schematic

and the moment of inertia in three dimensions to within  $\pm 0.25$  in-lb<sup>2</sup>. The maximum weight the instrument can measure is 300 lbs.

Center of gravity of a test article in two dimensions is determined by taking a set of measurements from a load cell located at the end of a moment arm. Two axes are measured with the vehicle in flight orientation. The center of gravity location in the third dimension is measured with the vehicle standing on end. The vehicle is fastened to the instrument with the use of a custom machined fixture provided by the user. The center of gravity is then balanced to the desired location using a series of calibrated weights. Determination of the moments of inertia of the test article is accomplished using a gas bearing, an internal braking system, and a rod of known torsional stiffness which acts as a torsional spring. Again two different orientations of the vehicle must be used to measure moments in all three axes.

Because the mass properties instrument is sensitive to air currents it is housed in a structure inside the high bay. The control console, an IBM PC located in the control room directly behind the CG/MOI room, is used both for instrument control and data acquisition. The CG/MOI instrument is depicted in Figure 7.

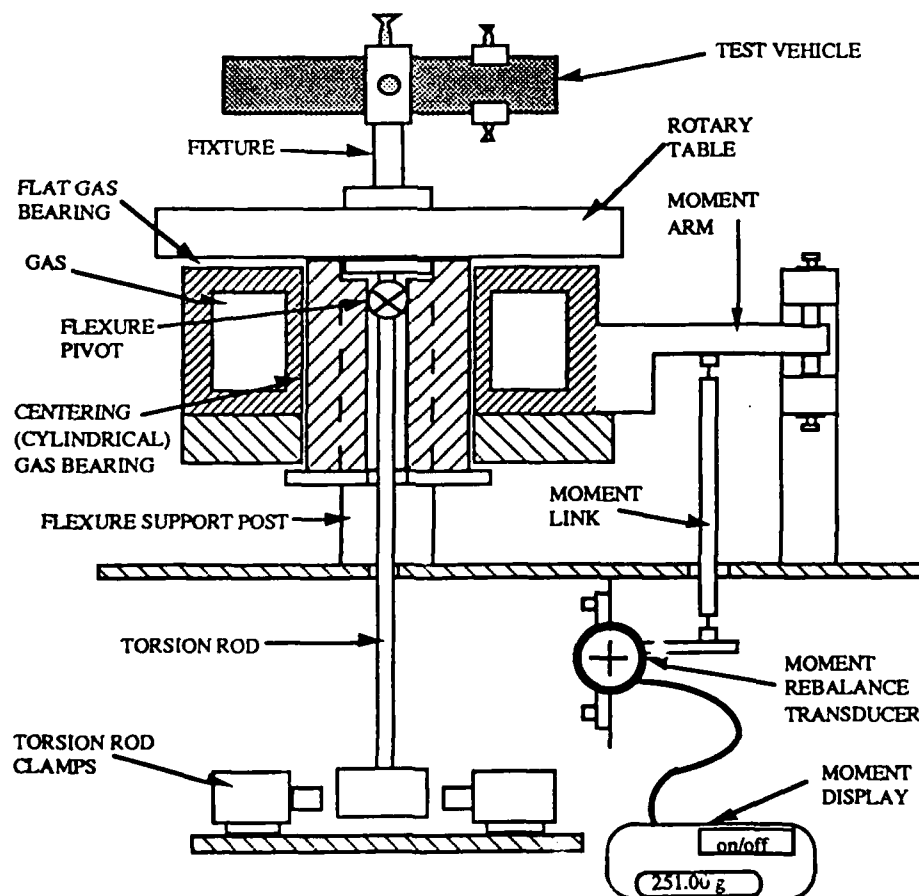


Figure 7. CG/MOI Instrument

## 2-6. AUDIO-VISUAL RECORDING

Audio-visual data is also of importance during vehicle testing. The facility has a number of still, high-speed movie, and video cameras installed throughout the high bay. These include three 16mm Milliken movie cameras at 100 feet per second, four Nikon still cameras at one or two frames per second, one high-speed Photosonics camera, and eight video cameras. The movie and still film can be processed post-test through AFFTC photographic support. Four Hitachi video cameras are mounted on motorized platforms which can be controlled from the control room. The other four cameras are mounted on the walls of the facility. Video and audio is recorded using eight high quality Mitsubishi 1/2" video cassette recorders located in the control room. The test time and date are recorded using eight time/date generators connected to the recorders.

The capability for recording the target simulator IR signature also exists using an Inframetrics Model 610 Dual Channel IR Imaging Radiometer with 3.4 and 5.1 micron filters. Simultaneous thermal imaging in both 3-5  $\mu\text{m}$  and 8-12  $\mu\text{m}$  spectral bands is available.

## 2-7. STATIC TEST FIXTURE

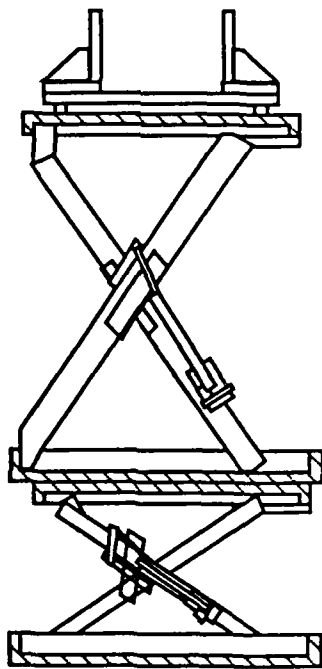
Static vehicle propulsion tests are performed with a static test stand using either flightweight or heavyweight propellant tanks. The fixture has been designed to withstand the high temperature hazardous exhaust plumes and thrust forces generated during the test while providing ready access to all propulsion system components. Test data can be downlinked using the flight telemetry data acquisition system or hardwired directly to the data acquisition computers. The current static test configuration can be easily modified to support any test article.

## 2-8. LAUNCH FIXTURE

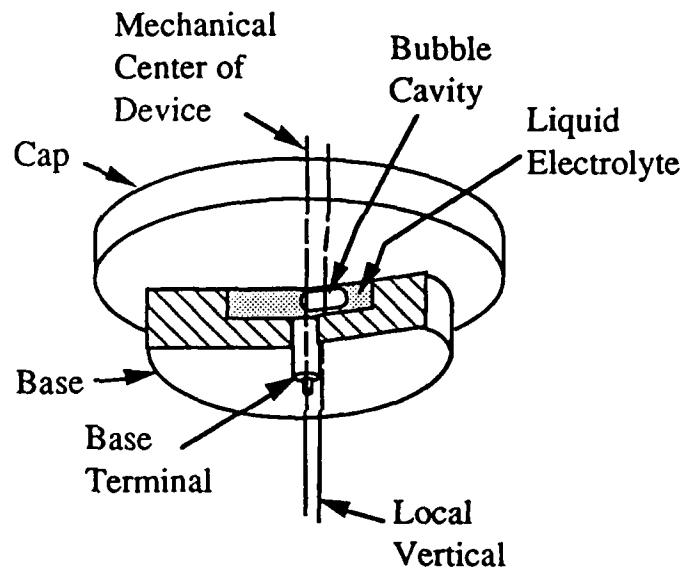
The launch fixture used to sustain the vehicle statically in the test volume for launch consists of four items: lift platform, launch cradle, leveling fixture, and biaxial tilt meter.

The lift platform consists of identical upper and lower stage hydraulic scissor jacks driven by a linear actuator which is operated from the Control Room. The platform maintains its position using a combination brake-clutch mechanism. Maximum extended and minimum retracted heights are 20 feet and 4.75 feet respectively. On launch a micro-switch in the cradle triggers the descent of the lift platform, lowering 58 inches in 3.0 seconds, limiting the exposure of the launch fixture in the flight volume during the test. The launch fixture can be easily relocated in the high bay and also has the capability for limited yaw positioning to allow for a direct line of sight of the target simulator.

The launch cradle that holds the vehicle is composed of two mechanically collapsing support stands using a frangible fiberglass and epoxy structures made to fail should a dynamic load 3 times greater than a normal static load impact the structure. The cradle collapse is triggered by the descent of the lift platform. The two support stands swing on hinges and lie flat against the lift platform further limiting flight volume exposure. The lift platform and launch cradle are shown in Figure 8. Because the cradle is vehicle specific, each test vehicle will require design and fabrication of its own cradle. The can be done in the facility by AL personnel.



Launch Fixture



Tilt Meter

Figure 8. Launch Fixture

The leveling fixture is used to balance the vehicle precisely and accurately on the cradle prior to launch. Three worm gear screw jacks driven by DC stepper motors accomplish this task. The leveling operator is remotely located in the control room and receives leveling feedback from the biaxial tilt meter mounted on the vehicle.

The biaxial tilt meter is a sensitive bubble meter mounted on the the vehicle. Resolution of  $\pm 0.1$  milliradian is accomplished using an electrical wheatstone bridge configuration. This device sends a signal to the operator corresponding to the position of the bubble in a volume of electrolytic fluid. The operator balances the vehicle in roll and pitch using the computer controlled stepper motors and an analog readout with four scales. In order to



insure that the thrust vector is aligned with the gravity vector, it is recommended that the tilt meter mount surface be machined at the same time as the divert thruster ring to a tolerance of  $\pm 0.1$  milliradian. A cut away view of the tilt meter appears in Figure 8.

## 2-9. PROPELLANT HANDLING AND PRESSURIZATION

The facility currently has storage areas for both Monomethyl Hydrazine (MMH) and Nitrogen Tetroxide (NTO) on site and the equipment necessary to load, decontaminate, and neutralize all on-site. The storage areas consist of shaded downwind barrel and tank placement of the propellants inside concrete berms that can provide 100% containment of the propellant amount stored. Safety equipment, showers and fire hoses are available at each site along with power and communication systems between the control room, high bay, and the visitor block house, if necessary. The facility will provide MMH, NTO, other Hydrazine blends, or other oxidizers as necessary.

AL personnel have been trained and are qualified to work on the Red Crew responsible for hazardous propellant servicing operations. For safety restrictions, only the AL will be permitted to handle hazardous propellants. Propellant service operations are performed using propellant carts which provide a totally contained system to load and neutralize the propellants. The propellant service system transfer cart is used to load a nominal amount of propellant in a transfer storage container, transport it to the vehicle loading area, and load the static test system or flight vehicle by either a vacuum or positive pressure fill. The propellant decontamination and neutralization system cart is used as a decontamination/neutralization system for hoses, tanks and fittings to downgrade the propellants below fuel grade. The propellant handling and decontamination carts are depicted in Figure 9.

Propulsion system pressurization with Helium is provided for using a special cart, shown in Figure 9, currently capable of up to 10,000 psig. Like propellant operations, pressurization will be performed exclusively by AL personnel.

The facility is equipped to supply large amounts of GN2 to anywhere in the building, providing support for the gas bearings for the CG/MOI machine, coolant to the vehicle electronics, remote access to the doors on the LRTS, or coolant to the engine valves during static tests. A compressed air controlled humidity cooling system is available for pre-test vehicle operations.

## 2-10. CLEANROOM

An operational class ?????????? cleanroom with support equipment is available. This section not yet completed.

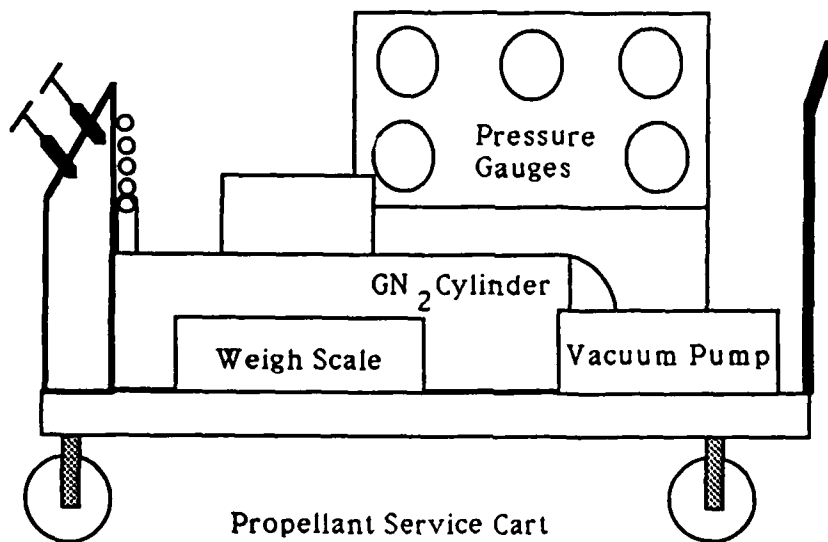
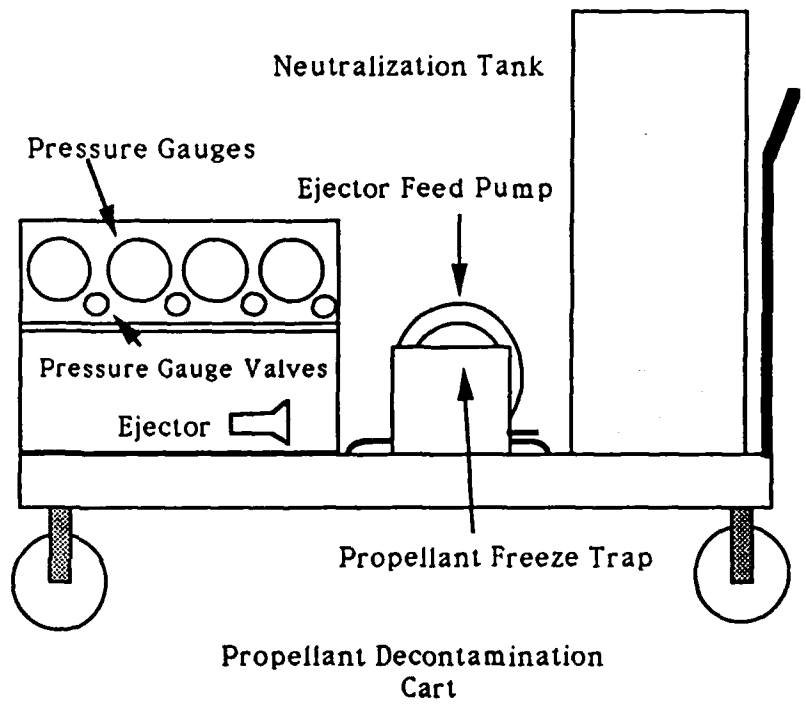
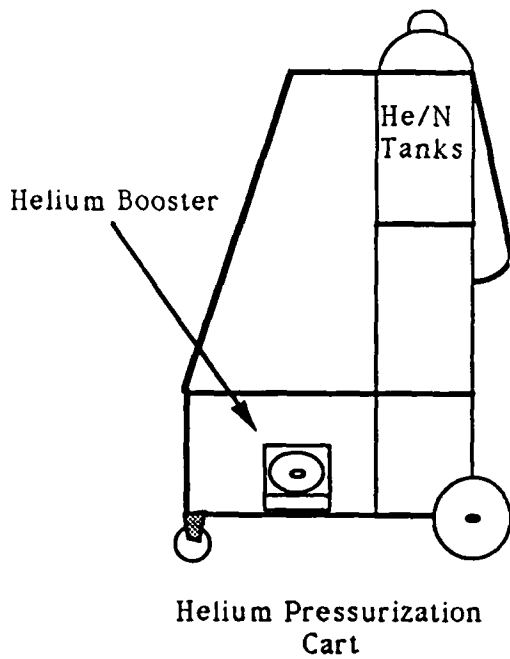


Figure 9. Propulsion System Service Carts

## 2-11. EHV TEST PLATFORM

A proven Experimental Hover Vehicle (EHV) test platform is available for flight testing KKV components. The EHV consists of a KKV propulsion and guidance system available for integration with seekers, avionics packages, and other critical components. The EHV was successfully flight tested in the Kinetic Kill Vehicle Hovered Interceptor Test (KHIT) program at the AL in April 1989.

The test structure consists of a carbon composite filament wound tube 11.5 inches in diameter and 70 inches long. The propulsion system consists of 4 divert engines each capable of providing 300 pounds (lbs) of thrust. The hover test uses the bottom divert to provide the thrust to null the effects of gravity. The 4 ACS thrusters provide pitch, roll, or yaw and deliver 5 lbs of thrust. The inertial reference unit is an AMRAAM IMU available as an off-the-shelf hardware item. The guidance and control algorithms are located on a central ground processor, which receives IMU and attitude information via a telemetry downlink, does the appropriate calculations for the next position change, and uplinks engine commands to the onboard avionics. The vehicle maneuvers by 'pogo control', where the ACS thrusters fire in combinations to induce roll or pitch and direct the divert thrust vector. This combination of bottom divert thruster firing approximately 50 percent of the time and the ACS engines controlling attitude keeps the 150 lb vehicle aloft and propels it in the commanded direction.

Integration of KKV components will require a combined AL/user effort to maintain vehicle system integrity and insure a successful test. Detailed information about the KHIT program and vehicle is available upon request.

## 2-12. TARGET SIMULATION

The facility is capable of providing simulated targets for infrared signature generation. The target stand simulates an infrared signature of an ICBM for KKV image processing and aimpoint shift testing. It consists of three components, the Ballistic Test and Evaluation System (BATES) stand, plume simulator and hardbody simulator.

The BATES stand is a test platform for firing solid rocket motors nozzle up. The BATES solid rocket test motors will be produced by the AL. Various combinations of propellants are available with burn times ranging from 4 to 10 seconds. BATES plume phenomenology data has been acquired and is available upon request.

The plume simulator is a calibrated ceramic heating element used when the BATES motor is not firing. A hardbody signature is generated using a heated aluminum plate contained inside a thermally insulated box. Six microprocessor controlled regions enable a temperature gradient from 120° C to 220° C to be produced across the hardbody simulator. Target stand data acquisition and control is done remotely from the control room. Figure 10 depicts the IR target simulator.

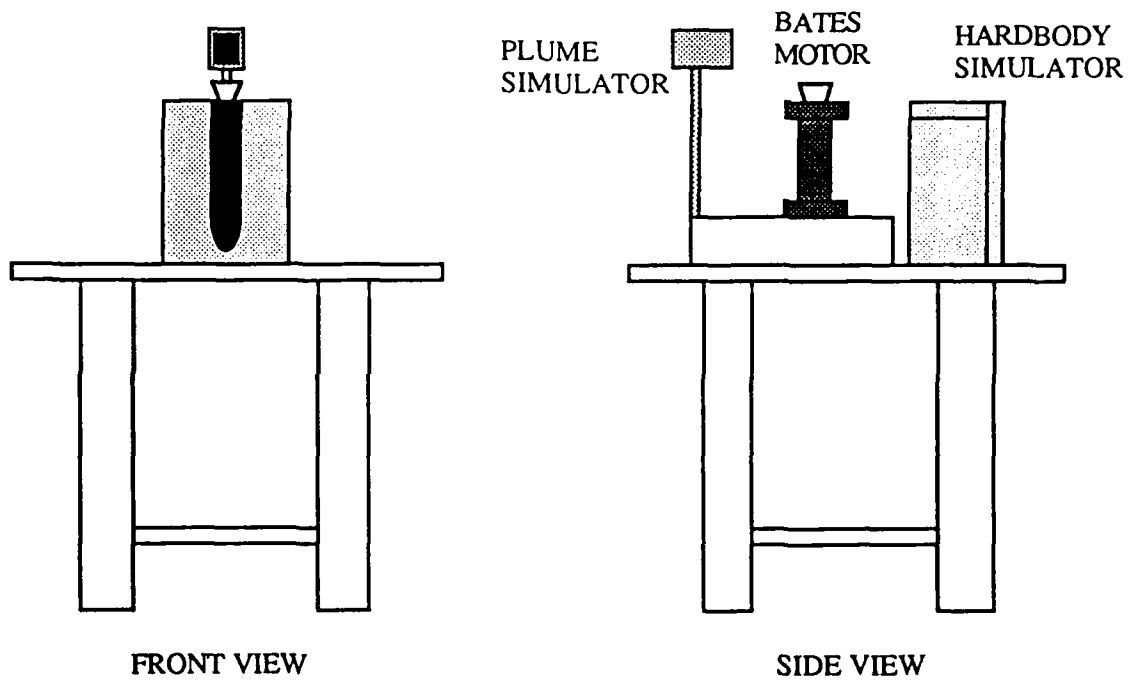


Figure 10. IR Target Simulator

### SECTION 3

#### FACILITY CHARACTERISTICS

##### 3-1. PROPELLANT CONTAINMENT

To allow for catastrophic failure of either propellant tanks in flight or on the launch fixture, a 2 inch concrete berm was built around the perimeter of the vehicle handling area inside the high bay and the propellant loading area. Given the volume of propellant typical used during a test and size of area, this berm contains 100% of the liquid volume. Special non-volatile putty has been used to seal excess holes, cracks and drainage pots in the high bay floor. Because exhaust gases are not contained in the high bay test area, the control room is sealed and placed on recirculated ventilation during hazardous operations.

##### 3-2. METEOROLOGICAL SUPPORT

Meteorological support is provided for test operations by the AL Safety Office and on-site facility personnel. Safety Office information has general weather information including current humidity, temperature, and wind conditions available. The Safety Office can also provide wind information specific to Area 1-125E, the location of the test facility available through its Micronet computer system. Historical weather information is available from the AFFTC Meteorological Office. On-site weather measurements include temperature, relative humidity, and wind information of the facility roof and at the IR Target Stand. A portable anemometer and weather computer set-up can be used to measure wind conditions inside the high bay in different test configurations.

##### 3-3. POWER SYSTEMS

The test facility is equipped to supply adequate power for test operations. The facility has a 15 KVA Uninterruptible Power Supply (UPS) in operation at all times. Approximately forty 120 vac utility outlets are available for user ground support equipment. Three phase 208 vac and 480 vac power is also available. A second smaller UPS rated at 7.5 KVA can provide 120 vac and 208 vac single phase power to special test equipment if test requirements dictate the use of a separate connection. Standard surge suppression and line filtering are performed by both power supplies.

### 3-4. ASSEMBLY ROOM

The assembly room is a dust-controlled environment used for vehicle integration and checkout. The workspace contains a vacuum oven, a laminar flow bench, and a flow bench for testing rocket engine components.

### 3-5. PERSONNEL COMMUNICATIONS

The personnel headset communications net allows communication between test personnel from their locations in the control room. Presently, approximately 40 headset outlets exist in the Control Room. In addition, direct communications between AL Safety Operations and the control room exist at all times.

### 3-6. TELEMETRY COMMUNICATIONS

Testing in the absence of hardwire instrumentation links, i.e. free-flight, is accomplished using an S-band telemetry link and a specialized antenna scheme. Multipath interference commonly found inside closed metal buildings was overcome using a combination of anechoic material placement and directional antennas.

The current configuration provides for an S-band command up-link, an S-band telemetry downlink, and a UHF range safety link. The directional telemetry link provides a volume which covers approximately 65% of the flight volume whereas the UHF range safety link covers the entire facility. Figure 11 shows the outdoor antenna configuration and the telemetry volume. The directional antenna has a gain of 14 dBs and the cable loss from antenna to receiver is 7 dBs.

Current available equipment can support telemetry operations in upper L band and lower S band. Expansion capability includes support for upper L band and lower S band. Four PCM bit synchronizers capable of 5 megabits per second are available along with a Loral ADS-100 Advanced Decommuation System with bit synchronizer and digital or analog outputs. Although data encryption is not presently supported, implementation of government standard encryption is possible.

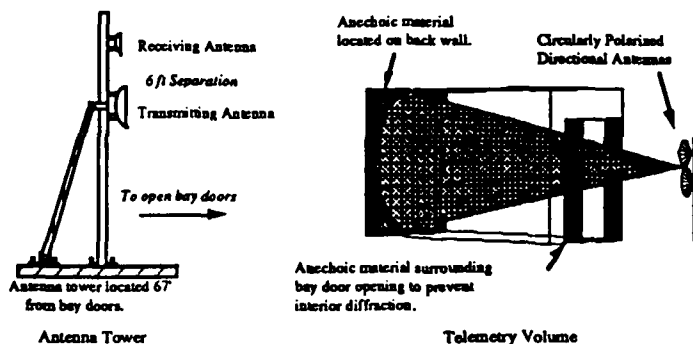


Figure 11. Telemetry Configuration

## SECTION 4

### FACILITY RANGE SAFETY

#### 4-1. GENERAL SAFETY POLICY

The Safety Policies Section has yet to be completed.

#### 4-2. FACILITY CONSIDERATIONS

The control room is constructed of 12" thick concrete walls rated at 7 psia overpressure blast resistance which gives an exceptional margin of safety for all operations and test personnel.

A primary component in the vehicle and facility flight range safety system is a nylon capture net. The net encompasses the entire volume of the high bay area, 10 feet off the ground and 12 feet from the side and top walls. The net serves as both a capture medium after the vehicle completes its maneuvers in the flight volume, and a safety net for the facility should the maneuvers become erratic before flight shutdown occurs. Nylon was chosen to minimize any multipath interference due to telemetry in the building.

The net is composed of 4 inch by 4 inch nylon squares and secured in a box volume of 30 ft. by 80 ft. by 35 ft. with a 3 inch plastic tubing frame. Polypropylene ropes are woven throughout the net between the tubing sides for reinforcement. A rectangular opening wide enough for the vehicle and cradle is cut in the middle of the lower section of the net. Separate straps allow that hole to be covered during flight testing.

The net has been subjected to repeated drop tests with a dummy load of 450 pounds from 35'. It did not break or allow the weight to fall through at any time. In addition, it was subjected to temperature gradients under a controlled 2000°F flame and results noted. The net burned through after 3-4 seconds of continued application. Net damage in flight tests to date has been minimal and contained to the area around the bottom divert thruster during capture.

#### 4-3. RANGE SAFETY SYSTEM IMPLEMENTATION

Flight termination can occur from three physical paths. Each path is independent of the other and any one can send the termination command. When a termination command is sent, two independent shutdown command signals are transmitted to the vehicle in flight, the S-band link and the UHF link. All test vehicles require the use of a redundant UHF range safety receiver to be provided by the AL. The range safety shutdown diagram is shown in Figure 12.

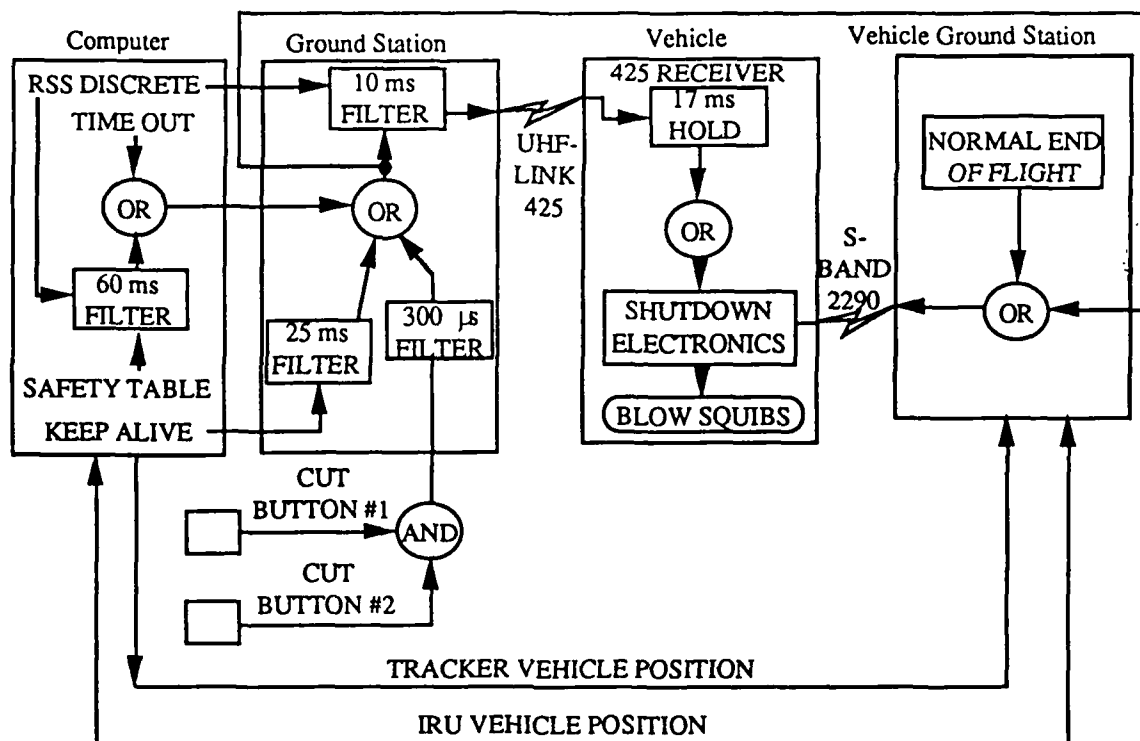


**Figure 12. Range Safety Shutdown Diagram**

The emergency termination path is the manual shutdown switch located in the observation window. A range safety officer sits in the window and observes the vehicle in flight. With the manual button he has the ability to override the flight and cause a shutdown.

The primary range safety shutdown system is the ground computer. The AL ground computer uses a combination of vehicle IMU and contrast tracker position data to determine the necessity of flight termination. Both vehicle IMU and contrast tracker position vectors are monitored every 10 milliseconds and matched to a predetermined set of safety tables. These safety tables are derived from predicted vehicle flight profile and performance. If either the IMU or the contrast camera position vectors exceed the limits of the bounds set in the safety tables, a terminate command is generated and sent to the flight termination paths. A sample of the ONTARGET safety table is shown in Table 3.



Table 3. ONTARGET Range Safety Table

| TIME<br>SEGMENT<br>(SEC) | TRANSLATIONAL POSITION (FT) |             |            | ANGULAR ATTITUDE (DEG) |               |               |
|--------------------------|-----------------------------|-------------|------------|------------------------|---------------|---------------|
|                          | X                           | Y           | Z          | ROLL                   | PITCH         | YAW           |
| [0 - 2]                  | $\pm 6.5'$                  | $\pm 16'$   | (+4',-16') | $\pm 10^\circ$         | $\pm 6^\circ$ | $\pm 6^\circ$ |
| (2 - 4]                  | $\pm 7'$                    | $\pm 16'$   | (-1',-20') | ↓                      | ↓             | ↓             |
| (4 - 6]                  | $\pm 7.5'$                  | $\pm 16'$   | (-4',-20') | ↓                      | ↓             | ↓             |
| (6 - 8]                  | (-8.5',+8')                 | $\pm 16'$   | ↓          | ↓                      | ↓             | ↓             |
| (8 - 10]                 | (-9.0',+8')                 | (-22',+16') | ↓          | ↓                      | ↓             | ↓             |
| (10 - 12]                | (-9.5',+8')                 | (-22',+16') | ↓          | ↓                      | ↓             | ↓             |
| (12 - 14]                | (-10',+8')                  | (-22',+16') | ↓          | ↓                      | ↓             | ↓             |

Onboard body rate safety table processing is permitted, however, an external position measurement system shutdown path is still required for flight tests. Implementation of the ground based range safety shut-down system requires access to IMU acceleration and angular rates in real-time via RS-232 or RS-422 computer interface.

Range safety external position measurement will be performed by the facility contrast tracking system. Safety table comparisons are computed by the AL ground station and a keep alive signal will be provided to the vehicle ground station along with a UHF flight termination command in the event of range safety shut-down.

## SECTION 5

### TEST DATA REDUCTION AND ANALYSIS

#### 5-1. DATA REDUCTION

While primarily responsible for the operation of the test facility, the Vehicle Systems Analysis and Integration section also performs a moderate analysis role. Test data can be reduced and results presented in a few days after test completion.

A variety of Macintosh scientific graphics packages are available to perform next day Quick-look data reduction. Detailed reduction is performed using the Matrix<sub>x</sub> software package on the AL Vax cluster and typically requires approximately one week to complete.

An Extended Kalman Filter (EKF) has been developed to estimate certain system states extract from flight performance data. The primary states to be estimated through the EKF are the individual engine thrust levels, divert thruster misalignments and the vehicle's CG travel. The actual vehicle states such as position and velocity are also outputs of the EKF, but they are not of interest since there are several other systems performing these measurements. The primary reason for interest in the thrust magnitudes, thruster misalignments, and the change in CG, is that these variables represent the disturbance torques to the vehicle, and the characterization of these torques is required in order to understand the performance of the system. EKF analysis requires approximately two weeks to complete.

#### 5-2. SIX DEGREE-OF-FREEDOM SIMULATION

A six degree-of-freedom computer simulation has been developed to analyze flight trajectory profiles. The simulation code was written to run on the AL Vax cluster using System-build, a simulation tool in Matrix<sub>x</sub>. The simulation examines vehicle dynamics and system response in alternate trajectory profiles. Implementation of user vehicle configuration requires detailed information including: mass properties, engine performance, vehicle geometry, and control algorithms.

## SECTION 6

### OTHER FACILITY TEST SUPPORT

#### 6-1. AL RESOURCES AND SUPPORT

The SDIO National Flight Test Facility is an integral part of the Astronautics Laboratory. The Fabrication Shop, Safety Office, and Propellant Laboratory are only some of the support received during vehicle testing. The Fabrication Shop has the ability to meet almost any short-term construction and machining task. The Safety Office closely coordinates test procedures and operations to meet Air Force Safety Regulations as well as supplying AL weather information. The Propellant Lab supports the Target Simulator by supplying the BATES test motor as well as the test personnel to fire it.

## SECTION 7

### FACILITY TEST HISTORY

#### 7-1. KHIT

The Kinetic Kill Vehicle Hovered Interceptor Test provided the proving ground for the SDIO National Flight Test Facility. On July 8, 1988 the Facility Activation Test (FAT) provided the first facility supported static test of the KHIT vehicle propulsion system. The test served to acquaint the test crew with the operation of the facility and the vehicle during actual test conditions. Test data was acquired through hardwire links between instrumentation and data acquisition computers. Since all test objectives were met and the propulsion system and facility performed as expected, this test was considered a complete success. Further information can be found in AFAL-TR-88-099 KHIT Facility Activation Test.

The second test of the vehicle propulsion test in the facility was a simulated Mission Duty Cycle (MDC). This successful test on July 21, 1988 again demonstrated the facility capability for static propulsion system testing using hardwired instrumentation. Documentation is available in AFAL-TR-88-113 KHIT Mission Duty Cycle Test.

The third static propulsion test consisted on a strap-down integrated vehicle test. The System Integration Test (SIT) was performed on October 5, 1988. Data acquisition and test control was accomplished using flight telemetry links. This successful use of the facility telemetry data acquisition system and ATIP is documented in KHIT System Integration Test, a soon to be published Astronautics Laboratory special report.

The first vehicle flight test attempt on November 18, 1988 was terminated after 3 seconds when the Range Safety system detected unsafe vehicle dynamics due to the failure of an Attitude Control Engine valve. Although the flight profile was not completed, 3 seconds of test data was obtained using flight telemetry links and the Range Safety Shutdown System was successfully demonstrated.

The second free flight test on November 18, 1988 was also terminated by the Range Safety System before launch occurred. The contrast tracking cameras locked on to a stray source of light present in the facility causing a shut-down at launch when the vehicle believed itself to be located outside of the flight volume. Modifications performed to the Range Safety System included software changes to disallow large tracker jumps and prevent unnecessary early termination of flight. The current Range Safety System is described above in Section 4.

The third free flight, performed on December 11, 1988, also resulted in an early termination by the Range Safety Shut-down System. Approximately one second into flight the Range Safety System was triggered by an unknown source of electromagnetic interference. Damage was sustained when the vehicle impacted with the cradle. Post-test modifications were performed on

the launch fixture to permit faster lowering and reduce the risk of the launch fixture in the flight volume. Electrostatic discharge and electromagnetic interference procedures and equipment considerations were subsequently implemented in the test facility.

On April 24, 1989 the first full duration hover flight of an integrated kinetic kill vehicle was demonstrated. The hover vehicle and test facility performed flawlessly as expected.

#### 7-2. ONTARGET

The ONTARGET section has not yet been completed.

Draft 8/2/89

SECTION 8  
USER REQUIREMENTS

The User Requirements section has not yet been completed.

FILAMENT WINDING PROJECT

Peter George

Jim Koury, Mentor

Astronautics Lab (AFSC)

Composite Structures Lab

Edwards AFB, CA

August 15, 1989

### Acknowledgments

I would like to extend a special thanks to my mentor, Jim Koury, for all his help and encouragement. Thanks also go to Tech. Sgt. Hamm, Staff Sgt. Goss, and Sgts. Lemley and Zinzow for answering all of my ridiculous questions.



### Objective

My goal this summer was to create a graphic-epoxy resin structure that can act as a rocket motor casing.

# Abstract

The construction of these prototyped rocket motor casing structures is a prolonged, tedious process. It involves using a mold as a basis for the desired shape of the rocket motor casing (sometimes referred to as a bottle). The procedure includes applying an insulator and then filament winding the bottle. To test the strength and inspect the bottle for faults, the bottle must be burst.

### Background

This structure is fabricated strictly of composite materials which make it lightweight and strong, as it must be durable enough to house the rocket motor.

## Experiment

Filament winding is a process of creating a graphite-epoxy resin structure. The first step in this procedure is making a solid form upon which to wind. The way that this is done is by using a mold, into which sand and sodium silicate is packed. The center is scooped out so that a shell is left with a thickness of 1 to 2 inches, and then it is baked. The hardened sand, which looks like a thick bowl, is taken out of the mold. Two of these sand mold halves are pressed together with a spackling powder around the rims, now giving it a bottle-shaped appearance. The sand bottle is covered with a layer of form-cut raw rubber which acts as an insulator. The rubber-covered bottle is put in a bag and cured in the autoclave with heat, a vacuum is pulled on the bag, and pressure is applied to the outside of the bag to make the rubber fit better on the sand mold.

When the cycle is complete and the bottle is cooled, it can be filament wound. This is a process of wrapping fibers with an epoxy resin tightly around the bottle. There are many different patterns and ways to wind a bottle. There are several types of fibers: a dry fiber, a prepreg fiber, both of which are black and a dry Kevlar fiber which is yellow. The dry fiber can be wound as is: dry, or it can be pulled through a heated liquid resin bath and then immediately wound onto the bottle. The prepreg fiber contains a slightly tacky resin and when wound it adheres fairly well to the bottle. After the pattern is chosen and is wound, the bottle goes into the autoclave for

another cure cycle. This last cycle is for the purpose of curing the fibers and will also prevent the fibers from unwinding on the bottle.

Next, the bottle is then prepared for a burst test, which will test the strength and the hoop fiber stress of the bottle. Because the original mold forms are made with sand and sodium silicate, it is water soluble and can be easily rinsed out. The bottle is placed in the burst chamber and a hose is attached to one end while the other end is plugged. The pressure is applied and water is forced into the bottle. When the bottle bursts, the burst test is complete. Data collected from the bottle test is evaluated and is utilized in ascertaining the faults and weak points of a bottle. This then completes the Filament Winding process of a bottle.

## Conclusions

My assessment of my summer work experience is a very positive one. The bottle fabrication process was interesting and exciting. I really enjoyed the time I spent here at the Astronautics Lab.

The conclusions related to the bottle making are as follows: when mixing the sand and the sodium silicate, if the ratio is not correct, then the mixture will not harden completely. There are special materials that must be wrapped around the rubber covered bottle when it is cured, otherwise when pressure is applied, the bottle can crack under the stress. Data collected from burst tests are placed in an equation to measure the hoop fiber stress and the strength of the bottle. If this data are positive, then it can be applied for future fabrication of rocket motor casings on a larger scale. Bottle fabrication is somewhat a new sector of Filament Winding. Filament Winding is also a new addition to the vast field of composites which will obviously be a positive to aerospace engineering.

# Filament Winding Procedure

August 1989

## Small (5.750 O.D.) Mandrel Procedure

### 1. Safety Procedures

- 1.1 Wear surgical gloves while handling M.E.K. or P.V.A. mixtures
- 1.2 Wear carbon-organic mask while using M.E.K. or plastil-ease
- 1.3. Use M.E.K. only in a well-ventilated area; mechanical ventilation or a hood is desired.

### 2. Equipment

- 2.1 Scale
- 2.2 Pair of surgical gloves
- 2.3 Acid brush or wood Q-tips
- 2.4 Exhaust hood and/or carbon filter mask
- 2.5 Bounceless hammer
- 2.6 Mold half (split)
- 2.7 Center rod 3/4" x 6 3/4"
- 2.8 2 (two) bosses: 7/8" - 14 internal threads
- 2.9 Sealed container of M.E.K. (4 oz.)
- 2.10 Mold compressor form
- 2.11 Can Esquire boot wax, neutral
- 2.12 Heat knife
- 2.13 Teflon tape

- 2.14 Vacuum tape
- 2.15 Vacuum - bagging material
- 2.16 Release material
- 2.17 Bleeder cloth
- 2.18 Nylon bleeder cloth
- 2.19 Squirt container of Acetone (8 oz.)
- 2.20 Spackling powder
- 2.21 Sand paper
- 2.22 Chemlok 205 and 220 Fast Tack adhesive
- 2.23 Steel wool

### 3. Ingredients

- 3.1 Sheet of uncured rubber: 1/30" thick
- 3.2 2 pieces, circular: 5 19/20" O.D. x 1 6/10" I.D.; or use template (for AFLAS rubber)
- 3.3 2 pieces, circular: 4 19/20" O.D. x 1 6/10" I.D.; or use template
- 3.4 2 pieces, circular: 2 3/5" O.D.; or use template
- 3.5 2 pieces 18" long, width varies as needed (for AFLAS)
- 3.6 2 pieces 1 1/4" wide X 18" long - for AFLAS; for raw rubber, only 1 piece is needed
- 3.7 Clean silica sand, 30 or 60 mesh, 1600 gm (1100 ml or 15 lbs)
- 3.8 Plastilease 512B; 200 ml - with ratio of 5 1/2 to 1 (sand to Plastilease); or 35 gm P.V.A. + 35 gm Methanol + .65 gm water, blended thoroughly with mixer until clear; or Sodium Silicate: 10% by weight or ratio of 15 to 1 (sand to Sodium Silicate) - all are hardeners



4. Mandrel Making Steps

- 4.1 Using steel wool and Acetone, thoroughly clean the split mold and rod
- 4.2 Assemble the split mold and rod
- 4.3 Thoroughly wax mold and rod with neutral Esquire wax
- 4.4 Mix sand and hardener
- 4.5 Fill mold with sand mixture. Pack sand tightly in mold, leaving cavity in center for compressor form.
- 4.6 Place compressor form into space in sand and press it down using the bounceless hammer
- 4.7 Smooth sand off to make it level on top and remove the compressor form
- 4.8 Place the mandrel in the oven at 300 degrees F for three hours, or 250 degrees for four hours
- 4.9 Remove cured mold half while hot, wearing insulated gloves
- 4.10 When cool, remove cured mandrel half from the mold by disassembling mold. Mark with grease pencil if sodium silicate.
- 4.11 If the, can be cleaned, clean the bosses and mandrel surfaces with sandpaper and M.E.K. If they cannot be cleaned, send them to Chalco to be grit blasted and resurfaced.
- 4.12 Rub two mandrel halves together for a smooth surface
- 4.13 Place the two cooled, cured mandrel halves together with a boss on each end on a threaded 3/4" diameter rod.

and seal together using a thickened mixture of water and spackling powder. Sand the seal smooth when dry.

4.14 Apply Chemlok 205 to surface to which rubber will be bonded. Dry 20 to 40 minutes.

4.15 Tighten bosses firmly and fill in gap between mandrel and boss with a small piece of rubber.

4.16 Place assembled mandrel in a vice or holding fixture

4.17 Lay a pre-cut circular piece of rubber on the dome area and smooth out the rubber. Continue laying on rubber until mandrel is covered with two complete layers.

4.18 Join rubber seams together with a heat knife.

4.19 Wrap release film around mandrel using teflon tape to seal it and wrap a thin layer of bleeder cloth over it.

4.20 After wrapping a nylon bleeder cloth around the mandrel as a cushion, make a vacuum bag and seal with teflon tape.

4.21 Mandrel is ready for a curing cycle in the autoclave.

This cycle includes a 6-hour run at 300 degrees F, with pressure applied and a vacuum pulled.

## 5. Data Sheet

5.1 Fill out Mandrel Prep data sheet with all relevant information. Write down comments as needed.

# Solid Rocket Propellants

Student: Sharron Groom

Mentor: Mary Arce

Place: Astronautics Laboratory, RKPL

Edwards AFB, CA 93523-5000

Date: August 17, 1989

A solid rocket propellant consists of two main ingredients: solids and binder ingredients. Some solid ingredients are aluminum (Al), ammonium perchlorate (AP), cyclotrimethylene trinitramine (RDX), cyclotetramethylene tetranitramine (HMX), combustion stabilizers, burn rate catalysts, zirconium (Zr), magnesium (Mg), and other fuels. Binders can be made of polymers, plasticizers, curatives, cross-linkers, bonding catalysts, and activators. A propellant always includes a polymer, oxidizer (solid), and a curative. Solid propellants are a mixture of fuel and oxidizer (both solids), usually in a granular form, which are cast and cured in a pressure vessel in which the propellant is burned. After this is ignited, combustion usually continues until the whole propellant grain is used up.

There are many ways in which solid propellants may be classified, some of which are binder type, safety characteristics (detonable vs. non-detonable), strength of the infrared emission of the exhaust plume as high or low signature propellants, and amount of smoke they produce. The amount of smoke is very important for tactical rocket weapons, and just about all modern tactical propellants are of the smokeless or reduced smoke type. They are presently classified into four groups:

### Metallized High Energy Propellants

These propellants contain 15 to 22% aluminum powder, have the highest energy (approximately 15 to 20 sec higher impulse than the non-metallized versions), and produce a large amount of smoke. To obtain the highest impulse of the system, they are formulated so that the oxidizer is about 10 mole percent in excess of the quantity required to burn all the aluminum to  $Al_2O_3$  and the carbon to CO. The hydrogen is essentially exhausted as  $H_2$ .

### Reduced Smoke Propellants

These do not contain metallic fuels, such as Al. They are now being used in air-launched missiles. Reduced smoke propellants require combustion stabilizers because there is no Al to absorb the high frequency oscillations that rocket motors produce.

### Minimum Smoke Propellants

These propellants contain neither Al nor AP (ammonium perchlorate) in their formulation. They are smokeless under all atmospheric conditions, except where some of the combustion catalysts may leave a faint trail. They are the most common among the "smokeless" propellants. Minimum smoke propellants are highly detonable. They

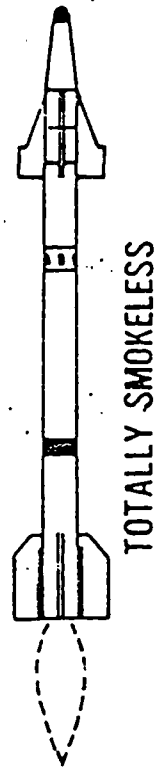
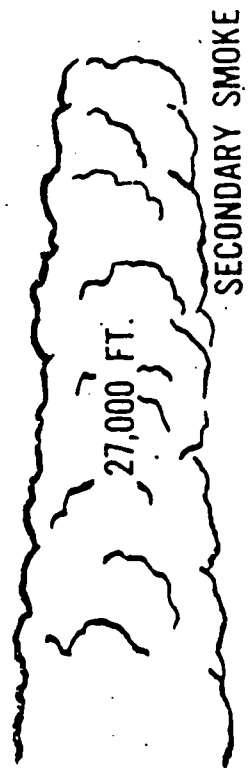
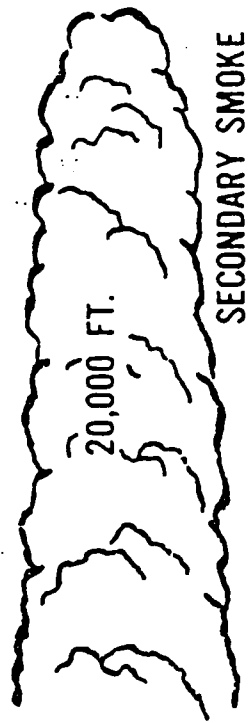
usually contain HMX or RDX as the oxidizer and are generally Class 1.1 explosives.

### Gas Generator Propellants

These are slow burning, non -metallized propellants that provide high-pressure gas to drive turbines, pumps and other control equipment used on large ICBM's or space missions. Their composition varies as much as their mission. AP,  $\text{NH}_4\text{NO}_3$ , HMX, or RDX are used as oxidizers.

The newest concern with air launch missiles is minimum signature, which is to reduce or eliminate enemy detection upon firing. Efforts are being directed at reducing the smoke/contrail formation and other identifiers as much as possible. The chart on the next page represents some of the types of propellants, specifically smoky, reduced smoke, minimum smoke, and smokeless. Smoky propellants contain metallic fuels that form a black oxide when they combust. This forms the dark, primary smoke. The white contrail, or secondary smoke, is produced by the condensation of water. Reduced smoke propellants contain no metallic fuels, so the primary smoke has been eliminated. However, they do have large amounts of ammonium perchlorate (AP) which combusts to form HCl. HCl forms

# DEFINITIONS



NO PRIMARY OR SECONDARY SMOKE

an excellent nucleating site on which water vapor condenses. The water is from the atmosphere and the combustion products. Minimum smoke propellants have taken out the AP as the primary oxidizer and replaced it with other non-halogen containing oxidizers such as HMX or RDX. These materials combust to form  $H_2O$ ,  $CO_2$ , and  $CO$ . Contrails are still formed due to water in the exhaust and atmosphere, but the contrail is reduced due to the lack of large numbers of nucleating sites.

A substance called GAP (glycidyl azide polymer) is currently being used by the Air Force in their efforts to produce a high performance, less sensitive and less smoky propellant. This summer, in addition to learning some of the basics of solid rocket propellants, I also worked on a database program containing information on GAP and other propellant ingredients. I researched some of the hazards of GAP, such as impact and friction sensitivity as well. Although my research was inconclusive, I feel that I am now more knowledgeable about rocket propellants and astronautics in general.



Common Solid Propellant Oxidizers<sup>a</sup>.

|  | $\Delta H_f/100g$ | Oxygen<br>balance <sup>b</sup> | Density,<br>g/cm <sup>3</sup> |
|--|-------------------|--------------------------------|-------------------------------|
| NH <sub>4</sub> NO <sub>3</sub>                          | -109.1            | +19.99                         | 1.72                          |
| NH <sub>4</sub> ClO <sub>4</sub>                         | -60.2             | +34.05                         | 1.95                          |
| RDX (hexogen,<br>cyclotrimethylene<br>trinitramine)      | +7.61             | -21.6                          | 1.85                          |
| HMX (octogen,<br>cyclotetramethylene<br>tetra nitramine) | +6.04             | -21.6                          | 1.90                          |
| NG (nitroglycerin)                                       | -39.2             | +3.50                          | 1.59                          |

<sup>a</sup>RDX, HMX, and NG are considered as oxidizers in aluminized propellants, where combustion is essentially to Al<sub>2</sub>O<sub>3</sub>, CO, and H<sub>2</sub>.

<sup>b</sup>Oxygen balance, the amount of oxygen, expressed in weight percent, liberated as the result of a complete conversion of the material to CO<sub>2</sub>, H<sub>2</sub>O, SO<sub>2</sub>, etc.

## References

Oberth, Adolf E. 1987. Principles of Solid Propellant Development.

Shelton, Chris. 1983. AFRPL Training Program for the Solid Rocket Division.

Willard, Dirk. 1984. Propellant Training Manual.

**Computer Support for the  
Minuteman III Demonstration Motor Test  
and the Advanced Solid Axial Stage**

Final Report  
by  
Lloyd Neurauter

Universal Energy Systems, Inc.  
Air Force Astronautics Laboratory  
AL/RKBA

Mentor: Mr. Terence Galati  
Work - (805) 275-5356

Period of Employment:  
26 June 89 to 1 Sep 89

### Acknowledgements

I would like to thank all of the people in RKBA for their support throughout the summer, particularly Mr Alex Sagers for all the times he helped me with the Amiga and Mr John Earls, whose computer support I could never have done without. I especially thank Mr Terence Galati, my mentor, for all the time, support and friendship he gave to me during my tour of the Laboratory. I would gladly welcome to opportunity to come back again in the future.

### Abstract

This summer I worked at the Astronautics Laboratory in the Engineering Design Evaluation Section (RKBA), Mr Terence Galati was my mentor. I was trained on the various terminals used here in the section such as the Tektronix 4208 and Raster Technologies 1/80. I used the VAX 8650 daily, but I also worked with two Amiga personal computers (an Amiga 1000 and an Amiga 2000) and with the DEC MicroVAX II/GPX workstation. I learned how to use many of the applications including T<sub>E</sub>X (a typesetting program), PATRAN (a CAD/CAM program), and X<sub>P</sub>LOT (A graphing program written by Mr Earls). During my tour of the Astronautics Laboratory I contributed to the Minuteman III Demonstration Motor (DMIII) data analysis effort and also did Advanced Solid Axial Stage (ASAS) graphics support. The DMIII support resulted in processing over 100 channels of motor performance data, culminating in an engineering animation of the high temperature thermocouples. The ASAS support consisted of plotting performance data and helping to prepare a technical paper and presentation for Mr Galati.

### Introduction

The Engineering Design Evaluation section, (RKBA) supports the Propulsion Division by providing timely technical analysis support for various ongoing programs. The many different computers, terminals, and software applications available to us are invaluable tools in our analysis work. PATRAN is a powerful modeling tool used in this section to evaluate rocket components. X<sub>P</sub>LOT, an inhouse graphing application, can handle a wide variety of data and can be customized to meet the needs of the user. T<sub>E</sub>X is used for final reports, evaluations and papers, such as this, in the section. With these software and hardware tools the section has the capability to perform complicated propulsion analysis tasks.

### DMIII Instrumentation Data Analysis

My first task at the Laboratory was taking the data collected from a Minuteman III 3rd stage (DMIII) test firing and organizing it into a form that could be easily examined and evaluated. (See Figure 1.) I plotted the data, such as temperature, pressure and thrust, in a series of graphs similar to those from previous tests so that the data from the different tests could be easily compared.

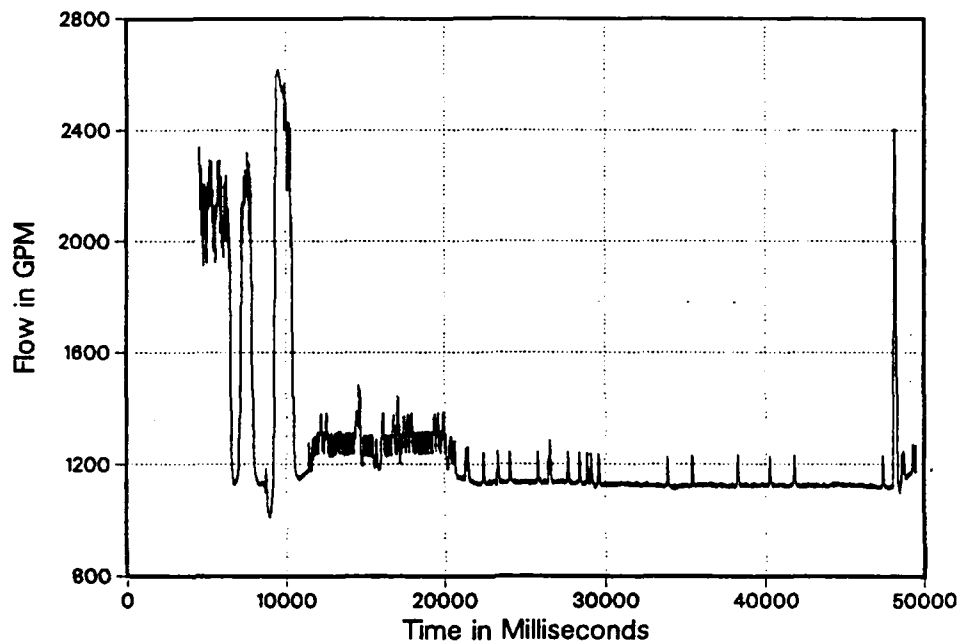


Figure 1

#### DMIII Test Cell Diffuser Flow

Next I was asked to combine the thermocouple data into an engineering animation sequence to give a visual presentation of the time-dependent data. I sorted through the data sets and pulled out the most consistent thermocouple data that I could find. I then made final checks and narrowed my selection down from ten readings on each instrumentation rake to only three to improve visualization. The entire animation consisted of 250 frames and provided a visual record of the thermal behavior during the firing.

Mr Earls, a Co-Op student also working in RKBA, wrote a data extraction utility that was used to extract the final data for the bar graphs used in the animation. The 250 data files for the animation frames were generated and plotted using X<sub>PLOT</sub>. I produced X<sub>PLOT</sub> command files for each of the frames. An Amiga 1000 was used as a terminal and each frame was saved to disk. Finally, Mr Alex Sagers, another summer hire, and I began using the Amiga to compress the files and transfer them from the Amiga to the

VAX cluster, where we generated the final animation using an inhouse program written by Mr Russ Leighton, another section member.

Mr Galati was pleased with the thermocouple animation. I decided to add some features to the animation such as a clock and a frame counter. I worked with Mr Alex Sagers on an Amiga 2000 to produce the final animation. The Amiga 2000 is a powerful personal computer that is well suited to this animation application. One now has the ability to animate large volumes of time-dependant data to aid instrumentation analysis.

### Advanced Solid Axial Stage (ASAS) Technical Support

During my tour at the Astronautics Laboratory I also worked with a Co-Op student named Mr Kent Chojnacki. He used the Solid Propulsion Prediction code (SPP) to analyze a beryllium propellant formulation of an advanced space booster. I took parametric data from SPP and plotted it using X<sub>PLOT</sub> to create viewgraphs and technical plots for analysis. I also used the graphics capability of the Amiga 2000 to create supporting viewgraphs. Figure 2 shows one of the viewgraphs I generated on the Amiga.

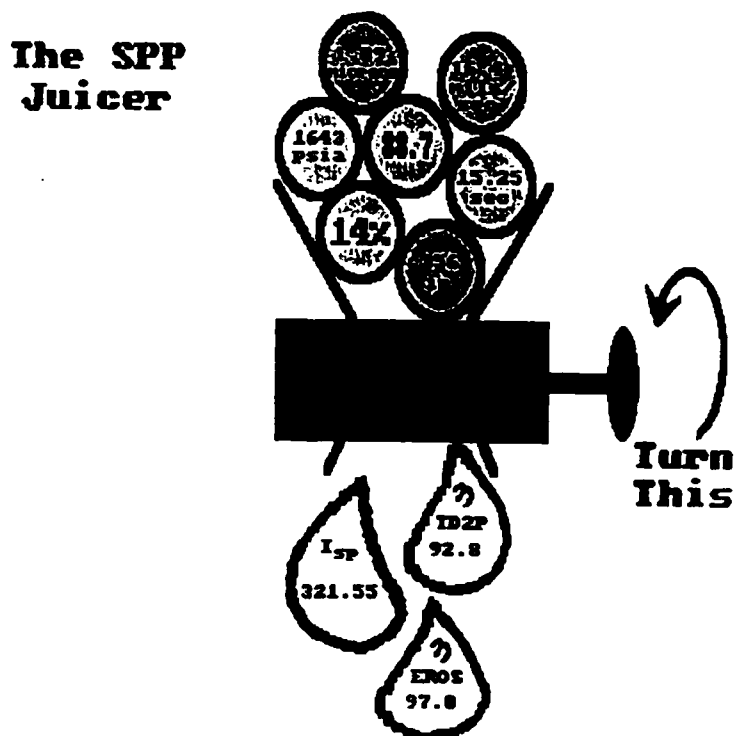


Figure 2

ASAS support slide generated on an Amiga 2000

Providing support for Mr Galati required that I apply everything that I had learned in a short period of time. I was generating graphs on the plotter and the laser printer non-stop for an entire week. Most of the time during that week one terminal was not enough to do all of the work, so I set up jobs on two terminals at once, and went back and forth between the two. The extensive networking in RKBA makes this high productivity possible.

### Miscellaneous Tasks

This summer was I was required to do a presentation for the summer hires at the third Summer Seminar. There were three Summer Seminars in all; each one had a different division's summer hires giving presentations explaining their assigned tasks. Most of the summer hires, including myself, used transparencies and viewgraphs to support our presentations. I generated all of my own transparencies using the Tektronix 4208 terminal and a Tektronix 4692 plotter in the next office. The seminar went well including the demonstration firing of a small solid rocket motor afterw -ds. The firing was especially interesting to me since I have been working with data from rocket motor firings all summer, but this was the first time I had witnessed one and seen the instrumentation and the data acquisition system in action.

Towards the end of my allotted eight week tour, as I was wrapping up my other projects I became involved with PATRAN and helped to prepare both the ASAS motor models and a simple model of the Liquid Plume Experiment (LPX) rocket for use by Dr. Alan Weston, who needed a color picture of the conceptual design for presentation purposes. (See Figures 3 and 4.)

### Conclusion

I was originally trained on X $\overline{\text{PLOT}}$  so that I could process the DMIII data. I spent the first half of my eight weeks here working on the graphs and the animation for the DMIII task. My remaining time here was spent doing various tasks with the many different kinds of hardware we have in this section. For example Mr Jerry Gallardo was trained on PATRAN just as I was in X $\overline{\text{PLOT}}$  , but one afternoon during about the fifth week I sat and watched him work and started using PATRAN to model the LPX rocket and the ASAS motor the same day, self training is the key to learning new software.

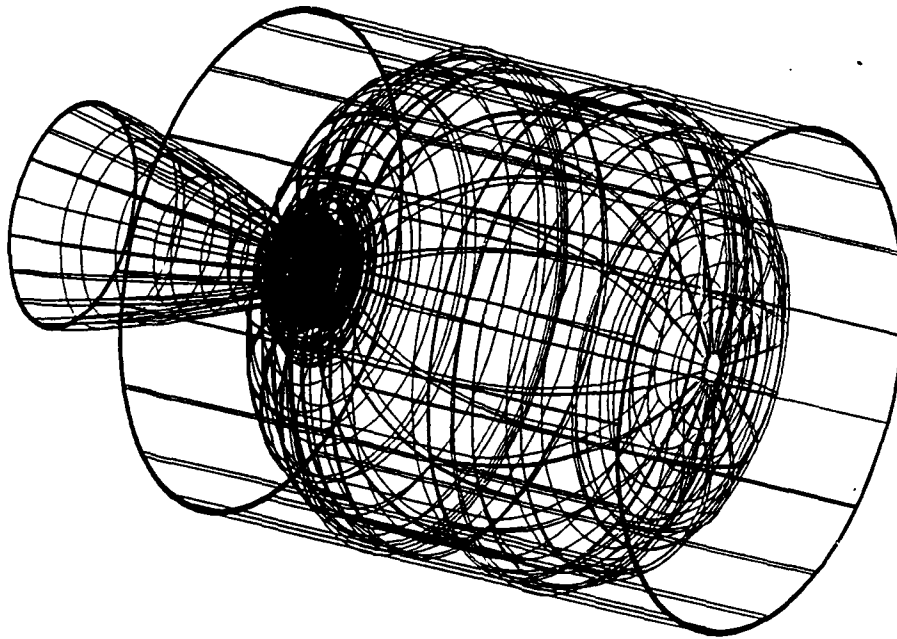


Figure 3

ASAS Motor model generated using PATRAN

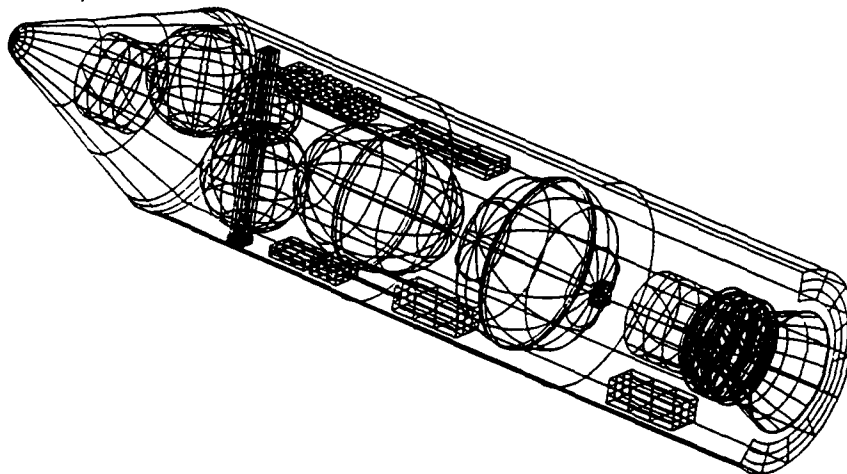


Figure 3

LPX Rocket model generated using PATRAN

I learned new things about computers, various hardware, and the Laboratory constantly throughout the summer. Each time I wanted to do something different on one of the computers I had to learn something new, writing these reports for example. I began writing my bi-weekly reports on a word processor on the Amiga, but since the Amiga was in such demand, I learned how to use  $\text{\TeX}$ , a program on the VAX cluster.



I have also learned how to operate almost all of the different terminals and other hardware in the section. Little things such as changing the paper in the laser printer or loading transparencies into the plotter can be important when you need results right away. Looking back I would say that I learned more about using different machines and software applications this summer than I have during all my years of taking computer courses in school.

I not only learned how to use computers this summer, but thanks to the instruction of my mentor I learned what to use them for. The DMIII animation taught me about displaying changing data in a way that people unfamiliar with high temperature thermocouple behavior could understand. My participation in the preparation of the ASAS briefing showed me how everyone's work comes together to form the end-product of our section.

THERMOPLASTIC BINDERS

by

SANDRA NOVAK

ASTRONAUTICS LABORATORY

EDWARDS AFB, CA

mentor

Dr. JOHN RUSEK

I would like to thank my mentor, Dr. John Rusek, for working with me this summer and for his help on my project. I would also like to thank Mary Arce for her help.

A solid rocket propellant is made up of three basic components. They are a fuel, an oxidizer, and a binder. The fuel is what burns and gives energy to the propellant, and the oxidizer supplies the oxygen and keeps the combustion going.

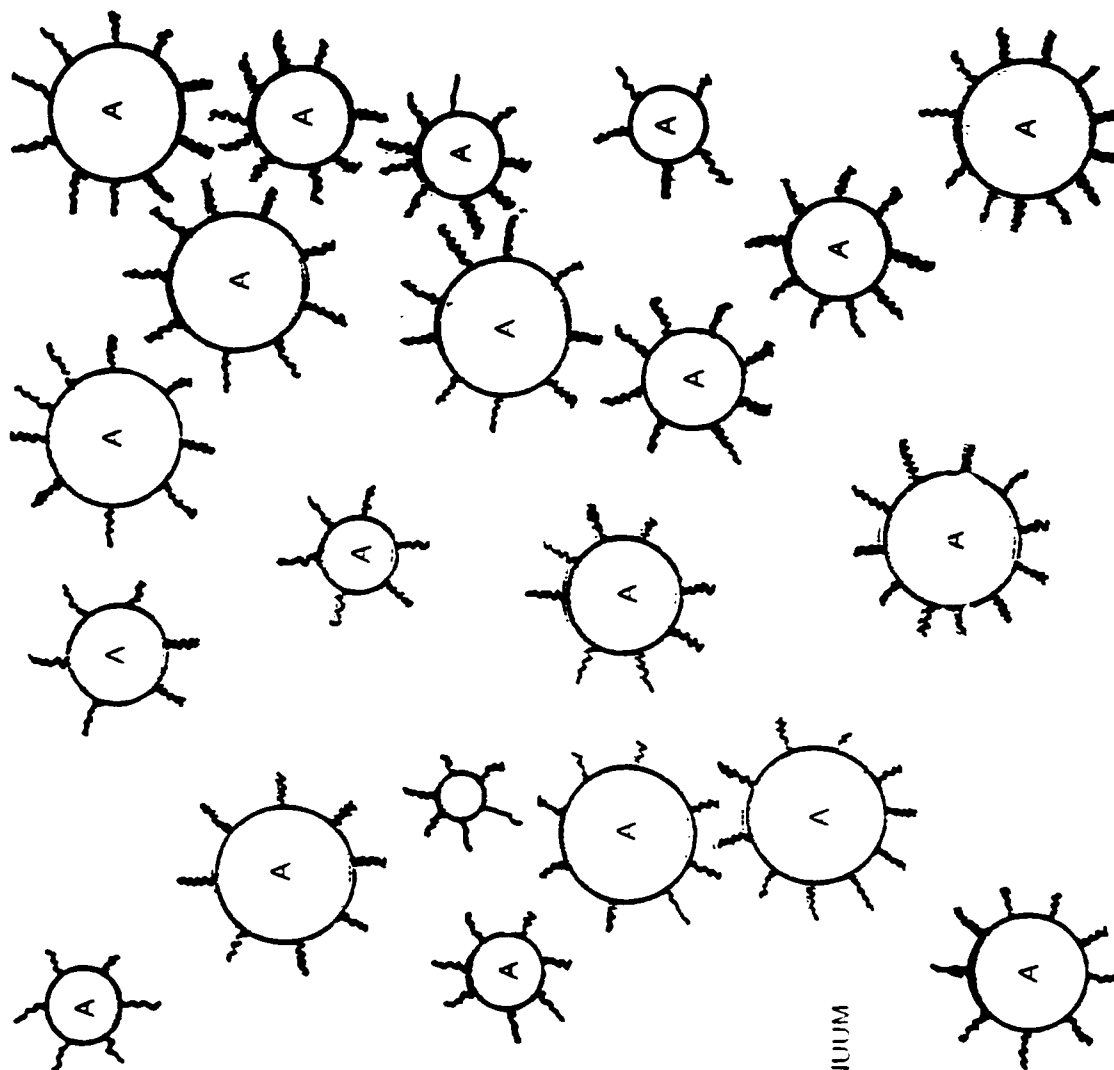
A binder holds solid rocket propellant together. This summer, I worked on developing a thermoplastic binder made up of an asphalt resin and Kraton D-1107, which is a type of rubber.

The ideal binder must be elastic at all temperatures that the rocket operates at. It also must have a high heat of combustion, so it can get the maximum thrust per unit weight of binder. Another important property is it must have long term chemical stability, so it can have a long shelf life and, it can be stored as long as it needs to be stored. One last important property is that it needs to be easy to handle and process.

Together, asphalt resin and Kraton D-1107 form a binder that fits these specifications. Alone, neither one of them has mechanical properties good enough to be a binder by itself. Asphalt resin alone is called a colloidal plasticizer, which means that it is made up two different components that don't mix. In the case of asphalt resin, two of the components, asphaltene and resin are combined, and together, they are suspended in an oil called maltene(See illustration 1).

It is because of this make-up that asphalt resin alone cannot be used as a binder. When the asphalt resin is heated, it becomes soft and sometimes

# Illustration 1



A: ASPHALTENES  
: RESINS  
MALTENE CONTINUUM

liquid. As stated above, a binder must be elastic at all temperatures. If the binder were to become soft, the propellant would not stay together, and it would be worthless. Also, if the asphalt resin got too cold, then it would crack. In a rocket motor, this could be disastrous, because a crack makes more surface area on the propellant, causing it to burn faster. Sometimes, the crack causes the propellant to burn faster and expel more gas than can escape from the nozzle. This causes the motor to explode.

Kraton D-1107 alone is called a thermoplastic elastomer. When it is added to the asphalt resin, it improves the mechanical properties. The asphalt no longer gets soft at high temperatures or cracks at low temperatures. This is because of the make-up of the Kraton. Kraton is a tri-block polymer. This means it is made up of three segments, a hardblock segment on either side of a softblock segment. When Kraton is mixed with the asphalt resin, the oil and the asphaltenes each mix with the two types of segments in the Kraton(See

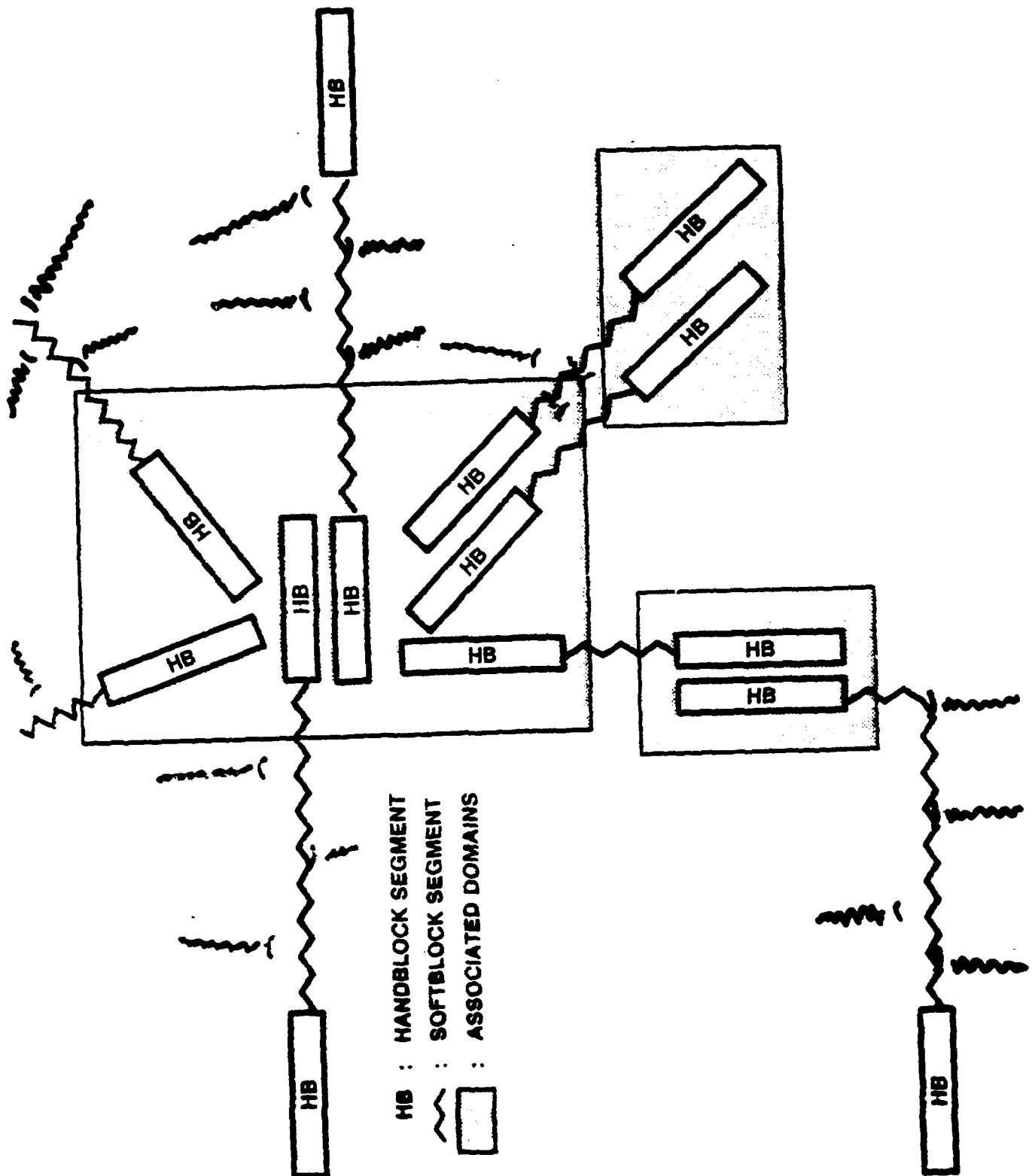
illustration 2). This way the entire mix is uniform, and there are no colloids. This way the binder that is made will have one melting point, and the mechanical properties are combination of the best of both materials.

The research that was done this summer was to find the best combination of these two materials. This was done by mixing different ratios together and comparing the results. Different types of asphalt resins were also used, and the results were compared.

Mixing the Kraton and the asphalt resin together is relatively simple. Each ingredient was measured out, and placed into a mixer. Then, they were left to sit for an hour at a temperature of 400<sup>0</sup>, in order for the Kraton to get soft enough to be mixed. Then they were mixed at the same temperature for an hour. Once mixed, it had to be cast immediately, because the elastomer in the mixes cooled off quickly, making the mix solid. The mix was cast onto teflon sheets, and then it was pressed out on these sheets to the width needed for testing.



Illustration 2

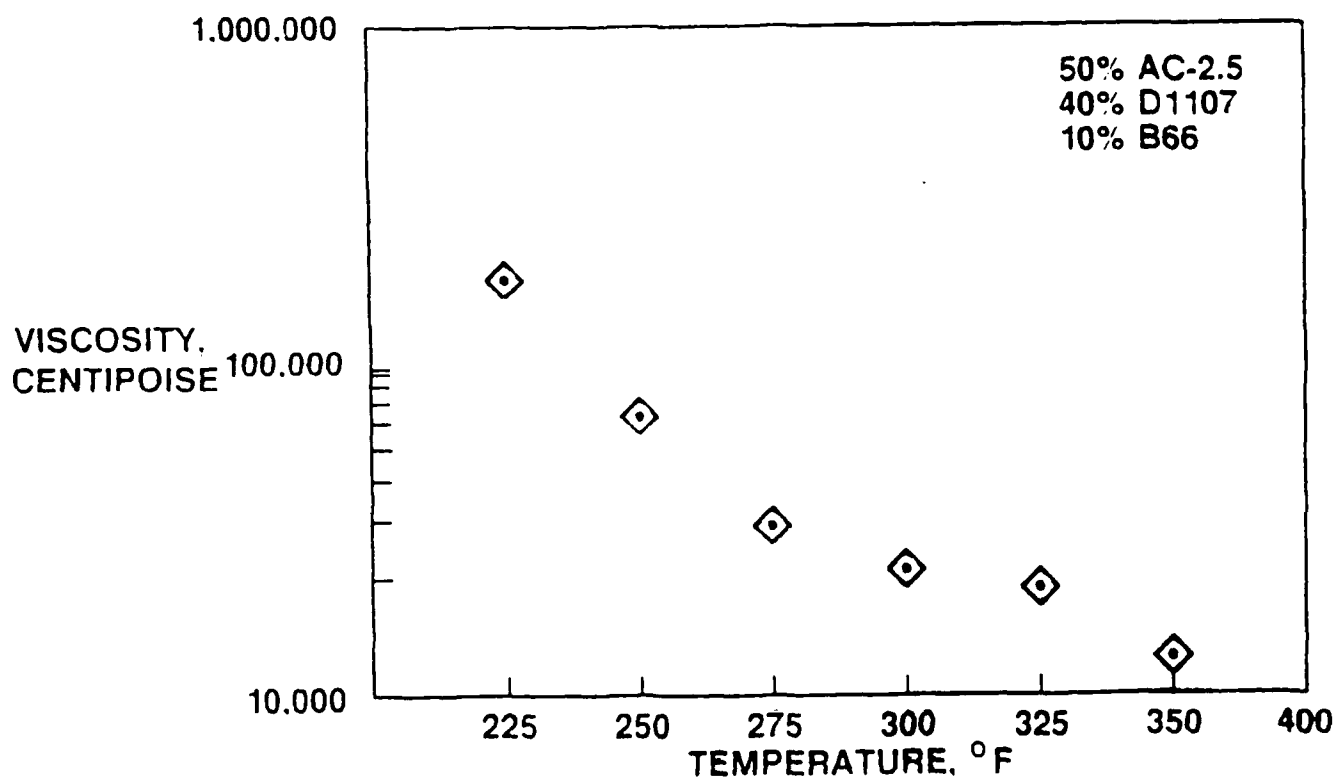
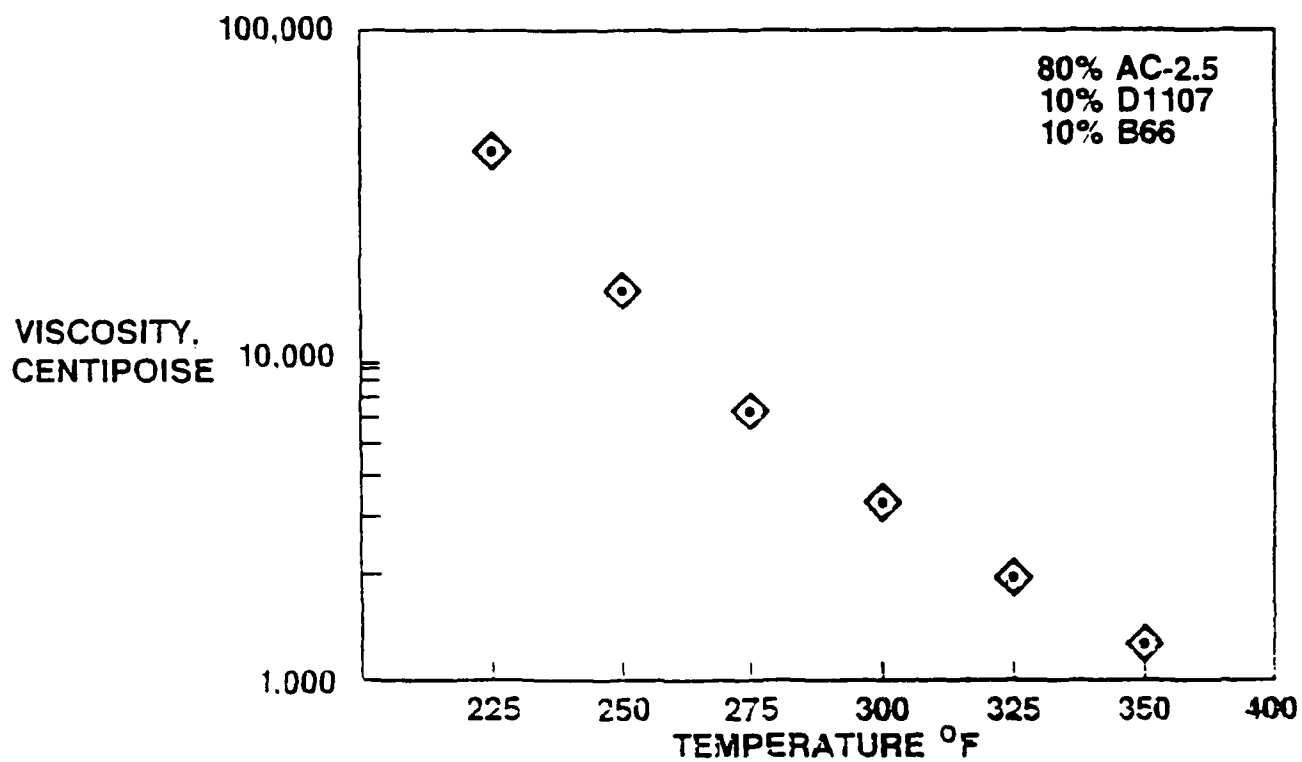


Also, some of the mix was placed on a microscope slide and into a container to be used for viscosity testing.

The reason some of the mix was tested for viscosity was to check for uniformity of the mix. A mix needs to be uniform for it to be good, because if it is not, when it is used in a propellant, part of the mix could melt or cool quicker than rest, which would cause the entire propellant to fail. Illustration 3 shows the difference between a good viscosity test and a bad viscosity test. The top graph shows a good test. The curve is smooth, and there are no bumps in it. The bottom curve had a bump in it, showing that the mix was not uniform. The bump was caused by the different melting points of the materials in the mix.

Another way to check the uniformity of a mix is by looking at it under a fluorescence microscope. A nonuniform mix will have blotches of the Kraton and the asphalt resin which are visible under a microscope. If the mix is uniform, there are no blotches, and everything is one even color.

Illustration 3



The testing that was done on these mixes was not completed during the time I was working. I had not gotten any numerical results back, but I knew that so far the mixes had turned out to be very elastic, which is what I had wanted them to be.

#### REFERENCES

Kraton Thermoplastic Rubber In Asphalt Products -  
Technical Bulletin by Shell Chemical Company

Dr. John Rusek - Astronautics Laboratory, Edwards,  
AFB

# **FINAL REPORT FOR SUMMER 1989**

Sonya Park

Mentor: Les Tepe

Supervisor: Ismail M. K. Ismail

Chemistry Laboratory

Edwards Air Force Base, Ca.

June 19, 1989 to August 11, 1989

## ACKNOWLEDGEMENTS

I would like to extend my appreciation to Universal Energy Systems for giving me the opportunity to work at the chemistry laboratory at Edwards Air Force Base. I would like to thank my mentor Les Tepe, my supervisor Dr. Ismail M.K. Ismail, and Dr. Wes Hoffman for his help. I would also like to thank Hong Phan and Melissa Rose, for their help with the TGA and analyzing data, as well as Matt Mahowald for his help and expertise with the computers.

## ABSTRACT

I am continuing work on the Thermogravimetric Analyzer (TGA). The samples I have been using in the TGA are Columbia Carbon N990 (washed in 2M HCl), and Columbia Carbon N762(washed in 2M HCl). The results from the Columbia Carbon N990 (washed in 2 M HCl) were compared to the results from the runs of Columbia Carbon N990 (unwashed). The results from the runs of Columbia Carbon N762 (washed in 2M HCl) were compared to the results from the runs of Columbia Carbon N762 (unwashed).

I am learning further how to use the Macintosh SE/30 and the programs Microsoft Word and Excel. Another task I completed in this period was refluxing a 50 gram sample of Columbia Carbon N330 with Nitric Acid and then washing the sample with double distilled water. The TGA is a routine experiment and will be continued by someone else when I leave.



## OBJECTIVES OF RESEARCH

My summer apprenticeship as a scientific aide at the chemistry laboratory, located at Edwards Air Force Base, in the area of Carbon Research had four main objectives. First, the main focus of my work was using a Thermogravimetric Analyzer (TGA) in order to explore the Chemical Vapor Deposition (CVD) of pyrolytic carbon on carbon fibers . Second was analyzing the data obtained from the TGA, by creating graphs, to see how they relate to the experimental parameters. Third, large amounts of carbon samples were oxidized and washed to open their porosity. Finally, I learned various programs on the Macintosh computer, such as Microsoft Word, Excel, and MacDraw II, and on the IBM computer, such as a word processing program.

## APPLICATION OF RESULTS

The main focus of the laboratory is rocket nozzle technology and in the fabrication of rocket nozzles, materials possessing a high strength to weight ratio are desirable. Among many ways to create this material, one process is Chemical Vapor Deposition. The CVD process can develop Carbon-Carbon composites which are very strong and can withstand high temperatures. The CVD process has been explored extensively, yet is still not fully understood. Thus, we are exploring the process further in order to propose a mechanism explaining CVD.

A sample of carbon fiber substrate is exposed to a mixture of 10% methane and 90% argon at temperatures between 1000 C and 1080 C. The methane gas has carbon-hydrogen bonds, and during the CVD process (Figure 1) the carbon - hydrogen bond in methane breaks, pyrolytic carbon

deposits onto the carbon fiber substrate, and a carbon-carbon composite is formed. The hydrogen from methane flows out of the system. Additional substrates like carbon particles were also used in my assignment (Figure 2).

## METHODOLOGY

The CVD process is explored using the Thermogravimetric Analyzer (TGA). The TGA records the weight gain or weight loss of a sample during chemical vapor deposition (CVD). The routine experiment (Figure 3) begins by placing a small amount of carbon sample (5-40mg) in a bucket, which is suspended on a Cahn RG Balance. Next, the system is evacuated to approximately  $10^{-4}$  Torr. Third, an inert gas, argon, is then introduced into the system to ambient pressure in order to prevent the oxidation (burning off) of the sample during subsequent heating. Fourth, the system is heated up under a flow of argon gas (150 cc/min) to the target temperature which is usually between 1000-1080 C. After the temperature has been stabilized for approximately thirty minutes, the methane/argon gas mixture is introduced to the system and the CVD process begins. These variable parameters (temperature and gas flow rate) are held for 3-20 hours. During the experiment, the IBM computer records the weight gain of the sample as the pyrolytic carbon deposits on the carbon substrate. After the run is completed, the system is cooled and the sample is oxidized overnight.

To explore the effects of oxidizing a carbon sample on the rate of CVD, a carbon sample is heated in concentrated Nitric Acid for 1-5 hours. To insure a reasonable oxidation of the sample, it was stirred and heated in a refluxing apparatus (Figure 4). The heating mantle heats up the mixture causing the  $\text{HNO}_3$ /carbon mixture to react. The cold water in the

condenser cools the inner tube and once the vapors come in contact with this inner tube, they condense and fall back into the round - bottom flask. This process, known as refluxing, creates mesopores and micropores in the carbon particles, which increases the surface area of the carbon black (Figure 5). Theoretically, it is believed that this process affects the rate of CVD.

After refluxing the sample, the mixture of carbon and  $\text{HNO}_3$  is poured into a filtration apparatus (Figure 6) to separate the oxidized carbon from the nitric acid. A vacuum pulls the liquid through the filter paper on the bottom of the Buchner funnel, leaving the particles of oxidized carbon. The carbon is then washed with distilled and double distilled water. Finally the sample is dried in a vacuum oven at 150 C and is then used for analysis in the TGA.

The particles of carbon contain certain ions which are suspected to catalyze the CVD rate. Thus to test the validity of this, a sample of carbon black was washed in 2 molar  $\text{HCl}$  to remove these ions from the surface of the particles. To wash the sample, 100 ml  $\text{HCl}$  was combined with 3 grams of columbia carbon in a beaker and was stirred overnight. in a similar manner as the oxidized samples, this sample was washed with distilled and double distilled water. It was then dried in a vacuum oven at 150 C and then analyzed in the TGA.

## ANALYSIS AND RESULTS

Using the Macintosh computer and the various programs, I created the first graph (Figure 7) in order to analyze the data. The graph shows the effect of flow rate of the methane gas on the deposition rate. Two different samples (VSB-32 fiber and V3G carbon black) are represented.

The large difference in the surface areas ( $VSB = 0.54 \text{ m}^2/\text{g}$  and  $V3G = 59.2 \text{ m}^2/\text{g}$ ) affect the deposition rate in two opposite ways. The smaller surface area carbon sample shows a decrease in the deposition rate with increasing flow rate. On the other hand, the larger surface area carbon sample shows an increase in the deposition rate with increasing flow rate.

The second graph (Figure 8) was created using a program on the IBM computer. This graph shows the effect of temperature on deposition rate. The sample (VSB-32) was heated to four different temperatures at a constant flow rate (150 cc/min) of the methane gas mixture. The graph shows that with increasing temperature, the deposition rate increases. The increase in the deposition rate with temperature shows that the temperature has an affect on the breaking of the C-H bond. This suggests that the breaking of the C-H bond occurs in the gas phase before the methane molecule reaches the surface of the substrate. As the temperature increases, the C-H bonds vibrate faster and thus break faster. Therefore, the faster the C-H bonds break, the more pyrolytic carbon is available for deposition.

Finally the third graph (Figure 9), also done on the IBM, suggests that the ions in the unwashed sample do catalyze the rate of deposition. However, more research is being done to make concrete conclusions on all three graphs.

## CONCLUSIONS

The things I learned this summer will be valuable for me in my college and later life. I understood the importance of carbon research and how it applies to rocket nozzle technology. I picked up some techniques in chemistry such as refluxing, filtering, and analyzing data. In addition, I

gained valuable knowledge with the computer which will be extremely useful in the next few years of college. I truly enjoyed the job and the work and overall it was an exciting and interesting experience for me.

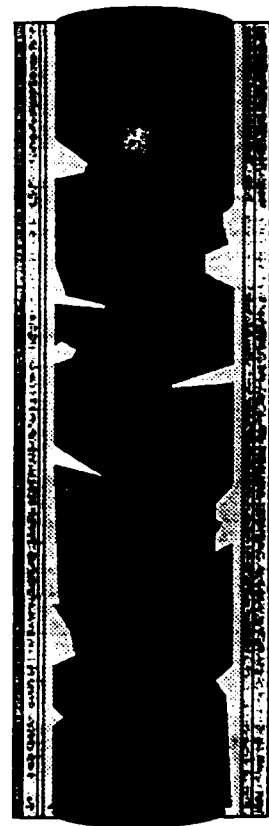
Figure 1 Deposition of Pyrolytic Carbon On Carbon  
Fibers During CVD



CARBON FIBER + CH<sub>4</sub>



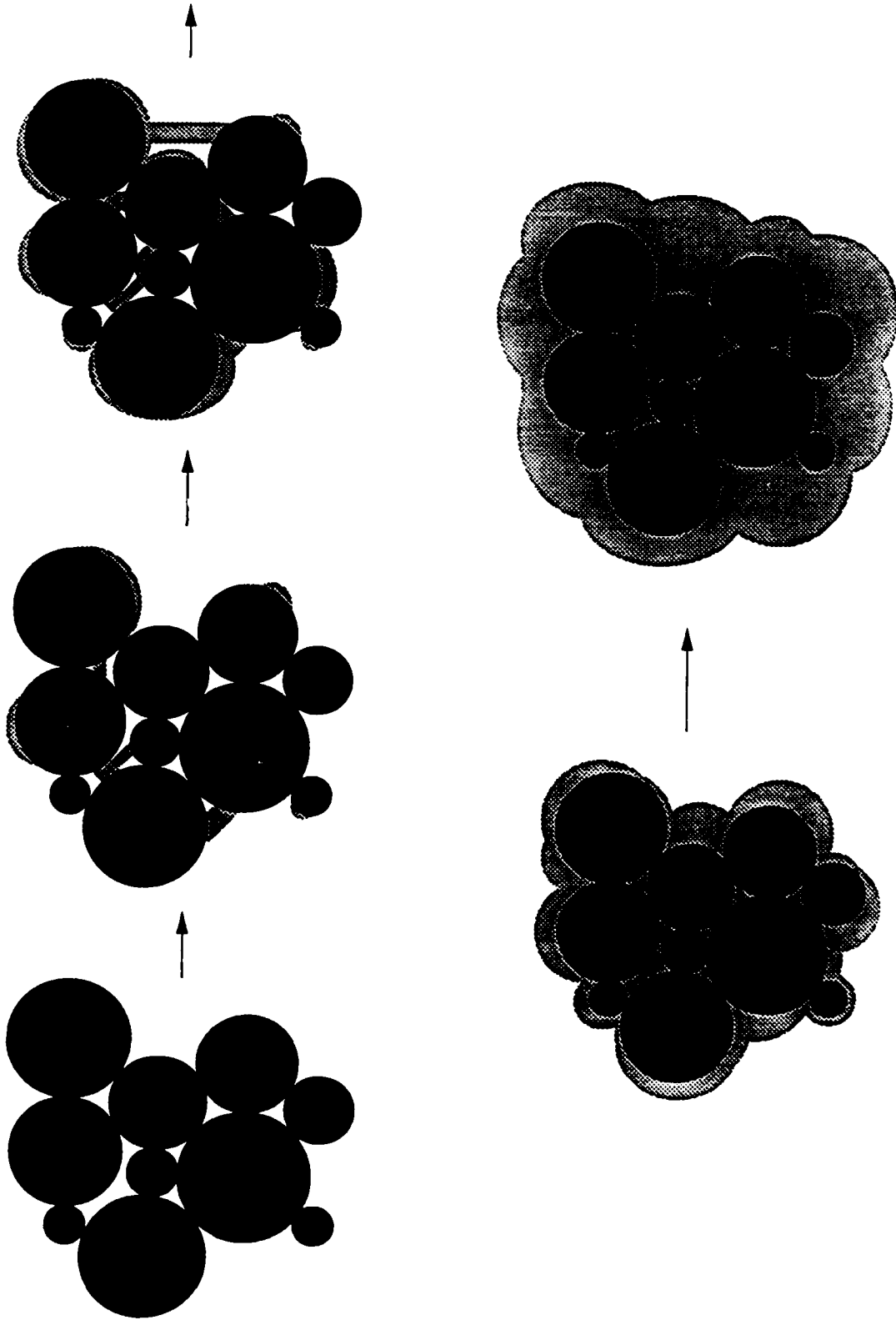
(HIGH TEMPERATURE)



+ H<sub>2</sub>

CARBON-CARBON COMPOSITE

Figure 2 Deposition of Pyrolytic Carbon On  
Carbon Particles During CVD



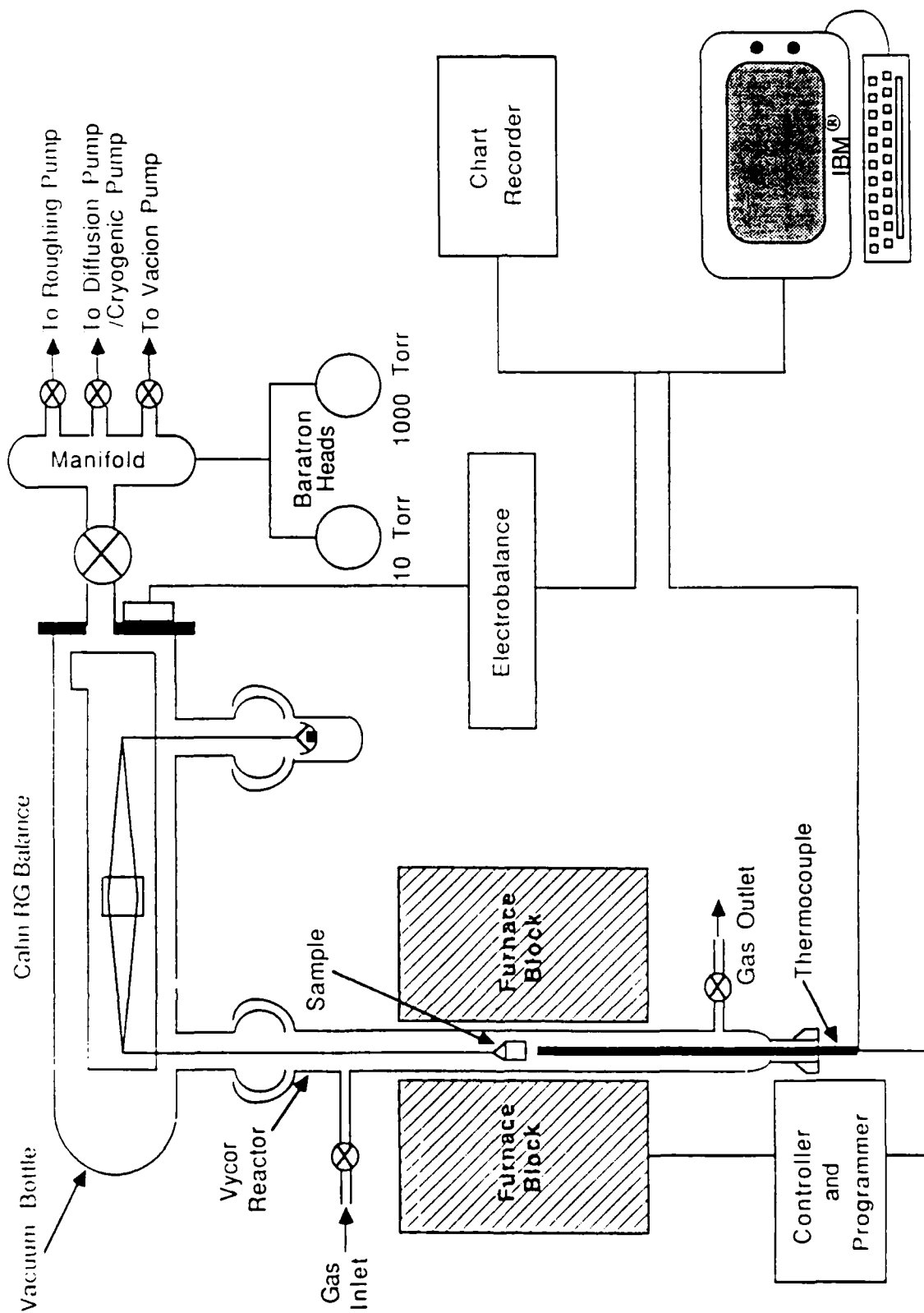


**Figure 3** Thermogravimetric Analyzer used in Deposition of Pyrolytic Carbon on Different Carbon Substrate



# Refluxing Apparatus for Nitric Acid

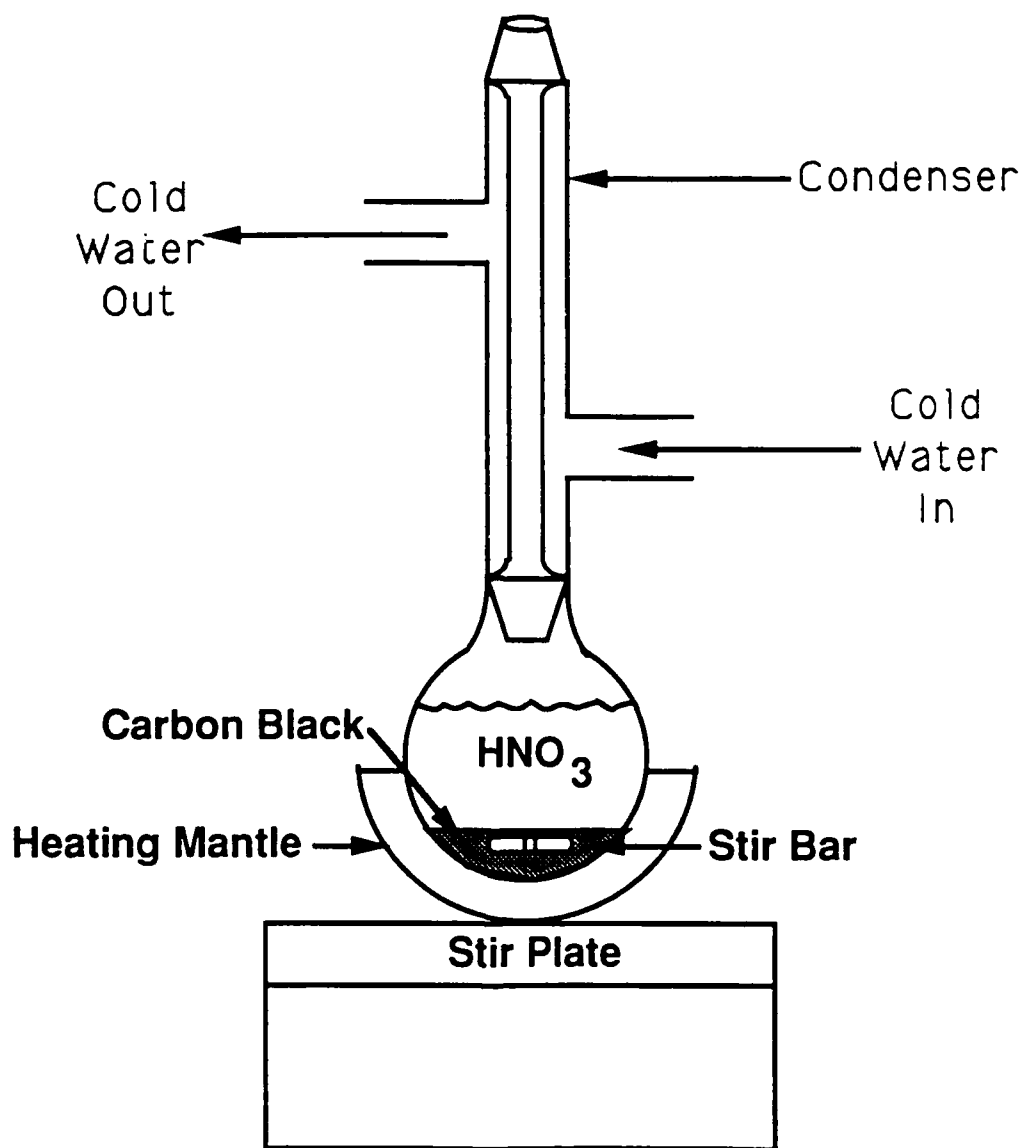


Figure 4

# Oxidation of Carbon Black

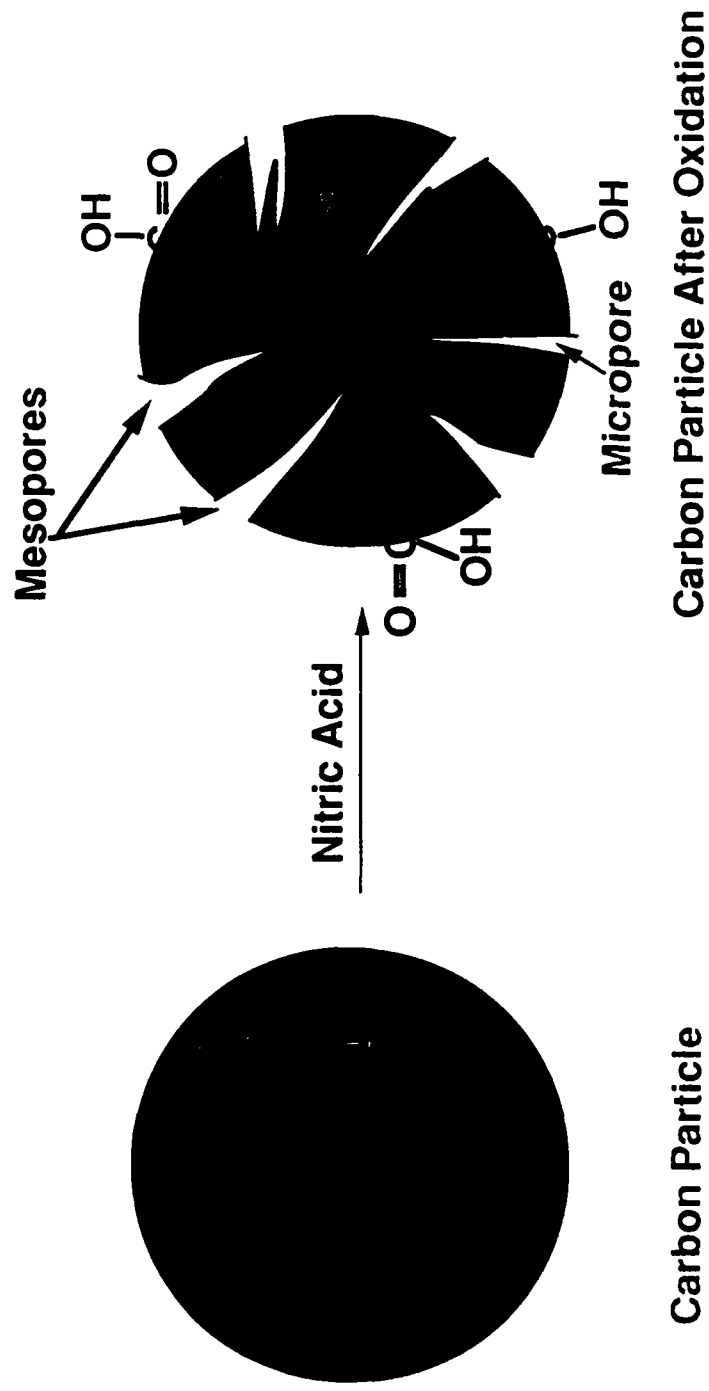


Figure 5

# Filtration Apparatus

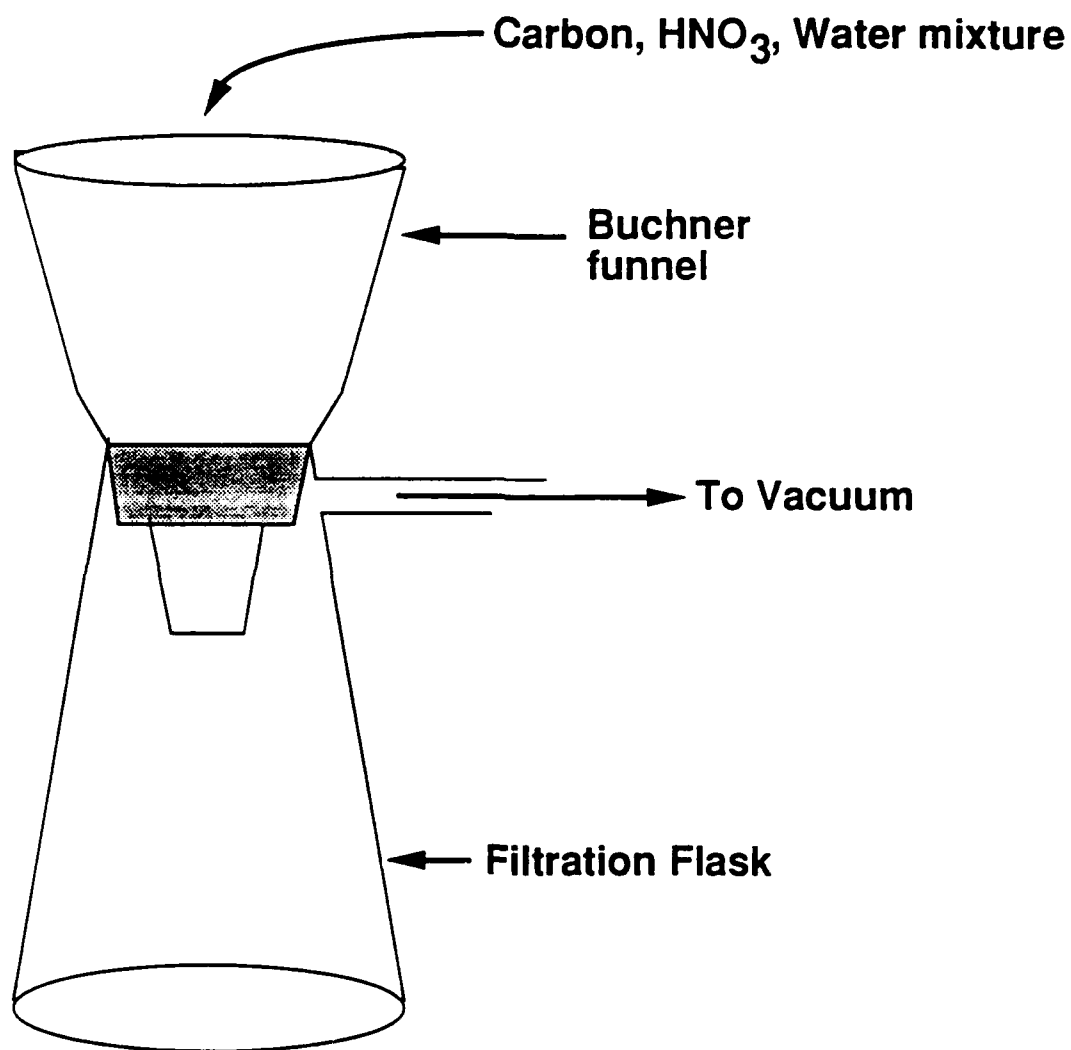
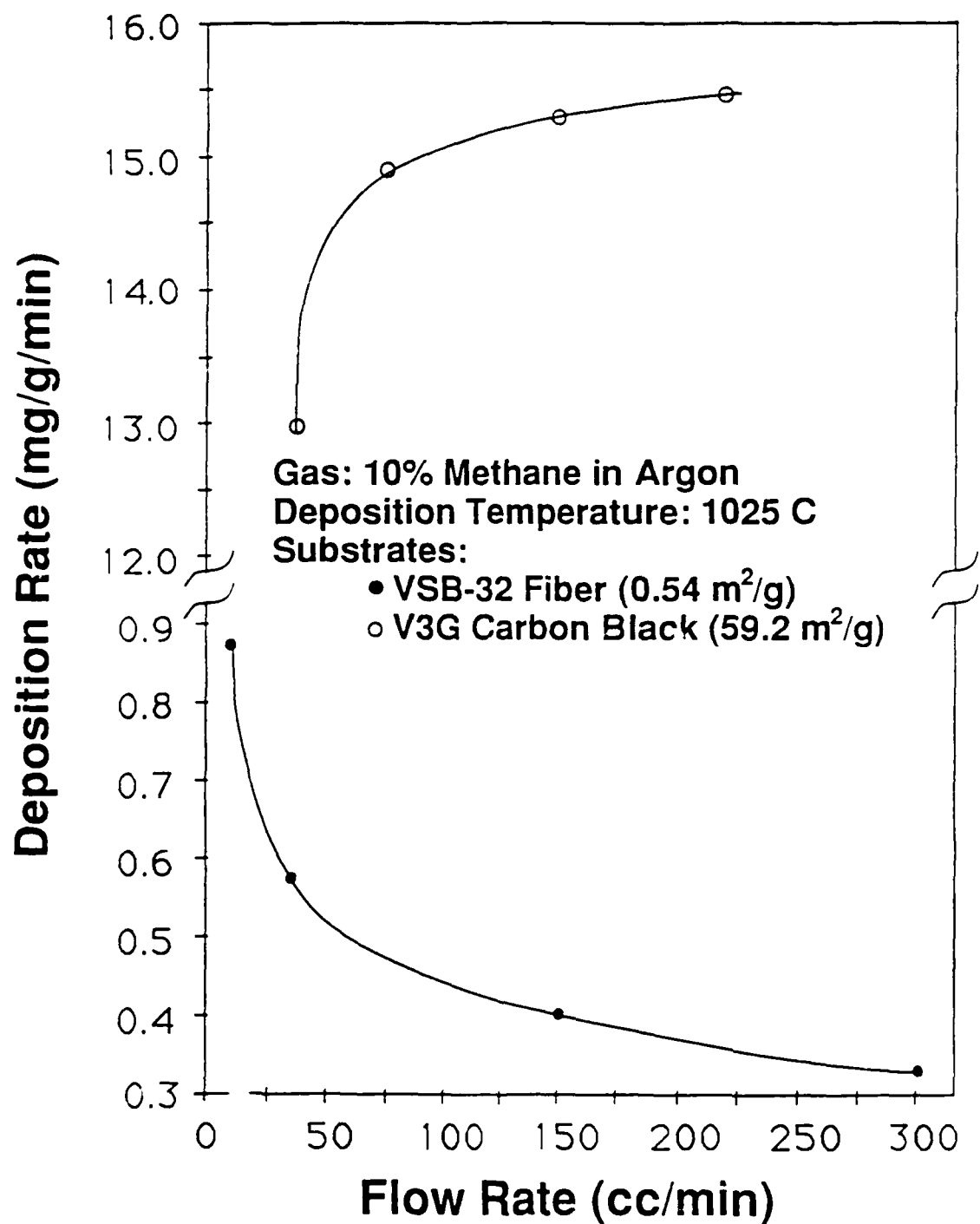
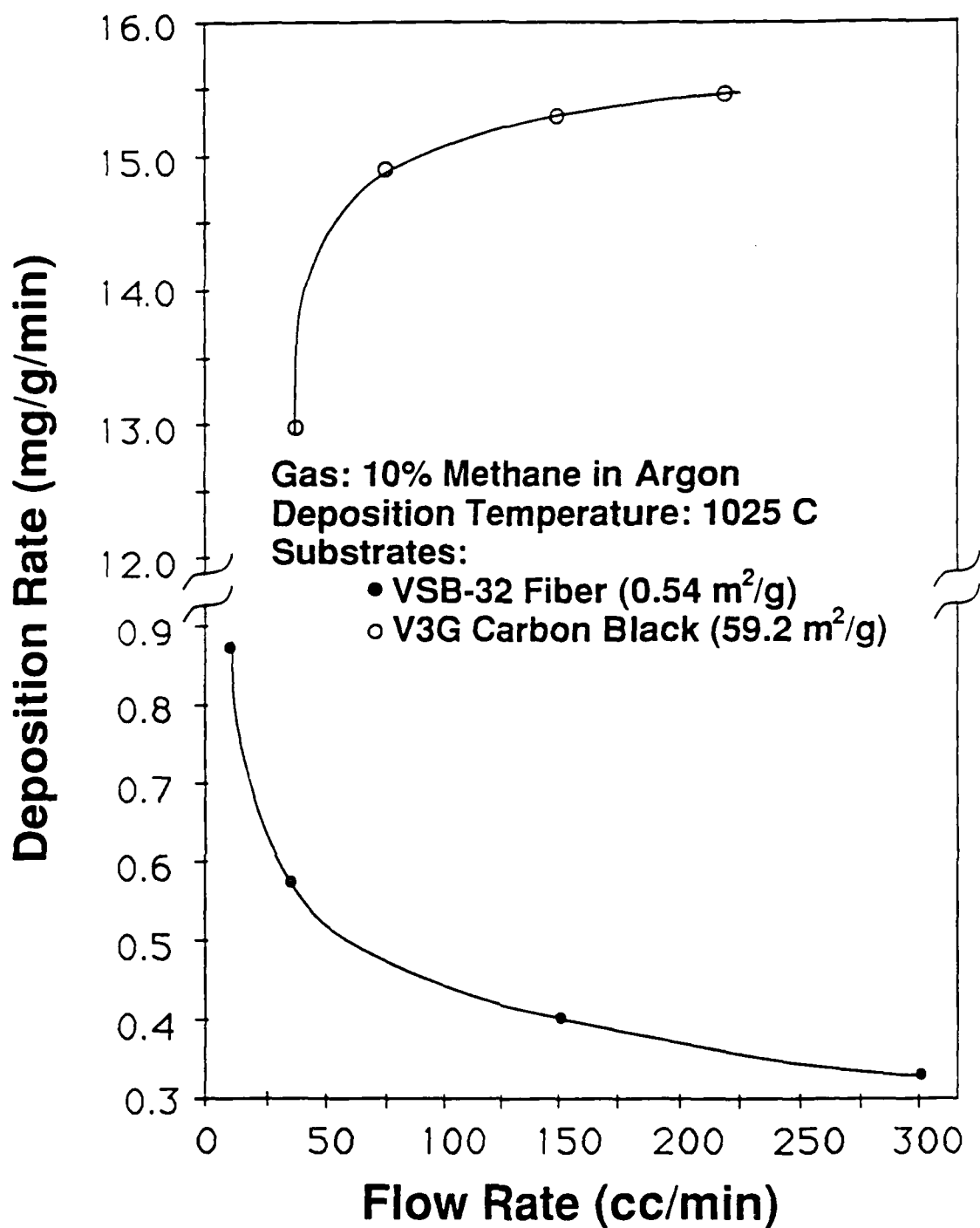


Figure 6



**Figure 7 Effect of Flow Rate on The Rate of CVD**



**Figure 7 Effect of Flow Rate on The Rate of CVD**

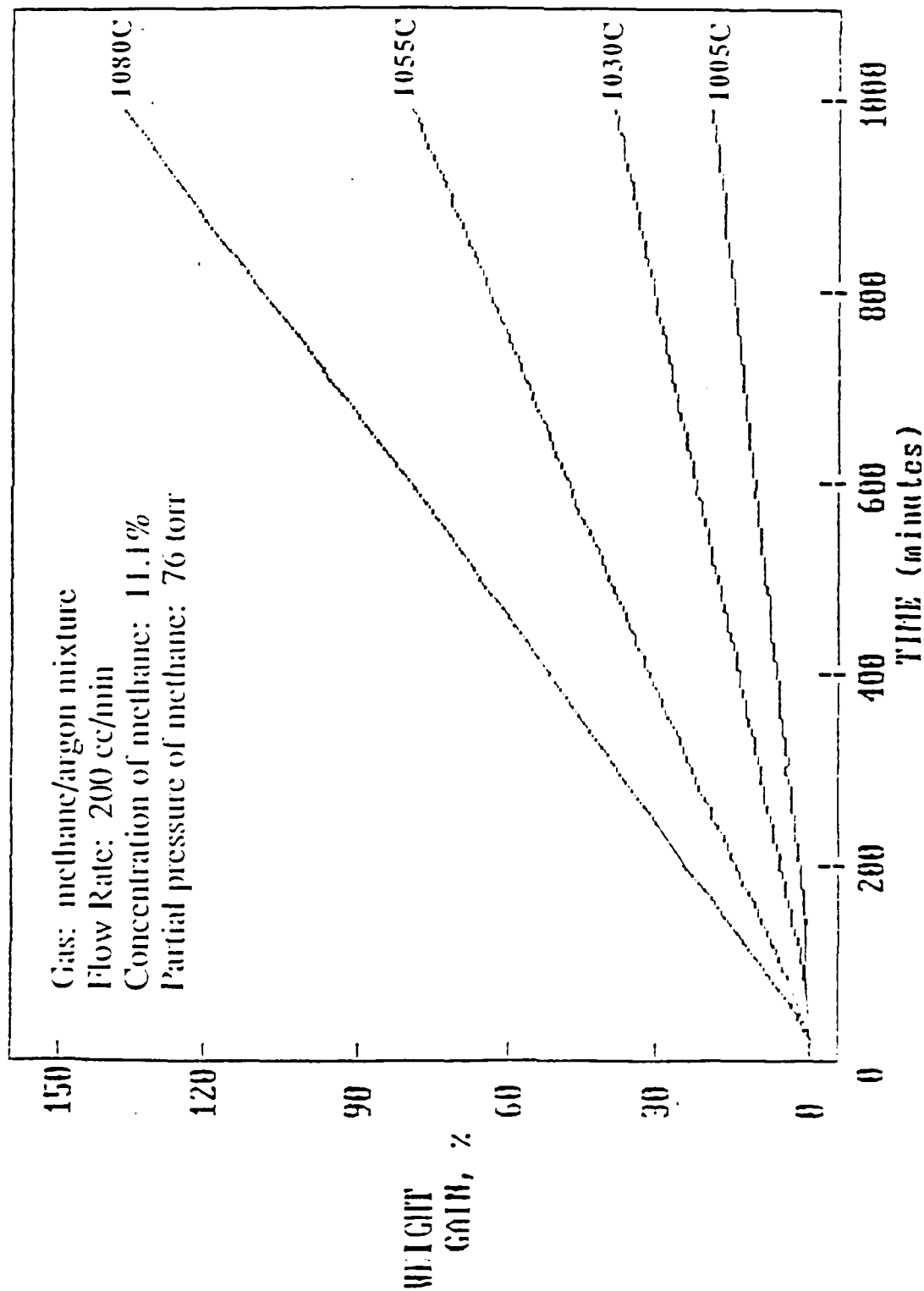
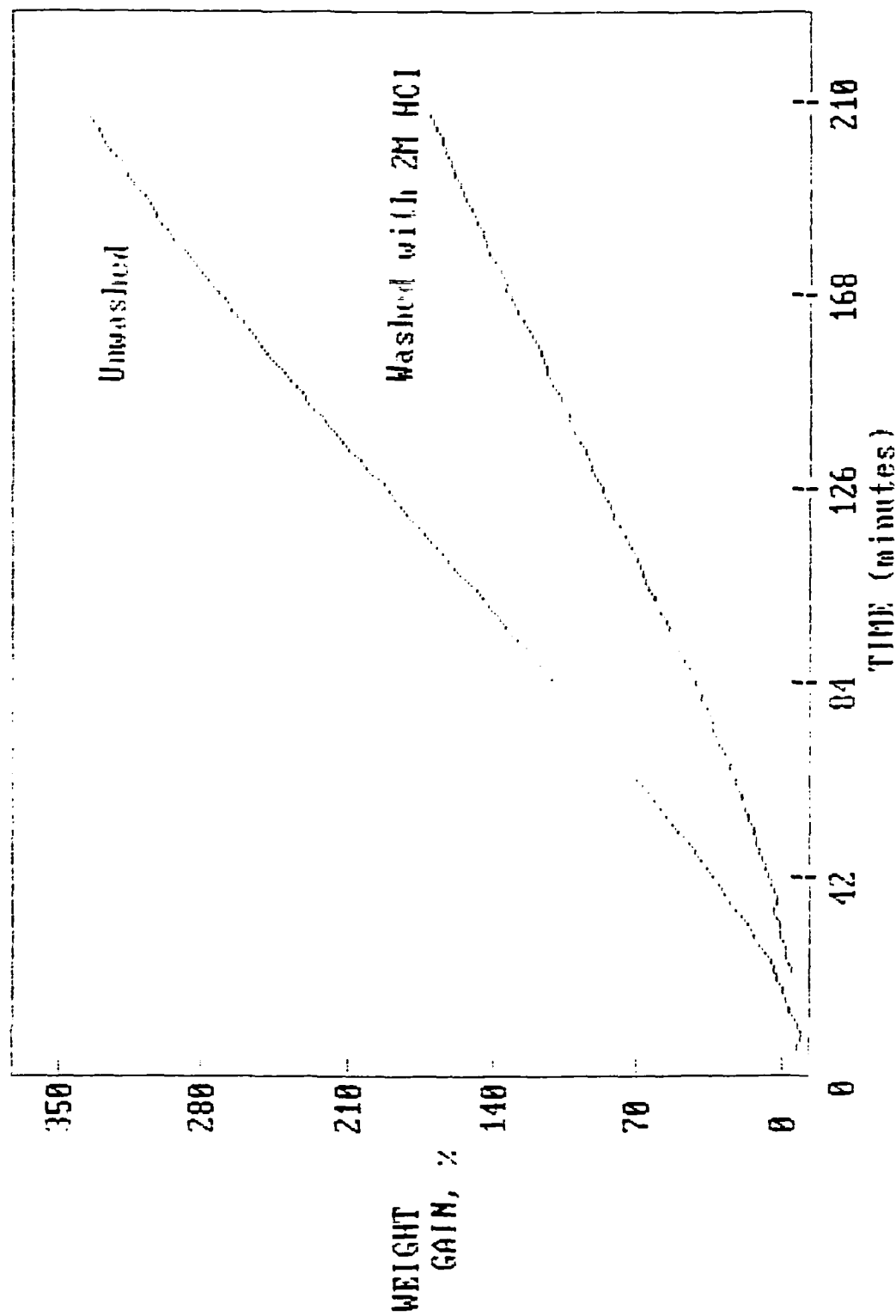


**Figure 8** Typical thermograms for methane cracking over VSB-32 fiber (flow system).

**Figure 9** CVD on Graphitized Columbia Carbon at 1000 C with 10% CH<sub>4</sub>



High School Apprenticeship Program Final Report

Astronautics Laboratory  
Edwards Air Force Base, California

June 19 - August 11, 1989

Mentor: Russ Leighton

Alexander Sagers



## High School Apprenticeship Program Final Report

This summer I was assigned to work at the Astronautics Laboratory at Edwards Air Force Base. The division I worked in was RKBA. My mentor was Russ Leighton. RKBA is primarily concerned with Engineering Design Evaluation. This involves extensive use of computer programs to simulate and evaluate solid rocket motors. When I started work on June 19, Russ was involved with creating programs on the VAX minicomputers to create picture formats which are readable on the Amiga microcomputer. The Amiga is used as a graphics workstation for the creation and presentation of high quality animations. It was on the Amiga that the vast majority of my work was done. My interests are in computer programming more than structural analysis so was projects were tailored for this interest.

Regarding my projects, the summer was roughly divided in half. The first half of the summer was spent on small projects that served two main purposes: better integration of the VAX and Amiga computers, and the allowing of me to become familiar and comfortable with the computer systems. I created quite a few programs to serve the mentioned purposes. The language used was ARexx. ARexx is the Amiga

version of the Rexx language, originally developed for IBM computers. ARexx is an interprocess communication language. Programs which support ARexx can be controlled by an ARexx program. On the Amiga, three programs I used directly supported ARexx: CygnusEd (a text editor), VLT (a terminal program), and T<sub>E</sub>X (a typesetting language). I wrote ARexx programs to integrate these three programs and make their use much more efficient. My first project was to create a integrated C program edit and compile environment using ARexx. I wrote programs which allowed compiling and debugging of programs from within CygnusEd. At the touch of a key, the current file would be run though the C compiler. If any errors occurred, the error message would be displayed and the proper line of code marked for editing. All interaction between the compiler and editor was controlled through the ARexx program. This integration proved very valuable in my later project.

With the completion of the editor-compiler integration I started on ARexx programs to manipulate VLT to allow easy file transfer between the Amiga and VAX minicomputer. I created two programs, one to send and one to receive files. At this time, Russ was creating images on the VAX that were to be displayed on the Amiga. My file transfer programs were ideally suited for transferring the images and were

frequently used for the remainder of the summer. T<sub>E</sub>X is a program used frequently in RKBA. It allows for the creation of typeset quality documents through a command language and compiler. It is not an interactive program. I wrote AR<sub>exx</sub> programs to make T<sub>E</sub>X more interactive. The programs essentially performed the same functions as the ones for the C compiler. The current document in CygnusEd was processed by T<sub>E</sub>X and then, if no errors occurred, was shown in the T<sub>E</sub>X previewer. After the document was finished, the resulting file could be transferred to the VAX, using my AR<sub>exx</sub> transfer program, and printed on a laser printer. Diagram 1 shows the interactions between AR<sub>exx</sub> and the other programs.

Along with the creation of AR<sub>exx</sub> programs, I was asked to create an animation which would be used as an introduction to videos created by RKBA. The video, which animates the "shield" symbols of the Astronautics Lab and AFSC, shows the incredible graphical power of the Amiga. Many animations of analysis data were created on the Amiga to better show the results of the data. I helped another summer hire create an animation which showed reading of thermocouples during a mishap of a Peacekeeper missile firing.

During the second half of the summer, I worked

extensively on one project: a graphing program. One of the people I worked with had written a graph shifting program on a Hewlett Packard computer. A version of this program was wanted for the Amiga and writing this program became my main project. Early on it was decided that my program would be a general purpose graphing program that could be used for shifting and other functions. I also decided to write the program in C (the original shifting program was written in BASIC). My ARexx programs were very beneficial during the development of the graph program. By the time my employment period was completed, I had developed an almost useable graph program which, with very few additions, could serve a wide range of purposes. The program can set a scale and draw, optionally, the axis, "ticks," and/or labels of the graph (diagram 2). A large portion of the development time was spent creating a parameter control requester (diagram 3). This requester allows the user to input attributes of the graph such as scale, axis intercept, and label format. By changing the values in the requester, the scale and other attributes of the graph are calculated and displayed. Diagram 4 shows the results of changes in the scale parameters and the corresponding changes to the displayed graph. Along the right side of the requester are three toggles to set what

is to be displayed in the graph. Diagram 5 shows the results of toggling off two of the "buttons." When the user is through modifying the graph parameters, selection of the "OK" button causes the parameters to take affect (diagram 6). For the plotting of data points, the program allows the specification of symbol attributes. The size, angle of rotation, color, and number of sides of the symbol polygon are specified. Diagram 7 shows four data point plotted using a five-sided polygon. In the lower right corner of the graph is a "sizing gadget." The sizing gadget allows the user to resize the graph as desired while maintaining its scale. Diagram 8 shows the same graph as diagram 7, but with the graph having been resized horizontally. All options of the program can be accessed through menu selection using the mouse. The final feature that has thus far been implemented in the graph program is the option to exit the program. This feature was the first to be implemented, for obvious reasons. When the user selects the "Quit" option from the menu, the program asks for confirmation of the action, shown in diagram 9. This graphing program should prove a versatile and useful tool for displaying and analyzing data.

I have found working in RKBA to be an interesting and productive use of my summer. This fall, when I enter

college, I am confident that the knowledge and experiences I have gained working this summer in RKBA will prove very advantageous. With my interests lying in computers and especially software programming, the projects I worked on have contributed greatly to the expansion of both my education and career oriented goals. I would certainly consider a program such as this apprenticeship program in the future as an educational opportunity.

### Acknowledgements

For their assistance, guidance, and friendship this summer, I would like to thank the following:

Wayne Roe  
Les Tepe  
Terry Galati

Durwood Thrasher  
Johnson Earls

and especially  
Russ Leighton

# Interprocess Communication

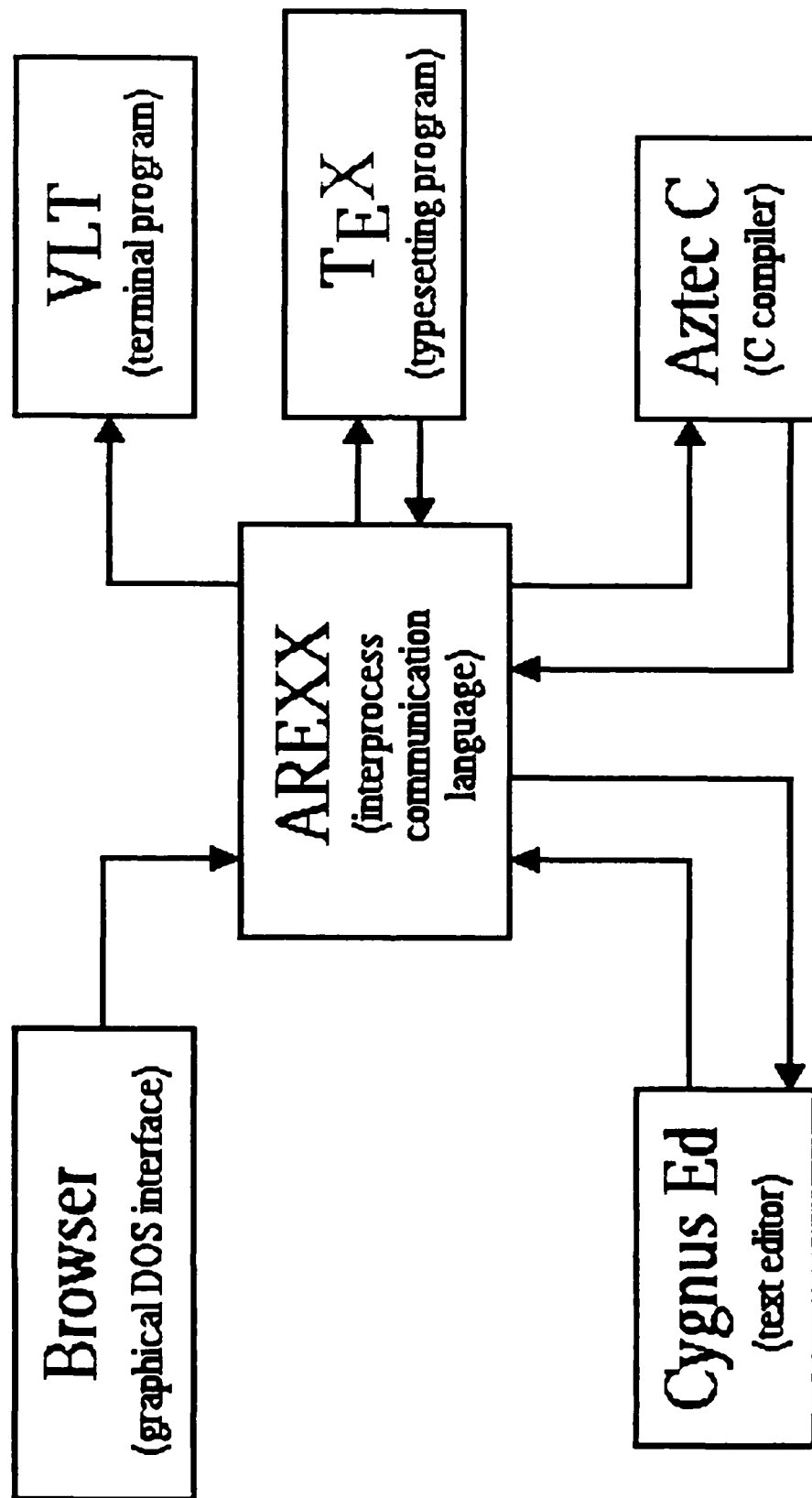
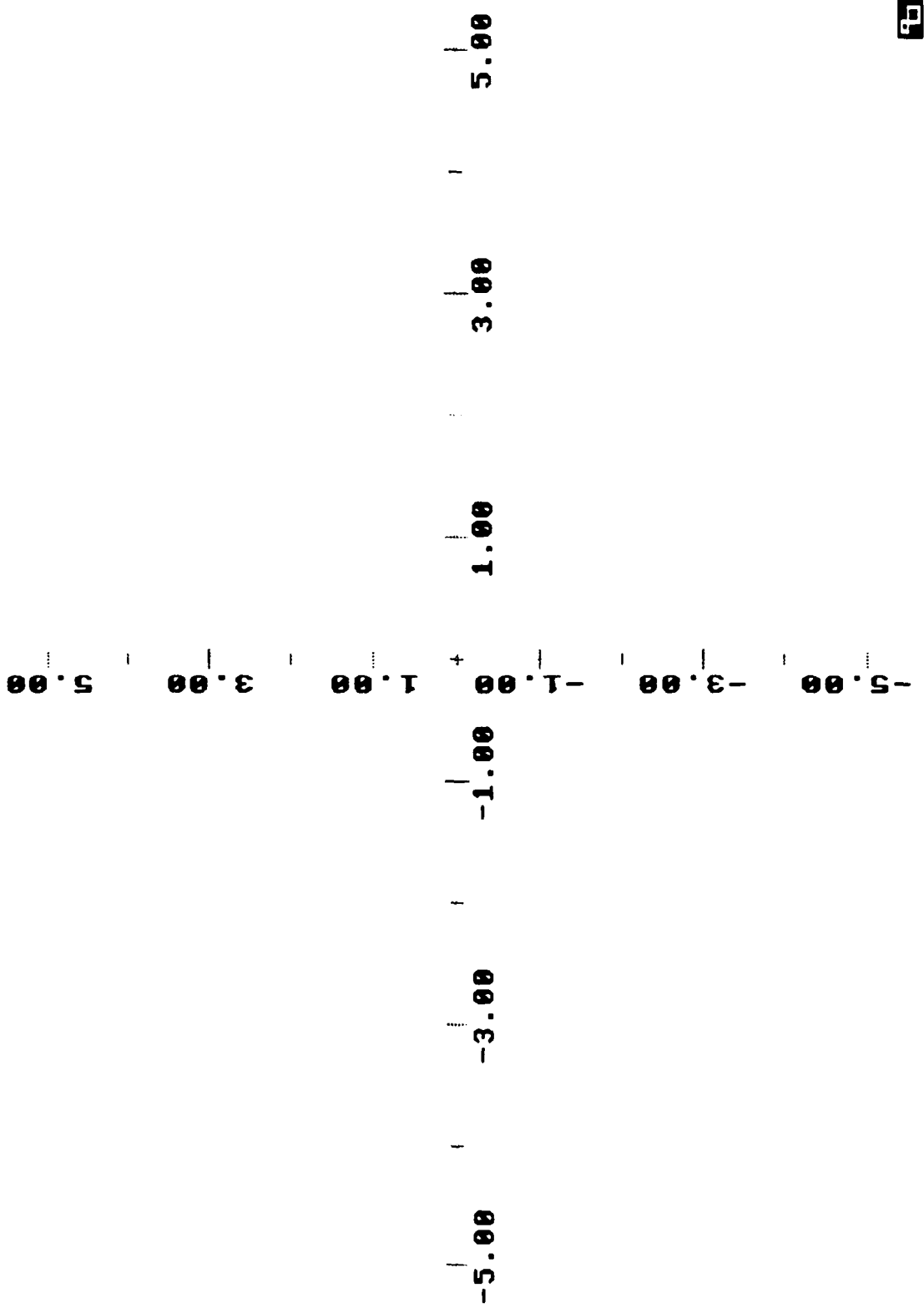


Diagram 1





| SCALE                             |         | Axis intercept coordinates |        | Axis is                               |                             |
|-----------------------------------|---------|----------------------------|--------|---------------------------------------|-----------------------------|
|                                   | Min     |                            | Max    |                                       | <input type="checkbox"/> ON |
| X                                 | -5.0000 |                            | 5.0000 | X                                     | 0.0000                      |
| Y                                 | -5.0000 |                            | 5.0000 | Y                                     | 0.0000                      |
| Tick Spacing                      |         |                            |        | Ticks are                             |                             |
|                                   | Minor   |                            | Major  |                                       | <input type="checkbox"/> ON |
| X                                 | 1.0000  |                            | 2      |                                       | Labels are                  |
| Y                                 | 1.0000  |                            | 2      |                                       | <input type="checkbox"/> ON |
|                                   |         |                            |        | Format                                |                             |
| X                                 |         |                            |        | X                                     | %.3g                        |
| Y                                 |         |                            |        | Y                                     | %.3g                        |
| <input type="button" value="OK"/> |         |                            |        | <input type="button" value="CANCEL"/> |                             |

-5.0

5.00

00.5

00.5

5

| SCALE        |        | Axis intercept coordinates |          | Axis is                             |                                     |
|--------------|--------|----------------------------|----------|-------------------------------------|-------------------------------------|
| Min          | Max    | X                          | Y        | Ticks are                           | Labels are                          |
| X -5.0000    | 15.000 | X 0.0000                   | Y 0.0000 | <input checked="" type="checkbox"/> | <input checked="" type="checkbox"/> |
| Y -8.0000    | 10.000 |                            |          |                                     |                                     |
| Tick Spacing |        | Format                     |          |                                     |                                     |
| Minor        | Major  | X                          | Y        |                                     |                                     |
| X 3.0000     | 1      | X % .3g                    |          |                                     |                                     |
| Y 2.0000     | 2      | Y % .3g                    |          |                                     |                                     |

-5.00

13.0

9b



| SCALE  |         | Axis intercept coordinates |  | Axis is |   |
|--|---------|----------------------------|--|---------|---|
|  | Min     | Max                        |  |         |   |
| X  | -5.0000 | 15.000                     | X  | 0.0000  | <input checked="" type="checkbox"/> ON            |
| Y  | -8.0000 | 10.000                     | Y  | 0.0000  | Ticks are <input checked="" type="checkbox"/> OFF |
| Tick Spacing                                 |         |                            | Labels are                                       |         |   |
|  | Minor   | Major                      |  | Format  | <input checked="" type="checkbox"/> OFF           |
| X  | 3.0000  | 1                          | X  | %.3g    |   |
| Y  | 2.0000  | 2                          | Y  | %.3g    |   |
| <input checked="" type="button" value="OK"/> |         |                            | <input checked="" type="button" value="CANCEL"/> |         |   |

Diagram 6

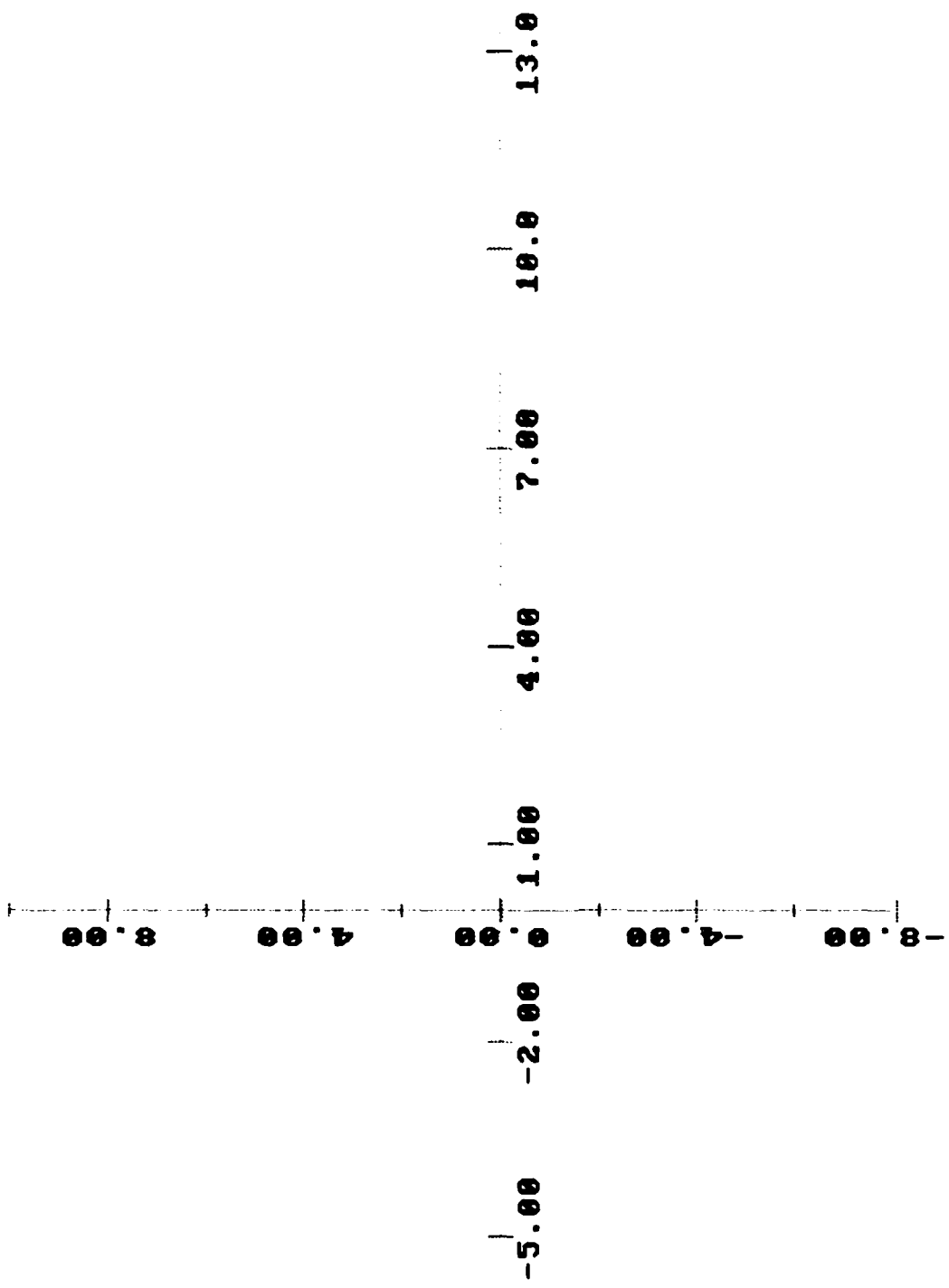
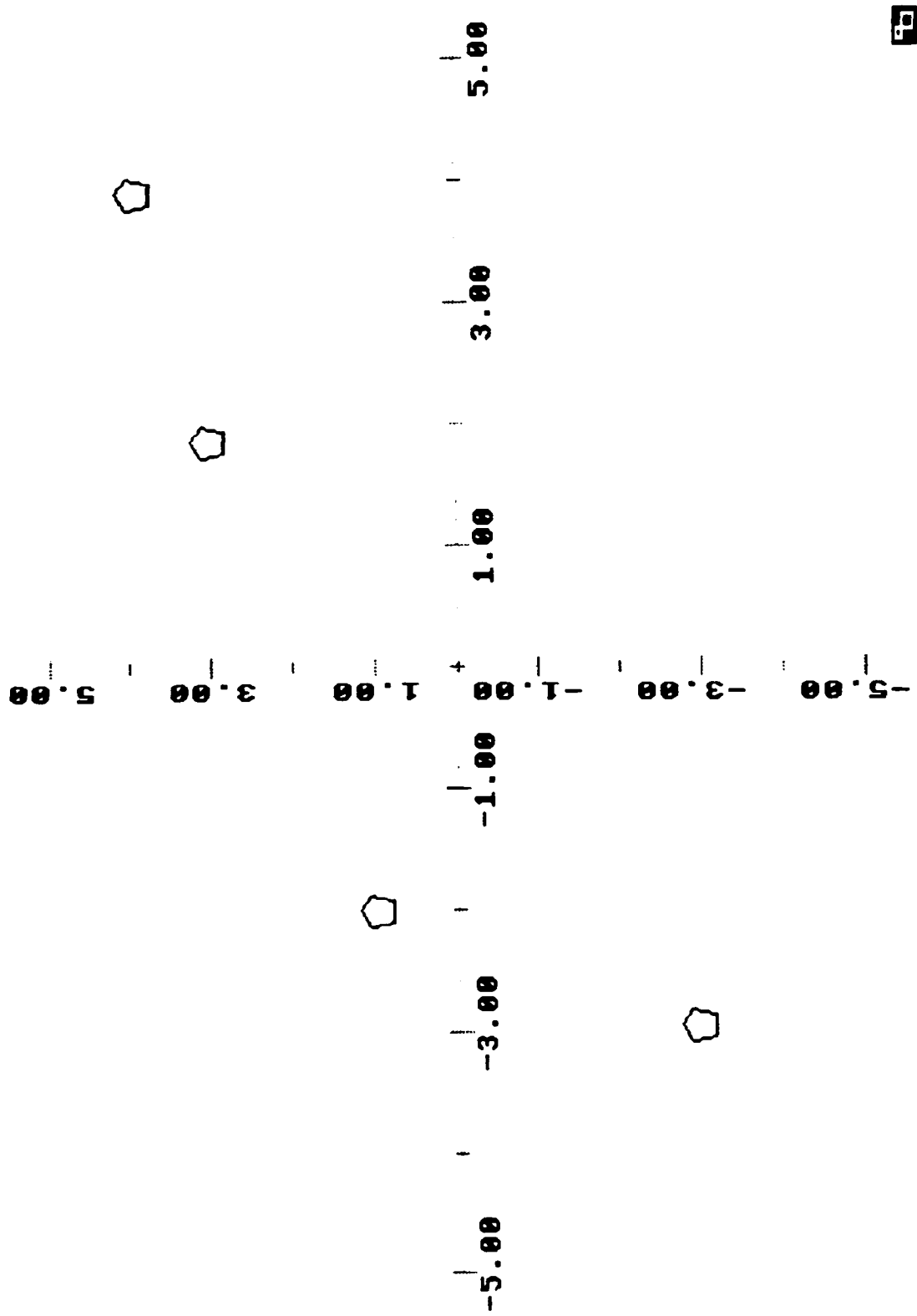


Diagram 7



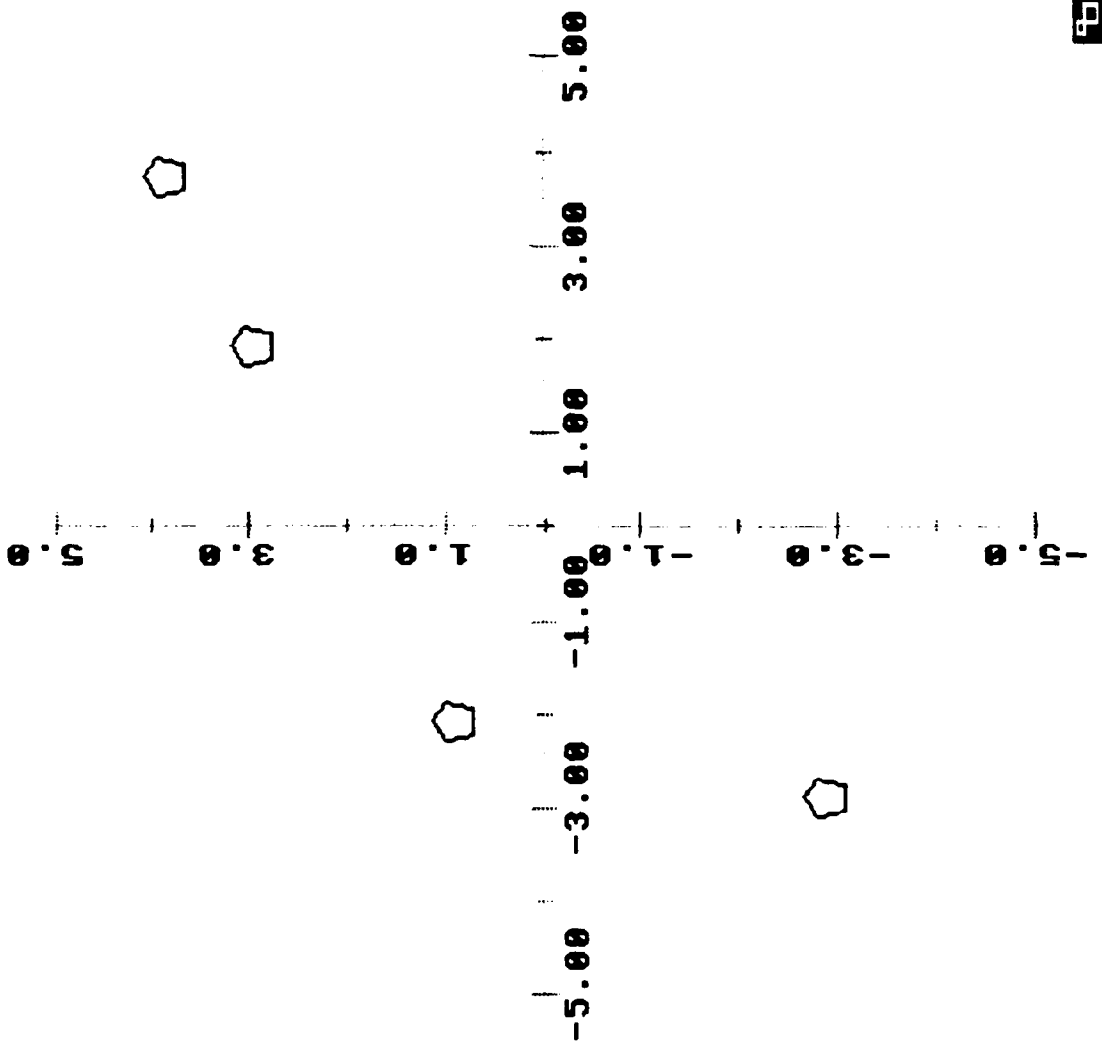
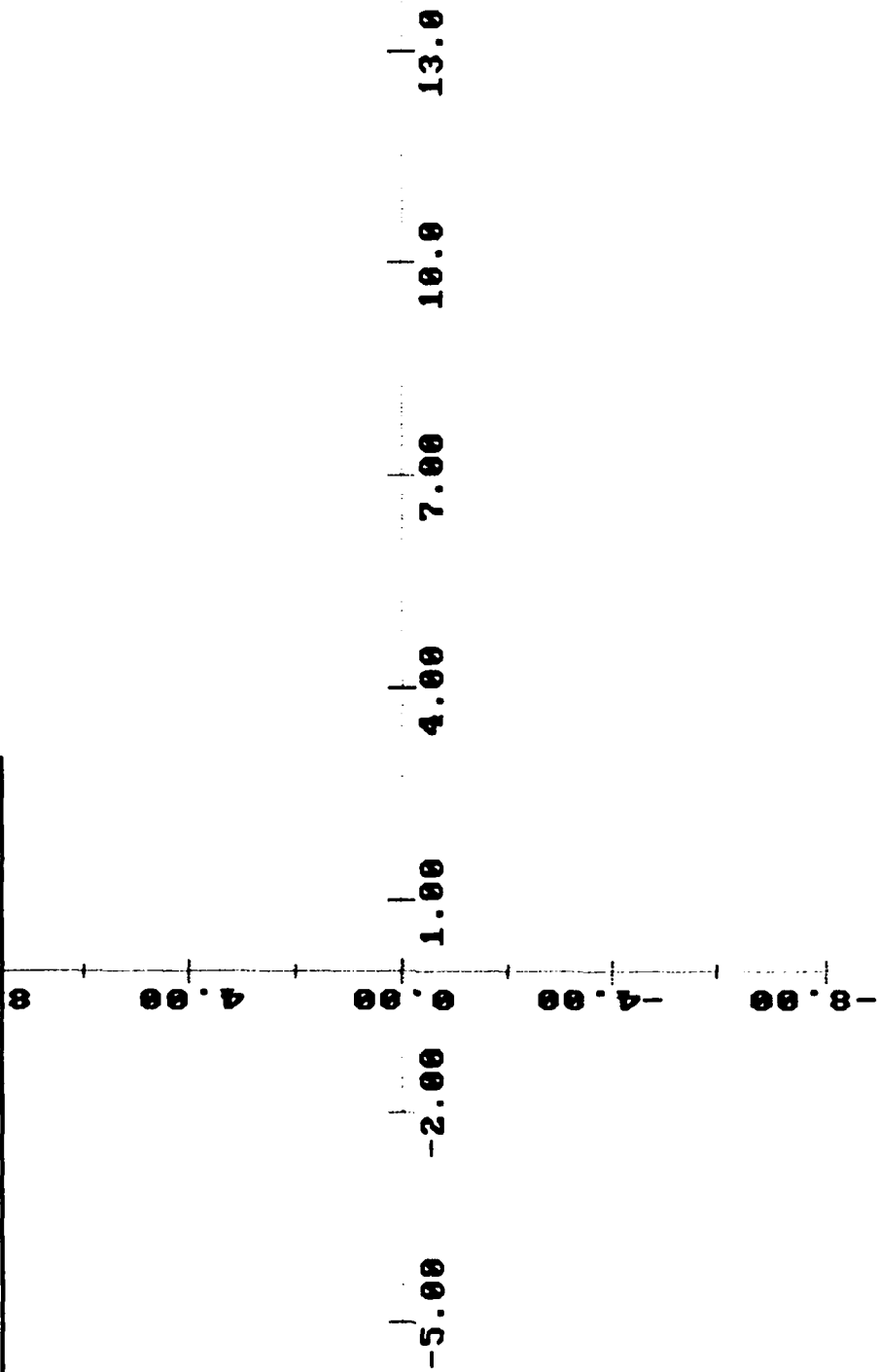
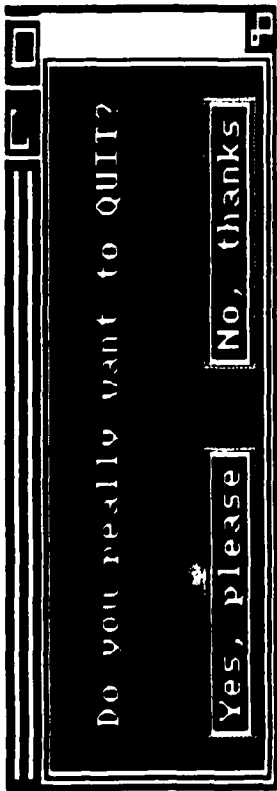


Diagram 8

Diagram 9



5



HIGH SCHOOL APPRENTICESHIP PROGRAM FINAL REPORT

Astronautics Laboratory

Edwards Air Force Base

August 16, 1989

Richard Sims

## ACKNOWLEDGEMENTS

I would like to thank the following people for all of the help they have given me during my brief stay here at the Astronautics Laboratory. First and foremost, I would like to thank my mentor, Pete Follock, for showing me what 'real science' is like. I would also like to thank all of the other students who worked under Pete along with me--Bruce Hinds, Beckv Peders, Jean Stojak, and Chris Kother. I also thank all of the scientists and technicians working at the Composites Laboratory for their help, especially Jim Naughton. I would also like to thank Gordy Wellman for his assistance in helping me find electronic equipment, and Roger Benedict who was always there to answer any questions I might have had.

## INTRODUCTION

This summer I worked with Pete Pollock, a mechanical engineer with the University of Dayton Research Institute. Pete is currently working with Carbon-Carbon, a composite structure which is incredibly strong, lightweight, and able to withstand very high temperatures for long periods of time. Pete also had four other apprentices working with him this summer. He had two Graduate students, Chris Kocher and Jean Stojak. Chris was testing the strength of the Carbon-Carbon under tension, compression, and other various tests, and the relationship between the strength of the Carbon-Carbon and its heat-treatment. Jean Stojak worked with another composite, Silicon Carbide, and was beginning to run various strength tests on it also. The other two students were Bruce Hinds and Becky Teders, both Undergraduates. Bruce worked on ways of replicating the surface cracks on the Carbon-Carbon so that one could be study it under the microscope, as well as on various projects of his own. Becky worked with a computer program, Patran, which is supposed to be able to create a model which would behave exactly as a real model would. Becky also studied the assorted cracks found in the Carbon-Carbon specimens.

There are other various projects that are also taking place at the Composites Lab at the same time. One such is the study of "smart" structures. These are structures that will hopefully be able to tell if they are damaged or if they are not behaving as they are supposed Lab are working on making structures that can sense if they are vibrating. This

... if someone could help when the structure is in trouble since there is no air to dampen the vibrations. If the structure is able to sense itself vibrating, and there is a mechanism in the structure which can stop those vibrations, the structure can be saved before it vibrates itself to pieces. I was chosen by Pete because I was interested in electrical engineering and because he has an interest in smart structures. He wishes to start working with smart structures next year and so wanted someone who could help him with his studies then. So he began to help me learn about electronics.

## MY SUMMER PROJECTS

Previously, I had only worked with very, very simple circuits, and then only on paper -- never actually working with a circuit. So I began the summer by learning more about R-C circuits, circuits with Resistors and Capacitors. One of the first things I learned was the importance of the constant  $e$ , which beforehand had only been the base of a natural logarithm. Now I know that it also has real world uses, specifically, relating to the RC time of a circuit.

Then Pete told me my summer project -- to build a radio from the spare parts laying around the Lab. So I started making a few different types of capacitors with aluminum plates separated by some Kevlar film, and from aluminum foil and Seran Wrap. This kind of work had many problems, mostly with the lack of supplies and the lack of time I had for the summer. So, we gave up this project and began a new one. This time Pete wanted me to try to simulate the neurons of the human brain with electronics -- using RC circuits. But again, the lack of supplies in the Astronautics Lab tried to stop us. So, while we were scrounging around for electronics equipment, I took apart some old solid-state equipment and found some Inductors. So I began experimenting with R-L-C circuits, R-C circuits with inductors.

After a while I had R-L-C circuits pretty much figured out. It was about that time we found a decent pulse generator. We needed the pulse generator to simulate a neuron that was sending out pulses to its adjoining circuits. The problem in finding one was that we needed a generator

and we varied the time between one pulse and the next, varying the length of the pulses themselves. But when we found this generator, we also found out that it put out pulses so weak that we could barely see them on the Oscilloscope. So we set out to find an isolation amplifier. After about a week, we found a good amplifier and set it up. So we set up some test to see if the Oscilloscope was turning out predictable results, and we found that it wasn't. We still do not know why it wasn't working, but were still thinking about it. This is what I did this summer as it relates to my project, but I also did some other work for various other people at the Lab.

Almost every day while the college students were at the Lab, there was work to be done helping them calibrate instruments, or polishing specimens to track, or taking data, or anything else they needed done desperately. I also helped the people working on the smart structures by helping them set up their structure, embed the strain gauges, and acquire test data from the vibrations that were occurring in the structure. Next year I hope I can be of further assistance to the people there, knowing more about electronics than I did this summer. I am very grateful for the teaching I got from Pete this summer. Just browsing through the college catalog, I have already learned most of what they are going to teach me through the second semester of my Sophomore year, and I haven't even entered college yet.

Final Report

by

Ben Sommers

### Acknowledgements

I would first like to thank my mentor, Captain Steven D. Thompson for being an exceptional boss, teacher, and friend. I must also thank Lieutenant Roeland van Opijnen for being around to help and give encouragement. Ed Miller was always around to help me out with any VAX related questions or to lighten things up with a joke. Sergeant Paul Adkison, Captain Tim Wiley, Jill Whitney, Lieutenant Thanh Mather, and Lieutenant Pete Dolan also deserve thanks for endless moral support. Dr. John Kenney gave some appreciated advice regarding college, and numerous other Dr.'s gave valuable help and provided interesting subjects for heated discussions. Finally, Dr. Steve Rodgers, as branch chief of LSX, and Cris Sandstrom, as ARIES secretary, must be thanked for their invaluable help.



### Introduction

This was my second summer working in the ARIES office under Captain Thompson. The main project in this office/laboratory is High Energy Density Matter, or HEDM. It has to do with nuclear chemistry and nuclear physics. A project related to this is anti-matter, also being researched in ARIES. Most of the projects in ARIES are in their early stages.

Most of my work in the ARIES lab was computer related, although I did help Dr. John Kenney with some wiring on a vacuum cooler in the cryogenics laboratory.

My main project was to create a database on the VAX network which could be used by anyone and everyone in the ARIES office. I therefore spent a good deal of time programming on the VAX, learning the operations of the mainframe system and also learning the database language of ORACLE.

The database form which I created will imminently be receiving data from everyone in LSX. All the experiments being conducted in the ARIES labs fall into a certain category, and each of these categories has a section in the database program.

My experience as an apprentice has been educational and fun. It will be a valuable asset in my future studies at college, and the exposure to a working environment will be a tremendous help when I enter the job market. I have learned computer programming and operating systems of several types of computers while working at the Astronautics Lab, and I will benefit greatly from this education.

# Space Structure

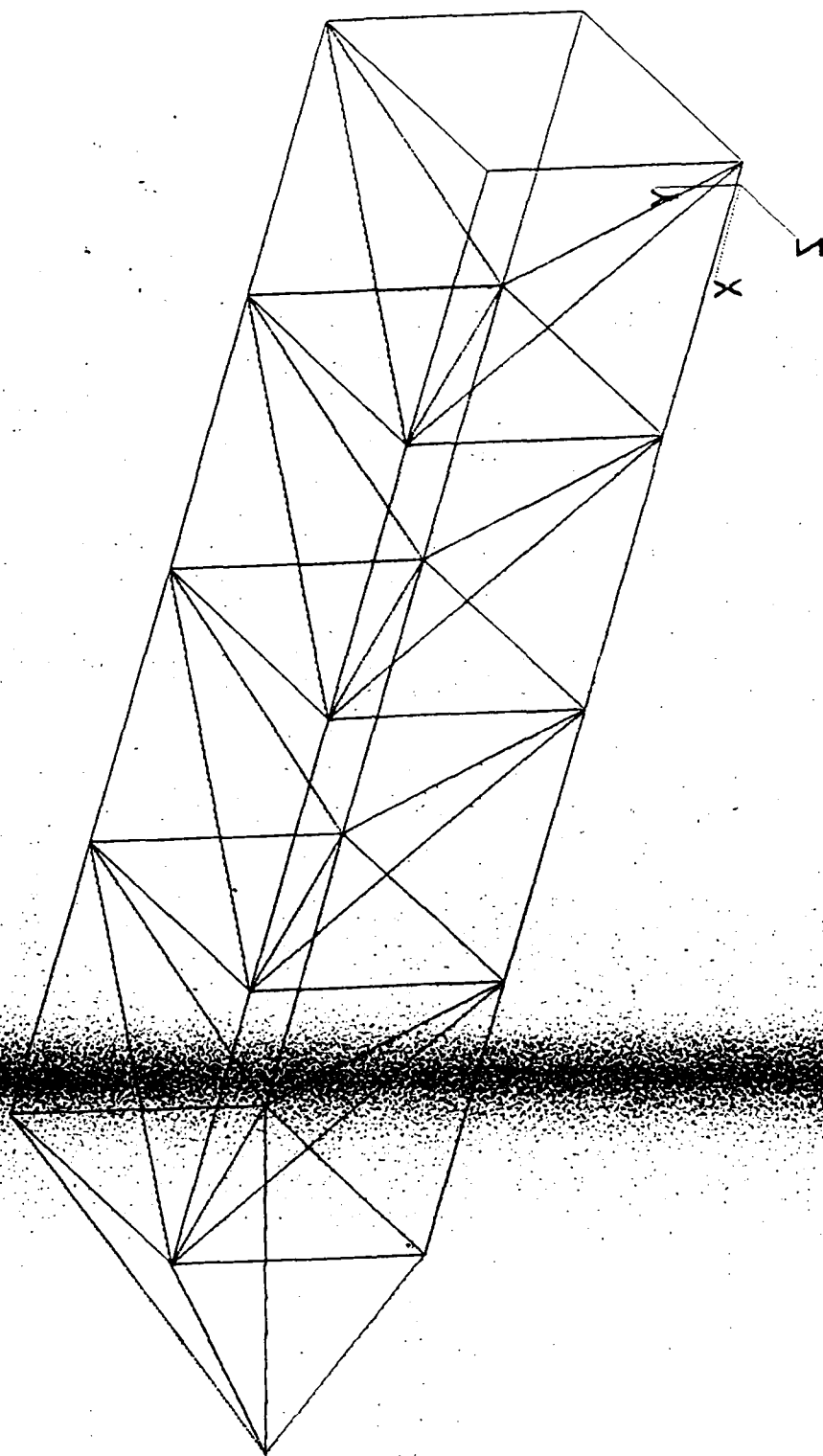
Shirley Williams

Captain Tim Strange

Astronautics Laboratory

Edwards AFB, CA

August 31, 1989



## Background

- \* Space Structures have increasing size requirements.
- \* Payload capabilities are not increasing to meet these requirements.
- \* As a result, the larger the space structure, the lower the stiffness of the truss.

## Requirement Effects

- \* In the design of the truss, two criteria must be met:
  1. It must be under the maximum mass set by rocket capabilities.
  2. It must be over the minimum stiffness to provide stability to the space structures.

Two cantilever models of a space truss were generated on the Patran system. One model, Case 1, had the diameter of its elements increased. The other model, Case 2, had twenty more elements added on to its structure. Nastran was used for finite element analysis. Matrix X created graphs that reflected node deflection to loads and stiffness to weight ratios.

The purpose for these two models was to determine which one was the stiffer. The space structures that the truss would be supporting would have increased size and weight, so the truss needs to be stiffer to support this increase. This truss has to meet the standard requirements of size and weight without going over and still be stiffer than the previous ones. The stiffer of the two models will be the better and stabler truss.

# Analysis Tools

**Patran**  
Graphics



**Nastran**  
Finite Element Analysis



**Matrix X**  
Graphical Results



The analysis tools used were Patran logged into a Vax, Nastran and Matrix X. Patran was developed to use the full potential of interactive engineering. Interactive engineering is the ability to construct, view, verify, analyze, manipulate, demonstrate and understand the nature and behavior of an object before it has been created.

#### Phase 1- Geometric Modeling.

The object of this phase was to generate a continuous geometry model of the truss. This means develop a set of mathematically defined regions so combined that it closely resembles the physical object of the truss.

#### Phase 2- Analysis Modeling.

In this phase the model can be subdivided to any required density for finite element model generation. The element used was aluminum and various loads from 100 to 300 N were applied.

#### Phase 3- Analysis.

Once the model has been made with its properties and loads, an analysis of its behavior can be made. The Neutral File was used which is a readable file that contains the raw information of a model. This information is needed to produce the input to an analysis program.

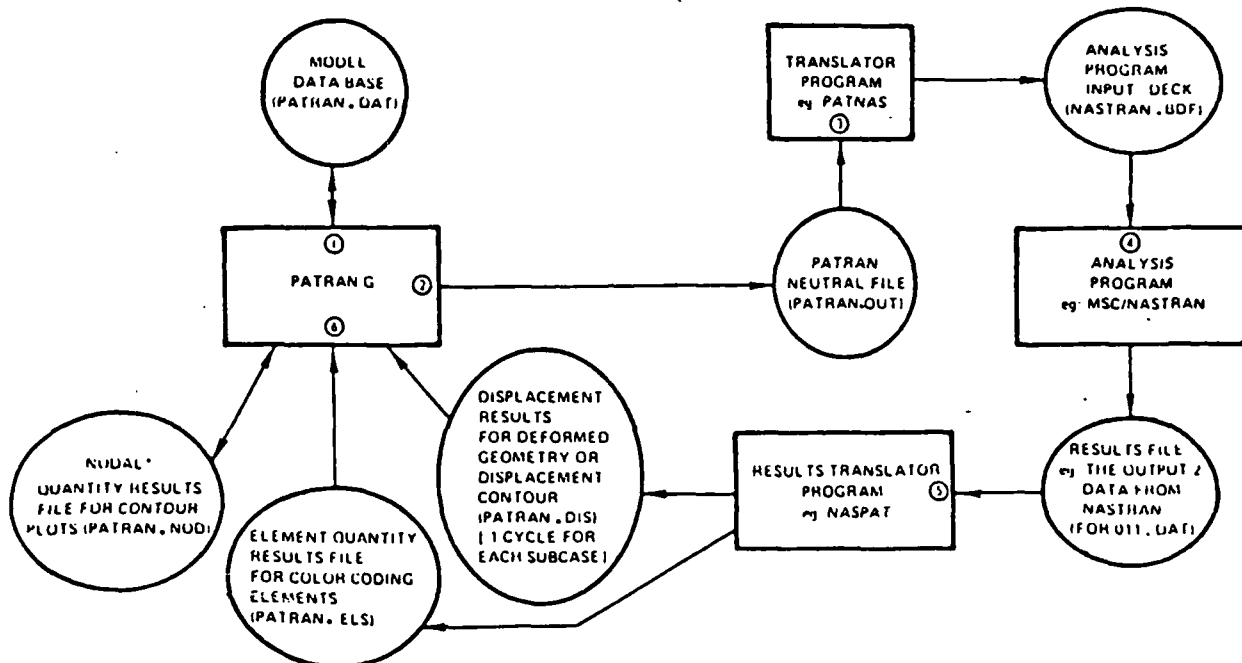
The neutral file is read by a program called the Analysis Translator. This is an external program that takes the information in the neutral file and gives the user an input file that is used by the analysis program. The analysis translator, PATNAS, reads the Patran's neutral file and creates a Nastran data deck.

Once the analysis is complete, the results can be read in either at an element or nodal level for post processing. Post processing is the process of reviewing and interpreting the results of an analysis. An Inverse Analysis Translator converts analysis programs into files which can be read by Patran.

#### Phase 4- Results Evaluation.

Once the analysis is done, the output from the analysis program like nodal quantities, displacement information and/or element quantities can be processed through a results translator and sent into Patran for interactive postprocessing of any quantity which can be calculated for any finite element or node.

## PATRAN-G POSTPROCESSING OVERVIEW



\* NOTE A NODAL QUANTITY FILE IS REQUIRED IN ORDER TO DO CONTOUR PLOT.  
IF YOU DO NOT HAVE A NODAL QUANTITY FILE PATRAN WILL ASK FOR  
THE NAME OF AN ELEMENT QUANTITY RESULTS FILE AND AUTOMATICALLY  
AVERAGE THOSE RESULTS AT NODES AND CREATE A PATRAN.NOD FILE.

Figure 20-1 PATRAN-G Postprocessing Overview

Nastran is a general purpose computer program based on finite element method, structural analysis, heat transfer, aeroelasticity, hydroelasticity and field type problems. The classes of input for Finite Element Analysis are Geometry, Element Connectivities, Element Properties, Material Properties, Constraints, Loads and Enforced Motion.

\*Geometry- The locations of the grid points and the orientations of the coordinate systems are used to record components of displacements and forces at the grid points.

\*Element Connectivities- The identification numbers of the grid points to which each element is connected.

\*Element Properties- Examples are the thickness of a surface element and the cross-sectional area of a live element. Each element type has a specific list of properties.

\*Material Properties- Examples are Young's Modulus, density and Thermal Expansion Coefficient. There are several material types available in Nastran. Each has a specific list of properties.

\*Constraints- These are used to specify boundaries, conditions, symmetry conditions and a variety of other useful relationships. They are necessary, because an unconstrained structure has free body movement, which will cause the analysis to fail.

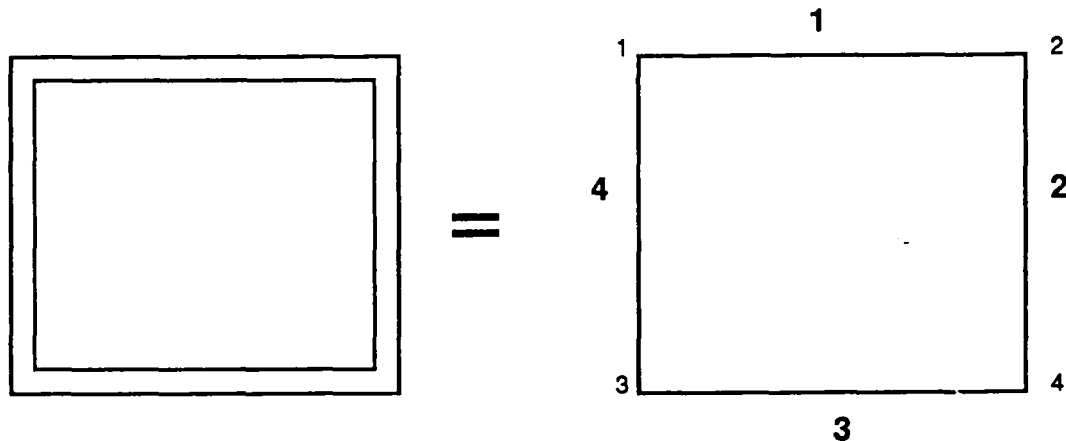
\*Loads and Enforced Motions- Loads may be applied at the grid points within elements, including point loads, distributed loads and implied loads. Enforced motions are applied at grid points.

The output received from finite element analysis are grid point

displacements, element data recovery: stresses, strain energy, internal forces and moments. Grid point data recovery are applied loads, forces and moments of constraint, forces due to elements.

# Finite Element Analysis

1. Large structures are divided into a large number of small elements.



2. Matrices with information about the structure's geometry are created.
3. These matrices are used in conjunction with basic spring mechanics to relate applied forces to deflections of the nodes. This results in a large number of equations, usually in matrix form.
4. Known applied forces and boundary conditions on the structure are plugged in to make the equations solveable.

What goes in: Geometry, Material Properties, Boundary Conditions, and Applied Forces

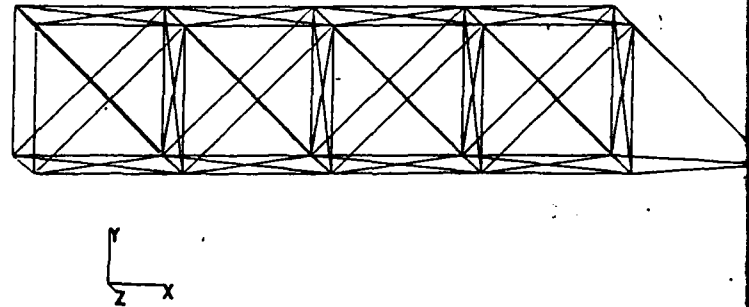
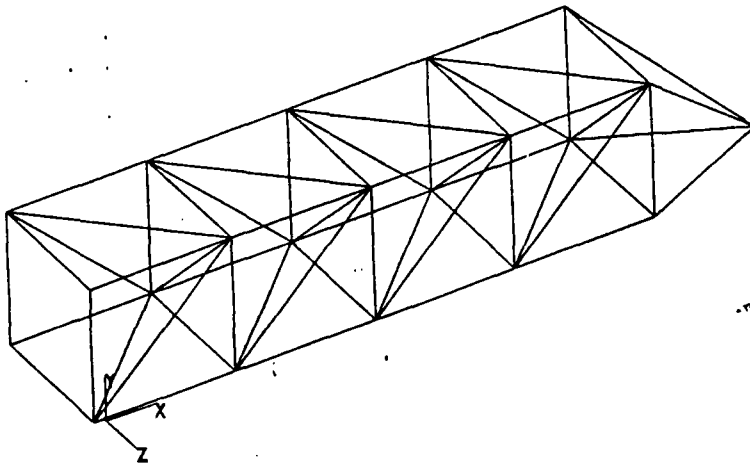
What comes out: Node Deflections, Member Forces, and Vibration Characteristics

To communicate with the VAX/VMS operating system, the user must use a terminal that is connected to the computer. The user tells the operating system what to do by typing a command on the terminal's keyboard. The system responds by executing the user's command. If the system cannot interpret what the user types, it displays an error message at the user's terminal; when the command is successfully executed, the user types another.

To begin, the user must log in. Logging in is getting the system's attention and the user's identification as an authorized user. Before the user can log into the system, the user must have an account. Accounts are set up by the system manager, or whoever is responsible at the user's installation for authorizing the use of the system. This person must provide you with a user name and a password. When the user logs in, the user must enter both his name and password.

# Problem

A space truss structure is needed with specific length and weight requirements. The stiffness must be maximized by either increasing the diameter or number of the members.



## Case 1

Member Length = 1m.

Total Length = 5m.

Number of members = 60

Member diameter = 1.1859 cm.

Total mass = 20.81 kg.

## Case 2

MemberLength = 1m.

Total Length = 5m.

Number of members = 80

Member diameter = 1.0 cm.

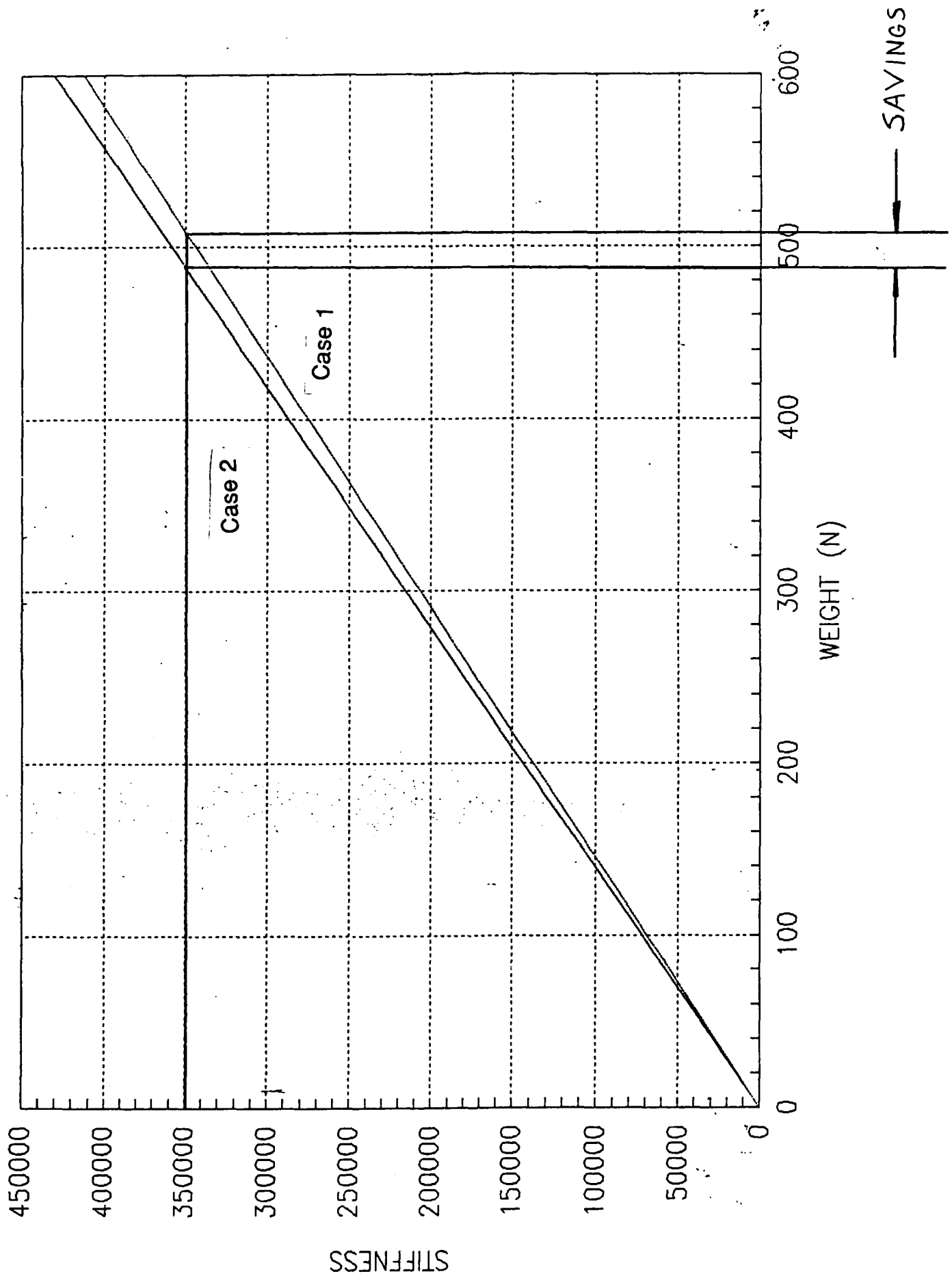
Total mass = 20.81 kg.

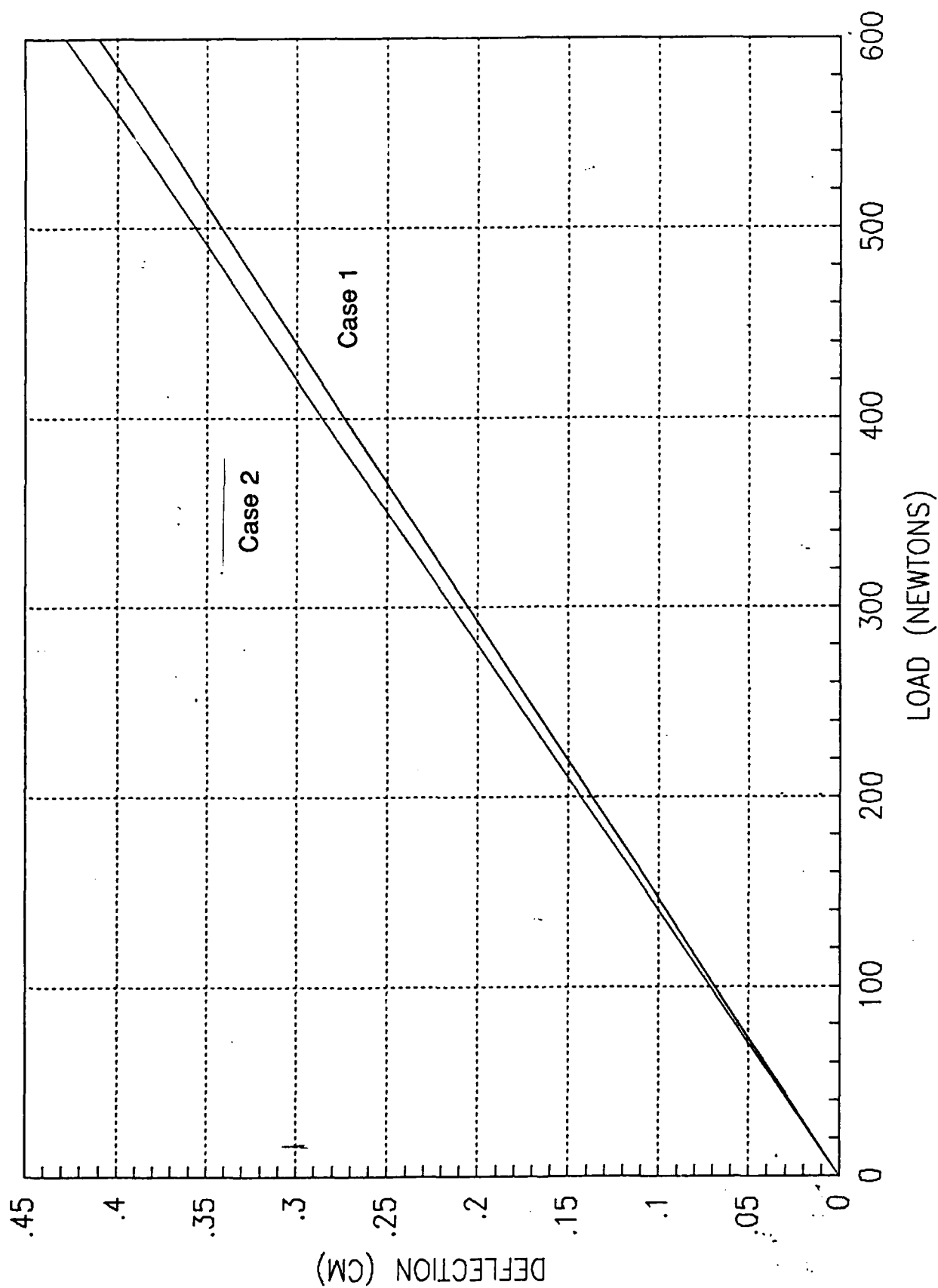


Matrix X is a powerful, programmable, matrix calculator with graphics. A user can solve complex, large-scale matrix problems in any engineering discipline. It has most of the matrix problems in any engineering discipline. It has most of the matrix analysis functions found in Eispack and Linpack, and several new algorithms which are not available on other systems. It was designed to have a good set of design and analysis functions for input/ output (classical) control and state-space (modern) control.

Data can be displayed with symbols, lines or a combination of both. When creating a graph, the data can be entered as a vector variable or expression. The Plot command accepts vector variables or expression in either row or column format. A vector is treated as if it were always in column format.

Axis labels and titles are specified with the Xlabel, Ylabel and Title keywords in the Plot command. The default labels may be suppressed, replaced or adjusted for font style.





# Solution

Generate stiffness data by creating a cantilever model of the truss, applying loads and analyzing deflection results.

|                          |              | Case 1 | Case 2 |
|--------------------------|--------------|--------|--------|
| Deflection (cm)          | Load = 100 N | 0.0713 | 0.0683 |
|                          | 200 N        | 0.1436 | 0.1368 |
|                          | 300 N        | 0.2611 | 0.2051 |
| Stiffness (N/m)          |              | 140255 | 146410 |
| Stiffness / Weight (1/m) |              | 687.0  | 717.2  |

## Conclusion

- \* Space structure are becoming larger and more flexible.
- \* In order to maximize the stiffness of a structure with rigid weight constraints, all possibilities and configurations should be considered.

## BIBLIOGRAPHY

Basic MSC/ Nastran Analysis- MSC -The Macneal-Schwendler

Corporation. 1963. 7442 North Figuero Street, Los Angeles, CA  
90041.

Guide to Using DCL and Command Procedures on Vax/ VMS. September

1984. Digital Equipment Corporation, 110 Spit Brook Road, Nashua,  
NH 03062-2698.

Matrix X User's Guide Engineering Analysis and Control Design

Version 6. May 1986. Integrated Systems Inc., 101 University  
Ave., Palo Alto, CA 94301-1695.

Patran-G User's Guide Vol 1. March 1984. PDA Engineering Software

Products Division, 1560 Brookhollow Drive, Santa Ana, CA 92705.

AVIONICS LABORATORY

# FINAL REPORT

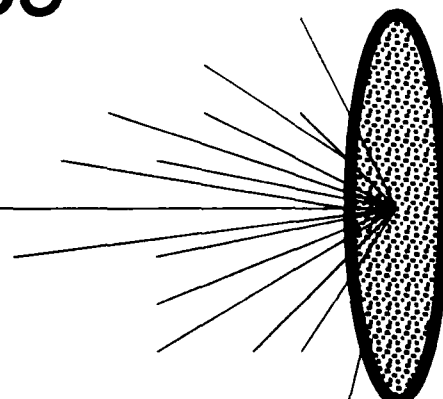
By:  
MATTHEW C. BREWER

Capt. JEFF BROWN  
Mentor

Electro-Optics Laboratory

11 AUG. 1989

HeNe Laser





## ACKNOWLEDGMENTS

I wish to thank Sam Addams for taking me around the workshop and taking the time to teach me about machining and electrical work. Thanks to Jim Grote for setting up the laser alignment experiment for me. Special thanks to Capt. John Hoeft for all his help on my model and his insight into the world of PCs, especially how to make one machine talk to another. Finally thank you to Capt. Jeff Brown for selecting me this summer and for taking the time to make this apprenticeship a great learning environment as well as a lot of fun.

## GENERAL DESCRIPTION OF THE TASK

My main assignment this summer was to create a computer model of a Lambertian surface. A Lambertian surface scatters light in such a way that the intensity of the scattered light decreases as the cosine of the scattering angle (see figure 1). This two-dimensional model generates a random surface for each trial, then simulates a laser beam striking the surface at any specified angle of incidence, and finally the model records the scatter from the surface and stores it to a data file for later evaluation.

There are many reasons for the construction of this model. First, the ideal reason would be to make a model that would perfectly simulate all the possible interactions between a laser beam and the surface, however this would be a very large task and would be too ambitious for one summer. Another reason is to find out more about how light is scattered. Since the existing formulas dealing with scatter are only applicable in certain situations, this model may help to show how light behaves in more random situations. Finally, this model as shown here should be directly applicable to scattering from a Lambertian surface. Since in reality contaminants, defects, and subsurface imperfections all effect light scattering, this model could form the groundwork for an all-encompassing model.

## DETAILED DESCRIPTION OF THE COMPUTER MODEL

The first part of the model was the surface generator. This routine had to create the random surface for each experiment. The first thing done in this section of the program is the defining of the variables and constants that will be used throughout the program. These variables include the X and Y coordinates for the facets, the ray variables, as well as constants like Pi. After these definitions, a starting point is set for the surface. A loop, beginning at this starting point, then generates the length of the facet and its angle  $\theta$  with respect to X-axis. The length L is randomly generated, and is between one and two microns. The angle is randomly generated between one and eighty-nine degrees, and is then randomly assigned a positive or negative sign. The X-coordinates and Y-coordinates of the facet end points are calculated using the formulas:

$$X = L\cos\theta \quad (1)$$

$$Y = L\sin\theta \quad (2)$$

The X-coordinate and Y-coordinate values are then added to the previous X-coordinate and Y-coordinate values and stored in the subscripted variables X(I) and Y(I) for later use in calculation. After the loop has finished and the entire surface has been generated (see Figure 2), the X and Y data

points are stored on disk in an ASCII (American Standard Code for Information Interchange) data file for viewing outside of the model.

The next routine generates the first reflection of the laser beam off of the surface. This routine starts by asking the user for some input values, the first being the incident angle of the beam with respect to the normal to the surface (see Figure 3). The angle of the ray is measured with zero being normal to the X-axis, and with negative values to the left and positive values to the right. The second input is the spot size, which is one-half of the laser beam diameter. The final input is the index of refraction of the material which is to be simulated. A loop is then started for each ray of the laser beam. The slope of the incoming beam is calculated using the formula:

$$M_1 = 1/\tan\theta \quad (3)$$

Next the Y-intercept of the incoming ray is calculated using the formula:

$$B_1 = -M_1X \quad (4)$$

Now that the formula for the incoming ray has been calculated, a second loop nested in the first is initiated. This loop is used to see which facet the incoming ray hits. The loop first calculates the slope of the facet using the formula:

$$M_2 = (Y_2 - Y_1) / (X_2 - X_1) \quad (5)$$

Then the Y-intercept of the facet is calculated using the formula:

$$B_2 = -M_2X + Y \quad (6)$$

Now that the formula for the facet has been calculated, the model calculates the intersection of the incoming ray and the line of the facet, point (E,F), using the following formula:

$$E = (B_2 - B_1) / (M_1 - M_2) \quad (7)$$

$$F = M_1E + B_1 \quad (8)$$

Then the model performs a test to see if the intersection of the ray and the line of the facet is on the actual facet (see Figure 4); if it is, the model continues the calculations, if it isn't the model goes to the next index of the loop and tests the next facet. Assuming now that the intersection of the incoming ray and the line of the facet was on the facet, the model continues by calculating the normal to the facet using the formula:

$$NF = -\arctan(M_1) \quad (9)$$

Next the incident angle of the incoming ray to the reference normal is calculated using the formula:

$$NI = -\arctan(-1/M_1) \quad (10)$$

Then the angle from the incident ray to the facet normal is calculated using the formula:

$$FI = NF - NI \quad (11)$$

Finally the model calculates the angle of the reflected ray using the formula (see Figure 5):

$$R = NF + FI \quad (12)$$

After the angle of the reflected ray is known, the relative power of the ray after the reflection is calculated using the following formulas:

$$\cos\theta_e = \{1 - [\sin(FI)/N_e]^2\}^{1/2} = TT \quad (13)$$

$$RE = ([N_e \cos(FI) - TT]/[TT + N_e \cos(FI)])^2 \quad (14)$$

$$PO = (RE) \exp[2A^2/W^2] \quad (15)$$

Next, the slope and Y-intercept of the outgoing reflected ray are calculated using the same process as previously described

(see equations 3 & 4). Lastly, the starting and ending points of the next loop are determined. The intersection point is the starting point and the ending point is the first facet if the ray is reflected left or the last facet if the ray is reflected right.

A third loop, also nested within the first loop, tests for the possibility of multiple reflections; that is, a reflected ray hitting another facet on the surface. The loop uses the same process as in the previous loop to test for possible intersection (see equations 5 through 8). If an intersection is found, then the same process as previously described is used to calculate the reflected ray and its relative power (see equations 9 through 15) and the loop is re-executed to test for more reflections.

When no more reflections are found, the final relative power of the ray is stored in a subscripted variable and saved on disk in an ASCII file for later evaluation. When the ray calculations are completed, the model goes on to calculate the power for all of remaining rays in the beam.

At this point, the data is sorted into bins, the bins being determined by the final reflected angle of the ray. The variable Z is then divided by the cosine of the angle which it represents. This division is done to normalize the data to a straight line. This normalized data is then stored on disk in an ASCII file for later evaluation.

This model was created on a Zenith Z-248 personal computer using Zenith GW-Basic "TM" version 3.10. Data produced by this

model was processed and analyzed using PC-MATLAB, a scientific math software package by The MathWorks Inc. See Appendix for a listing of the code.

Data was imported into the PC-MATLAB environment from ASCII data files. Inside of the PC-MATLAB program many functions could be preformed such as a histogram of the data or a curve fit to the data. The PC-MATLAB program was used for the majority of data manipulation and analysis.



## RESULTS

In conclusion, consider the results of the model. Instead of looking at the model as a whole, consider each part of the model as it was coded and tested.

The first part of the model is the surface generator. In diagram one, a sample surface generated by the model is shown. The random surface generated by the model is suitable for this exercise and gives a good representation of the real surface. If time would have permitted however, other features such as facet angles over ninety degrees and overlapping facets should be added to give a more realistic view of an actual Lambertian surface.

The next part of the model that was coded was the ray reflection routine. If the generated surface is truly a Lambertian surface, the rays should be scattered in a cosine curve; that is, the number of rays at any angle should be proportional to the cosine of that angle with the most rays reflecting off at zero degrees and the least reflecting off at ninety degrees. In diagram two, a histogram of the reflected rays of one test is shown. This graph shows how more rays were reflected off at the lesser angles (those closer to zero), and fewer at the steeper angles. This shows that the model was giving an accurate representation of the Lambertian surface. To further illustrate the cosine curve of the data, a curve fit was done to the data. In diagram three, the points represent the number of rays per angle and the curve is the

best fit to those points. This plot is a good representation of a cosine curve. The reflection part of the model is as complete as possible. But if more time was allowed, this model should allow for the possible transmittance of a ray as well as reflection.

Calculations for the reflectance and the power output was the next part of the model to be written. Diagram four shows the power output per ray of the beam. The diagram plainly shows a Gaussian curve for the power output of the beam, which is typical of a real laser beam. The highest parts of the curve show where only one reflection has taken place, while the lower spots and gaps in the curve represent multiple reflection where more power is absorbed by the surface. By contrast, the total power per angle should be in the shape of a cosine curve, and in diagram five the power per angle is shown. To expand this part of the model, the complex part of the index of refraction should be considered when calculating the reflectance and the power output.

The final part of this model is the normalization of the power. The power output is normalized by dividing by the cosine of the angle. If the data was in a perfect cosine curve, this normalization should produce a straight line at the maximum value of the power of the input beam (in this case one). Diagrams six, seven, and eight all show different normalized sets of data. The points on the graphs represent the normalized power per angle. The line is a curve fit to those data points. This curve shows, through its linear nature

and magnitude at one, that the model was indeed producing a cosine data set.

There are still several situations that the model can not handle besides those already mentioned. One problem that could not be solved was interference. Since the rays ending up at one particular angle all didn't travel the same distance, in a real world situation interference patterns would be present. Several problems arose from this, first the distance must be kept track of. Starting and ending points must be set for every ray in the beam. This put too much strain on the computer and slowed down calculations so much that the idea had to be dropped due to time constraints.

The problem of memory size also limited the model to two dimensions. The number of arrays and subscripted variables that the computer had to keep track of in order to do the necessary calculations slowed it down greatly. In order to expand this model to three dimensions, either a change in computer or a switch to a higher level language would be needed.

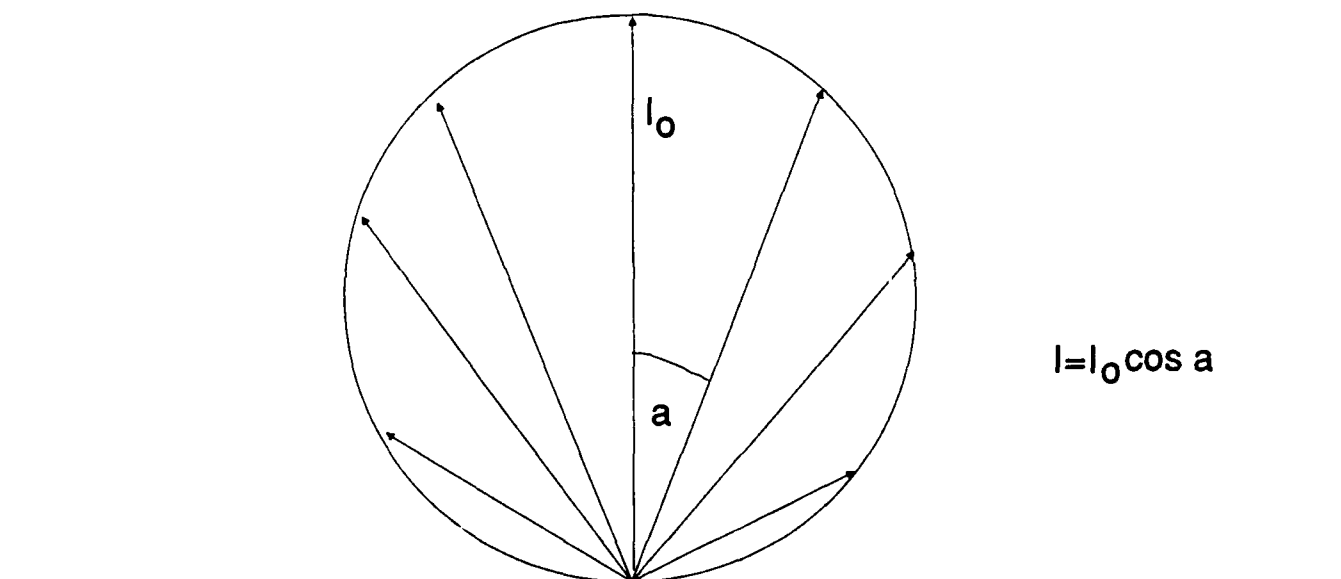
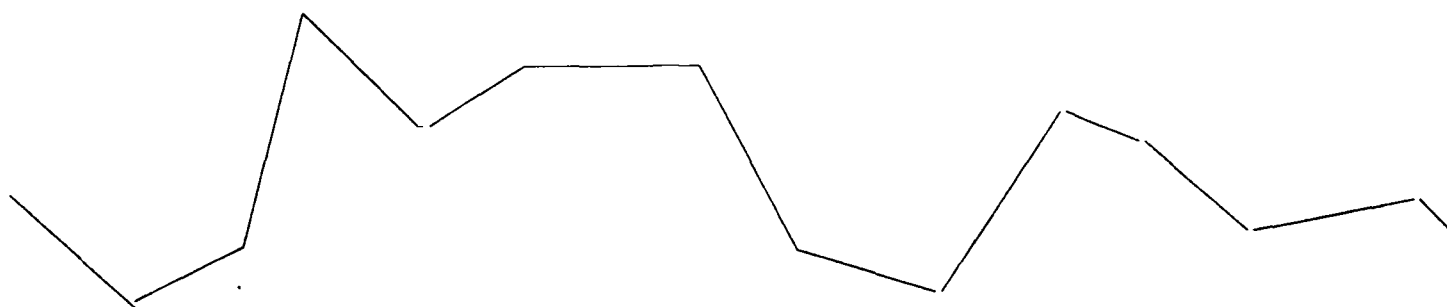


Fig. 1



**Fig. 2**

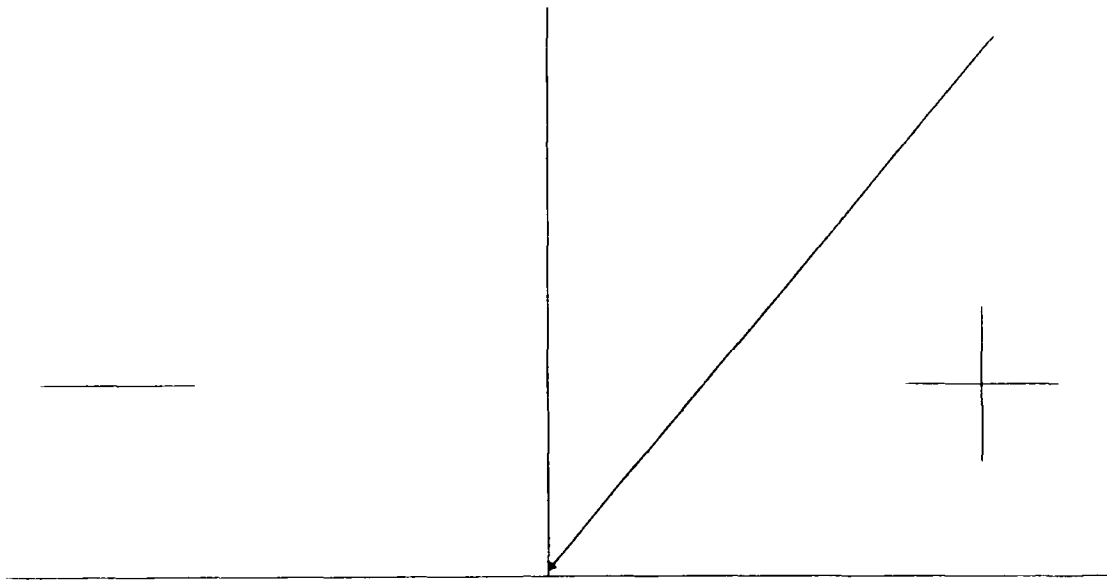


Fig. 3

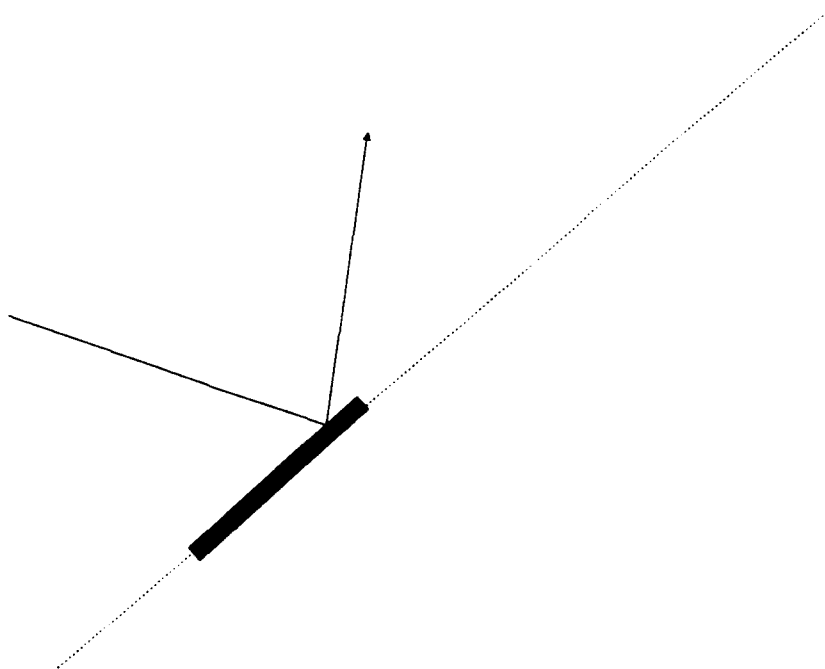


Fig. 4

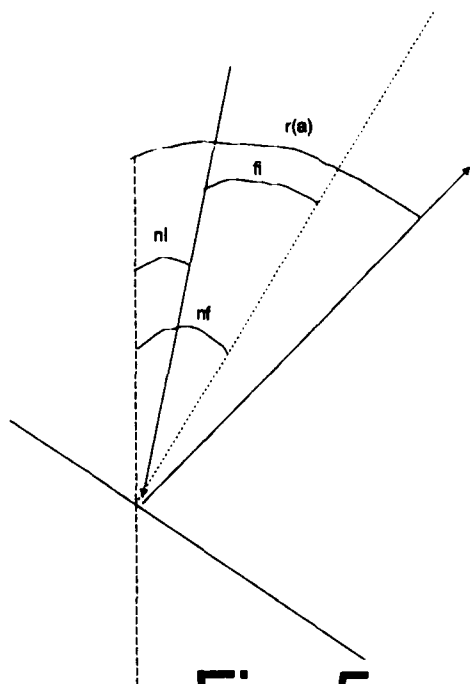
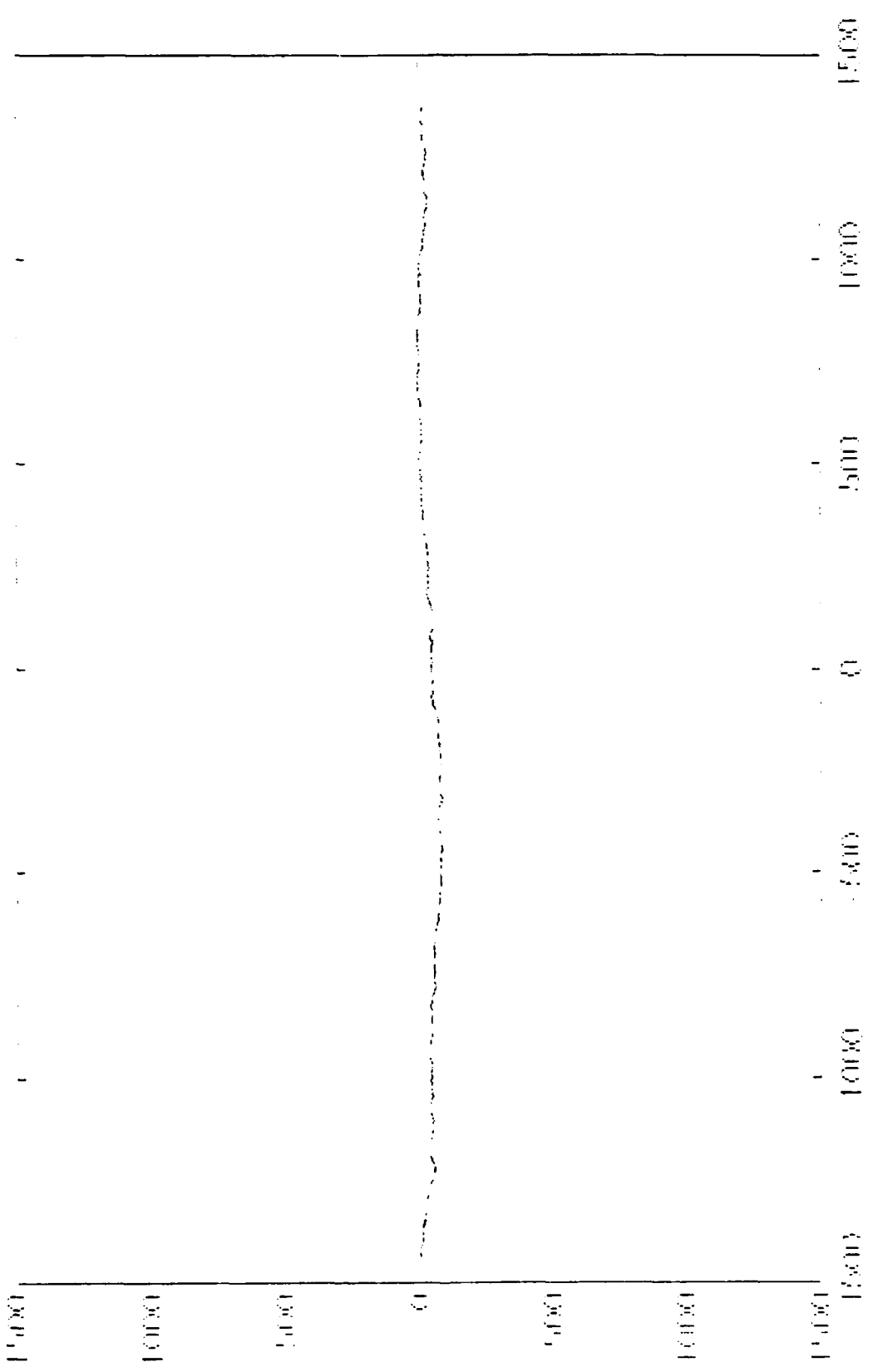


Fig. 5



# DIAGRAM 1 SAMPLE SURFACE



X COORDINATE (in inches)

DIAGRAM 2 HISTOGRAM OF THE REFLECTED RAYS

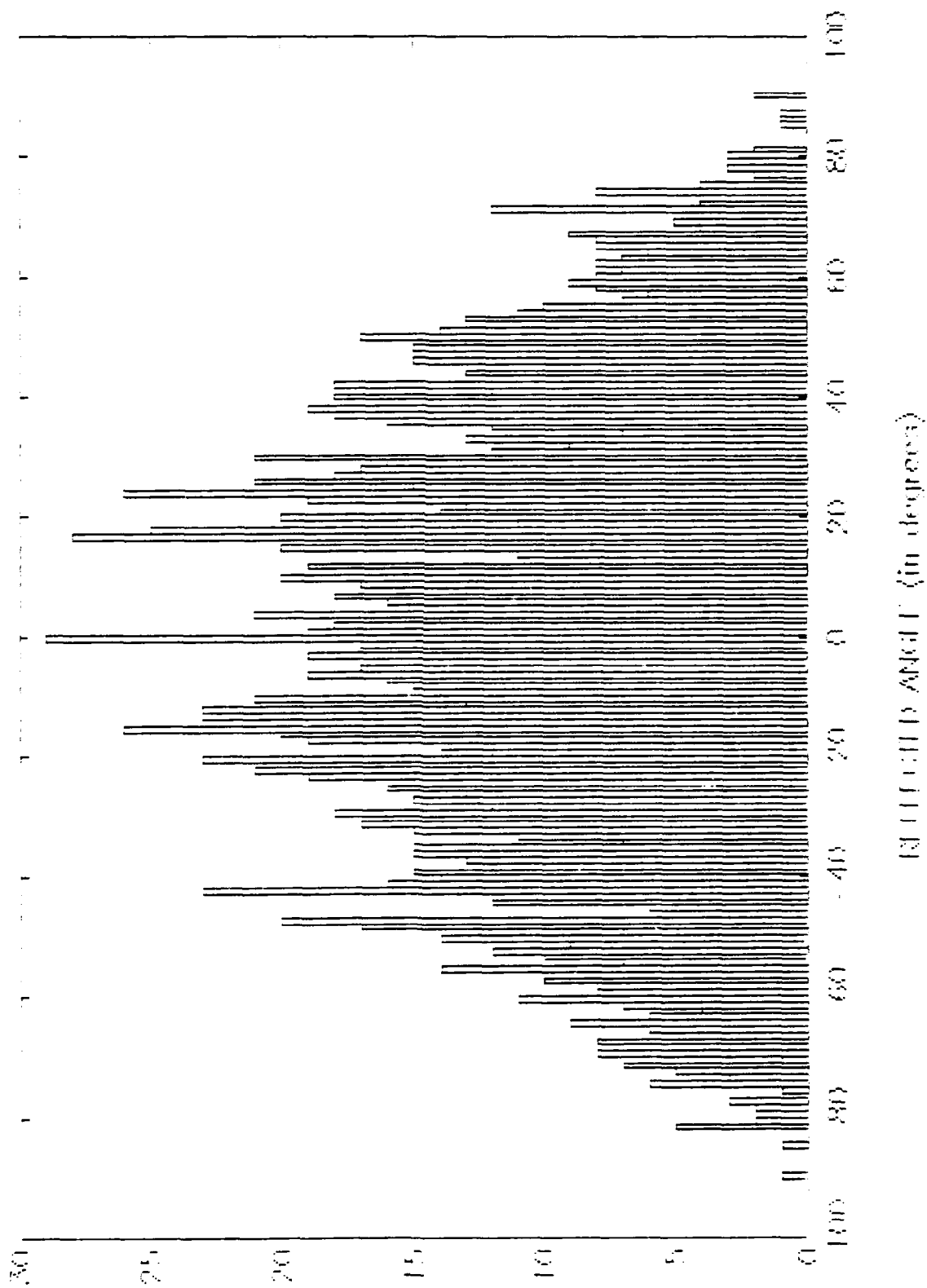


DIAGRAM 3. CURVE III TO DATA

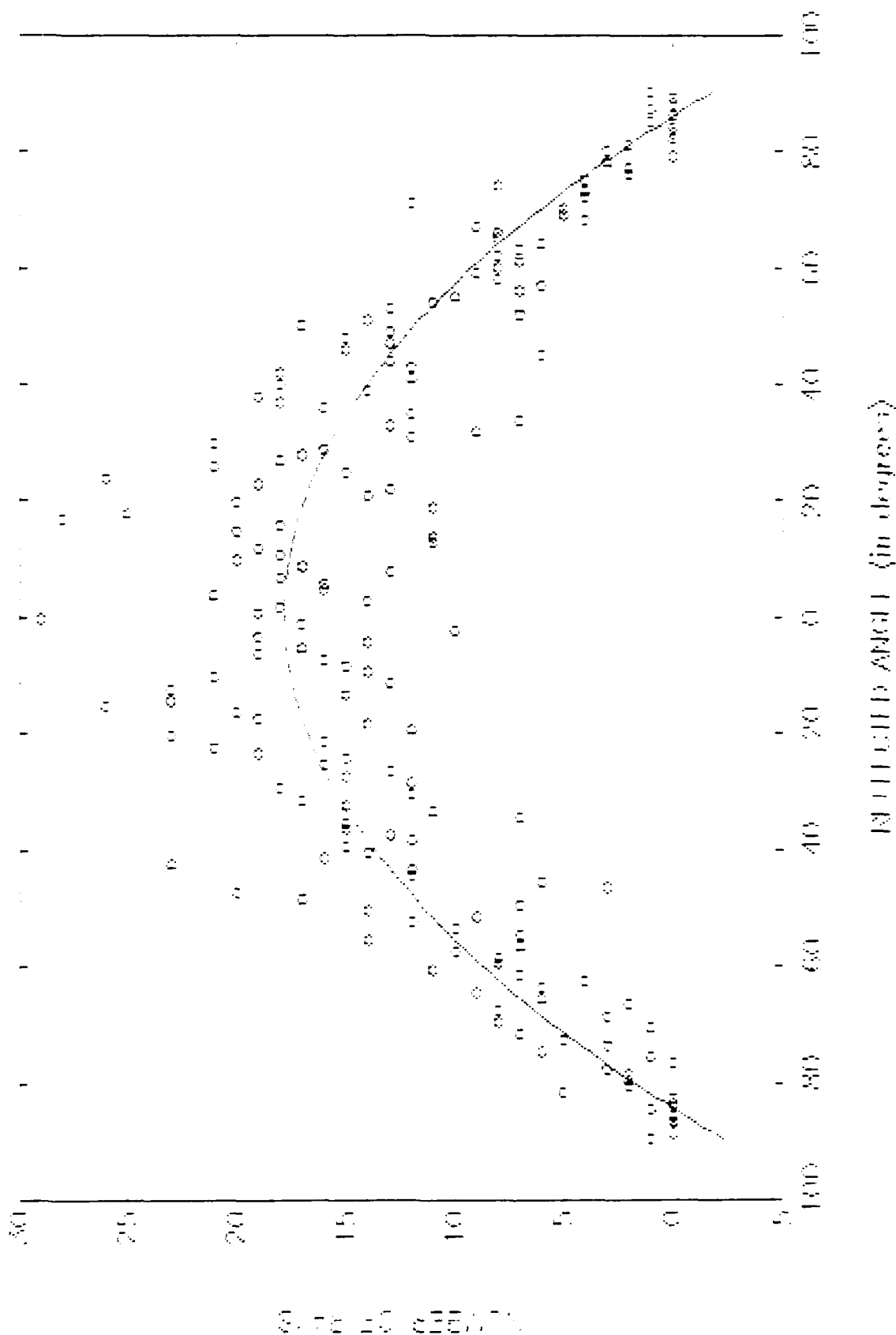
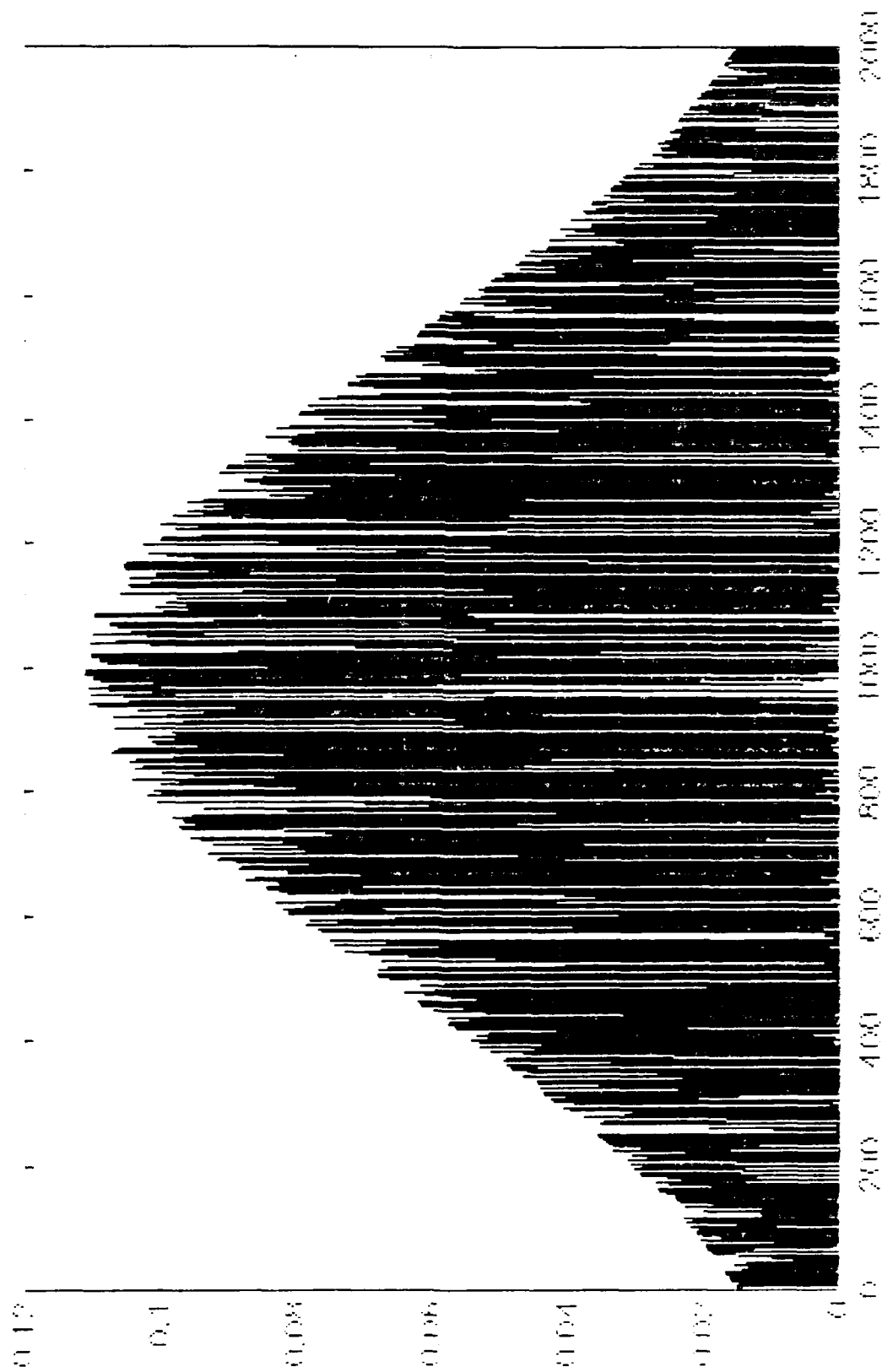


DIAGRAM 4 POWER PER RAY



RAY NUMBER

DIAGRAM 5--POWER PER ANGLE

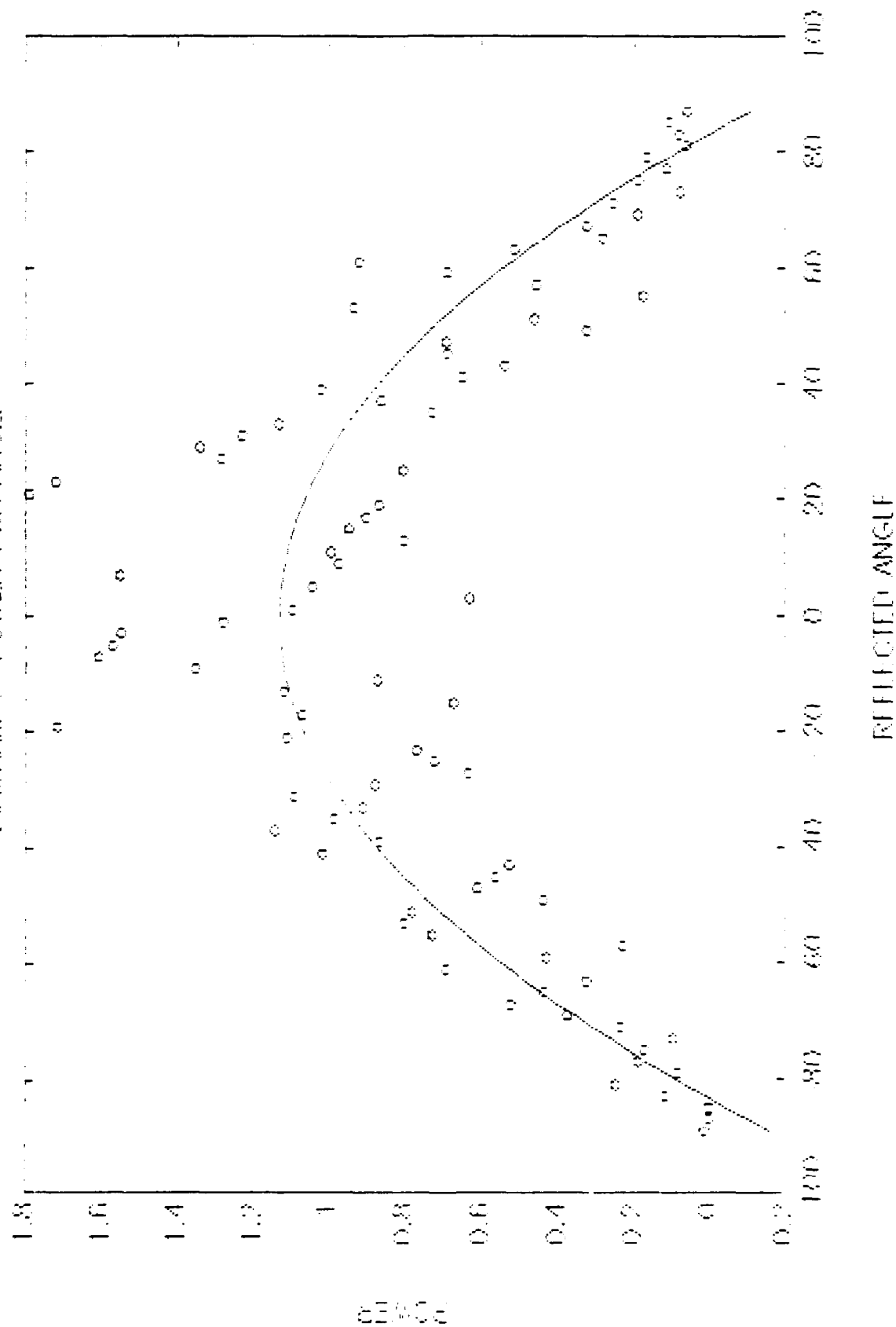
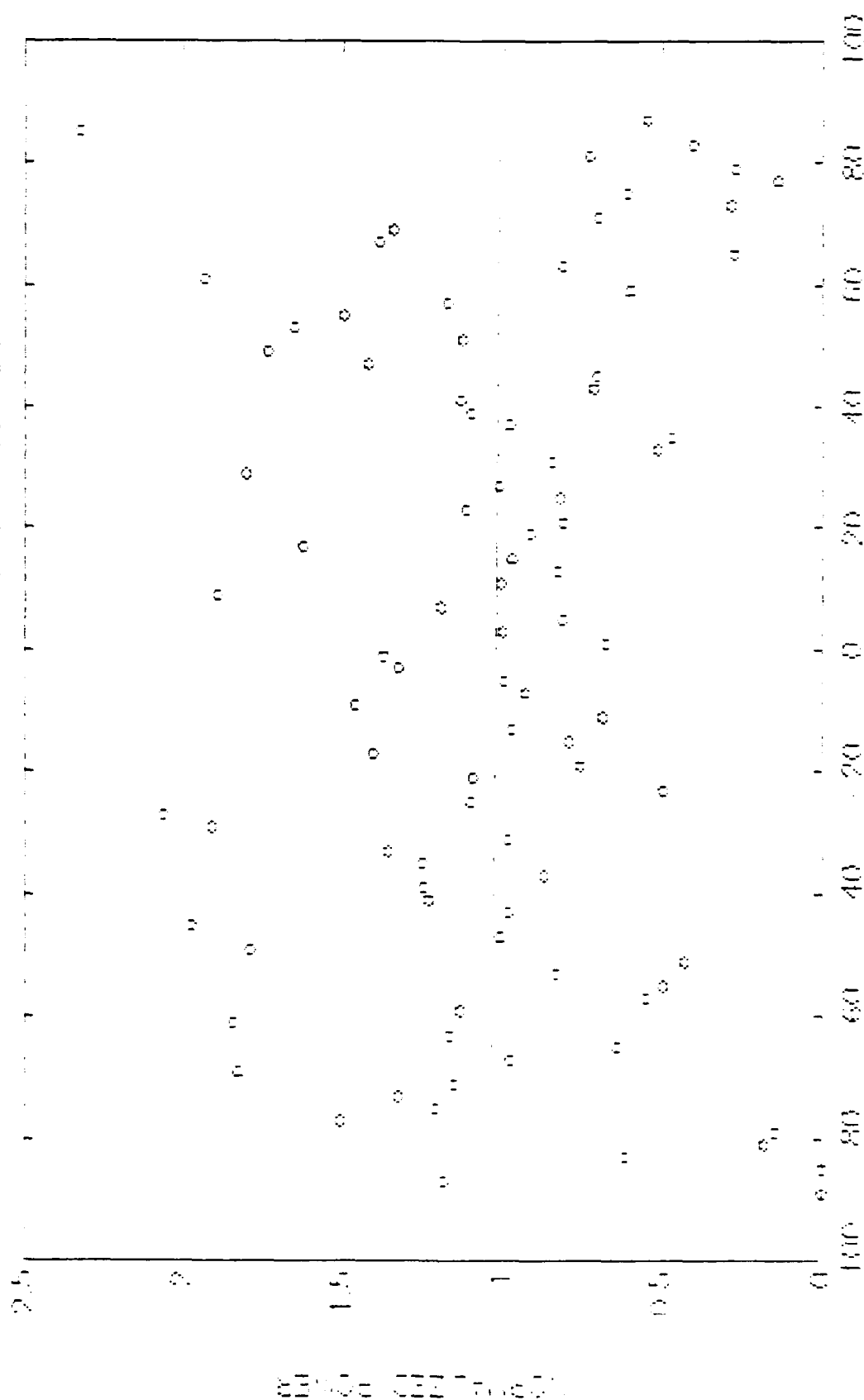
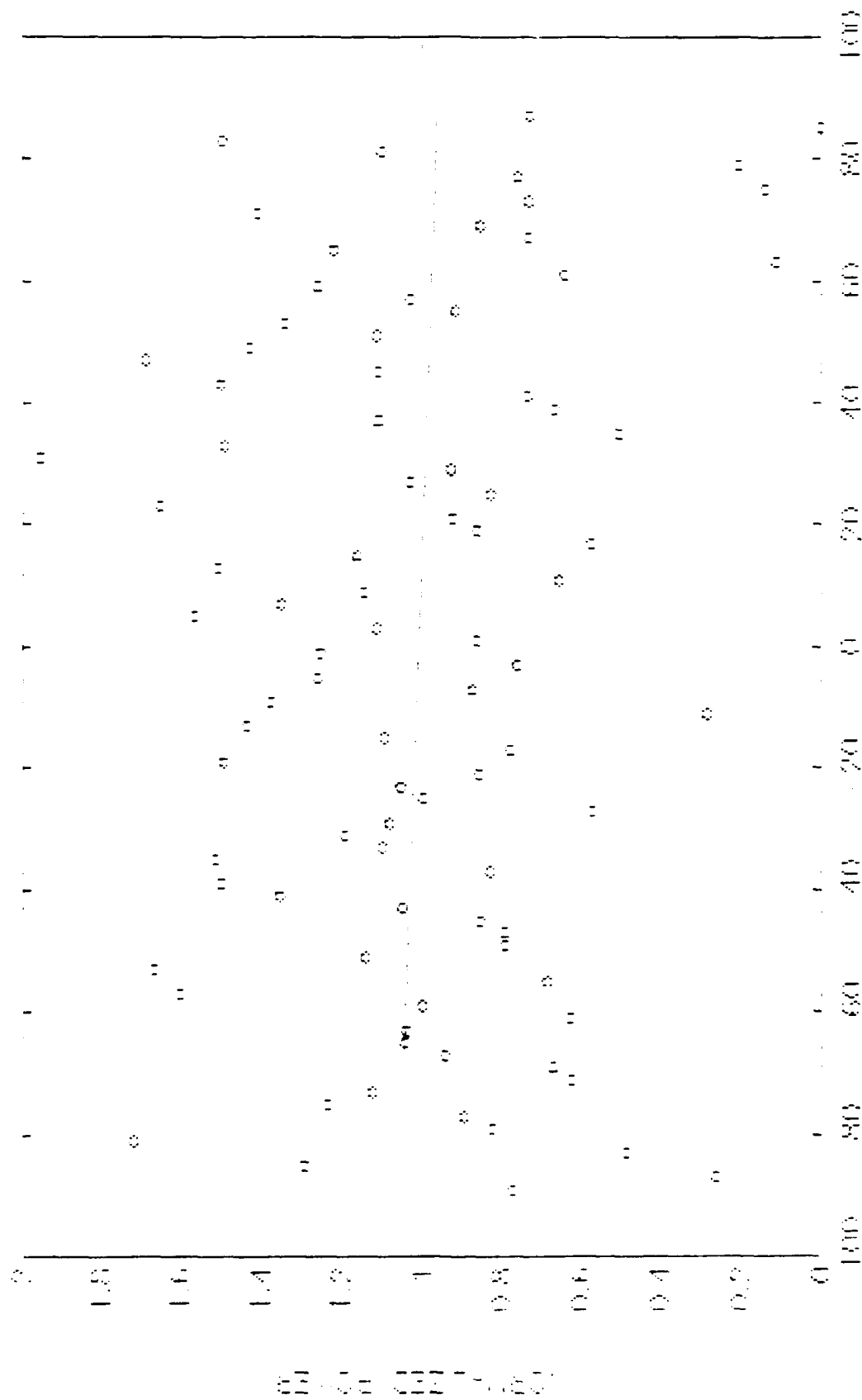


DIAGRAM 6--NORMALIZED DATA WITH CURVE FIT



REFLECTED ANGLES (in degrees)

DIAGRAM 7 NORMALIZED DATA WITH CURVE FIT



REFLECTED ANGLE (in degrees)

DIAGRAM 8. NORMALIZED DATA WITH CURVE FIT

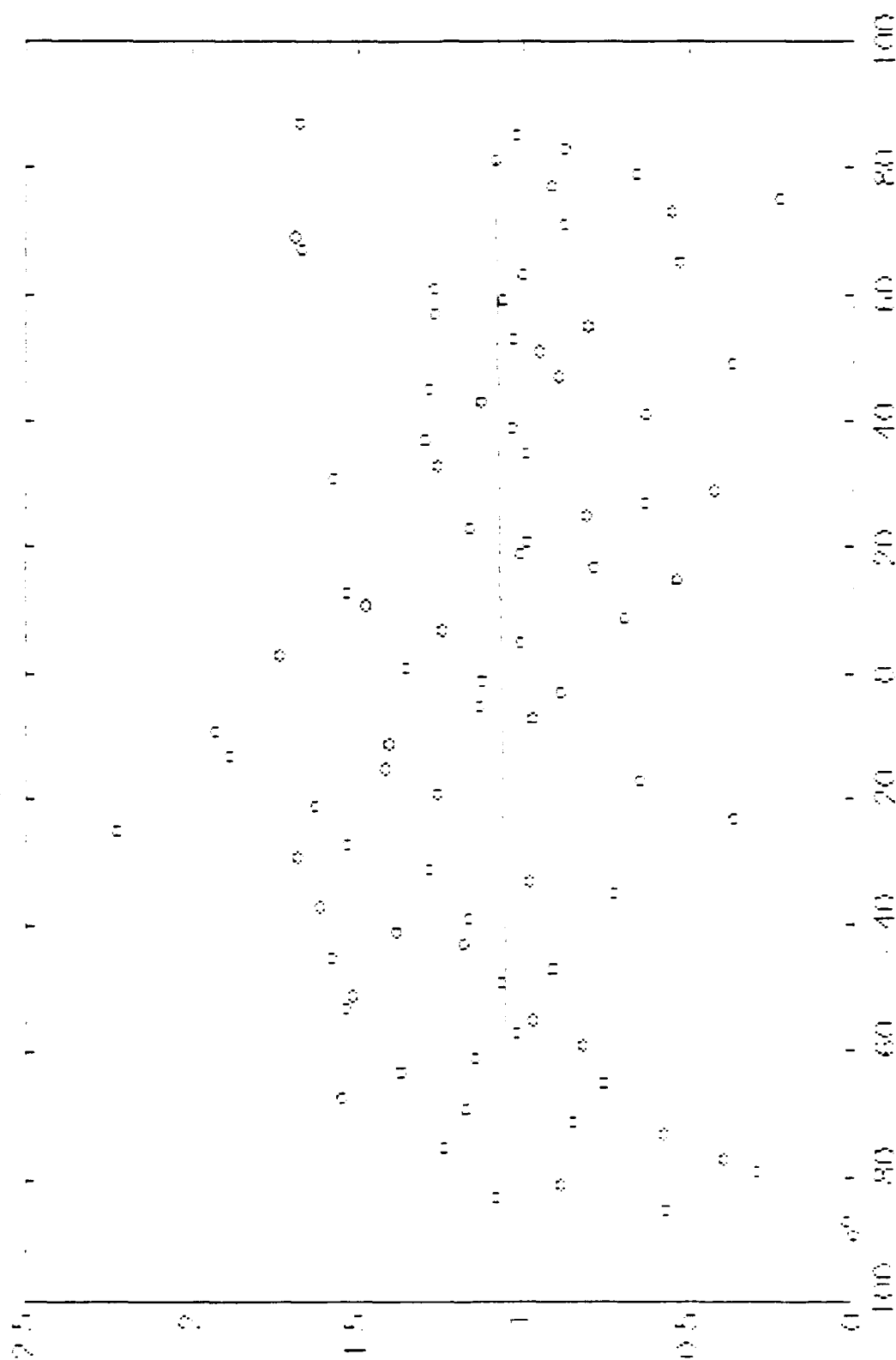


DIAGRAM 8. NORMALIZED DATA WITH CURVE FIT



## REFERENCES

Azzam, R. M. A. and N. M. Bashara. Ellipsometry and Polarized Light. Amsterdam: North Holland Physics Publishing, 1978.

Hecht, Eugene and Alfred Zajac. Optics. Reading, Massachusetts: Addison-Wesley Publishing Company, 1974.

Thomas, George B., Jr. and Ross L. Finney. Calculus and Analytical Geometry. Reading, Massachusetts: Addison-Wesley Publishing Company, 1979.

Apprendices can be obtained from  
Universal Energy Systems, Inc.

F-15 RADAR SIMULATION

SOOK HEE CHOUNG

AVIONICS LAB

GREG POWER

### ACKNOWLEDGEMENTS

I would like to extend my appreciation to Universal Energy Systems and Wright-Patterson Air Force Base for giving me this opportunity. The High School Apprenticeship program has given me insight on engineering and much needed experience. Greg Power and all the people in the Radar Branch of the Avionics Lab especially deserve my immense gratitude for all of their help and hospitality.

## INTRODUCTION

The F-15 radar display simulation was developed to reproduce the radar capabilities of the F-15. The air to ground radar control panel displays a radar image taken from Lowville, New York. The image proceeds to move as if the plane were in motion. This is one example of how the project was developed as realistically as possible.

## THEORY

### GRID

The co-ordinates the program needed to draw the grid for both of the radar screens were derived by setting an arbitrary variable as the center thus allowing one to easily change the center position. The essential co-ordinates needed to plot points were then calculated by adding or subtracting the proper amount to the center value. The value of each co-ordinate was dependent on the center value. The grid was then completed by utilizing the UIS\$ graphics commands.

### AIR TO GROUND GRID

Diagram D-1 is the portion of the radar control panel where the radar image is located. The raw image data is a 512 x 512 square character array. The radar image to be viewed must be the same configuration as the figure so the image can be laid on it easily. Since the figure is not a regular figure, the figure must be filled in three parts, triangle ABC, rectangle BDEC, and arc DE.

The starting point and ending point of each line is needed so that the essential radar piece of each line can be identified. To do so the distance from the center (203) to end of the line must be calculated.

Angle ACF is a 30 degree angle therefore angle XAC is 60 degrees making triangle XAC is a special 30-60-90 degree triangle. This makes calculating the distances

easier. If the line AX was 10 pixels long then line XC would be  $10 \cdot \text{SQRT}(3)$  pixels long. Since the line Ax is variable, an equation must be established such as to calculate the line xC dependent on line AC.

$$1. XC = \text{SQRT}(3.0) \cdot AX$$

$$2. \text{Start} = 203 - XC$$

$$3. \text{End} = 203 + XC$$

Rectangle BCDE has the same length therefore the start and end point only need to be calculated once. The length would be set as the last line xC value.

As arc DE converges to point Z angle GAH becomes larger and is not a definite value. To calculate that angle, use the radius and height which is the line number as shown in the equation to the right. When the angle is determined the line zE can be calculated.

$$AG = 240$$

$$4. GAH = \text{Arcsin}(GH/GA)$$

$$Ah = zE$$

$$5. Ah = 240 \cdot \cos(GAH)$$

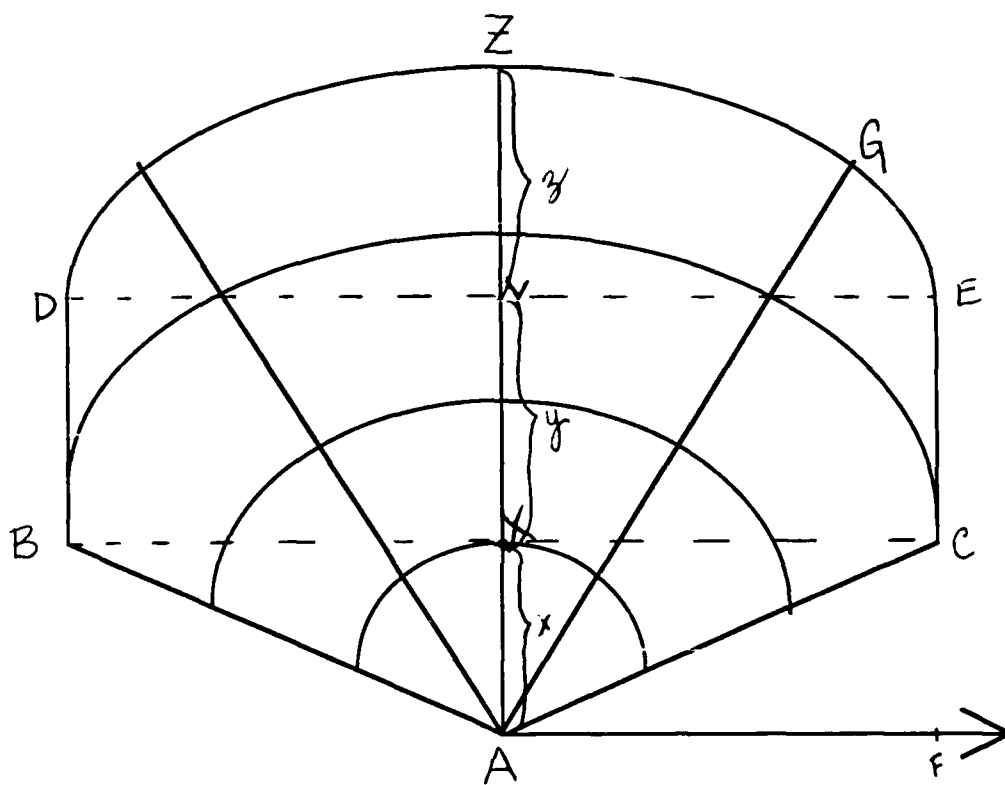


Diagram D-1



## PROGRAM DESIGN

The Radar Display program contains three levels in  
ADDSARDEMO.FOR.

LEVEL I: DISPLAY\_SCREEN

LEVEL II: AIR\_TO\_AIR\_MODE, SHOWMONO

LEVEL III: PUT\_PANEL, DRAW\_EDGE, PUT\_GRID, PUT\_SCREEN  
AIR\_TO\_GROUND\_GRID, AIR\_TO\_GROUND\_EDGE,  
LOAD\_CHAR

The main program, DISPLAY\_SCREEN, calculates the co-ordinates needed to draw each grid. The program then branches into two subroutines, AIR\_TO\_AIR\_MODE and SHOWMONO. AIR\_TO\_AIR\_MODE calls PUT\_PANEL, DRAW\_EDGE, PUT\_GRID, PUT\_SCREEN while SHOWMONO calls PUT\_PANEL, AIR\_TO\_GROUND\_GRID, AIR\_TO\_GROUND\_EDGE, and LOAD\_CHAR. Both subroutines utilize the PUT\_PANEL subroutine since they both use the generic panel. All the EDGE, GRID and SCREEN subroutines complete the diagrams by drawing the insides of the panel. SHOWMONO takes the specified 512 X 512 character array and moves the image down one pixel at a time to create the effect of an actual radar image movement when flying. SHOWMONO then proceeds to call LOAD\_CHAR to load each character into a separate array to fit in the form of the air\_to\_ground grid image.

## CONCLUSION

Concerning the air to ground portion of this project, the radar movement was implemented, but problems developed. One problem was that the grid was drawn after the image in the shape of the figure was painted. This was done each time after the movement. The problem was that the grid did not paint fast enough so therefore a blinking effect occurred. The solution developed was to put the grid onto the array before the image was put onto the screen. Due to the lack of time only part of that solution was implemented, but it was successful thus indicating its feasibility.

This project seemed impossible at times but with the help and patience of my mentor, Mr. Greg Power, I was able to see other solutions. I was able to work with graphics programming which I would not have even experienced had I not been in this program and had I not had my mentor.

**High School Apprenticeship Program**  
**Final Report**  
detailing work performed at  
**Air Force Wright Research and Development Center**  
**WRDC/AARI-3**  
**June - August 1989**

by Sheri Cody

### Acknowledgements:

Many people this summer were very helpful to me and deserve special thanks for all their efforts. First of all, I would like to thank 1st Lt. Brian Figie, my mentor this summer, for all his help and instruction and for the great opportunity of working on base these past two months. I would also like to thank Jeff Sweet for giving me the chance to work on the EOSMS Vax. In addition, I would like to thank the following people who were always willing to assist me with any problems (especially computer related) that I encountered: John Carr, Tony Absi, Capt. Pat Marshall, Bob Muse, Dan Smith, and Pat Woodworth. Finally, I would like to thank Rich Hill for the exciting tank ride.

## 1. Introduction

I am Sheri Cody, a 1989 graduate from Centerville High School, and this summer I worked with WRDC in the Avionics Laboratory in Building 622 for 1st Lt. Brian Figie as a part of the Apprenticeship Program. My summer has been a rewarding and enriching experience thanks to the opportunities this program has provided me. I have learned a great deal from this summer's work and am very thankful for this opportunity.

I worked with the group AARI-3, which analyzes electro-optic sensors. The first couple of days of work were filled with all kinds of new information, from FLIRs (forward-looking infrared sensors) to the MS DOS computer language. Throughout the summer, I learned a lot about the various types of work and projects taking place in my building.

## 2. Infrared Tactical Design Aid

I spent the majority of my summer working on a project for Lt. Figie that involved computer predictions of infrared sensors. The sensors the computer programs are designed to model are part of the Air Force's Tactical Design Aid. The TDA involves mounting an infrared sensor on a plane that will approach a target. The pilot can then monitor the picture sent out by the sensor in order to help him recognize the target before he actually gets in visible range of the target. Essentially, the computer models use data from weather, target, and background observations to determine a sensor's performance in a particular situation. For instance, with the given information the computer model would determine how close a pilot would have to approach the target before he could actually detect the target on his screen. The model would also predict how close the pilot must approach to obtain both lock-on and launch ranges on the target. Because the computer's calculations become long and time-consuming, the Air Force has three grades of the model. The most complicated version is the Research Grade TDA (RGTD), which is so large it is run on the Electro Optics Sensor Modeling System (EOSMS) Vax. This version is then simplified and reduced into the Intermediate Grade TDA

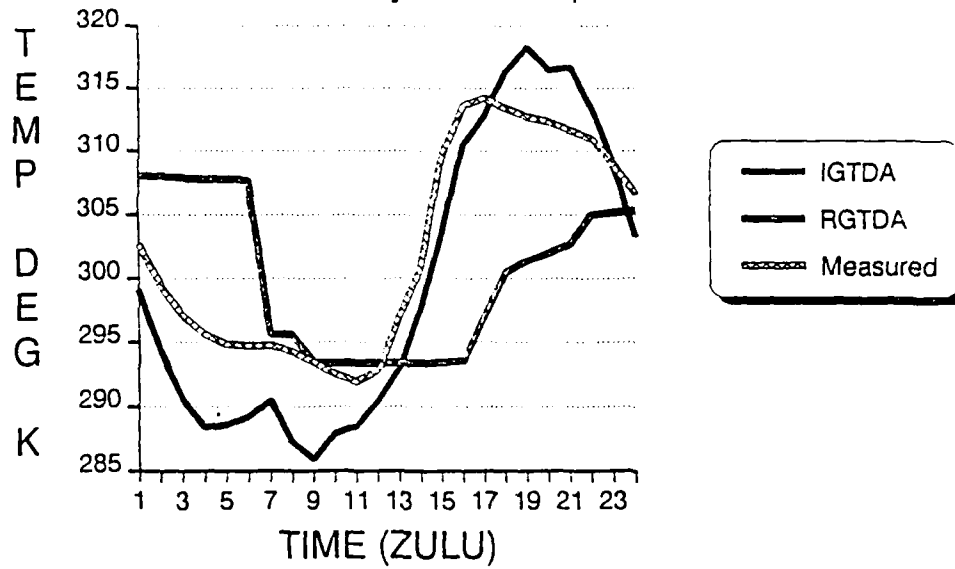
(IGTDA), which is run on a personal computer. Finally, the model is simplified even further for more practical application to the Operational TDA, which is the version actually utilized by the operational Air Force.

This summer my job was to input all the necessary data from an actual test flight into the personal computer version, the IGTDA. I then collected all the computer's predictions for ranges, target temperatures, and background temperatures. Meanwhile, a co-op student, Geoff Deep, ran the same tests on the RGTDA. When we were finished, we compiled the predictions from both models into graphs. Through the graphs, we compared the predictions of the IGTDA to those of the RGTDA, and then compared both sets of graphs to the actual measured temperatures. By this method, we were able to determine the accuracy of the computer model's predictions.

Our results were different than what we had expected. The RGTDA should have tracked closer to the measured values than the IGTDA; however, the IGTDA tended to track better. One possible explanation was that the RGTDA might not have received all the updates as the IGTDA has. The following graphs are just a sample of the various graphs we generated using our results.

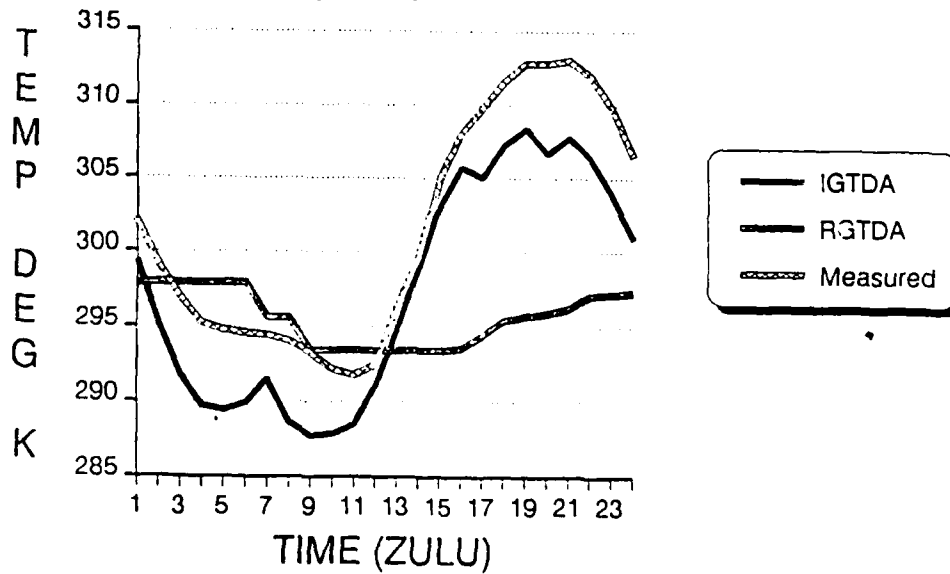
## FACET 1 (TOP OF TANK)

June 15 -- Physical Temp.



## FACET 2 (RADIMETRIC TEMP)

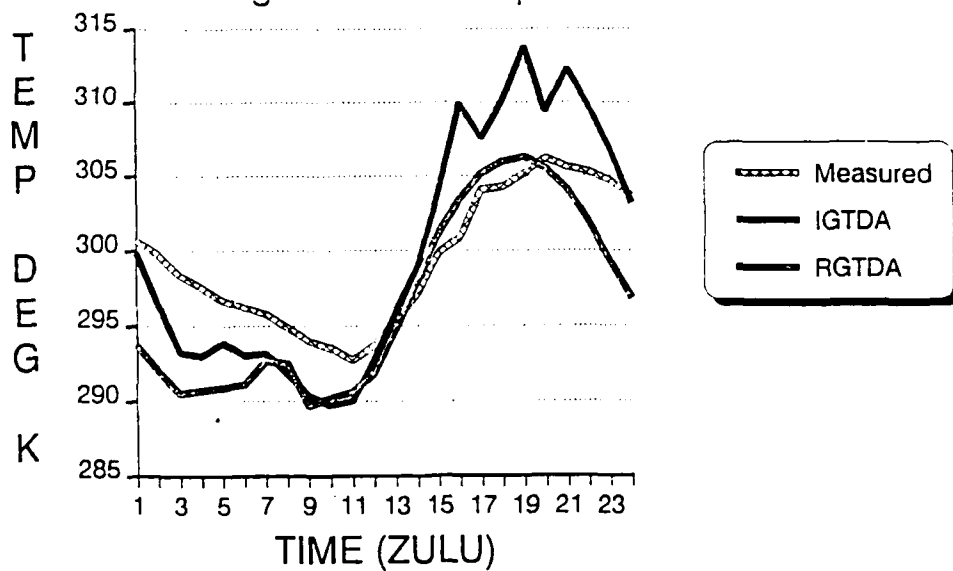
June 15





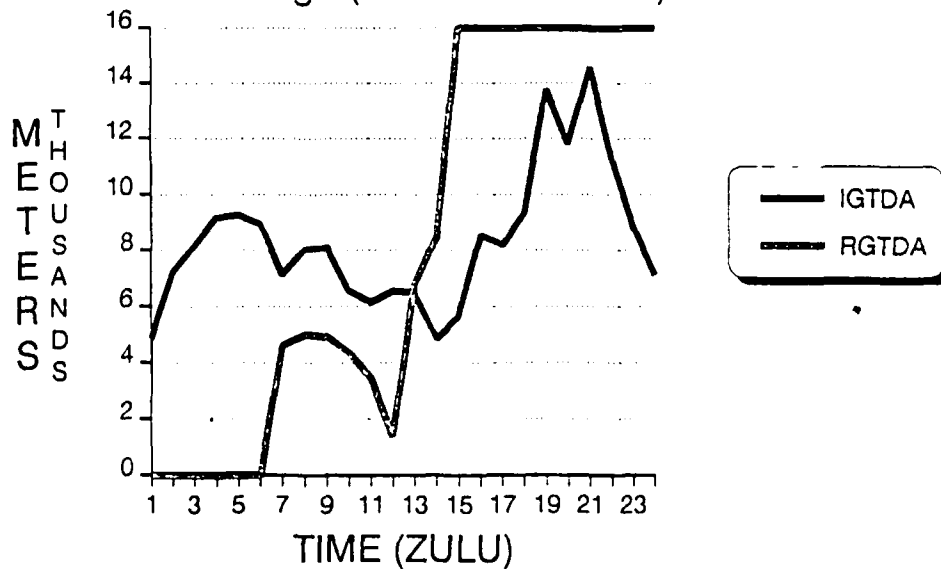
## JUNE 15 (WHITE TANK)

### Background 34 Temp



## JUNE 15 (WHITE TANK)

### Detection Range (IGTDA vs RGTDA)



### 3. Unify Database

During the latter part of the summer I worked on the Unify database, which is run on the EOSMS. Prior to this work, I took a class from Digital Equipment Corporation that taught me how to use the database. The class lasted a week, and covered the basic applications of Unify. I learned how to create a new database, write inquiries, generate reports, and a variety of other operations. After finishing the class, I performed work for Jeff Sweet, the EOSMS Manager, on Unify. I created a new database and wrote various inquiries and reports. This programming was very useful to me because it helped me to become more familiar with programming. It also helped me to become familiar with the Unix system (used by the EOSMS), which I will be using this year at Purdue.

### 4. In Conclusion

This summer has been a great experience for me. I have observed engineers at work and obtained more of an idea about my future profession. This opportunity has helped me to better understand where all my hard work is leading, and to show me what I have to look forward to in the future. Also, I learned about infrared sensors and have been able to see some interesting equipment at work.

For instance, I had the chance to look at a foggy morning scene with the aid of a infrared sensor. Another day I looked through the dark using a pair of night vision goggles. Not only did I learn a lot from my work this summer, I enjoyed the work that I did. The Apprenticeship Program has been a positive experience for me that will be helpful to me long after the summer has ended.

Christine Kay Garcia

Darrell Barker

Computer Circuitry

14 August 1989

I would like to thank Universal Energy Systems for giving me the opportunity to work at Wright Patterson Air Force Base.

I would also like to thank everyone with whom I worked for all of their assistance and for making my summer experience an enjoyable and valuable one.

I would especially like to thank my mentor, Darrell Barker, for his kindness and patience in teaching me more about the job of computer and electrical engineers.

The Computer Aided Design Branch of the Microelectronics Division is involved with the creation of various computer circuits. These circuits are then produced on wafers by other branches of this division. Since the Microelectronics Division is a part of the Wright Research and Development Center, its main purpose is to gather information from the wafers it produces.

The integrated circuits are not packaged because this is only the research stage. The wafers allow the engineers to become more knowledgeable. From this stage, the engineers publish papers on their new discoveries. When companies read them, they may continue to do more research on the specified chips or may manufacture the computer circuits to be installed in Air Force weapon systems.

This summer the apprentice worked with the Mentor Graphics Computer System. She learned the functions of the most common integrated circuits using Transistor-Transistor (TTL) Logic. These chips consist of flip-flops, registers, magnitude comparators, arithmetic logic units, gates, and adders. By connecting many circuits together, one is able to design a computer that performs a specified function.

Mentor Graphics, a Computer Aided Design computer, is used for the drawing of integrated circuits. This system provides the user with a method to simulate any particular circuit. By simulating the created design, the user is able

to insure that his design performs the desired function. This is done by forcing input values and making comparisons with the given truth table.

The following subsections include specific gates and chips that were used in the understanding of TTL Logic:

**AND GATE-** This gate uses Boolean expressions and binary numbers to determine whether the given statements are "true" or "false." In order for the circuit to emit a high voltage, both input voltages must be high. For two input variables, Figure 1.0 is the truth table.

AND TRUTH TABLE

| X | Y |  | Z |
|---|---|--|---|
| 0 | 0 |  | 0 |
| 0 | 1 |  | 0 |
| 1 | 0 |  | 0 |
| 1 | 1 |  | 1 |

Figure 1.0

**NAND GATE-** This gate uses Boolean expressions and binary numbers to determine whether the given statements are "true" or "false." The nand gate reverses the function of the and gate, producing a reverse truth table as seen in Figure 1.1.

# NAND TRUTH TABLE

| X | Y | Z |
|---|---|---|
| 0 | 0 | 1 |
| 0 | 1 | 1 |
| 1 | 0 | 1 |
| 1 | 1 | 0 |

Figure 1.1

**OR GATE-** This gate uses Boolean expressions to determine whether the given statements are "true" or "false." In order for the output to be high, only one of the inputs must be of a high voltage. Figure 1.2 demonstrates the truth table for the two input or gate.

# OR TRUTH TABLE

| X | Y | Z |
|---|---|---|
| 0 | 0 | 0 |
| 0 | 1 | 1 |
| 1 | 0 | 1 |
| 1 | 1 | 1 |

Figure 1.2

**NOR GATE-** This gate uses Boolean expressions and binary numbers to determine whether the given statements are "true" or "false." The nor gate reverses the function of the or gate, producing a reverse truth table. Figure 1.3 represents the nor truth table for two input values.



NOR TRUTH TABLE

| X | Y | Z |
|---|---|---|
| 0 | 0 | 1 |
| 0 | 1 | 0 |
| 1 | 0 | 0 |
| 1 | 1 | 0 |

Figure 1.3

**INVERTER-** This gate reverses the signal of the output of the previous component. One inverter immediately following another changes the signal to its original state.

**7474-** The dual d-type positive-edge-triggered flip-flop with preset and clear is used as a storage unit and may preset and clear the original signals (see Figure 1.4).

**7483-** This 4-bit full adder with fast carry has the capacity to add two 4-bit numbers (see Figure 1.5).

**7485-** This 4-bit magnitude comparator is used to determine whether one 4-bit binary number is less than, equal to, or greater than the other given 4-bit binary number. For numbers greater than 4-bits, comparisons may be made by connecting the least significant outputs to the cascading inputs ( $A > B$ ,  $A = B$ ,  $A < B$ ) of the more significant magnitude comparator (see Figure 1.6).

**74153-** This dual 4-line to 1-line data selector/multiplexer is used to select the desired set of binary numbers (see Figure 1.7).

**74181-** The arithmetic logic unit (ALU) /function generator performs 16 binary arithmetic functions on 4-bit binary numbers. For numbers larger than 4-bits, the ALU may be used by connecting a net from the carry out (CN\_PL\_4) pin of the least significant unit to the carry in (CN) of the more significant one (see Figure 1.8).

**74191-** The synchronous up/down counter with down/up mode control counts up or down and is dependent upon the initialized value and the phase of the clock (see Figure 1.9).

**74194-** The 4-bit bidirectional universal shift register stores data for a specified amount of time and has the ability to move the data from left to right (see Figure 1.10).

The apprentice also assisted the Research Division of the Electronic Technology Laboratory this summer. She translated the Proximity Correction Program for the Electron Beam Lithography System from BASIC to FORTRAN. This program will be used to help regulate the dose of electrons applied onto the individual geometric features of a chip in order to prevent the overcharge of electrons onto nearby features.

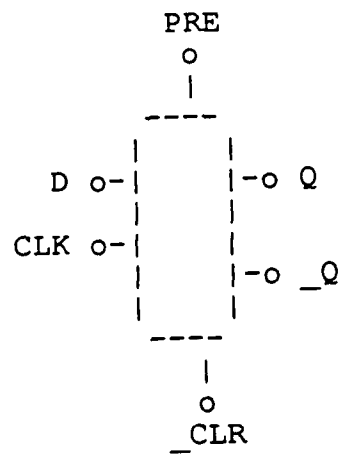


Figure 1.4

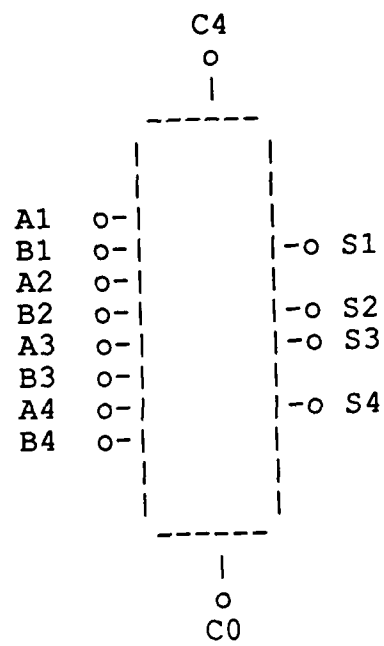


Figure 1.5

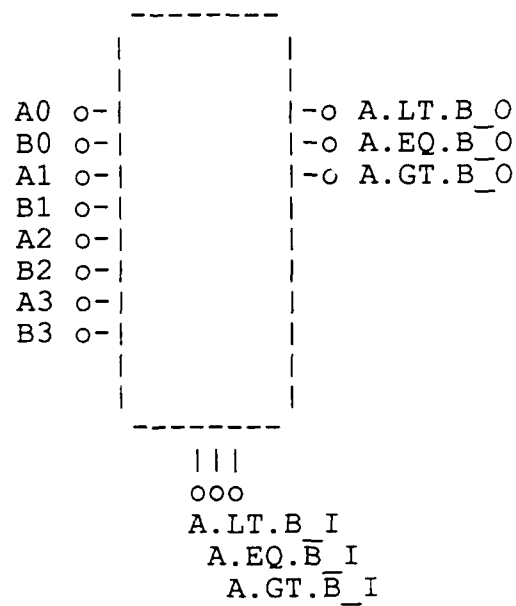


Figure 1.6

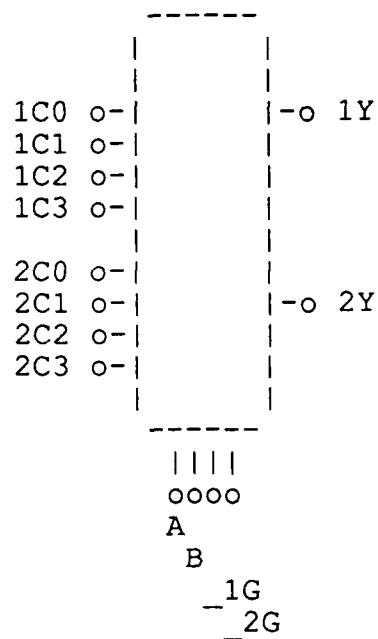


Figure 1.7

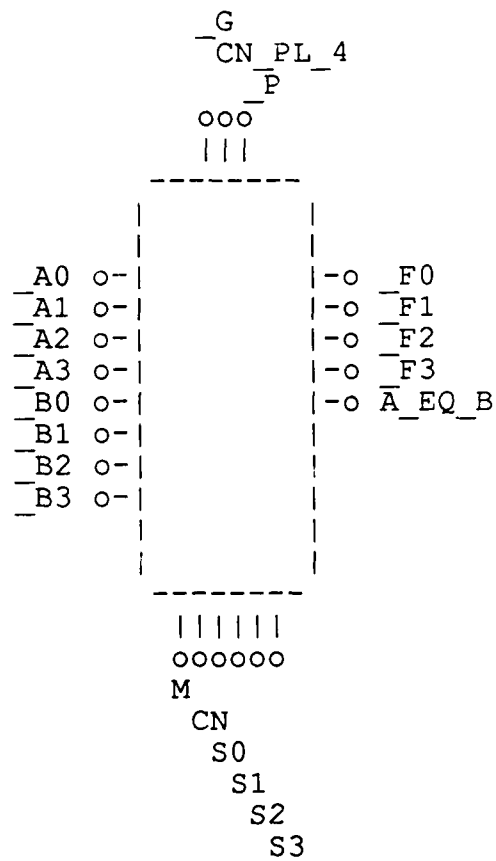


Figure 1.8

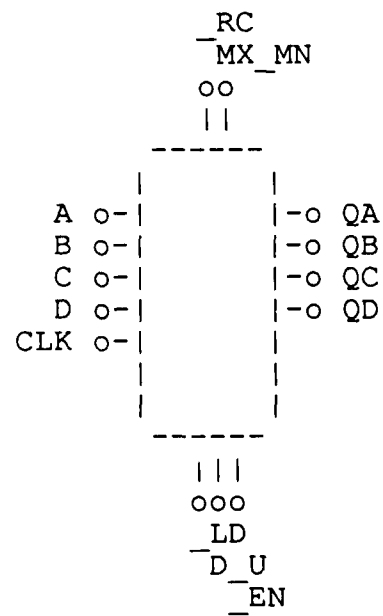


Figure 1.9

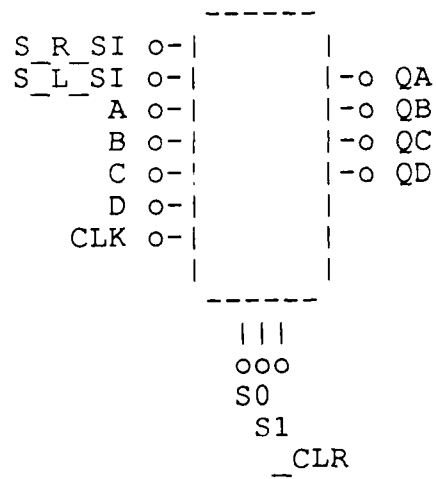


Figure 1.10

## BIBLIOGRAPHY

- Gschwind, Hans W. and McCluskey, Edward J., Design of Digital Computers. Springer-Verlag: New York, 1975.
- The TTL Logic Data Book. Texas Instruments: Dallas, 1988.

### EVALUATION

I feel Wright Patterson Air Force Base has an excellent apprenticeship program. I worked in the Microelectronics Division of the Electronic Technology Laboratory. The atmosphere was one of professionalism. My mentor treated me as an equal and gave me the opportunity to discover the job of an engineer. While I was under his supervision, he allowed me to work at my own pace and solve problems on my own.

Had I not been a high school senior this year, I would have liked to return next summer. I believe that this program should be advertised more in order to give more students the same opportunity.



*Universal Energy Systems*

*\*\*\* ROTATE IMAGE \*\*\**

*Lori A. Harris*

*Greg Power*

*Summer, 1989*

*- \* TABLE OF CONTENTS \*-*

- 1. Acknowledgments*
- 2. Introduction*
- 3. User Instructions*
- 4. Conclusion*

*- \* ACKNOWLEDGMENTS \**

*I would like to thank Universal Energy Systems and Wright-Patterson Air Force Base for making the High School Apprenticeship Program a type of program that gives high school students an excellent opportunity to gain the experience and knowledge they will later need to help further their careers. I'd also like to give a special thanks to my mentor, Greg Power, for giving me a project that was not only challenging, but also beneficial.*

*- \* INTRODUCTION \**

*Since 1978, the shuttle has been providing synoptic radar geologic imagery of the earth's surface. By studying these images, Shuttle Imaging Radar (SIR-B), provides a better understanding of the Earth's regions, geologic features, and structural mapping. However, these images are not in a position referenced to true north.*

*ROTATE IMAGE is a program that reads data from a 725 X 725 array into a 512 X 512 array. The position the image is read is the same position the shuttle processed the data.*

*ROTATE IMAGE will then rotate the image from the position it was processed to the position that corresponds to the angle the user wants to see the image rotated. This will be beneficial in viewing the image in it's true north position.*

*- \* USER INSTRUCTIONS \*-*

1. *Type RUN ROTATE\_IMAGE at the dollar sign prompt.  
Press RETURN.*

*>> The message "50 records read" will appear on the  
screen. Similar records will appear on the screen  
thereafter in increments of 50 up to 700. These  
messages inform the user that data from a 725 X 725  
array is being read into ROTATE IMAGE.*

2. *Enter the angle the image is to be rotated. Press  
RETURN.*

*>> After the data has been read in, the message "What  
angle do you want the image to be rotated?" will  
appear on the screen. Along with positive numbers,  
ROTATE IMAGE also accepts real and negative numbers  
for the angle. Type the desired angle and press*

*RETURN. The user might want to view the position the image is read in the program since that is the position the image is rotated from. To view that position, enter 0 for the angle and press RETURN.*

*\*-----\**  
*ROTATE IMAGE creates a file, DATARRAY.DAT, which is an output file that stores the data from the rotated image. Since DATARRAY.DAT is not in the correct format to print an image, ROTATE IMAGE creates a file called DATARRAY.PRT. DATARRAY.PRT will be in the correct format to print an image, and thus will be used for doing so.*

*\*-----\**

*9. Type INIT1 at the dollar sign prompt and press RETURN.*

*>> INIT1 is used to initialize the system that will*

*print out the image.*

4. *Type MSHOCMS and press RETURN.*

*>> The message "Enter the mono image file spec >" will*

*appear on the screen. Type DATARRAY.DAT and press*

*RETURN. A second message will appear on the screen*

*just like the previous message. Ignore the second*

*and just press RETURN. MSHOCMS is an optional command*

*which is used to show the image on a printing terminal*

*before a hardcopy of the image is printed. Enter this*

*command every time the angle at which the image to be*

*rotated changes. However, it is not necessary to enter*

*INIT1 every time the angle changes. INIT1 should only*

*be used once to initialize the system.*

5. *Type PIMAGE at the dollar sign prompt. Press RETURN.*

>> A message "Enter input and output names:" will appear on the screen. Type DATARRAY.DAT, leave a space, and then type DATARRAY.PRT. DATARRAY.DAT is the input file that will enter data into the output file called DATARRAY.PRT. DATARRAY.PRT is the file that will be used to print out a hardcopy of the rotated image. In a couple of minutes the statement "You will find the laser formatted data in DATARRAY.PRT" will appear on the screen. This is message informing the user that the file DATARRAY.PRT is ready to print a hardcopy of the image.

6. Type BORDERPRT at the dollar sign prompt. PRESS RETURN.

>> The screen is now in BORDERPRT mode. Where the statement "Input Imaging File:" appears on the screen,



*type DATARRAY.PRT. Press the down arrow in order to move to the "Title:", "First Subtitle:", and "Second Subtitle:" fields. Press the E key to erase the field and enter new data. The user can use these fields to type information about the rotated image he wants displayed. Press the P key to print the image. Press Q to exit BORDERPRT.*

*- \* CONCLUSION \*-*

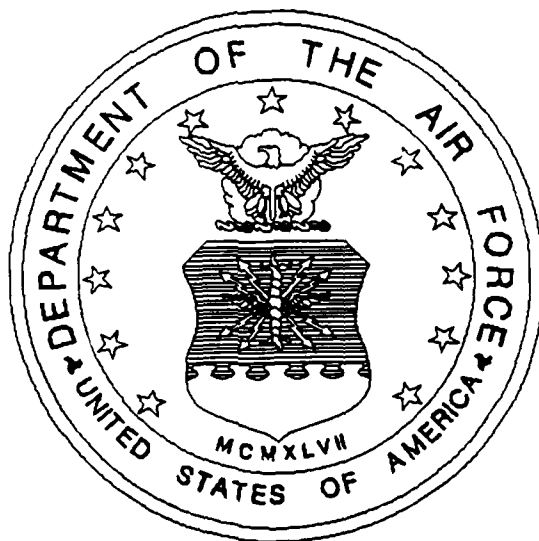
*In concluding my report, I'd like to say that I've enjoyed the challenge ROTATE IMAGE has given me. This was my first time working with Fortran, and I feel that the experience and knowledge I have gained this summer will be extremely beneficial in helping me in the computer courses I will take this fall at the University of Cincinnati.*

*ROTATE IMAGE has a modification that has yet to be done.*

*The modification is one of scaling the size of the array in order to make the image larger or smaller.*

# **AFOSR**

## **High School Apprenticeship Program**



**Final Report**  
**Summer 1989**

**Amy Teresa Listerman**  
**Mentor : Captain Marc J. Pitarys**  
**WPAFB, OH**

## INTRODUCTION

Webster's II New Riverside University Dictionary notes that the word "apprentice" originates from the Old French verb "aprendre" meaning "to learn." This summer has indeed been a learning experience for me. I have been exposed to and learned about things that I had never even heard of before my apprenticeship began. In this final report I will discuss the work that I have done during my apprenticeship and also note some observations that I have made.

## Table of Contents

I. Acknowledgements

II. General Description of Work

III. Detailed Description of Work

IV. Observations

V. Bibliography

## I. Acknowledgements

Firstly, I thank my mentor Captain Marc J. Pitarys for his time and interest. Captain Pitarys has introduced me to many of the operations of the Laboratory and has taught me how to use many specific computer systems and packages. I appreciate the fact that he has allowed me to work on a variety of projects and has also allowed me to do special work in areas of personal interest.

I also thank Mr. Kenneth Littlejohn, Captain Pitarys' office mate, for his time and concern. Mr. Littlejohn has been a "second mentor" to me and has taught me a lot, especially concerning the office computers and Ada programming.

Everyone that I have met in this branch (WRDC/AAAF) has been very helpful and friendly to me and I thank them all for it.

And finally, I thank the Air Force Office of Scientific Research (AFOSR) and Universal Energy Systems (UES) for making this summer apprenticeship program possible.

## II. General Description of Work

The majority of work that I have done this summer fits into one of two categories: Ada programming and specific computer packages and systems. The following is a general description of these categories. More detailed descriptions can be found in section III.

### (A) Ada Programming

Ada is a high-level computer programming language developed by the Department of Defense for real-time embedded computer applications. It also is a good general purpose programming language. I started learning to write Ada code by studying programs which my mentor had written and then reusing the code structure for my own programs. Later, I used the Ada-Tutr (Interactive Software by John S. Herro, PhD) course on a PC and gained a much deeper understanding of Ada. I have now written many Ada programs ranging from numerical analysis to benchmark timing programs.

Programs written in Ada must be compiled before they can be run by the computer. Errors in the Ada code are detected during compilation and must be corrected. Not only did I compile my own programs, but I also entered and compiled prewritten programs for my mentor.

### (B) Specific Computer Packages and Systems

I have worked with various packages and systems for many different purposes throughout the summer. The two that I most frequently worked with were Guide Hypertext and Harvard Graphics. A detailed description of these will follow in section III.



### III. Detailed Description of Work

#### (A) Ada Programming

"The programming language Ada is the result of an effort by the U.S. Department of Defense to control the increasing cost of its software. A study conducted between 1973 and 1974 revealed that the department was spending \$3 billion each year on computer software, over half of it for embedded computers." (Cohen, Norman H., Ada as a Second Language, McGraw-Hill Book Company, New York, 1986,p.1) Ada was developed by the DoD in the late 1970's to cut down both on the proliferation of computer languages within the DoD and on life-cycle support costs of weapon systems. As was stated in section II, Ada was designed for real-time embedded computer applications.

When I started my apprenticeship, I knew almost nothing at all about Ada. My only previous programming experience has been with BASIC. I started learning about Ada by studying some simple programs that my mentor had written. I also reviewed the chapter concerning Ada Statements in the book Ada as a Second Language (Cohen, Norman H., pp.156-187). The first few Ada programs that I wrote came from reviewing the book Applied Numerical Methods for Digital Computation with Fortran ( James, Smith, and Welford, International Textbook Company, Scranton, Pennsylvania, 1967). Using the flow charts in this book, I wrote programs that performed linear interpolation, trial-and-error determination of a root, and the Gaussian probability function. I found this

flowcharting exposure to be an asset while writing more difficult programs.

I had trouble with my first few programs and eventually my mentor would help me work out the bugs in each one. Thus I was learning about Ada as I was trying to write code. It wasn't a very organized process. I then found out about a computer based Ada course called Ada-Tutr (Herro, John S., PhD, Ada-Tutr, Software Innovations Technology, 1988). Ada-Tutr goes through the many various aspects of Ada programming and explains when and how to use different options. It is interactive software in that it asks questions about the material covered that the user must answer and gives (and checks) outside assignments. I got a copy of Ada-Tutr and worked with it for a few weeks. I now understand and recognize most of the common features of Ada. I completed the outside assignments given by Ada-Tutr and went on to write more Ada programs for my mentor ( such as a timing program and an average program ). Since Ada-Tutr was so useful, several other individuals in the Laboratory have obtained copies and are now learning Ada from them.

Part of my project for this summer dealt with Ada compilations. I entered pre-written Ada programs into the computer, compiled them, and then corrected the compilation errors. One of these programs in particular was the Dhrystone Benchmark. This program was published in the journal Ada Letters. The program consists of several mathematical operations that together measure the execution speed of Ada compilers. This benchmark has already been executed on several

computers by my mentor.

(B) Specific Computer Packages and Systems

Throughout the course of my apprenticeship I also had the opportunity to become acquainted with various computer systems in the office. The two that I used most often are: (1) Guide hypertext system and (2) Harvard Graphics (HG).

(1) Guide hypertext system

"Hypertext is a high-speed, automated way of browsing through information. Up until now, most computer software for most users has been designed to make it easier to put information on paper . . . (Hypertext) include(s) capabilities that go beyond paper." (Guide Hypertext for the PC, OWL International, Inc., 1988.) Most documents are confined to the paper on which they are written. They are one-dimensional. Hypertext allows one to escape these confines of paper. With hypertext, there can be different levels of text and different "paths" of information (see figure III-B-1). This allows the reader to find and use only the information she needs. For example, a hypertext document might read --

The price of gismos has risen remarkably (graph) in the last three years. Most analysts claim that the recent shortage (chart) of raw materials accounts for this sharp increase. There are, however, dissenting opinions (\*) from world renowned economists P.W. Herman and I.M. Smart. The gismo . . .

If the reader wanted to know the definition of "gismo" she could

move a pointer to the word "gismo" and then click a button. The definition of "gismo" would appear. Likewise if the reader wanted to view the graph of gismo prices or the chart of raw material shortages he would click on those words and the picture would appear on an overlapping screen. If the reader wanted to read about the dissenting opinions, she could click on the \* and open a entirely different "path" of information.

Hypertext has many advantages and promises to become an important means of information transfer in the future.

## Hypertext

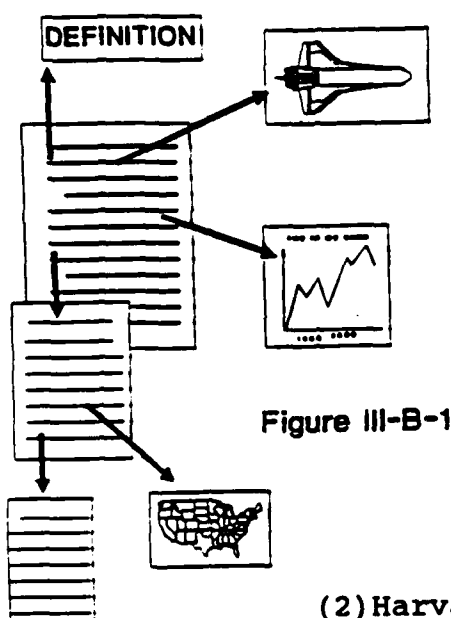


Figure III-B-1

### (2) Harvard Graphics

Harvard Graphics is a brand of software that is used to make charts, graphs, signs, coversheets, lists, and so on. It is very useful in the office. I worked on HG to make charts and graphs of data, slides for presentations, a slide show, lists of information, and numerous other projects for my mentor. The coversheet of this report, in fact, was made on HG. I

enjoyed working with HG and my mentor has never had better charts. Note that Figure III-B-1 which illustrates a hypertext document is one of the many applications of Harvard Graphics.

#### IV. OBSERVATIONS

One of the reasons that I applied to be an AFOSR apprentice was to observe a scientific work place. Throughout high school, my attitudes and thoughts regarding engineering and computer science had not been based upon any fact or first-hand knowledge. While I had done some reading about these fields and spoken to some, people involved in them, I had no "feel" for what it would be like to be an engineer or scientist. And now, although I realize that I have only worked with one small group of scientists, I have gained some useful experience in a scientific field.

I was very fortunate to have been able to work with some of latest computer technology such as Hypertext and Ada. It was not only a learning experience but also a definite personal advantage to have been exposed to this technology so early in my academic career.

It was also a good experience simply to work in a "real" office setting. It certainly is a different atmosphere than my previous summer jobs as a lifeguard and a theater concessionist.

I have learned many things this summer. Some, such as Ada programming, are specific to a particular field. Others, such as word processing software, hypertext, and graphics packages, are things that I will be able to use in any office situation. I know that these skills, and this entire experience in itself, will help me in other endeavors.

I definitely recommend this program to any student

interested in a scientific field.

## V. Bibliography

Cohen, Norman H., Ada As A Second Language, McGraw-Hill Book Company, New York, 1986.

Guide Hypertext for the PC, OWL International, Inc., 1988.

Herro, John S., PhD, Ada-Tutr, Software Innovations Technology, 1988.

James, Smith, and Wolford, Applied Numerical Methods for Digital Computation with Fortran, International Textbook Company, Scranton, Pennsylvania, 1967.

Other resources that I used for this report but did not make direct reference to --

Booch, Grady, Software Engineering with Ada, The Benjamin/Cummings Publishing Company, Reading, Massachusetts, 1983.

VAX Ada Language Reference Manual, Digital Equipment Corporation, Maynard, Massachusetts, 1985.



*AN INVESTIGATION  
OF THE GaAs MESFET*

*PRESENTED TO  
Universal Energy Systems*

*By Joan McManamon  
August 10, 1989*

## ABSTRACT

The Gallium Arsenide (GaAs) Metal-Semiconductor Field Effect Transistor (MESFET) is an important part of MMICs, Microwave Monolithic Integrated Circuits. These MMICs are used in military electronics systems in a variety of applications. A GaAs MESFET was fabricated using various processing techniques, and then electrically characterized. Values for the MESFET performance parameters were found to be  $g_m = 135 \text{ mS/mm}$ ,  $V_p = 1.7 \text{ V}$ , and  $I_{ss} = 35.6 \text{ mA}$ . A MESFET single stage amplifier circuit was then constructed demonstrating amplification.

## ACKNOWLEDGEMENTS

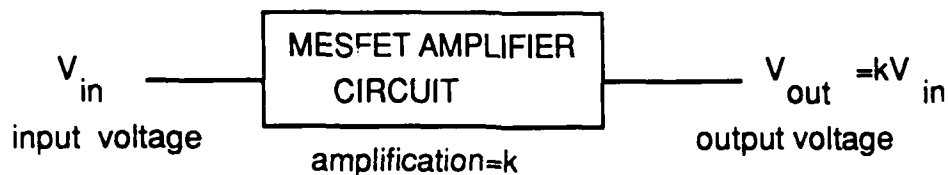
I very much appreciate the opportunity I have had this summer to work in a professional engineering environment. I have been introduced to Electrical Engineering as an interesting and exciting career which I hope to pursue in the future. I would like to thank all the people I have come in contact with for their helpfulness and understanding. I would especially like to thank Kitt Reinhardt for all the time, guidance, and encouragement he has given me over the summer, and for the extra effort he put forth to make sure my eight weeks here were a rewarding, learning experience.

## I. INTRODUCTION

At the present time employees in ELM, a division of the Electronic Technology lab at Wright Patterson Air Force Base, are conducting in-house work on the development of MIMICs, Microwave/Millimeter Wave Monolithic Integrated Circuits. The purpose of this program is to develop the capability to produce large quantities of highly reliable Gallium Arsenide, GaAs, monolithic circuits for use in military electronics systems. Possible uses include radar, communications, electronic warfare, and smart munitions.

The GaAs Metal-Semiconductor Field Effect Transistor, MESFET, forms the basis of these MIMICs. The MESFET has had a major influence on microwave technology in the past few years and is being used more and more in microwave amplifiers for civilian and military systems.

*A MESFET, like all transistors, is an integral part of an amplifier circuit.*



It is built onto a semiconductor substrate, in this case GaAs, by various processing techniques. The substrate does not conduct electricity in its purified state so the top layer is doped. This can be done by many techniques. The most common are ion implantation, where dopant atoms are shot into the substrate, and molecular beam epitaxy, where a thin layer of semiconductor is grown up from the substrate. In the

most common type of GaAs MESFET, this doped layer is rich in electrons. It is called n-type material and contains donor atoms which readily give up electrons for conduction. There is also p-type material which is deficient in electrons, or rich in holes. Typically n-type material is used for MESFETs at microwave frequencies because it has better frequency response, and higher amplification can be achieved due to its superior material properties.

The MESFET has three terminals, the source, gate, and drain, as shown in Figure 1.1.

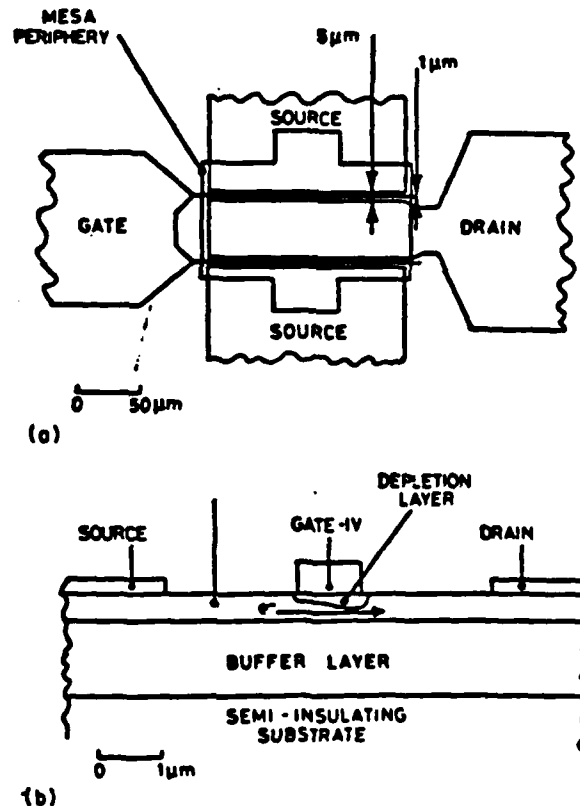


Figure 1.1 GaAs MESFET: (a) plan view; (b) cross section

The basic principle of operation for a MESFET involves the modulation of a conductive channel by applying voltages to the gate. The gate is a Metal-semiconductor Schottky contact which acts as a rectifying diode, a device which allows current to pass only in one direction. The gate modulation controls current from the drain to the source. Reverse-biasing the gate forms a non-conducting region underneath the gate called the depletion region. Applying a negative voltage to the gate of an n-type MESFET modulates this depletion region. The depth of the depletion region can be increased to the point where the conduction channel is pinched off. This allows the basic function of amplification and also enables the MESFET to be used as a switch.

A typical way of characterizing a transistor is to analyze its current-voltage(I-V) characteristics, shown in Figure 1.2. A curve tracer is an instrument that can be used to measure these I-V characteristics.

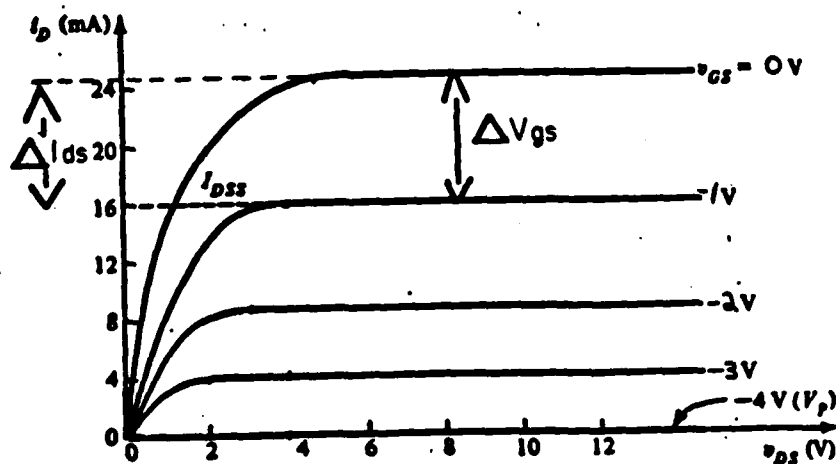


Figure 1.2 I-V Characteristics

$$g_m = \frac{\Delta I_{ds}}{\Delta V_{gs}}$$

Equation 1.1

Transconductance ( $g_m$ ) is a measure of admittance, the inverse of resistance. Its unit is the siemen (S), which is the inverse of ohms. The pinch-off voltage ( $V_p$ ) is the gate voltage at which the conducting channel is pinched closed by the depletion region. The saturation current ( $I_{ds}$ ) is the maximum value of current that can be passed from the drain to the source through the conducting channel. An application of the MESFET is shown in the single stage amplifier circuit below.

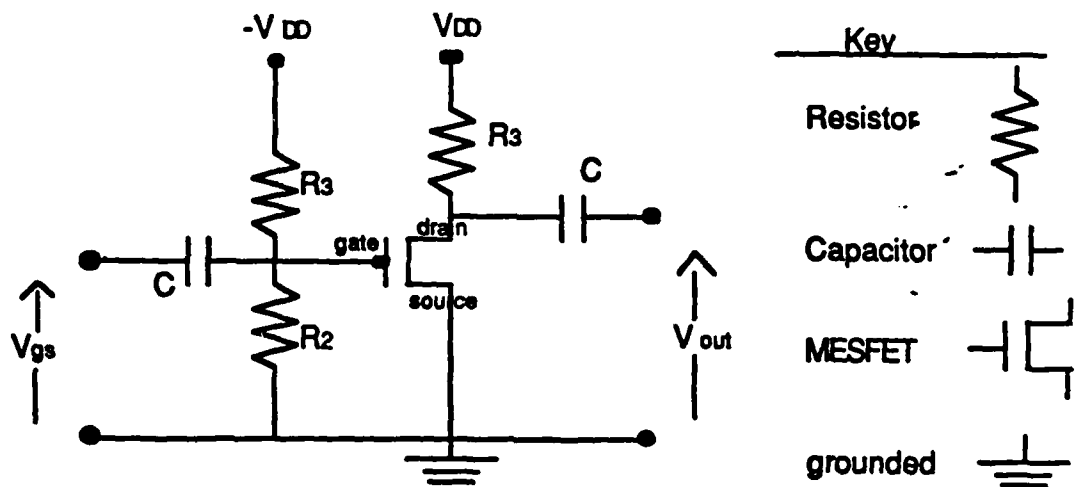


Figure 1.3 MESFET Amplifier Circuit

The gain is the number of times the input signal is amplified.

$$\text{gain} = \frac{V_{out}}{V_{gs}} = -g_m R_3 \quad \text{Equation 1.2}$$

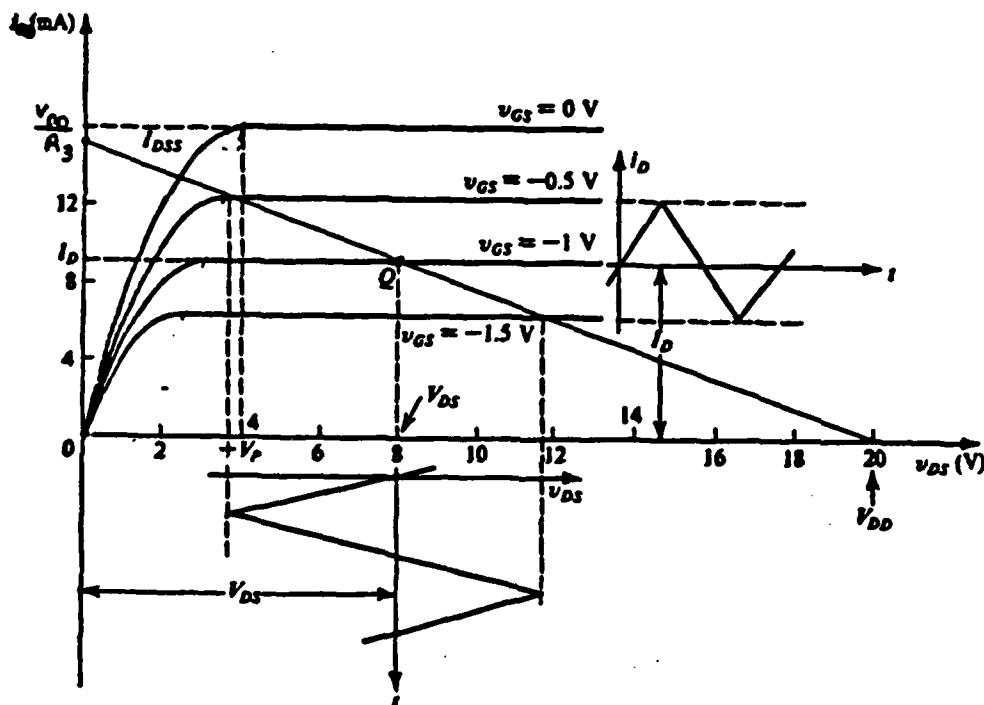


Figure 1.4 Graphical analysis of MESFET amplifier circuit

All combinations of current and voltage fall on the load line during circuit operation. An example of the single stage MESFET amplifier circuit is shown above in Figure 1.3. The gate is biased by a negative voltage,  $-V_{DD}$ , through a voltage divider



resistor circuit to restrict its operation to a specified point on the load line. The input to this amplifier is an AC signal,  $V_{gs}$ , which causes excursions up and down the load line. These changes in gate voltage cause a modulation of the depletion region which modulates the current flow from the drain to the source. The change in current will cause a change in the voltage drop across the resistor,  $R_d$ . The resulting voltage is an amplified inverted AC signal.

## II. MESFET FABRICATION

The first step in the fabrication of a GaAs MESFET is to design the mask set. The mask set is a set of quartz plates which define the photoresist pattern that are required for the various processing steps, such as substrate etching, ohmic contact, and gate metalization. The side of the mask containing the chrome pattern is placed in vacuum contact with the photoresist coated wafer. Ultraviolet light shining through the mask enables the exposed areas to be developed away, leaving behind a photoresist pattern. The photoresist patterning techniques are used to pattern the mesa, ohmic metal contacts, and Schottky gate contacts, and are explained in detail below.

## STEP1 - MESA PHOTOLITHOGRAPHY (MP1400-27 PROCESS)

1. Visually inspect wafer surface. Record any dirt or dust specks in comments. Degrease using acetone, methanol, isopropyl alcohol - 30 seconds each on spinner. Record comments.
2. Bakeout - 150 C - 15 minutes. Record actual time and temperature.
3. Spin on resist - cover entire surface with MF1400-27 - spin at 4000 RPM for 30 seconds (approx. 1.3 thick). Record actual data.
4. Softbake - 90 C - 20 minutes. Record actual time and temperature.

### MAS6

5. Align and expose mesa mask - ~~MAE-5~~ - 320 nm - 12 mw/cm<sup>2</sup> - 20 second exposure. Record all actual values. Record chamber vacuum during exposure.  
NOTE: Place wafer on chuck with flat down (towards operator).
6. Develop (spin speed: 200 rpm) - AZ351:DIW (1:5) - approx. 2 minutes. Rinse with DIW for 30 seconds. Blow dry with filtered N<sub>2</sub>.
7. Visual Inspection - microscope - Record all comments.
8. Hardbake - 100 C - 30 minutes. Record actual time and temperature.
9. Descum - Oxygen Plasma, LFE Etcher, 30 seconds, 100 Watts, Oxygen flow=3. Record all actual values.

## STEP2 - MESA ETCH

1. Check step height of resist with Dektak.
2. Etch sample - HF:H<sub>2</sub>O<sub>2</sub>:DIW (1:1:8) for 20 seconds (~110 A/sec) Rinse with DIW for 30 seconds and blow dry with nitrogen gas.
3. Inspect under microscope. Check for pattern lifting. Record any comments.
4. Measure VBD at three positions across diameter of wafer (perpendicular to major flat). Record in electrical comments.  
Calculate average and record. Check etch depth with Dektak and record TP015.
5. Strip Resist - Acetone, methanol, isopropyl, DIW rinse - 30 sec each on spinner - 1000 RPM - Blow wafer dry with N<sub>2</sub>.
6. Measure mesa height on Dektak in same three places as above. Record in comments. Calculate average and record in TP278.

### STEP3 - OHMIC CONTACT PHOTOLITHOGRAPHY (MP1400-27/CHLOROBENZENE)

1. Visually inspect wafer surface. Record any dust or dirt specks. Degrease with Acetone, Methanol, DIW rinse -30 seconds each on spinner. Record in comments.
2. Bakeout - 150 C - 15 minutes.
3. Spin on MP1400-27 at 4000 RPM - 30 seconds (Approx. 1.3 um).
4. Softbake - 90 C - 20 minutes.
5. Soak in Chlorobenzene approximately for 15 minutes and postbake at 90 C approximately for 15 minutes. Record actual soak time, temperature and postbake time.
6. Align and expose - MJB3 or MA56 Aligner - 320 nm - 12 mw/cm2 -20 seconds. Record actual values and comments.
7. Develop - MP351:DIW (1:5) - 2.5-3.5 minutes spin/spray - 200 RPM. Record actual values.
- B. Visual inspection - red light - microscope - check fork patterns. Record any comments.

### STEP4 - OHMIC METAL SEQUENTIAL DEPOSITION (Au/Ni/Au/Ge/Ni)

1) Pre-metal clean - 30 sec. BHF:DIW (1:1) dip, 30 sec. DIW rinse, THOROUGH blow dry with N2. Load into vacuum chamber IMMEDIATELY.

2) Sequential Deposition - E-Gun, stationary:

| METAL | DESIRED THICKNESS |
|-------|-------------------|
| Ni    | 50 Angstroms      |
| Ge    | 170 Angstroms     |
| Au    | 330 Angstroms     |
| Ni    | 150 Angstroms     |
| Au    | 2000 Angstroms    |

3) Record rate and total thickness.

#### STEP5 - OHMIC METAL LIFTOFF

1. Soak in acetone for 10 min. Record actual soak time.
2. Using 50 PSI acetone spray gun, spray wafer surface while still in teflon carrier in beaker. Fan from center to wafer edge, then reverse direction and spray back to opposite edge. Continue to spray until wafer appears clear of unwanted metal. DO NOT ALLOW ACETONE TO DRY ON SURFACE.
3. If metal will not lift off, place acetone bath in ultrasonic cleaner for no more than 5 min. Record any comments. Try step 2 again if necessary.
4. Without allowing wafer surface to dry, rinse with acetone, methanol, DIW. Blow dry with nitrogen.
5. Strip/Descum residual resist - Oxygen Plasma, 10 min.@ 100 W.

#### STEP6 - RTA ALLOY - SPIKE

1. Heatpulse 210
2. Cycle =
3. Record actual peak temp and any comments
  - Soak temp
  - Soak time
  - Peak temp
  - Peak timeIf soak is not used record only peak temp and time.
4. Recommended alloy temp: 430 C for 30 sec for 2E17 peak carrier concentration

#### STEP7 - POST SOURCE DRAIN MEASUREMENTS

1. MEASURE AND RECORD THE FOLLOWING ACROSS THE WAFER:
  - (a) CROSS BRIDGE MESA ( 23 )
  - (b) BRIDGE MESA ( 25 )
  - (c) CROSS BRIDGE S/D ( 31 )
  - (d) BRIDGE S/D ( 34 )
  - (e) CONTACT RESISTANCE ( 40 )
  - (f) ISOLATION TEST ( 15 )
  - (g) TEST RESISTORS ( 58 )
  - (h) S/D SPACINGS ( 28 )
  - (i) OHMIC METAL THICKNESS ( 12 )
  - (j) IDSS ( 230 )
2. ATTACH ALL GRAPHS AND PLOTS.

**STEPB -GATE LITHOGRAPHY (MP 1400-27/CHLORO BENZENE)**

1. Visually inspect wafer surface. Record any dust or dirt specks. And clean with Acetone, Methanol and DIW rinse - 30 seconds each on spinner and dry with N2. Record any comments.
2. Bakeout - 150 C -15 minutes. Record actual time and temp.
3. Spin on MP1400-27 -4000 RPM - 30 seconds (Approx.1.3 um).
4. Softbake - 90 C - 20 minutes. Record actual time and temp. CB soak for 15 minutes. Bake at 90 C for 15 minutes.
5. Align and expose -MJB3 Aligner -320 nm - 12 mw/cm2 - 20 seconds. Record actual values and comments.
6. Develop - MP351:DIW (1:5) - 2.5 minutes spin/spray - 200 RPM. Record actual values.
7. Visual inspection - red light - microscope - check for patterns. Record any comments.

**STEP9 - GATE RECESS ETCH - [NH4OH:H2O2:DIW(3:1:1000)] - BEAKER**

1. Before processing gate etch, reference post ohmic IDSS.  
Etch gate pattern using NH4OH:H2O2:DIW (3:1:1000) (40 A/sec) by dipping the sample in a beaker. Rinse in DIW for 30 seconds and blow dry with N2. Start with desired etch time.
2. Measure Source/Drain saturation current. Target value is --  
(for 1x200 um gate FET: target current approx. 50-55 mA)
3. Repeat Etch/Test procedure using 5-10 second intervals until saturation current goal is obtained.

### STEP10 TEST #3: SOURCE/DRAIN SATURATION CURRENT

1. Max. Peak Volts should be set at 75 V and minimum series resistance. Curve tracer should be set to measure  $BV_{ceo}$ .  
Polarity = AC                      Mode = NORMAL  
Horizontal = 5V/Div.              Vertical = 5  $\mu$ A/Div.  
Switch = Left Test Ports          Var. Coll. Supply = 0 Volts.
2. Connect test probes to Emitter and Collector jacks on Curve Tracer.
3. Place wafer on chuck and turn on vacuum. Lower the two test probes so that each one contacts one of the two Source/Drain pads of an FET pattern. Lower the probes gently so that they JUST touch the wafer surface. Turn off stage illumination. Record exact FET probed.
4. Increase variable collector supply until saturation occurs. Calculate the saturation resistance using the linear region of the I-V curve. Record  $R_{sat}$ .
5. Record any comments.

### STEP11- Ti/Pt/Au DEPOSITION

1. (a) Dip in BOE:DIW (1:1) solution for 30 seconds. Rinse in DIW for 30 sec.

LOAD INTO VACUUM CHAMBER IMMEDIATELY.

2. Sequential deposition:

| Metal | Desired thickness (angstroms) | Alternatives |
|-------|-------------------------------|--------------|
| Ti    | 200                           | 1000         |
| Pt    | 700                           | 0            |
| Au    | 8100                          | 5000         |

## STEP12 GATE LIFTOFF - ACETONE

1. Soak in acetone for 10 minutes. Record actual soak time.
2. Using 50 PSI acetone spray gun, spray wafer surface while still in teflon carrier in beaker. Spray from center of wafer to one edge, then reverse direction and spray back to opposite edge. Continue to spray until wafer appears clear of unwanted metal. DO NOT ALLOW ACETONE TO DRY ON WAFER SURFACE. Record comments.
3. If metal will not lift off, place acetone bath in ultrasonic cleaner for no more than 5 minutes. Try step2 again if necessary. Record comments.
4. Without allowing wafer surface to dry, rinse with acetone, methanol, isopropyl alcohol and DI water. Blow dry with N2.

## STEP13- POST GATE MEASUREMENTS

1. MEASURE AND RECORD THE FOLLOWING:
  - (a) I-V PLOTS ( 230 )
  - (b) GATE LENGTH ( 74 ) AND ALIGNMENT
  - (c) SOURCE/GATE SPACING ( 24 )
  - (d) GATE/DRAIN SPACING ( 26 )
  - (e) GATE METAL THICKNESS ( 12 )
  - (f) GATE METAL RESISTANCE ( 56 )
  - (h) FAT FET ( 144 )
  - (i) C-V PLOT ( Kiethley )
  - (k) RF TEST ( 61,62,63,64 )
  - (l) PINCH OFF VOLTAGES ( $V_p$  (V))


### III. TESTING AND RESULTS

Testing was completed following the procedures listed in the fabrication steps in the previous section. The mesa step height was measured using a profilometer and found to be  $3000\text{\AA}$ , as shown in Figure 3.1. The source drain metal thickness was similarly found to be  $2400\text{\AA}$  and is shown in Figure 3.2.

Post source drain measurements mentioned in step 7 showed the source drain contacts to be ohmic, metal-semiconductor bonds which allow current flow in either direction. A plot of the resistance between the source and drain is pictured in Figure 3.3. The linear characteristics show the contact to be ohmic. By Ohms law the resistance from the drain to the source, across the channel, is 39.9 ohms, 37 of which is known to be from the active layer. The rest is due to ohmic contact resistance.

$$R = \frac{V}{I} = \frac{2.000V}{50.12mA} = 39.9\text{ohms} \quad \text{Equation 3.1}$$

Figure 3.4 shows the I-V characteristics of the MESFET before the gate recess etch step. The current saturation shown occurs because the electrons have reached a maximum speed, termed the electron drift saturation velocity. This saturation velocity is a result of the physical properties of a semiconductor.

The gate is a Schottky contact, a metal-semiconductor junction which passes current in only one direction. Figure 3.5 shows the I-V characteristics from the gate to the source and demonstrates a typical diode characteristic. A diode is a two terminal device with the symbol , that allows current flow only in one direction. The

modulation of the channel in a MESFET is made possible by reverse-biasing the Schottky junction. Figure 3.6 shows the final I-V characteristics for the gated MESFET.



Fig. 3.1 Mesa Height

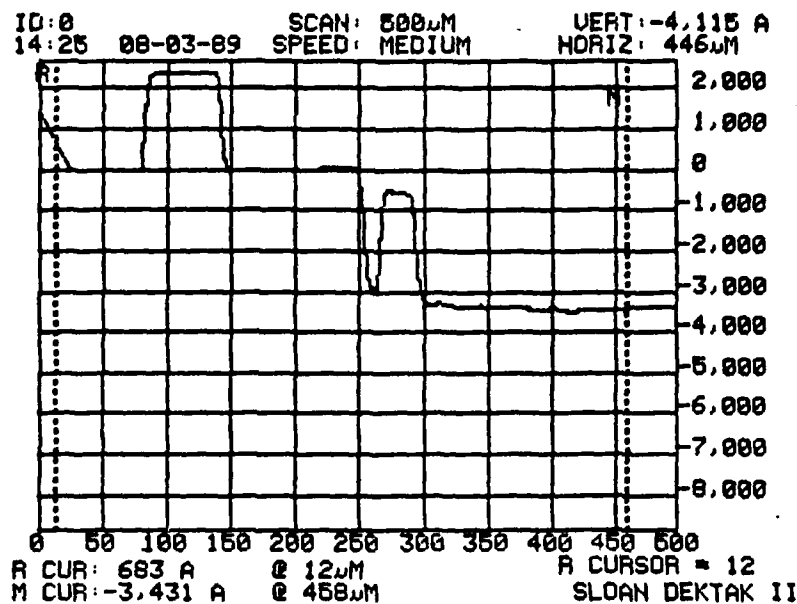
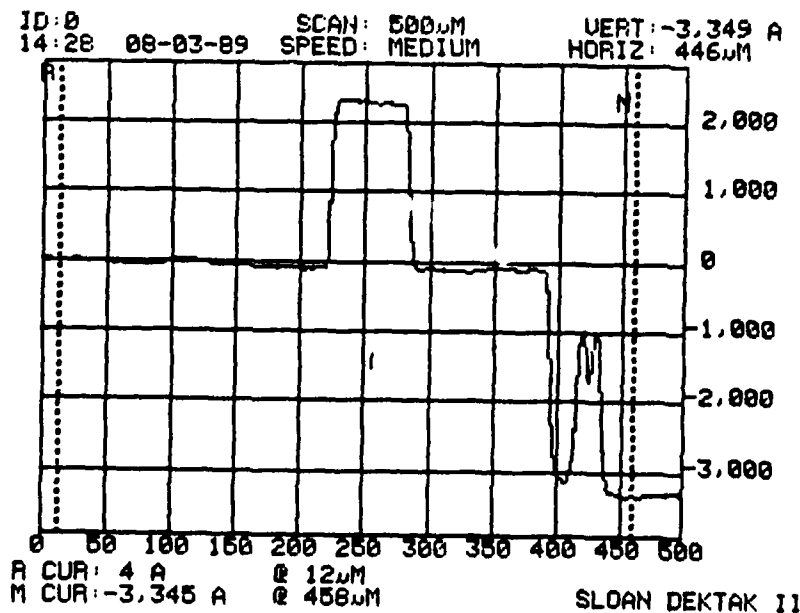
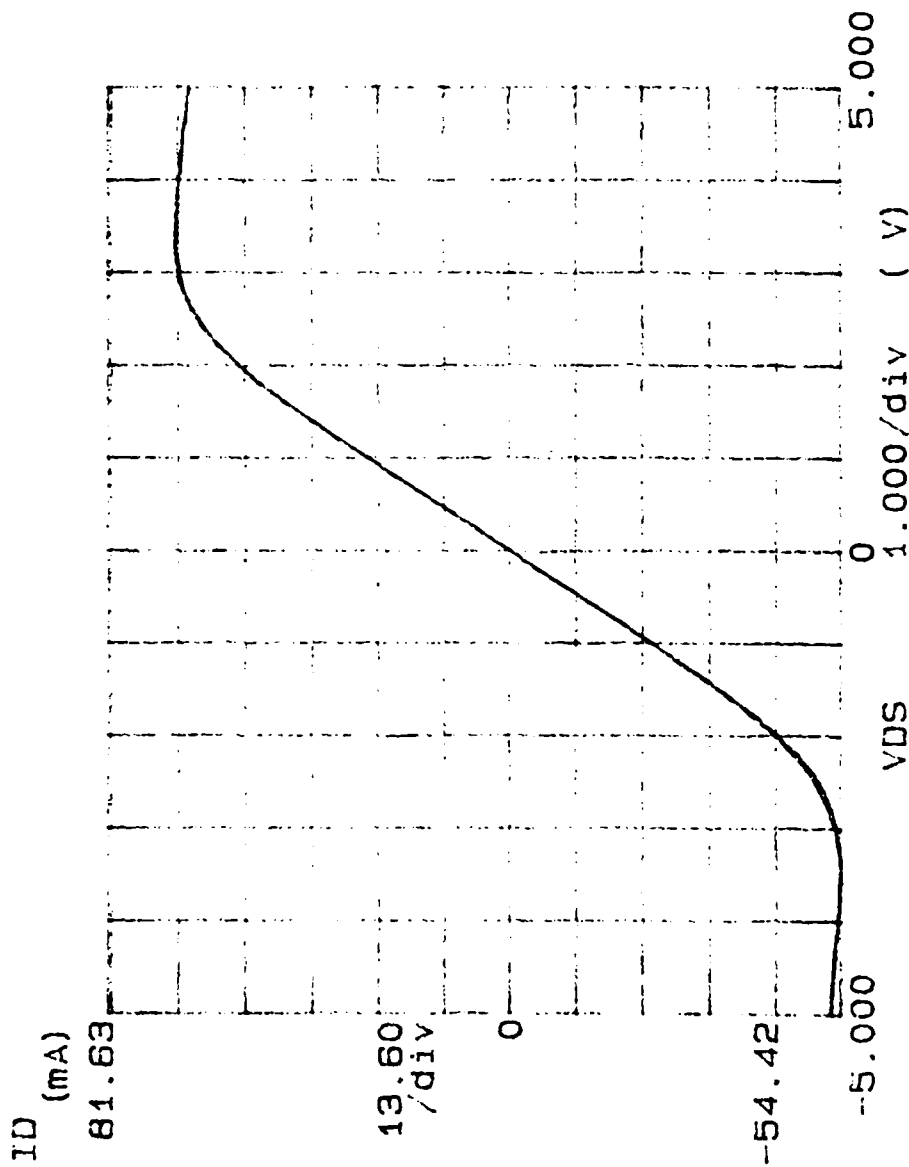


Fig 3.2 Source/Drain Metal Thickness



\*\*\*\*\* GRAPHICS PLOT \*\*\*\*\*  
OHMIC CONTACT RESISTANCE



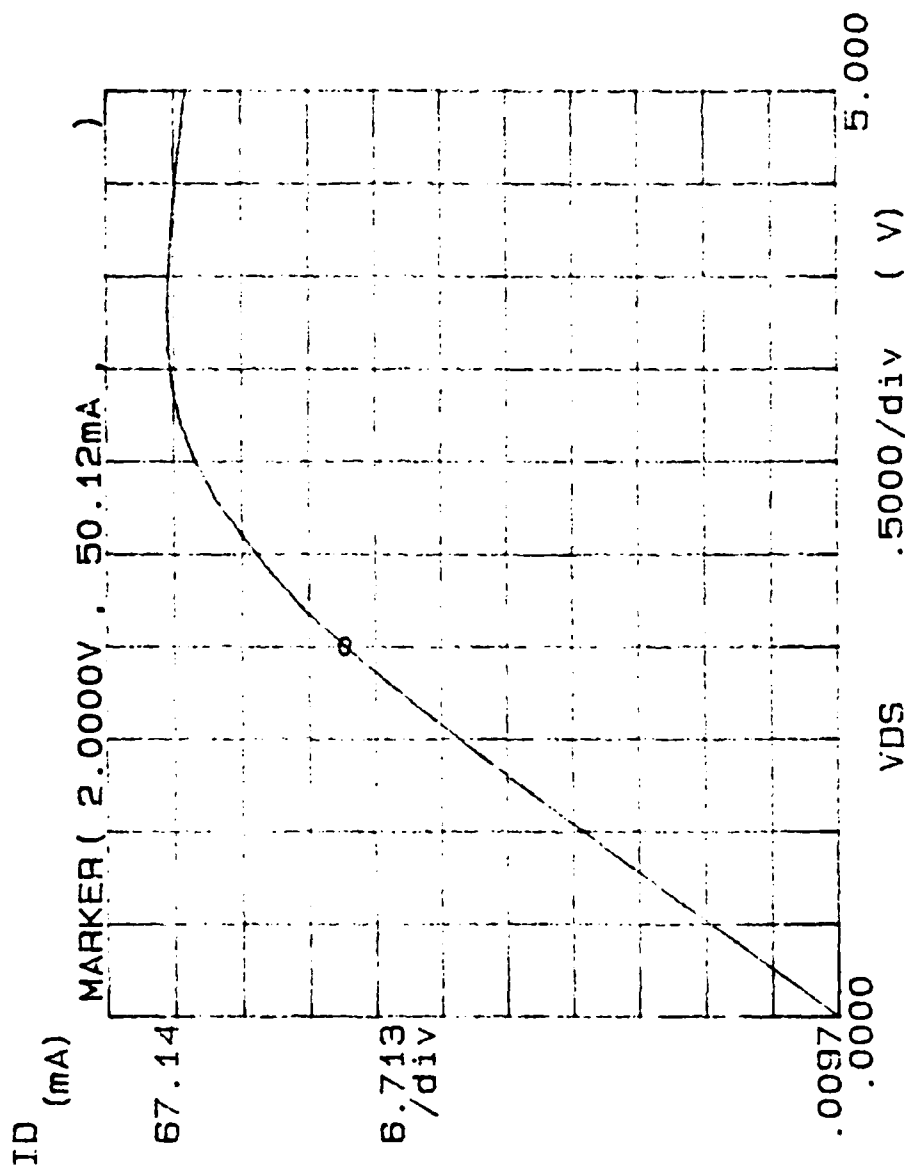
Variable1:  
VDS -Ch2  
Linear sweep  
Start -5.0000V  
Stop 5.0000V  
Step .2000V

Variable2:  
VG -Ch3  
Start .0000V  
Stop -5.5000V  
Step .5000V

Constants:  
VS -Ch1 .0000V

Figure 3.3 Ohmic Contact Resistance

\*\*\*\*\* GRAPHICS PLOT \*\*\*\*\*  
I-V BEFORE RECESS



Variable1:  
VDS -Ch2  
Linear sweep  
Start .0000V  
Stop 5.0000V  
Step .2000V

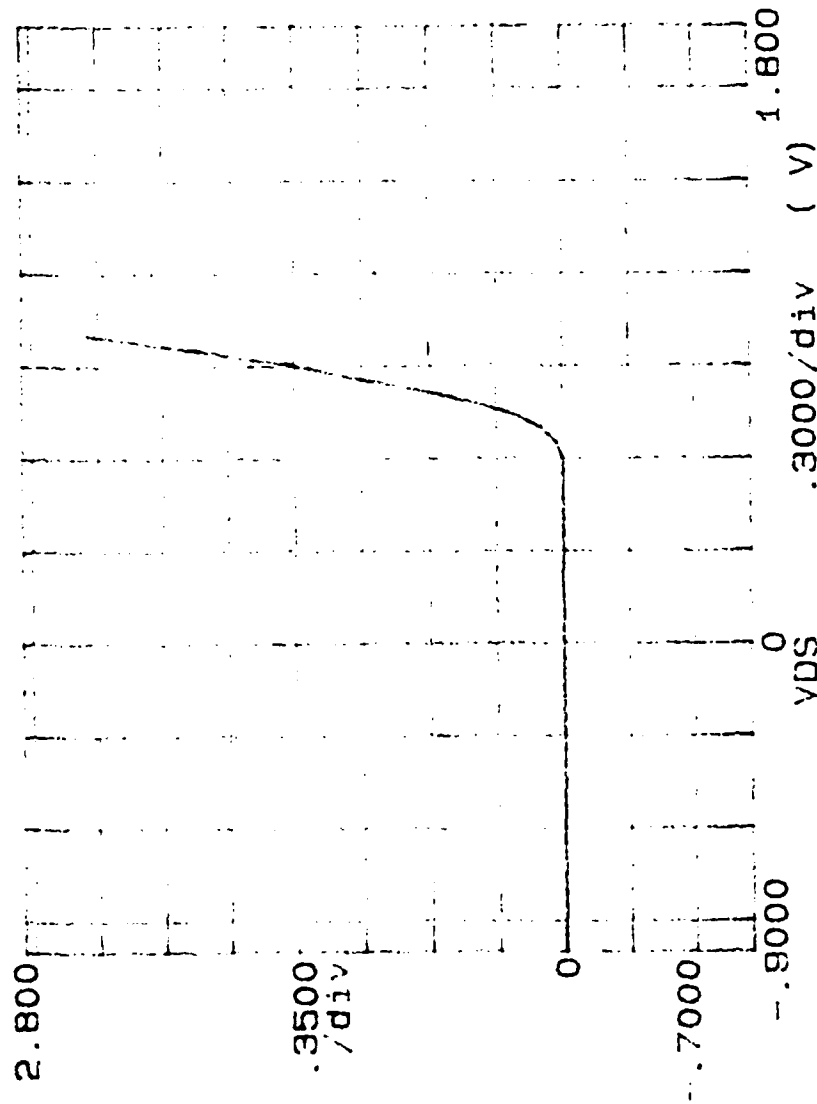
Variable2:  
VG -Ch3  
Start .0000V  
Stop -5.5000V  
Step - .5000V

Constants:  
VS -Ch1 .0000V

Figure 3.4 I-V Characteristics Before Gate Recess

\*\*\*\*\* GRAPHICS PLOT \*\*\*\*\*  
 SCHOTTKY DIODE CHARACTERISTIC

ID (mA)



Variable1:  
 VDS -Ch2  
 Linear sweep  
 Start -1.0000V  
 Stop 1.0000V  
 Step .0500V

Variable2:  
 VG -Ch3  
 Start .0000V  
 Stop -5.5000V  
 Step -.5000V

Constants:  
 VS -Ch1 .0000V

Figure 3.5 Diode Characteristic

\*\*\*\*\* GRAPHICS PLOT \*\*\*\*\*

Variable1:  
 VDS -Ch2  
 Linear sweep  
 Start .0000V  
 Stop 5.0000V  
 Step .2000V

Variable2:  
 VG -Ch3  
 Start .0000V  
 Stop -4.5000V  
 Step -.5000V

Constants:  
 VS -Ch1 .0000V

Idss = 35.6mA @ Vds = 3V  
 Vp = 1.7V @ Vds = 3V  
 gm = 135mS/mm @ Vgs = 0V

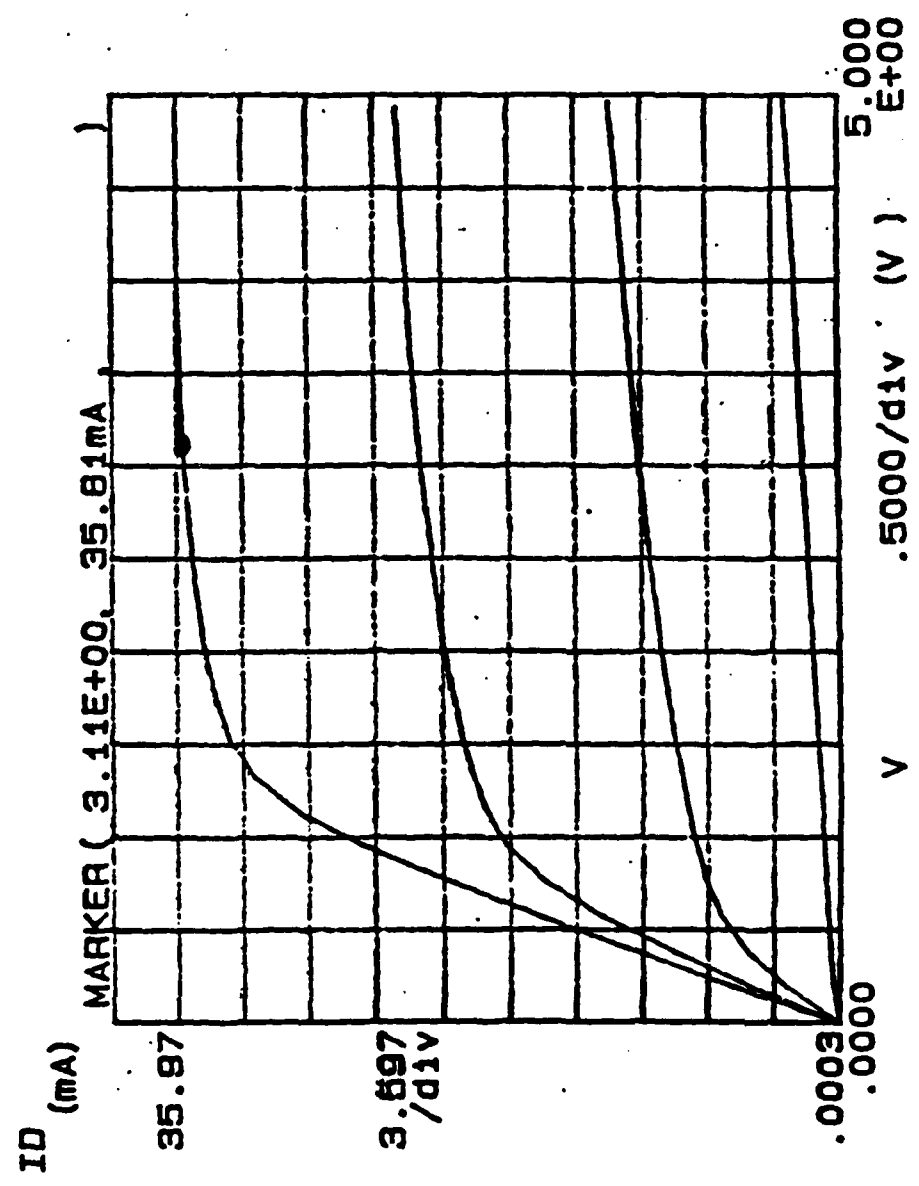


Figure 3.6 I-V Characteristics for Gated MESFET

## CONCLUSION

In this project the GaAs MESFET was studied, fabricated, tested, and inserted into a single stage amplifier circuit. Various Semiconductor processing techniques were studied and then utilized to produce 75 micron GaAs MESFETs having gate lengths of 1 micron. Testing showed the source drain contacts to be ohmic and the gate to be a Schottky contact. These MESFETs were electrically characterized and found to exhibit typical performance parameter values of  $g_m = 135 \text{ mS/mm}$ ,  $V_p = 1.7 \text{ V}$ ,  $I_{dss} = 35.6 \text{ mA}$ . A typical MESFET was then inserted into a single stage amplifier circuit demonstrating a typical application of amplification.

# The Optical Spectroscopy of $\text{Ti}^{3+}$ doped $\text{YAlO}_3$

Allison L. Potter

Universal Energy Systems

## I. INTRODUCTION

This project investigated the optical properties of  $\text{Ti}^{3+}:\text{YAlO}_3$  and its potential as a laser source.  $\text{Ti}^{3+}:\text{YAlO}_3$  crystals have not performed well as laser sources in the past, and because of this the investigation was begun. A large single crystal sample grown by Heraeus was provided to us by R. Simms of the Naval Air Development Center. Prior crystals investigated in this lab were grown by Airtron. Since Heraeus had a different method for growing the crystal, we wanted to investigate it to see if it might be a better source for lasing. Absorbance, fluorescence, annealing, and lifetime measurements were planned.

The crystal of  $\text{Ti}^{3+}:\text{YAlO}_3$  was grown by Heraeus in West Germany by using the modified Czochralski method under stringent vacuum conditions. It is .1 at% Ti by melt and it has a beige-orange tint. The crystal's measurements were 1.026 cm by 1.509 cm by 3.05 cm (see figure 1). A rectangular parallelepiped of size .3 cm by 1.026 cm by 1.01 cm was cut from the original crystal. The sample was cut with faces perpendicular to crystallographic axes. The crystal's imperfections are pits that were made on the bc faces.

## II. EXPERIMENT

### Absorption Measurements

An IR9 Spectrophotometer with a polarizer/depolarizer unit, made by Perkin-Elmer, was used to measure polarized transmission in the crystal utilizing the six orientations possible (e.g. E11a and k11c or k11b; E11b and k11a or k11c; E11c and k11a or k11b; where E = the electric field and k = beam direction). The scan was from 300 nm to 2000 nm in increments of one nanometer.

An annealing experiment was carried out by baking the crystal for fifteen and a half hours in an oven at 200°C. The absorption spectra were measured again with the spectrophotometer to see if the broadband peak around 800-1000 nm would change in any way.

### Fluorescence Measurements

Krypton lamp scans first were carried out to calibrate wavelength for fluorescence measurements using the SPEX 1269 Spectrometer and a 1200 g/mm grating blazed at 750 nm. The controller used with the spectrometer was a SPEX Datamate DM1 controller. Wavelength calibration was done by making several scans of the krypton lamp spectrum. All of the scans were done in the range of 500 to 800 nm. Two different types of scans were used. The first used a PIN silicon detector made by United Detector Technologies Inc. and the second used the R928 photomultiplier tube made by Hamamatsu.



After changing the grating so short wavelength fluorescence could be measured, it was necessary to do another calibration of wavelength for the fluorescence measurements using the SPEX 1269 Spectrometer and a 1200 g/mm grating blazed at 400 nm. Scans were made between 400 nm and 800 nm with the R928 photomultiplier tube made by Hamamatsu. The slit size was 10  $\mu$ m and data was taken at increments of 0.2  $\text{\AA}$ .

Fluorescence measurements were taken to further investigate the optical properties of this crystal. Fluorescence scans of intensity versus wavelength at room temperature were taken with the crystal in twenty-four different orientations (see figure 2). The laser beam pumping the crystal and the fluorescence entering the spectrometer were both polarized. The slits in the spectrometer were set at 50  $\mu$ m. A Spectra Physics 165 argon ion laser was used at a power of 500 mW and the two pump wavelengths of 488 nm and 514.5 nm were used in the experiment. Each run was a scan between 500 and 800 nm with increments of 1 nm.

#### Fluorescence Lifetime Measurements

Measurements of fluorescence lifetime with increasing temperature were also performed. In these measurements the need for accurate temperature monitoring was vital, so a comparison was done among a Cole-Farmer Digi-Sense Model 2168-80 Temperature Controller, a Bailey Instruments Co. Inc Wide Range Thermometer, Model BAT-7, and a calibrated thermometer. This was done by placing thermocouples, connected to each monitor, and the thermometer into a beaker of oil to be heated up to 220°C (according to the thermometer). Temperatures of the three temperature meters were recorded and compiled in a graph (see figure 3).

The  $\text{Ti}^{3+}:\text{YAlO}_3$  crystal was placed in a vacuum oven on top of a copper block. The temperature controller's thermocouple was attached to the top of the crystal. The controller was connected to the heating element in the copper block and an air pump cooling system. The other thermocouple was mounted inside the copper block and monitored by the wide range thermometer. The crystal was tested for lifetime at room temperature and then at 50° increments up to 235°C. The Hastings Vacuum Gauge, model VT-4S2, measured a vacuum of .7 mm of mercury. For the lifetime measurements, the argon ion laser was operated at 488 nm with a power of one Watt. An acousto-optical switch was used to select pulses from the beam that were 100  $\mu\text{s}$  long and had rise and fall times (10%-90%) of 1-2  $\mu\text{s}$ . The fluorescence was detected at 600 nm.

Further fluorescence scans were made as a function of temperature. The laser was pumping at 488 nm with 100 mW of power. The slits on the spectrometer were 300  $\mu\text{m}$  apart and the spectrometer took data in increments of 1 nm.

### III. RESULTS AND DISCUSSION

#### Transmission measurements

The results of the transmission measurements were manipulated to show the absorption coefficient with these two equations :

$$\begin{aligned} T &= I/I_0 = e^{-(\alpha l)} \\ T &= I/I_0 = 10^{-x} \end{aligned}$$

where  $x$  = absorbance,  $l$  = crystal thickness or beam pathlength,  $T$  = transmission,  $I$  = intensity,  $I_0$  = incident intensity and  $\alpha$  = absorption coefficient. Taking the natural log of both equations gives,

$$-\alpha l = -x (\ln 10)$$

or

$$\alpha = x (\ln 10) / l$$

By utilizing the final equation the distance that the laser traveled through the crystal was taken out so it would not be a factor. In this basic data manipulation, the absorption coefficient ( $\alpha$ ) was found.

Before using the final equation a correction for Fresnel losses (reflection losses) had to be made. The reflection loss was calculated by first figuring out how much of the beam is reflected when it hits the first face of the crystal. This is calculated using the formula,

$$R = (n_0 - n_1)^2 / (n_0 + n_1)^2$$

where  $n_0$  = refractive index of the atmosphere,  $n_1$  = refractive index of Ti<sup>3+</sup>:YA10; (Ella  $n_1$  = 1.97; Ellb  $n_1$  = 1.96; Ellc  $n_1$  = 1.94, where  $E$  is the electric field). The resulting fraction is the amount of light reflected from the first face. The same percentage of the beam is reflected back into the crystal when the beam strikes the second face of the crystal. This reflection is again reflected and transmitted at the first face; the same percentage of the reflected light is reflected, but the transmitted percentage at the first face the second time is to be added to the reflected light from the first face. This summed percentage is

subtracted from 100%. The negative log of this decimal percentage is subtracted from the absorbance in order to subtract out the reflection loss (see figure 4 for a calculation example). Then this value can be used in the final equation as the absorbance ( $x$ ) to find the absorption coefficient ( $\alpha$ ).

#### Absorption coefficient graphs

The graphs of absorption were very much alike in that there were peaks at around 450 nm and 500 nm, which are known to be  $Ti^{3+}$  absorption peaks from the AFWAL TR Final Report by K.L. Schepler.<sup>1</sup> Between 800 nm and 1000 nm several things happened. First, at 819.2 nm there was a glitch in the graph due to the spectrophotometer changing it's detector. Second, there was a broad absorption band in the near infrared, peaking around 950-1000 nm. With these two details occurring in such close proximity, the graph is distorted (see figure 5).

Comparing the absorption features at different polarizations, EIIa and EIIc were found to be greater at the 450 and 500 nm peaks and less, compared to the EIIf spectrum, in the broadband near-infrared peak. Comparing EIIa and EIIc where the electric field pointed along the y-axis and the magnetic field pointed perpendicular to the electric field and the laser propagation (laser vertically polarized), EIIa was found to be greater overall. When the electric field pointed along the x-axis and the magnetic field pointed perpendicular to the electric field and the laser propagation (laser horizontally polarized) EIIa was greater at the 450 and 500 nm peaks and

---

<sup>1</sup> "Spectroscopy and Laser Performance of  $Ti^{3+}$  Doped and  $Cr^{3+}, Nd^{3+}$  Co-doped Crystals", AFWAL-TR-88-1125, Aug. 1988.

less at the 950 nm wide band (see figure 6).

#### Ti:YAlO<sub>3</sub> Crystal Annealed

In the spectra that were done after the annealing experiment, only one changed dramatically. That spectrum, with E11a, k11b (k is the propagation direction), and vertically polarized light, had noticeably less loss at all wavelengths and the broadband peak decreased in height. The high temperature anneal appears to have removed some color center or defect from the crystal. Whether this improvement is permanent or not remains to be seen.

#### Consistency Investigation

Due to the results we observed in the annealing experiment, the uniformity of the crystal needed further investigation. Runs were made in the spectrophotometer with the crystal in the same position each time except for a slight movement. The absorbance measurements produced have very similar Ti<sup>3+</sup> peaks but at 1000 nm the broad band peak shows up on some scans more than others. (see figure 7). Then a Spectra Physics helium-neon laser was passed through the crystal. The crystal was moved so that the laser beam passed through different areas of the crystal. Cloudy areas of the crystal caused the laser beam to scatter and this scattering occurred mainly on the crystal's outer edges. The middle area produced a fairly low amount of scattering beam when the laser was passed through it. Thus, different parts of the crystal were found to have different amounts of scattering. The annealing experiment changes may have been caused by

changes in the beam position rather than any annealing effects.

#### Krypton scan

The krypton scans for wavelength calibration were done by comparing the measured peaks with the recorded peaks. The first calibration was done with both the silicon detector and the photomultiplier tube. The results are in the following table.

TABLE OF  $\lambda$ 's FOR 750 NM BLAZE GRATING

1) Main peaks found with the silicon detector, 1 mm slits, and increments of 1 Å

| EXPECTED PEAKS(Å) | MEASURED PEAKS(Å) | OFFSET(Å) |
|-------------------|-------------------|-----------|
| 5570.3            | 5573.             | 2.7       |
| 5870.9            | 5874.             | 3.1       |
| 7587.4            | 7590.             | 2.6       |
| 7601.5            | 7604.             | 2.5       |
| 7685.2            | 7688.             | 2.8       |
| 7694.5            | 7697.             | 2.5       |

Average Offset = 2.7

2) Main peaks found with the FMT, 100  $\mu\text{m}$  slits, and increments of .01  $\text{\AA}$   
 (measured peaks rounded to one decimal place.)

| EXPECTED PEAKS ( $\text{\AA}$ ) | MEASURED PEAKS ( $\text{\AA}$ ) | OFFSET ( $\text{\AA}$ ) |
|---------------------------------|---------------------------------|-------------------------|
| 5570.3                          | 5571.9                          | 1.6                     |
| 5870.9                          | 5872.6                          | 1.7                     |
| 7587.4                          | 7588.9                          | 1.5                     |
| 7601.5                          | 7603.1                          | 1.6                     |
| 7685.2                          | 7686.8                          | 1.6                     |
| 7694.5                          | 7696.2                          | 1.7                     |
| 7854.8                          | 7856.6                          | 1.8                     |

Average Offset = 1.6

3) Main peaks found with the FMT, 10  $\mu\text{m}$  slits, and increments of .01  $\text{\AA}$   
 (measured peaks rounded to one decimal place for comparison with expected.)

| EXPECTED PEAKS ( $\text{\AA}$ ) | MEASURED PEAKS ( $\text{\AA}$ ) | OFFSET ( $\text{\AA}$ ) |
|---------------------------------|---------------------------------|-------------------------|
| 5570.3                          | 5571.9                          | 1.6                     |
| 5870.9                          | 5872.7                          | 1.9                     |
| 7587.4                          | 7589.3                          | 1.9                     |
| 7601.5                          | 7603.5                          | 2.0                     |
| 7685.2                          | 7687.2                          | 2.0                     |
| 7694.5                          | 7696.4                          | 1.9                     |
| 7854.8                          | 7856.6                          | 1.8                     |

Average Offset = 1.9

Full width at half maximum with the FMT, 10  $\mu$ m slits, and increments of .01  $\text{\AA}$ .

| RIGHT $\lambda$ ( $\text{\AA}$ ) | LEFT $\lambda$ ( $\text{\AA}$ ) | DIFFERENCE ( $R\lambda-L\lambda$ ) |
|----------------------------------|---------------------------------|------------------------------------|
| 5572.22                          | 5571.67                         | .55                                |
| 5873.00                          | 5872.54                         | .46                                |
| 7589.60                          | 7589.09                         | .51                                |
| 7603.80                          | 7603.25                         | .55                                |
| 7687.46                          | 7686.97                         | .49                                |
| 7696.69                          | 7696.18                         | .51                                |
| 7856.88                          | 7856.35                         | .55                                |

Average Offset = .52

The main offset of the silicon detector data has been determined to be due to the inaccuracy of an angle at which one of the mirrors inside the spectrometer was situated.

The second calibration for the change to a grating blazed at 400 nm was done and this is data comparing the peaks found with the recorded peaks for krypton. This was used to find the spectrometer's deviation from the correct wavelength.



# TABLE OF $\lambda$ 'S FOR 400 NM BLAZE GRATING

1) Main peaks found with the PMT, 10  $\mu$ m slits, and increments of .2  $\text{\AA}$ .

| EXPECTED PEAKS ( $\text{\AA}$ ) | MEASURED PEAKS ( $\text{\AA}$ ) | OFFSET ( $\text{\AA}$ ) |
|---------------------------------|---------------------------------|-------------------------|
| 5993.9                          | 5986.0                          | 7.9                     |
| 5879.9                          | 5872.0                          | 7.9                     |
| 5870.9                          | 5863.0                          | 7.9                     |
| 5672.5                          | 5664.4                          | 8.1                     |
| 5570.3                          | 5562.2                          | 8.1                     |
| 4502.4                          | 4493.8                          | 8.6                     |
| 4463.7                          | 4455.2                          | 8.5                     |
| 4453.9                          | 4445.4                          | 8.5                     |
| 4376.1                          | 4367.6                          | 8.5                     |
| 4362.6                          | 4354.2                          | 8.4                     |
| 4319.6                          | 4311.0                          | 8.6                     |
| 4274.0                          | 4265.6                          | 8.4                     |

Average Offset = 8.3

2) Main peaks found with FMT, 10  $\mu$ m slits, and 0.1  $\text{\AA}$  increments.

| EXPECTED PEAKS( $\mu$ ) | MEASURED PEAKS( $\text{\AA}$ ) | OFFSET( $\text{\AA}$ ) |
|-------------------------|--------------------------------|------------------------|
| 4319.6                  | 4310.9                         | 8.7                    |
| 4362.6                  | 4354.2                         | 8.4                    |
| 4376.1                  | 4367.8                         | 8.3                    |
| 5870.9                  | 5862.9                         | 8.0                    |
| 5879.9                  | 5872.0                         | 7.9                    |
| 5993.9                  | 5986.1                         | 7.8                    |

Average Offset = 8.2

#### Fluorescence Measurements at Room Temperature

The results of the fluorescence measurements at room temperature showed the typical broadband peak for  $\text{Ti}^{3+}$  ions. Due to the non-uniformity of the crystal, discussion of the dependence of intensities on pump and fluorescence polarizations and directions could not be performed. The pump beam direction, the fluorescence direction, and the pump beam electric field all influence the intensity, therefore, these three variables can not accurately be compared. So, the intensities were normalized to be equal and the wavelengths where the maximum intensity occurred were compared. In this comparison a pattern was found to be present. Where E was the electric field of the fluorescence, E<sub>11a</sub> was found to peak at 601 nm, then E<sub>11c</sub> peaked at 613 nm, and finally E<sub>11b</sub> peaked at 626 nm (see figure 8).

#### Fluorescence and Lifetime Measurements at High Temperatures

The results in the lifetime and fluorescence measurements in high temperatures showed that the intensity peak of the fluorescence decreased with increasing temperature (see figure 9). The intensity varied from 100% (arbitrary percentage) at 23.4°C to 49% at 238°C. The integrated intensity was also found by finding the sum of the intensities between 500 and 800 nm. The sum intensity values were then multiplied by a constant of 4.1 to make them comparable in numerical value to the lifetime results (see figure 10).

The equation of fluorescence intensity as a function of time after an initial excitation pulse is given by,

$$I = I_0 e^{-t/\tau}$$

where  $I_0$  = the intensity at time = 0,  $t$  = time and  $\tau$  = lifetime. When the natural log of this equation is taken it results in:

$$\ln I = \ln I_0 - t/\tau$$

When the following substitutions are made:  $\ln I = y$ ;  $\ln I_0 = mx$ ;  $-t/\tau = b$ , this equation can be reorganized as the equation for a straight line. Lifetimes were calculated by setting the left and right parameters at 16000  $\mu s$  and 36000  $\mu s$  (the pump pulse turns off after 10240  $\mu s$ ) and then finding the least-square fit to the slope of the log of the intensities. If the plot of log (intensity) versus time is a straight line then only one lifetime is being measured. Graphs of log (intensity) versus time are shown in figure 11. In these graphs the lifetime can be compared on the

basis of slope; the steeper the slope the shorter the lifetime. The lifetime measurements were found to decrease as temperatures increased; similar to the integrated intensity except that the lifetime decreased at a quicker rate at first and then proceeded at the same rate as the integrated intensity (see figure 10).

#### IV. SUMMARY

Absorbance measurements were taken and Ell<sub>a</sub> was the maximum for the Ti<sup>3+</sup> peaks and Ell<sub>b</sub> was the maximum for the broadband peak. The fluorescence measurements at room temperature showed the typical broadband peak for Ti<sup>3+</sup> and produced a pattern of maximum peaks which occurred in the order : Ell<sub>a</sub> at 601 nm, Ell<sub>c</sub> at 613 nm, Ell<sub>b</sub> at 626 nm. The fluorescence measurements as a function of temperature resulted in the conclusion that as temperature increases intensity decreases and that the nonradiative loss is increasing with temperature. Lifetime measurements of the fluorescence were taken and compared to the integrated intensity; the fluorescence lifetime was found to decrease at a faster rate than the integrated intensity.

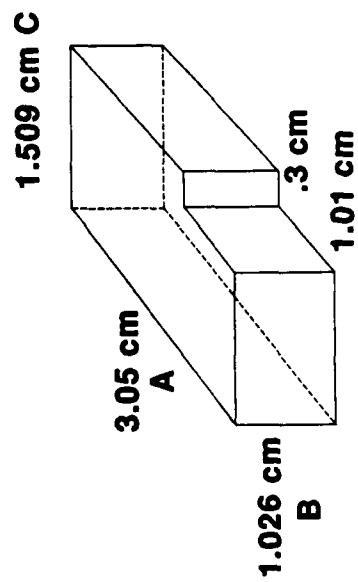
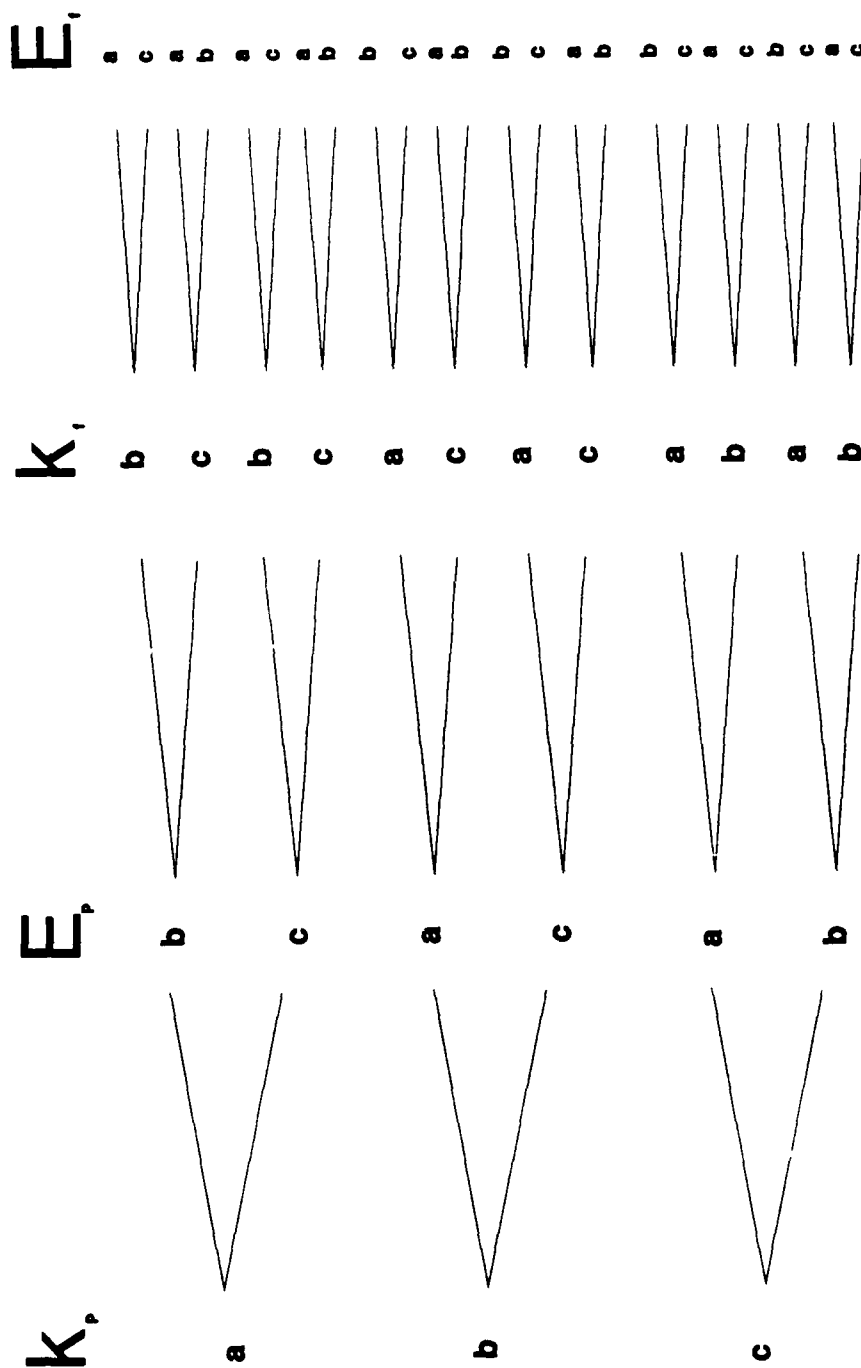


**Figure 1: Diagram of the Ti:YAlO Crystal**

**Figure 2: Crystal Pumping Configurations**

$k_p$  = pump beam direction       $E_p$  = pump beam polarization  
 $k_f$  = fluorescence direction       $E_f$  = fluorescence polarization



# A Comparison of a Standard Thermometer, a Temperature Controller, and a Temperature Meter

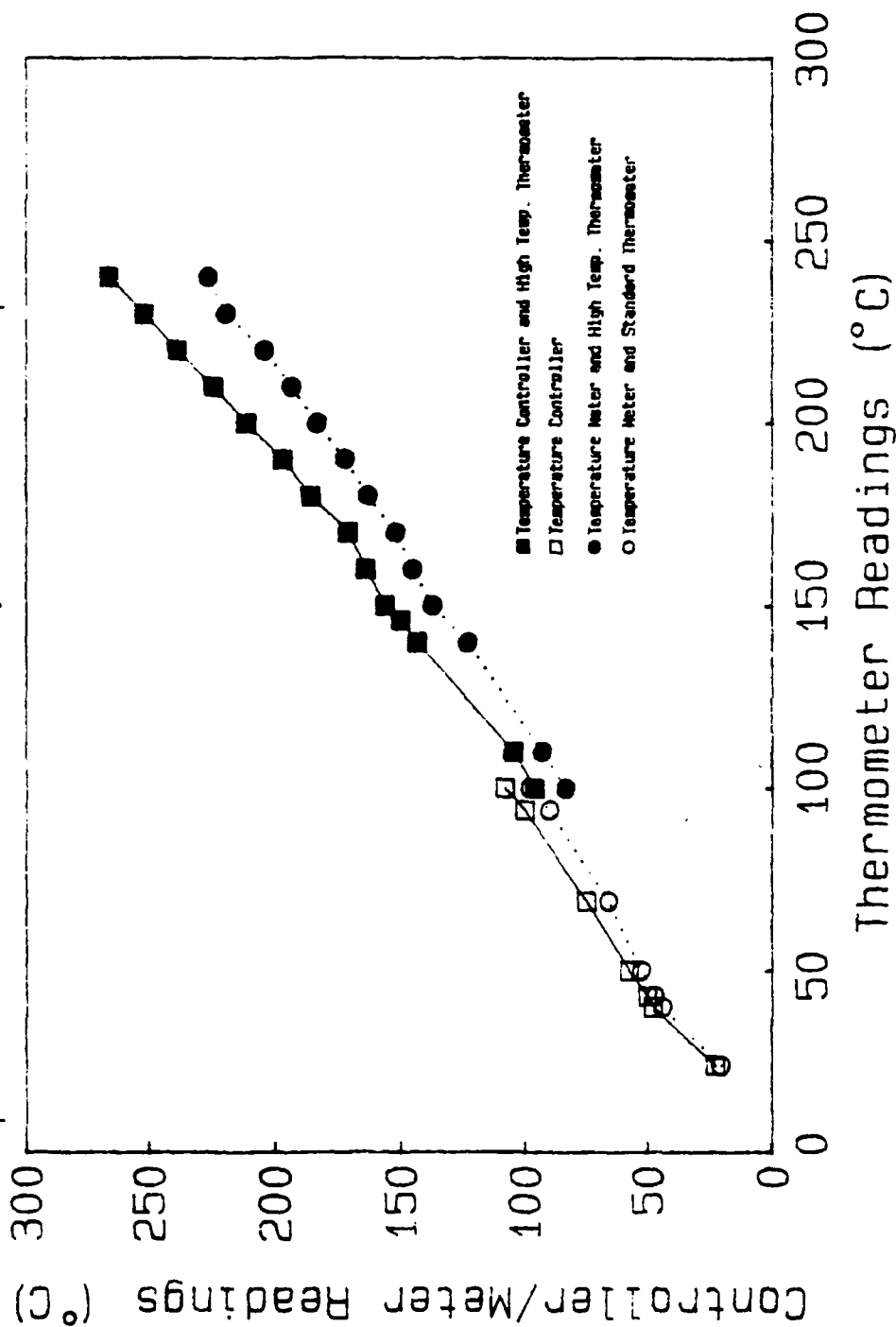


Figure: 3

**Figure 4: An example of Fresnel Loss calculation**

$$R = (N - n)^2 / (N + n)^2$$

**N = Refractive Index of the Atmosphere**

**n = Refractive Index of Ti:YAlO<sub>3</sub>; Ell<sub>a</sub> = 1.97**

**Ell<sub>b</sub> = 1.96**

**Ell<sub>c</sub> = 1.94**

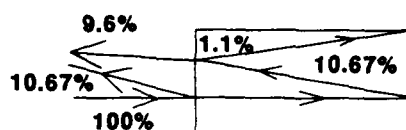


**Diagram of a laser beam going  
through the Ti:YAlO<sub>3</sub> crystal**

$$\begin{aligned} \text{Ell}_a &= (1 - 1.97)^2 / (1 + 1.97)^2 = .1067 \\ &= 10.67\% \end{aligned}$$

$$10.7\% + 9.6\% = 20.3\%$$

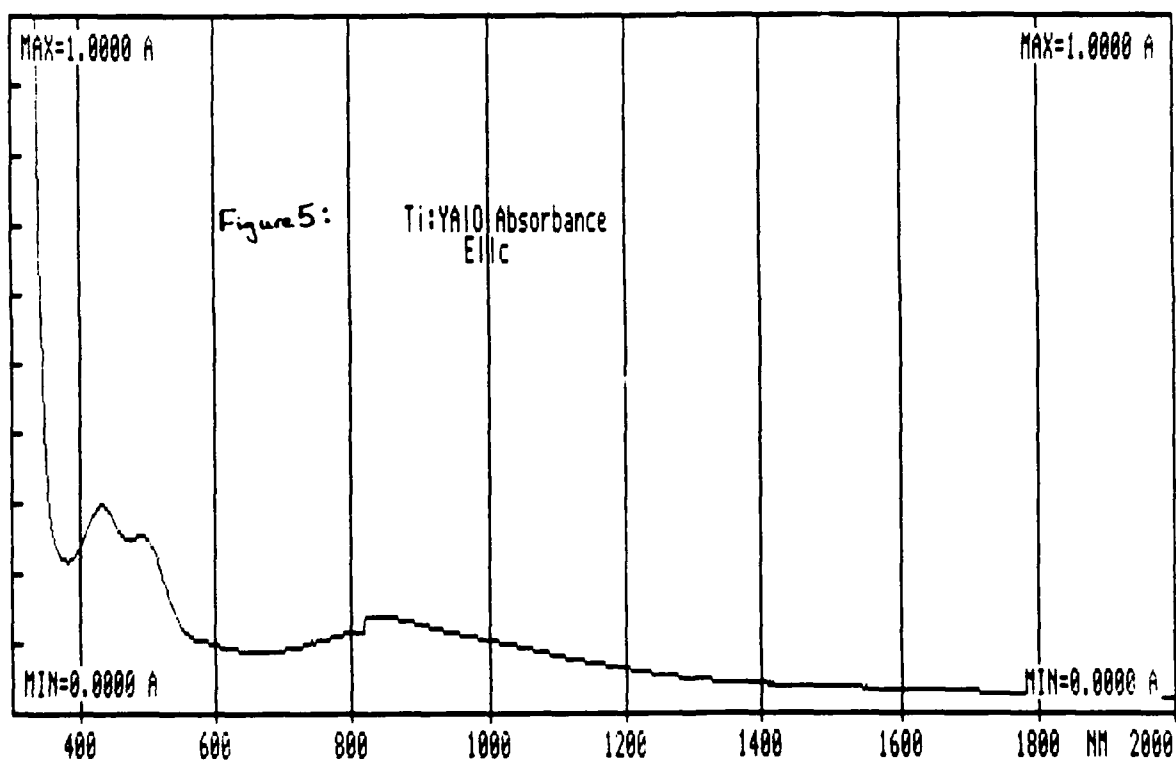
$$100\% - 20.3\% = 79.7\%$$

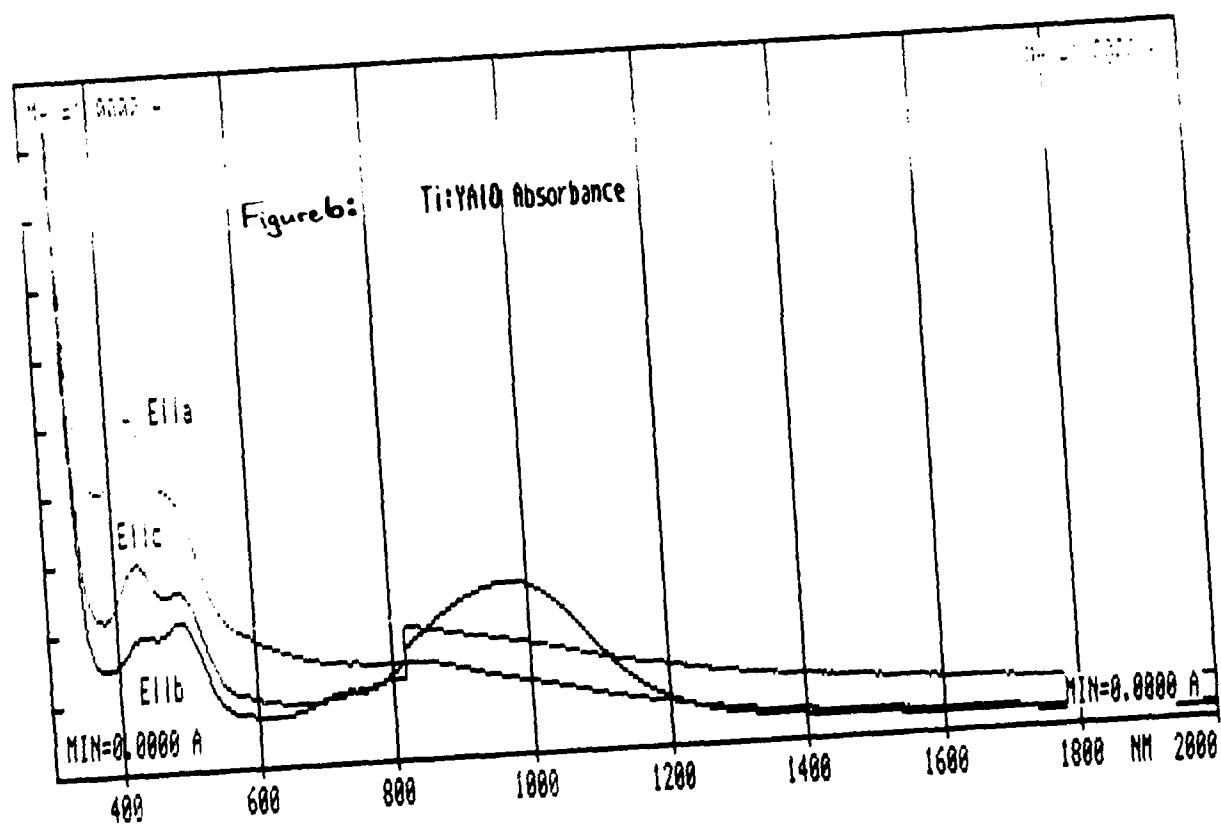
$$\text{FRESNEL LOSS} = -\log(.797)$$

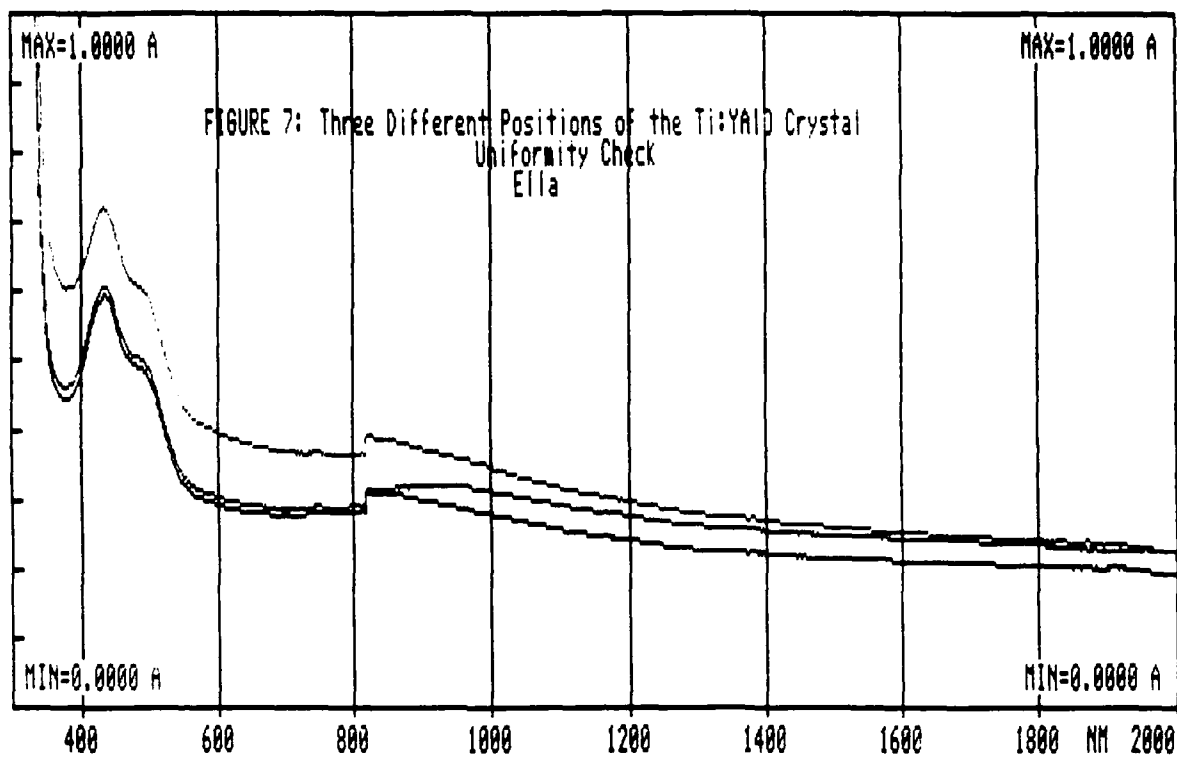
**CORRECTED ABSORBANCE**

$$= X - \text{FESNEL LOSS}$$









# TI:YALO ROOM TEMPERATURE FLUORESCENCE

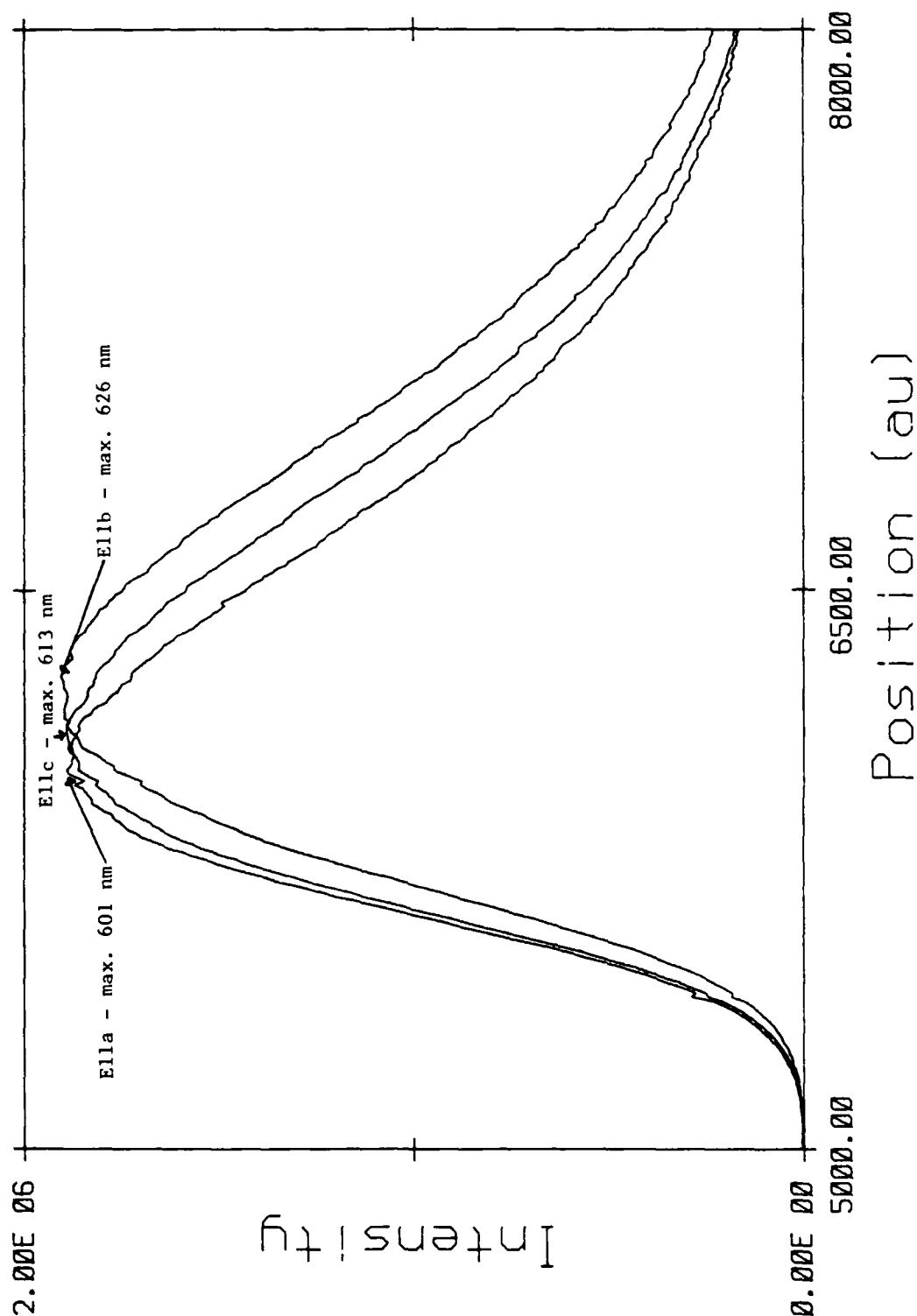


Figure 8

— TI:YALO FLUORESCENCE AT VARIOUS TEMPS

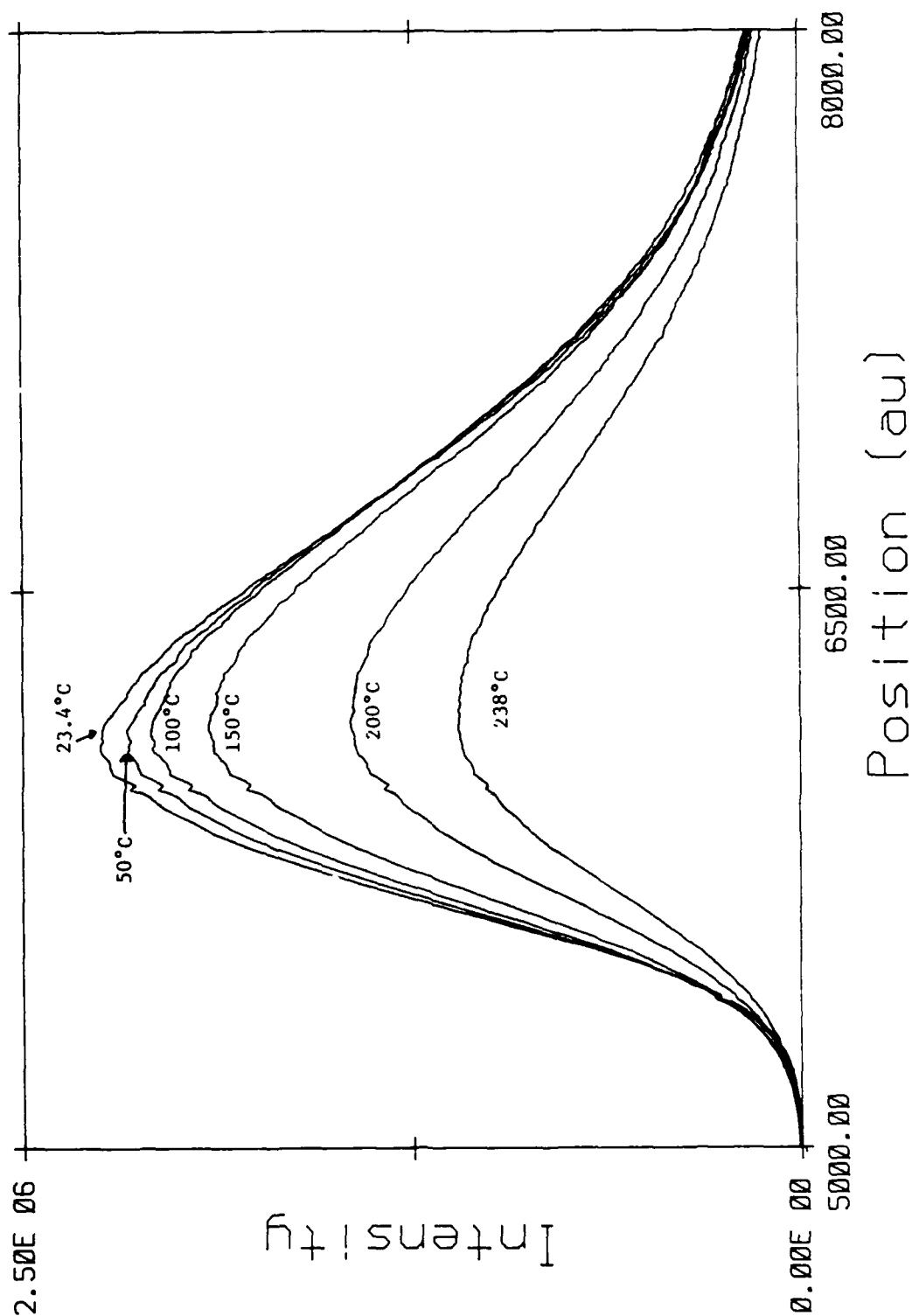
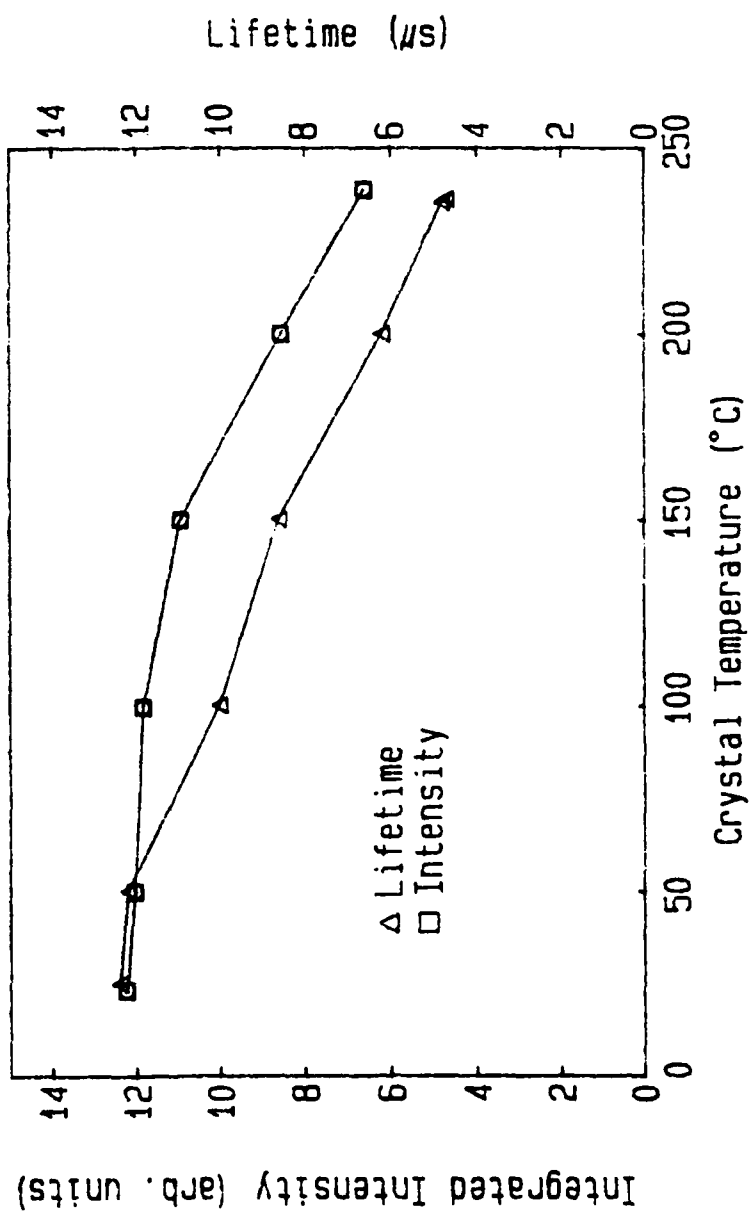


Figure 9

Figure : 10  
 Ti: YAlO<sub>3</sub> Fluorescence Lifetime and Integrated Intensity  
 High Temperature Measurements



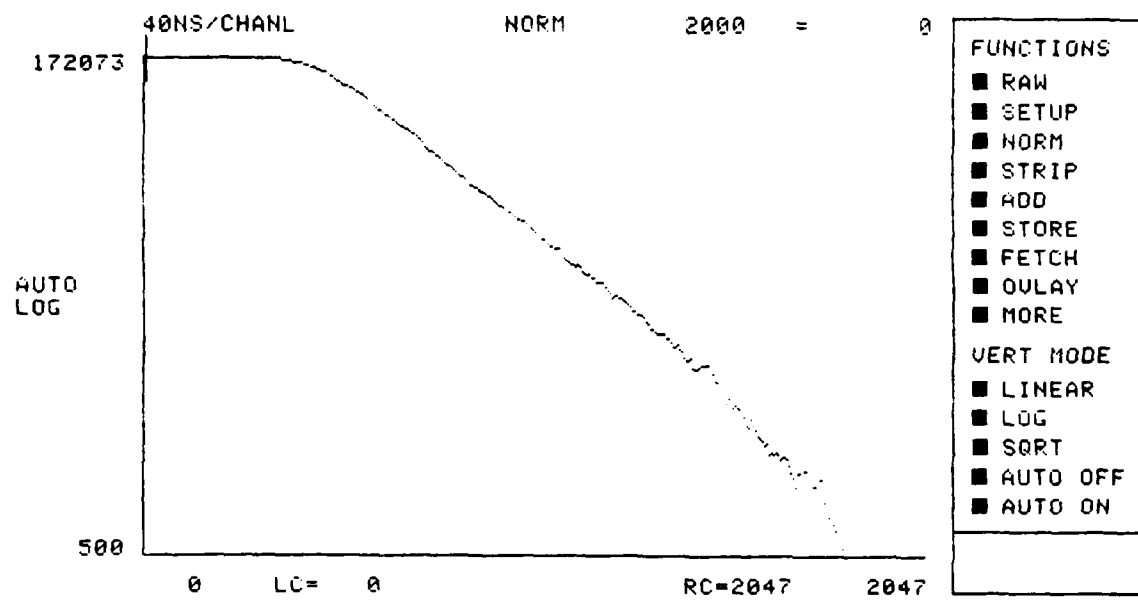


Figure 11: Ti:YAlO at 50°C Fluorescence Lifetime of 12.2  $\mu$ s.

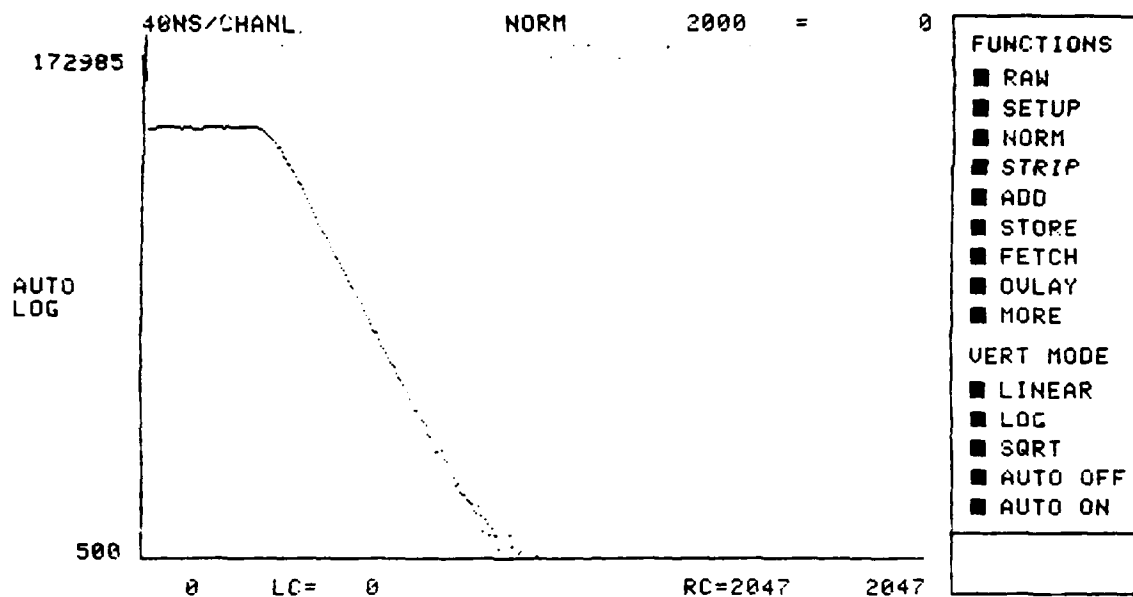


Figure 11: Ti:YA10 at 235°C Fluorescence Lifetime of 4.8  $\mu$ s.



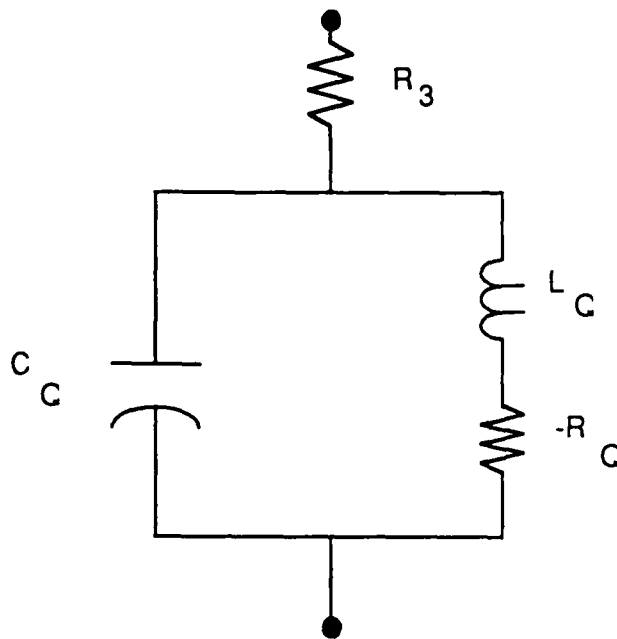
*The Research and  
Development Division*

*WRDC/ELRD*

*Presented to  
Universal Energy Systems*

*By  
Renee Roesner  
August 14, 1989*

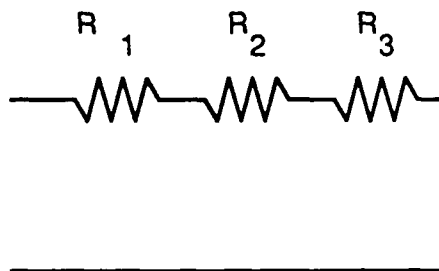
**INTRODUCTION:** The Electronic Technology Laboratory's Research Division employs dedicated workers and has a state-of-the-art clean room that contains sophisticated equipment. The team of scientists and technicians research and develop advanced electronic devices using elements from columns III and V of the periodic table such as Gallium (Ga) and Arsenic (As). This type of research is possible because of recent advances in crystal growth technologies. One of these, Molecular Beam Epitaxy (MBE), allows precise control of the doping (number of impurity atoms per square cm) and thickness of ultra-thin high quality crystal layers. Growth of semiconductor crystals with alternating layers of different materials is possible, allowing researchers to design electronic devices using synthetic or man-made crystals with properties not available from natural semiconductors. One of these novel electronic devices is the resonant tunneling diode (RTD) which is the research area of my mentor. He extracted an equivalent circuit of his diodes to study the high frequency characteristics.



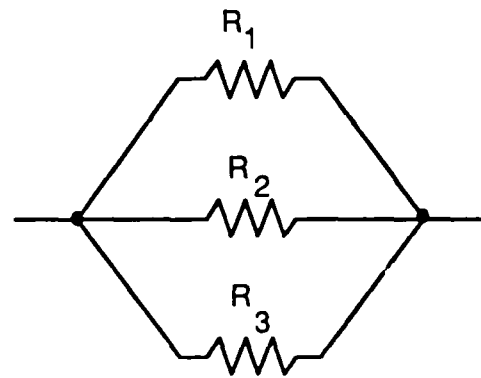
This study resulted in a presentation and publication in the IEEE/CORNELL conference. My project was to learn and assist my mentor in his research efforts.

**OBJECTIVE:** To learn about semiconductor processing of RTDs in WRDC/EL Device Research facility. To meet this objective, I worked in these areas: basic circuit theory and some important wafer processing steps; cleaning, developing, and etching.

**OBSERVATIONS:** To understand the operating principle of RTDS and other electronic devices, I studied basic circuit theory. My mentor showed and explained the different kinds of circuits and its components. I learned about Ohm's law, capacitance and the difference between parallel/series circuits.

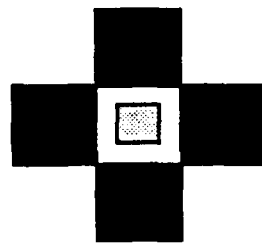


Series circuit

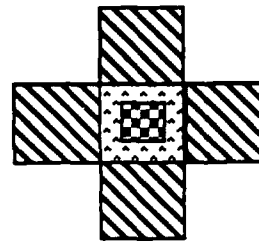


Parallel circuit

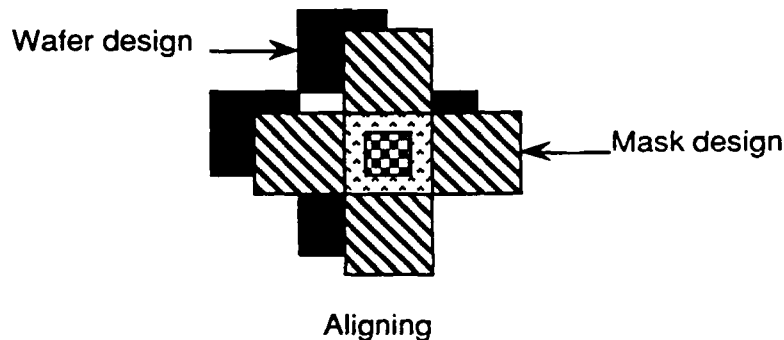
After the overview of basic circuits, I learned some of the processing steps needed to make RTDs. Specifically, I learned three of the more critical steps. The first and most critical step is the cleaning of the wafer. To insure reproducibility and performance, the wafer must be kept perfectly clean. The effort of maintaining a class 100 facility (100 particles with a diameter of  $.5\mu\text{m}$  or greater ) would be wasted if the wafers were not kept as clean as possible. Any particles such as dust or pollen must be removed. The cleaning step involves using a series of solvents to remove any particles or organic matter present on the wafers surface. The first solvent, Acetone, is the strongest and removes almost all of the contaminants. Methanol is used next to remove the Acetone which would contaminate the wafer surface if it was allowed to dry. Finally, Isopropyl removes the Methanol. The wafer can be safely blown dry with pure nitrogen gas with isopropyl on the surface. The cleaning process is done on a machine called a spinner. The wafer is held into place with a vacuum on a chuck, a platform that the wafer is laid on, in the center of a basin which catches the liquid that is spun off. The chuck can be rotated at speeds ranging from 100 to 6000 rpm. The spinning action improves the cleaning. The solvents are sprayed onto the wafer while it is spinning.. It is then blown dry with the nitrogen mentioned above. The next most critical step is applying, exposing and developing photoresist. Almost every other step involves the use of photoresist on the wafers. The devices are built using a series of steps requiring photoresist. First of all, the wafer is covered with photoresist and baked for thirty minutes at 90 C in an oven in the clean room. After it cools in the dry box, it can then be put on the mask aligner. The mask aligner is a machine that aligns the wafer with the mask design ( see on next page ).



Wafer design



Mask design



When the mask is perfectly aligned or close to perfect, the operator of the machine pushes the exposure button and exposes the photoresist that was not protected by the mask. The photoresist that is exposed washes away when developed. The final step that I learned was the etching of wafers in phosphoric acid. The purpose was to test the etching rate to see how deep the etchant went. The procedure is as follows: the wafer is placed in a plastic holder and then immersed in the etchant for four seconds, after those four seconds, it is removed from the acid and placed in Deionized water (extremely pure ) to wash off the acid. It is then blown dry by nitrogen gas. The wafer is then measured, which I will write about in the next paragraph, and etched again.

The last area that I worked in was the measuring of wafers with the Mercury Probe and a Keithly work station. After every etch, the wafer is placed on the probe. The

Mercury Probe is machine that has a platform with a hole in the center where mercury, when the switch is turned on, will come out and make contact with the wafer thereby creating a vacuum and having good conductance with the wafer. Then the operator uses a program that measures the depth of the etching and compares the depth and the doping by producing a graph (p. 6 ). The computer will then print out the graph. By this information you can figure out the etching rate. The procedure of etching is then repeated until it has reached the depth desired.

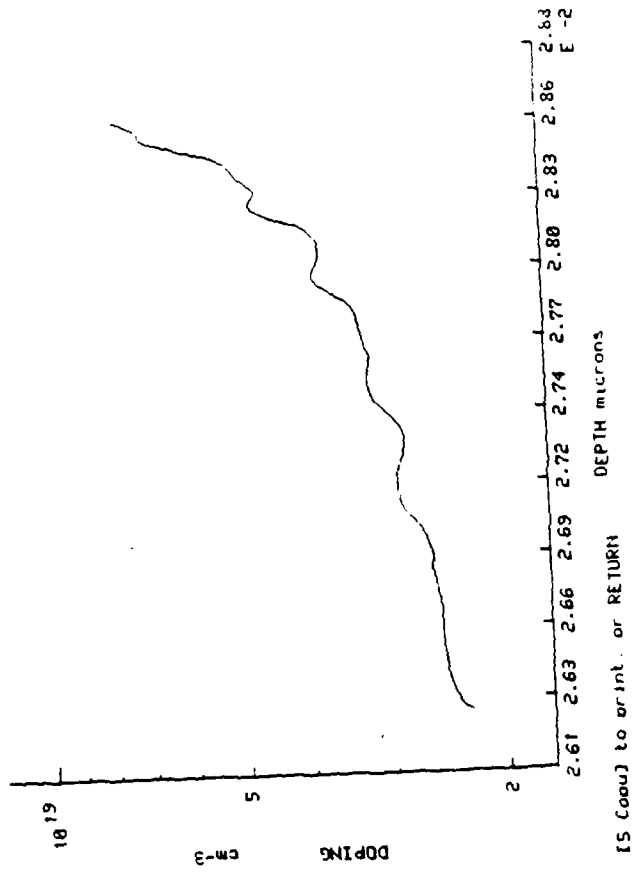
In addition to the areas mentioned, I helped prepare the publication and presentation of my mentor's paper for the IEEE/CORNELL Conference on Advanced Semiconductor Devices and Circuits. In the back of the report, you will find some examples of my view graphs and drawings I made on the Macintosh computer.

**ACKNOWLEDGEMENTS:** The opportunity to work in a professional engineering atmosphere has been an interesting and rewarding experience. For this I have to thank Lt. Michael Paulus, Captain Chris Bozada, Belinda Johnson and the rest of the Research Division.

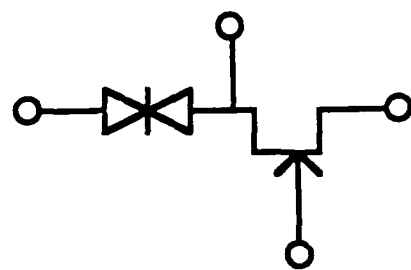
300 Å

# DOPING ETCH DATA 4 SEC

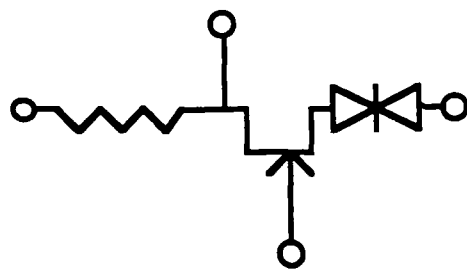
H89B



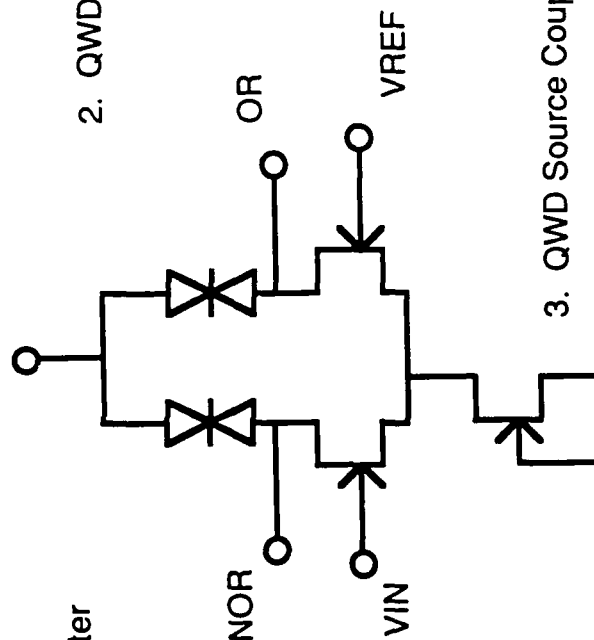
# PROPOSED DIGITAL GATES



1. QWD Inverter



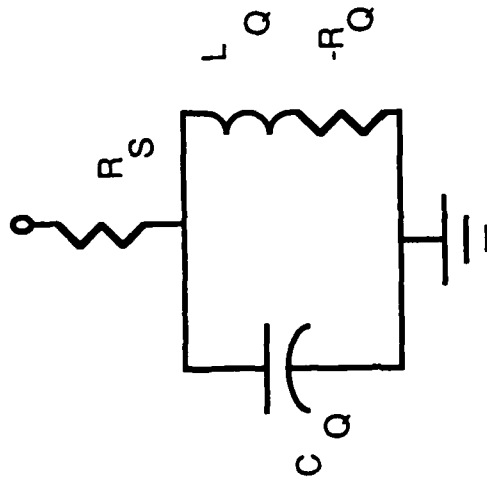
2. QWD Flip Flop



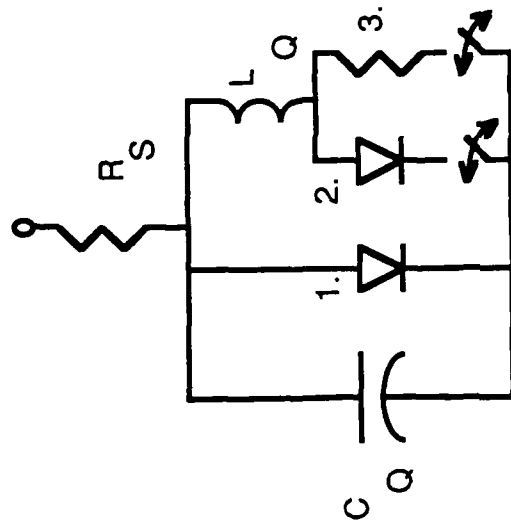
3. QWD Source Coupled Gate



## QUANTUM WELL DIODE MODELS



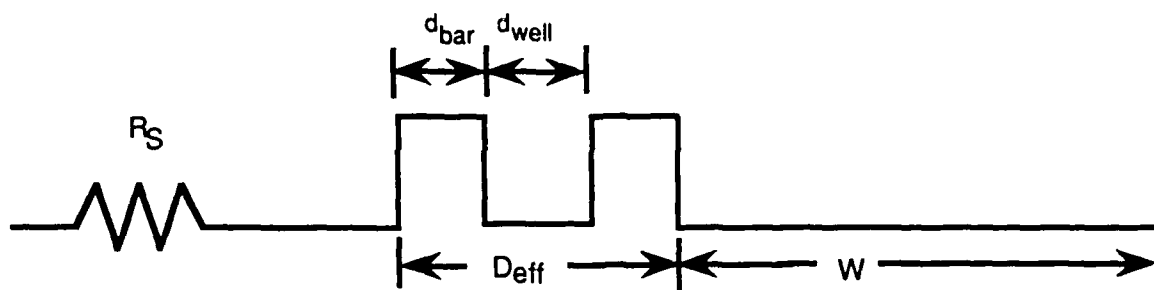
Negative resistance  
Small Signal  
Model



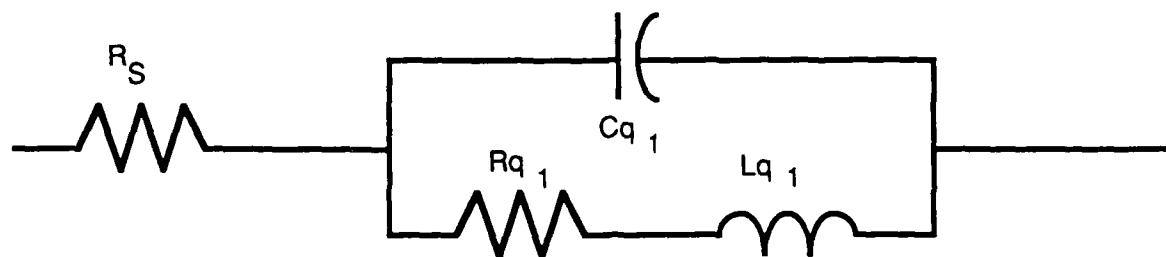
Schematic of  
Large Signal  
SPICE Model

- 1) Non Resonant tunneling current
- 2) Positive resonant conductance
- 3) Negative resonant conductance

# QWD or QWITT

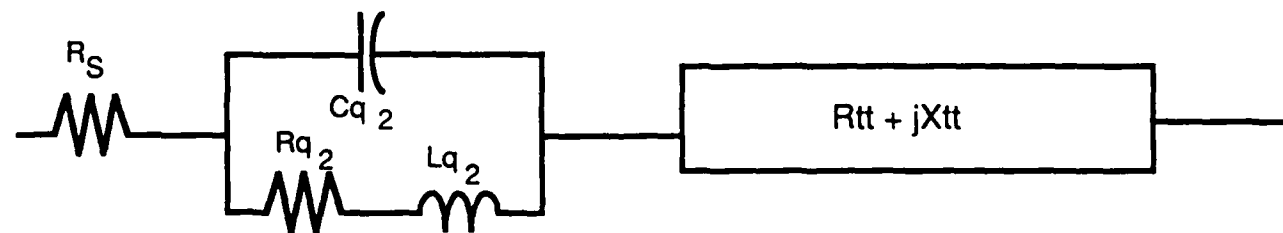
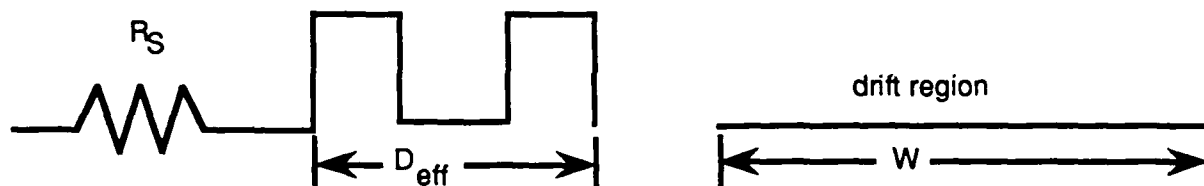


## QWD



(a)

## QWITT



(b)

# **QUANTUM WELL DIODE - FIELD EFFECT TRANSISTOR DIGITAL CIRCUIT STUDY**

**BRIEFER:** Lt. Michael Paulus

**CONTRIBUTORS:** Lt. Eric Koenig  
Dr. Dennis Whitson

**RELATED CONTRACT:** AFOSR Research Fellowship to Dr. Whitson

**OBJECTIVE:** Incorporate quantum well diodes into circuits employing existing device technology in order to evaluate quantum well diode usefulness as a circuit element.

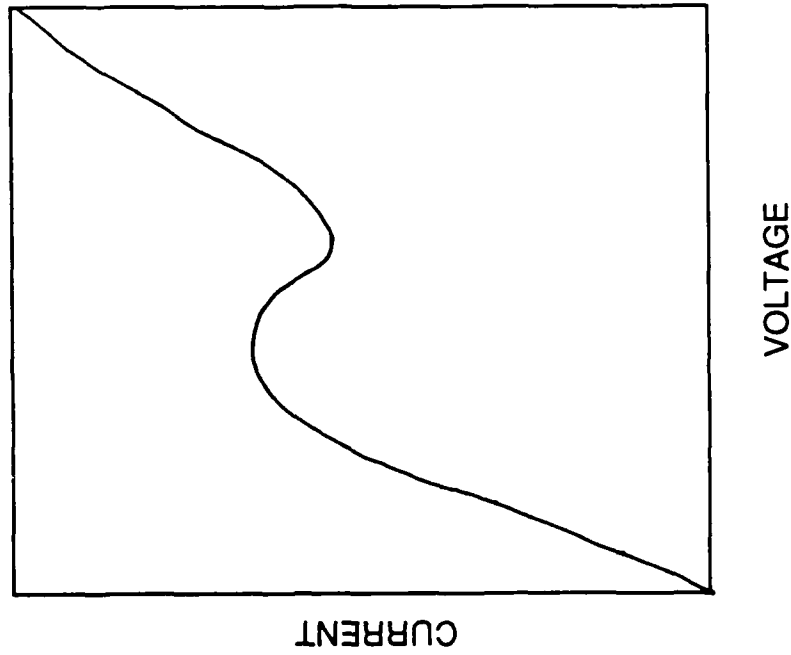
## SIGNIFICANT ACCOMPLISHMENTS

- Demonstrated circuit feasibility using discrete circuit elements.
- Developed SPICE model for quantum well diode.
- Proposed a novel small signal model
- Fit model parameters to measured *r.f.* reflection coefficients with 0.4% error function.
- Abstract describing the small signal model was accepted for the 1989 IEEE/Cornell Conference
- Designed New Mask Set (Received May 1989)
- Fabricated Working QWD-FET gates

## BACKGROUND

- For the last 3 years, ELRD has studied Physics of quantum well diodes
  - Hold world record for GaAs/ AlGaAs peak to valley ratios
  - Developed physical first principle numerical model
  - Characterized quantum states using thermionic emission theory
- This task studies applications for quantum well diodes
  - Quantum well diode design requirements for high speed digital circuits
  - Potential circuits whose performance would be improved by the use of quantum well diodes

## WHY USE A QUANTUM WELL DIODE ?

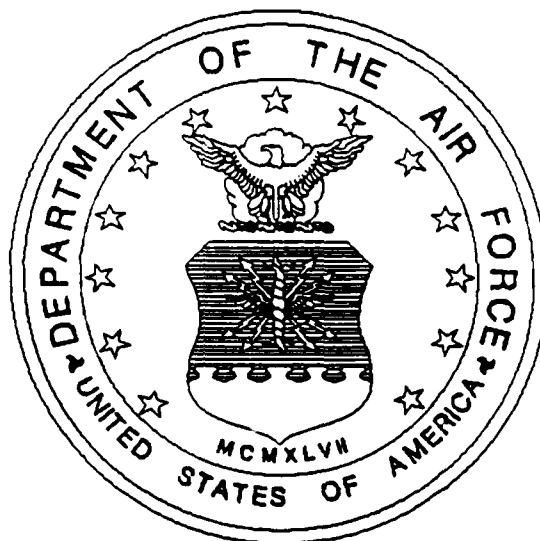


- Negative resistance
  - Useful as r.f. oscillator
    - State of art    420 GHz
    - ELRD            40 GHz
- Tunneling mechanism switches very quickly
  - State of art    ~ 0.1 ps
  - ELRD           ~ 6.0 ps
- NDR Introduces hysteresis useful for improving digital noise margin

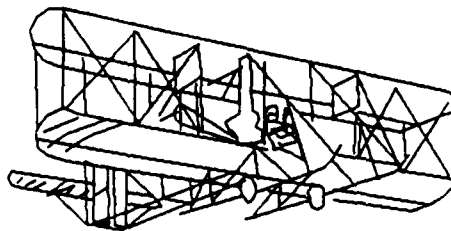
# **AFOSR**

## **High School Apprenticeship Program**

### **WRDC/AAAF-3**



**Final Report**  
**Summer 1989**



**Apprentice : Jerard Wilson**  
**Mentor : Captain Marc J. Pitarys**  
**WPAFB, OH**

### Acknowledgements

I gratefully acknowledge the contributions of the following people, all of whom were of great assistance in my summer success: Capt. Marc J. Pitarys, Kenneth Littlejohn, Bob Harris, Jimmy Williamson, Creshanna Workman, Maddie Tillman, and everyone else in the WRDC/AAAF-3 branch and at UES who helped get the program on it's feet.

Naturally, one of the above persons stood out from the rest; of course it was none other than Capt. Pitarys, whose unyielding time, patience, energy and guidance was greatly received.



## Table of Contents

- I. Acknowledgements
- II. General Description of Research
- III. Detailed Description of Research
- IV. Observations
- V. Bibliography
- VI. Appendixes

## General Description of Research

I began work with the Software Concepts Group (AAAF-3) under the Air Force Office of Scientific Research High School Apprenticeship Program. During my time there I assisted my mentor, Capt. Marc J. Pitarys, in evaluating Ada compilers, and in addition, I worked with computer graphic design tools since I have had classes in Computer Aided Design. I have learned to work with various systems and have gained more experience in word processing and computer programming (especially since my previous experience was very limited). All in all, I feel I have done my part in contributing to the Software Concepts Group mission. (See Appendix I.)

## Detailed Description Of Research

Since everything in my division revolves around Ada, it was necessary to learn many aspects of the language - even its history. Ada is a high level programming language designed for embedded computer systems and based upon a set of specific language requirements. I started learning about the language itself by reading from a Grady Booch book Software Engineering with Ada. After learning about some of the basic traits of Ada programs, I was on my way to writing simple programs based upon flowcharts. This skill was further enhanced when my mentor taught me how to take a flowchart (or program) written in some other language (i.e. FORTRAN or BASIC) and use its structure to write an Ada program. After completing and editing a program, one must compile it. I quickly learned to do this and even learned how to debug a program to find out exactly where the problem occurs. Thus my mentor was an "Ada teacher" for the first part of the summer, until we received an instructional program called Ada-Tutr. Ada-Tutr, by John Herro, PhD, is interactive software that teaches Ada to beginners. Though the first part of Ada-Tutr was review, the package proved to be very helpful in assisting me to write more complicated programs and grasp a better understanding of Ada. When not writing, editing, or compiling programs, I assisted my mentor in evaluating different Ada compilation systems. I was given the chance not only to run evaluation programs but also to take data derived from various sources and compute and graph measurements.

This data was sent to other Air Force organizations to aid them in making decisions concerning compilers which use Ada in embedded computers. My work on this project was not only a learning experience, but also a real contribution to the Air Force. During this time, another apprentice, Amy Listerman, and I helped out with the new revised Dhrystone Benchmark program and helped to run the program for the very first time since its revision! These two activities really let me know my work does help help the DoD. Through using such graphic tools as Harvard Graphics, I was able to make wonderful charts, graphs, lists, and images efficiently for some of the many presentations that my mentor gave or will give. I have even made a branch slide show for my mentor which saved him time, therefore allowing him to labor in areas of higher priority. Although I cannot explain the complete importance of Harvard Graphics, it was a necessity for my job. Other packages, such as wordstar, helped to make my job worthwhile. Wordstar is a highly flexible and very visible word processing package. In the middle of the summer, I began to work on a higher release of Wordstar, Wordstar 4, which had even more speed and versatility as the previous version. Because of Wordstar, I can now type and edit any kind of text (i.e. letters, reports, memos, etc.). My only setback with this is that I don't have a computer at home, therefore, I can't use Wordstar for school. Lastly, I worked on the supreme system for personal computing, OWL Company's Guide hypertext (more complicated than word processing) ,a high-speed, automated way of browsing through information making the use of windows the utmost value. With

this, Amy Listerman and I created, from scratch, hypertext for the F-16 Fire Control Computer.

## Observations

This summer has been one of fun, hard work and learning. Again I am glad to have taken part in the AFOSR High School Apprenticeship Program. The time and effort allotted for my participation and advancement this summer has definitely paid off. This is just the start of a long life dedicated to the scientific field, and I look forward to returning as a third year apprentice and gaining that extra boost of knowledge and work-force experience.

## Bibliography

Birns, Peter, Brown, Patrick, Muster, John, UNIX for People,  
Prentice-Hall, Incorporated, Englewood Cliffs, New Jersey, 1985.

Booch, Grady, Software Engineering with Ada, The  
Benjamin/Cummings Publishing Company, Reading, Massachusetts,  
1983.

Herro, John S., PhD, Ada-Tutr, Software Innovations  
Technology, 1988.

## Appendix I

The Software Concepts Group mission is:

To perform research, development, assessments, and evaluations in software technologies for advanced-capability, supportable avionics systems. To provide a center-of-excellence of knowledge and software engineering practices associated with real-time, embedded computers. To provide the Air Force with quality avionics software that is mission-supportable throughout its lifecycle by combinations of in-house research and contracted efforts. To establish software science for advanced avionics architectures. To support logistics engineering concepts for software using technology innovations and state-of-the-art practices. To perform research in the following areas: software tools and engineering environments, operational flight programs, computer aided software engineering, Ada language, reusable avionics software, fault-tolerant reusable software, reliability, and compiler evaluations.

---



# Appendix II

WITH TEXT\_IO; USE TEXT\_IO;  
PROCEDURE HYDROCARBON IS

PACKAGE MY\_FLOAT IS NEW FLOAT\_IO(FLOAT);  
USE MY\_FLOAT;  
PACKAGE EGER\_IO IS NEW INTEGER\_IO(INTEGER);  
USE EGER\_IO;

Z : CHARACTER := 'Y';  
COUNT : NATURAL;  
C, E, H, N, O, S : FLOAT;  
O2, A, A1, F, M : FLOAT;  
C2, S2, H2, O3, N2 : FLOAT;  
HP4 : FLOAT;

BEGIN

FOR II IN 1 .. 21 LOOP  
NEW\_LINE;  
END LOOP;  
PUT\_LINE("THIS PROGRAM COMPUTES THE PERCENTAGES OF THE PRODUCTS");  
PUT\_LINE("PRODUCED BY HYDROCARBON COMBUSTION .");  
NEW\_LINE;  
LOOP  
PUT\_LINE("FOR INSTRUCTIONS TYPE Y FOR YES AND N FOR NO --> "); GET (Z);  
SKIP\_LINE;  
IF Z = 'N' THEN EXIT; END IF;

PUT\_LINE("THE AMOUNT OF EACH ELEMENT MUST BE ENTERED IN FLOATING POINT");  
PUT\_LINE("NUMBERS, EVEN IF THE AMOUNT IS ZERO. FOR EXAMPLE: ");  
PUT\_LINE("METHANE(CH4) MUST BE ENTERED AS C--> 1.0, H--> 4.0");  
PUT\_LINE("O--> 0.0, S--> 0.0, N--> 0.0 ");  
NEW\_LINE;

END LOOP;

LOOP

PUT("REMEMBER THAT ALL NUMBERS ARE FLOATING POINT!"); NEW\_LINE;  
PUT(" "); NEW\_LINE;  
PUT(" "); NEW\_LINE;  
PUT("ENTER CARBON(C) --> "); GET (C);  
PUT("ENTER HYDROGEN(H) --> "); GET (H);  
PUT("ENTER OXYGEN(O) --> "); GET (O);  
PUT("ENTER SULFUR(S) --> "); GET (S);  
PUT("ENTER NITROGEN(N) --> "); GET (N);  
PUT(" "); NEW\_LINE;  
PUT(" "); NEW\_LINE;  
PUT(" "); NEW\_LINE;  
PUT(" ENTER THE PERCENTAGE OF EXCESS AIR, AND IF IT IS ZERO PUT 0.0;");  
PUT("FOR EXAMPLE: 34% WOULD BE ENTERED AS 34.0 -->"); GET (E);  
NEW\_LINE;

E := 1.0 + (E / 100.0);  
O2 := C + S + (H / 4.0) - (O / 2.0);  
A := O2 \* E \* 4.762;  
A1 := 1.8094 \* A;

```

F := (0.7507 * C) + (0.063 * H) + (2.004 * S);
F := (0.875 * N) + O + F;
A1 := A1 / F;
M := A + (HP4) + (O / 2.0) + (N / 2.0);
C2 := (C * 100.0) / M;
S2 := (S * 100.0) / M;
H2 := (H * 100.0) / (2.0 * M);
O3 := (100.0 * (E - 1.0) * O2) / M;
N2 := (100.0 * ((3.762 * E * O2) + (N / 2.0))) / M;

```

```

PUT("THE AIR-FUEL RATIO WITH RESPECT TO MOLES = "); PUT (A); NEW_LINE;
NEW_LINE;
PUT("THE AIR-FUEL RATIO WITH RESPECT TO MASS = "); PUT (A1); NEW_LINE;
NEW_LINE;
PUT("THE TOTAL MOLES OF THE PRODUCT = "); PUT (M); NEW_LINE;
NEW_LINE;
PUT(" ***** PERCENTAGE VOLUME OF PRODUCTS ***** "); NEW_LINE;
PUT("CARBON DIOXIDE = "); PUT (C2); NEW_LINE;
PUT("SULPHUR DIOXIDE = "); PUT (S2); NEW_LINE;
PUT("WATER = "); PUT (H2); NEW_LINE;
PUT("OXYGEN = "); PUT (O3); NEW_LINE;
PUT("NITROGEN = "); PUT (N2); NEW_LINE;
PUT(" ***** COMPLETE COMBUSTION ASSUMED ***** "); NEW_LINE;

```

```

PUT_LINE("DO YOU WANT TO TRY ANOTHER COMPOUND. Y OR N?");
GET(Z);
SKIP_LINE;
IF Z = 'N' THEN EXIT; END IF;

```

```

END LOOP;
FOR III IN 1 .. 21 LOOP
  NEW_LINE;
END LOOP;
  PUT("THANK YOU AND HAVE A NICE DAY!");

```

```

END HYDROCARBON;

```

**ENGINEERING AND SERVICE CENTER**

A 'Lowly' Student's  
Summer Job

Student, Greg Dixon  
Mentors, Cpt. D. Miller  
Jim Murphy  
RDCS/RDCP  
Aug 11, 1989

Acknowledgements:

To: Jim Busi  
Charlie Smith  
Drew Bareiss  
Jim Murphy  
and  
Daryll

For all the rides, tips, and stories.

This summer I spent eight weeks as an apprenticeship student. I worked for the Air Force Office of Scientific Research High School Apprenticeship Program at Tyndall Air Force Base, FL.

My first mentor was to be Capt. Diane Miller. She introduced to my work place and the people I would be working with. After a few days, Capt. Miller let me begin to work for Jim Murphy. There was not enough work in Capt. Miller's department at the time to make sufficient use of me, and Mr. Murphy's project had several tasks that could use my assistance. So, after three days, I was transferred to the area I'd be spending the rest of my summer in.

Mr. Murphy's project was the study of the effect of simulated aircraft loading (F-4's and F-15's) on asphalt concrete pavement. There were many aspects to this study and I was to carry out one of them. I was to weigh trafficked pavement cores in air and water to obtain their densities and compare these densities to the densities of non-trafficked pavement cores. This study and the resulting theories are explained in the enclosed report that thoroughly covers the majority of my eight weeks work.

After this portion of the study was completed, I then participated in the tasks of involved with recording Multi-Deflectometer-Detector(MDD) readings from a section of test pavement that was currently being trafficked. An MDD measures the amount of deflection (bend or give) that occurs in some pavement when a vehicle runs over it or very near it. It measures in thousandths of inches and is a very delicate device. We suffered many problems with the devices due to bad weather conditions and the stress of trafficking.

The loadcars used were not an average 'vehicle'. They were large diesel trucks weighed down with blocks of lead. This was to make the weight placed upon its 'load' wheel (an actual F-4 or F-15 tire) equivalent to that of an F-4 or an F-15. The heavier load car weighed actually 30,000 lbs, just on the loadwheel!

The task of MDD recording was quite a menial task, but still a necessary one. It consisted of manning a computer program outside at the test pad and setting the MDD to record the next desired pass. It was not a difficult task, but one absent of any other possible operator than a human.

So, this was how I spent my last weeks at Tyndall. It wasn't a bad job and I still continued to learn things. And considering the eight weeks of employment as a whole, I learned some invaluable things while gaining irreplaceable, useful work experience.

The report of the core study follows. It describes in detail what I did for the majority of the eight weeks.

Theorized Effects of  
Simulated Aircraft Loading  
on the density of  
Asphalt Concrete Pavements

Student  
Greg Dixon  
Aug 10, 1989  
RDCP

The comparison of the bulk specific gravity and density of pretraffic cores and posttraffic cores is a necessary step in determining the effects of simulated aircraft loading on asphalt concrete pavements. Many separate steps are required in such a study. Drilling cores, determining and identifying various significant aspects of the pavement such as asphalt content, percent fines, percent air voids, etc, that effect the BSG (Bulk Specific Gravity) and density, and the actual determining of the BSG and density of the cores are of few of the necessary tasks. The following is a paraphrase of the test method used for finding the BSG and density of the pavement cores as determined in the 1986 Annual Book of ASTM Standards (D2726-83).

Once the necessary cores were acquired, each core was weighed after having had enough time to cool or warm up to room temperature (25°C, 77°F). This weight is called the "in air" weight and will be referred to as weight A.

The cores were then immersed in a tub of water equipped with an overflow outlet for maintaining a constant volume. After 2 to 3 minutes of immersion, the weight of the core still in water was recorded. This weight is called the "in water" weight and will be referred to as weight C. The temperature of the water was also a factor. The ideal temperature of the water was 25°C. If the temperature varied from that desired one by more than one degree (which it did), a conversion factor was to be utilized to correct the BSG.

Immediately after the "in water" weight was recorded, the cores were taken out of the water and blotted dry with a towel. They were then placed on the scale and the core's "saturated surface-dry" weight was recorded. This weight will be referred to as weight B.

This concluded all the necessary weighing. The next step was to calculate the cores' BSGs from the three different weights. This was done using the following formula:

$$\text{Bulk sp gv} = A / (B - C)$$

where:

- A = mass of dry core in air
- (B-C) = mass of water absorbed by core
- B = weight of saturated surface-dry core in air
- C = weight of core in water

This formula produces an absolute number with no units (specific gravity). So, it must be converted to density in order for it to be used in calculations that require units. This conversion is made by multiplying the specific gravity at a certain temperature by the density of water at the same temperature.

This test method produced the necessary data for a basis of comparison for pre-traffic and post-traffic cores. The resulting comparisons will hopefully offer explanations of the effects of trafficking on the density of airfield pavements and produce beneficial ideas or insights for future airfield pavements construction.



### Findings:

The only method of comparison that offered rational findings in the change of density after so many passes was a study of individual trucks. This was because different trucks had different asphalt pavement compositions and densities. This meant that each lane could not be studied as a whole since its characteristics changed down the lane (it took six or seven trucks for a lane's construction).

What was found seemed quite logical. As the number of passes increased (within a certain section of pavement as defined by a "truckload of mix") the densities also increased. But the compaction only continued to a point. Then the densities began to decrease.

A popular explanation for that occurrence is that the trafficking would compact the pavement to a point. That is, the trafficking would be compacting the pavement and lowering the amount of voids in the pavement. Eventually, all or mostly all of the voids would be gone and then attempting to compact the pavement more would begin to destroy it. So, as the voids decreased, the density would increase, and then when there were no more air voids to eliminate, the density had reached its maximum.

Attached is the data retrieved for the core weighing, and several graphs that show the trends of density changes already discussed.

At first, the graphs showing the findings of the spreadsheet, which was just a compilation of the data taken from the core weighing, didn't seem to make any comprehensive sense. The line that represented the densities of the cores seemed to wave up and down without much rule.

This was very confusing at first, and at this point it was discovered that a complex curve was evolving due to the complexities of the varying asphalt pavement. Then using the information for lanes one and three concerning the pre-trafficking densities of the pavement, the data was divided into common densities. These were then loosely called "truckloads". This was when the data began to show some signs of order.

The graphs concerning lanes one and three (labeled "as a whole", "individually", and "by 'truckload'") show the development of the data's cohesiveness. The first graph showing the lane "as a whole" shows the wavy, senseless appearing line. Then when the points are examined "individually", certain distinct "groups" may seem discernable. For instance on the graph of the "individual" densities for lane one, a rather distinct group of three points can be seen just above the two-thousand pass mark. That group of points also marks the end of an extreme drop off on the graph showing the lane "as a whole".

The graphs of lane three also show this characteristic. The first "as a whole" graph again shows the densities going up and down and up and down. Then, when once again, examined

"individually", there seems to be "groups" of points. For example, on that graph, the dots seem to be steadily rising until about the three-thousand pass point, after that, three distinct groups are observable. The first three points after the three-thousand mark, the next three (above the four), and the last four points all seem to be similiar.

These groups are not just coincidentally similiar. When the "truckloads" are identified, their starting and ending points superbly match the starting and ending points of these groups. It seemed that anywhere on the graph of the lane "as a whole" there was a drastic change in the determined densities, that was where the next "truckload" began.

The data examined from this new perspective made much more sense. Within individual truckloads, the densities seemed less erratic. When examined from one to next, the densities seemed to be following good wave pattern. On the graph of lane one with densities represented "by 'truckload'", a pattern can be examined when following from one "truckload" to the next.

For example the first "truckload" rises up. The second continues to rise and then to fall. The third continues this downward trend, but seems to begin to level out at the end. The fourth follows this level trend, and the last then begins to rise up again. In other words if the "truckloads" were connected end to end, they would form a rather nice wave. This point of view and resulting information would validate the theory that the trafficking would at first increase the density of the pavement, then decrease the density of the pavement (by destroying it after its maximum density was reached), and then possibly begin to re-densify the pavement and restart the cycle.

This hypothesis is still questionable, but after studying the resulting data from weighing cores, it is the most popular theory and the one this test suggests to be true.

## Density II

3 3  
lbs/ft lbs/ft

| LANE | STATION | CORE | AIR(g) | WATER(g) | SSD(g) | BSG   | DENS   | AVG.DENS | PASSES | TRUCK |
|------|---------|------|--------|----------|--------|-------|--------|----------|--------|-------|
| 1    | 20      | A    | 1247.2 | 732.4    | 1248.6 | 2.416 | 151.01 |          |        |       |
| 1    | 20      | B    | 1730.4 | 1016.6   | 1733.5 | 2.414 | 150.86 |          |        |       |
| 1    | 20      | C    | 1228.3 | 721.4    | 1229.4 | 2.418 | 151.12 |          |        |       |
| 1    | 20      | D    | 1751.1 | 1030.5   | 1757.2 | 2.408 | 150.48 |          |        |       |
| 1    | 20      | E    | 1277.6 | 752.5    | 1278.4 | 2.429 | 151.83 |          |        |       |
| 1    | 20      | F    | 1724.9 | 1018.1   | 1728   | 2.430 | 151.86 | 151.19   | 300    | TK1   |
| 1    | 26      | A    | 1784.6 | 1043.3   | 1790.3 | 2.389 | 149.31 |          |        |       |
| 1    | 26      | B    | 1296.8 | 764.8    | 1297.7 | 2.433 | 152.09 |          |        |       |
| 1    | 26      | C    | 1813.4 | 1064.9   | 1815.6 | 2.416 | 150.98 |          |        |       |
| 1    | 26      | D    | 1276.8 | 755.7    | 1277.5 | 2.447 | 152.93 |          |        |       |
| 1    | 26      | E    | 1806.8 | 1068.2   | 1808.1 | 2.442 | 152.62 |          |        |       |
| 1    | 26      | F    | 1306.1 | 776.3    | 1307.3 | 2.460 | 153.73 | 151.94   | 600    | TK1   |
| 1    | 32      | A    | 1320.4 | 796.4    | 1321.9 | 2.513 | 157.04 |          |        |       |
| 1    | 32      | B    | 1885.3 | 1135     | 1886.2 | 2.510 | 156.86 |          |        |       |
| 1    | 32      | C    | 1900.3 | 1144.3   | 1901.1 | 2.511 | 156.94 |          |        |       |
| 1    | 32      | D    | 1321   | 798.7    | 1321.3 | 2.528 | 157.98 |          |        |       |
| 1    | 32      | E    | 1982.3 | 1193     | 1983.3 | 2.508 | 156.77 |          |        |       |
| 1    | 32      | F    | 1300   | 781.2    | 1301   | 2.501 | 156.31 | 156.98   | 900    | TK1   |
| 1    | 42      | A    | 1331.9 | 805.3    | 1333   | 2.524 | 157.75 |          |        |       |
| 1    | 42      | B    | 2215.5 | 1331     | 2217.4 | 2.499 | 156.21 |          |        |       |
| 1    | 42      | C    | 1333.6 | 805.7    | 1334.8 | 2.521 | 157.53 |          |        |       |
| 1    | 42      | D    | 2203.4 | 1332.2   | 2205.8 | 2.522 | 157.64 |          |        |       |
| 1    | 42      | E    | 1338.1 | 809      | 1339.3 | 2.523 | 157.71 |          |        |       |
| 1    | 42      | F    | 2221   | 1330.9   | 2223.4 | 2.489 | 155.53 | 157.06   | 1200   | TK1   |
| 1    | 56      | A    | 2287.4 | 1333.6   | 2291   | 2.389 | 149.32 |          |        |       |
| 1    | 56      | B    | 1257.7 | 736.7    | 1259.2 | 2.407 | 150.44 |          |        |       |
| 1    | 56      | C    | 2233.6 | 1309.1   | 2242.3 | 2.393 | 149.59 |          |        |       |
| 1    | 56      | D    | 1256.8 | 734.9    | 1257.8 | 2.404 | 150.22 |          |        |       |
| 1    | 56      | E    | 2314   | 1345.5   | 2318.5 | 2.378 | 148.64 |          |        |       |
| 1    | 56      | F    | 1256.5 | 734      | 1257.5 | 2.400 | 150.01 | 149.70   | 1430   | TK2   |
| 1    | 80      | D    | 2411.7 | 1416.9   | 2415.5 | 2.415 | 150.94 |          |        |       |
| 1    | 80      | E    | 1269.5 | 750.8    | 1270.1 | 2.445 | 152.79 |          |        |       |
| 1    | 80      | F    | 2377.9 | 1400.9   | 2380.7 | 2.427 | 151.68 | 151.81   | 1730   | TK2   |
| 1    | 92      | A    | 2254.7 | 1324     | 2256.7 | 2.417 | 151.09 |          |        |       |
| 1    | 92      | B    | 1252.8 | 737.9    | 1253.7 | 2.429 | 151.80 |          |        |       |
| 1    | 92      | C    | 2269.7 | 1327.8   | 2273.4 | 2.400 | 150.02 |          |        |       |
| 1    | 92      | D    | 1251.8 | 731.9    | 1252.9 | 2.403 | 150.17 |          |        |       |
| 1    | 92      | E    | 2252.6 | 1310.4   | 2255.1 | 2.384 | 149.03 |          |        |       |
| 1    | 92      | F    | 1241.8 | 726.6    | 1243.1 | 2.404 | 150.27 | 150.40   | 2000   | TK2   |
| 1    | 104     | A    | 1284.5 | 761.6    | 1285.4 | 2.452 | 153.27 |          |        |       |
| 1    | 104     | B    | 2266.6 | 1349.7   | 2269   | 2.466 | 154.10 |          |        |       |
| 1    | 104     | C    | 2251.7 | 1345.5   | 2253.7 | 2.479 | 154.96 |          |        |       |
| 1    | 104     | D    | 1306.4 | 762.2    | 1307.9 | 2.394 | 149.62 |          |        |       |
| 1    | 104     | E    | 2211.3 | 1319.1   | 2213.6 | 2.472 | 154.51 |          |        |       |
| 1    | 104     | F    | 1292.3 | 775.5    | 1292.7 | 2.499 | 156.17 | 153.77   | 2300   | TK3   |
| 1    | 116     | B    | 1297.7 | 779.9    | 1298.4 | 2.503 | 156.42 |          |        |       |

|   |     |   |        |        |        |       |        |        |      |     |
|---|-----|---|--------|--------|--------|-------|--------|--------|------|-----|
| 1 | 116 | C | 2070   | 1239   | 2073.3 | 2.481 | 155.07 |        |      |     |
| 1 | 116 | D | 1295.2 | 777.4  | 1296.7 | 2.494 | 155.88 |        |      |     |
| 1 | 116 | E | 2091.8 | 1250.8 | 2093.4 | 2.483 | 155.16 |        |      |     |
| 1 | 116 | F | 1302   | 780.9  | 1302.6 | 2.496 | 155.98 | 155.70 | 2600 | TK3 |
| 1 | 128 | A | 1266.7 | 752.5  | 1267.9 | 2.458 | 153.61 |        |      |     |
| 1 | 128 | B | 2004.2 | 1182.9 | 2005.4 | 2.437 | 152.29 |        |      |     |
| 1 | 128 | C | 1266.1 | 749.3  | 1266.7 | 2.447 | 152.94 |        |      |     |
| 1 | 128 | D | 1994.1 | 1180.5 | 1996.2 | 2.445 | 152.79 |        |      |     |
| 1 | 128 | E | 1281.1 | 760.5  | 1282.2 | 2.456 | 153.48 |        |      |     |
| 1 | 128 | F | 2011.9 | 1188.6 | 2013.6 | 2.439 | 152.42 | 152.92 | 2900 | TK3 |
| 1 | 140 | A | 1937.7 | 1129.8 | 1939.8 | 2.392 | 149.51 |        |      |     |
| 1 | 140 | B | 1216.2 | 711.1  | 1218.2 | 2.398 | 149.90 |        |      |     |
| 1 | 140 | C | 1952.5 | 1136.1 | 1956.1 | 2.381 | 148.82 |        |      |     |
| 1 | 140 | D | 1210.7 | 707.7  | 1212.2 | 2.399 | 149.94 |        |      |     |
| 1 | 140 | E | 1968.4 | 1149.3 | 1970.3 | 2.398 | 149.85 |        |      |     |
| 1 | 140 | F | 1196.8 | 700.9  | 1197.9 | 2.408 | 150.50 | 149.75 | 3200 | TK3 |
| 1 | 146 | A | 1941.1 | 1134.2 | 1943.1 | 2.400 | 149.98 |        |      |     |
| 1 | 146 | C | 1202.7 | 699.5  | 1203.4 | 2.387 | 149.17 |        |      |     |
| 1 | 146 | D | 1944.8 | 1131.8 | 1946.2 | 2.388 | 149.25 |        |      |     |
| 1 | 146 | E | 1204.6 | 701.2  | 1205.6 | 2.388 | 149.26 |        |      |     |
| 1 | 146 | F | 1945   | 1132.6 | 1947.4 | 2.387 | 149.19 | 149.37 | 3500 | TK3 |
| 1 | 166 | A | 1928.6 | 1136.1 | 1930.5 | 2.428 | 151.73 |        |      |     |
| 1 | 166 | B | 1930.5 | 1134.2 | 1932.7 | 2.418 | 151.10 |        |      |     |
| 1 | 166 | C | 1961.7 | 1150.1 | 1963.5 | 2.412 | 150.73 |        |      |     |
| 1 | 166 | D | 1945.6 | 1147.4 | 1947.2 | 2.433 | 152.05 |        |      |     |
| 1 | 166 | E | 1928.4 | 1133.9 | 1929.6 | 2.424 | 151.47 |        |      |     |
| 1 | 166 | F | 1933.1 | 1122.9 | 1940.4 | 2.365 | 147.79 | 150.81 | 3800 | TK4 |
| 1 | 178 | C | 2026.3 | 1209.1 | 2046.6 | 2.419 | 151.22 | 151.22 | 4000 | TK4 |
| 1 | 188 | B | 1997.1 | 1171.7 | 2000.4 | 2.410 | 150.62 |        |      |     |
| 1 | 188 | C | 1977   | 1159.4 | 1978.7 | 2.413 | 150.81 |        |      |     |
| 1 | 188 | D | 1989.1 | 1167.7 | 1990.8 | 2.417 | 151.04 |        |      |     |
| 1 | 188 | F | 1957.9 | 1141.3 | 1959.7 | 2.392 | 149.52 | 150.50 | 4300 | TK4 |
| 1 | 200 | B | 1985.1 | 1168.7 | 1990.1 | 2.417 | 151.05 |        |      |     |
| 1 | 200 | C | 1996   | 1173.5 | 1998.4 | 2.420 | 151.23 |        |      |     |
| 1 | 200 | F | 1997.1 | 1168.1 | 2000.3 | 2.400 | 149.99 | 150.75 | 4600 | TK5 |
| 1 | 220 | B | 1816.4 | 1089.7 | 1818.1 | 2.494 | 155.86 |        |      |     |
| 1 | 220 | D | 1812.8 | 1080.9 | 1815.7 | 2.467 | 154.19 |        |      |     |
| 1 | 220 | F | 1768.5 | 1055.2 | 1770.6 | 2.472 | 154.50 | 154.85 | 5000 | TK5 |
| 1 | 232 | A | 1857.9 | 1125.6 | 1859   | 2.533 | 158.33 |        |      |     |
| 1 | 232 | B | 1909.3 | 1155   | 1910.2 | 2.528 | 158.01 |        |      |     |
| 1 | 232 | C | 1870.8 | 1127   | 1872   | 2.511 | 156.95 |        |      |     |
| 1 | 232 | D | 1948   | 1113   | 1848.7 | 2.512 | 156.99 |        |      |     |
| 1 | 232 | E | 1862.1 | 1123.8 | 1863   | 2.519 | 157.44 |        |      |     |
| 1 | 232 | F | 1899.5 | 1148   | 1900.8 | 2.523 | 157.70 | 157.57 | 5500 | TK5 |
| 1 | 238 | B | 1722.7 | 1040.2 | 1724   | 2.519 | 157.46 |        |      |     |
| 1 | 238 | C | 1673.4 | 1010   | 1674.4 | 2.519 | 157.42 |        |      |     |
| 1 | 238 | E | 1722.1 | 1041.9 | 1723.1 | 2.528 | 158.00 | 157.63 | 6000 | TK5 |

| LANE | STATION | CORE | AIR(g) | WATER(g) | SSD(g) | BSG   | DENS   | AVG.DENS | PASSES | TRUCK |
|------|---------|------|--------|----------|--------|-------|--------|----------|--------|-------|
| 3    | 20      | A    | 1284.5 | 756      | 1285.7 | 2.425 | 151.56 |          |        |       |

|   |     |   |        |        |        |       |        |        |      |     |  |
|---|-----|---|--------|--------|--------|-------|--------|--------|------|-----|--|
| 3 | 20  | B | 1902.1 | 1116.7 | 1909.1 | 2.400 | 150.03 |        |      |     |  |
| 3 | 20  | C | 1267.1 | 746.9  | 1269.3 | 2.426 | 151.60 | 151.06 | 300  | TK1 |  |
| 3 | 26  | A | 1842.1 | 1082.9 | 1844.5 | 2.419 | 151.17 |        |      |     |  |
| 3 | 26  | B | 1268.8 | 749.5  | 1270.9 | 2.433 | 152.09 |        |      |     |  |
| 3 | 26  | C | 1686.8 | 995.6  | 1691.8 | 2.423 | 151.43 |        |      |     |  |
| 3 | 26  | D | 1281.5 | 757.2  | 1282.2 | 2.441 | 152.56 |        |      |     |  |
| 3 | 26  | E | 1697.5 | 1003.5 | 1702.9 | 2.427 | 151.69 |        |      |     |  |
| 3 | 26  | F | 1259   | 739.4  | 1260.2 | 2.417 | 151.09 | 151.67 | 600  | TK1 |  |
| 3 | 32  | A | 1322.1 | 784.7  | 1322.9 | 2.457 | 153.53 | 153.53 | 900  | TK1 |  |
| 3 | 42  | A | 1908.1 | 1112.8 | 1911.3 | 2.390 | 149.35 | 149.35 | 1200 | TK2 |  |
| 3 | 56  | A | 2010.5 | 1196.3 | 2012.9 | 2.462 | 153.88 |        |      |     |  |
| 3 | 56  | B | 2007.7 | 1195.9 | 2009.7 | 2.467 | 154.19 |        |      |     |  |
| 3 | 56  | C | 1322.8 | 790.9  | 1324.1 | 2.481 | 155.05 |        |      |     |  |
| 3 | 56  | D | 1339.6 | 800.7  | 1341   | 2.479 | 154.96 |        |      |     |  |
| 3 | 56  | E | 1339.6 | 802.9  | 1340.9 | 2.490 | 155.62 |        |      |     |  |
| 3 | 56  | F | 1903.8 | 1130.9 | 1906.1 | 2.456 | 153.49 | 154.53 | 1430 | TK2 |  |
| 3 | 80  | A | 1304.5 | 783.5  | 1307.5 | 2.490 | 155.59 |        |      |     |  |
| 3 | 80  | B | 2023   | 1211.9 | 2026.2 | 2.484 | 155.27 |        |      |     |  |
| 3 | 80  | C | 1303.6 | 781.5  | 1305.1 | 2.490 | 155.61 |        |      |     |  |
| 3 | 80  | D | 2062.4 | 1232.1 | 2064.8 | 2.477 | 154.80 |        |      |     |  |
| 3 | 80  | E | 2051.8 | 1218.9 | 2055.4 | 2.453 | 153.30 |        |      |     |  |
| 3 | 80  | F | 1294.2 | 770    | 1295.5 | 2.463 | 153.92 | 154.75 | 1730 | TK2 |  |
| 3 | 92  | A | 2091.3 | 1251.5 | 2093.3 | 2.484 | 155.27 |        |      |     |  |
| 3 | 92  | B | 2148.5 | 1289.2 | 2150.3 | 2.495 | 155.94 |        |      |     |  |
| 3 | 92  | C | 2110.6 | 1268.1 | 2112.5 | 2.500 | 156.22 |        |      |     |  |
| 3 | 92  | D | 2113.8 | 1272.2 | 2115.7 | 2.506 | 156.62 |        |      |     |  |
| 3 | 92  | E | 2109.6 | 1261.6 | 2112.1 | 2.480 | 155.03 |        |      |     |  |
| 3 | 92  | F | 2136.3 | 1283.8 | 2138.3 | 2.500 | 156.25 | 155.89 | 2000 | TK3 |  |
| 3 | 104 | A | 2089.6 | 1253   | 2092.6 | 2.489 | 155.55 |        |      |     |  |
| 3 | 104 | B | 2079.5 | 1246.4 | 2081.1 | 2.491 | 155.71 |        |      |     |  |
| 3 | 104 | C | 2059.2 | 1230.1 | 2061.4 | 2.477 | 154.82 |        |      |     |  |
| 3 | 104 | D | 2092.2 | 1255.7 | 2094.4 | 2.495 | 155.91 |        |      |     |  |
| 3 | 104 | E | 2049.2 | 1229.7 | 2051.5 | 2.494 | 155.85 |        |      |     |  |
| 3 | 104 | F | 2007.3 | 1198.2 | 2010.5 | 2.471 | 154.45 | 155.38 | 2300 | TK3 |  |
| 3 | 116 | A | 2218.7 | 1329.2 | 2221.5 | 2.486 | 155.41 |        |      |     |  |
| 3 | 116 | B | 1334.8 | 806.1  | 1336.4 | 2.517 | 157.32 |        |      |     |  |
| 3 | 116 | C | 1314.5 | 794.9  | 1316   | 2.522 | 157.63 |        |      |     |  |
| 3 | 116 | D | 2234.9 | 1341.4 | 2236.8 | 2.496 | 156.00 |        |      |     |  |
| 3 | 116 | F | 2206.6 | 1315.2 | 2209.5 | 2.467 | 154.21 | 156.11 | 2600 | TK3 |  |
| 3 | 128 | A | 1295   | 770    | 1295.7 | 2.463 | 153.96 |        |      |     |  |
| 3 | 128 | D | 1269.9 | 749.3  | 1270.7 | 2.436 | 152.22 |        |      |     |  |
| 3 | 128 | E | 1261.6 | 749.4  | 1262.9 | 2.457 | 153.58 |        |      |     |  |
| 3 | 128 | F | 1928   | 1137   | 1932.2 | 2.425 | 151.53 | 152.82 | 2900 | TK4 |  |
| 3 | 140 | A | 1209.2 | 712    | 1210.1 | 2.428 | 151.73 |        |      |     |  |
| 3 | 140 | B | 1228   | 723.1  | 1228.9 | 2.428 | 151.74 |        |      |     |  |
| 3 | 140 | C | 1222.8 | 723.7  | 1223.9 | 2.445 | 152.79 |        |      |     |  |
| 3 | 140 | D | 2079.7 | 1230.2 | 2081.2 | 2.443 | 152.71 |        |      |     |  |
| 3 | 140 | E | 2079.7 | 1225.8 | 2081.5 | 2.430 | 151.90 |        |      |     |  |
| 3 | 140 | F | 2075.4 | 1215.4 | 2077   | 2.409 | 150.55 | 151.90 | 3200 | TK4 |  |
| 3 | 146 | A | 2090.2 | 1228.6 | 2094.1 | 2.415 | 150.94 |        |      |     |  |
| 3 | 146 | B | 2042.5 | 1198   | 2045.5 | 2.410 | 150.63 |        |      |     |  |

|   |     |   |        |        |        |       |        |        |      |     |
|---|-----|---|--------|--------|--------|-------|--------|--------|------|-----|
| 3 | 146 | C | 2046.7 | 1208.4 | 2048.5 | 2.436 | 152.27 |        |      |     |
| 3 | 146 | D | 1994.6 | 1167.4 | 1997.1 | 2.404 | 150.25 |        |      |     |
| 3 | 146 | E | 2008.1 | 1171.5 | 2011.2 | 2.391 | 149.47 |        |      |     |
| 3 | 146 | F | 1971.8 | 1151.5 | 1974.6 | 2.396 | 149.72 | 150.55 | 3500 | TK4 |
| 3 | 166 | A | 1841.3 | 1093.7 | 1843.9 | 2.454 | 153.40 |        |      |     |
| 3 | 166 | B | 1808.2 | 1072.1 | 1811.1 | 2.447 | 152.93 |        |      |     |
| 3 | 166 | C | 1806.4 | 1069.5 | 1810   | 2.439 | 152.46 |        |      |     |
| 3 | 166 | D | 1808.7 | 1068.1 | 1810.7 | 2.436 | 152.23 |        |      |     |
| 3 | 166 | E | 1804.1 | 1065.4 | 1805.6 | 2.437 | 152.33 |        |      |     |
| 3 | 166 | F | 1799.8 | 1065   | 1802   | 2.442 | 152.63 | 152.66 | 3800 | TK5 |
| 3 | 178 | A | 1824.1 | 1083.2 | 1825.9 | 2.456 | 153.50 |        |      |     |
| 3 | 178 | B | 1805.8 | 1067.3 | 1808.7 | 2.436 | 152.23 |        |      |     |
| 3 | 178 | C | 1801.7 | 1065.8 | 1804.3 | 2.440 | 152.48 |        |      |     |
| 3 | 178 | D | 1806.7 | 1069.5 | 1809.4 | 2.442 | 152.61 |        |      |     |
| 3 | 178 | E | 1822.1 | 1080.5 | 1823.9 | 2.451 | 153.19 |        |      |     |
| 3 | 178 | F | 1820.2 | 1078.4 | 1821.4 | 2.450 | 153.11 | 152.85 | 4000 | TK5 |
| 3 | 188 | A | 1878.3 | 1109.7 | 1881.1 | 2.435 | 152.18 |        |      |     |
| 3 | 188 | B | 1878.3 | 1113.7 | 1880.8 | 2.449 | 153.04 |        |      |     |
| 3 | 188 | C | 1877.5 | 1110   | 1879.4 | 2.440 | 152.51 |        |      |     |
| 3 | 188 | D | 1510.9 | 904.9  | 1513.8 | 2.481 | 155.08 |        |      |     |
| 3 | 188 | E | 1712.7 | 1027.3 | 1715.5 | 2.489 | 155.54 | 153.67 | 4300 | TK5 |
| 3 | 200 | A | 1814.8 | 1077.1 | 1817.7 | 2.450 | 153.15 |        |      |     |
| 3 | 200 | B | 1849   | 1094.4 | 1851.4 | 2.443 | 152.66 |        |      |     |
| 3 | 200 | C | 1842.4 | 1085.8 | 1846.1 | 2.423 | 151.45 |        |      |     |
| 3 | 200 | D | 1865.7 | 1103.4 | 1867.1 | 2.442 | 152.65 |        |      |     |
| 3 | 200 | E | 1832.8 | 1075.1 | 1834.9 | 2.412 | 150.76 |        |      |     |
| 3 | 200 | F | 1810.6 | 1061.8 | 1812.1 | 2.413 | 150.82 | 151.92 | 4600 | TK6 |
| 3 | 220 | A | 1763.8 | 1041.1 | 1765.9 | 2.433 | 152.09 |        |      |     |
| 3 | 220 | B | 1733.9 | 1022.3 | 1736.3 | 2.428 | 151.78 |        |      |     |
| 3 | 220 | C | 1726.9 | 1019.5 | 1729.7 | 2.432 | 151.97 |        |      |     |
| 3 | 220 | D | 1745.4 | 1034.4 | 1749.3 | 2.441 | 152.59 |        |      |     |
| 3 | 220 | E | 1901.1 | 1122.1 | 1903.4 | 2.433 | 152.08 |        |      |     |
| 3 | 220 | F | 1906.7 | 1122.7 | 1908.5 | 2.426 | 151.65 | 152.03 | 5000 | TK6 |
| 3 | 232 | A | 2000.2 | 1179.6 | 2002.9 | 2.429 | 151.84 |        |      |     |
| 3 | 232 | B | 2021.9 | 1192.1 | 2023.5 | 2.432 | 152.00 |        |      |     |
| 3 | 232 | C | 2030.4 | 1192.8 | 2031.8 | 2.420 | 151.25 |        |      |     |
| 3 | 232 | D | 2043.8 | 1208.2 | 2045.9 | 2.440 | 152.49 |        |      |     |
| 3 | 232 | E | 2067   | 1219.7 | 2068.5 | 2.435 | 152.20 |        |      |     |
| 3 | 232 | F | 2133.9 | 1260.9 | 2135.6 | 2.440 | 152.47 | 152.04 | 5500 | TK6 |
| 3 | 238 | A | 2033.9 | 1194.5 | 2036.4 | 2.416 | 150.99 |        |      |     |
| 3 | 238 | D | 2012.5 | 1182.4 | 2014.1 | 2.420 | 151.23 |        |      |     |
| 3 | 238 | E | 1984.2 | 1167.3 | 1985.8 | 2.424 | 151.51 |        |      |     |
| 3 | 238 | F | 1957.2 | 1150.2 | 1958.9 | 2.420 | 151.26 | 151.25 | 6000 | TK6 |

| LANE | STATION | CORE | AIR    | WATER  | SSD    | BSG   | DENS   | AVG.DENS | PASSES | TRUCK |
|------|---------|------|--------|--------|--------|-------|--------|----------|--------|-------|
| 4    | 20      | B    | 1642.6 | 980    | 1644.4 | 2.472 | 154.52 |          |        |       |
| 4    | 20      | C    | 1601.3 | 954.6  | 1603.2 | 2.469 | 154.30 |          |        |       |
| 4    | 20      | D    | 1690.1 | 1003.3 | 1691.8 | 2.455 | 153.42 |          |        |       |
| 4    | 20      | E    | 1602   | 953.3  | 1603.7 | 2.463 | 153.94 |          |        |       |
| 4    | 20      | F    | 1561.4 | 929.7  | 1563.3 | 2.464 | 154.02 | 154.04   |        |       |
| 4    | 26      | A    | 1495.9 | 886.2  | 1498.3 | 2.444 | 152.74 |          |        |       |
| 4    | 26      | B    | 1481.3 | 874.4  | 1483.1 | 2.434 | 152.10 |          |        |       |

|   |     |   |        |        |        |       |        |        |
|---|-----|---|--------|--------|--------|-------|--------|--------|
| 4 | 26  | C | 1535.6 | 908.6  | 1537.3 | 2.443 | 152.66 |        |
| 4 | 26  | D | 1495.9 | 886.9  | 1497.4 | 2.450 | 153.14 |        |
| 4 | 26  | E | 1506.2 | 896.2  | 1507.9 | 2.462 | 153.89 |        |
| 4 | 26  | F | 1513   | 901.4  | 1514.3 | 2.469 | 154.29 | 153.14 |
| 4 | 32  | B | 1292.4 | 770.8  | 1293.5 | 2.473 | 154.53 |        |
| 4 | 32  | C | 1543.5 | 918    | 1544.4 | 2.464 | 154.01 |        |
| 4 | 32  | D | 1315   | 784.7  | 1316.1 | 2.475 | 154.66 |        |
| 4 | 32  | E | 1516.9 | 905    | 1518.3 | 2.473 | 154.58 |        |
| 4 | 32  | F | 1308.3 | 782.2  | 1309.1 | 2.483 | 155.19 | 154.59 |
| 4 | 42  | A | 1862.8 | 1105.7 | 1865   | 2.453 | 153.33 |        |
| 4 | 42  | B | 1367.9 | 1110.2 | 1869.6 | 2.460 | 153.73 |        |
| 4 | 42  | C | 1847.2 | 1094.5 | 1848.8 | 2.449 | 153.06 |        |
| 4 | 42  | D | 1900   | 1138.2 | 1902   | 2.488 | 155.47 |        |
| 4 | 42  | E | 1898   | 1132.3 | 1900.2 | 2.472 | 154.48 |        |
| 4 | 42  | F | 1884.8 | 1122.8 | 1887   | 2.466 | 154.15 | 154.04 |
| 4 | 56  | A | 2184.5 | 1301.8 | 2186.1 | 2.470 | 154.39 |        |
| 4 | 56  | B | 1229.5 | 733.2  | 1230.3 | 2.473 | 154.58 |        |
| 4 | 56  | D | 1184.8 | 698.5  | 1185.6 | 2.432 | 152.02 |        |
| 4 | 56  | E | 1199.3 | 705.1  | 1200.3 | 2.422 | 151.37 |        |
| 4 | 56  | F | 2206.6 | 1304.4 | 2209.5 | 2.438 | 152.37 | 152.95 |
| 4 | 66  | A | 2178.8 | 1290.2 | 2181.5 | 2.445 | 152.78 |        |
| 4 | 66  | B | 1207.3 | 713.3  | 1208.1 | 2.440 | 152.50 |        |
| 4 | 66  | D | 1207.5 | 712.2  | 1208.4 | 2.433 | 152.09 |        |
| 4 | 66  | E | 1206   | 713.9  | 1206.7 | 2.447 | 152.95 | 152.58 |
| 4 | 78  | A | 1334.5 | 800    | 1335.3 | 2.493 | 155.81 |        |
| 4 | 78  | B | 2467.3 | 1477.6 | 2470.1 | 2.486 | 155.37 |        |
| 4 | 78  | C | 1334.4 | 798.6  | 1335.6 | 2.485 | 155.31 | 155.50 |
| 4 | 82  | D | 2339.7 | 1355.6 | 2342.2 | 2.472 | 154.48 |        |
| 4 | 82  | E | 1307.1 | 776.5  | 1308   | 2.459 | 153.70 |        |
| 4 | 82  | F | 2363.3 | 1409.6 | 2365.1 | 2.473 | 154.59 | 154.26 |
| 4 | 92  | A | 2399.1 | 1434   | 2400.8 | 2.481 | 155.09 |        |
| 4 | 92  | B | 1326.4 | 790.9  | 1328.1 | 2.469 | 154.32 |        |
| 4 | 92  | D | 2466.7 | 1476.8 | 2468.2 | 2.488 | 155.51 |        |
| 4 | 92  | E | 1301.7 | 776.4  | 1302.3 | 2.475 | 154.70 |        |
| 4 | 92  | F | 1308   | 780.5  | 1308.6 | 2.477 | 154.80 | 154.88 |
| 4 | 104 | B | 2568.7 | 1532   | 2570.3 | 2.474 | 154.62 |        |
| 4 | 104 | C | 1307.9 | 783.2  | 1308.6 | 2.489 | 155.58 |        |
| 4 | 104 | D | 1305.6 | 778.1  | 1306.5 | 2.471 | 154.43 |        |
| 4 | 104 | E | 2476.3 | 1466.9 | 2480.5 | 2.443 | 152.69 |        |
| 4 | 104 | F | 2518.5 | 1488.6 | 2520.8 | 2.440 | 152.50 | 153.96 |
| 4 | 116 | A | 2106.3 | 1259.2 | 2108.9 | 2.479 | 154.93 |        |
| 4 | 116 | B | 1274.9 | 750.2  | 1276.4 | 2.423 | 151.43 |        |
| 4 | 116 | C | 1260.8 | 742.8  | 1262.4 | 2.426 | 151.66 |        |
| 4 | 116 | D | 2447   | 1435.1 | 2450.3 | 2.410 | 150.65 |        |
| 4 | 116 | E | 1284.6 | 755    | 1285.7 | 2.421 | 151.29 |        |
| 4 | 116 | F | 2471.4 | 1467.9 | 2474   | 2.456 | 153.53 | 152.25 |
| 4 | 128 | C | 1352.4 | 817.4  | 1353.1 | 2.525 | 157.78 |        |
| 4 | 128 | D | 2261.4 | 1359.7 | 2263.1 | 2.503 | 156.45 |        |
| 4 | 128 | E | 1358.7 | 819.1  | 1360.2 | 2.511 | 156.94 | 157.06 |
| 4 | 140 | A | 1326.4 | 792.4  | 1327.2 | 2.480 | 155.01 |        |
| 4 | 140 | B | 2277.3 | 1366.3 | 2278.7 | 2.496 | 156.00 |        |

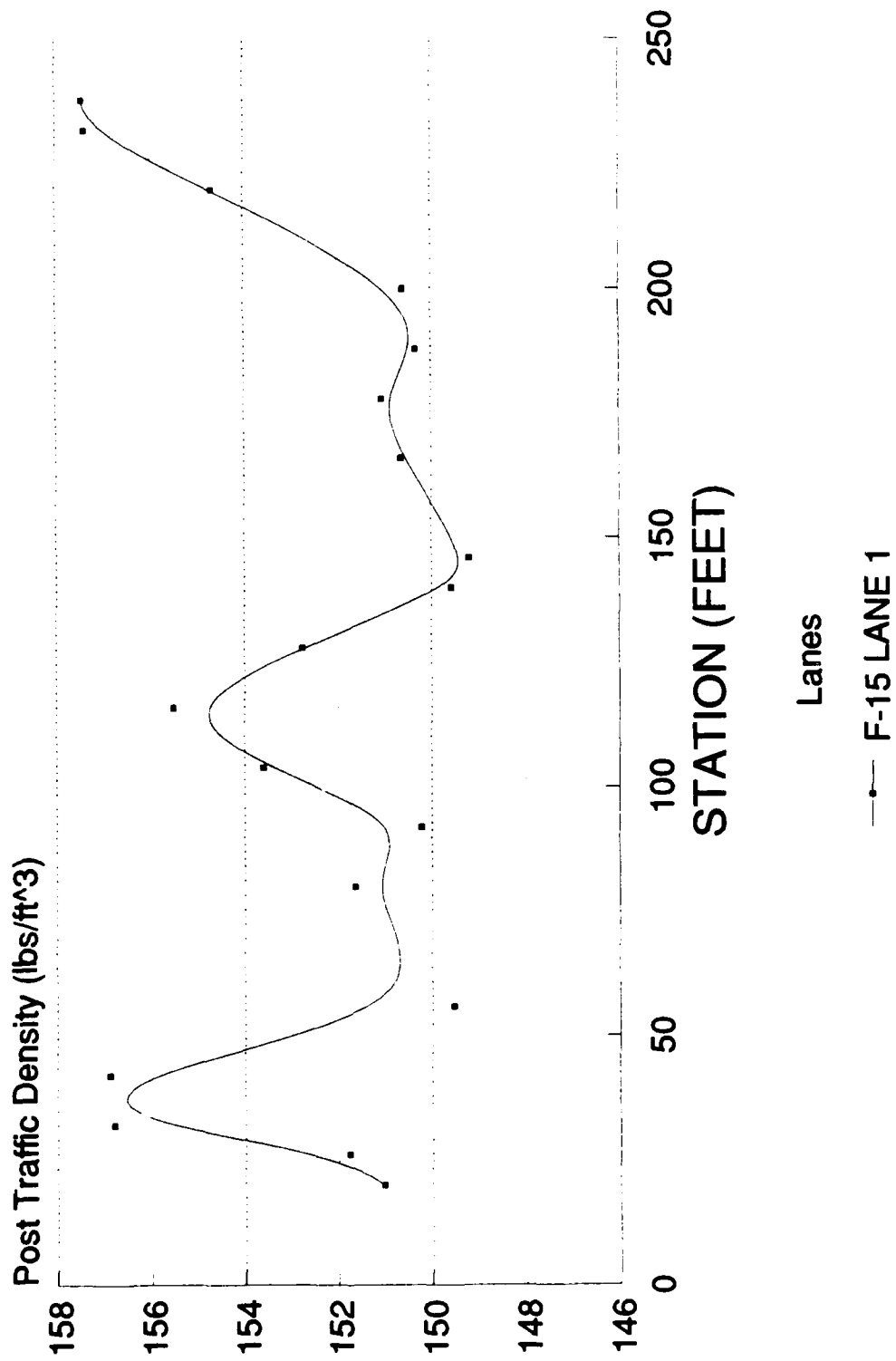
|   |     |    |        |        |        |       |        |        |  |
|---|-----|----|--------|--------|--------|-------|--------|--------|--|
| 4 | 140 | C  | 1349.9 | 808.4  | 1350.8 | 2.489 | 155.55 |        |  |
| 4 | 140 | D  | 2282.8 | 1369.4 | 2284.3 | 2.495 | 155.95 |        |  |
| 4 | 140 | E  | 1324.5 | 793    | 1325.8 | 2.486 | 155.37 |        |  |
| 4 | 140 | F  | 2267.5 | 1359.7 | 2269.5 | 2.492 | 155.77 | 155.61 |  |
| 4 | 146 | C  | 2372.4 | 1413.4 | 2374.6 | 2.468 | 154.26 |        |  |
| 4 | 146 | D  | 2211.7 | 1327.5 | 2213.9 | 2.495 | 155.95 |        |  |
| 4 | 146 | E  | 2276.1 | 1365.3 | 2277.9 | 2.494 | 155.88 | 155.36 |  |
| 4 | 166 | B2 | 1915.1 | 1120.3 | 1918.3 | 2.400 | 149.99 | 149.99 |  |
| 4 | 178 | B  | 1877.8 | 1112.9 | 1879.6 | 2.449 | 153.07 |        |  |
| 4 | 178 | C  | 1862.5 | 1103.4 | 1863.8 | 2.449 | 153.09 |        |  |
| 4 | 178 | D  | 1835.9 | 1090.3 | 1837   | 2.459 | 153.67 | 153.28 |  |
| 4 | 188 | B  | 1293.7 | 746.8  | 1294.7 | 2.361 | 147.57 |        |  |
| 4 | 188 | D  | 1313.1 | 780.7  | 1314.1 | 2.462 | 153.86 |        |  |
| 4 | 188 | E  | 1906.4 | 1131.4 | 1908   | 2.455 | 153.43 |        |  |
| 4 | 188 | F  | 1291.7 | 763.3  | 1293   | 2.439 | 152.41 | 151.82 |  |
| 4 | 200 | C2 | 2061.7 | 1189   | 2063.4 | 2.358 | 147.37 |        |  |
| 4 | 200 | D2 | 1282.9 | 743.1  | 1283.5 | 2.374 | 148.37 | 147.87 |  |
| 4 | 232 | B  | 2215.7 | 1313.7 | 2216.6 | 2.454 | 153.37 | 153.37 |  |

| LANE | STATION | CORE | AIR(g) | WATER(g) | SSD(g) | BSG   | DENS   | AVG.DENS | PASSES | TRUCK |
|------|---------|------|--------|----------|--------|-------|--------|----------|--------|-------|
| 5    | 20      | A    | 2131.6 | 1257.2   | 2136.7 | 2.424 | 151.48 |          |        |       |
| 5    | 20      | B    | 2155.7 | 1264.5   | 2166.6 | 2.390 | 149.35 |          |        |       |
| 5    | 20      | C    | 2156.1 | 1268.7   | 2166.6 | 2.401 | 150.08 |          |        |       |
| 5    | 20      | E    | 1919.1 | 1108     | 1933.2 | 2.326 | 145.35 |          |        |       |
| 5    | 20      | F    | 2031.3 | 1183.7   | 2045.2 | 2.358 | 147.37 | 148.73   | 300    |       |
| 5    | 26      | D    | 1918.6 | 1115.1   | 1926.3 | 2.365 | 147.82 |          |        |       |
| 5    | 26      | E    | 1908.1 | 1106.7   | 1912.7 | 2.367 | 147.96 | 147.89   | 600    |       |
| 5    | 32      | A    | 1847.6 | 1084.6   | 1850   | 2.414 | 150.87 |          |        |       |
| 5    | 32      | B    | 1836.1 | 1079     | 1838.4 | 2.418 | 151.11 |          |        |       |
| 5    | 32      | C    | 1794.7 | 1046.2   | 1798.6 | 2.385 | 149.08 |          |        |       |
| 5    | 32      | D    | 1760.8 | 1016.7   | 1764.8 | 2.354 | 147.11 |          |        |       |
| 5    | 32      | E    | 1759.8 | 1019.6   | 1763.6 | 2.365 | 147.83 | 149.20   | 900    |       |
| 5    | 42      | F    | 1864.6 | 1081.1   | 1870   | 2.364 | 147.72 | 147.72   | 1200   |       |
| 5    | 56      | A    | 2050.9 | 1235.7   | 2053.7 | 2.507 | 156.70 |          |        |       |
| 5    | 56      | B    | 2054.7 | 1228.7   | 2056.9 | 2.481 | 155.06 |          |        |       |
| 5    | 56      | C    | 2077.8 | 1240.5   | 2079.6 | 2.476 | 154.76 |          |        |       |
| 5    | 56      | E    | 2097.8 | 1239.7   | 2100.5 | 2.437 | 152.31 |          |        |       |
| 5    | 56      | F    | 2079.8 | 1227.1   | 2083.1 | 2.430 | 151.85 | 154.14   | 1500   |       |
| 5    | 66      | A    | 1280.9 | 760.3    | 1281.8 | 2.456 | 153.51 |          |        |       |
| 5    | 66      | B    | 2335.6 | 1392.4   | 2337.9 | 2.470 | 154.39 |          |        |       |
| 5    | 66      | C    | 2339.2 | 1402.4   | 2341.6 | 2.491 | 155.66 |          |        |       |
| 5    | 66      | D    | 1309.4 | 785.7    | 1310.3 | 2.496 | 156.00 |          |        |       |
| 5    | 66      | E    | 1292.5 | 761.5    | 1293.8 | 2.428 | 151.76 |          |        |       |
| 5    | 66      | F    | 2291.1 | 1346.5   | 2293.6 | 2.419 | 151.19 | 153.80   | 1800   |       |
| 5    | 80      | A    | 2521   | 1476     | 2523.6 | 2.406 | 150.40 |          |        |       |
| 5    | 80      | C    | 2560   | 1500.5   | 2567.3 | 2.400 | 149.98 |          |        |       |
| 5    | 80      | E    | 2555.5 | 1488.3   | 2558   | 2.389 | 149.31 |          |        |       |
| 5    | 80      | F    | 2610.4 | 1531.6   | 2614.6 | 2.410 | 150.65 | 150.09   | 2000   |       |

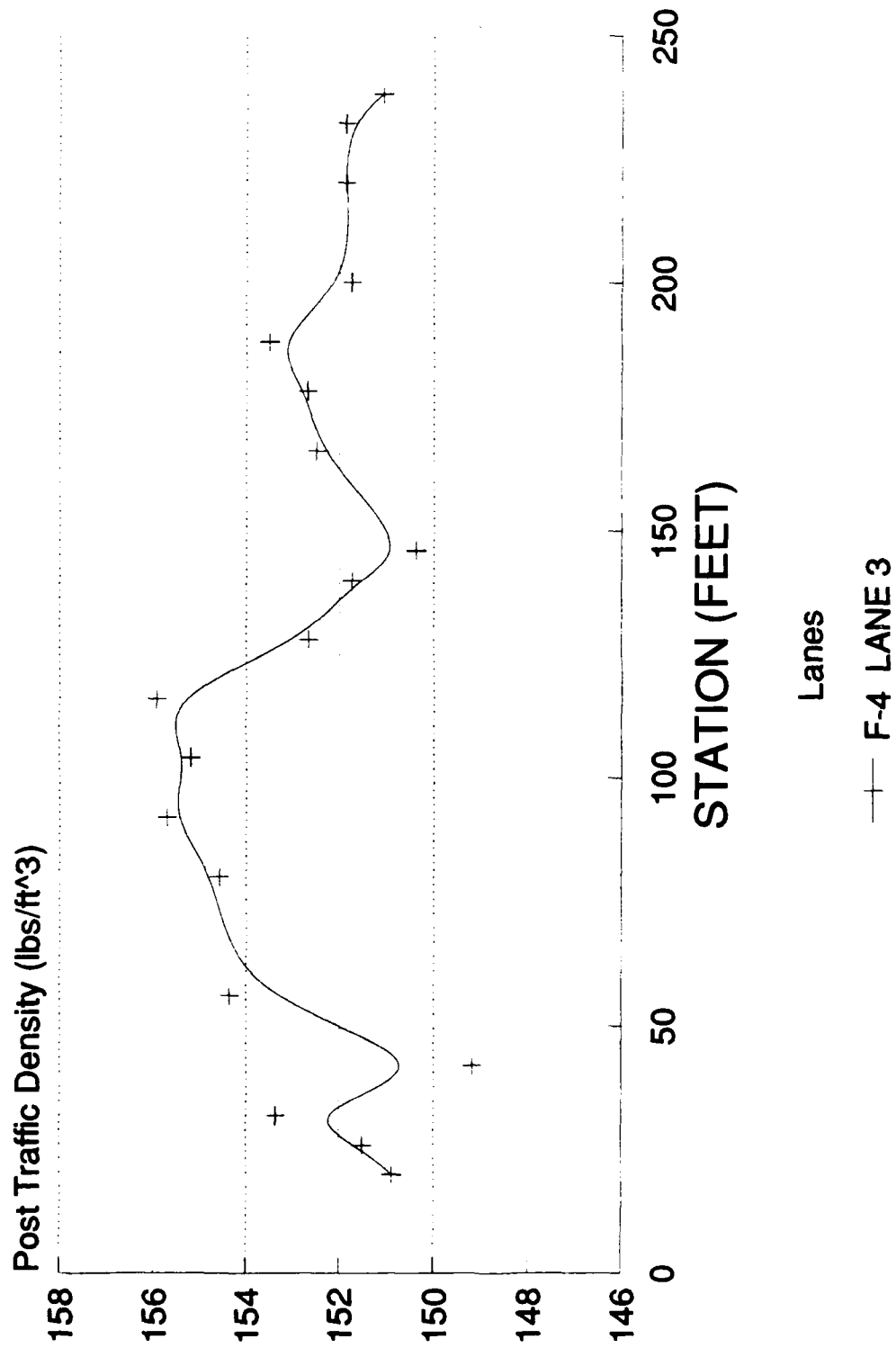


|   |     |    |        |        |        |       |        |        |      |
|---|-----|----|--------|--------|--------|-------|--------|--------|------|
| 5 | 92  | A  | 2521.3 | 1476.4 | 2526.9 | 2.400 | 150.01 | 150.01 | 2300 |
| 5 | 116 | A  | 2292.9 | 1341.4 | 2295.8 | 2.402 | 150.15 |        |      |
| 5 | 116 | C  | 2265.6 | 1323.2 | 2268.1 | 2.398 | 149.86 |        |      |
| 5 | 116 | D  | 2275.7 | 1334.8 | 2278.1 | 2.412 | 150.78 |        |      |
| 5 | 116 | E  | 2274.4 | 1335.2 | 2276.3 | 2.417 | 151.05 |        |      |
| 5 | 116 | F  | 2280.4 | 1338.2 | 2282.6 | 2.415 | 150.92 | 150.55 | 2900 |
| 5 | 128 | A2 | 2104.1 | 1240.3 | 2106.1 | 2.430 | 151.89 | 151.89 | 3200 |
| 5 | 166 | A2 | 1417.9 | 825.4  | 1419.2 | 2.388 | 149.24 |        |      |
| 5 | 166 | B2 | 1476   | 855.9  | 1477.7 | 2.374 | 148.36 | 148.80 | 3800 |
| 5 | 188 | A0 | 1481.9 | 863.8  | 1483.8 | 2.390 | 149.39 |        |      |
| 5 | 188 | B0 | 1458   | 844    | 1461.8 | 2.360 | 147.50 |        |      |
| 5 | 188 | C0 | 1484.8 | 860.6  | 1486.8 | 2.371 | 148.20 |        |      |
| 5 | 188 | D0 | 1528.6 | 884.4  | 1530.3 | 2.367 | 147.91 |        |      |
| 5 | 188 | E0 | 1518   | 877.1  | 1520.8 | 2.358 | 147.39 | 148.08 | 4300 |

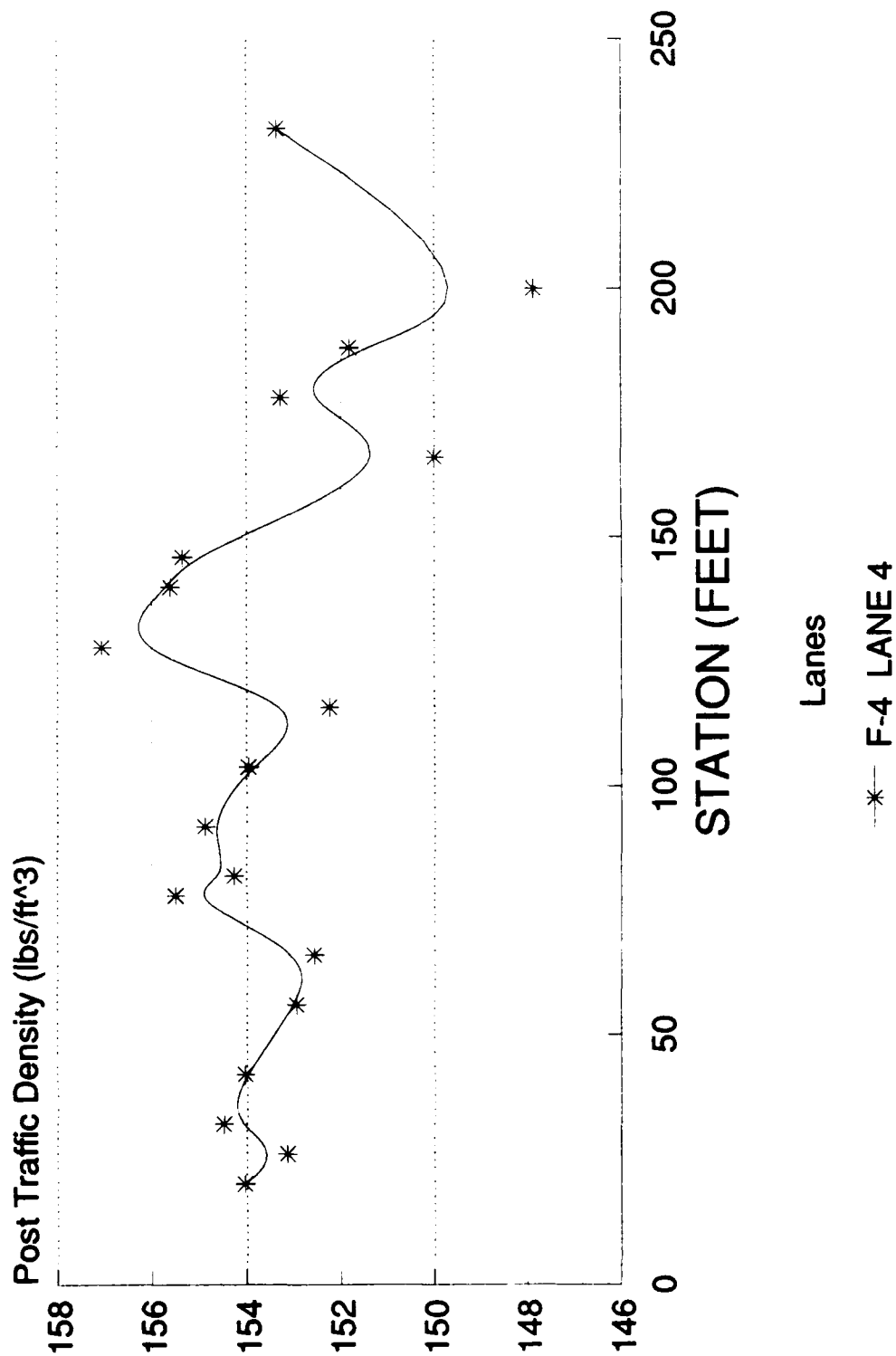
# Summary of Lane 1



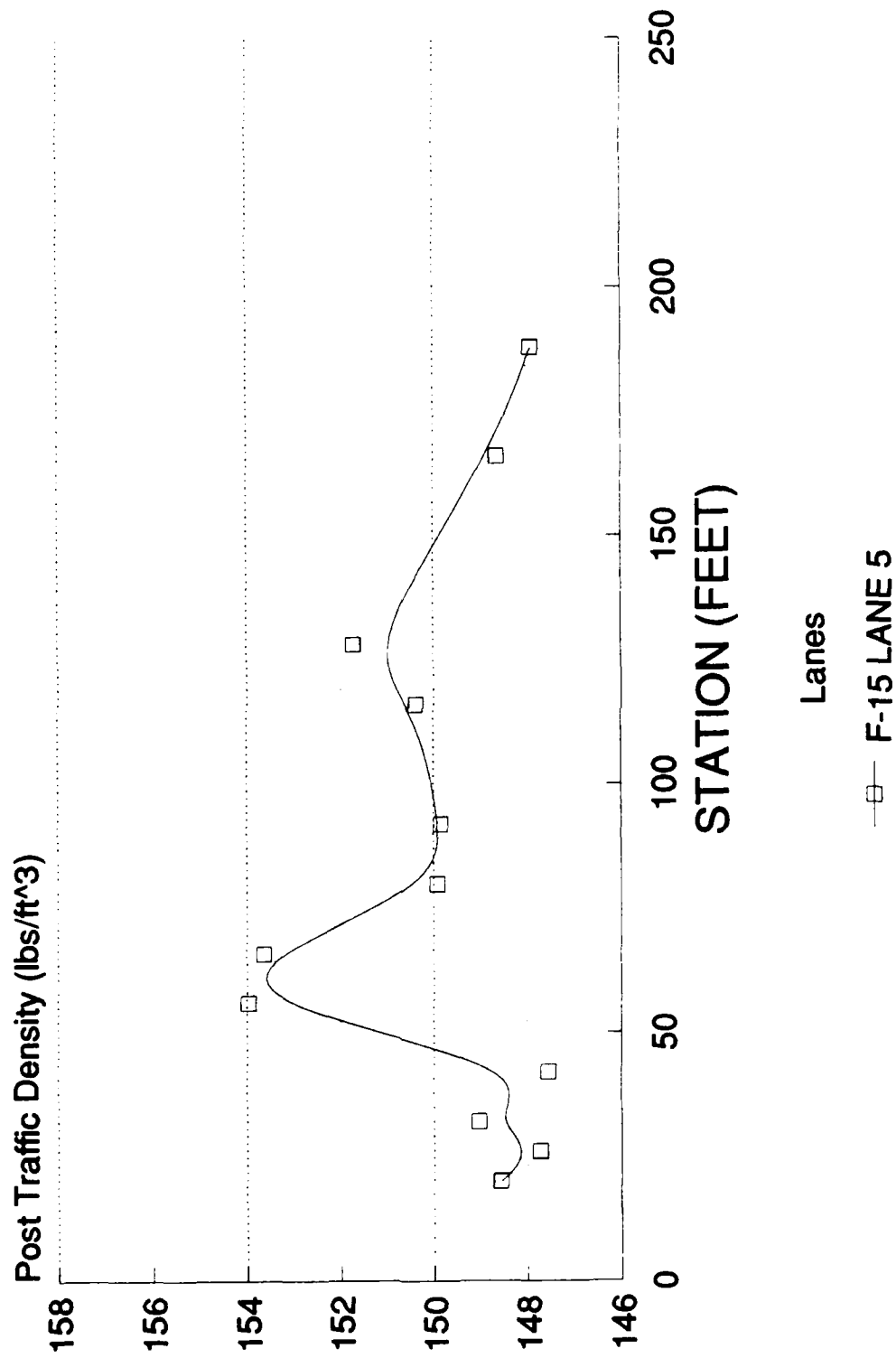
# Summary of Lane 3



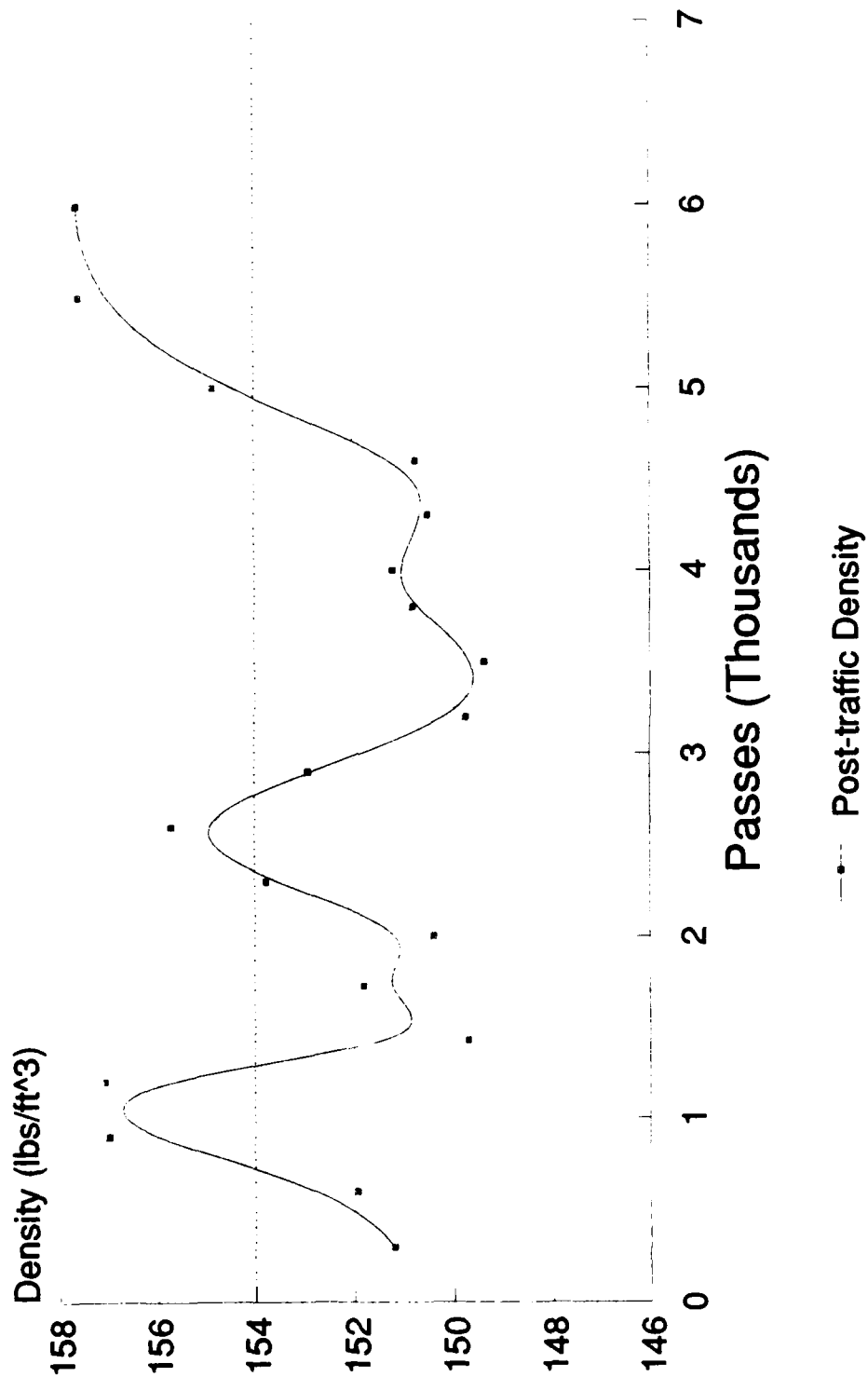
# Summary of Lane 4



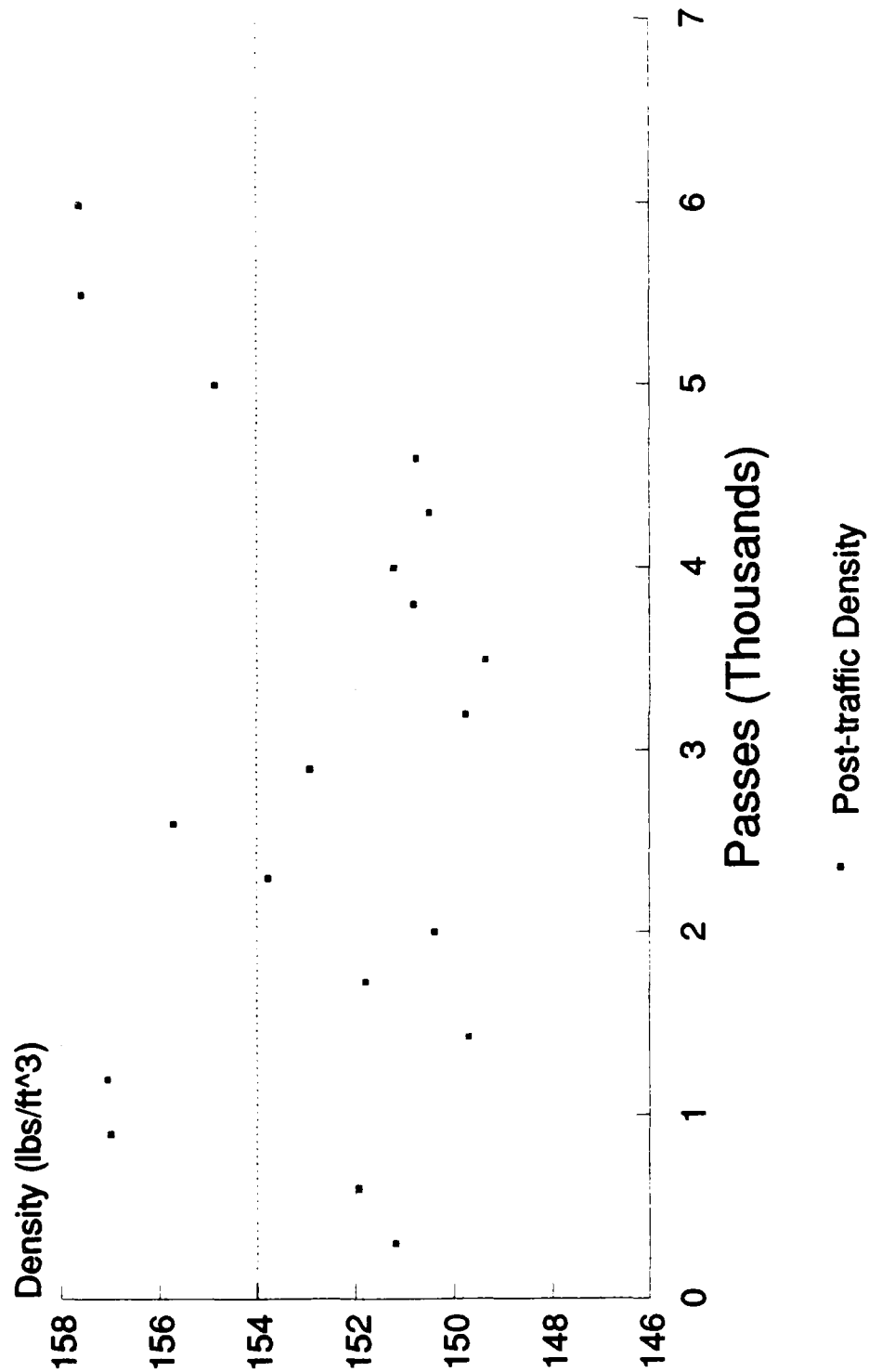
# Summary of Lane 5



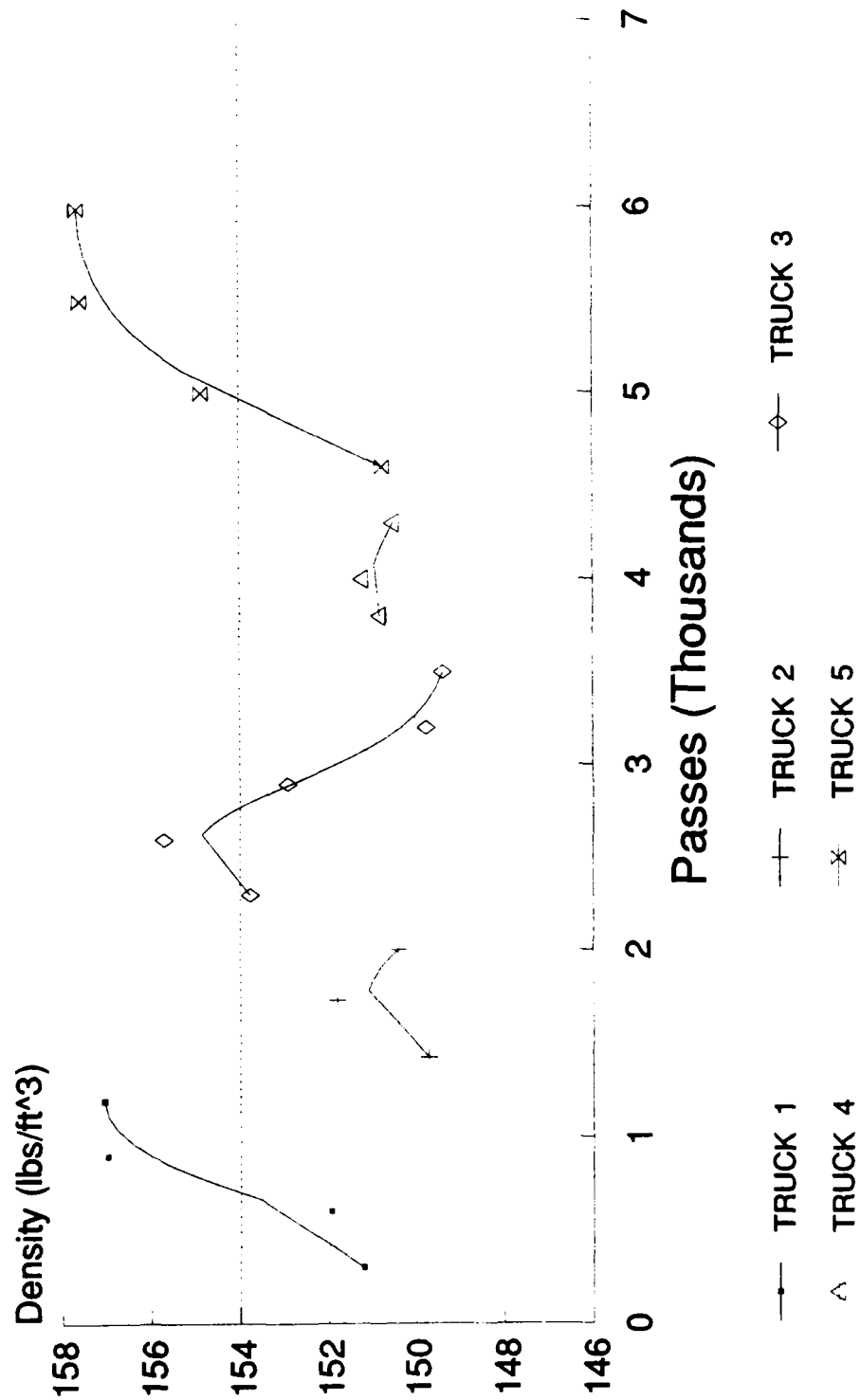
## Densities of Lane 1 (As a Whole)



# Densities of Lane 1 (Individually)

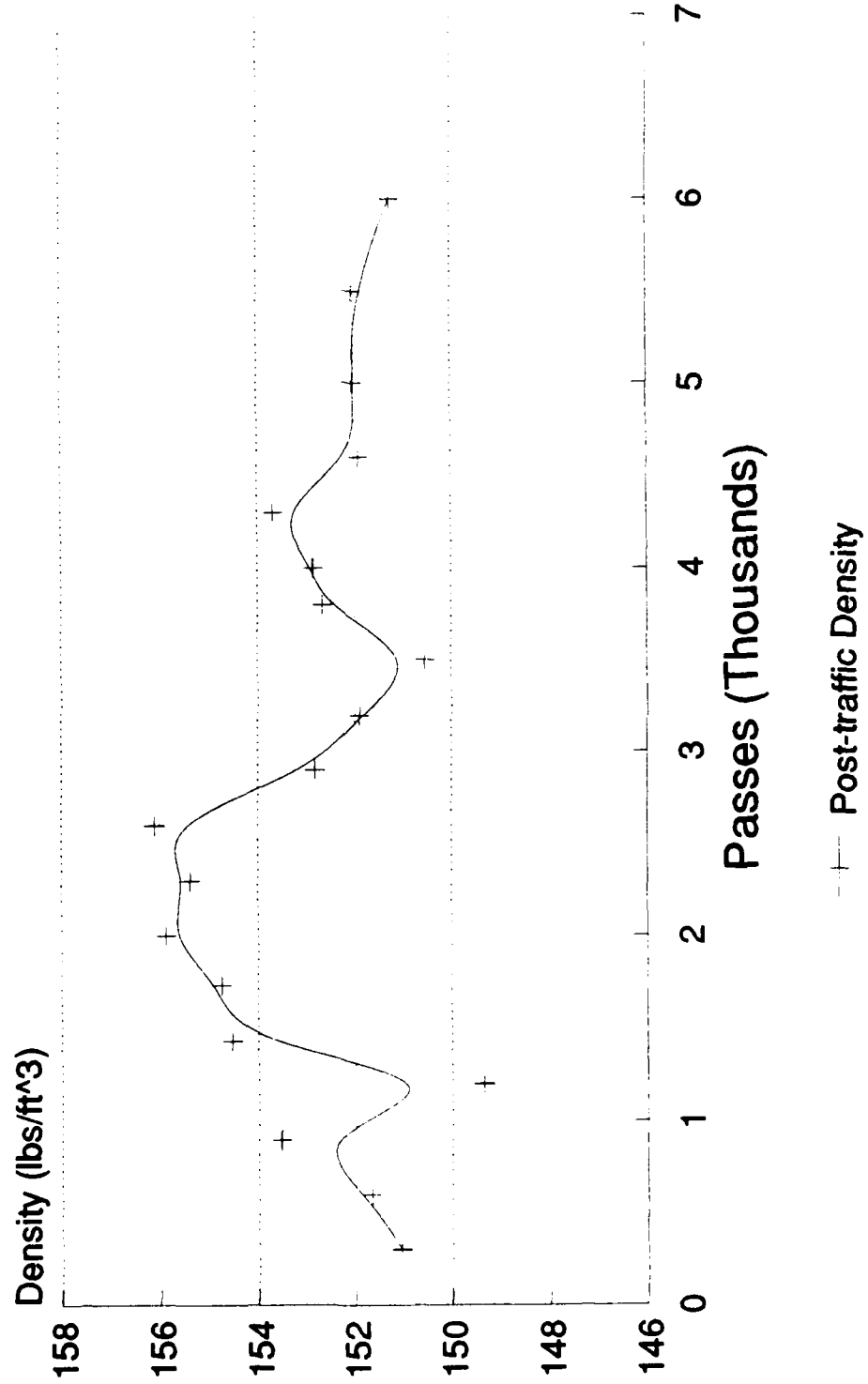


# Densities of Lane 1 (By "Truckload")

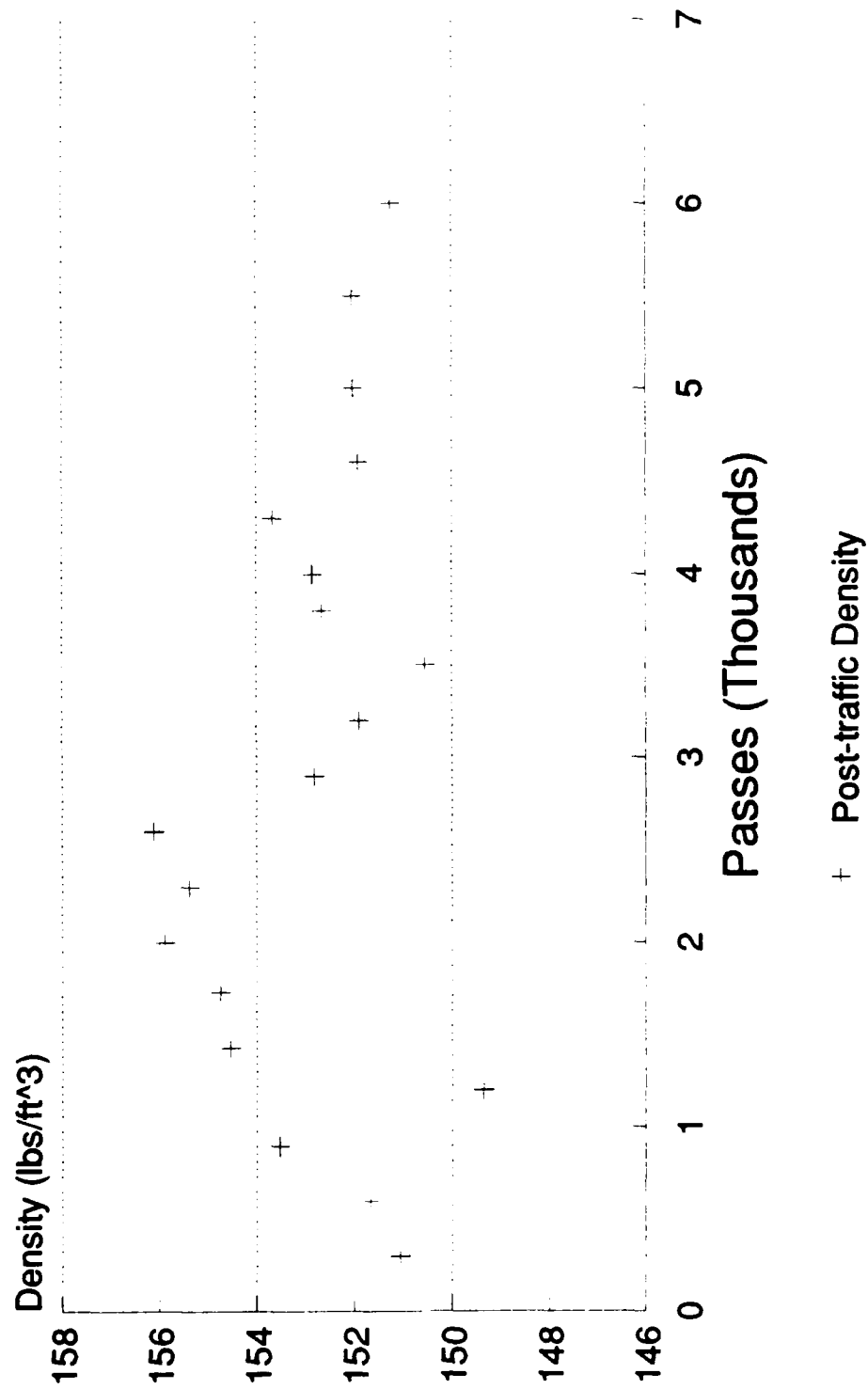




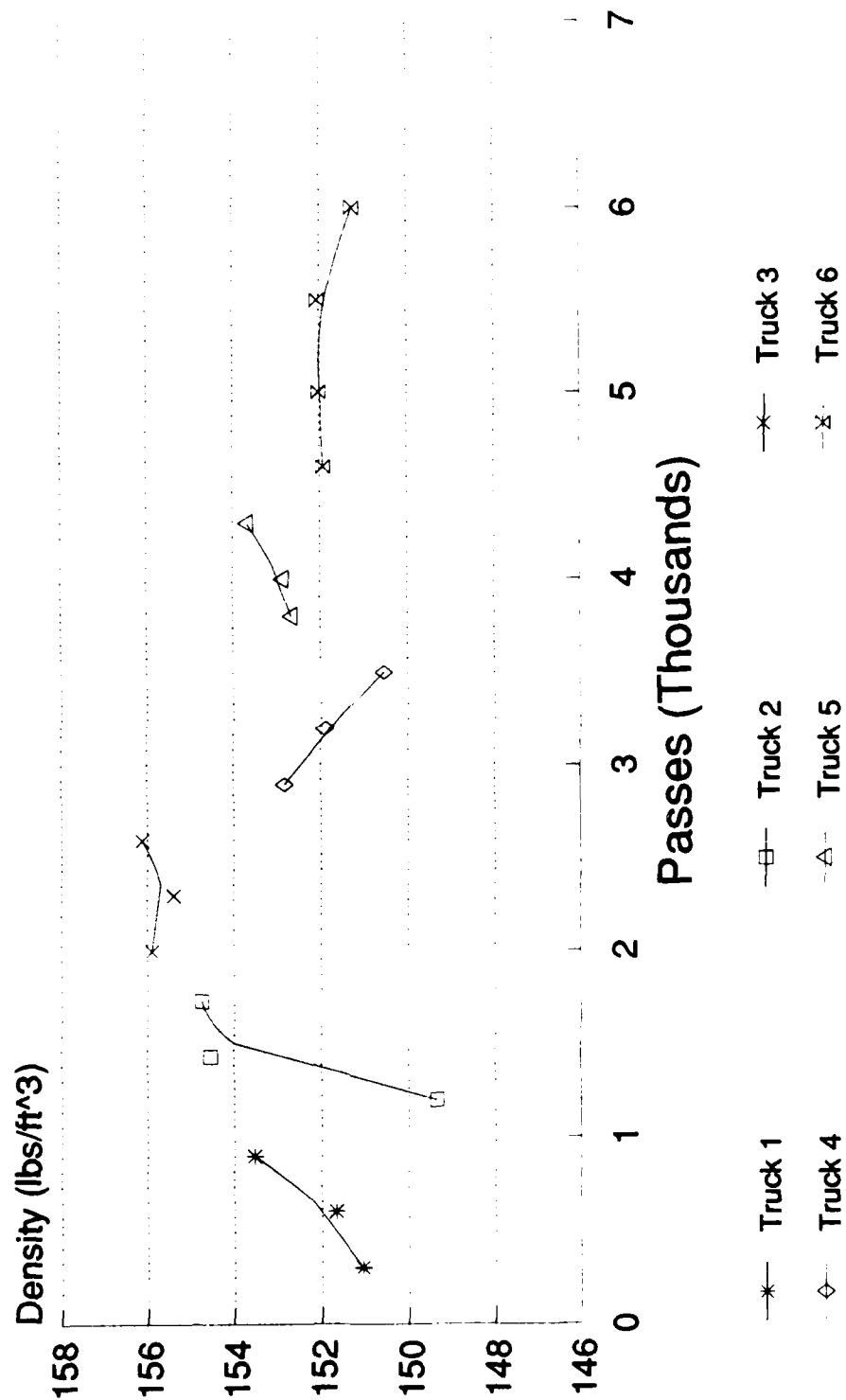
# Densities of Lane 3 (As a Whole)



# Densities of Lane 3 (Individually)



# Densities of Lane 3 (By "Truckload")



1989 USAF - UES HIGH SCHOOL APPRENTICESHIP PROGRAM

Sponsored by the  
AIR FORCE OFFICE OF SCIENTIFIC RESEARCH

Conducted by  
UNIVERSAL ENERGY SYSTEMS, INC.

FINAL REPORT  
ENVIRONMENTAL SIMULATION CHAMBER STUDIES  
OF THE ATMOSPHERIC CHEMISTRY OF HYDRAZINE

|                    |   |
|--------------------|---|
| Prepared by:       | Dorothy M. Iffrig   |
| High School:       | Rutherford High School<br>Panama City, FL 32401               |
| Research Location: | Environics Laboratory<br>USAF Engineering and Services Center |
| Mentor:            | Dr. Daniel A. Stone, PhD.                                     |
| Date:              | 19 June - 11 August 1989                                      |

**Acknowledgements:**

My thanks must go to Dr. Daniel A. Stone for his never ending patience and optimistic outlook! Also thanks to Mr. Mike Henley, Dr. Howard Mayfield, and Dr. Pratt Mounfield for their patience and assistance in helping me to learn and keep busy throughout my eight weeks here at the Center.

## I. Introduction

The main objective of the Environics Laboratory hydrazine research program is to determine the effects and eventual fate of this substance in the atmosphere. The results, which are determined through use of a spherical environmental simulation chamber and an infrared spectrometer, allow for more effective handling, disposal, and spill clean up of this chemical found in several US Air Force weapons systems. My part in this project was to assist Dr. Stone in his research and to learn as much as I could while doing so.

## II. General Description of Research

My assistance consisted of various responsibilities. Principally, these were to sort and graph data files from both previous and current runs in the spherical chamber, to wash and rinse chrome-plated steel plates and aluminum plates for placement within the spherical chamber, to learn to operate the Nicolet computer for conducting experimental runs done in the spherical chamber, to run samples in and plot results from the spherical chamber, to measure absorbance values of various peaks in the calibration plots, and to make graphs to compare the assorted values found with different amounts of water and different lengths of time in which water samples were in the chamber.

### III. Detailed Description of Research

#### A. Spectrometer

A principal requirement of being able to function in the laboratory is to become acquainted with one or more computers. For my part there was no exception. The commands, programs, and capabilities of the Zenith (model Z-248) had to be learned, as did such programs as Lotus 123 (Reference 1), WordPerfect (Reference 2), Harvard Graphics (Reference 3), and Reflections (Reference 4). This was accomplished in quite some detail both by moving through the tutorials and by trial and error. The Lotus 123 program was the most important one to be learned, as this is what is generally used to modify and graph data files from the spherical chamber runs. A typical data file is shown in Figure 1.

File manipulation ensued when the Lotus 123 program had been learned. However, first it was necessary to transfer those files from the original disks they were stored on to the Zenith hard disk. This was done using the HP150 and the HP1000, and is clearly explained in Figure 2. After this file transfer the data was stored in the Zenith so that the extraction could easily be done. Extracted was the information needed to make a graph for each file showing the comparison between the elapsed time and the concentration of hydrazine. These files were from any time between August 1988 to June 1989. An example of a modified file and its graph can be found in Figures 3 and 4.

hydrazine + oxygen (20%) in helium [1st series, 7  
(30 Aug 88 -- 31 Aug 88)

| E-time<br>(hr) | E-time<br>(total) | T (int)<br>(deg C) | Conc.<br>HZ | norm.<br>Conc. | Conc.<br>NH3 |
|----------------|-------------------|--------------------|-------------|----------------|--------------|
| .000           | 87.550            | 20.7               | 1.085       | 1.000          | 0.000        |
| 0.329          | 87.879            | 20.7               | 1.049       | 0.967          | 0.028        |
| 0.656          | 88.206            | 20.7               | 0.992       | 0.914          | 0.016        |
| 0.986          | 88.536            | 20.8               | 1.030       | 0.949          | 0.000        |
| 1.313          | 88.863            | 20.9               | 0.943       | 0.869          | 0.000        |
| 2.352          | 89.902            | 21.0               | 0.954       | 0.879          | 0.000        |
| 3.389          | 90.939            | 21.0               | 0.837       | 0.771          | 0.025        |
| 4.428          | 91.978            | 20.9               | 0.761       | 0.701          | 0.000        |
| 5.465          | 93.015            | 21.1               | 0.670       | 0.618          | 0.000        |
| 6.505          | 94.055            | 21.2               | 0.604       | 0.557          | 0.011        |
| 7.543          | 95.093            | 21.0               | 0.551       | 0.508          | 0.012        |
| 8.586          | 96.136            | 21.2               | 0.498       | 0.459          | 0.001        |
| 9.624          | 97.174            | 21.3               | 0.462       | 0.426          | 0.011        |
| 10.668         | 98.218            | 21.1               | 0.391       | 0.360          | 0.044        |
| 11.705         | 99.255            | 21.0               | 0.353       | 0.325          | 0.034        |
| 12.745         | 100.295           | 20.9               | 0.317       | 0.292          | 0.053        |
| 13.781         | 101.331           | 20.9               | 0.273       | 0.252          | 0.075        |
| 14.820         | 102.370           | 20.9               | 0.237       | 0.218          | 0.062        |
| 15.857         | 103.407           | 20.6               | 0.213       | 0.196          | 0.078        |
| 17.895         | 105.445           | 20.7               | 0.181       | 0.167          | 0.098        |
| 18.932         | 106.482           | 20.6               | 0.161       | 0.148          | 0.094        |
| 19.970         | 107.520           | 20.6               | 0.136       | 0.125          | 0.124        |
| 21.007         | 108.557           | 20.6               | 0.116       | 0.107          | 0.122        |
| 18.044         | 105.594           | 20.4               | 0.099       | 0.091          | 0.124        |
| 23.080         | 110.630           | 20.4               | 0.077       | 0.071          | 0.118        |
| 24.118         | 111.668           | 20.5               | 0.059       | 0.054          | 0.139        |

Figure 1. Hydrazine data taken in the spherical chamber,  
from a Lotus 1-2-3 file.



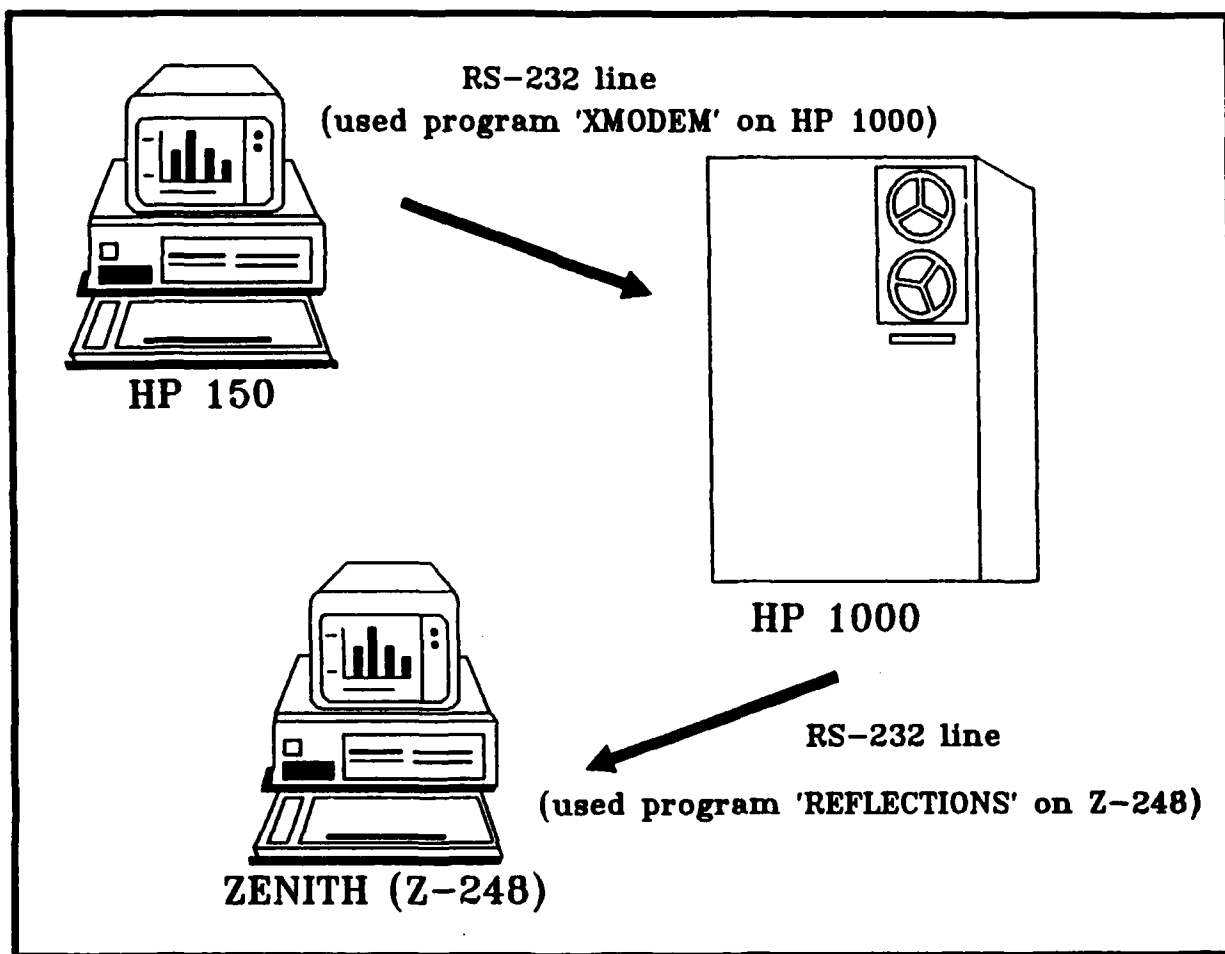


Figure 2. Schematic diagram of data transfer protocol.

|        |       |
|--------|-------|
| 0      | 1.085 |
| 0.329  | 1.049 |
| 0.656  | 0.992 |
| 0.986  | 1.03  |
| 1.313  | 0.943 |
| 2.352  | 0.954 |
| 3.389  | 0.837 |
| 4.428  | 0.761 |
| 5.465  | 0.67  |
| 6.505  | 0.604 |
| 7.543  | 0.551 |
| 8.586  | 0.498 |
| 9.624  | 0.462 |
| 10.668 | 0.391 |
| 11.705 | 0.353 |
| 12.745 | 0.317 |
| 13.781 | 0.273 |
| 14.82  | 0.237 |
| 15.857 | 0.213 |
| 17.895 | 0.181 |
| 18.932 | 0.161 |
| 19.97  | 0.136 |
| 21.007 | 0.116 |
| 18.044 | 0.099 |
| 23.08  | 0.077 |
| 24.118 | 0.059 |

MD30AG88.PRN

Figure 3. The elapsed time and hydrazine concentration data as extracted from the file in Figure 1.

# HZ + O<sub>2</sub> (20%) IN HELIUM

1st SERIES, 7th RUN

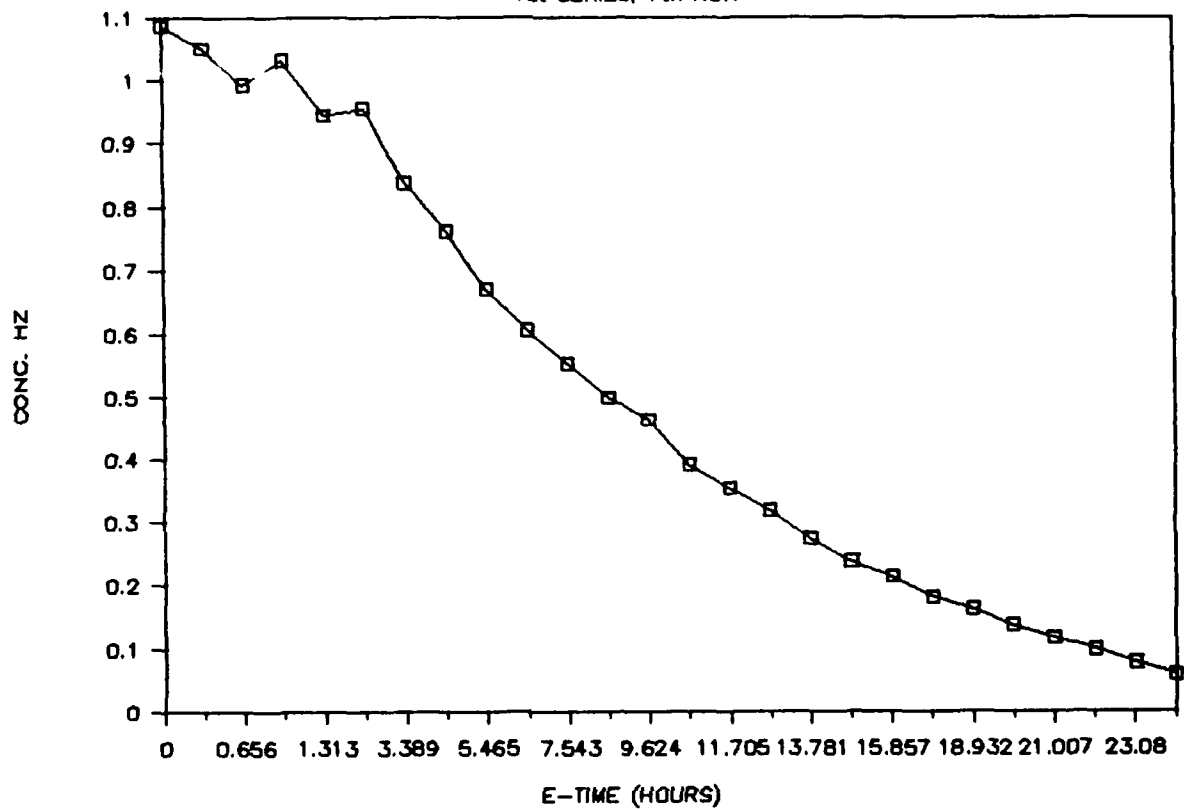


Figure 4. A plot of hydrazine concentration versus time.

Upon completion of the extractions and graphs, 20 chrome-plated steel and 20 aluminum plates were prepared for surface-effects experiments in the chamber. They were washed in a laboratory cleaning solution ('Micro'), rinsed in tap water, rinsed in distilled water, and finally rinsed in a solution of 50% acetone and 50% methanol. This procedure was followed so that the plates could be reproducibly used in chamber experiments.

Details of the software on the Nicolet computer were also learned. The FT-IR program operates the spectrometer to acquire infrared spectra from the chamber and stores these spectra for future reference or graphing. Various manuals and also trial and error were used to accomplish this task. Especially helpful in understanding the computer was a Nicolet manual titled FT-IR Theory (Reference 5); this explained in the simplest manner how the spectrometer works, and some different applications for it. To explain how it works and why it is used is best summed up in this quote from the manual: "The goal of IR (infrared) spectroscopic applications is to determine the chemical functional groups contained in a particular material. Each functional group absorbs characteristic frequencies of infrared radiation uniquely. Thus, a plot of radiation intensity versus frequency (the infrared spectrum) fingerprints the identifiable chemical groups in the unknown." The "particular material"s in this project are hydrazine (or water), methane (which is used as

an internal standard), and whatever varying substance is used to react with the hydrazine. Although the identities of the particular materials are known, the spectra show how hydrazine reacts with the addition of different substances, and with the passing of time.

The operation of the infrared spectrometer can be understood by referring to Figure 5 (Reference 1), while its relationship to the spherical chamber can be easily seen in Figure 6.

#### B. Chamber

The procedure for conducting experiments in the spherical chamber is quite complex. In runs using injections of liquid water as a means to obtain the data necessary for a water calibration curve, the procedure includes the following steps:

First, the turbomolecular pump is shut off and the main pumping valve is closed. Then the internal fan is turned on to equilibrate the chamber. Next, in the case of liquid samples, the temperature of the external glass sample manifold is raised so that the water injected turns to vapor before entering the chamber. When the manifold is hot enough, a very small amount of water (1 to 20 microliters) is injected into the manifold through a silicon septum and is flushed into the chamber with dry helium. Then the internal standard, methane (10 cubic centimeters at 1.0 atmosphere pressure), is also injected. The helium flows into the chamber until it reaches

1. Collimated radiation from the broadband infrared source, A, is directed into the interferometer and impinges on the beamsplitter, B (basically a very thin film of germanium). As its name implies, the beamsplitter "splits" the incoming beam into two "arms" of about equal energy.
2. Approximately 50% of the light is transmitted through the film and is directed onto the fixed mirror, C. The remainder of light reflects off the beamsplitter and is directed onto the moving mirror, D.
3. The beams reflect off the surfaces of the two mirrors and recombine at the beamsplitter. Here constructive and destructive interference occurs, depending on the position of the moving mirror relative to the fixed mirror.
4. The resulting beam passes through the sample where selective absorption takes place, and then continues on to the detector.

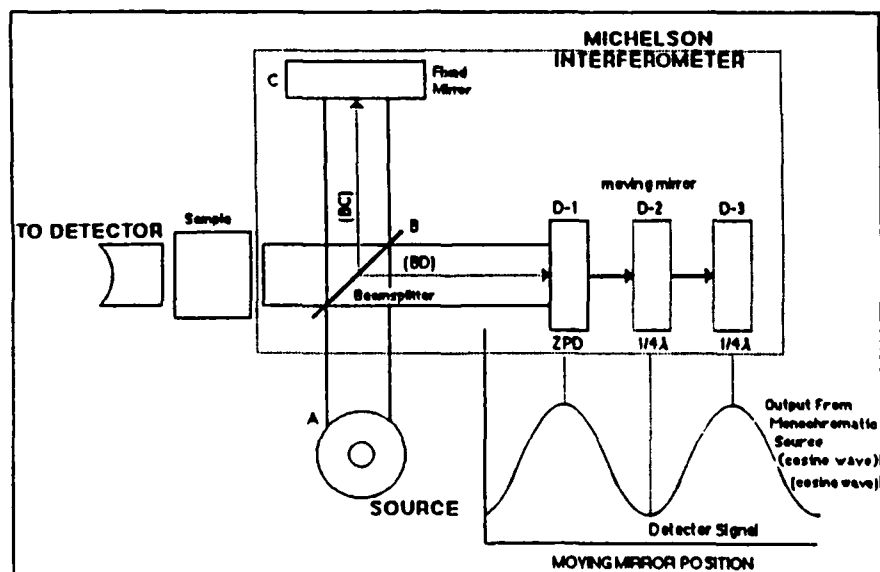


Figure 5. Schematic diagram of an FT-IR spectrometer with a brief overview of its operation.

## Controlled Environment Chamber Experiments

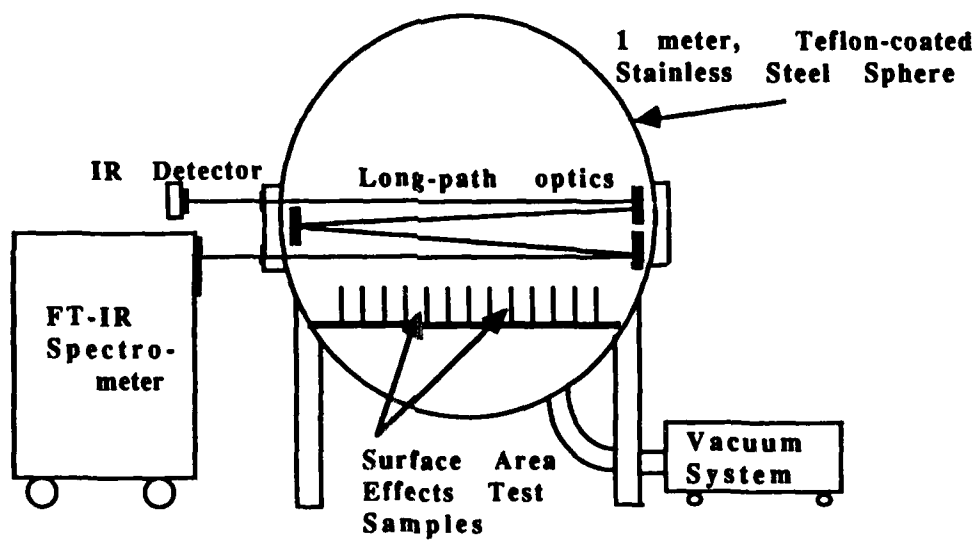


Figure 6. Schematic diagram of FT-IR spectrometer coupled with the spherical reaction chamber.

the desired pressure (usually 760 or 600 Torr). The FT-IR co-adds 512 single scan interferograms and converts them into one single spectrum. Over a period of approximately one hour, four separate spectra are acquired for each sample. These spectra are then ratioed against a background spectrum and plotted in absorbance. Figure 7 shows an entire water calibration spectrum.

The purpose of plotting all of the different spectra is to allow one to make comparisons between runs. In the case of water spectra, two different absorbance features were selected as possible analytical peaks. A range of the spectrum which included these two features was plotted and used to measure peak heights. To select this range and plot individual spectra, a macro written by Dr. Stone was used. Of course, the same x axis range is chosen for every plot of the same experiment to enable easy comparisons between different peaks and their absorption values to be made. An example of a plot showing the chosen water peaks can be seen in Figure 8.

Measuring the chosen water peaks is a very straightforward procedure: a baseline must be drawn from which all measurements are based. A ruler is used to measure the length of each chosen peak in millimeters, and that value is multiplied times the increment value (or distance between steps) of the y axis. The result is the absorbance of the water at that point in time.

As data (absorbance peaks) were collected, they were recorded and a graph was made showing the comparisons between



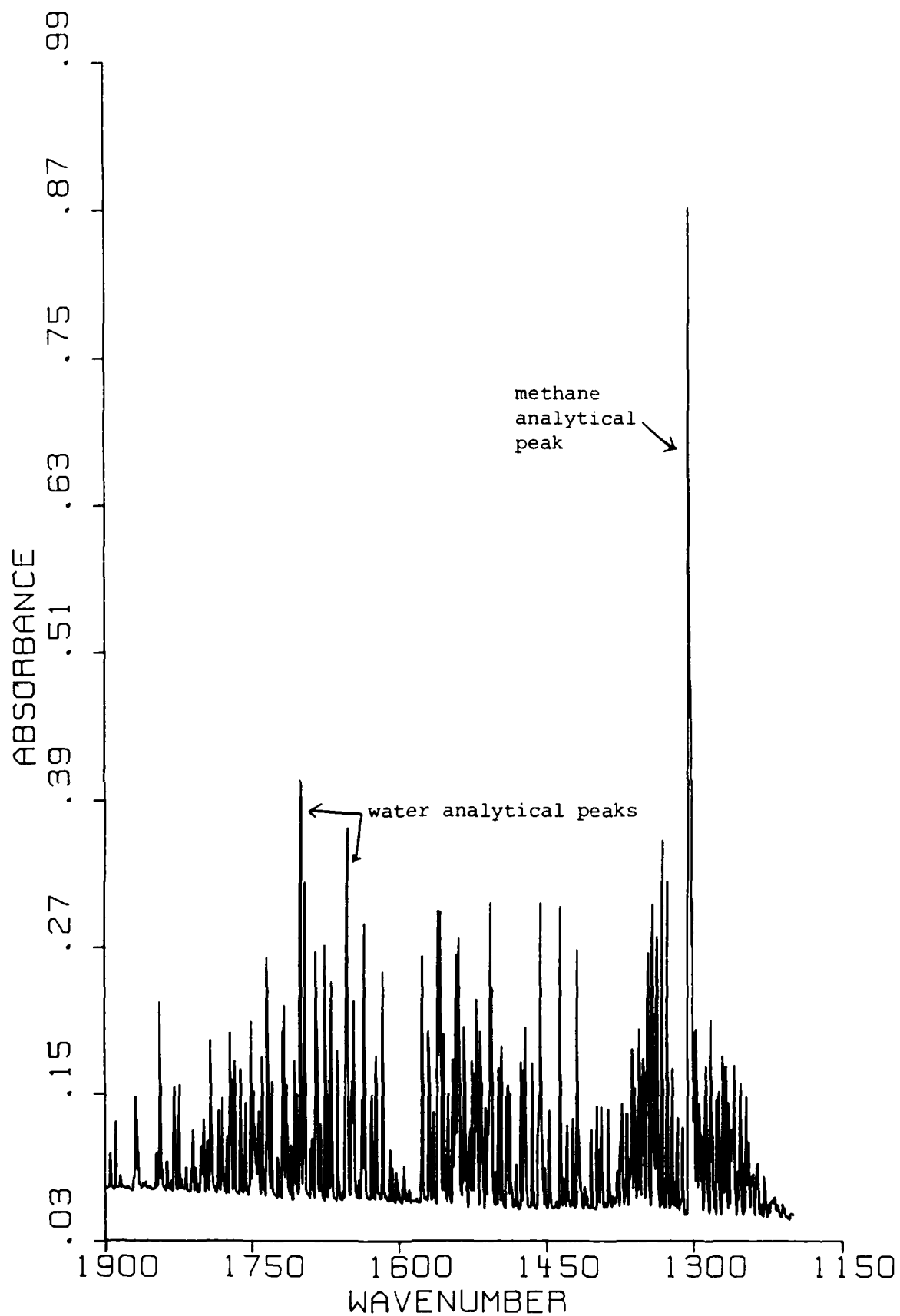


Figure 7. A plot of the spectral region used for water calibrations.

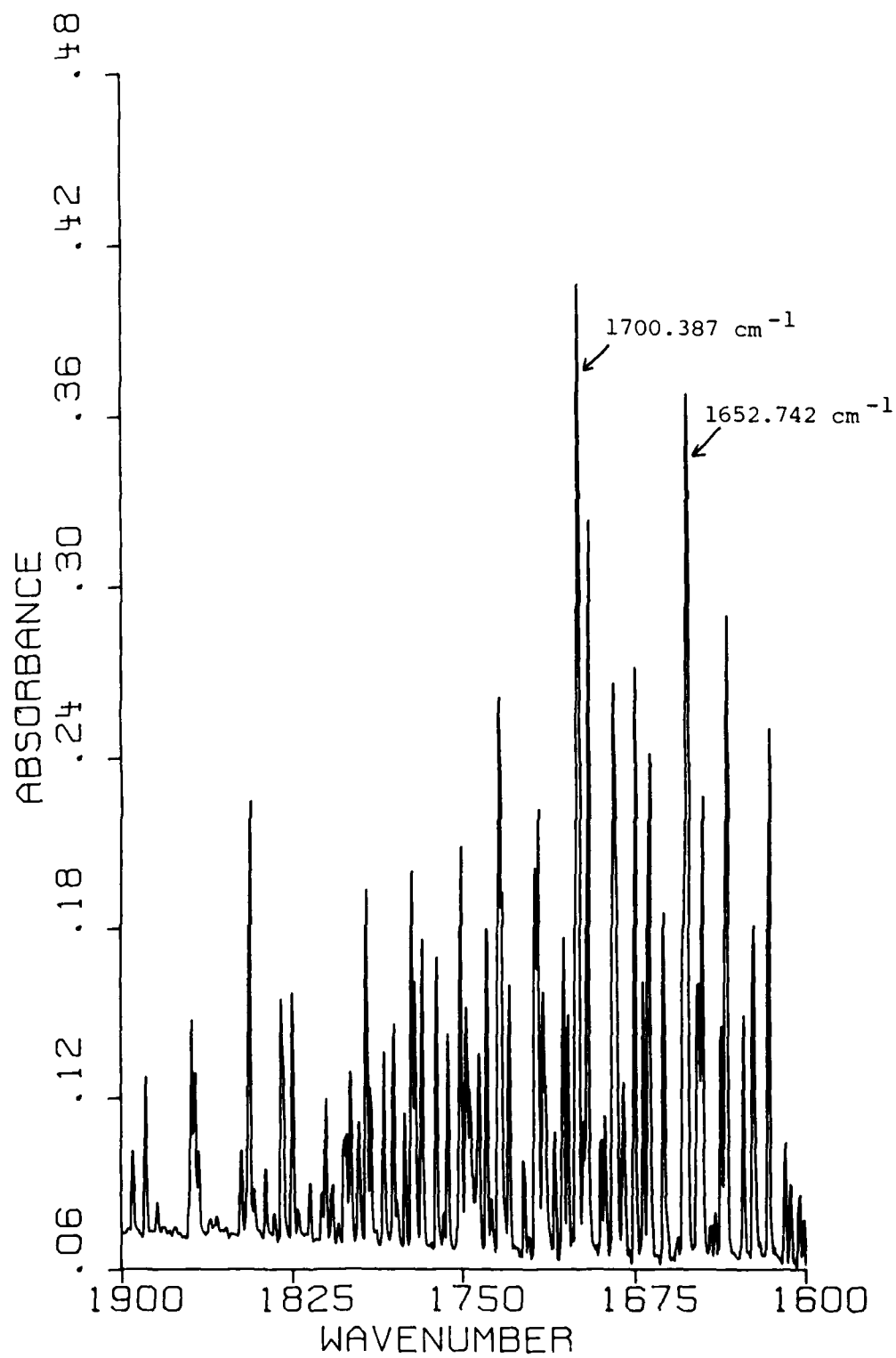


Figure 8. An expanded spectrum of the water bands showing the two analytical peaks.

vapor samples and liquid samples. These comparisons can be seen in Figure 9.

#### IV. Results

The very first runs attempted with the spherical chamber were done using hydrazine in dry helium and 20 chrome-plated steel plates. Only one sample was run, however, because Dr. Stone decided shortly after starting the hydrazine sample that it would be more practical to do the water calibrations, as this is important in understanding hydrazine reactions. The behavior of water and any other aspect of the hydrazine runs should be known, so that should an adverse reaction take place with the addition of a new component (like chrome-plated plates), the scientist would be certain that what was affected was actually the hydrazine.

Before the calibrations were done using injections, they were attempted in a different manner which proved unsuccessful. The initial procedure followed to do the water calibrations was one in which the water was entered into the chamber as vapor and measured according to its pressure rather than being injected as a liquid. Runs were done in a range of 1 to 15 Torr before the faults with this method were discovered. The absorbance rates of the samples were not decreasing at a rate proportional to their pressure; therefore it was concluded that an undetermined amount of water vapor was sticking to the sides of the sample bulb,

## H2O CALIBRATIONS

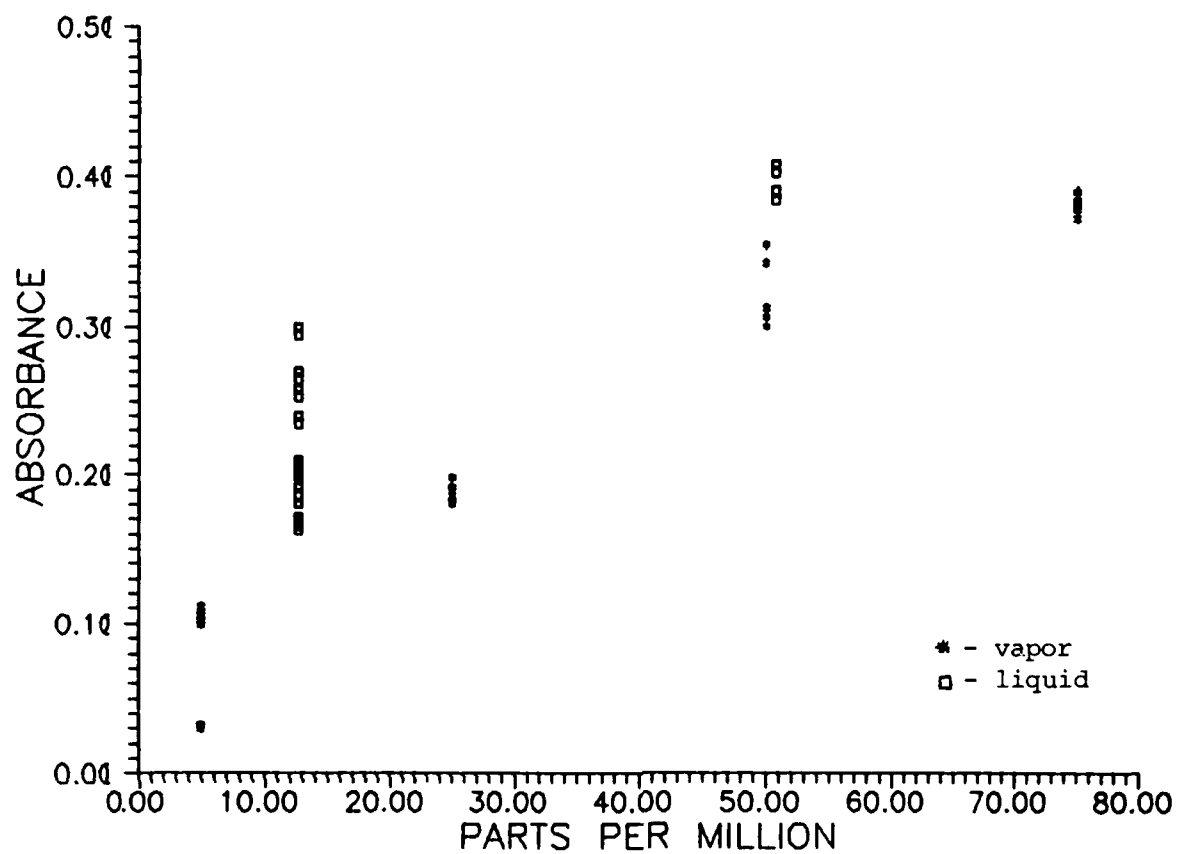


Figure 9. Comparison between vapor and liquid water samples.

consequently making the results from the spectrometer incorrect.

After this was determined, the decision was made to continue the water calibrations using liquid injections. Initially, however, in these liquid injections the peaks still were not in proportion to the amount of water that had been injected. Therefore, the decision was made to leave each sample in the chamber for longer periods of time to determine how long it would take for the peaks to come to their (theoretical) maximum. Samples have been left in the chamber and periodically checked for their progress for up to four days. They seem to be approaching an asymptotic value, however, they have not yet reached this value, so the experiment continues.

#### V. Interesting Observations and Lessons Learned from Summer Experience

My participation in this summer apprenticeship program has definitely been a memorable experience. It has led me to discover much about a laboratory environment, how to work together successfully with others, the detail and exactness involved with all scientific projects, the reliance on computers, and many other things. As this was the first time I had ever been employed, I feel that I was very lucky in having the opportunity to have a job that allows for learning as well as pay. I also feel I was lucky to have this job

experience as my first, because it encouraged rather than dampened my enthusiasm for working, and my coworkers/advisors were all helpful and pleasant people.

The interaction of the people who work here in the Center has also impressed me. Every person whom I came across seems to be very willing to assist anyone who needs their help, yet does not interfere with anyone else's project. The cooperation among coworkers here in the lab is very nice, and possibly very rare. I enjoyed it very much.

## REFERENCES

1. Lotus 1-2-3 User Manual, Lotus Development Corporation MA, 1986.
2. WordPerfect for IBM Personal Computers, WordPerfect Corp., USA, 1988.
3. Harvard Graphics, Software Publishing Corp., USA, 1987.
4. Reflection 1/7 User Manual, Walker Richter and Quinn, Inc., WA, 1988.
5. FT-IR Theory, Nicolet Instrument Corp., Madison, WI, 1986, p. 1-7.

Universal Energy Systems/AF Office of Scientific Research  
High School Apprenticeship Program

HQAFESC Technical Information Center

Final Report

Tyndall Air Force Base

Tyndall, FL

Prepared by: Byron Kuhn

Mentor: Andrew Poulis

Date: August 11, 1989



### Acknowledgments

During the period that I worked at the Air Force Engineering and Services Center in the Technical Information Center, there were many people who deserve a thanks for their guidance and support. To Mr. Andrew Poulis who was my mentor and lent administrative support, thanks. Thanks also to Virginia Davis who helped me with all of the problems that I came across. I would also like to thank Janet Davis, Lela Fletcher and Linda Baker for all the help that they gave me in many areas. For all of his help with and knowledge of BASIS, I would like to thank Fred Nagel. Finally, I would like to thank all of the wonderful people at the Air Force Engineering and Service Center who helped me throughout the summer.

## Final Report

During my term of apprenticeship at the Technical Information Center, I was exposed to many new concepts, ideas, and projects. These projects ranged from barcoding library books to writing report files for the WANG data base, BASIS.

When I first began work, I started off by learning the basics of BASIS, the data base that is used by TIC (Technical Information Center) to store bibliographic records of all of the materials available in the library. As a beginning, I learned the basic process of manipulating the data and how to enter the data using the fields that were allocated for each type of report or book. The first week was basically a familiarization period as to the workings of the data base.

After I became familiar with the workings of BASIS, I began to learn more about how to write reports and profiles.

Reports and profiles are small programs that are written in a language used by BASIS to manipulate data in the data base by creating sets of items and displaying or printing them in a certain fashion. This was accomplished by many hours of reading and trial and error on the reports. Through it all there were many things that I discovered about the workings of the database and the extents of its use.

I created a few reports that were to be used by a group that was researching centrifuges and entering their collection of literature on to the BASIS system. I had to design a model or basic structure of a report that would print the needed fields to a printer and to a file on a disk. I proceeded to do this but only to run into a problem with printing the file to the disk. With the help of the computer department and my previous knowledge of the WANG, it was soon taken care of.

Now that the file was on disk on the WANG, we needed to find a way to transfer this data to a PC (Personal Computer) in order to be able to manipulate it in a word processor and save it on disk, for distribution. This posed a small problem. We needed a communications program that would be able to interface with the WANG, as well as do a transfer of files back and forth

between the WANG and the PC. Our first attempt using Procomm was a failure because the function keys on the WANG did not coincide with the keys that Procomm used. Faced with this dilemma we began searching for another communications program. The computer department (SI) at AFESC let us borrow a copy of VsCom, a communications utility designed for use with the WANG. An attempt to use this program brought immediate success.

Now that we had accomplished this communication with the WANG, we were able to transfer the files using a utility on the WANG called MHUTIL. This program allowed us to transfer the files with ease back and forth between the WANG and the word processor on the PC. The only problem with this system was that if a different type of report was desired, then it would have to be made with the WANG editor and then be restored and compiled for use in BASIS. What we needed was to be able to easily capture the text that we wanted it and place it in a text file on the PC instead of having to write the report each and every time.

Procomm Plus has a feature that allows the user to capture text in a file on the PC for later use. The problem with using Procomm Plus was that it was not sending the proper codes that the

WANG needed to process the commands. I obtained a list of the codes that the WANG needed to receive in order to process the different applications from Major Combs in the SI department. With this list of codes, I was able to enter them into Procomm Plus with it's special key mapping feature. I configured the Procomm Plus program to utilize as closely as possible the same key configuration that VsCom utilized. This took a little time but was easily achieved.

Now the file could be obtained by logging a copy of the information displayed on the screen instead of getting it from a print file on the WANG. This eliminated the steps in creating the report file on BASIS and the transfer of the print file from the WANG to the PC. The only draw back to this was that Procomm Plus could not do a transfer back to the WANG if it was needed, but the advantages outweighed the disadvantages, therefore Procomm Plus was the better choice.

Because I was working in the library I was also required to barcode and catalog a few books while I was there. At first the barcoding was new and interesting however it did become a little tedious at times. While I was working, a new barcoder arrived so I got the chance to configure it to the proper

settings for the type of barcodes that the library used. This consisted of changing some dip switches and connecting the cables to their proper connectors for interface with the WANG terminal.

I also had a chance to do some on-line searching for books and reports while I worked at TIC. This was my favorite part of the summer. I was taught how to search and update records on OCLC, a library cataloging utility that is utilized for bibliographic verification in reference and for inter-library loans. The records are used for cataloging as well as to facilitate libraries sharing resources in a network of library loans. I also did some searching on DTIC, the Defense Technical Information Center, a data base which has hundreds of areas for use. This was a complicated on-line searching service and can be quite costly for some searches. When on DTIC the object was to narrow down a broad subject to find a listing of books, magazines and reports on a specific subject or experiment.

These two on-line data bases when used together by the library creates a vast expanse of materials available to the people at AFESC. A subject area would be searched on DTIC, OCLC or other on-line services and a listing of possible sources of information were gathered and given to the person requesting the search. That person then

looked over the listing and selected the materials that he need and returned the list to the library. At this point the books were then searched for on OCLC and a request would be made for an inter-library loan of that book. Some times the book would be unavailable but if it was available then the request would be made and the responding library would send the requested material for a period of time that usually lasted a month. At that time the book would then need to be sent back to the original library.

As with any job, there were some other smaller tasks that were required of me, like shifting books, but these fell in to the schedule of my other duties. In closing, it was a very interesting summer and well worth the time I spent working. It would have been nice if the program could have lasted longer but I still enjoyed it.

## Creating REPORTS on the WANG Editor.

In order to utilize the WANG editor, please follow the following instructions for creating reports for BASIS.

1) The first thing that must be done is to load the editor. In order to do this you must run the program "EDITOR" from a run screen. \*! From the main menu, type a F12 {Shift=F2} to enter the Basic Utilities Menu. From this menu, depress and F31 {Alt-F1} to Run a Program. For the program name, type in "Editor" and press enter. !\*

2) The language that will be used is FORTRAN. This must be specified at the beginning of the edit.

3) If you are creating a NEW report file then simply depress enter and the EDITOR will take you to the creation screen.

4) If you are editing an OLD file then tab over in order to type in the Name, Library, and Volume to specify the file that you wish to edit. If you are editing an old file then the editor will tell you that it must number the program, just press enter to allow it to number the program lines.

5) When you EDIT, you will have to follow the instructions on the editor. They are pretty straight forward. When editing, I suggest you use the functions keys to move to the place in the report that you want to edit then press F9 to modify.



After the modifications are complete, simply press enter. If you need to insert or delete lines, those options are available on the screen.

6) When making NEW reports, simply use the Insert (F11) {Shift-F1} command to make the report.

7) Once you have modified or created the report, then you need to save it. Press F16 {Shift-F6} to go to the editor menu. At the editor menu, select the create command (F5) to save it as a new file or (F6) to overwrite the old file. You will then be asked for the filename, library, and volume, as well as if you want the report compressed and with line numbers. The report should be compressed and SELECT NO LINE NUMBERS, IF YOU ALLOW LINE NUMBERS, THEN THE FILE WILL NOT OPERATE PROPERLY!

8) After the file has been saved, exit the editor by pressing F16 {Shift-F6} in order to exit the editor. Continue pressing F16 {Shift-F6} until you come to the main menu.

## Getting the Report in BASIS.

Before you can use a report that you created in the Wang editor for BASIS, you must restore the file to your profile and compile it. Only after this is done can you can utilize the report. Follow the following instructions in order to create the report for use on BASIS.

- 1) Log on to BASIS using your BASIS ID.
- 2) Exit the MENUS.
- 3) Enter report mode by typing in "report" and pressing enter.
- 4) For this report we will be using the sample report included to perform these functions. Simply modify the filename, library and volume to fit your system. This report was called "ARARPT" in the library, "RXLRPTS", on the volume, "USR1".
- 5) Type in "restore all file fil=ARARPT lib=RXLRPTS vol=USR1" and press enter. This will restore the file to your profile.
- 6) Now the file MUST be compiled. Type in "compile" and press enter.

- 7) If ANY errors occur then you will need to go back into the EDITOR, make the changes then save them and repeat the restoring process.
- 8) After the compilation is successful you may exit the report mode by typing "quit" to exit BASIS or "BASIS" to go to BASIS.

## Sample Report.

The following report was created by Byron Kuhn on July 5, 1989 for utilization with BASIS to produce output needed for a bibliography. Below is a listing of the report that will be explained in detail. We will call this report "ARARPT" which will be located in library "RXLRPTS" on volume "USR1". The name of the file, library and volume may vary from system to system. The Library should be the users personal library or a library that is universal to the BASIS system. The file name is anything that the user would like to name the report. This report was written in the Wang VS Integrated Editor - Version 7.02.18 in the Fortran mode. THIS FILE SHOULD BE SAVED WITHOUT LINE NUMBERS! If the report is saved with line numbers then it will not function properly. After the report is created, enter BASIS and type "report" to enter the report mode. Then type in "restore all file fil=(filename {ARARPT}) lib=(library name {RXLRPTS}) vol=(volume name {USR1})" and press enter. When the restore is completed, type in "compile" and press enter to compile the report. Once this is completed, return to BASIS and the report has been added for you to utilize. In the following listing, the lines will be numbered in order to be able to refer back to them.

```

010      *RPT* ARARPT
020      */
030      */ Report file for ARA BASIS record conversion
040      */
050      BEGIN
060      SET(PUT.FILE="FIL=ARATST,LIB=RXLRPTS,VOL=USR1")
070      OPEN(NAME=PUT.FILE,DEV=Q,MODE=OUTPUT)
080      */
090      */          Begin loop
100      */
110      REPEAT.A
120      */          Get Document
130      */
140      GET
150      BREAK.A WHEN (END.OF.SET)
160      */
170      PUT(T=5;AU AS <X(60)< IN ROWS=(1:5))
180      SKIP(1)
190      PUT(T=5;CORP AS <X(60)< IN ROWS=(1:5))
200      SKIP(1)
210      PUT(T=5;TI AS <X(60)< IN ROWS=(1:9))
220      SKIP(1)
230      PUT(T=5;PUBL AS <X(60)< IN ROWS=(1:9))
240      SKIP(1)
250      PUT(T=5;CONF AS <X(60)< IN ROWS=(1:9))
260      SKIP(1)
270      PUT(T=5;EDTN AS <X(60)< IN ROWS=(1:9))
280      SKIP(1)
290      PUT(T=5;SERIES AS <X(60)< IN ROWS=(1:9))
300      SKIP(1)
310      PUT(T=5;NOTES AS <X(60)< IN ROWS=(1:9))
320      SKIP(2)
330      */
340      */          Stop if no more Documents
350      */
360      UNTIL.A (END.OF.SET)
370      END

```

This listing is the report that creates the Wang Print file that will be used to download to the PC. Following is an explanation of how this REPORT operates and possible modifications that can be made to it.

```
{ *RPT* ARARPT } - 010
```

This line is used to specify that this program is a REPORT. BASIS uses other procedures that are called profiles, but those will not be discussed. The {\*RPT\*} specifies the REPORT status. {ARARPT} is the name that the report will be called, this can be different than the name that the file is saved as.

```
{ */ } - 020+
```

This prefix on a line, tells the computer that this is just a remark about the program, this does NOT perform any actual functions.

{ BEGIN } - 050

This line MUST be at the beginning of where the actual program starts but after the { \*RPT\* } line.

{ SET(PUT.FILE="FIL=ARATST,LIB=RXLRPTS,VOL=USR1") } - 060

This line tells the computer the name of the file that will be created when the report is run. It sets the variable {PUT.FILE} equal to the file name. This can be easily changed to accommodate your needs.

{ OPEN(NAME=PUT.FILE,DEV=Q,MODE=OUTPUT) } - 070

This line opens the file for input by BASIS. The parameters at the end {DEV=Q} and {MODE=OUTPUT} can be changed if needed. (See the BASIS manual for details.)

{ REPEAT.A } - 110

{ BREAK.A WHEN (END.OF.SET) } - 150

{ UNTIL.A (END.OF.SET) } - 360

These statements form the loop in the program. The program will end the loop once the end of the set of documents is reached.

{ GET } - 140

This takes the next document from the document set.

{ PUT(T=5;AU as <X(60)< IN ROWS=(1:5)) } - 170+

This line (used as an example) is the line that sends the data to the print file. The { T=5 } statement tells the computer to tab over 5 spaces first. This line calls the { AU } author field from the document. This field will be displayed within 60 characters per line { <X(60)< }. The { IN ROWS=(1:5) } statement tells the computer that it may take up to 5 lines to display the Author field of that document. If only one row is desired, then the ROWS command may be omitted from the line. Therefore this line will display up to 300



characters for the Author field. The other lines include the corporate author field { CORP }, the title field { TI }, the publication { PUBL } field, the conference field { CONF }, the edition field { EDTN }, the series field { SERIES }, and the notes field { NOTES }. These can be changed to what ever fields may be desired by the user. (NOTE: When a report is created, it MUST be restored and compiled!! See your BASIS manuals for more details on how this is done.)

{ SKIP(1) } - 180

{ SKIP(2) } - 320

These lines tell the computer to skip a line in the file.

{ END } - 370

This designates the end of the REPORT.

## Making the BASIS print file.

To create a print file for download, follow the following step-by-step instructions.

\*\*\*\*\*NOTE\*\*\*\*\* Before you run the report, MAKE SURE THAT YOUR PRINT SETTINGS ARE SET TO "K" FOR KEEP. You do not want it set to "S" to spool it to the printer, unless you want a hard copy of the output. If you are going to spool to the printer, then you must "quit" BASIS after it has been sent, then BASIS will que the file to the printer.

- 1) Create the desired set in BASIS. (EX: find loc=ARA)
- 2) After the set has been created, make sure it is the previous set. (EX: if you are on line 4 then the set should be on line 3)
- 3) Type in { Report execute ARARPT ( <- this name should be the REPORT name. This is the name given to the report on the "\*RPT\*" line.) }.
- 4) Wait for the report to complete its run.
- 5) After the report is done, type quit to exit BASIS

## Modifying the Report.

There will probably be a need to change that sample report to fit the individual needs of the users, I have included a few simple possible modifications that can easily be made. If there are any major changes to be made, then I recommend consulting the manual on writing reports provided with BASIS.

In the lines 170-310 of the Sample Report, there was the statement "IN ROWS=(1:5)".. This can be modified to reflect the number of lines that you would like to limit the field to. It will only utilize all of the lines if needed, therefore it will not print out 4 blank lines if 5 were allocated and only one was needed.

Also in lines 17-310 there is a statement "<X(60)<". This statement allocates the number of characters allowed per line for that field. For example a field for the ISBN number would only need 10 to 12 spaces for it, depending on whether dashes were used. That line could then be written like:

```
PUT(T=5;ISBN AS <X(10)<)
```

If you would like to add a line before the data saying what the data is, then it can be added by putting a line like the following just before the line that outputs the data.

```
PUT("ISBN" AS <X(4)>)
```

\_\_\_\_\_ this number represents the  
number of  
characters that the prefix  
takes up.

## Using VsComm to Convert the Print File.

To begin, you will need to have the two VsComm diskettes. It is HIGHLY recommended that these disks be installed on a hard drive. This can be done by creating a directory like "\TERM" and copying the files from both disks to this sub-directory.

Following are STEP-BY-STEP instructions for utilizing VsComm for downloading a PRINT file from the Wang. VsComm has many other utilities but this report will concentrate solely on the conversion of a print file from the Wang to an ASCII file on a PC.

Before beginning, you must first set up a call file on VsComm. This file is used to dial the Wang. Create the file and name it "WANG".

- 1) Press F1 to call the Wang, when prompted for the call file, type in "WANG" or the name that you gave that file. This will dial the Wang and connect to it.
- 2) Log-On to the Wang, using your user ID.

- 3) Goto where you RUN a program or procedure. (In this case it is an F12 {Shift-F2} (The Basic Utility Menu) then an F31 {Alt-F1} (Run a program) The conversions are located in the VsComm manual for all the different function keys, or you can press {Alt-Z} to get a listing on the screen.
- 4) The program that you will need to run is called "MHUTIL". You can leave the other options for library and volume blank. Type in "MHUTIL" and press Enter.
- 5) Select F1 - Document/File Transfer Functions.
- 6) Select F4 - Wang print files to PC ASCII Files.
- 7) Type in the correct volume and library of the file. In this report we used Library=RXLRPTS and Volume=USR1.
- 8) Select the file desired by tabbing and pressing the F1 key to select the file that was specified in line 060 of the accompanying report. In this case, that file is "ARATST". Then press the Enter key to continue the process.
- 9) Now select the path on the PC for the file. We will use C: because we are using a hard drive and \TERM as a directory for the file to go to. If you want it to go to a floppy (A:) then just enter an A: for the drive specification and nothing for the Path.

- 10) After these selections have been made, the transfer will begin.
- 11) When the transfer is complete, press enter and wait for the menu to come back up. Log-Off the Wang ( a few F16's {Shift-F6} should take you out.
- 12) After you have logged off of the Wang, you will need to terminate the connection to the Wang. This is done by pressing {Ctrl-A} to get the options menu of the VsComm program. At this menu press the F3 key to "Terminate the Connection". The program will ask you to confirm this, simply press the "Y" key and the program will terminate the connection.
- 13) After you have terminated the connection, Press the ESC key to exit to DOS.
- 14) Now use the PC's Word Processor to edit the file.

GAS CHROMATOGRAPHIC INVESTIGATION  
OF  
JET FUEL EVAPORATION

PREPARED BY:  
SCOTT T. LAMB

MENTOR:  
HOWARD T. MAYFIELD  
AFESC ENGINEERING AND SERVICES CENTER  
ENVIRONICS LABORATORY, TYNDALL AFB

From  
June 19, 1989  
through  
August 12, 1989



## ACKNOWLEDGEMENTS

Special recognition must be given to Universal Energy Systems and the Air Force Engineering and Services Center for establishing the program and giving me the chance to further my scientific interests. The Apprenticeship Program has indeed furthered my interest in science and helped in creating and broadening my future goals because it has enhanced my knowledge of chemistry and allowed me to experiment with extremely advanced equipment. Thanks again for the opportunity.

I would also like to thank Mr. Mike Henley and my mentor, Dr. Howard Mayfield, both of whom patiently and thoroughly answered my many questions. Thanks must also be given to the many friendly people at the Center who helped in my learning what it is like in an actual laboratory environment.

## INTRODUCTION

An Air Force Engineering and Services Center project, "Marker Identification of JP-4 in Ground Water," has studied the gas chromatographic profiles of various aviation and jet fuels in their neat forms and from their water-soluble fractions [1,2,3]. Little information was known about the chromatographic profiles and the effect on the identification of these fuels after the affects of weathering processes such as evaporation, absorption, and biodegradation. This project attempts to simulate the processes of evaporation and absorption in laboratory experiments. Gas chromatographic profiles of laboratory "weathered" fuel samples will yield information relevant to the identification of jet fuels when natural weathering processes occur.

Spills occuring during jet refueling and from leaking underground fuel tanks pose environmental problems. Often times the source of a spill is unknown. Therefore the fuel which was spilled becomes important. The experiments in this study will demonstrate the problems associated with the identification of fuels after the effects of weathering. This experiment also attempts to simulate the actual soil and evaporating conditions in order to provide an estimate of the time elapsed before JP-4 and JP-8 have similar component make-ups.

## PROCEDURE

The first experiment was set up using 1 uL of JP-4 and JP-8 fuel samples in 1 gram of two different types of soil; Chipola and Mississippi in 22 ml VOA vials. The soils had been sterilized with mercuric chloride to prevent the effects of biodegradation. After weighing the samples it became apparent that 1 uL of fuel could not be detected by the scale, as it recorded negative weights. This problem was probably due to the presence of moisture contained in the soil. Control bottles were set up in all four sections of the fume hood to account for the loss or gain of moisture in the bottles. After sacrificing a vial each day and extracting the fuel from the soil, it was then injected into the gas chromatograph. A detailed look at the extraction procedure and extraction solvent preparation can be found in Table 1.

Analyses were performed on the HP5890 Gas Chromatograph (Hewlett Packard, Co.)\* This instrument utilized a fused silica capillary column measuring 30m with a 25mm inner diameter. The column was coated with 1.0um of poly 95% methyl 5% phenyl siloxane (DB-5, J&W Scientific, Inc.)\*. A detailed description of chromatographic settings can be found in Table 2.

The chromatograms from the first experiments showed that the organic compounds of the fuel were undetectable. Due to

apparent negative weights and low analytical response from the first experiment, the project was restarted using 25 uL of fuel in hopes that this fuel sample would be more easily detectable and measured. Again, 46 bottles were filled with 1 gram each of Mississippi type soil and 46 were filled with Chipola soil. After the addition of the 25 uL of the different fuel to the soils, the samples were placed under the fume hood in a condition of relatively constant wind velocity. Weights were taken on a daily basis to attempt to account for the loss of organics in the fuel over time. The same procedure was used in extracting and injecting as in the first experiment.

After several injections using the automatic sampler, the syringe became clogged with soil particles. These particles were caused by the small amount of extraction solvent used which in turn caused some of the soil to be pipeted during the transfer from the VOA vile to the auto sampler vile. The result of this was that all of the samples were injected manually so that the syringe could be cleaned better between injections. A detailed list of manual injections can be found in Table 3.

Following weighing, extraction, and injection, the integration reports containing a list of peak areas were then analyzed. The Laboratory Automation System (LAS) was the primary program used in collecting and storing data. The plotting of the chromatograms was done using the CPLOT program. Following data collection, the reports were then

transduced into data vectors using the SETUP gas chromatographic transducing program.\* Three "marker peaks" were chosen to standardize the retention times.

---

\*Mention of the products above does not constitute Air Force endorsement or rejection of this product, and use of information contained herein for advertising purposes without obtaining clearance according to existing contractual agreements is prohibited.

## RESULTS AND CONCLUSIONS

JP-4 and JP-8 jet fuels become indistinguishable after about 4 days, under the conditions I used to perform this experiment. After 4 days the volatile materials present at time 0 in JP-4 have had time to evaporate out, leaving a chromatogram similar to that of JP-8 as is shown in Figures 1-4. Although there is more JP-8 still present, the components are the same, and the chromatographic profiles are similar. The type of soil had no effect, as one type of soil did not impede the progress of evaporation more than the other. However, compared to the fuel sample not placed in any kind of soil, the effects that the soil had on the evaporation is clearly seen. The amount of fuel placed in an empty 22ml vial which evaporated in 8.5 hours, was about the same as after 2 days in the soil bottles. See Figures 5-6. The total peak areas also were the same after about 6 days as seen in Figure 7.

In another experiment, vials were used which had less surface area than the 22ml VOA viles. These vials contained 100 uL of fuel and were also analyzed over a daily period. Their chromatographic profiles show that they still have many of their components after 21 days, Figures 8 and 9. A long-term study would be needed to figure out exactly how long before these components are completely gone. Soil blanks were extracted and analyzed after 22 days to measure any extractable organics in the soil, and to determine whether or not the fumehoods might have permitted cross contamination of the

sample by exchanging vapor phase organics. Figure 10 illustrates that there was no contamination evident after 22 days.

In future experiments involving the weighing of soil, one recommendation would be to use glass beads or totally dry the soil, if possible in order to bypass any confusion resulting from the presence of moisture. In order to acquire extremely accurate data concerning the weight of 1 uL of fuel it would be necessary to avoid this confusion. Another aspect of the experiment which proved challenging was the clogging of the plunger in the auto sampler due to the particles from the soil. Perhaps centrifuging the samples longer or at a higher rate, or perhaps using some type of filter would overcome this problem.

Further research is needed to simulate all conditions and sizes of spills, but this experiment provides sufficient data to give an accurate illustration of the evaporation of fuel and the effects that soil has upon it.

## REFERENCES

1. H. T. Mayfield and M.V. Henley, Database Management and Pattern Recognition Analysis for the Interpretation of Gas Chromatographic Profiles, Proceedings of the Pittsburgh Conference, March 6-10, 1989, Atlanta, GA.
2. M.V. Henley and H.T. Mayfield, Analysis of Water Soluble Fractions for Aviation Fuel Classification, Proceedings of the Pittsburgh Conference, March 6-10, 1989, Atlanta, GA.
3. H.T. Mayfield, Ph.D. Dissertation, University of Alabama, University, AL (1984).
4. H.T. Mayfield and W. Bertsch, Computer Applications in the Laboratory, 1 (1983) 130.
5. H.T. Mayfield, Personal Communication, HQ AFESC/RDVC, Tyndall AFB, FL. 1989.
6. M. Henley, Personal Communication, HQ AFESC/RDVC, Tyndall AFB, FL. 1989.



Table 1

PREPARATION OF CARBON DISULFIDE SOLVENT

- 1 Measure 20 ml of Carbon Disulfide into small serum vial
- 2 Pipet 22.4 ml of D<sub>10</sub> Ethyl Benzene (1.07 g/L)
- 3 Add to Carbon Disulfide
- 4 Close vial and crimp it shut

EXTRACTION PROCEDURE

- 1 Measure 1 gram of soil into 22 ml VOA vial
- 2 Add 1 uL of fuel
- 3 Weigh the sample
- 4 Add 1 ml of Carbon Disulfide
- 5 Place in shaker for 5 minutes
- 6 Centrifuge for 10 minutes at 2.18 x 1000 RPM
- 7 Extract using fisher transfer pipets
- 8 Put in auto sampler vials and label

TABLE 2  
CHROMATOGRAPH SETTINGS

|                      |  |
|----------------------|--|
| F.I.D Hydrogen flow- | 75 ml per minute                                       |
| F.I.D Air flow-      | 230 ml per minute                                      |
| Carrier gas flow-    | 1.8 ml per minute                                      |
| Purge flow-          | 2.75 ml per minute                                     |
| Split vent flow-     | 31 ml per minute                                       |
| Carrier gas-         | Helium   |
| Injection temp-      | 250°C  |
| Temperature program- | Initial temp., 40°C<br>rate, 3.0 deg/min. to 250°C     |
| Equilibration time-  | 1.00 minute  |
| Sample size-         | 1 uL   |
| Injection method-    | Splitless for soil extracts<br>Split for fuel extracts |

TABLE 3

## SOIL EXTRACTION SAMPLE LISTING

S= SOIL (1-CHIPOLA SOIL) (2-MISSISSIPPI SOIL)

JP-4 AND JP-8 TYPE FUELS

T= TIME IN DAYS

FE= FUEL EVAPORATION

\*ALL SOIL EXTRACTION SAMPLES WERE RUN SPLITLESS\*

\*ALL FUEL EXTRACTION SAMPLES WERE RUN SPLIT\*

| <u>SA#</u> | <u>SAMPLE NAME</u> | <u>PROC-FILE</u> | <u>RAW FILE</u> | <u>STD AMOUNT</u> |
|------------|--------------------|------------------|-----------------|-------------------|
| 1          | S1JP4T0            | PEV054           | REV054          | 1.00000           |
| 2          | S1JP8T0            | PEV055           | REV055          | 1.00000           |
| 3          | S2JP4T0            | PEV056           | REV056          | 1.00000           |
| 4          | S2JP8T0            | PEV057           | REV057          | 1.00000           |
| 5          | S1JP4T1            | PEV058           | REV058          | 1.00000           |
| 6          | S1JP8T1            | PEV059           | REV059          | 1.00000           |
| 7          | S2JP4T1            | PEV060           | REV060          | 1.00000           |
| 8          | S2JP8T1            | PEV061           | REV061          | 1.00000           |
| 9          | S1JP4T4            | PEV062           | REV062          | 1.00000           |
| 10         | S1JP8T4            | PEV063           | REV063          | 1.00000           |
| 11         | S2JP4T4            | PEV064           | REV064          | 1.00000           |
| 12         | S2JP8T4            | PEV065           | REV065          | 1.00000           |
| 13         | S1JP4T7            | PEV066           | REV066          | 1.00000           |
| 14         | S1JP8T7            | PEV067           | REV067          | 1.00000           |
| 15         | S2JP4T7            | PEV068           | REV068          | 1.00000           |
| 16         | S2JP8T7            | PEV069           | REV069          | 1.00000           |
| 17         | S1JP4T6            | PEV070           | REV070          | 1.00000           |
| 18         | S1JP8T6            | PEV071           | REV071          | 1.00000           |
| 19         | S2JP4T6            | PEV072           | REV072          | 1.00000           |
| 20         | S2JP8T6            | PEV073           | REV073          | 1.00000           |
| 21         | S1JP4T8            | PEV074           | REV074          | 1.00000           |
| 22         | S1JP8T8            | PEV083           | REV083          | 1.00000           |
| 23         | S2JP4T8            | PEV084           | REV084          | 1.00000           |
| 24         | S2JP8T8            | PEV085           | REV085          | 1.00000           |
| 25         | S1JP4T11           | PEV086           | REV086          | 1.00000           |
| 26         | S1JP8T11           | PEV087           | REV087          | 1.00000           |
| 27         | S2JP4T11           | PEV088           | REV088          | 1.00000           |
| 28         | S2JP8T11           | PEV089           | REV089          | 1.00000           |
| 29         | STD 7-7-89         | PEV090           | REV090          | 1.00000           |
| 30         | STD 7-7-89         | PEV091           | REV091          | 1.00000           |
| 31         | S1JP4T12           | PEV092           | REV092          | 1.00000           |
| 32         | S1JP8T12           | PEV093           | REV093          | 1.00000           |
| 33         | S2JP8T12           | PEV094           | REV094          | 1.00000           |
| 34         | S2JP4T12           | PEV095           | REV095          | 1.00000           |
| 35         | S1JP4T13           | PEV096           | REV096          | 1.00000           |
| 36         | S1JP8T13           | PEV097           | REV097          | 1.00000           |
| 37         | S2JP4T13           | PEV098           | REV098          | 1.00000           |
| 38         | S2JP8T13           | PEV099           | REV099          | 1.00000           |
| 39         | S1JP4T14           | PEV100           | REV100          | 1.00000           |
| 40         | S1JP8T14           | PEV101           | REV101          | 1.00000           |
| 41         | S2JP4T14           | PEV102           | REV102          | 1.00000           |
| 42         | S2JP8T14           | PEV103           | REV103          | 1.00000           |

TABLE 3, Cont.

|    |           |        |        |         |
|----|-----------|--------|--------|---------|
| 43 | NSJP4T0   | PEV104 | REV104 | 1.00000 |
| 44 | NSJP8T0   | PEV105 | REV105 | 1.00000 |
| 45 | NSJP4T4.5 | PEV106 | REV106 | 1.00000 |
| 46 | NSJP8T4.5 | PEV107 | REV107 | 1.00000 |
| 47 | S1JP8T12  | PEV108 | REV108 | 1.00000 |
| 48 | NSJP4T8.5 | PEV109 | REV109 | 1.00000 |
| 49 | NSJP8T8.5 | PEV110 | REV110 | 1.00000 |
| 50 | S1JP4T15  | PEV111 | REV111 | 1.00000 |
| 51 | S1JP8T15  | PEV124 | REV124 | 1.00000 |
| 52 | FE4JP8T8  | PEV125 | REV125 | 1.00000 |
| 53 | S2JP4T15  | PEV126 | REV126 | 1.00000 |
| 54 | FE4JP8T8  | PEV127 | REV127 | 1.00000 |
| 55 | S1JP8T15  | PEV128 | REV128 | 1.00000 |
| 56 | FE3JP4T11 | PEV129 | REV129 | 1.00000 |
| 57 | S2JP8T15  | PEV130 | REV130 | 1.00000 |
| 58 | S1JP4T18  | PEV131 | REV131 | 1.00000 |
| 59 | S1JP8T18  | PEV132 | REV132 | 1.00000 |
| 60 | S2JP4T18  | PEV133 | REV133 | 1.00000 |
| 61 | S2JP8T18  | PEV134 | REV134 | 1.00000 |
| 62 | S1JP8T15  | PEV135 | REV135 | 1.00000 |
| 63 | S1JP4T2   | PEV136 | REV136 | 1.00000 |
| 64 | S1JP8T2   | PEV137 | REV137 | 1.00000 |
| 65 | S2JP4T2   | PEV138 | REV138 | 1.00000 |
| 66 | S2JP8T2   | PEV139 | REV139 | 1.00000 |
| 67 | FE4JP8T1  | PEV140 | REV140 | 1.00000 |

FIGURE 1

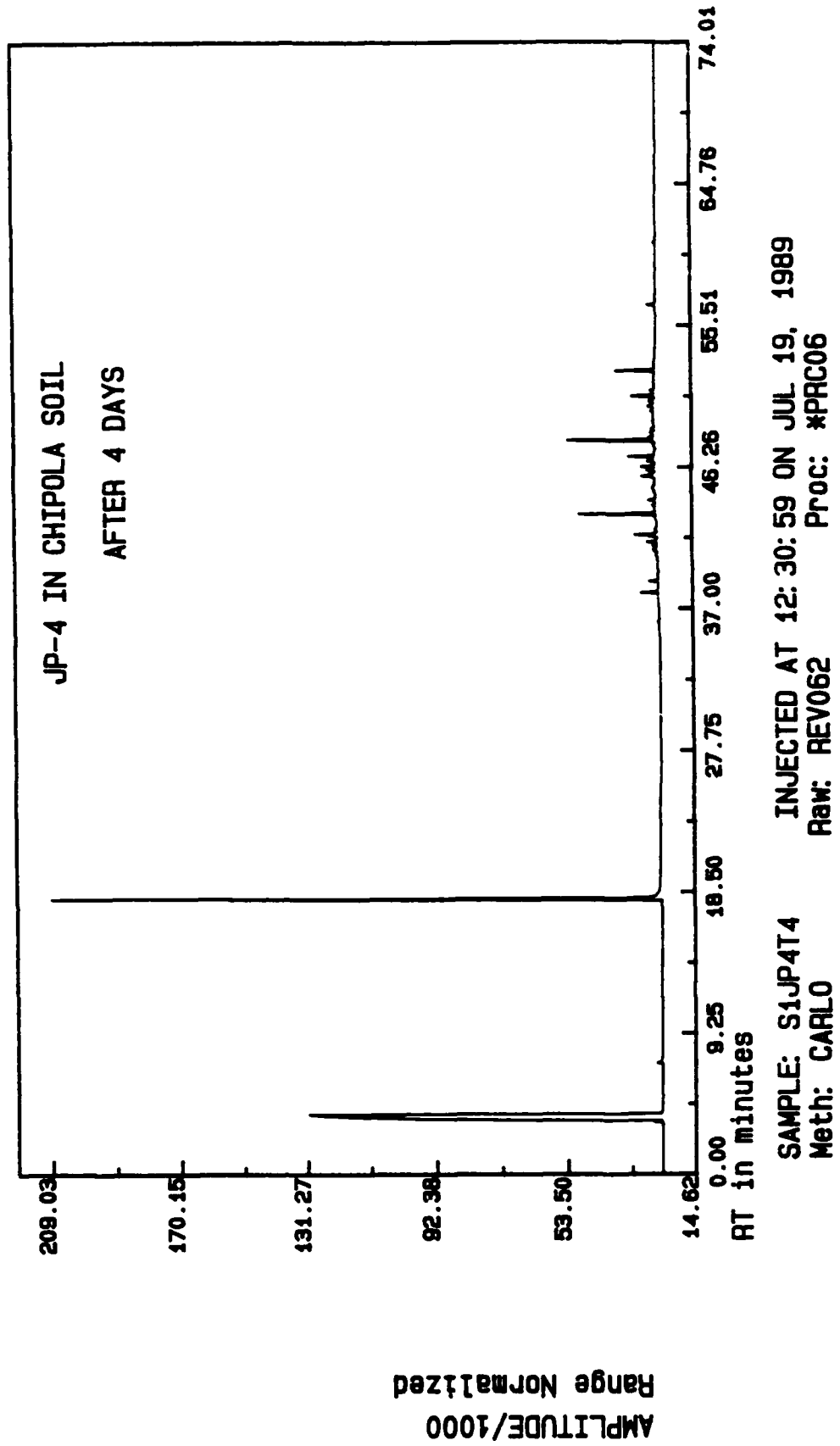
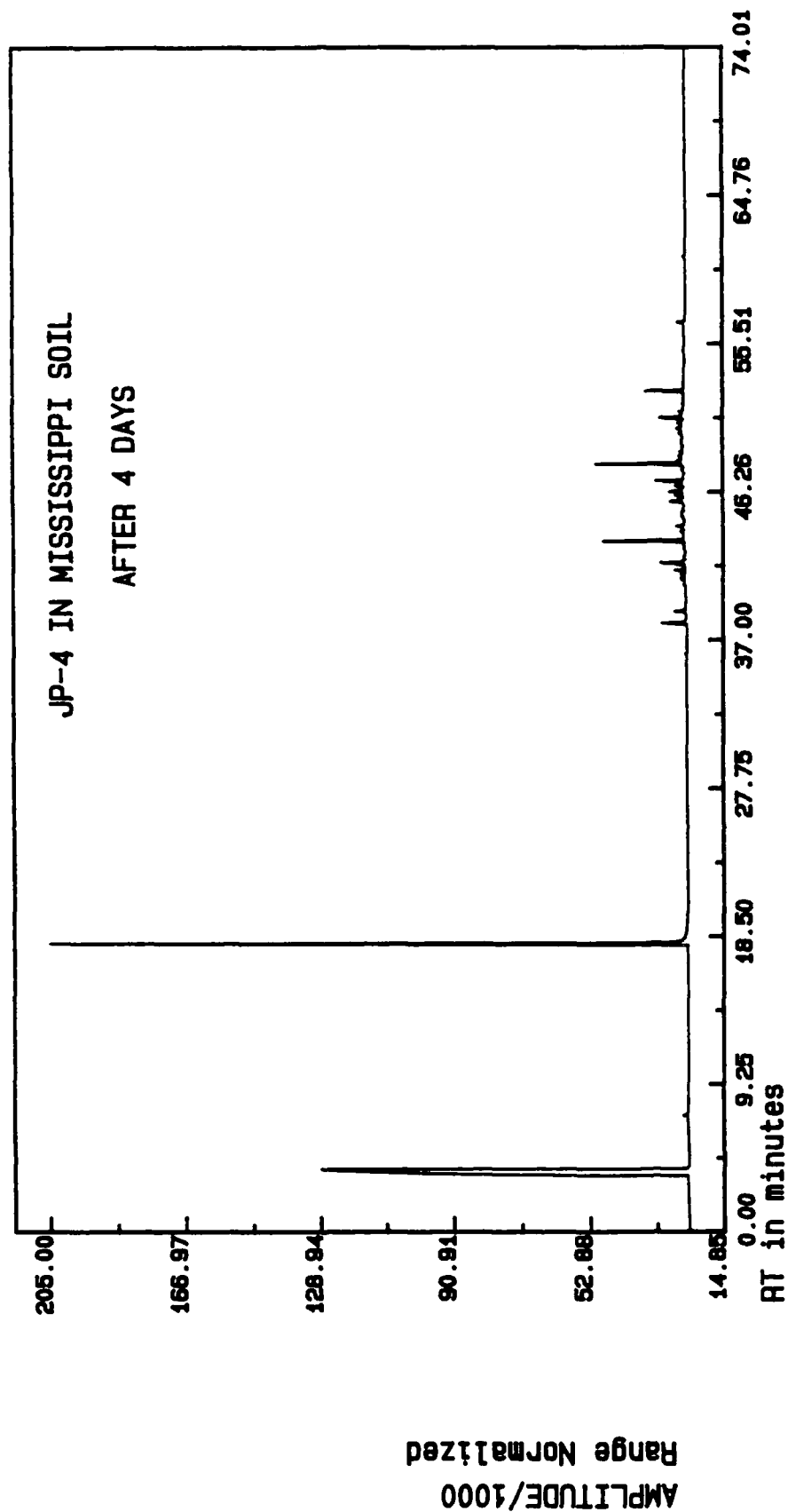


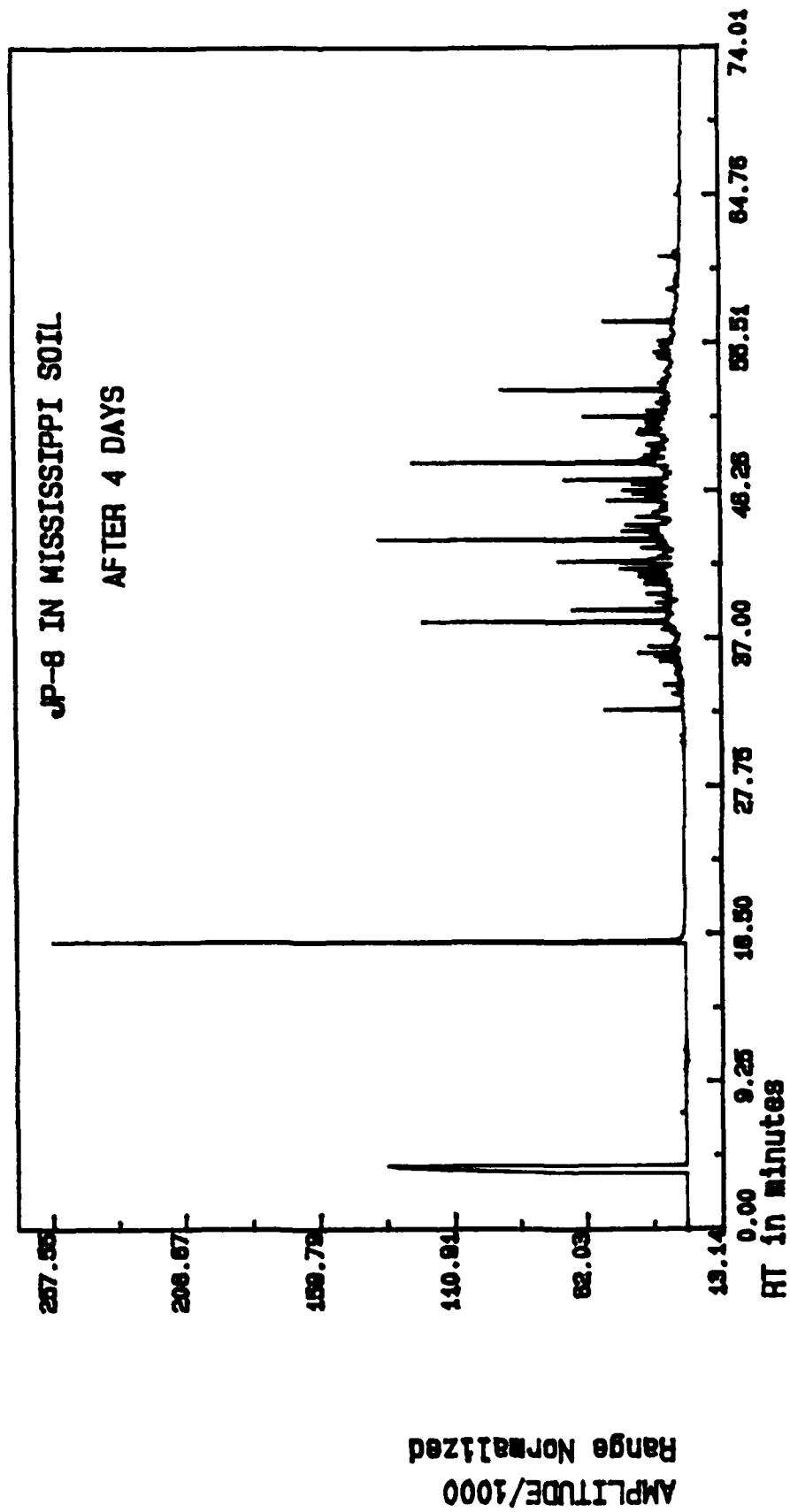
FIGURE 2



SAMPLE: S2JP4T4  
Meth: CARLO

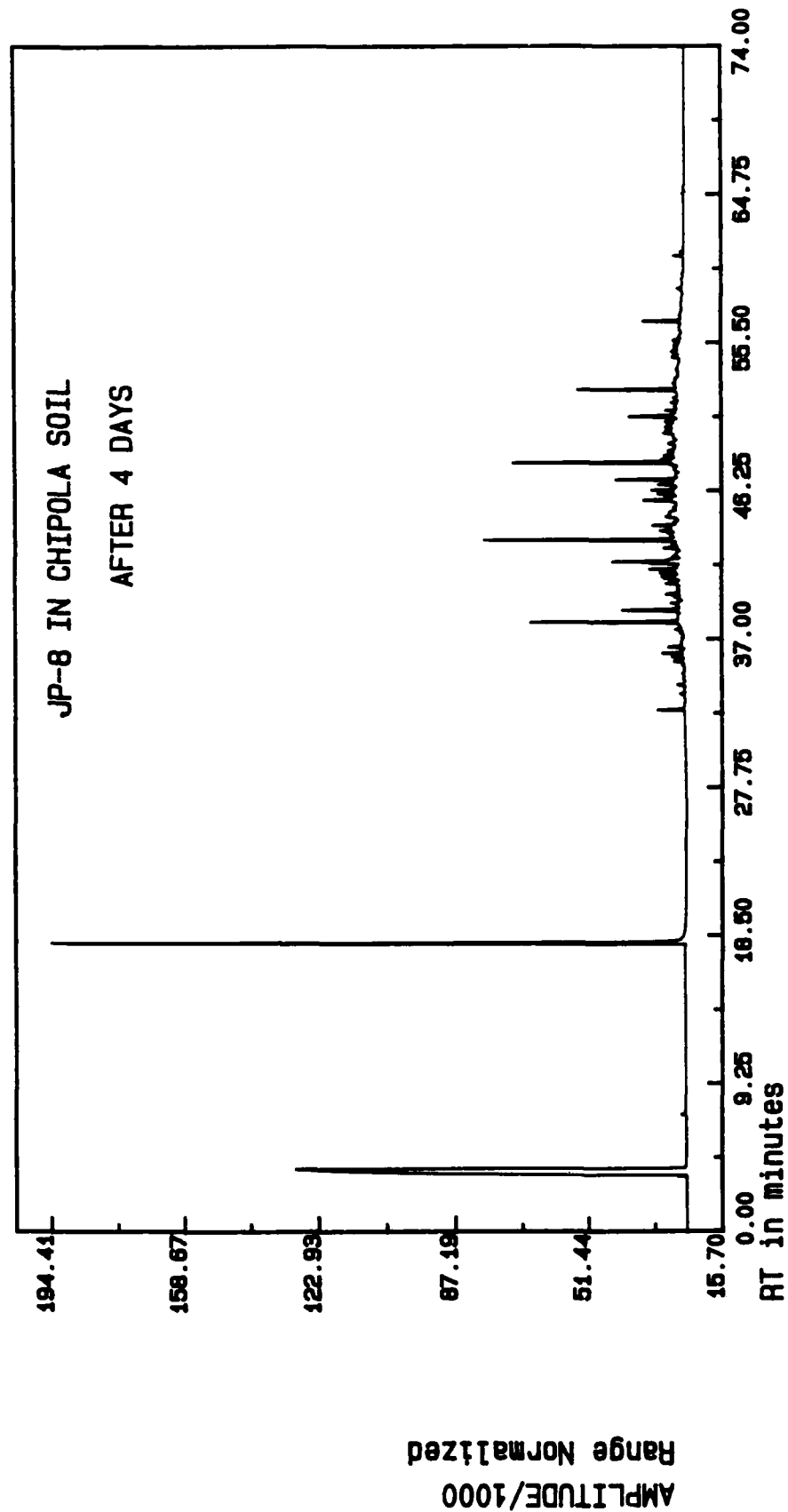
INJECTED AT 15:18:39 ON JUL 19, 1989  
Raw: REV064 Proc: \*PRC06

FIGURE 3



SAMPLE: S2JP8T4  
Meth: CARLO  
INJECTED AT 6:56:43 ON JUL 20, 1989  
Raw: REV065 Proc: \*PRC06

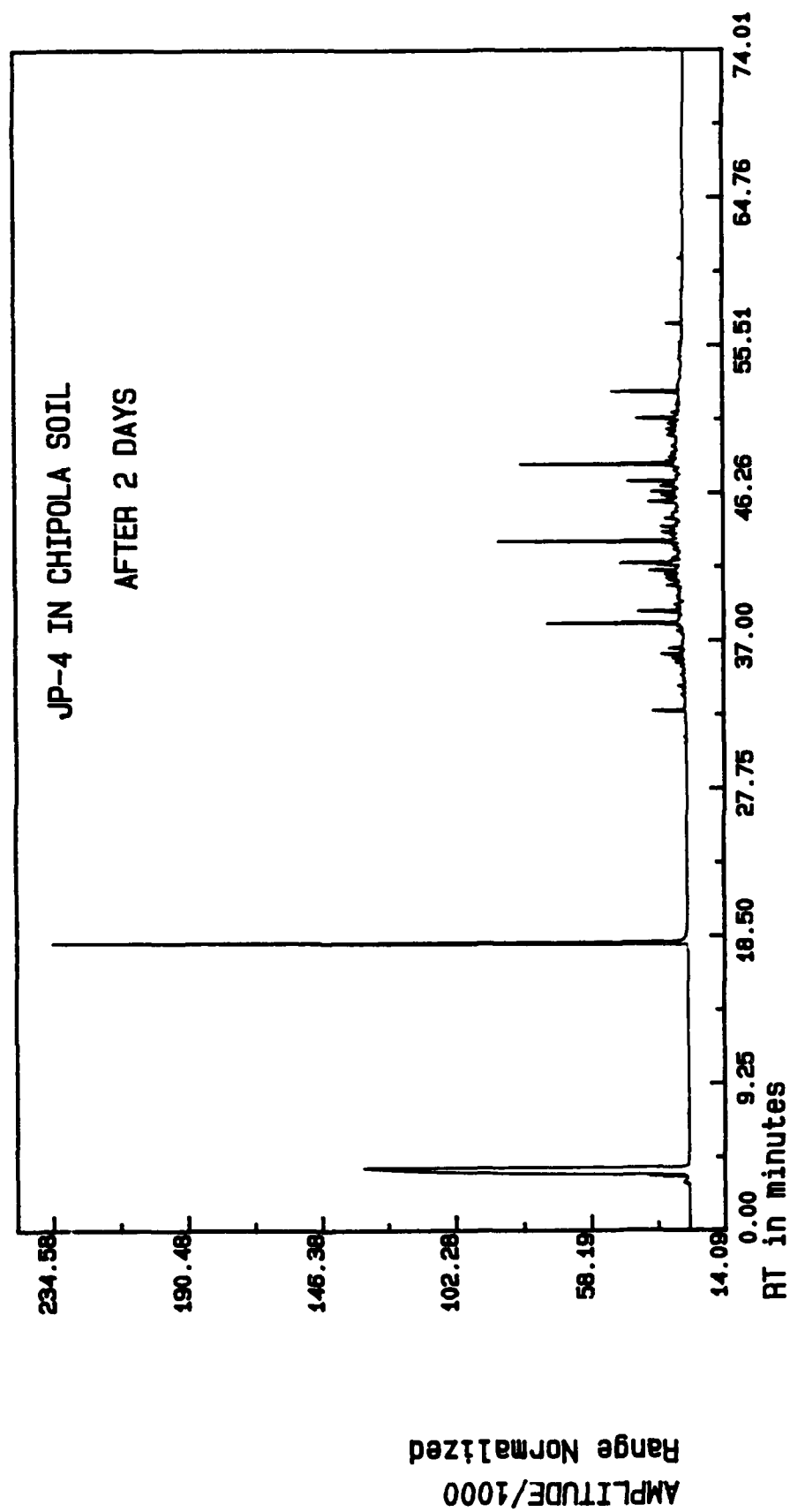
FIGURE 4



SAMPLE: S1JP8T4  
Meth: CARLO  
INJECTED AT 13:55:15 ON JUL 19, 1989  
Raw: REV063  
Proc: \*PRC06

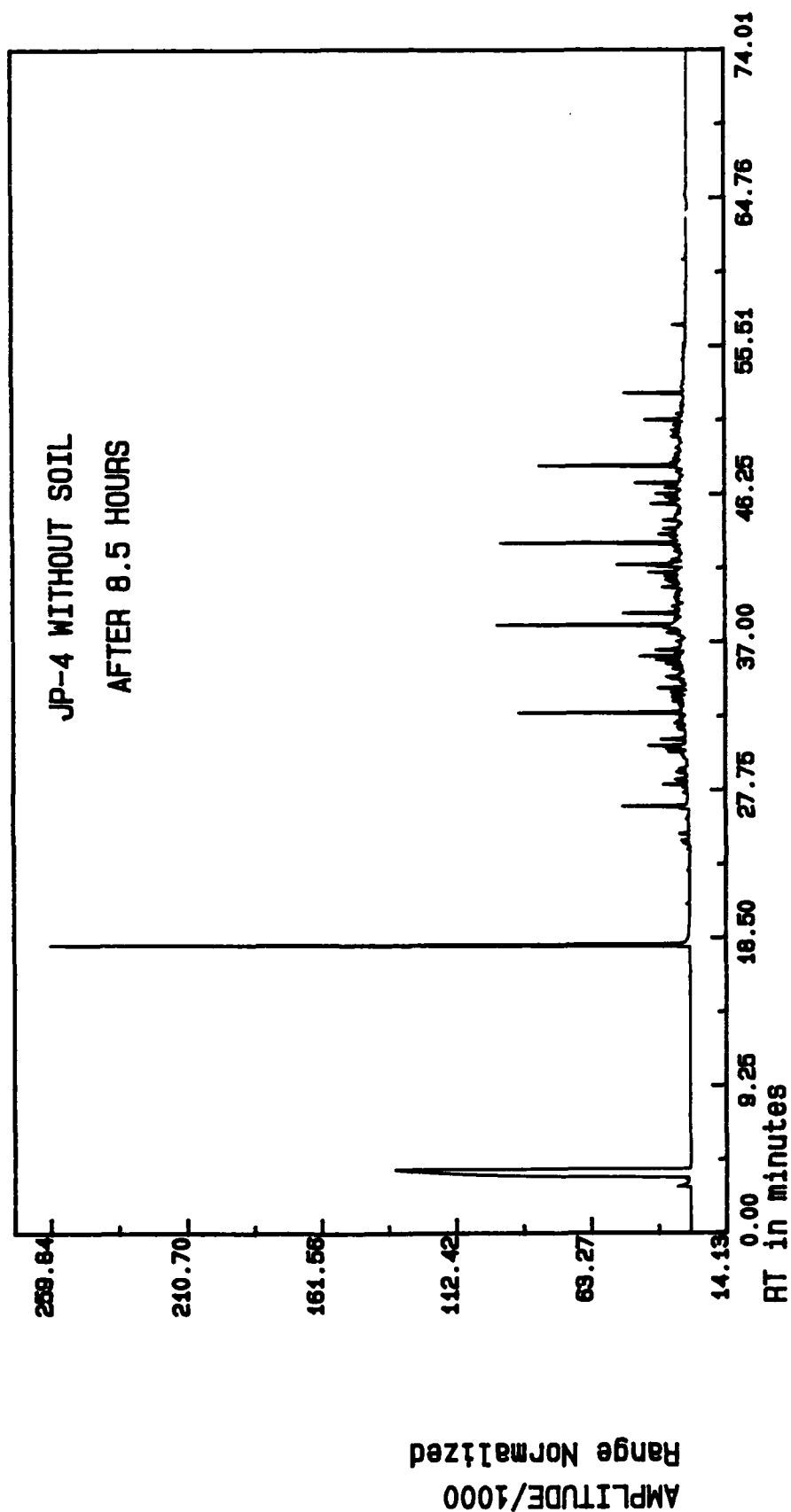


FIGURE 5



SAMPLE: S1JP4T2  
Meth: J8METH  
INJECTED AT 10:08:06 ON AUG 4, 1989  
Raw: REV136  
Proc: PEV136

FIGURE 6



SAMPLE: NSJP4T8.5 INJECTED AT 11:12:58 ON JUL 31, 1989  
Meth: J8METH Raw: REV109 Proc: PEV109

FIGURE 7

# PLOT OF RESPONSE VARIABLE VERSUS TIME FOR JP-4 AND JP-8 IN TWO DISSIMILAR SOILS

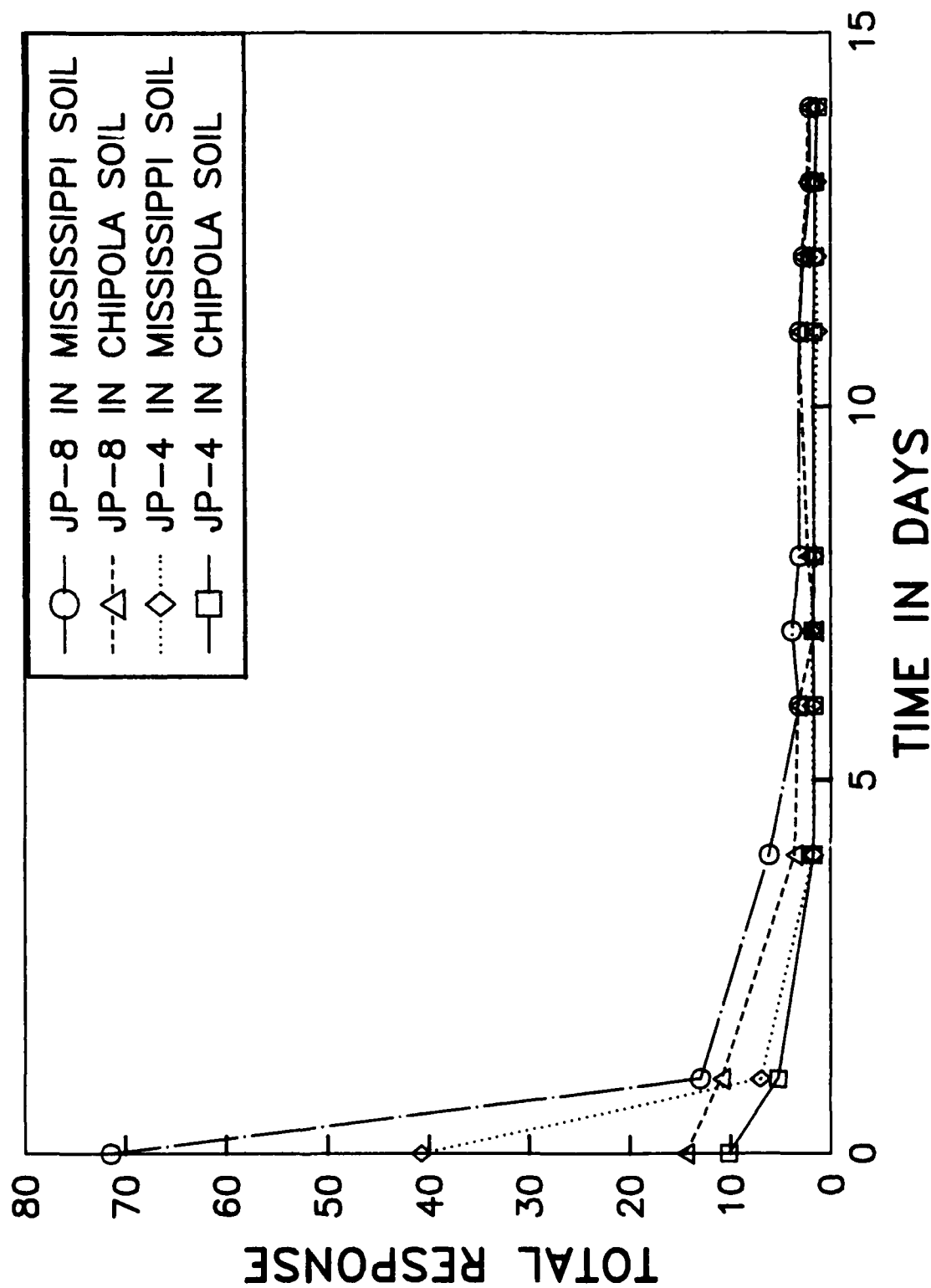


FIGURE 8

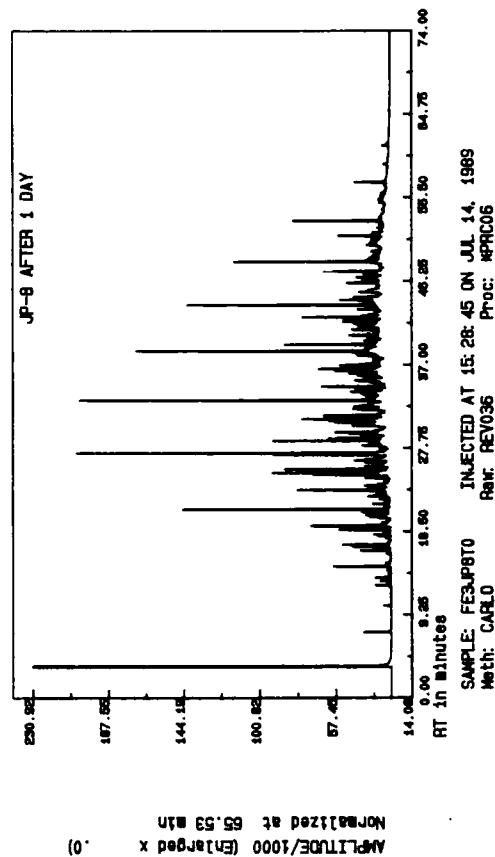
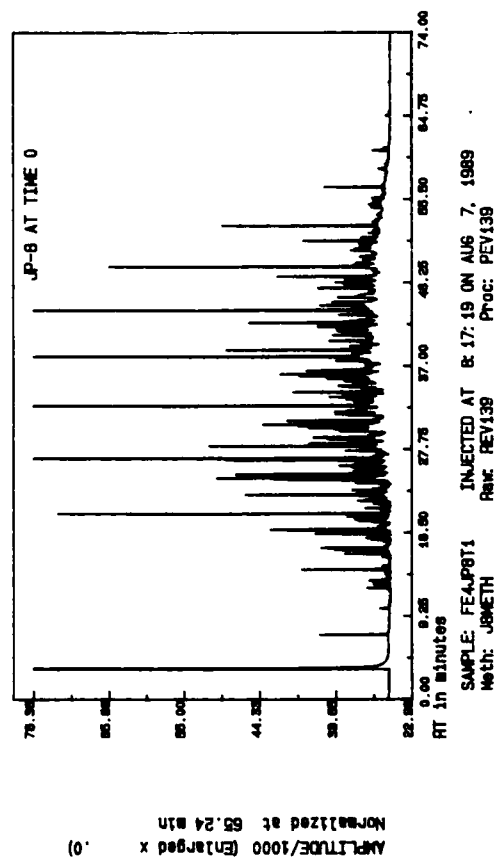
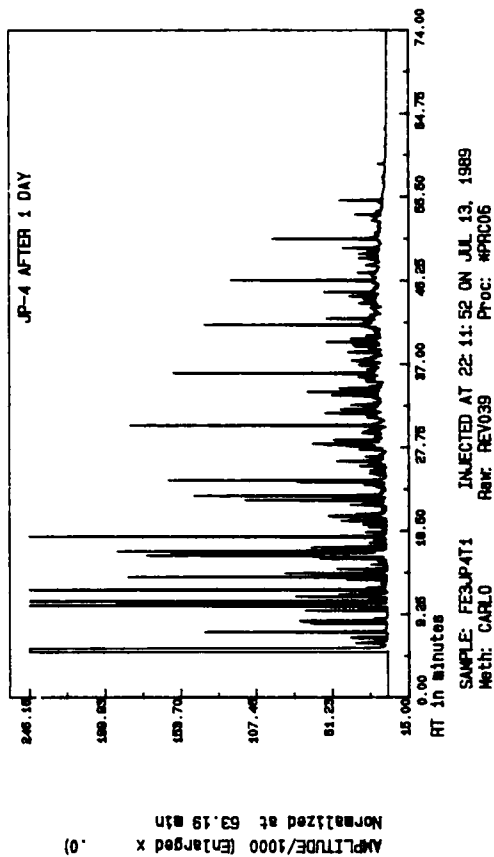
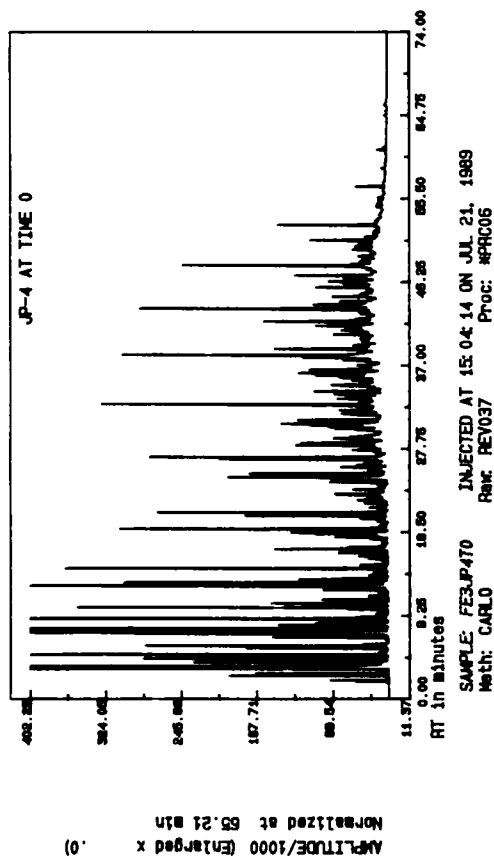


FIGURE 9

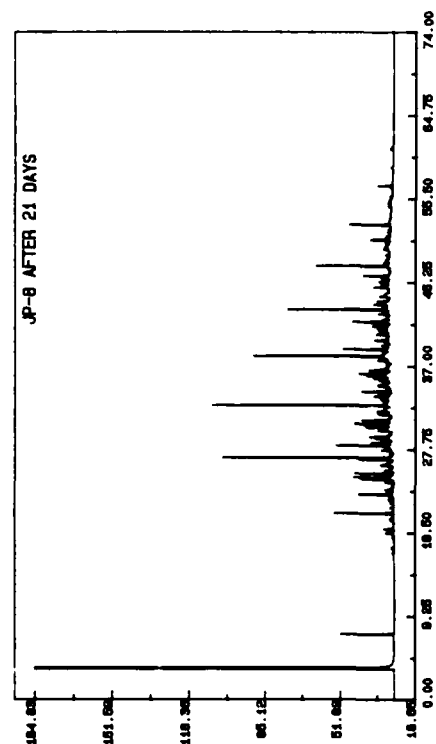
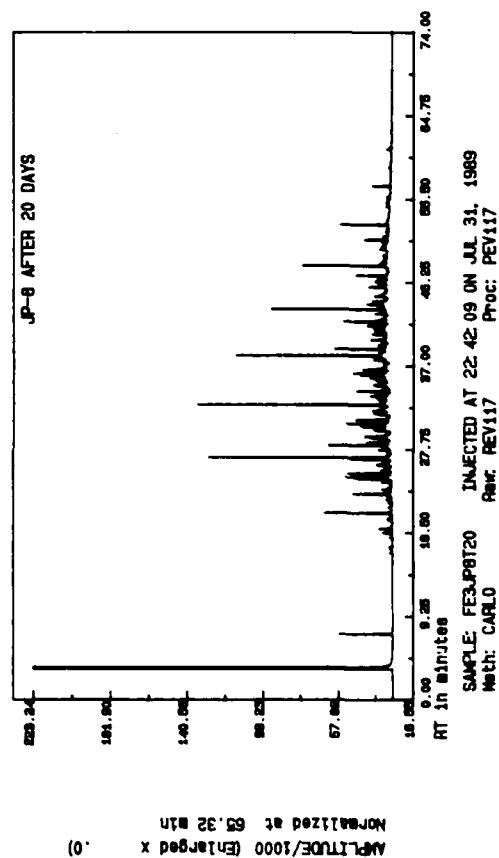
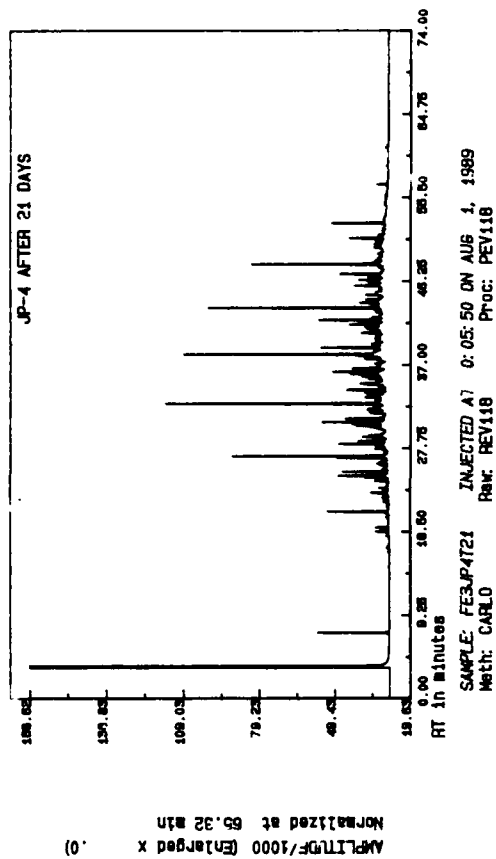
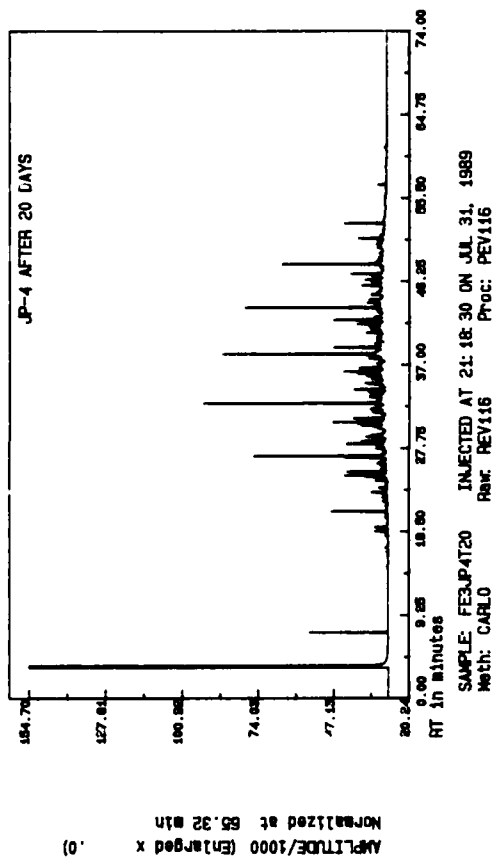
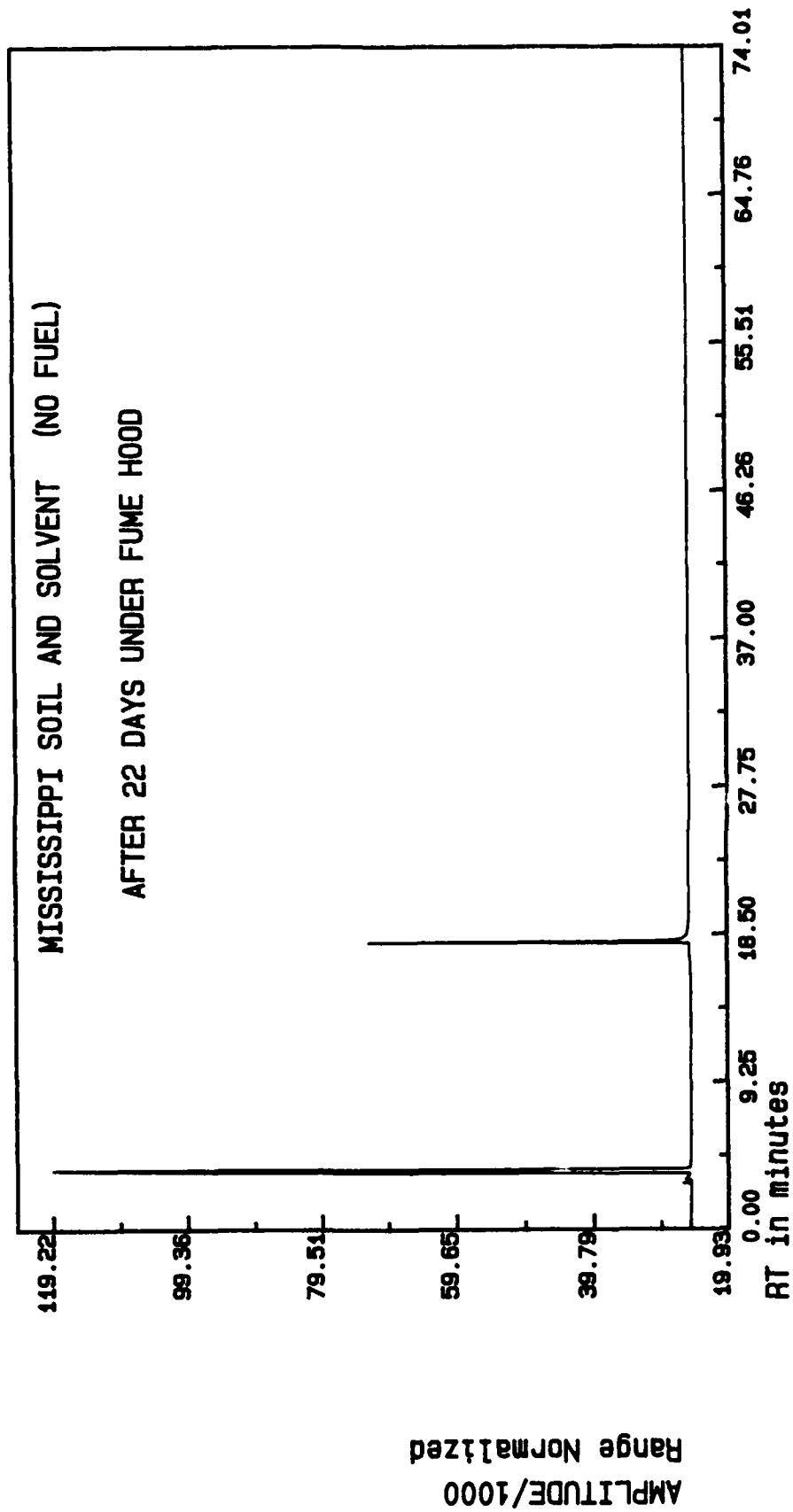


FIGURE 10



SAMPLE: S2NFT22 INJECTED AT 9:42:16 ON AUG 7, 1989  
Meth: J8METH Raw: REV141 Proc: PEV141

1989 USAF-UES High School Apprenticeship Program

Sponsored by the

Air Force Office of Scientific Research

Conducted by the

Universal Energy Systems, Inc.

Final Report

Piping Code and FEA program reviews

Prepared by: Keith Levesque

Research Location: Engineering Serviced Center

Tyndall AFB, FL

USAF Mentor: Capt. Isaac Shantz

Date: August 11, 1989

Contract Number:

#### ACKNOWLEDGEMENT

During the time in which I worked in the RDCE branch at the Tyndall Engineering and Services Center, many people helped me out with the literary research that I was conducting. These people made many things easier and possible for me to do. Thank you Capt. Shantz, for your patience in having to explain my objective to me to what seems at least twice a week, and in always being around for me to ask you lots of other questions about what I was doing, they were many and often. Thank you Mr. Gee Brindly and Mr. Langsford for fixing up the computer during the first week of my job. Thank you Mr. Hardy, Mr. Haselden, and everyone else here for treating me like a co-worker and not just some seventeen year old kid. And finally the library staff , without you I would never have gotten past square one.



Scientists and engineers depend on many different computer programs to aid and simplify their jobs. Finite Element Analysis (FEA) is a powerful tool in engineering, with it an engineer can model an object and run various tests on it such as fatigue, stress, thermal analysis. Using a computer, engineers can save hours of time and even make computations that could never be accomplished if done by hand.

My job consisted of a search for different FEA programs that would help predict the effect of a blast from a conventional weapon on underground piping systems. If a blast was close enough to a pipe, it would burst, relieving the pipe of its internal pressure, but if the pipe did not break, it still would be directly affected by the shock waves produced by the blast. The shock travels through the soil into the pipe. The medium within the pipe carries the shock wave through it, increasing the pressure tremendously as it is a dynamic case. When the surge of pressure finally reaches the end of the pipe, the valve or any other attachment at the end has a good chance of breaking or bursting right off the end of the pipe.

In the beginning I didn't know the first thing about FEA but I started out in the library at AFESC. I read about FEA, what it is and what it can do. Books on FEA weren't going to get me any closer to a solution. In the back of some of the books, they had listed computer programs, most of which led to be FEA programs on a mainframe computer. Since I was looking for PC FEA programs, this was little help. The library did a literary search on my subject with key words like FEA, 3-D, computer program. In a short while they were

able to give me pages upon pages of different books or articles on FEA programs that were PC based. When you request a book, it doesn't usually get there the next day, in fact usually a little over a week, because they need to "import" it from another library, sometimes from overseas. The biggest asset to the search would be a Data Sources book put out by Unix. When looking under the subject structural analysis, or civil engineering, there were many PC programs that could fit into the needed description. The companies that make or sell the programs are listed and their address or phone numbers are printed in the back. I got in touch with four of the companies that would best fulfill the requirements. Out of the four that I contacted, three said they would send me the information that I requested about a particular program. The other one seemed to be out of business because they had cancelled their telephone number and not left a new one. Even the Unix hotline couldn't find a new number and had even erased their listing of the company from their Data Sources files. The operator at Unix tried to call the San Francisco operator, but could never get through due to a strike. Out of those three, only two sent me back information. When I finally decided that the third company wasn't going to send me any information, I called them up again and requested that they send me some brochures on the particular computer program. They said they would, but the information they said will be sent will not be in time to include them in the final report to Capt. Shantz. About the same time this was happening, the library was able to get many different articles on the FEA programs I was reviewing, however most of these articles were not really recent enough

to be accurate. Since programs are continually updated and bettered, the reviews themselves were pretty much of no use in my report to Capt. Shantz. Because of this, the report relied heavily on the information that the companies had sent about their own products.

Using the FEA programs on the PC turned out to be Step three in a three step process. These programs could only show stress on the valves of the pipes due to pressure exerted on them, but they couldn't calculate the pressure on the inside of the piping system, or figure out the stress created within the pipes due to the internal pressure. Step two would be to find out how the pressure affected the pipes and Step one would be to calculate the pressures. When looking through the Data Sources book, I saw a program called Caepipe made by SST systems inc. When I called, they sent information on their entire Cae (Computer Aided Engineering) line. One program PS+Caepipe could calculate stress on a network of pipes when an internal pressure was given. A man that I talked to there told me that Step one could be found in a program called Flownet, and after searching for a long time, I was able to come up with a company that made this program they were talking about because there are many programs called Flownet from different companies. When I explained the problem to Ronald Bradshaw, the owner of R.T. Bradshaw inc., he told me that the program I needed was pulsenet. He sent me the information about it and others, but it arrived early in week eight, and as it turns out, Pulsenet will not actually work the way we need it to and so I find that I cannot quite complete the goal I set out for.

Even though I didn't finish what I started, I learned valuable things about doing literary research. One of the biggest things is that if you get stuck or run into a dead end, don't get frustrated because there is always a different direction that you can take. Also the library is going to be your biggest help on where to start. If you don't even know the slightest bit about what it is your researching, you can read about it and soon enough you will at least know something that will help you get started in the right direction.

Other things that I did this summer would be: learning about the bureaucracy involved with the Air Force, communicating better with others around me, and the different types of engineers and what they are expected to do on the job. I also learned how to use the word processor on the Wang computer, and most of all organize myself so that I could always find what I was looking for once I already had it.

AIR FORCE  
HIGH SCHOOL  
APPRENTICESHIP PROGRAM

By: Cyrus L. Riley

Tyndall AFB, Florida  
June 18-August 11, 1989

## INTRODUCTION

My second summer with the Air Force High School Apprenticeship Program was an enriching experience. I learned a great deal about a variety of fields, including civil engineering, computer science, and electronics. I also learned the importance of teamwork and how a group of people work on different tasks in order to achieve a common goal.

This year, I helped in the operation of the centrifuge at the 9700 area. The centrifuge tests that were conducted this summer had many purposes. First and foremost was to obtain data to be used in association with the hyperbolic paraboloid that the Air Force is experimenting with. Through a series of cratering and blasting tests, we were able to determine certain depths at which the structure could be built underground safe from the harm of attack.

Another purpose of our testing was to fully-establish the newly-developed testing facilities. By running tests and utilizing the available equipment, we were able to familiarize ourselves with the use of the equipment in order to better serve incoming researchers.

This summer was very productive and a great goal was achieved. However, due to the lack of necessary equipment,

our progress was hampered and we were not able to fully accomplish everything that was planned. Still, this summer was quite a success and I am proud to have been a part of it.

During the first weeks of my apprenticeship, we ran some tests in the 9700-area centrifuge. We used various types of soil along with different bucket sizes. The purpose of this was to establish a design chart and equipment parameters for incoming researchers. I assisted in test preparation by pluviating the various soils and loading the buckets onto the centrifuge cradle. Later in the summer I even helped repair a faulty chain in the drive motor.

Safety was also taken seriously and I assisted in this area also. I would sound the warning horn at the appropriate times, which would inform everyone in the centrifuge building when a test was either about to begin, underway, or just completed. I would also execute several other safety maneuvers, including taking steps to exclude personnel from entering the centrifuge bay area during tests.

Toward the middle of the summer there was some down-time when the centrifuge was not in action. As mentioned earlier, some vital parts had not yet come in and our progress was slowed. It was during this time that I was sent up to the Engineering and Services Center, Building 1120, to do some data input in the technical library. Researchers that would come to our facilities would need access to certain reference materials. It was my duty to establish a "centrifuge library" of sorts which would contain any information needed to assist these researchers.



I input 73 items into the 1120 data base and differentiated them from the proceeding text by giving them different library prefixes. Thus, to access the information, all one had to do was call upon this certain library prefix and all of the information would be displayed. This information was later translated into Air Force Standard Form.

As the end of the summer approached, I began to spend some time at the 9700 Instrumentation Shop. There, I repaired halon extinguishers, corrected faulty wire connections, and did some data transfer between two different computer terminals. During some free time, I spent some time at the mortician's laboratory and discovered how the remains of human bodies were identified.

My last major project was the construction of a one-g testing apparatus. The structure was designed to set up a gun perpendicular to the ground and fire a bullet into a soil sample below it. Unfortunately, the gun was a piece of equipment that did not arrive during the summer so we had to improvise, as usual. However, the test was successfully completed.

On the last day of my apprenticeship, I was a part of history. For the first time anywhere, an onboard data acquisition unit was used in a centrifuge operation. We did a cratering test in the centrifuge and was able to create a graph within minutes after the test was completed with the help of a Pacific Instruments Data Acquisition Unit.

In closing, I would like to thank everyone that I

worked with this summer. They made this a very fun affair and I could not have learned so much without them. I would also like to thank Rod Darrah and UES for selecting me to the Apprenticeship Program for another year. You all have truly enriched my life with this experience.

### ACKNOWLEDGEMENTS

I would like to thank the following people, without whom this summer would not have been so enjoyable:

Mr. Walt Bucholtz  
Dr. Wayne Charlie  
Mrs. Virginia Davis  
Mr. Frank Doerle  
Mr. Duane Hemmerich  
SMSgt. Carl Hollopeter  
Mr. Jim Jones  
Lt. Steve Kuennen  
Mr. Ed Lockhart  
Mr. William Naylor  
Mr. Andrew Poulis  
Mr. Tom Provost  
Dr. Allan Ross  
Mr. Clarence Schell  
Mr. George Strickland  
Dr. Teresa Taylor  
Mr. Jeff Thompson  
Mr. Mike Womack  
Dr. George Veyeras

UES SUMMER  
HIGH SCHOOL  
APPRENTICESHIP PROGRAM  
JUNE 12 - AUGUST 4  
ROBIN WOODWORTH  
TYNDALL AIR FORCE BASE  
FLORIDA

## TABLE OF CONTENTS

- I. List of Figures/Tables
- II. Material Testing System
- III. Split-Hopkinson Pressure Bar
- IV. Discription of Sand
- V. Sample Preparation
- VI. Compaction
- VII. Running of Tests
- VIII. Information Recieved
- XI. Results
- X. Refrences

## ACKNOWLEDGEMENTS

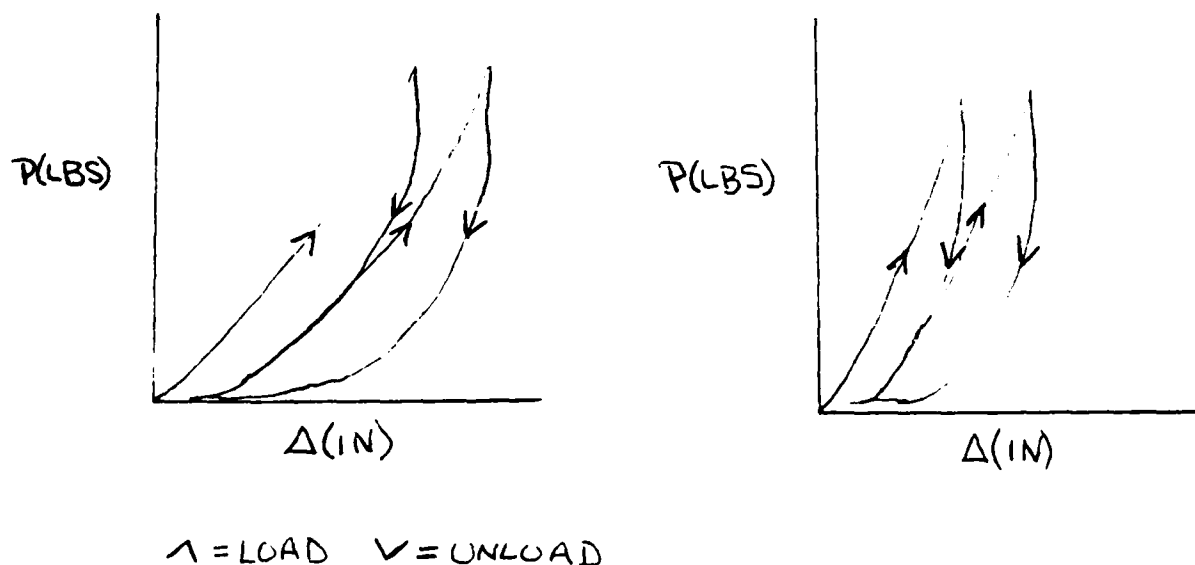
I'd like to thank Dr. Allen Ross for being so helpful to me throughout the summer and for bringing himself to my level and explaining the answers in a way that I could understand them.

and to Lt. Steve Kuennen for starting me out on the right foot and introducing me to the variety of projects that were being performed and tested.

## INTRODUCTION

During the summer of 1989 at AFESC/RDCM, Tyndall AFB, Dr. Allen Ross, Dr. George Veyera from University of Rhode Island, Dr. Wayne Charlie from Colorado State University, Lt. Steve Kuennen and myself with the UES Summer Apprenticeship Program, performed many types of tests on partially saturated sands. The saturation levels used with these sands varied from 20 percent to 80 percent by intervals of 20%. The machines that we used were the Material Testing System (MTS) and the Split-Hopkinson Pressure Bar (SHPB). These machines will be described later in this report. All test were run the same way on four different types of sand so that a consistant factor was present and the information could be compared at the end.

The Material Testing System (MTS) is a machine that statically measures time vs. pressure. The set up of this machine is very simple with two major parts (see fig. 1) but running it takes skill and knowledge. First of all there is a digital display consol with many buttons and knobs of choices to choose from to get different readings. This display is connected with wires to strain gauges that are placed on to your sample which pick up any minute movement. The sample itself sits on a round steal plate that moves upward with the programmed amount of pressure per second. When the machine is running an x-y plotter plots the curve of the strain verses stress. On the tests we performed we plotted the load and unload by  $\Delta(\text{in})$  vs.  $P(\text{LBS})$ . When the tests were finished we looked at the plotted curves. If the curves were long and drawn out then the sample was much weaker in strength than if the curves were shorter and steeper.





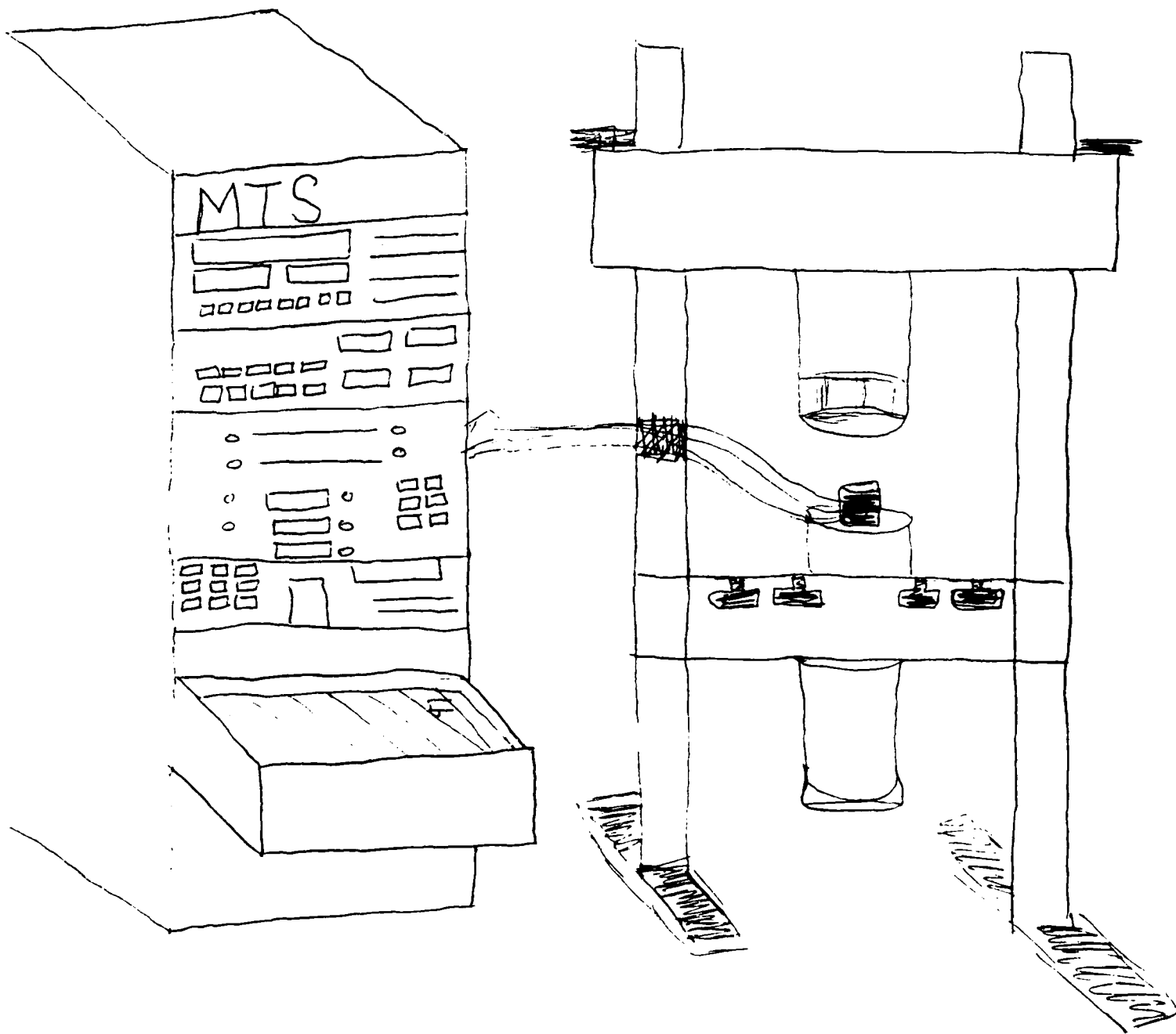
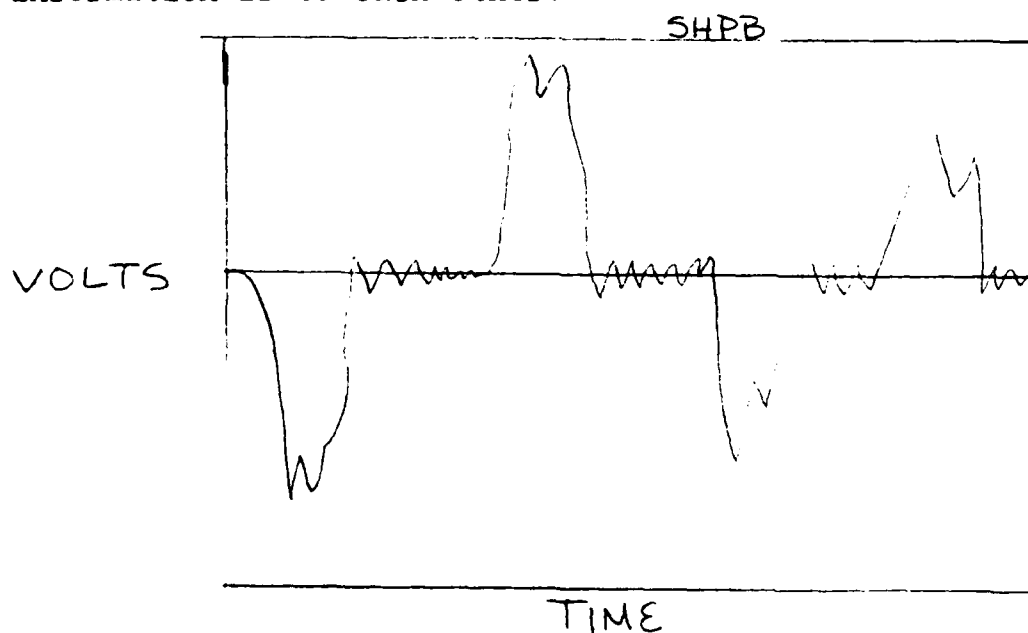


Figure 1 Material Testing System

The Split-Hopkinson Pressure Bar (SHPB) is used to measure the strength of the stress wave, propagation on velocity, and how much energy was absorbed by the sample. The SHPB is made of a striker bar (20.23cm) an incident bar (3.66m) and a transmitter bar (3.35m). On each bar a strain gauge is attached measuring the strength of the stress wave. All the information is then transfered to the Nicolet Digital Storage Oscilloscope. Here is where we can determine the time between the incident stress wave and the transmitted stress wave. The points plotted from the SHPB were much different from the MTS because on the MTS they were curves and on the SHPB the points were plotted as sharp lines connecting each and every change. As you can see in figure 2 the Split-Hopkinson Pressure Bar is shaped much different than the Material Testing System, but further on in this report you will be able to see how closely related the information is to each other.



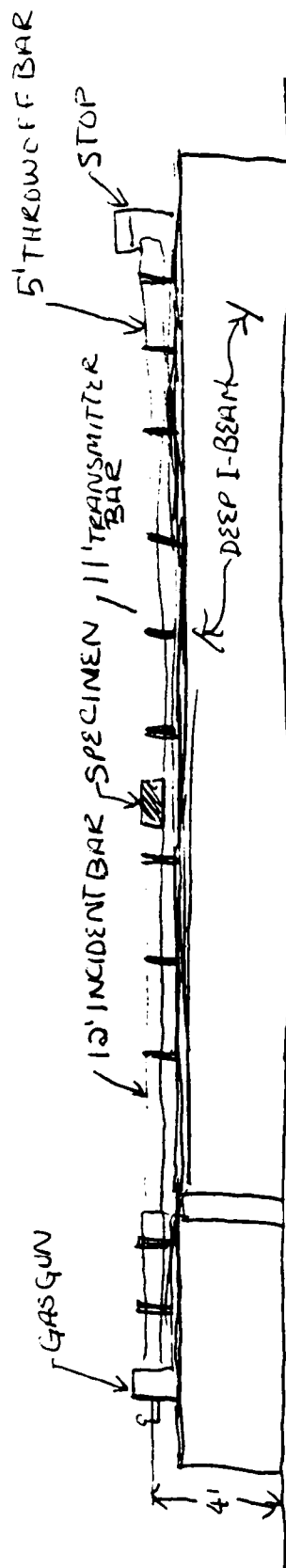


Figure 2 Split-Hopkinson Pressure Bar

From the samples tested, we had four different kinds of sand. Of these sands we had BASE sand off the beach of Tyndall AFB, EGLIN sand off the beach of Eglin AFB, and two kinds of sand sent from Ottawa Indiana. The names of these sands are F-58(for the fine sand) and 20-30(for the coarse sand). Each of these sands are very unique in their own way. Although the Base Sand and F-58 Sand are very fine the F-58 Sand has somewhat rounded smooth particles, where the Base Sand has somewhat angular particles.(See fig 3a and 3b) The Eglin Sand is called well graded sand because of the variety of size particles it contains.(see fig 4a) The 20-30 Sand is different from the rest of the sands, its particles are smooth and round and is much larger in size than the rest.(See fig 4b) In figures 3 and 4 the sand particles were magnified the same magnitude to show the difference between each sand.

In preparing our samples we measured one sample into four seperate layers at the same density. Reason for this was to maintain a constant factor between the samples. also had to use the same density and weight because of the difference between the sands. To each of the layers with the same density we add the same amount of water to maintain the proper saturation level for the test that were being run,

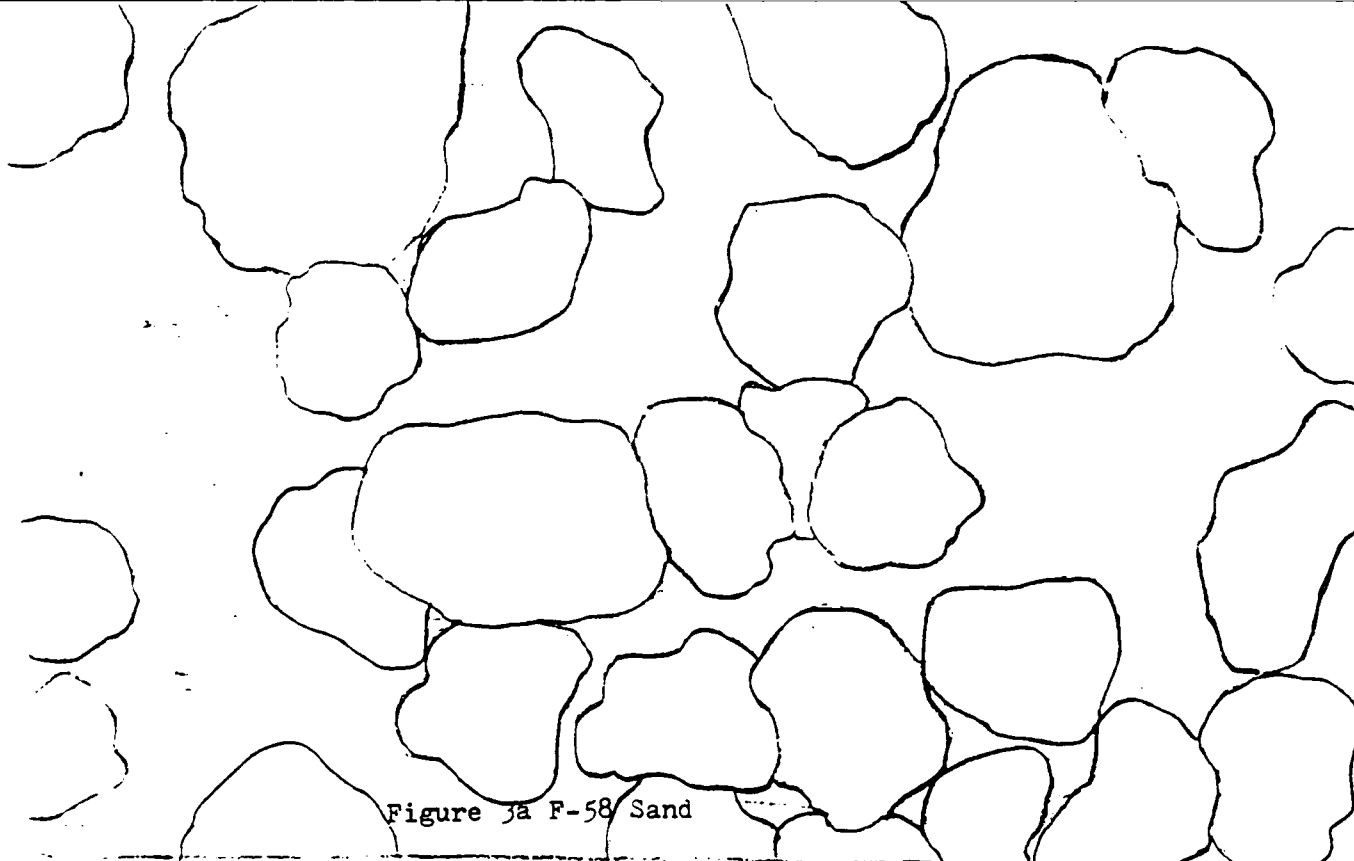


Figure 3a F-58 Sand

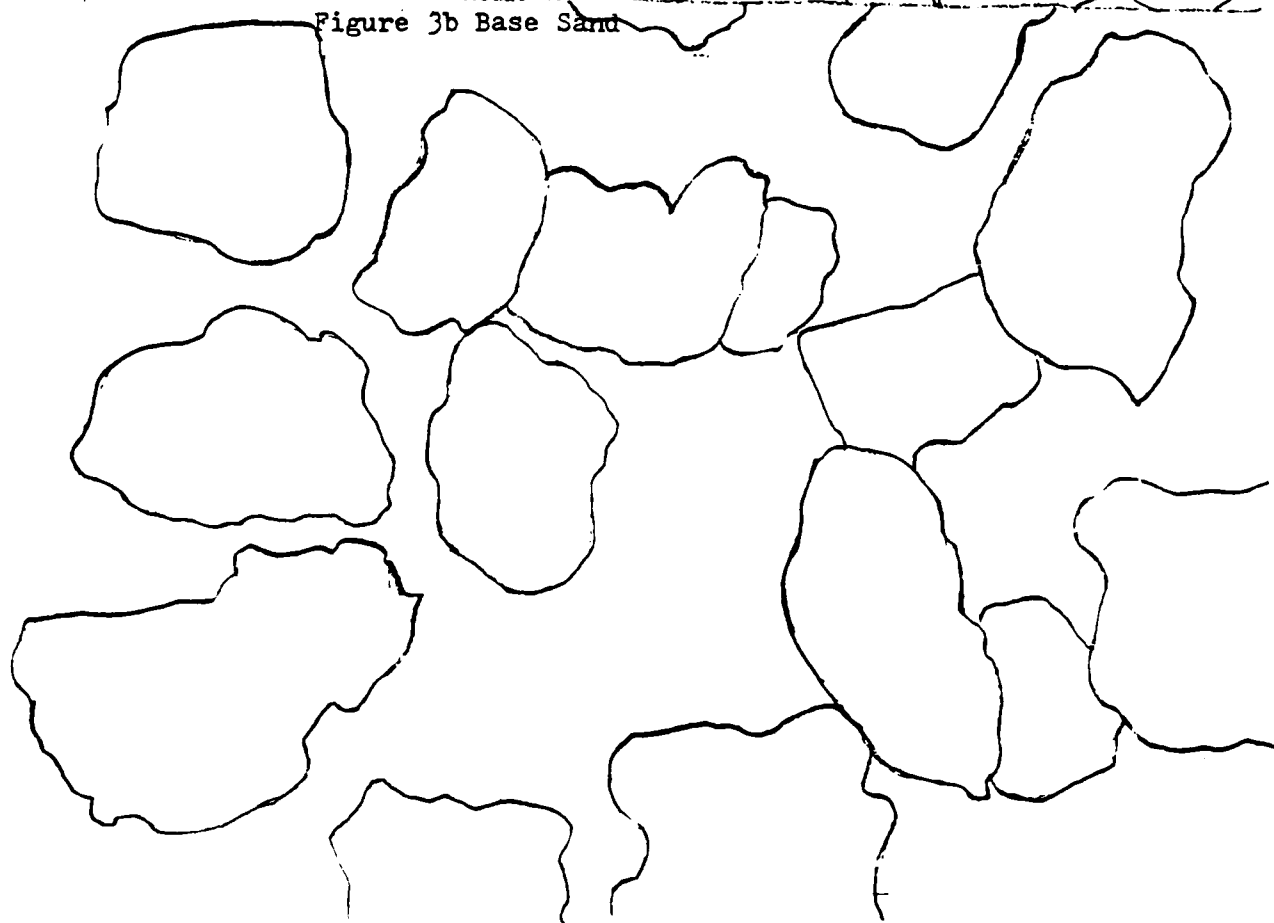


Figure 3b Base Sand

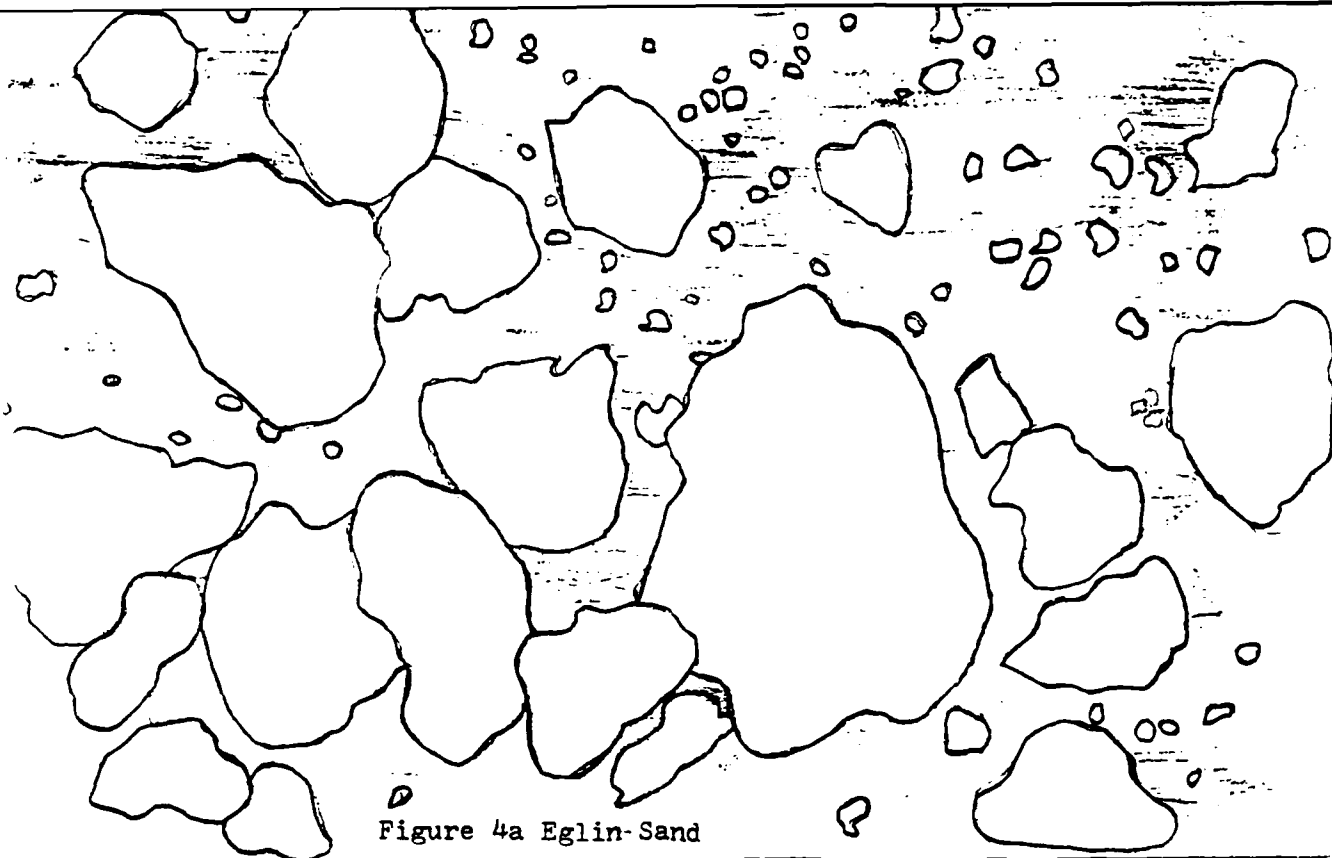


Figure 4a Eglin-Sand

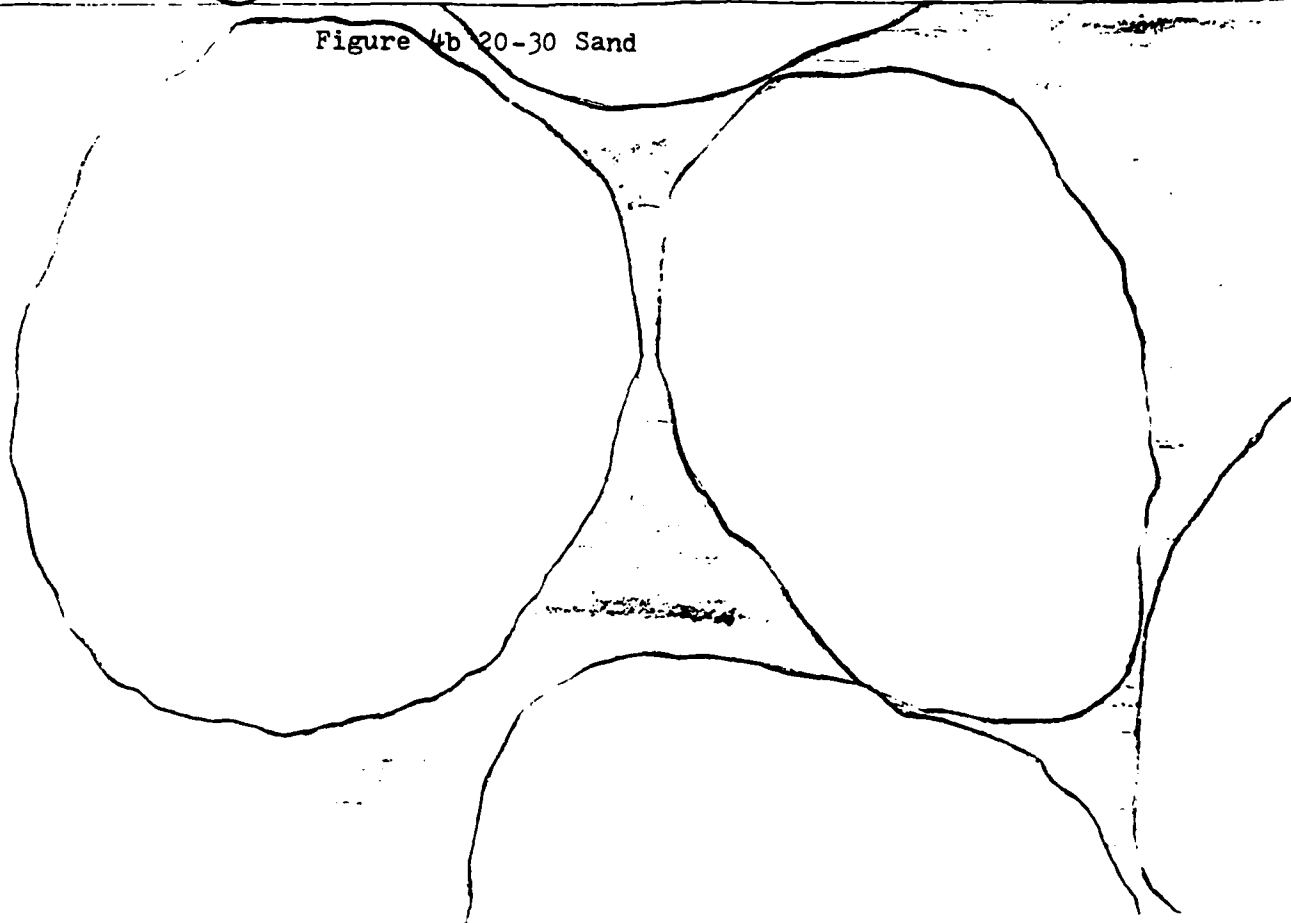


Figure 4b 20-30 Sand

As you can see in Table 1 and 2 the amount of sand and water that was used to complete each sample. For example if you were to use Eglin Sand for one layer you would measure out 102.5g of dry sand. Then if you were to measuring 20% saturation you would put 3.95g of water and mixing it in with the dry amount of sand. When measuring these samples you need to be very precise with each layer or your information will vary.

Once the sample has been weighed and the water mixed in, we <sup>PLACED</sup> layer by layer into a 6 inch stainless steel tube with the diameter of 2.130 inches. One layer was put in and then compacted with a <sup>STANDARD</sup> proctor hammer. To make sure the layer of sand was compacted to the proper level a compactor rod was placed on top with lines carved around the side one inch apart. The  $5\frac{1}{2}$  pound weight falls on the compactor rod from 12 inches up thus giving the same compaction pressure on each sample and individual level. After the fourth level has been compacted and all the blows of the hammer has been totalled, a wafer with an O-ring is placed on the top along with the bottem of the sand inside of the steel tube. The main reasons for the wafers are to remove the air and to hold the sample in place. When loading the sample a little bit of grease is applied to the ends to provide true contact.

6/14

SAMPLE PREPARATION: EGLIN SAND, OTTAWA 20-30 - USED BASE REDESIGN

FOR ALL SAMPLES:

$$\gamma_D = 1.755 \text{ g/cm}^3 \text{ (109.5 PCF)}$$

$$G_s = 2.65$$

$$e = 0.510$$

$$W_s = 410 \text{ g}$$

COMPACTED IN 4 LAYERS OF 102.5 g (DRY SOIL) PER LAYER

$$G_s w = S e \quad w = S e / G_s \quad W_w = w W_s$$

| S (%) | w (%) | W <sub>w</sub> (g) |           |
|-------|-------|--------------------|-----------|
|       |       | TOTAL              | PER LAYER |
| 0     | 0     | 0                  | 0         |
| 20    | 3.85  | 15.78              | 3.95      |
| 40    | 7.70  | 31.56              | 7.87      |
| 60    | 11.55 | 47.34              | 11.84     |
| 80    | 15.40 | 63.12              | 15.78     |
| 100   | 19.25 | 78.91              | 19.73     |

Table 1



Table 2

6/14

SAMPLE PREPARATION: BASE SAND, F58 OTTAWA - USED BASE FEDERAL

FOR ALL SAMPLES:

$$\gamma_d = 1.600 \text{ g/cm}^3 \text{ (100 PCF)}$$

$$G_s = 2.65$$

$$e = 0.656$$

$$W_s = 374.73 \text{ g}$$

COMPACTED IN 4 LAYERS OF 93.6 g (DRY SOIL) PER LAYER

$$G_s w = Se \quad w = Se/G_s \quad W_w = w W_s$$

| F (%) | w (%) | $W_w$ (g) | $W_w$ (g) |
|-------|-------|-----------|-----------|
|       |       | TOTAL     | PER LAYER |
| 0     | 0     | 0         | 0         |
| 20    | 4.95  | 18.54     | 4.63      |
| 40    | 9.90  | 37.08     | 9.27      |
| 60    | 14.85 | 55.61     | 13.90     |
| 80    | 19.80 | 74.14     | 18.54     |
| 100   | 24.75 | 92.69     | 23.17     |

\* COULD NOT COMPACT TO  $1.755 \text{ g/cm}^3$  (109.5 PCF)

\*\* - 1ST ROUND OF TESTS ON 11/15: ORIGINALLY HAD  $W_s = 102.5 \text{ g/LAYER}$ , SAMPLES PREPARED WITH MOISTURE; PRIOR TO TEST, SAMPLE HEIGHTS WERE REDUCED PROPORTIONATELY TO GET  $\sim 1.600 \text{ g/cc}$ , BUT THIS MAY HAVE CAUSED PROBLEMS (INCONSISTENT # BLADES VS SAMPLE TEST.)

When loading the sample holder in the Material Testing System we placed it on a pedestal to hold it up. On top of the sample holder we just left the compactor rod after our last layer was compacted. Reason for this was, when the programmed amount of pressure had been started on the sample we just wanted to compact the sample and not the sample holder. When testing samples on the Split-Hopkinson Pressure Bar we did not use the compactor rod. The last O-ring was placed inside and turning the sample horizontally in the sample holder we loaded it in the SHPB. One side fit smoothly around the incident bar, and the other side against the transmitter bar. As said earlier, grease was used to reduce friction and to provide true contact.

After the sample was prepared, compacted and loaded it was time to set up for the test. First of all, the data sheet was close to write all settings and calibrations. Next, the machine itself had to be ready. For example on the MTS your sample had to be attached to the strain gauges properly, all your displays of what was to be recorded had to be programmed, and your time was to be set for how long you wanted the test to run. On the SHPB all your displays have to be zeroed out, your time on zero and the bar itself should be ready by putting the piston back, closing the valve to keep the gas in, and putting the protector in at the end so when fired the bar will not go over the side.

Information was recorded before, during, and after each and every test. In Tables 3 and 4 you can see just how much was recorded. In Figures 5 and 6 you can see the type of curve was recorded from each machine. In tables 5 to 9 you can see all the information recorded from each sand in each test we take these numbers and input them into an IBM computer where we can produce graphs. (See figs. 7 to 10)

TEST NO. EGUN Doo T1 DATE 11 July 87 TIME 1450 DISK - 14

\*\*\*\*\*  
ROOM TEMP 75

STRIKER BAR LENGTH 8" GUN CHAMBER PRESS 25 psi

COUNTER TIME  $5.7 \times 10^{-3}$  COMPUTED VELOCITY \_\_\_\_\_

COMPUTED INC. STRESS \_\_\_\_\_ THEOR. VELOCITY \_\_\_\_\_

\*\*\*\*\*

SOIL SAMPLE DESCRIPTION Eglin Day strain gaged st tube

T1

SOIL SAMPLE LENGTH 4.0" SOIL SAMPLE MASS 410g

SOIL SAMPLE DENSITY 1.755 g/cc SOIL SAMPLE MOISTURE 0.0 Actual 1.47.

SOIL SAMPLE LENGTH AFTER TEST 3.88" DENSITY AFTER SHOT \_\_\_\_\_

SOIL SAMPLE CONFINEMENT Ko

\*\*\*\*\*

#### TRANSDUCER SETUP

INCIDENT STRESS GAGE VFS 4 2.50  
EXC 10 AMP GAIN 100 NICHOLET VOLTS 2.30 DT 0.5  $\mu$ s

TRANSMITTED STRESS GAGE Ext...  
#1 EXC 10 AMP GAIN 1000 VFS 1.0 NICHOLET VOLTS 1.08 DT 0.5  $\mu$ s  
#2 EXC \_\_\_\_\_ AMP GAIN \_\_\_\_\_ VFS \_\_\_\_\_ NICHOLET VOLTS \_\_\_\_\_ DT \_\_\_\_\_

SOIL PRESSURE GAGE VFS 1.0 TR = 0.047

TYPE GAGE ST GAGE S/N \_\_\_\_\_ SENSITIVITY \_\_\_\_\_ GAIN 100

COMMENTS .536 V max  
Changed TRANS VFS to 2.0

$\mu = 0.277$   $\beta = 1.40 \%$

1st C.A. + 2 blows  
2nd C.A. + 12 blows  
3rd C.A. + 11 blows  
4th C.A. + 9 blows  
Total 34 blows

Velocity through sample - 15  $\mu$ s  
$$V = \frac{4.0''}{\frac{1560 \text{ ft} + 57860 \text{ ft}}{59261 \text{ sec}}} = \frac{4.0''}{\frac{180 \text{ ms}}{21 \text{ ft}}} = \frac{40 \text{ ft}}{21 \text{ ft}} = 1.9$$

LOAD = 11100 #/MIN  
UNLOAD = 3000 #/MIN

MTS

DATE: 28 JULY 89

01

Table 4  
SAMPLE BASE SAND

FILE ID BASE 500 T2 S111

" " LOAD  
" " RADIAL

PRE-TEST

DRY UNIT WEIGHT 101 #/FT<sup>3</sup>

VOID RATIO .656

SATURATION 0%

WATER CONTENT

| LAYER        | 1 | 2 | 3 | 4      |
|--------------|---|---|---|--------|
| NO. OF BLOWS | 5 | 6 | 5 | 6 = 22 |

RADIAL STRAIN GAGE ID #2

$V_{OR} = 7.6211V$  [AFTER COMPACTION]

FIRST LOAD-UNLOAD CYCLE

$P_{MAX_1} = 55.44 \pm$   $V_P = 0.253V$   $t_P = 32.15 \text{ SEC}$

$\Delta_{MAX_1} = .062''$   $V_{\Delta_1} = 1.025V$   $V_{R_1} = .659V$

$\Delta_{O_1} = .021''$   $V_{OR_1} = -.057V$  [AT  $P=0$  - UNLOAD]

SECOND LOAD-UNLOAD CYCLE

$P_{MAX_2} = 55.11 \pm$   $V_{P_2} = 0.258V$   $t_{P_2} = 70.7 \text{ SEC}$

$\Delta_{MAX_2} = .041''$   $V_{\Delta_2} = 1.107V$   $V_{R_2} = .671V$

$\Delta_{O_2} = .024''$   $V_{OR_2} = 111.621V$  [AT  $P=0$  - UNLOAD]

$t_{FINAL} = 874$  [TOTAL TEST TIME]

END OF TEST

$V_{FR_1} = .097V$  [RADIAL STRAIN GAGE AT  $P=0$ ]

Figure 5 Plot from Material Testing System

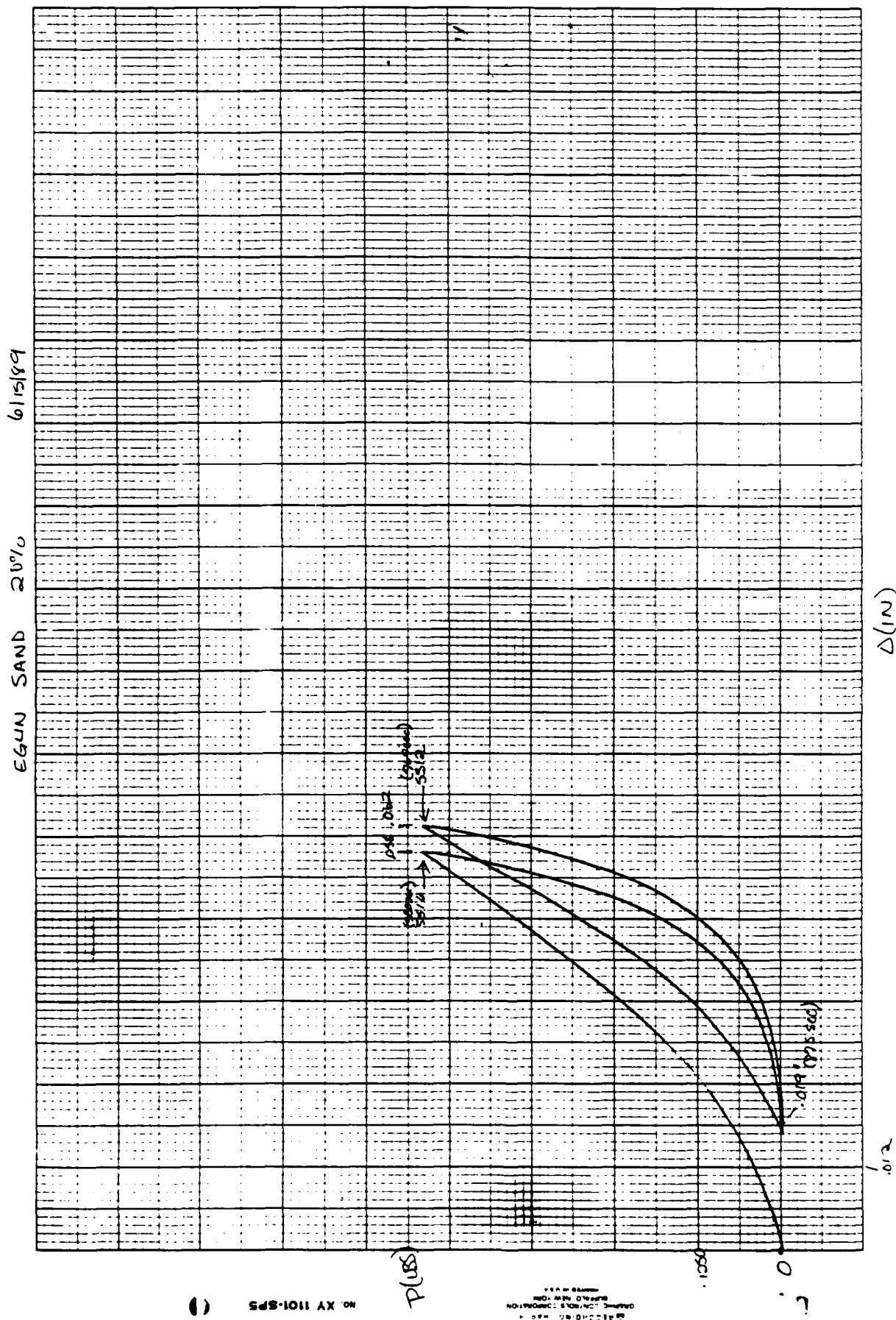


Figure 6 Plot from the Split-Hopkinson Pressure Bar

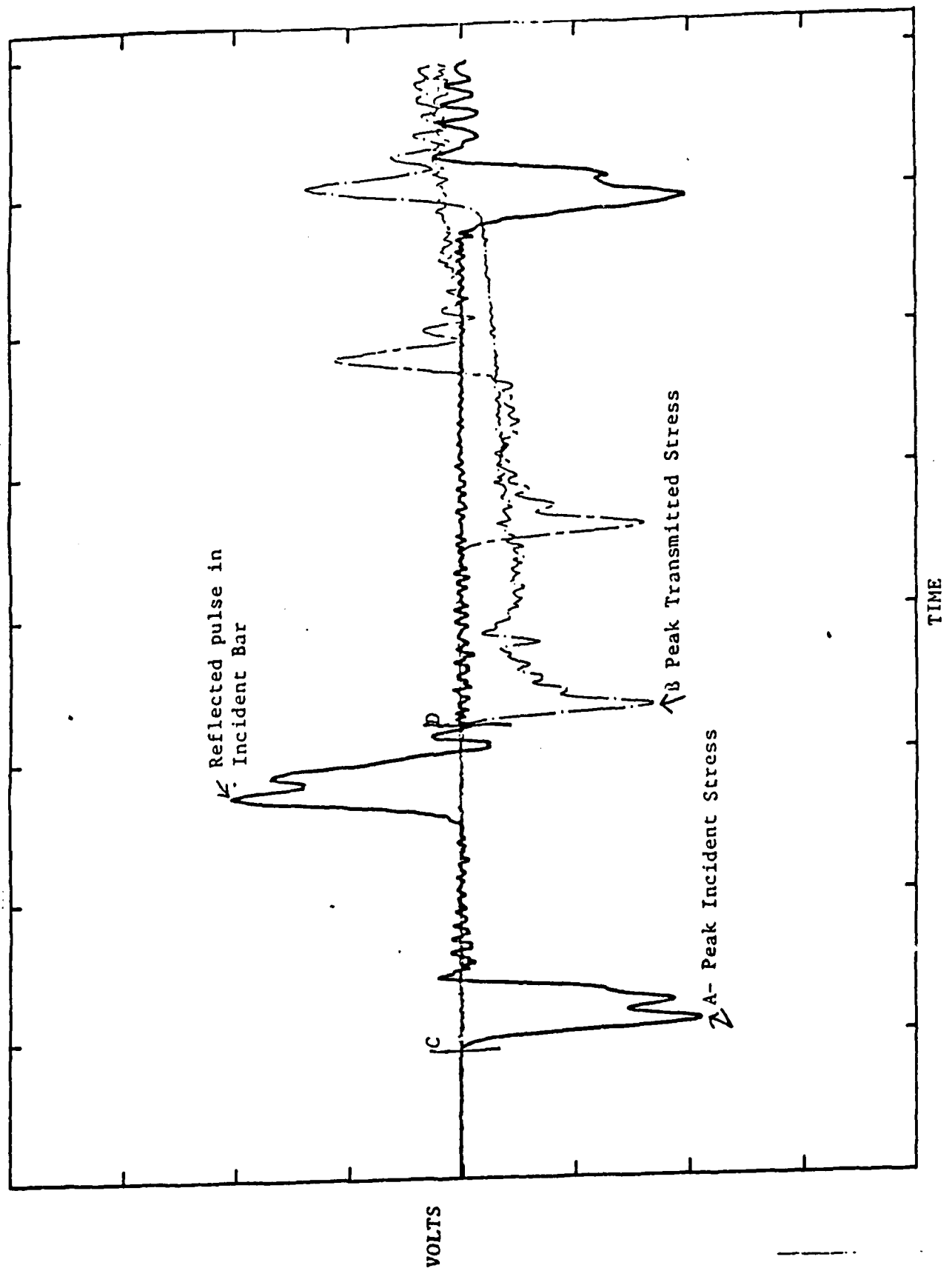


Table 5

OTTAWA 20

| IDENT.<br>NUMBER       | SATUR<br>(%) | TIME<br>seconds | F-BRIDGE<br>volts | LOAD<br>volts | STRESS<br>AX psi | SLOPE<br>OF LINES | BRIDGE/<br>LOAD | HORIZ<br>STRESS<br>(PSI) | LATERAL<br>STIFF<br>K <sub>o</sub> |
|------------------------|--------------|-----------------|-------------------|---------------|------------------|-------------------|-----------------|--------------------------|------------------------------------|
| OS00T1                 | 0            | 332             | 0.822             | -2.202        | 1544.93          | 0.000532          | 0.373297        | 535.122                  | 0.346372                           |
|                        |              | 443             | 0.822             | -0.002        | 1.4032           | 0.000518          |                 |                          |                                    |
|                        |              | 773             | 0.825             | -2.202        | 1544.93          | 0.000520          |                 |                          |                                    |
|                        |              | 884             | 0.827             | -0.002        | 1.4032           | 0.000516          |                 |                          |                                    |
| OS20T1                 | 20           | 332             | 0.861             | -2.224        | 1560.36          | 0.000551          | 0.387140        | 560.511                  | 0.359219                           |
|                        |              | 443             | 0.031             | -0.024        | 16.838           | 0.000537          |                 |                          |                                    |
|                        |              | 773             | 0.855             | -2.218        | 1556.15          | 0.000535          |                 |                          |                                    |
|                        |              | 884             | 0.0305            | -0.014        | 9.822            | 0.000533          |                 |                          |                                    |
| OS40T1                 | 40           | 332             | 0.905             | -2.214        | 1553.347         | 0.000582          | 0.408762        | 589.155                  | 0.379290                           |
|                        |              | 443             | 0.048             | -0.012        | 8.419            | 0.000554          |                 |                          |                                    |
|                        |              | 770             | 0.912             | -2.194        | 1539.315         | 0.000564          |                 |                          |                                    |
|                        |              | 884             | 0.052             | -0.01         | 7.016            | 0.000561          |                 |                          |                                    |
| OS60T1                 | 60           | 328             | 0.88              | -2.19         | 1536.51          | 0.000572          | 0.401826        | 572.88                   | 0.372844                           |
|                        |              | 438             | 0.03              | -0.016        | 11.2256          | 0.000557          |                 |                          |                                    |
|                        |              | 766             | 0.892             | -2.194        | 1539.32          | 0.000564          |                 |                          |                                    |
|                        |              | 884             | 0.052             | -0.01         | 7.016            | 0.000548          |                 |                          |                                    |
| OS80T1                 | 80           | 328             | 0.855             | -2.192        | 1537.912         | 0.000555          | 0.390054        | 556.605                  | 0.361922                           |
|                        |              | 439             | 0.034             | -0.01         | 7.016            | 0.000536          |                 |                          |                                    |
|                        |              | 766             | 0.866             | -2.192        | 1537.912         | 0.000543          |                 |                          |                                    |
|                        |              | 883             | 0.033             | -0.01         | 7.016            | 0.000544          |                 |                          |                                    |
| SUMMARY OF FIRST LINES |              |                 |                   |               |                  |                   |                 |                          |                                    |
| OS00T1                 | 0            | 332             | 0.822             | -2.202        | 1544.93          | 0.000532          | 0.373297        | 535.122                  | 0.346372                           |
| 535122                 |              |                 |                   |               |                  |                   |                 |                          |                                    |
| OS20T1                 | 20           | 332             | 0.861             | -2.224        | 1560.36          | 0.002527          | 0.387140        | 560.511                  | 0.359219                           |
| 560511                 |              |                 |                   |               |                  |                   |                 |                          |                                    |
| OS40T1                 | 40           | 332             | 0.905             | -2.214        | 1553.347         | -0.00627          | 0.408762        | 589.155                  | 0.379290                           |
| 589155                 |              |                 |                   |               |                  |                   |                 |                          |                                    |
| OS60T1                 | 60           | 328             | 0.88              | -2.19         | 1536.51          | 0.001484          | 0.401826        | 572.88                   | 0.372844                           |
| .57288                 |              |                 |                   |               |                  |                   |                 |                          |                                    |
| OS80T1                 | 80           | 328             | 0.855             | -2.192        | 1537.912         | -0.01783          | 0.390054        | 556.605                  | 0.361922                           |
| 556605                 |              |                 |                   |               |                  |                   |                 |                          |                                    |



Table 6

F-58 SAND

| IDENT.<br>NUMBER       | SATUR<br>(%) | TIME<br>seconds | F-BRIDGE LOAD<br>volts | LOAD<br>volts | STRESS<br>AZ psi | SLOPE<br>OF LINES | BRIDGE/<br>LOAD | HORIZ<br>STRESS<br>(psi) | LATERAL<br>STIFF<br>No |
|------------------------|--------------|-----------------|------------------------|---------------|------------------|-------------------|-----------------|--------------------------|------------------------|
| FS00T1                 |              | 0               | 347                    | 1.26          | -2.192           | 1537.91           | 0.000819        | 0.574817                 | 820.26 0.533360        |
|                        |              |                 | 457                    | 0.105         | -0.01            | 7.016             | 0.000754        |                          |                        |
|                        |              |                 | 784                    | 1.254         | -2.19            | 1536.508          | 0.000751        |                          |                        |
|                        |              |                 | 898                    | 0.121         | -0.004           | 2.8064            | 0.000738        |                          |                        |
| FS20T1                 |              | 20              | 356                    | 1.205         | -2.19            | 1536.508          | 0.000784        | 0.550228                 | 784.455 0.510544       |
|                        |              |                 | 466                    | 0.052         | -0.01            | 7.016             | 0.000753        |                          |                        |
|                        |              |                 | 794                    | 1.205         | -2.194           | 1539.31           | 0.000752        |                          |                        |
|                        |              |                 | 910                    | 0.057         | -0.006           | 4.2096            | 0.000747        |                          |                        |
| FS40T1                 |              | 40              | 381                    | 1.265         | -2.18            | 1529.491          | 0.000827        | 0.580275                 | 823.515 0.538424       |
|                        |              |                 | 493                    | 0.051         | -0.004           | 2.806             | 0.000795        |                          |                        |
|                        |              |                 | 821                    | 1.267         | -2.192           | 1537.911          | 0.000792        |                          |                        |
|                        |              |                 | 931                    | 0.051         | -0.004           | 2.806             | 0.000792        |                          |                        |
| FS60T1                 |              | 60              | 350                    | 1.191         | -2.192           | 1537.911          | 0.000774        | 0.543339                 | 775.341 0.504152       |
|                        |              |                 | 460                    | 0.061         | -0.001           | 7.016             | 0.000738        |                          |                        |
|                        |              |                 | 788                    | 1.21          | -2.198           | 1542.121          | 0.000743        |                          |                        |
|                        |              |                 | 900                    | 0.05          | -0.008           | 5.6128            | 0.000754        |                          |                        |
| FS80T1                 |              | 80              | 343                    | 1.301         | -2.204           | 1546.33           | 0.000841        | 0.590290                 | 846.951 0.547716       |
|                        |              |                 | 454                    | 0.0125        | -0.03            | 21.048            | 0.000844        |                          |                        |
|                        |              |                 | 782                    | 1.283         | -2.206           | 1547.734          | 0.000832        |                          |                        |
|                        |              |                 | 893                    | 0.117         | -0.024           | 16.8384           | 0.000761        |                          |                        |
| SUMMARY OF FIRST LINES |              |                 |                        |               |                  |                   |                 |                          |                        |
| FS00T1                 |              | 0               | 347                    | 1.26          | -2.192           | 1537.91           | 0.000819        | 0.574817                 | 820.26 0.533360        |
| FS20T1                 |              | 20              | 356                    | 1.205         | -2.19            | 1536.508          | 0.039229        | 0.550228                 | 784.455 0.510544       |
| FS40T1                 |              | 40              | 381                    | 1.265         | -2.18            | 1529.491          | -0.00855        | 0.580275                 | 823.515 0.538424       |
| FS60T1                 |              | 60              | 350                    | 1.191         | -2.192           | 1537.911          | -0.00878        | 0.543339                 | 775.341 0.504152       |
| FS80T1                 |              | 80              | 343                    | 1.301         | -2.204           | 1546.33           | 0.013065        | 0.590290                 | 846.951 0.547716       |

Table 7

## EGLIN SAND

| IDENT. NUMBER          | SATURAL (%) | TIME seconds | F-BRIDGE volts | LOAD volts | STRESS AX psi | SLOPE OF LINES | BRIDGE/LOAD | STRESS (181) | STIFF E <sub>s</sub> |
|------------------------|-------------|--------------|----------------|------------|---------------|----------------|-------------|--------------|----------------------|
| -----                  |             |              |                |            |               |                |             |              |                      |
| ES00T1                 | 0           | 350          | 1.174          | -2.188     | 1535.105      | 0.000764       | 0.536563    | 764.274      | 0.497864             |
|                        |             | 460          | 0.04           | -0.012     | 8.419         | 0.000742       |             |              |                      |
|                        |             | 787          | 1.179          | -2.188     | 1535.105      | 0.000746       |             |              |                      |
|                        |             | 898          | 0.039          | -0.004     | 2.8064        | 0.000743       |             |              |                      |
| ES20T1                 | 20          | 338          | 1.215          | -2.19      | 1536.508      | 0.000799       | 0.554794    | 790.965      | 0.514780             |
|                        |             | 448          | 0.041          | -0.008     | 5.6129        | 0.000766       |             |              |                      |
|                        |             | 775          | 1.218          | -2.183     | 1535.105      | 0.000769       |             |              |                      |
|                        |             | 886          | 0.04           | -0.002     | 1.4032        | 0.000768       |             |              |                      |
| ES40T1                 | 40          | 344          | 1.201          | -2.186     | 1533.7        | 0.000783       | 0.549405    | 781.851      | 0.509780             |
|                        |             | 454          | 0.034          | -0.012     | 8.42          | 0.000765       |             |              |                      |
|                        |             | 781          | 1.204          | -2.188     | 1535.105      | 0.000766       |             |              |                      |
|                        |             | 892          | 0.039          | -0.004     | 2.806         | 0.000760       |             |              |                      |
| ES60T1                 | 60          | 339          | 1.287          | -2.284     | 1609.475      | 0.000799       | 0.563485    | 837.837      | 0.520560             |
|                        |             | 448          | 0.146          | -0.12      | 84.192        | 0.000748       |             |              |                      |
|                        |             | 776.5        | 1.285          | -2.298     | 1612.28       | 0.000745       |             |              |                      |
|                        |             | 887          | 0.145          | -0.116     | 81.386        | 0.000744       |             |              |                      |
| ES60T2                 | 60          | 338          | 1.282          | -2.2204    | 1546.33       | 0.000823       | 0.577373    | 834.582      | 0.539717             |
|                        |             | 448          | 0.06           | -0.016     | 11.2256       | 0.000796       |             |              |                      |
|                        |             | 775          | 1.278          | -2.194     | 1539.315      | 0.000797       |             |              |                      |
|                        |             | 885          | 0.072          | -0.012     | 8.419         | 0.000787       |             |              |                      |
| ES80T1                 | 80          | 347.5        | 1.167          | -2.19      | 1536.508      | 0.000759       | 0.532876    | 759.717      | 0.494444             |
|                        |             | 457          | 0.046          | 0.004      | 2.8064        | 0.000730       |             |              |                      |
|                        |             | 790.5        | 1.169          | -2.186     | 1533.7        | 0.000733       |             |              |                      |
|                        |             | 900.5        | 0.057          | 0.01       | 7.016         | 0.000728       |             |              |                      |
| SUMMARY OF FIRST LINES |             |              |                |            |               |                |             |              |                      |
| ES00T1                 | 0           | 350          | 1.174          | -2.188     | 1535.105      | 0.000764       | 0.536563    | 764.274      | 0.497864             |
| 764274                 |             |              |                |            |               |                |             |              |                      |
| ES20T1                 | 20          | 338          | 1.215          | -2.19      | 1536.508      | 0.000799       | 0.554794    | 790.965      | 0.514780             |
| 790965                 |             |              |                |            |               |                |             |              |                      |
| ES40T1                 | 40          | 344          | 1.201          | -2.186     | 1533.7        | 0.000783       | 0.549405    | 781.851      | 0.509780             |
| 781851                 |             |              |                |            |               |                |             |              |                      |
| ES60T1                 | 60          | 339          | 1.287          | -2.284     | 1609.475      | 0.000799       | 0.563485    | 837.837      | 0.520560             |
| 837837                 |             |              |                |            |               |                |             |              |                      |
| ES60T2                 | 60          | 338          | 1.282          | -2.2204    | 1546.33       | 0.000823       | 0.577373    | 834.582      | 0.539717             |
| 834582                 |             |              |                |            |               |                |             |              |                      |
| ES80T1                 | 80          | 347.5        | 1.167          | -2.19      | 1536.508      | 0.000759       | 0.532876    | 759.717      | 0.494444             |
| 759717                 |             |              |                |            |               |                |             |              |                      |

Table 8

|        |     |       |        |       |          |          |         |          |
|--------|-----|-------|--------|-------|----------|----------|---------|----------|
| 1389T3 | 528 | 0.736 | -2.182 | 1531  | 0.000480 | 0.337305 | 479.136 | 0.312956 |
|        | 458 | 0.41  | -0.016 | 11.22 | 0.000214 |          |         |          |
|        | 765 | 0.717 | -2.194 | 1539  | 0.000299 |          |         |          |
|        | 874 | 0.01  | -0.022 | 15.44 | 0.000464 |          |         |          |

| IDENT. | SATUR | AVG      | AVG      | HORIZ    |
|--------|-------|----------|----------|----------|
| LABEL  | (%)   | HORIZ    | RO       | STRESS   |
|        |       | STRESS   |          | KSI      |
| 1389   | 0     | 574.182  | 0.373971 | 0.574182 |
| 1320   | 20    | 653.2785 | 0.424630 | 0.653278 |
| 1349   | 40    | 665.6475 | 0.434131 | 0.665647 |
| 1359   | 60    | 514.29   | 0.335876 | 0.51429  |
| 1382   | 80    | 506.044  | 0.328997 | 0.506044 |

TZ IS AT 100 PCF

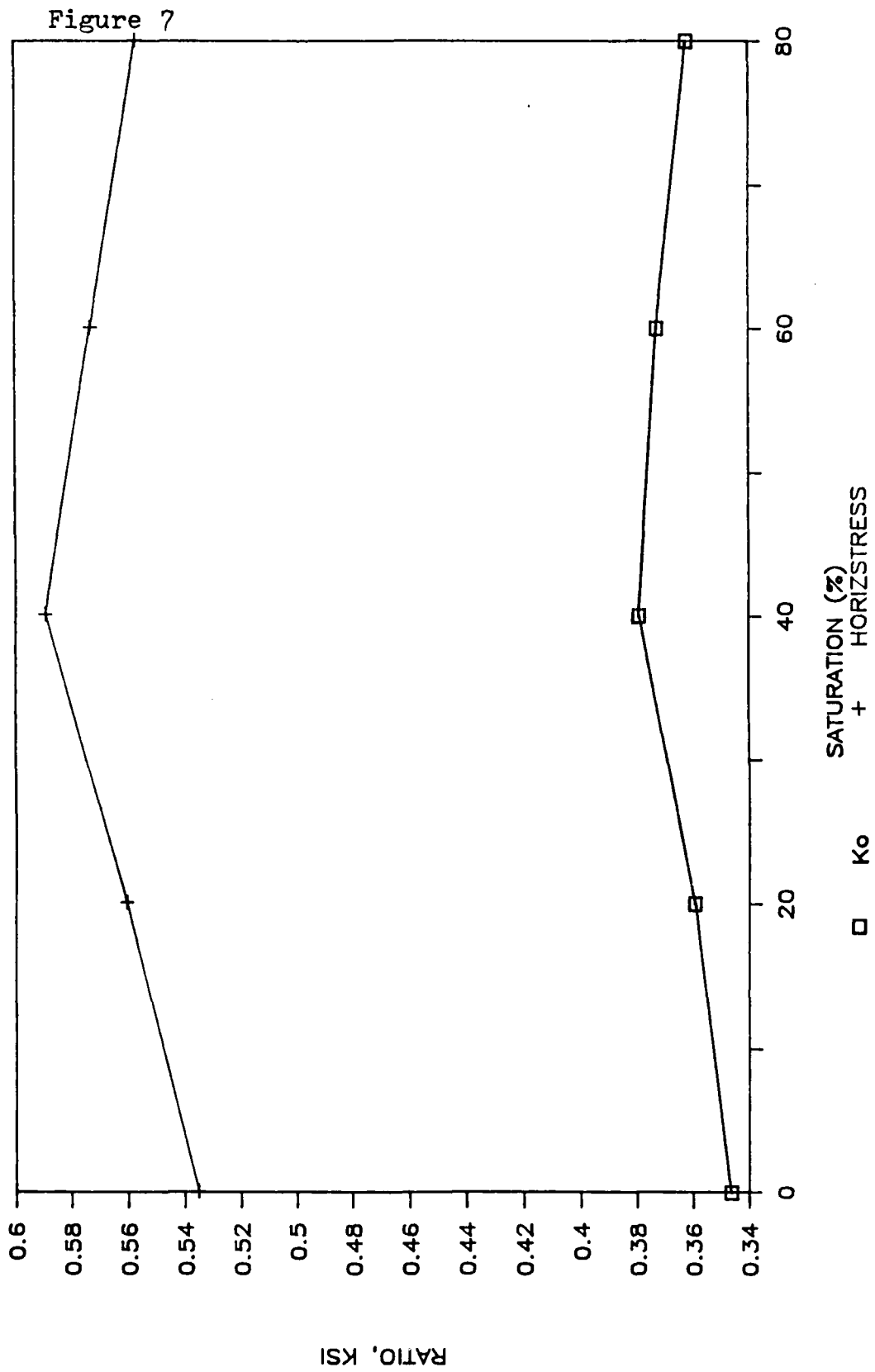
T1 SERIES

Table 9

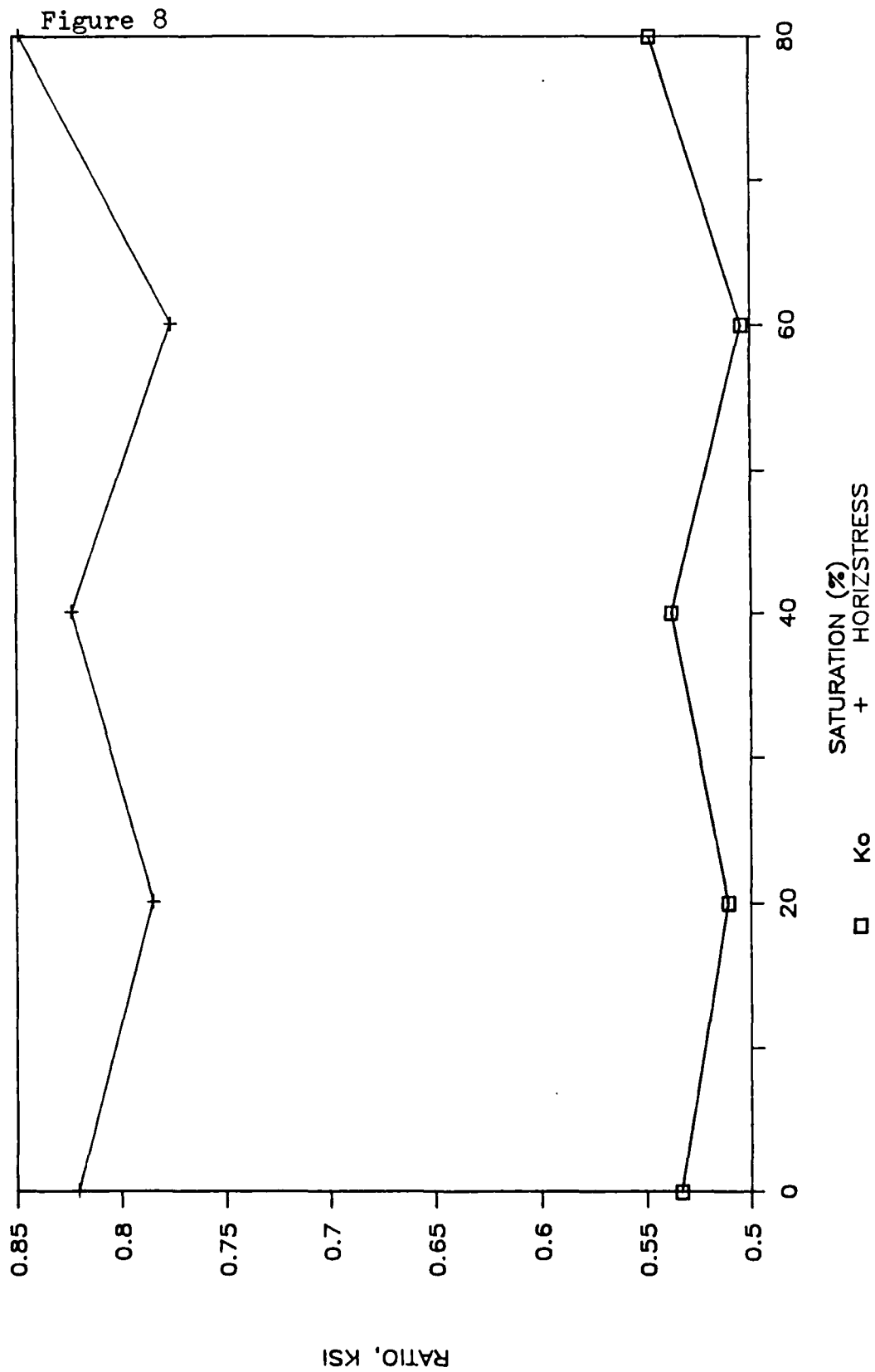
BASE SAND (110 PCF)

| TEST NUMBER | TIME seconds | F-BRIDGE LOAD volts | LOAD volts | STRESS AX psi | SLOPE OF LINES | BRIDGE LOAD | VERT STRESS (PSI) | LATERAL STIFF (ksi) |
|-------------|--------------|---------------------|------------|---------------|----------------|-------------|-------------------|---------------------|
| BS60T1      | 349          | 1.115               | -2.185     | 1533.7        | 0.000727       | 0.519064    | 725.165           | 0.473277            |
|             | 418          | 0.040               | -0.002     | 1.403         | 0.000697       |             |                   |                     |
|             | 786          | 1.116               | -2.186     | 1533.7        | 0.000698       |             |                   |                     |
|             | 805          | 0.037               | -0.002     | 1.043         | 0.000704       |             |                   |                     |
| BS60T2      | 327          | 0.649               | -2.12      | 1528          | 0.000421       | 0.225       | 422.199           | 0.274706            |
|             | 448          | 0.056               | -0.026     | 18.24         | 0.000390       |             |                   |                     |
|             | 765          | 0.663               | -2.206     | 1548          | 0.000396       |             |                   |                     |
|             | 877          | 0.075               | -0.018     | 12.63         | 0.000382       |             |                   |                     |
| BS20T1      | 330          | 1.13                | -2.19      | 1536.5        | 0.000735       | 0.511981    | 735.63            | 0.478769            |
|             | 450          | 0                   | -0.008     | 5.613         | 0.000738       |             |                   |                     |
|             | 777          | 1.145               | -2.19      | 1536.5        | 0.000747       |             |                   |                     |
|             | 886          | 0.015               | -0.026     | 18.24         | 0.000744       |             |                   |                     |
| BS20T2      | 328          | 0.877               | -2.196     | 1541          | 0.000569       | 0.339362    | 570.927           | 0.370491            |
|             | 433          | 0.036               | -0.0106    | 74.37         | 0.000573       |             |                   |                     |
|             | 766          | 0.836               | -2.194     | 1539          | 0.000546       |             |                   |                     |
|             | 877          | 0.027               | -0.014     | 9.82          | 0.000529       |             |                   |                     |
| BS40T1      | 348          | 1.13                | -2.18      | 1529.49       | 0.000738       | 0.518348    | 735.63            | 0.480964            |
|             | 458          | 0.012               | -0.017     | 11.93         | 0.000736       |             |                   |                     |
|             | 784          | 1.145               | -2.18      | 1529.49       | 0.000746       |             |                   |                     |
|             | 894          | 0.022               | -0.006     | 8.402         | 0.000738       |             |                   |                     |
| BS40T2      | 328          | 0.915               | -2.192     | 1529          | 0.000594       | 0.417437    | 595.665           | 0.387298            |
|             | 433          | 0.036               | -0.0106    | 74.37         | 0.000600       |             |                   |                     |
|             | 765          | 0.913               | -2.188     | 1535          | 0.000600       |             |                   |                     |
|             | 875          | 0.015               | -0.012     | 8.42          | 0.000588       |             |                   |                     |
| BS60T1      | 354          | 1.163               | -2.182     | 1530.895      | 0.000759       | 0.532997    | 757.113           | 0.494555            |
|             | 464          | 0.294               | -0.004     | 2.806         | 0.000568       |             |                   |                     |
|             | 790          | 1.185               | -2.178     | 1528.08       | 0.000584       |             |                   |                     |
|             | 900          | 0.034               | -0.01      | 7.016         | 0.000756       |             |                   |                     |
| BS60T2      | 328          | 0.417               | -2.184     | 1532          | 0.000272       | 0.190934    | 271.467           | 0.177197            |
|             | 438          | 0.439               | 0.012      | 8.419         | -0.00001       |             |                   |                     |
|             | 766          | 0.171               | -2.184     | 1532          | -0.00017       |             |                   |                     |
|             | 877          | 0.377               | 0          | 0             | -0.00013       |             |                   |                     |
| BS80T1      | 342          | 0.928               | -2.198     | 1542          | 0.000601       | 0.422202    | 604.128           | 0.391782            |
|             | 452.5        | 0.028               | -0.012     | 8.419         | 0.000586       |             |                   |                     |
|             | 780.5        | 1.02                | -2.199     | 1543          | 0.000646       |             |                   |                     |
|             | 890          | 0.021               | -0.01      | 7.016         | 0.000650       |             |                   |                     |
| BS80T2      | 328          | 0.668               | -2.196     | 1540.7        | 0.000421       | 0.304103    | 434.868           | 0.282253            |
|             | 438          | 0.133               | -0.02      | 13.07         | 0.000350       |             |                   |                     |
|             | 765          | 0.781               | -2.188     | 1535          | 0.000421       |             |                   |                     |
|             | 875          | 0.036               | -0.018     | 12.62         | 0.000482       |             |                   |                     |

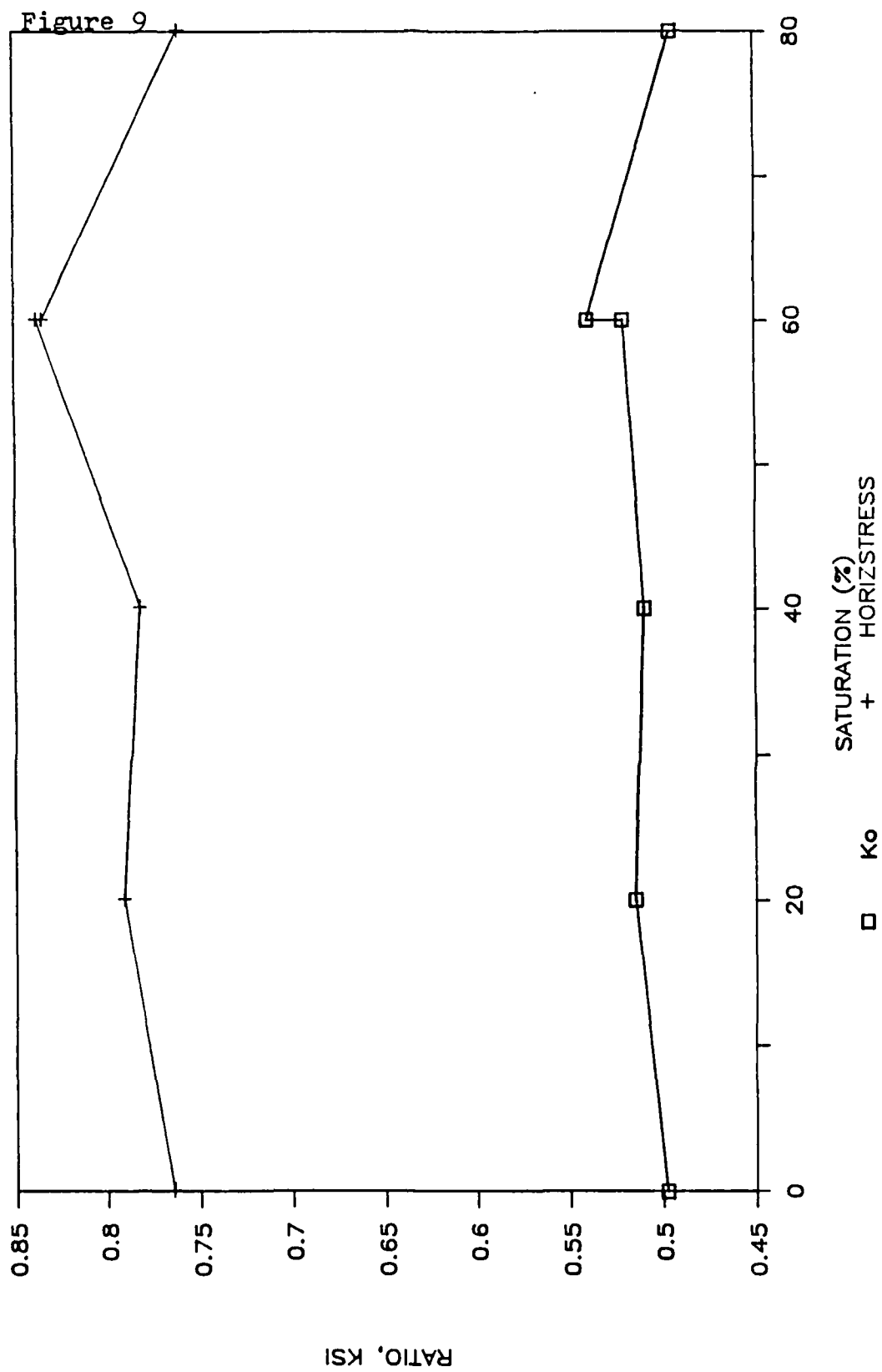
# OTTAWA 20-30 SAND



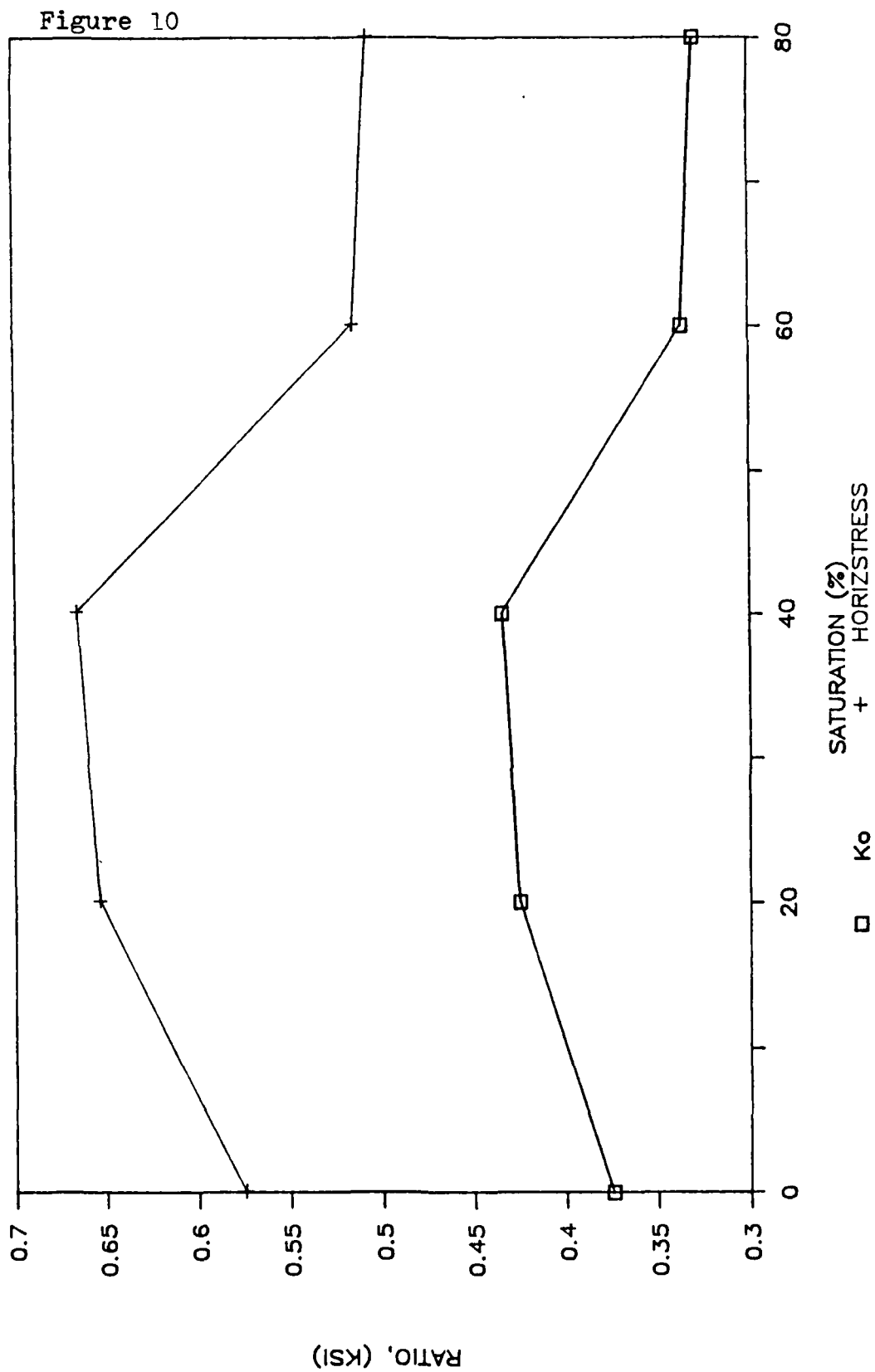
# F-58 SAND



# EGLIN SAND



# BASE SAND





UNLOAD =

INTS

DATE: \_\_\_\_\_

SAMPLE \_\_\_\_\_

FILE ID \_\_\_\_\_

PRE-TEST

DRY UNIT WEIGHT \_\_\_\_\_

VOID RATIO \_\_\_\_\_

SATURATION \_\_\_\_\_

WATER CONTENT \_\_\_\_\_

LAYER

1

2

3

4

NO. OF BLOWS

RADIAL STRAIN GAGE ID \_\_\_\_\_

 $V_{OR} =$  \_\_\_\_\_ [AFTER COMPACTION]FIRST LOAD-UNLOAD CYCLE $P_{MAX_1} =$  \_\_\_\_\_  $V_{P_1} =$  \_\_\_\_\_  $t_{P_1} =$  \_\_\_\_\_ $\Delta_{MAX_1} =$  \_\_\_\_\_  $V_{\Delta_1} =$  \_\_\_\_\_  $V_{R_1} =$  \_\_\_\_\_ $\Delta_{O_1} =$  \_\_\_\_\_  $V_{OR_1} =$  \_\_\_\_\_ [AT  $P=0$  - UNLOAD]SECOND LOAD-UNLOAD CYCLE $P_{MAX_2} =$  \_\_\_\_\_  $V_{P_2} =$  \_\_\_\_\_  $t_{P_2} =$  \_\_\_\_\_ $\Delta_{MAX_2} =$  \_\_\_\_\_  $V_{\Delta_2} =$  \_\_\_\_\_  $V_{R_2} =$  \_\_\_\_\_ $\Delta_{O_2} =$  \_\_\_\_\_  $V_{OR_2} =$  \_\_\_\_\_ [AT  $P=0$  - UNLOAD] $t_{FINAL} =$  \_\_\_\_\_ [TOTAL TEST TIME]END OF TEST $V_{FR} =$  \_\_\_\_\_ [RADIAL STRAIN GAGE AT  $P=0$ ]

## SOIL TEST DATA

### SPECIMEN DATA

Test No \_\_\_\_\_ Date \_\_\_\_\_ Time \_\_\_\_\_ Room Temp \_\_\_\_\_  
Striker Bar Length \_\_\_\_\_ Gun Chamber Press. \_\_\_\_\_  
Counter Time \_\_\_\_\_ Computed Incident Stress \_\_\_\_\_  
Soil Specimen Description \_\_\_\_\_  
Soil Specimen Length \_\_\_\_\_ Specimen Mass \_\_\_\_\_  
Specimen Density \_\_\_\_\_ Moisture Content \_\_\_\_\_  
Specimen Confinement Press. \_\_\_\_\_ Desaturation Press. \_\_\_\_\_

-----

### Instrumentation (Nicolet 4094)

#### Incident Strain Gage

Exc. Volts \_\_\_\_\_ Amp. Gain \_\_\_\_\_ Time Step \_\_\_\_\_  
Peak Volts \_\_\_\_\_ Ave. Volts \_\_\_\_\_ Calibration  $\left(\frac{\text{Strain}}{\text{Volts}}\right)$  \_\_\_\_\_

#### Transmitted Strain Gage

Exc. Volts \_\_\_\_\_ Amp. Gain \_\_\_\_\_ Time Step \_\_\_\_\_  
Peak Volts \_\_\_\_\_ Ave. Volts \_\_\_\_\_ Calibration  $\left(\frac{\text{Strain}}{\text{Volts}}\right)$  \_\_\_\_\_

Strain Ratio (Peak Transmitted/Peak Incident) \_\_\_\_\_

Specimen Transit Time \_\_\_\_\_ Specimen Wave Speed \_\_\_\_\_

Disk Storage \_\_\_\_\_

Cyl. Strain Gage Exc. V. \_\_\_\_\_ Amp. Gain \_\_\_\_\_ Peak V. \_\_\_\_\_ Time Step \_\_\_\_\_ VFS \_\_\_\_\_

COMMENTS: \_\_\_\_\_  
\_\_\_\_\_  
\_\_\_\_\_  
\_\_\_\_\_  
\_\_\_\_\_

**WATER CONTENT DETERMINATION**

Data Sheet 1

Project \_\_\_\_\_ Job No. \_\_\_\_\_

Location of Project \_\_\_\_\_

Description of Soil \_\_\_\_\_

Tested By \_\_\_\_\_ Date of Testing \_\_\_\_\_

Date of Weighing \_\_\_\_\_

|                       |  |  |  |  |  |
|-----------------------|--|--|--|--|--|
| Boring no.            |  |  |  |  |  |
| Container no. (cup)   |  |  |  |  |  |
| Wt. of cup + wet soil |  |  |  |  |  |
| Wt. of cup + dry soil |  |  |  |  |  |
| Wt. of cup            |  |  |  |  |  |
| Wt. of dry soil       |  |  |  |  |  |
| Wt. of water          |  |  |  |  |  |
| Water content, $w\%$  |  |  |  |  |  |

|                       |  |  |  |  |  |
|-----------------------|--|--|--|--|--|
| Boring no.            |  |  |  |  |  |
| Container no. (cup)   |  |  |  |  |  |
| Wt. of cup + wet soil |  |  |  |  |  |
| Wt. of cup + dry soil |  |  |  |  |  |
| Wt. of cup            |  |  |  |  |  |
| Wt. of dry soil       |  |  |  |  |  |
| Wt. of water          |  |  |  |  |  |
| Water content, $w\%$  |  |  |  |  |  |

## REFERENCES

1. Bowles, E.J., "Engineering Properties of Soils and their measurement"
2. Ross, C.A., Nash, P.T., and Friesenhahn, G.T., "Pressure Waves in Soils Using a Split-Hopkinson Pressure Bar," ESC-TR-86-29 Engineering and Service Laboratory, Air Force Engineering and Service Center, Tyndall AFB FL. July 1986
3. Bshbach, W.O., Souders, M., "Handbook of Engineering Fundamentals" third edition, John Wiley & Sons, Inc , 1975.

FLIGHT DYNAMICS LABORATORY

1989 USAF-UES SUMMER HIGH SCHOOL APPRENTICE ENGINEER

CREATION OF A F-15/F-16 AIRCRAFT DATA BANK

Prepared by: Tremayne Dion Anderson

Academic rank: Junior

High School: Patterson Career Center

USAF Researcher: Monika K. Hilb/Paul C. Ulrich  
Flight Dynamics Laboratory  
Landing Gear Test Facility  
August 11, 1989

## ACKNOWLEDGEMENT

Before I let my fingers and my head get away from myself, I would like to thank Mr. Paul Ulrich for taking a chance with me. Had he not given me the opportunity to showcase my abilities, I would not have been able to exceed. What I mean is he allowed me to manifest my knowledge and talents while in return I was able to acquire an intense degree of learning pertaining to my career choice which is engineering. I thank Mr. Paul Ulrich again for allowing me to enhance my knowledge of engineering. I'm quite sure this knowledge will be of great use to me in a few years to come.

I would like to thank Ms. Monika Hilb, my official mentor. She was to me a very becoming person. She was not at all what I was expecting a female boss to be like. That's not a bad trait, it's a good one. Ms. Hilb made my 8 weeks satisfying. It seemed as though her motto was "the way you treat me is the way you are treated." With that I developed some trust between her and myself. She explained the do's and don'ts of the facility in a respectable manner. She was a very open minded person and she got right to the point. The one trait that stood out the most was the fact that she was very versatile. Ms. Hilb was able to adjust to changes quite easily. I admire that in a boss and I thank Ms. Monika Hilb for making me feel more at ease and comfortable during the 8 weeks.

Robert Maggio was another colleague of mine. He and I worked neatly in the same office. Mr. Maggio didn't carry himself as if he was my boss, but he was very helpful. He was also very encouraging. As I noticed that he acted himself around me, that justified that it was ok to act myself around him. That was very relaxing. He too made my 8 weeks comfortable. I thank Mr. Maggio for an intriguing work experience.

Ron Gillum, an employee for SRL, was another person to be graciously commended. In every household, every classroom, every work area there is a clown. In the Flight Dynamics Laboratory, Mr. Ron Gillum was the clown. Though he had more fun than the other workers, he was a hard worker. Mr. Gillum made SRL sufficient money with every mandrel he constructed. He was young but he was also wise. Mr. Gillum was one of the few people to open up to me this past summer. Each time he and I talked it was about something interesting and I could relate quite easily. It was easy for me to relate because he spoke of some experiences he had encountered and I understood because I underwent the same experience. Mr. Gillum was relaxed with his job and didn't mind conversating with me while he continued his work. From many of our conversations, I learned something about SRL and FIVMA. I enjoyed talking to Mr. Ron Gillum because he was an interesting person to speak with and I want to thank him for devoting so much of his time to me these past eight weeks.

Jim Burgess, electrical engineer for SRL, deserves a tremendous warm thank you from me. Mr. Burgess, from our conversations, gave me a head start in the field of engineering. He opened my eyes a little further and showed me what exactly it would take to become an engineer. Basically, within these 8 weeks, Mr. Burgess told me how to become an engineer, crossing every obstacle, and what to expect once I became a certified engineer. I want to thank Mr. Jim Burgess for his encouraging remarks. Especially when he said he had faith that I would succeed. Words such as those can increase a persons confidence a great deal and I thank him for being so candid and for sharing his knowledge with me.



Deborah Flagg, buyer employed under Systems Research Laboratory, Inc. (SRL), was an exceptional woman. Mrs. Flagg was friendly with everyone and of course everyone was friendly toward her. She had two lovely children in which she adored too death. Though she was a mother of two and a wife, I didn't think of her as one at work. To me I saw her as a very close friend. One whom I could turn to whenever I was in need of someone to talk to. It seemed as though she was always there just as a mother should be. Even though she was approximately twenty years older than me, had children of her own to take care of, and had a hectic job that accumulated a considerable amount of her time during the day, she found time to show concern for my well-being. If there were any problems that may have been on my conscience or if I just wasn't cheerful that day, Mrs. Flagg had a way of lifting up my spirits and making the day brand new. I admired that. To be totally candid, looking back at the eight weeks, I would have to recognize Mrs. Flagg as more of a mom than a co-worker. And now I would like to thank Mrs. Deborah Flagg for adopting me those past eight weeks. I enjoyed her company and every conversation we had was informative and learning. It was a pleasure and again thank you.

Dave Morris was another influential character at Wright Patterson Air Force Base. The words from Mr. Morris' mouth came so fluently and I became interested when I heard him mention that he was an engineer. He too offered me a few words of encouragement as far as how to prepare for four years of engineering. From the conversation Mr. Morris and I had, it seemed as though achieving his degrees and maintaining an interesting career was not a challenge at all. I gathered, that with an attitude of such about college, he must be an intelligent human being. Mr. Morris informed me that if I applied myself a bit more in college than I did in high school and don't hang with the wrong crowd, I'll do just fine. Now that I had that talk with Mr. Morris, I must say that his attitude about college has sort of rubbed off on me. Hopefully I'll be as successful as Mr. Morris. An encouraging word or two is just as good as a helping hand. If only there were more people willing to share those confidence boosters. Thank you Mr. Morris for sharing your experiences with me. I hope in the near future I can be as helpful to you.

I would just like to thank once again all those people kind enough to open up and shed light in places I did not know existed. I will always be grateful and I wish you the best of luck in what your future brings. Thank you.

SECTION I  
INTRODUCTION

My primary project for the 8 weeks at WPAFB was to create a data bank based on the F-16 and F-15 aircrafts. Eventually it will be necessary to possess data banks on all aircrafts. The limitation of my work period only allowed me to begin a methodology on these two planes. The reason I was assigned this task was because it was mandatory that SRL, the contractors, the engineers, and every other employee in the Flight Dynamics Laboratory have data banks on the aircrafts and parts tested in FIVMA. Basically it's convenient for all the workers. It allows them to retrieve information when needed on specific aircrafts. This eliminates searching all over for one piece of information when it could be located in a single booklet. The workers now will have the information necessary when performing tests on tires, brakes, wheels, strut, anti-skid, load deflection, and flotation. Information on the size and weight of wheels and tires can be obtained and also assembly numbers can be determined from these data banks. The data stored in these booklets will provide for adequate convenient information to the employees. These particular data filled booklets are more helpful to the workers. The entire laboratory can refer back to the data banks when in need of information. Each book will serve as an information center for the entire Flight Dynamics Laboratory while at the same time provide for a new personnel trainee guide or booklet.

The methodology I created was exactly like the outline shown:

The F-16 and F-15 Model Aircraft

- I Introduction
  - A. Describe Facility
    - a. background of WRDC/FIVMA
- II Tires
  - A. Profile
  - B. Size
  - C. Weight
  - D. Flotation
  - E. Load Deflection
  - F. Curves
  - G. Specification
  - H. Stock #
  - I. Photographs
- III Wheels
  - A. Stock #
  - B. Assembly #
  - C. Specification
  - D. Photographs
  - E. Profile
  - F. Size
  - G. Weight
- IV Brakes
  - A. Assembly #
  - E. Stock #
  - C. Performance Programs
  - D. Temperature
  - E. Fatigue
  - F. Fraction Mechanics
  - G. Specification
  - H. Photographs
- V Strut
  - A. Assembly #
  - B. Stock
  - C. Metering Pin
  - D. Photographs
- VI Anti-Skid
  - A. Stock
  - B. Photographs

SECTION II

APPARATUS

The apparatus involved in this project were USAF Technical Manuals or T.O.'s and files. To be more specific I used T.O. 1F-16A-2-32JG-40-1 and T.O. 1F-16A-2-32JG-50-1, 1F-16A-2-32JG-60-1. These two particular T.O.'s contained data on nosewheel steering and landing gear wheels and brakes of the F-16. Information was also obtained from the Goodyear Aircraft Tire Manual & Data Book and the B. F. Goodrich Aircraft Tires Engineering Data Book. The two latter manuals provided for me adequate information on both the F-16 and F-15 aircraft.

My primary sources of information were not machines. Meaning, in other words, I did not receive information from equipment. But the data bank I am creating will act as a succor to SRL when tests are being performed on various pieces of machinery as the dynamometers, the drop towers, the shaker, and the console, which was manufactured by SRL. The data was analyzed by my colleagues of higher rank. The information I retrieved was compared to the data in the T.O.'s. The data was also analyzed by the computers. If the information was invalid the test would be a failure. Therefore the information proposed must be valid.

During the installation of data into the data bank, I had discovered that the F-16 and F-15 aircrafts are not of the same popular name nor company. F-16 is referred to as a Fighting Falcon manufactured by General Dynamics. The F-15 model aircraft is a product of the McDonnell-Douglas Company. The popular name of this particular aircraft is Eagle. I also made an observation of the size and weight of the main and nose gear wheels and tires of the F-16 and compared the gathered data to the size and weight of the wheels and tires of the F-15. The results of the comparison proved that the size and weight of the F-15 aircraft was definitely greater than that of the F-16 aircraft. Other observations lead me to conclude that the F-15 and F-16 aircrafts were designed to perform different tasks. The F-15 aircraft is strictly a fighter plane, while the F-16 is not. The different designs of the two planes clears up the controversy about which aircraft does what. The F-16 may bomb but the F-15 is the fighter aircraft. The components of the F-15 are sturdier than those of the F-16 because the F-15 was equipped to undergo a substantial amount of pressure and combat. The F-16, on the otherhand, was not. After making these observations, I began to interpret the data as being factual information used to distinguish one particular aircraft or part from the other. Data concerning one aircraft could not be used to depict another aircraft.

SECTION III

OBSERVATION

There were many interesting observations I took note of this summer and of course I obtained a tremendous amount of knowledge concerning not just FIVMA but of Wright Patterson Air Force Base also. I was uplifted with the information. Before I began working at WPAFB, I had never witnessed a tire explosion. On July 20, 1989, I observed a F-16 main gear tire blow after being taxied at an excessive speed for only a short period of time. I was not able to account for the explosion, but it was quite a vision. The tire was destroyed and before any further major tests could be made it had to be removed from the mandrel and be replaced with another F-16 tire. I also made an observation of tire footprints that were developed from a tire test. The fascinating part about it was that each time you applied more pounds of pressure the footprints became larger. At 5,000 psi the footprints were relatively small compared to what they looked like at 25,000 psi. Each time I traveled through the mandrel build up I paid special attention to the procedure in which the mandrels were built. From time to time there were scheduled tour and I always managed to find time to join in and learn something new about the facility. One of my supervisors and myself took a tour of the Survivability Enhancement Building. There we observed the gun range where trained engineers programed machines to shoot specific parts of the fuel tank area of an aircraft. The test is performed to see if it is possible to find a means of constructing a bullet proof type material to prevent the aircrafts fuel tank from exploding. Right now I'm in the process of viewing an upper carriage being placed on top of the 192 dynamometer. The significance of this carriage is that in the near future the space shuttle's landing gear will be mounted on this carriage. The purpose is to run tests on the landing gear to see if FIVMA can develop a mechanism that allows the space shuttle to stop after a landing without destroying the entire landing gear. Before my work period comes to an end, I have a desire to get some hands on experience and assist some of the engineers in constructing mandrels and running tire tests. That next Monday, July 24, I was able to fulfill my desire. I didn't quite get to build a mandrel or run a tire test yet, but I did learn how to arc weld, how to operate a mill, and I learned what exactly could be constructed on a mill. I also learned what a lathe was and what can be constructed when the use of the two machines are combined (mill and lathe). Everything was quite interesting.

The most important thing I learned this summer was that with my status in school and my mentality level, Wright Pat is the place for me as far as developing a career in engineering. The base is crawling with engineers and I'd like to be one of those who are employed with the government. With this experience I also learned that there are obstacles both good and bad that you have to over come in order to be successful. Things aren't always going to be the way you expect them to be, but that must not discourage you. You were born to be somebody and you were hired to do a job. No one can take that away from you. So I'd say that the most meaningful thing I learned is my position as far as wealth, rank, occupation, and reputation in life. The majority of the people I have spoken with while working at WPAFB have visualized a truly promising picture of myself with a high ranking business position in the very near future. My biggest fear presently is that some where down the line I will undergo a major set back that will seize my chances of advancement. I would just like to say that I am grateful for the confidence so, so many people possess in me and to show my appreciation I will work now to prevent any delays and I will only strive for excellence.



With all due respect this work experience was a pleasure and I would be more than happy if you (UES) and you (Mr. Paul Ulrich) allowed me to return next summer. Please consider the request and thank you.

Sincerely

Tremayne Anderson

Tremayne Anderson

SECTION IV  
REFERENCE

## Bibliography

T.O. 1F-16A-2-32JG-40-1

T.O. 1F-16A-2-32JG-50-1, 1F-16A-2-32JG-60-1

T.O. 4W1-7-1203, 4W1-8-73

A-A-1 F-16

A-A-1 Pictures F-16

A-A-1 Qualification Test Reports F-16

A-A-1 Qualification Test Reports F-15

A-A-1 Specification F-15

AFWAL-TM-82-221-FIBE

9.C-12-8 F-15 Response to Runway

F-15 Taxi Simulation Computer Program User's Manual - Volume 1

B. F. Goodrich Aircraft Tires Engineering Data

Goodyear Aircraft Tire Manual and Data Booklet

A-A-1 Landing Gear F-16

EVALUATION OF SEVERAL METHODS FOR PREDICTING SURFACE  
PRESSURES IN THE SHADOW REGIONS OF AEROSPACE VEHICLES

Eric W. Bailey - Apprentice  
Robert E. McCarty - Mentor

Aircrew Protection Branch  
Vehicle Subsystems Division  
Flight Dynamics Laboratory  
Wright Research and Development Center  
Wright-Patterson Air Force Base, Ohio 45433

August 1989

HIGH SCHOOL APPRENTICESHIP PROGRAM  
AIR FORCE OFFICE OF SCIENTIFIC RESEARCH

## TABLE OF CONTENTS

### SECTION

- I. ACKNOWLEDGEMENTS
- II. INTRODUCTION
- III. DESCRIPTION OF RESEARCH
- IV. RESULTS
- V. CONCLUSIONS AND RECOMMENDATIONS
- VI. OTHER INTERESTING OBSERVATIONS AND  
LESSONS LEARNED FROM SUMMER EXPERIENCE
- VII. REFERENCES/BIBLIOGRAPHY

# LIST OF SYMBOLS

|               |  |
|---------------|--|
| $C_p$         | Pressure coefficient   |
| $C_{p_s}$     | Shadow region pressure coefficient                                     |
| $L$           | Length of analytic body, in.   |
| $M_\infty$    | Freestream Mach number   |
| $P$           | Local static pressure  |
| $P_\infty$    | Freestream static pressure   |
| $P_{t_2}$     | Total (stagnation) pressure pressure downstream of a normal shock wave |
| $Q_{INF}$     | Freestream dynamic pressure  |
| $\rho_0$      | Local static density   |
| $\rho_{0INF}$ | Freestream static density  |
| $T$           | Local static temperature   |
| $T_{INF}$     | Freestream static temperature  |
| $V_\infty$    | Freestream velocity  |
| $x$           | Distance along the X axis of the analytic body, in.                    |

LIST OF SYMBOLS (Concluded)

(Others are defined in the text and in the figures)

|          |  |
|----------|--|
| $\alpha$ | Angle of attack, deg   |
| $\gamma$ | Ratio of specific heats  |
| $\delta$ | Body slope angle, the angle between the freestream flow direction and the tangency plane of a point on a body, deg |

## I. ACKNOWLEDGEMENTS

I would like to thank everyone in the Aircrew Protection Branch for making this summer an educational, rewarding, and enjoyable experience. I would like to thank both Robert E. McCarty and Charles A. Babish III in particular. Mr McCarty, the Group Leader of the Aircrew Protection Branch, allowed me to work as an apprentice in the Flight Dynamics Laboratory and served as my mentor. Mr Babish, Flight Dynamics Laboratory aerospace engineer, served as the principle engineer for my project. Both men were always happy to answer my questions and help me with any problems I had.



## II. INTRODUCTION

We evaluated methods for predicting surface pressures in shadow regions of aerospace vehicles (see Figure 1). In other words, we ran tests on different equations which predicted the pressures generated on the area of where an airplane's body slopes are negative, to see which equation was the most accurate at subsonic, transonic, supersonic, and hypersonic speeds. The most accurate, and therefore best, method will be used for a FORTRAN computer program that simulates the aerothermodynamic heating effects of high speeds on aircraft forebodies and their transparencies. This program, called STAPAT\* II, will help produce windshields, canopies, and windows that can better withstand the harsh effects of pressure variation as well as aerothermodynamic heating and cooling. This improvement, if combined with other technological advances within the Aircrew Protection Branch, could produce the ideal canopy that would resist crazing, bird strike and delamination, provide better optics to the pilot, be lightweight, and affordable.

---

\*STAPAT is the acronym for Specific Thermal Analyzer Program for Aircraft Transparencies.

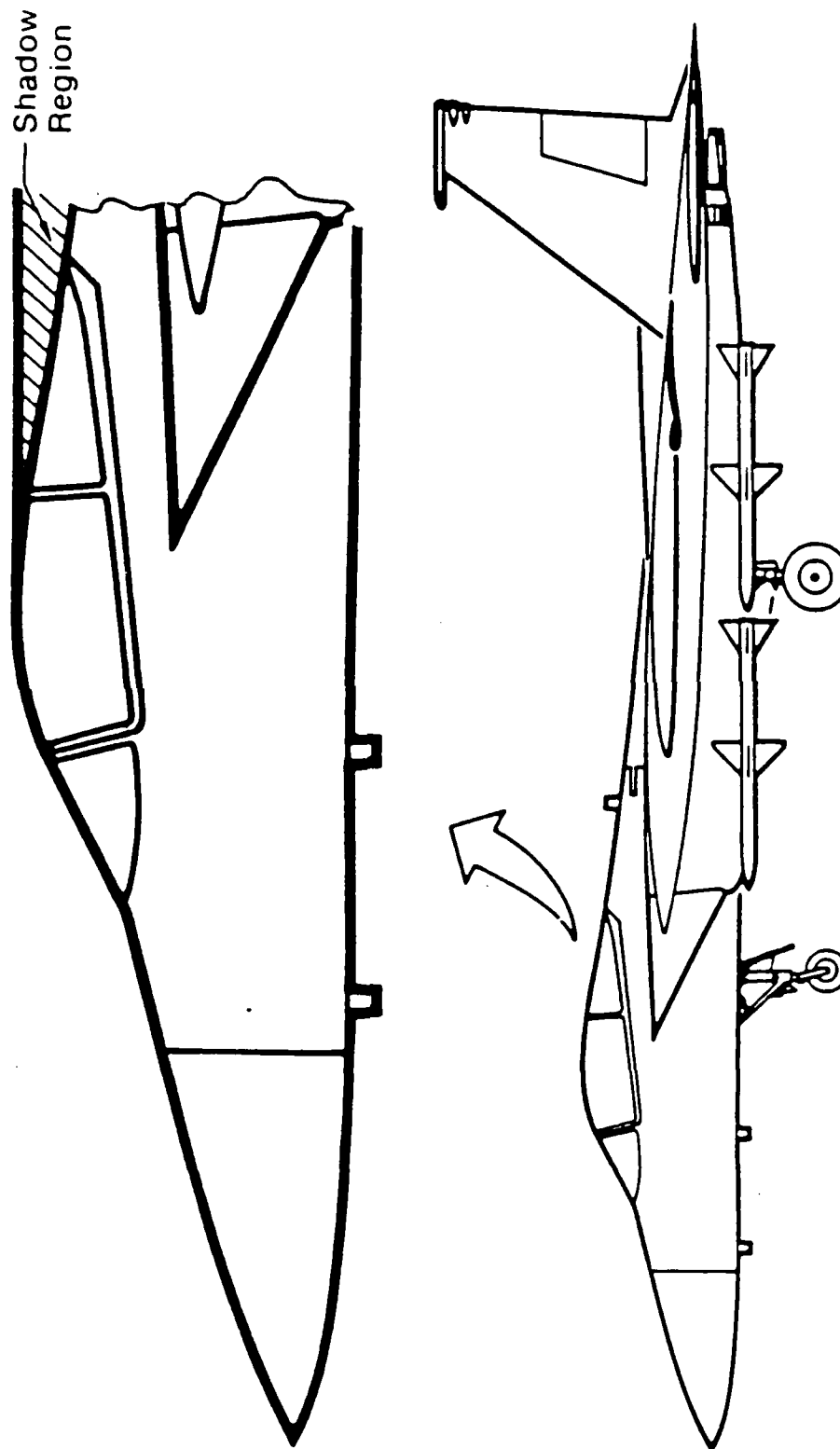


Figure 1. Aircraft Canopy Shadow Region Location

### III. DESCRIPTION OF RESEARCH

The four shadow region surface pressure prediction methods evaluated were Babish, Prandtl-Meyer, Dahlem-Buck, and ACM. Using the VAX computer system, we predicted surface pressures from the method equations and compared them with wind tunnel data to see which method was the best. First of all, we used a computer program called GEOMPLT to plot different aircraft forebodies from several different perspectives (see Figure 2 and 3). Secondly, we made runs using a STAPAT subprogram called STAHET (see Figure 4). Later, we plotted pressures using HEATPLT (see Figure 5). Next, we tabulated predicted pressures from these plots. Then, we extracted, tabulated, and plotted wind tunnel data, for comparison with the predicted pressures from the methods (see Figure 6 thru 9). Finally, we concluded which prediction method was the most accurate.

The equations for calculating shadow region surface pressures and the computer code limits are presented on the following pages.

STAPAT calculations of the inviscid surface streamlines and heating rates are dependent upon surface pressure distributions. These distributions are determined from a modified Newtonian pressure coefficient relationship, that is

$$C_p = C_{p_s} \sin^2 \delta \quad (1)$$

where

$$C_{p_s} \equiv \left( P_{t_2} - P_\infty \right) / \left( 0.5 \gamma P_\infty M_\infty^2 \right) \quad (2)$$

and

$$C_p \equiv \left( P - P_\infty \right) / \left( 0.5 \gamma P_\infty M_\infty^2 \right) \quad (3)$$

This method gives acceptable results on forward facing portions of aerospace vehicles but is not applicable to rearward facing portions where body slope angles are negative; i.e., in shadow regions such as the canopy backside area shown in Figure 2.

In shadow regions (where  $\delta < 0.0$  deg) STAPAT sets the surface pressure,  $P$ , equal to the freestream static pressure,  $P_\infty$ , that is  $C_{p_s} = 0.0$ . In reality, the flow expands into shadow regions yielding lower than freestream surface pressures.

As an enhancement of STAPAT, a shadow region pressure prediction method is proposed for incorporation into STAPAT II (Reference 8). Four prediction methods were reviewed and evaluated for possible incorporation: (1) Babish correlation (Reference 7); (2) Prandtl-Meyer expansion (Reference 9); (3) Dahlem-Buck mirror (reference 10); and (4) ACM empirical (Reference 11).

The BABISH correlation method was developed using experimental data from supersonic wind tunnel tests such that the resulting shadow region pressure would:

1. be continuous in  $M_\infty$  for  $0 \leq M_\infty \leq \infty$ ,
2. be continuous in  $\delta$  for  $-90 \leq \delta \leq 0^\circ$ ,
3. yield negative  $C_p$  values for negative  $\delta$  values,
4. yield larger negative  $C_p$  values for larger negative  $\delta$  values,
5. yield  $C_p$  values that follow the general trend of, and are essentially bounded by, the  $P = 0$  versus  $M_\infty$  relationship for  $M_\infty > 1.0$ , and
6. yield  $C_p$  values that agree reasonably well with available data in terms of magnitude and variation with  $M_\infty$ .

The shadow region pressure coefficient correlation equation selected was

$$C_{p_S} = -AR (0.7) M_\infty^{1/2} \sin^{1/3} (-\delta) \quad (4)$$

for  $-90 \leq \delta \leq 0^\circ$  and where

$$AR = 1 / [ (1 - M_\infty^2)^2 + M_\infty^2 ]^{1/2} \quad (5)$$

The PRANDTL-MEYER expansion method makes use of the equations for a uniform, two-dimensional supersonic stream which expands isentropically while flowing over a convex bend. The shadow region pressure coefficient is calculated from

$$C_{p_s} = \frac{2}{\gamma M_1^2} \left( \frac{P_2}{P_1} - 1 \right) \quad (6)$$

where:

$C_{p_s}$  = shadow region pressure coefficient  
 $P_1$  = pressure upstream of expansion  
 $M_1$  = Mach number upstream of expansion  
 $P_2$  = pressure downstream of expansion

$P_2$  is computed from the following:

$$v_1 = \sqrt{\frac{\gamma+1}{\gamma-1}} \tan^{-1} \sqrt{\frac{\gamma-1}{\gamma+1} (M_1^2 - 1)} - \tan^{-1} \sqrt{M_1^2 - 1} \quad (7)$$

$$v_2 = v_1 + \delta \quad (8)$$

$v_1, v_2$  = Prandtl-Meyer expansion angles  
 $\delta$  = body slope

$M_2$ , the Mach number downstream of expansion, is calculated from:

$$v_2 = \sqrt{\frac{\gamma+1}{\gamma-1}} \tan^{-1} \sqrt{\frac{\gamma-1}{\gamma+1} (M_2^2 - 1)} - \tan^{-1} \sqrt{M_2^2 - 1} \quad (9)$$

then:

$$P_2 = P_1 \left[ \frac{1 + \frac{\gamma-1}{2} M_2^2}{1 + \frac{\gamma-1}{2} M_1^2} \right]^{-\gamma/(\gamma-1)} \quad (10)$$

The DAHLEM-BUCK minor correlation method calculates the shadow region pressure coefficient from

$$C_{pS} = - C_{pDB} \left[ \frac{C_{p \text{ cone } (M < 20)}}{C_{p \text{ cone } (M = 20)}} \right] \quad (11)$$

where:

$C_{pS}$  = shadow region pressure coefficient

$$C_{pDB} = \overbrace{\left[ \frac{1.0}{(\sin 4(-\delta))^{3/4}} + 1.0 \right]}^B \sin^2(-\delta) \text{ for } -\delta \leq 22.5^\circ \quad (12)$$

$$= 2 \sin^2(-\delta) \text{ for } -\delta > 22.5^\circ \quad (13)$$

$\delta$  = body slope

$$\frac{C_{p \text{ cone } (M < 20)}}{C_{p \text{ cone } (M = 20)}} = 1.0 + A (-\delta)^n \quad (14)$$

$$A = (6.0 - 0.3 M_\infty) + \sin \left[ \frac{(\ln M_\infty - 0.588)}{1.2} \pi \right] \quad (15)$$

$$n = -1.15 - 0.5 \sin \left[ \frac{(\ln M_\infty - 0.916) \pi}{3.29} \right] \quad (16)$$

The ACM empirical method was developed based upon shadow region pressure data obtained at Mach 4.0 on an Aerodynamic Configured Missile. The shadow region pressure coefficient is calculated from

$$C_{p_s} = - \frac{1}{16} \frac{\delta}{M_\infty^2} \quad (17)$$

### 3.5 Limiting Pressure Values

In addition to the limit placed on shadow region pressure coefficient values calculated by the PRANDTL-MEYER expansion method due to separated flow considerations, overall limiting pressure values were incorporated in the STAPAT II computer code. They are as follows:

#### 1. CODE LIMIT 1

$$\text{If } C_{p_s} < - \frac{1}{M_\infty^2} \quad \text{then } C_{p_s} = - \frac{1}{M_\infty^2} \quad (18)$$

$$\text{i.e., if } P < -0.3 P_\infty \quad \text{then } P = -0.3 P_\infty \quad (19)$$

#### 2. CODE LIMIT 2

$$\text{If } C_{p_s} < - \frac{2}{8} \frac{1}{M_\infty^2} \quad \text{then } C_{p_s} = - \frac{2}{8} \frac{1}{M_\infty^2} \quad (20)$$

$$\text{i.e., if } P < 0.0 \quad \text{then } P = 0.0 \quad (21)$$



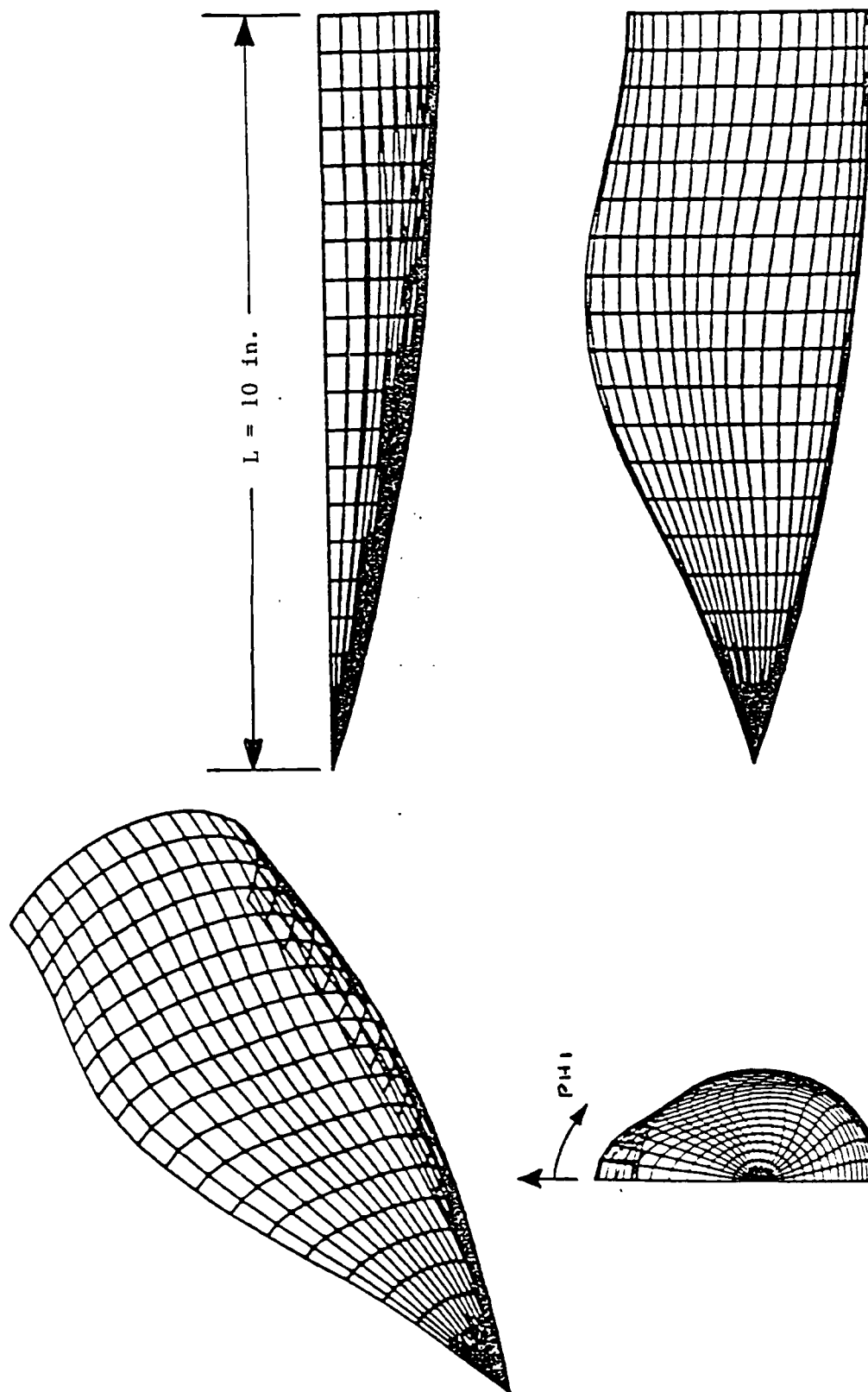


Figure 2. Four Views of the STAPAT II Geometry of the Analytic Model

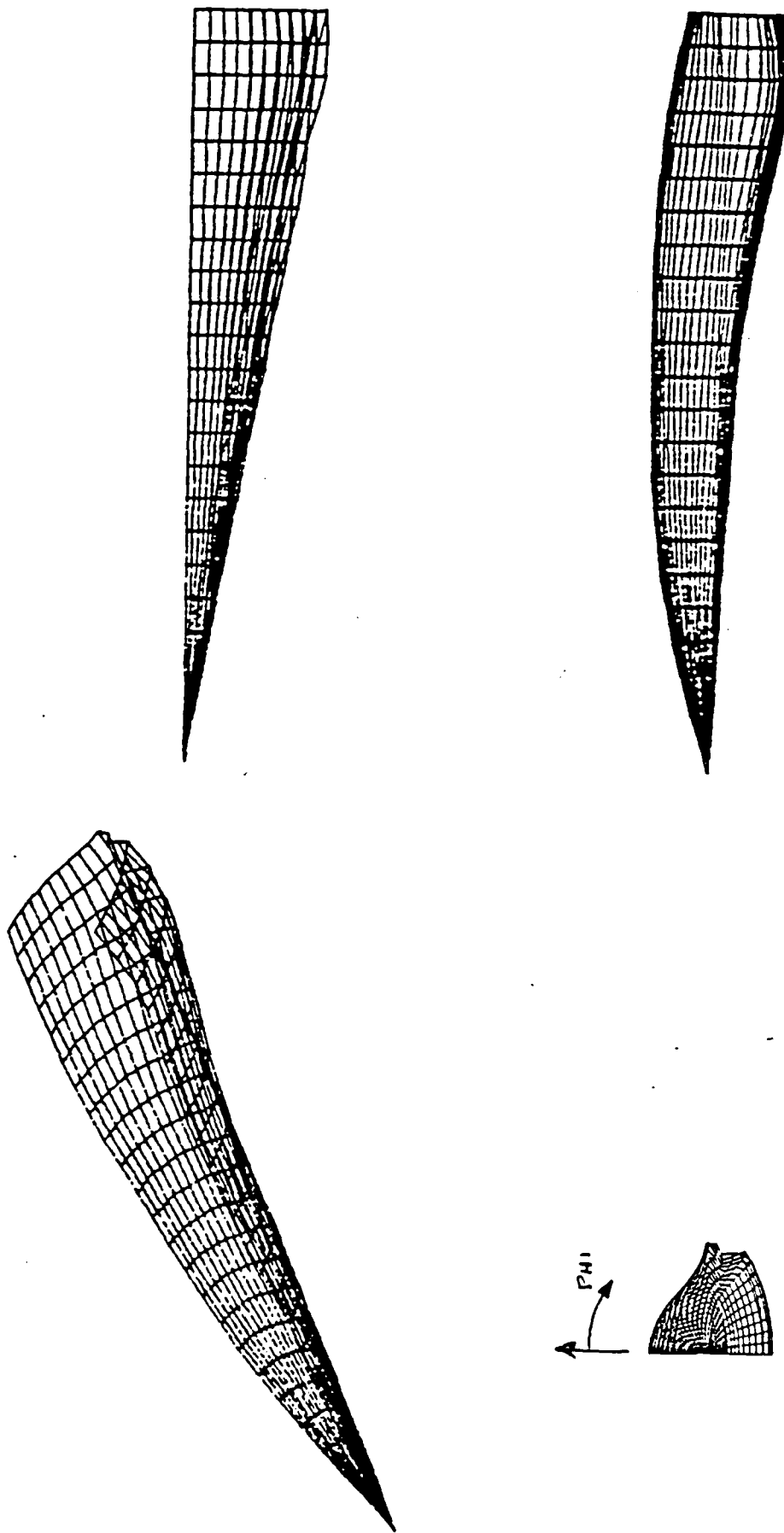


Figure 3. Four Views of the STAPAT II Geometry of the  
Blended Wing Body (BWB) Model

| <u>MODEL</u> | <u>M<sub>∞</sub></u> | <u>α (deg)</u> | <u>CODE LIMIT</u>      | <u>SHADOW REGION<br/>PRESSURE METHODS*</u> |
|--------------|----------------------|----------------|------------------------|--|
| ANALYTIC     | 1.70                 | 0, 10, 20      | P = 0.3 P <sub>∞</sub> | 1, 2, 3, 4                                 |
| ANALYTIC     | 2.50                 | 0, 10, 20      | P = 0.3 P <sub>∞</sub> | 1, 2, 3, 4                                 |
| ANALYTIC     | 3.95                 | 0, 10, 20      | P = 0.3 P <sub>∞</sub> | 1, 2, 3, 4                                 |
| ANALYTIC     | 4.50                 | 0, 10, 20      | P = 0.3 P <sub>∞</sub> | 1, 2, 3, 4                                 |
| BWB**        | 11.32                | 0              | P = 0.3 P <sub>∞</sub> | 1, 2, 3, 4                                 |
| BWB          | 11.31                | 6              | P = 0.3 P <sub>∞</sub> | 1, 2, 3, 4                                 |
| ANALYTIC     | 4.50                 | 10             | P = 0                  | 1, 2, 3(a), 4                              |
| BWB          | 11.31                | 6              | P = 0                  | 1, 2, 3(a), 4                              |
| ANALYTIC     | 0.60                 | 10             | P = 0                  | 1, 2, 3(a), 4                              |
| ANALYTIC     | 1.00                 | 10             | P = 0                  | 1, 2, 3(a), 4                              |

| <u>*METHOD</u> | <u>TYPE</u>          |
|----------------|----------------------|
| 1 -            | BABISH               |
| 2 -            | PRANDTL-MEYER        |
| 3 -            | DAHLEM-BUCK          |
| 3(a) -         | MODIFIED DAELEM-BUCK |
| 4 -            | ACM                  |

\*\* NASP BLENDED WIND BODY

NOTE: A TOTAL OF 72 RUNS

Figure 4. Summary of the STAPAT II Simulation Runs

HEATING MODULE ISO- AND STREAMLINE CONTOURS

ALTITUDE OR TIME . 1. MACH NO. . 4.50 TU/TO-INF. 0.800

Friday 21-JUL-83 13:31:33 PLOT # 1

STREAMLINES

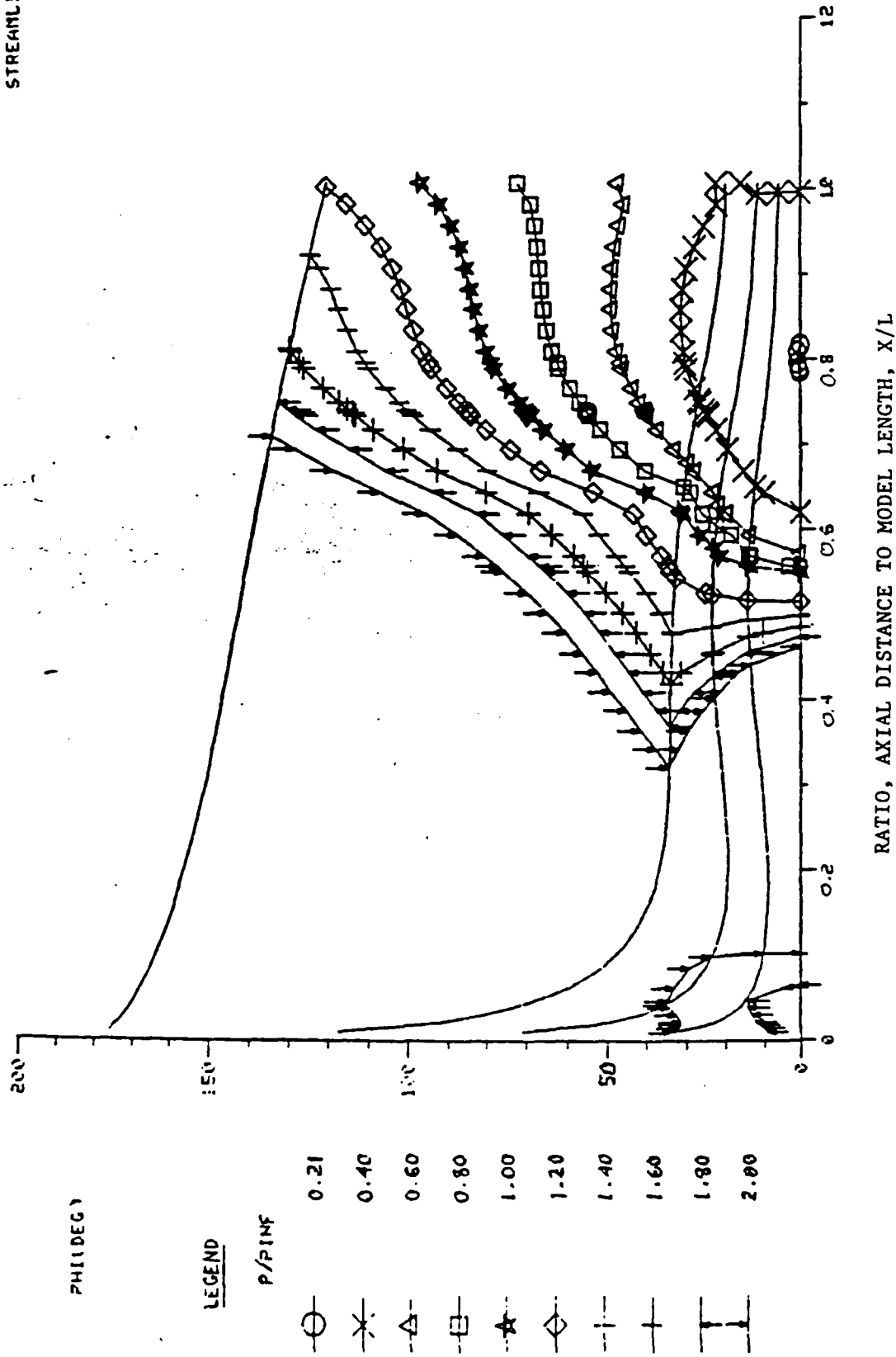


FIGURE 5. HEATPLT pressures

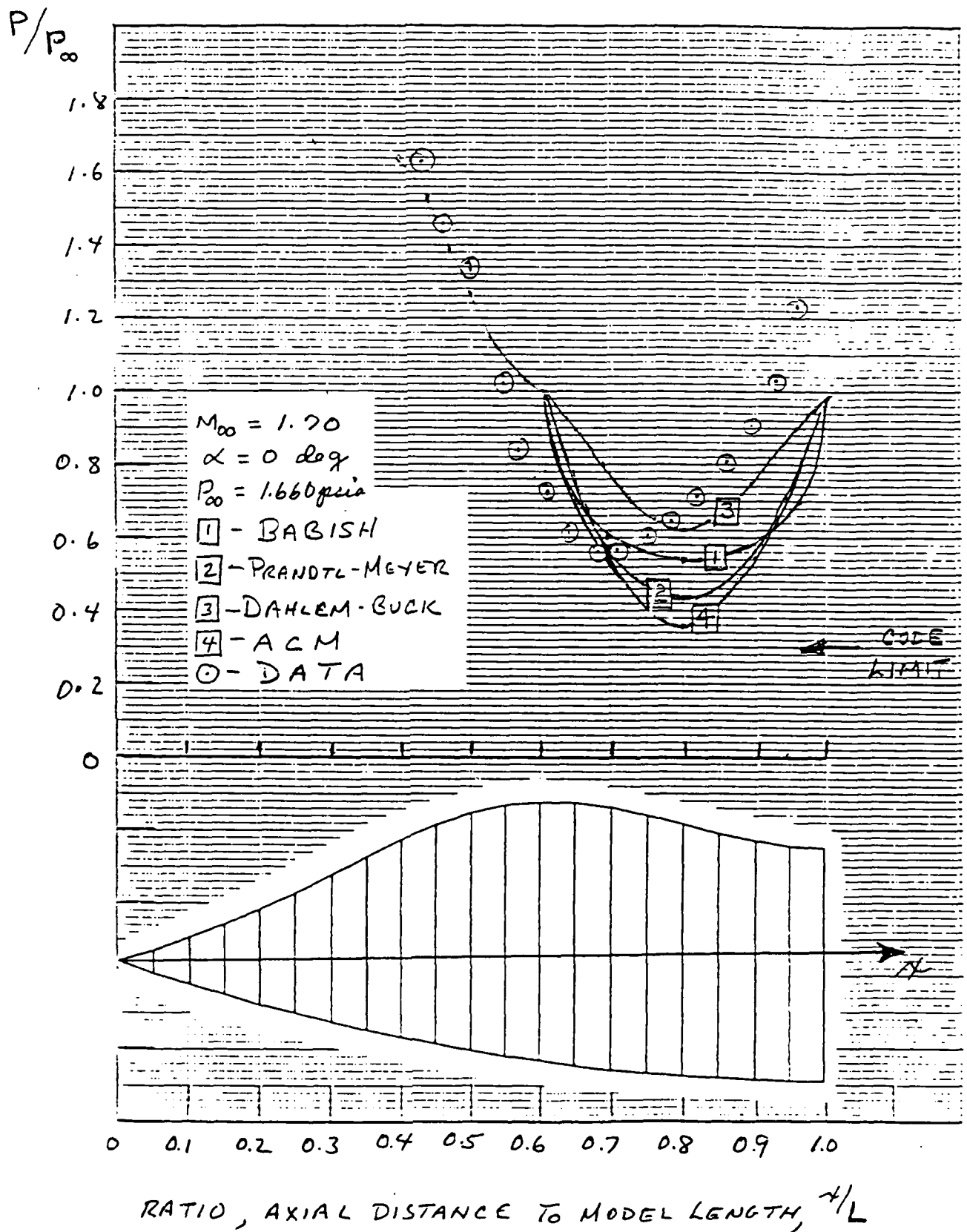


Figure 6. Comparisons of STPAT II Predictions With Wind Tunnel Data for the Analytic Model (Code Limit 1)

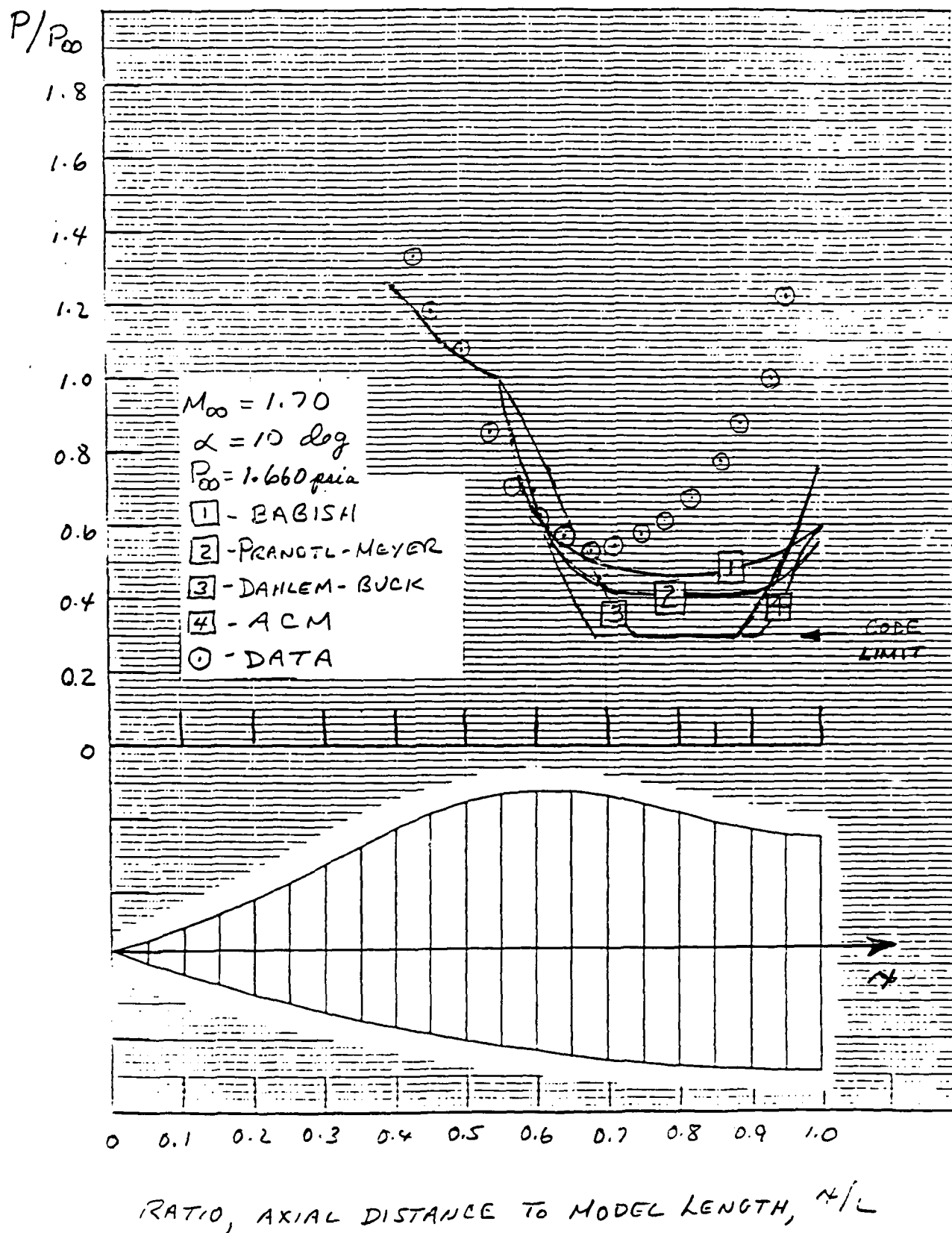


Figure 6. Continued

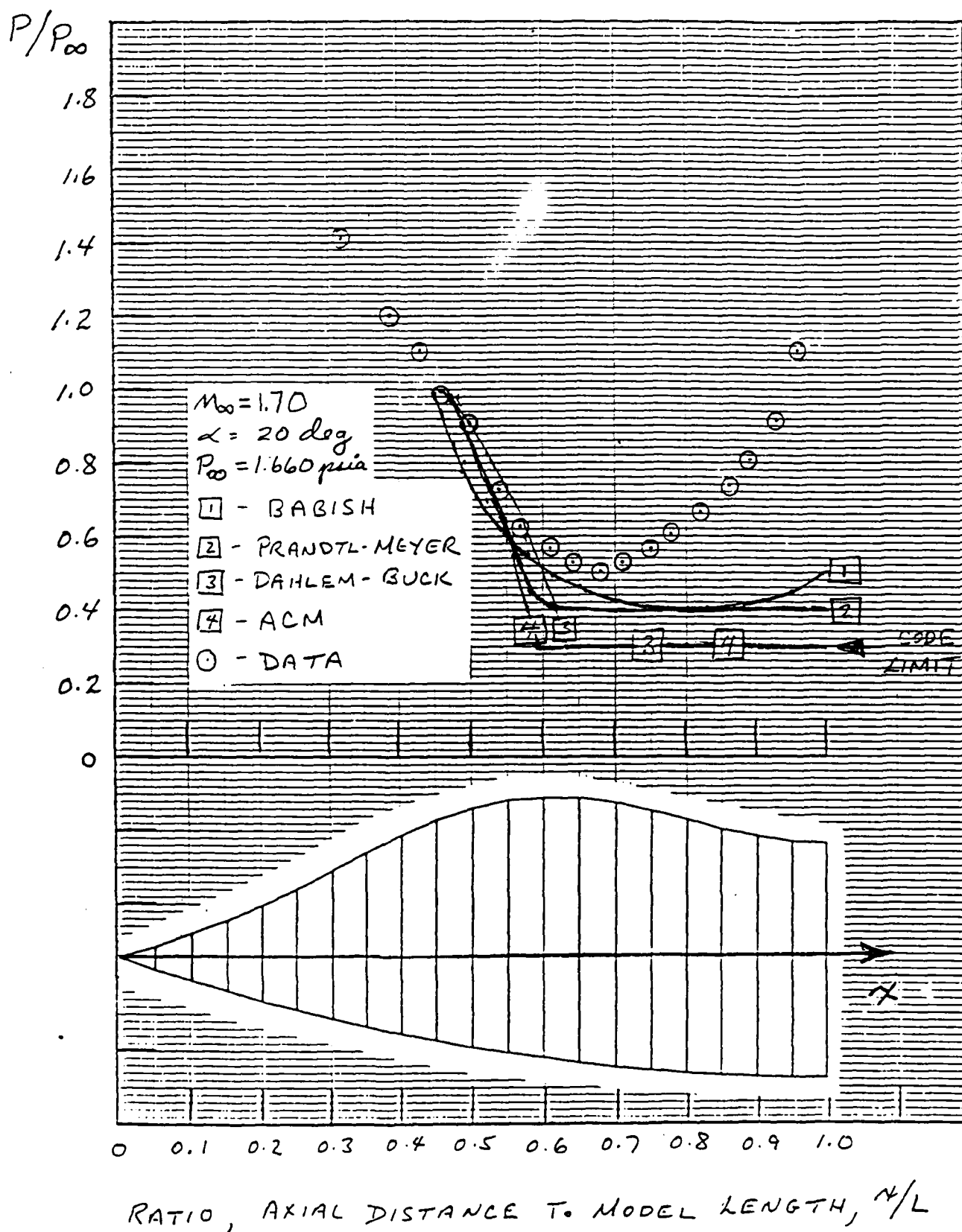
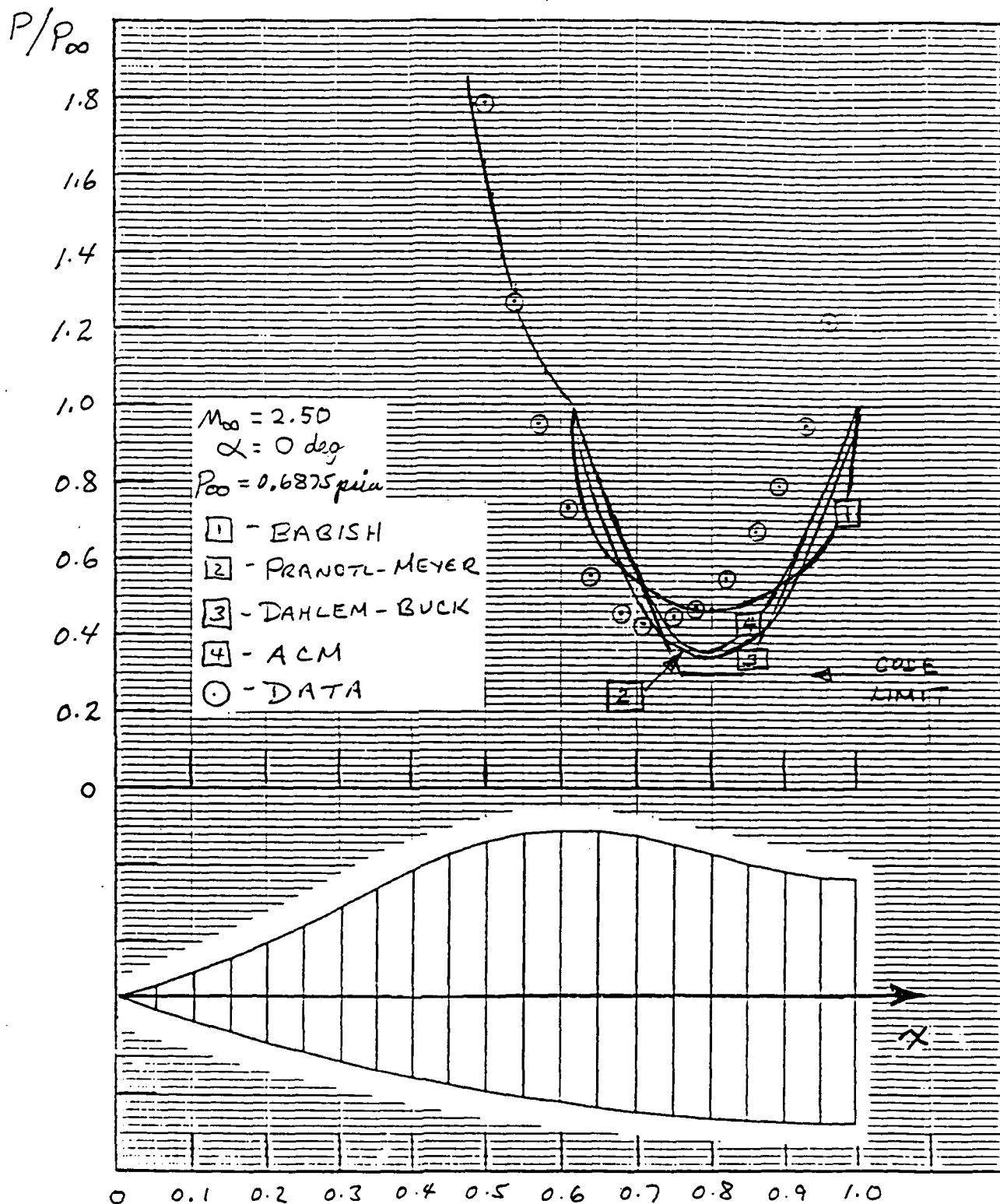


Figure 6. Continued



RATIO, AXIAL DISTANCE TO MODEL LENGTH,  $x/L$

Figure 6. Continued



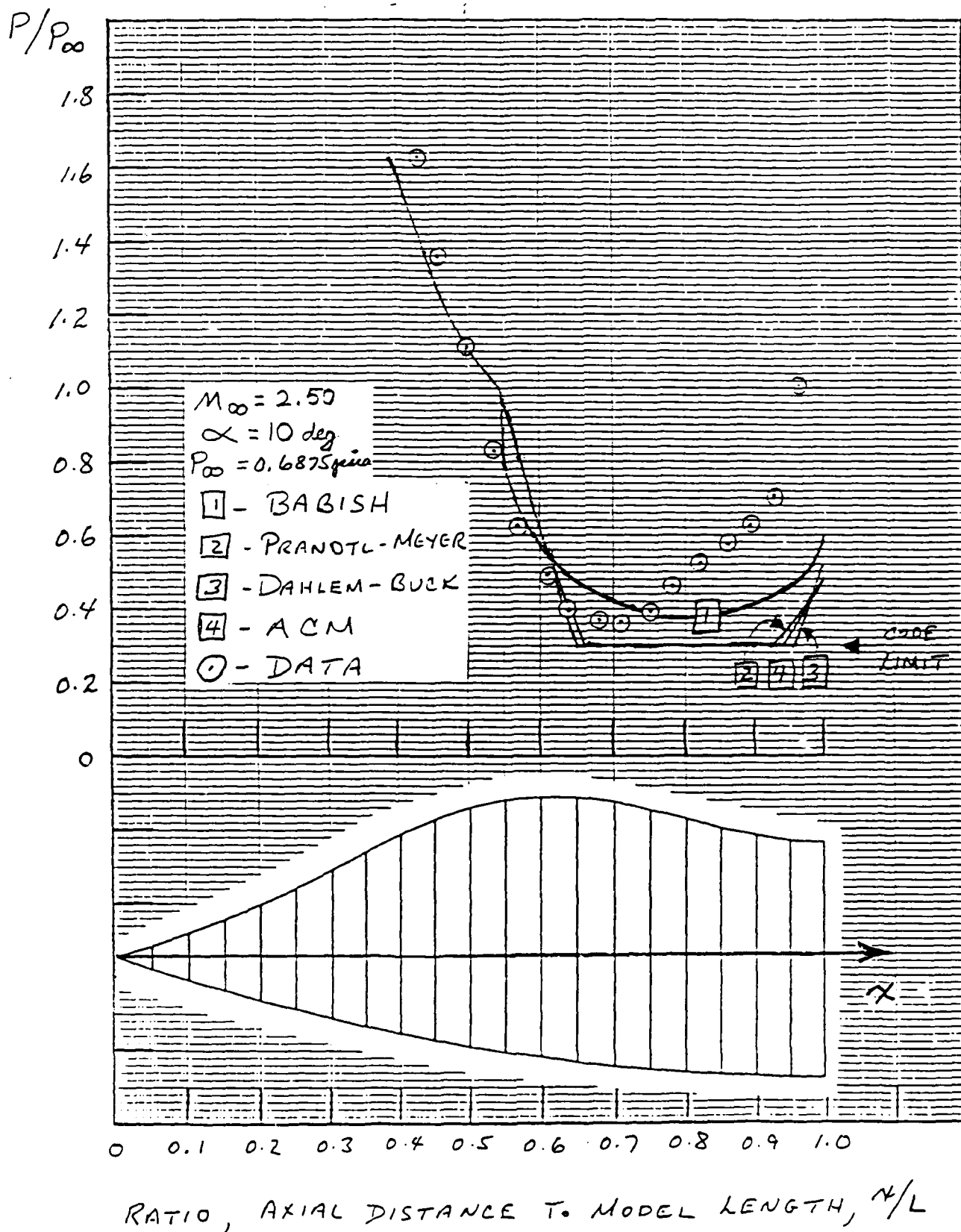
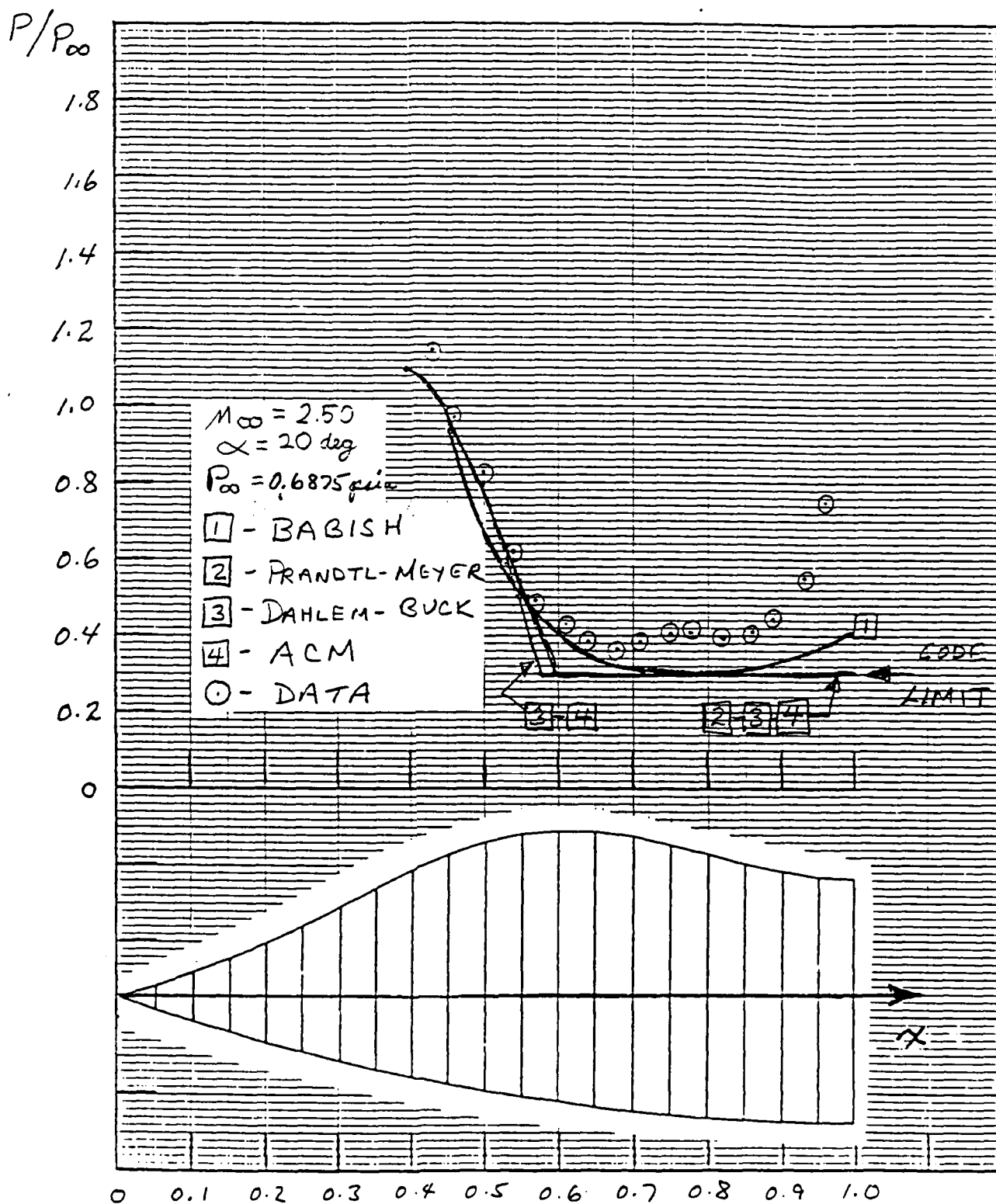


Figure 6. Continued



RATIO, AXIAL DISTANCE TO MODEL LENGTH,  $x/L$

Figure 6. Continued

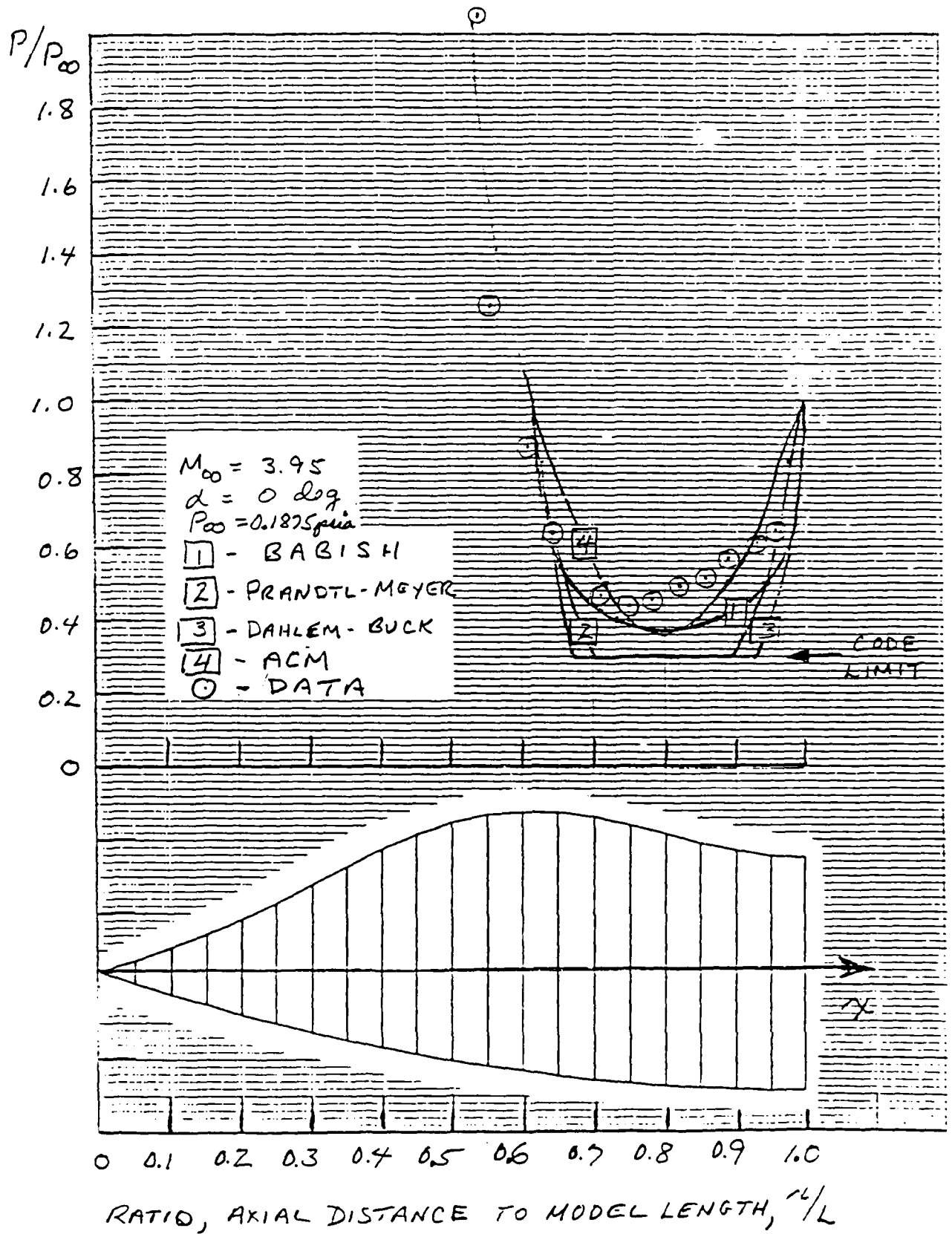
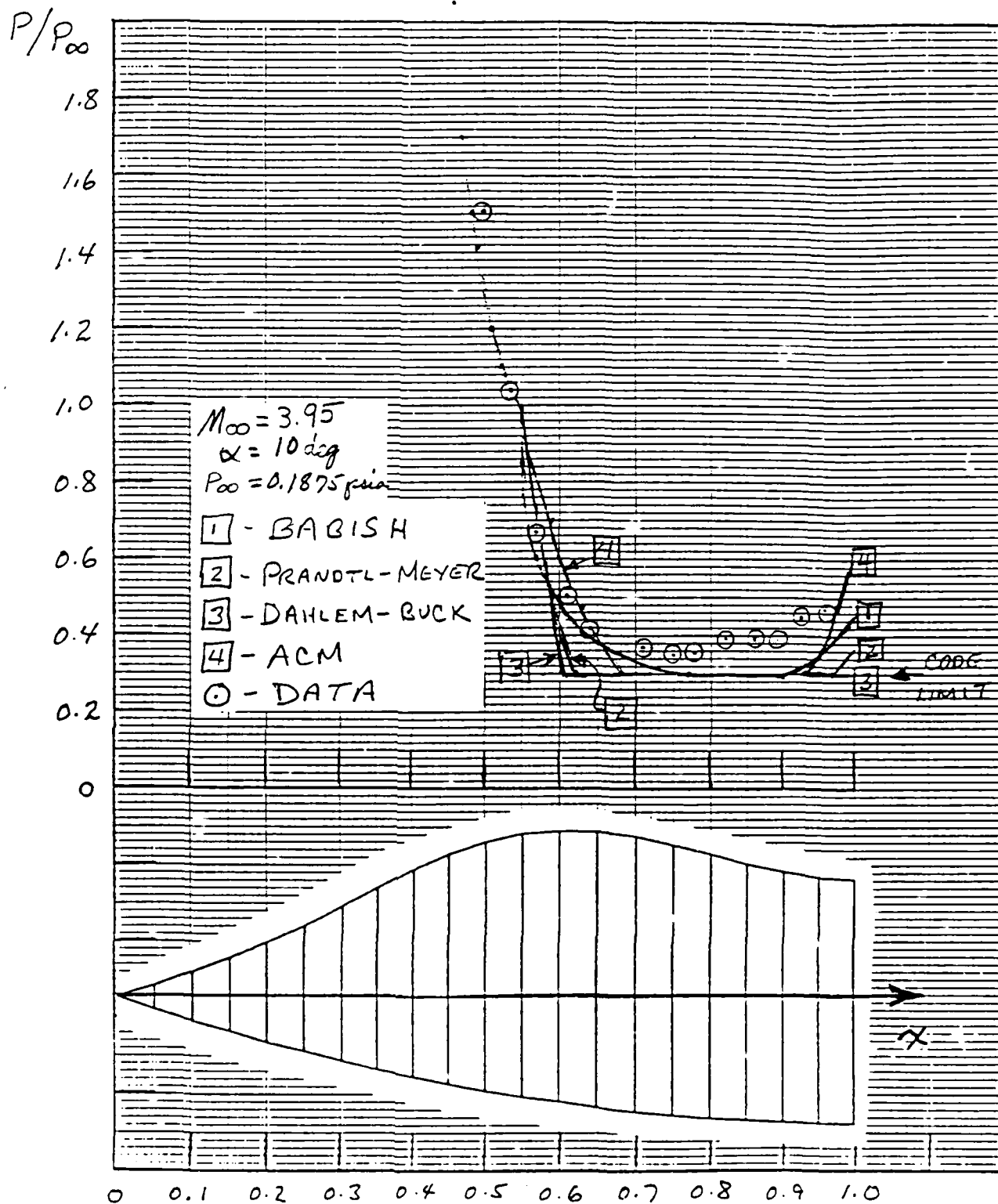


Figure 6. Continued



RATIO, AXIAL DISTANCE TO MODEL LENGTH,  $x/L$

Figure 6. Continued

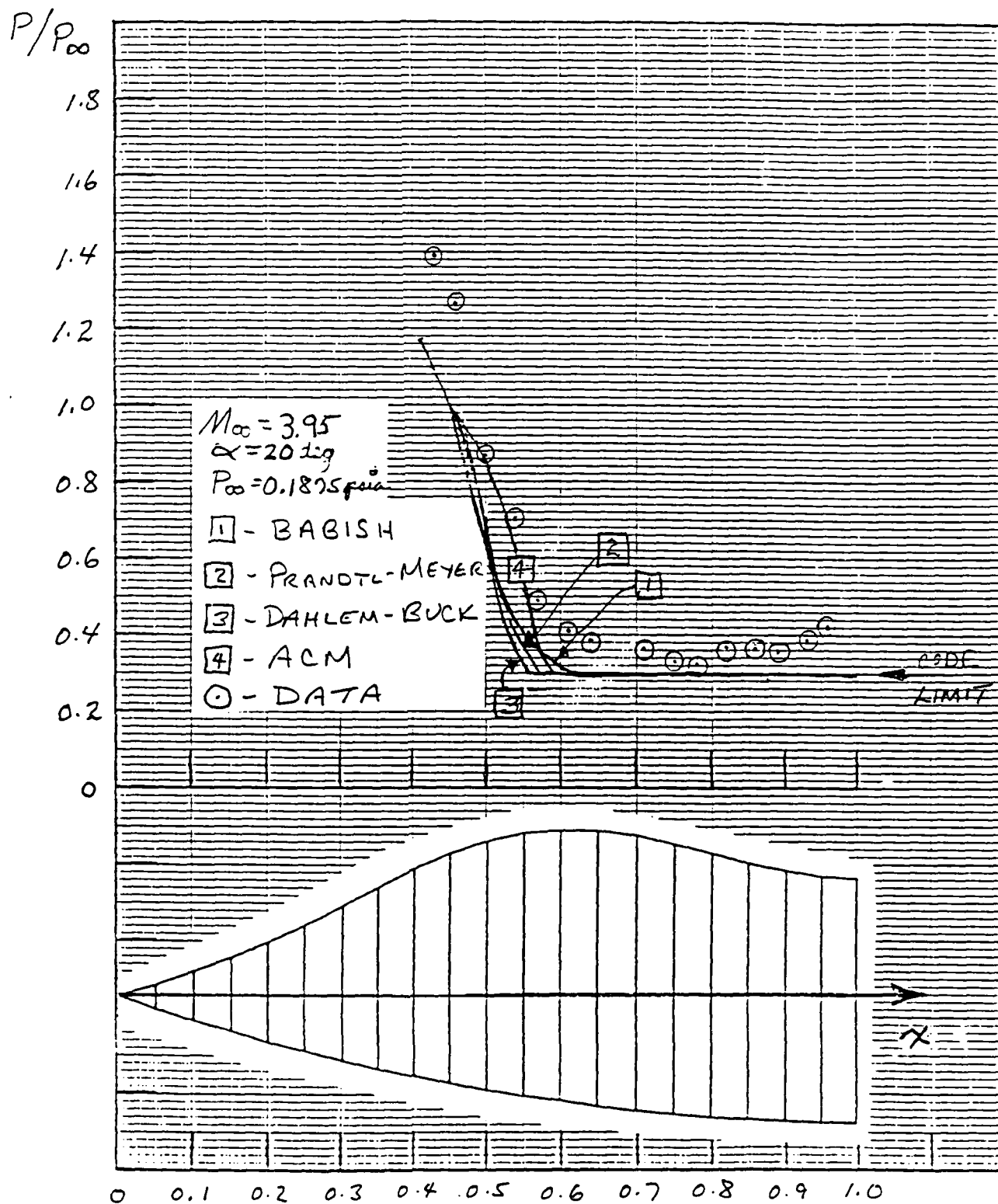
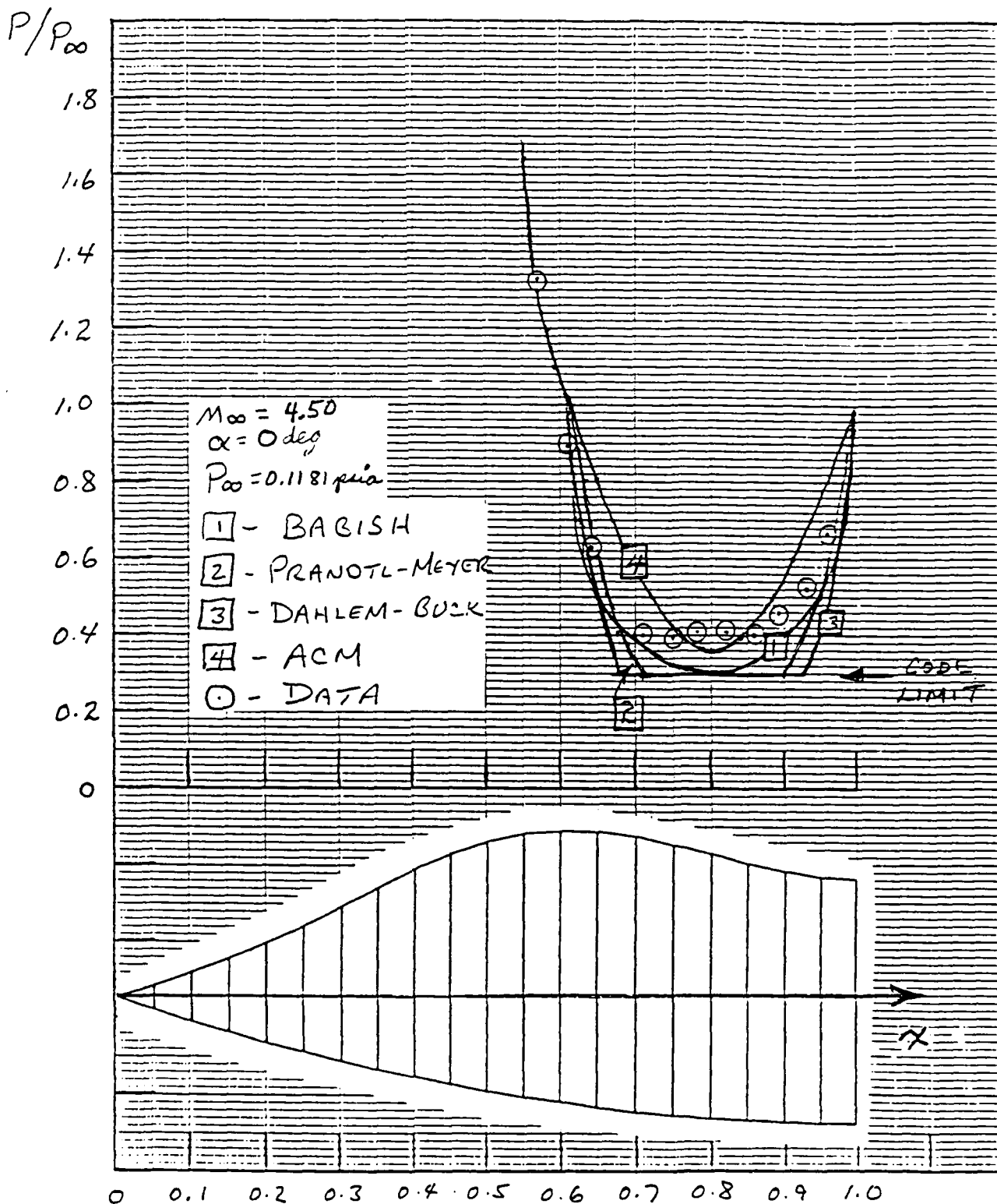


Figure 6. Continued



RATIO, AXIAL DISTANCE TO MODEL LENGTH,  $x/L$

Figure 6. Continued

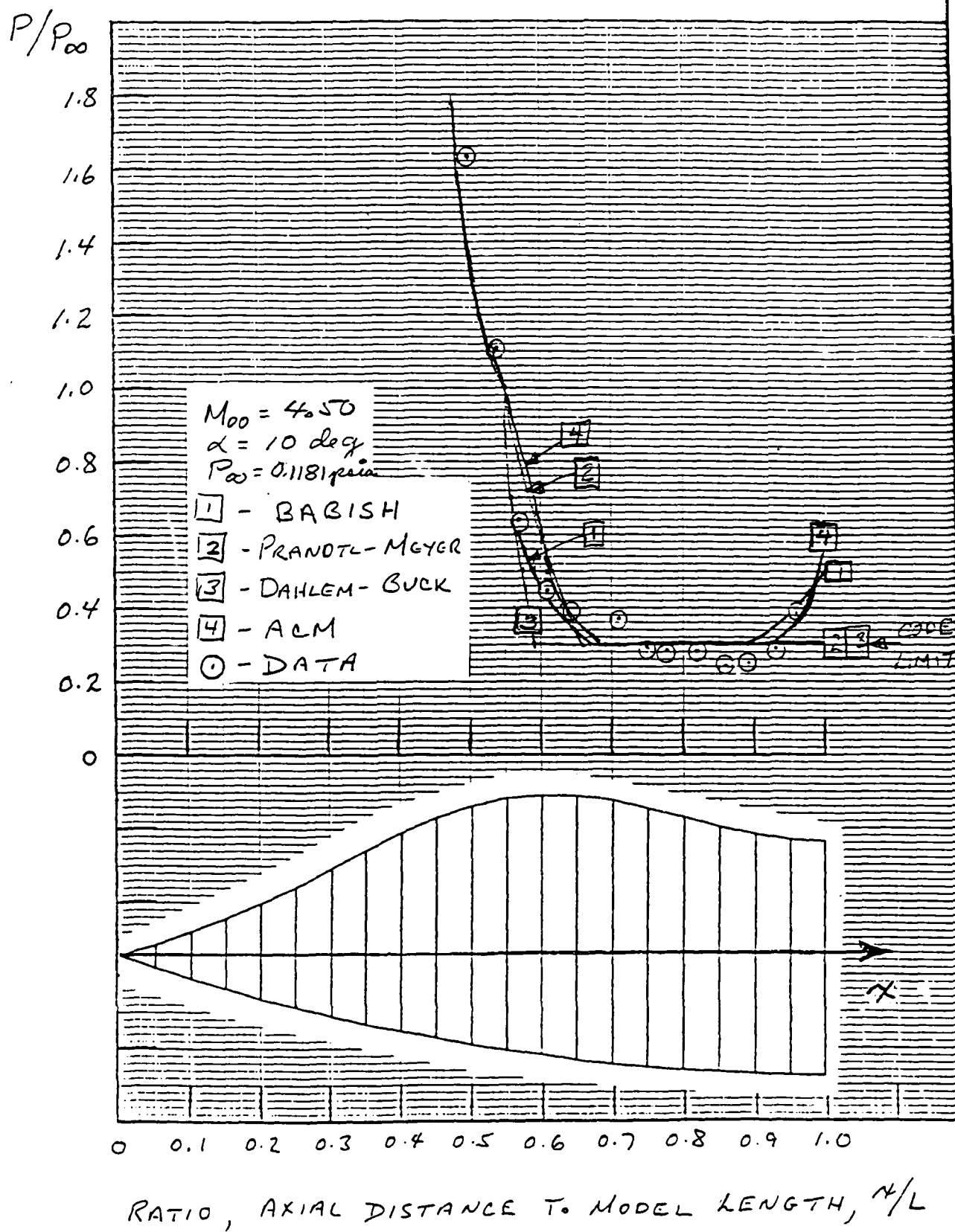


Figure 6. Continued

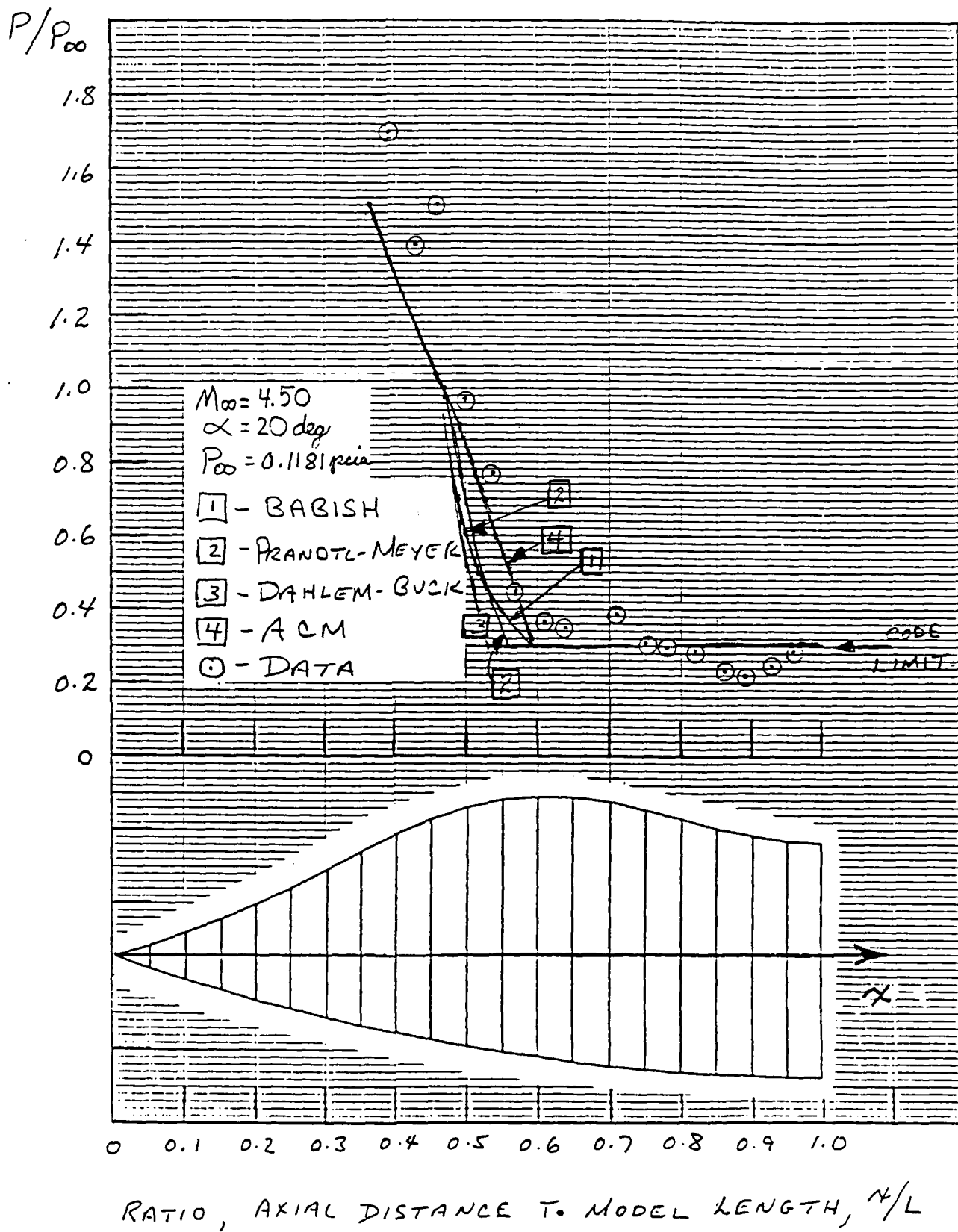


Figure 6. Concluded



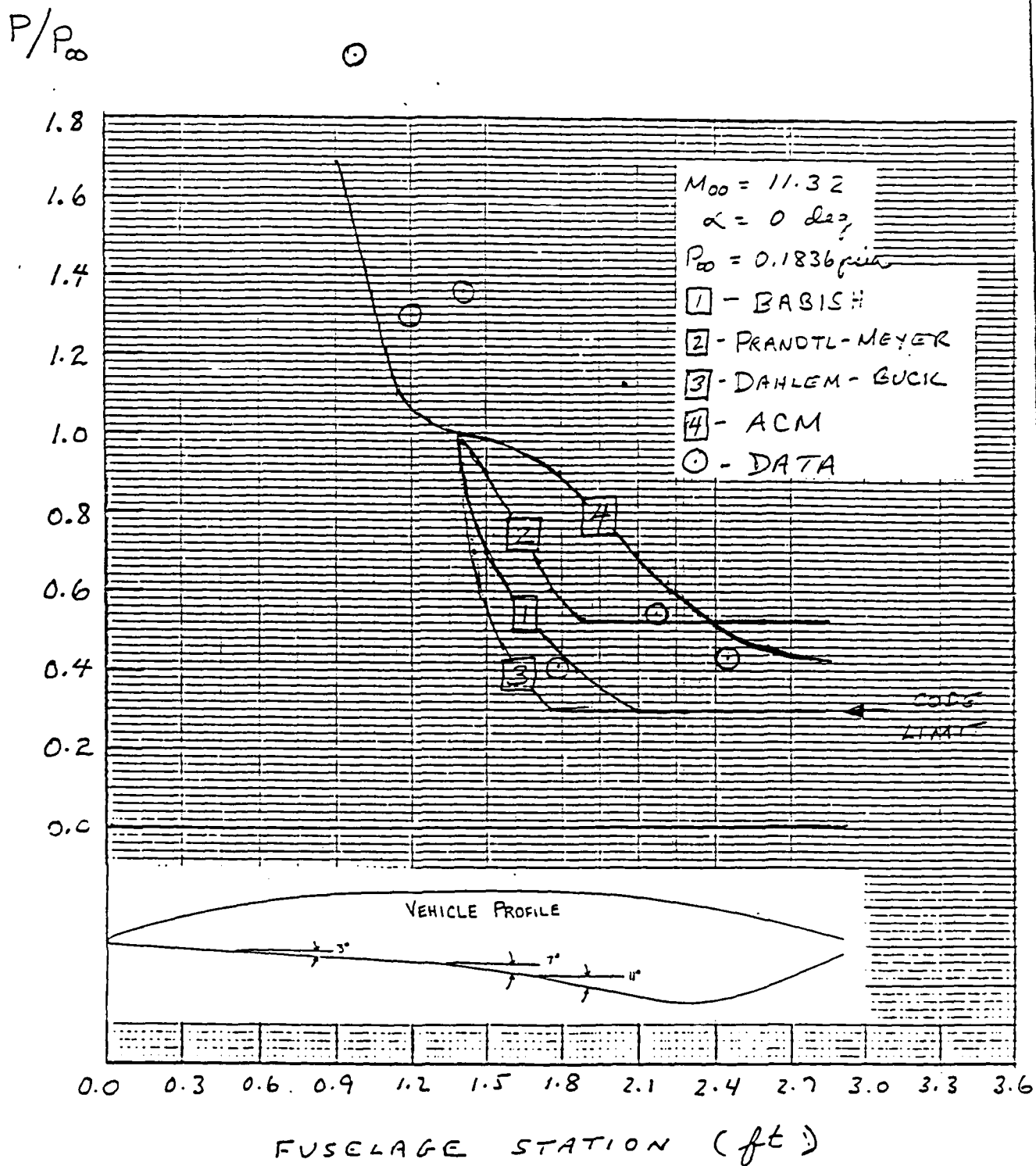


Figure 7. Comparisons of STAPAT II Predictions With Wind Tunnel Data for the BWB Model (Code Limit 1)

$P/P_\infty$

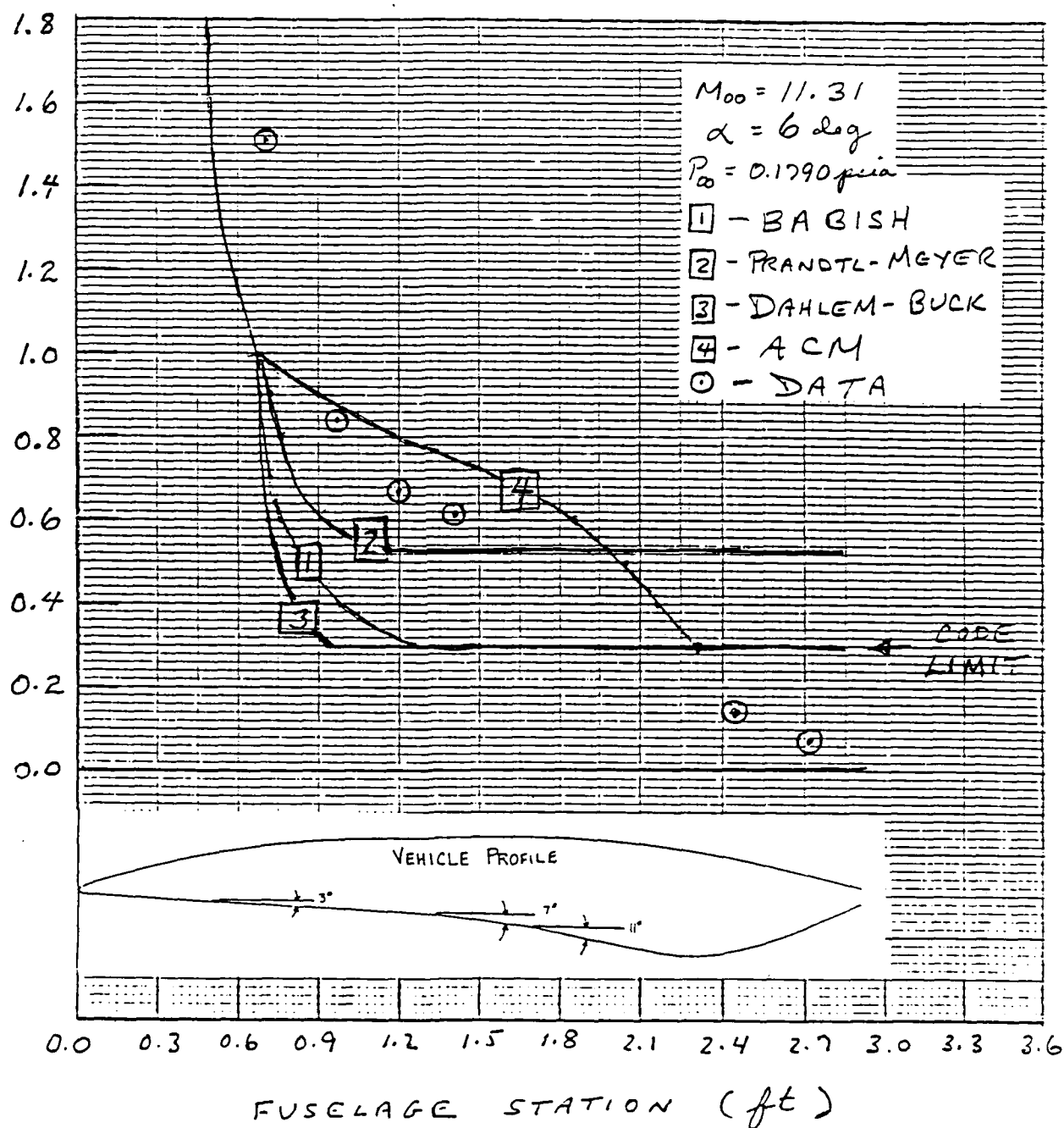


Figure 7. Concluded

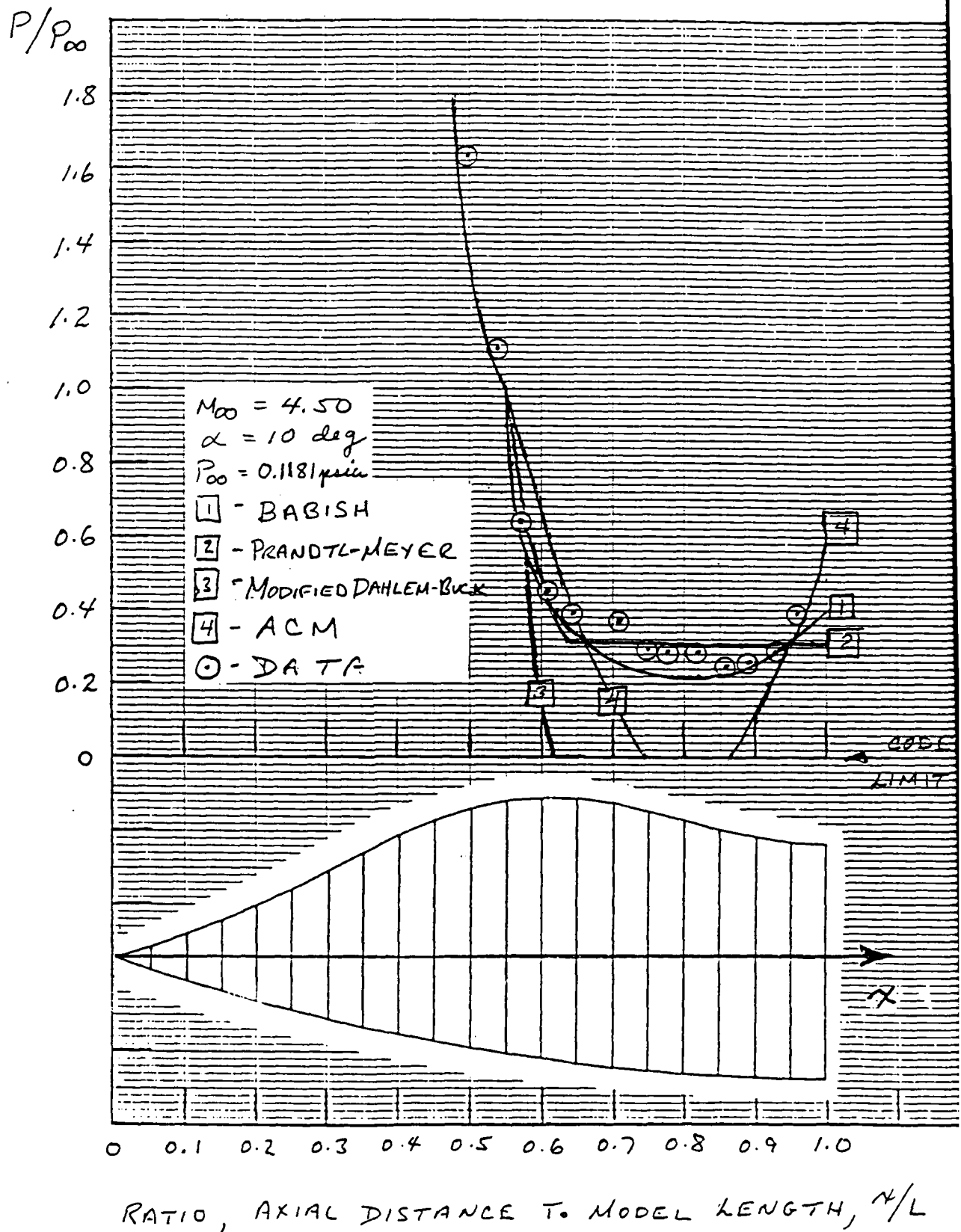


Figure 8. Comparisons of STAPAT II Predictions With Wind Tunnel Data for the Analytic and BWB Models (Code Limit 2)

$P/P_\infty$

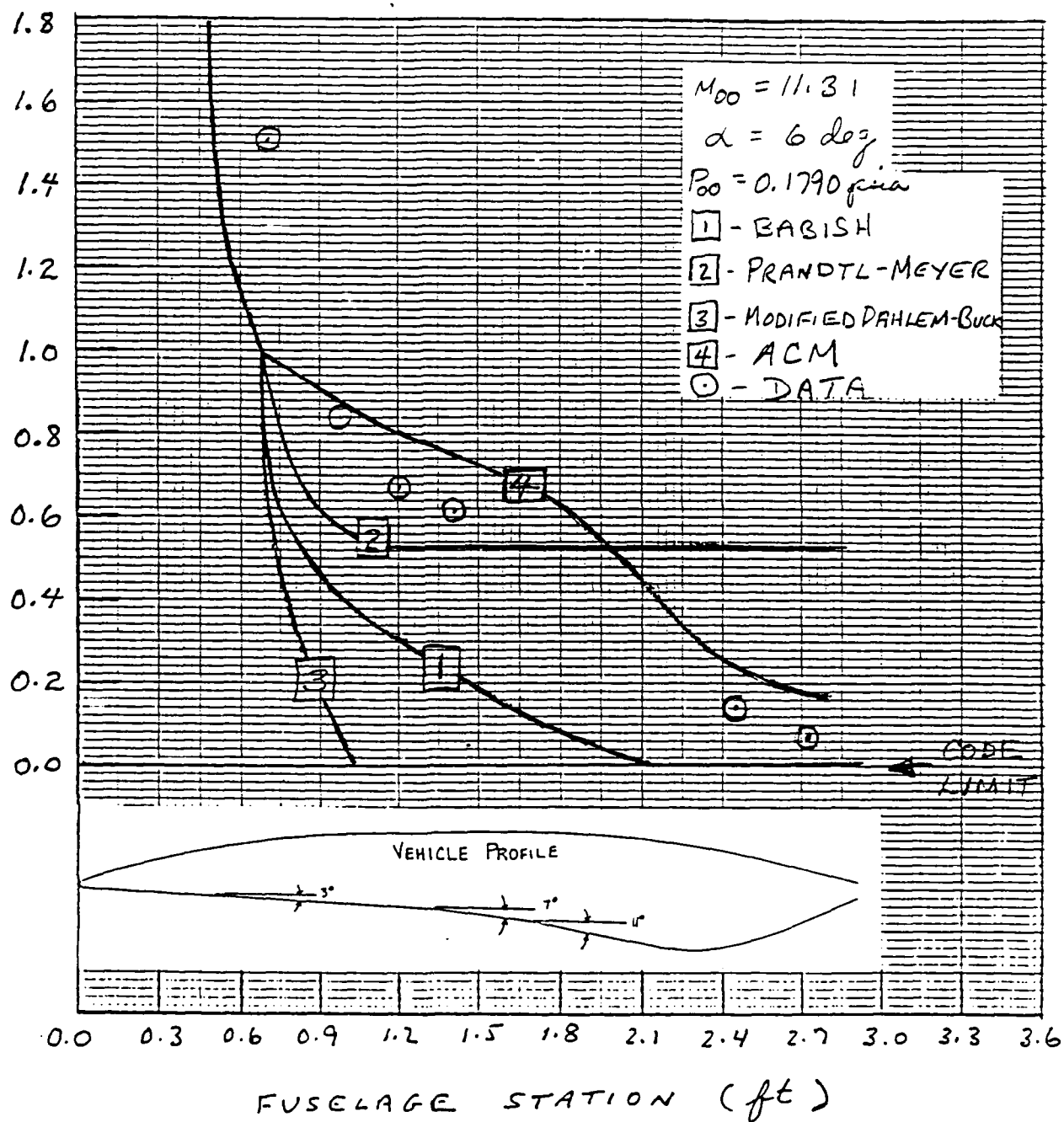


Figure 8. Concluded

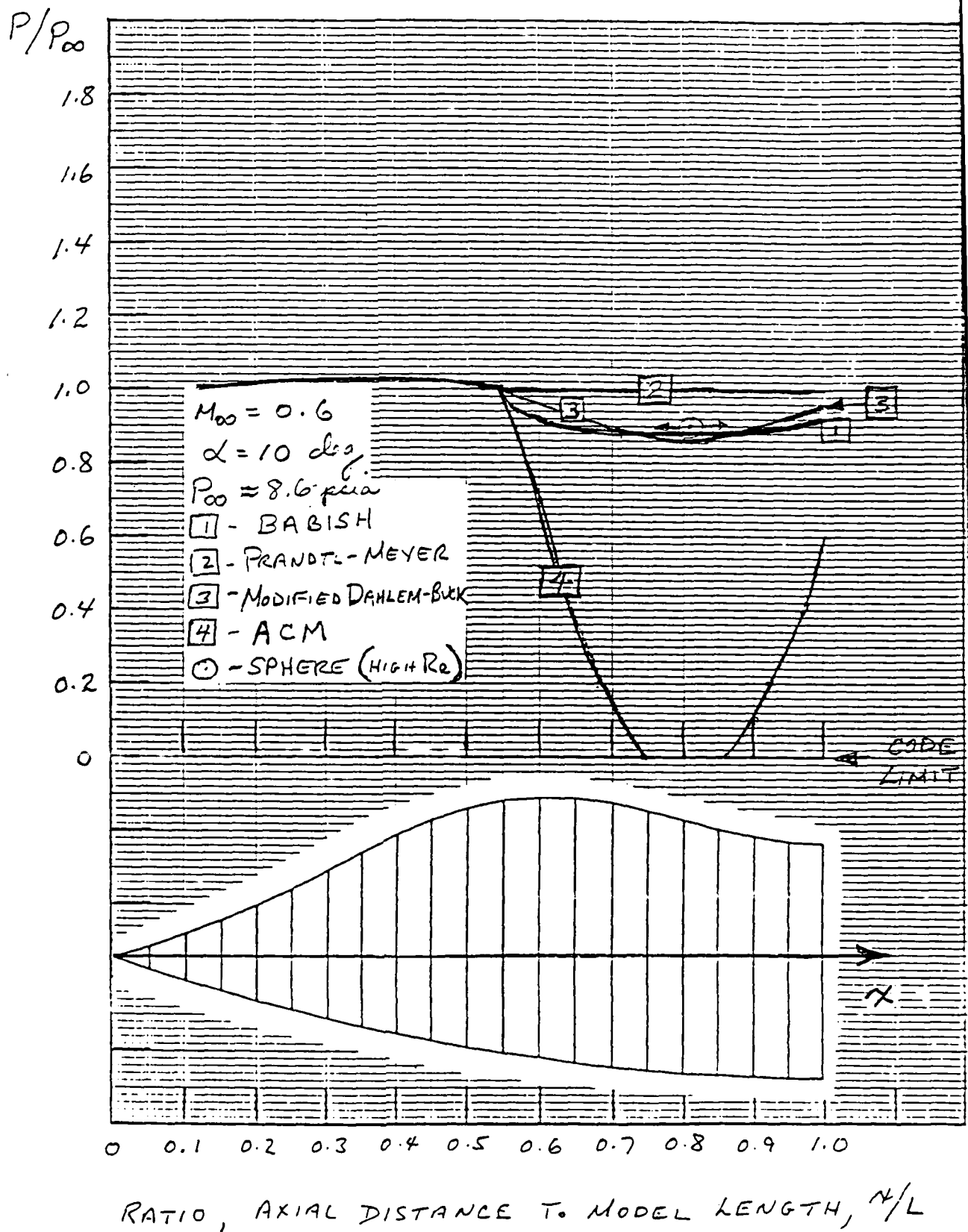
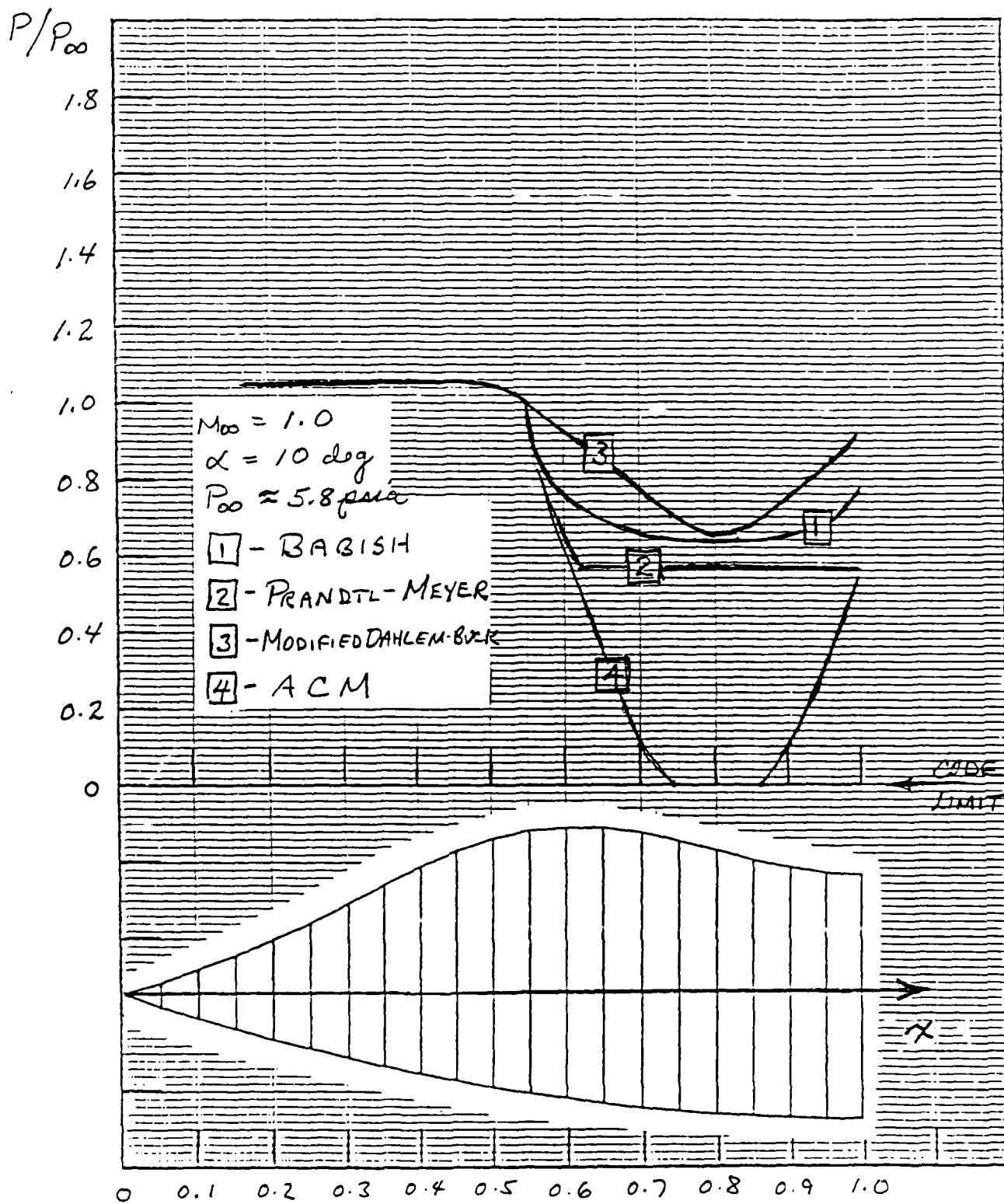


Figure 9. Comparisons of Prediction Methods for the Analytic Model at Transonic Speeds (Code Limit 2)



RATIO, AXIAL DISTANCE TO MODEL LENGTH,  $x/L$

Figure 9. Concluded

#### IV. RESULTS

We concluded which prediction method was the most accurate by plotting the predicted shadow region pressures and the wind tunnel data and then comparing the predicted pressures to the data. The model that followed the data most closely is the best.

Using Code Limit 1, Figure 6 shows the prediction methods using the analytic model at supersonic speeds. At Mach numbers 1.70 and 2.50, all four prediction methods closely agreed with the wind tunnel data on the upstream portion of the shadow region, but they under-predicted the data on the downstream portion. At these Mach numbers, the BABISH method showed better agreement with the data than the other three methods and it never reached Code limit 1 as the other three did.

At zero degrees angle of attack, Mach numbers 3.95 and 4.50 (Figure 6), the BABISH method gave superior agreement and never reached the code limit. All prediction methods showed excellent agreement with the data at 10 and 20 degrees angle of attack, but were aided by Code Limit 1 in the downstream portion of the shadow region.

The ACM method showed the best agreement for the blended wing body, at zero and six degrees angle of attack and hypersonic speeds (Figure 7). While the other three methods under-predicted pressures in the upstream portion and over-predicted in the downstream portion, the ACM method remained relatively close to the data.

Figure 8 is identical to two comparisons in Figure 6 with the only differences being Code Limit 2 and a modified DAHLEM-BUCK (MDB) mirror method. (The MDB method limits the parameter B of Equation 12 to values of 2 through 5.) Both the analytic model and blended wing body model were used, but in different conditions. For the analytic model, at Mach 4.5 and an angle of attack of ten degrees, the Code Limit 2 resulted in the ACM and DAHLEM-BUCK methods under-predicting nearly the entire portion of the shadow region, while it slightly improved the BABISH method and had no

effect on the PRANDTL-MEYER method. For the blended wing body model, at Mach 11.31 and an angle of attack of six degrees, the ACM method never reached the code limit and showed excellent agreement with the wind tunnel data. The BABISH method agreed poorly in the upstream portion of the shadow region but it improved from Code Limit 2 as it neared the downstream portion. The use of Code Limit 2 worsened the agreement of the DAHLEM-BUCK method, but it did not effect the PRANDTL-MEYER predictions.

The prediction methods in Figure 9 are compared at transonic speeds using Code Limit 2. The BABISH and modified DAHLEM-BUCK methods showed excellent agreement. The ACM method showed poor results at both Mach 0.6 and Mach 1.0. The PRANDTL-MEYER method was created to predict only supersonic speeds, it is therefore useless at transonic speeds.



## V. CONCLUSIONS AND RECOMMENDATIONS

Although all four methods showed relatively good agreement with the wind tunnel data, there are different methods which are the most accurate at specific speeds. The BABISH method showed the best agreement at low supersonic speeds. The best at hypersonic speeds was the ACM method. The BABISH and DAHLEM-BUCK were the most accurate at subsonic speeds.

From the above conclusions, we made the following recommendations:

The BABISH correlation method should be used in STAPAT II with Code Limit 2 for all speeds.

The PRANDTL-MEYER expansion method should be used in STAPAT II with the limit of freestream pressure for subsonic speeds, the expansion criteria limit for supersonic speeds, and Code Limit 1 or 2 for hypersonic speeds.

The DAHLEM-BUCK (or MODIFIED DAHLEM-BUCK) mirror method should be used in STAPAT II with Code Limit 1 for subsonic and supersonic speeds. The DAHLEM-BUCK mirror method should not be used at hypersonic speeds.

The ACM empirical method should be used in STAPAT II with the limit of freestream pressure for subsonic speeds, Code Limit 1 for supersonic speeds, and Code Limit 2 for hypersonic speeds.

Either the BABISH method or the ACM method should be used as the STAPAT II default shadow region pressure prediction method.

## VI. OTHER INTERESTING OBSERVATIONS AND LESSONS LEARNED FROM SUMMER EXPERIENCE

In addition to the work I did at the Flight Dynamics Laboratory, I also went on a tour of the Aircraft Transparency Life Cycle Durability Facility. In this facility, transparency systems are exposed to typical flight temperature gradients, net pressure loadings, and flight line cleaning solutions to determine their durability. The temperature gradients are provided by three duct loops (see Figure 10). One loop circulates air heated by six large heaters at 1000°F. Another loop circulates air cooled by liquid nitrogen at -100°F. Yet another loop combines the two previous loops and directs the air over the transparency being tested. This testing process is a vital area in the designing of new transparencies because a problem can be identified and corrected before being placed on an actual plane on an actual flight.

The High School Apprenticeship Program gave me a first-hand experience as to how an engineer works. It showed me the hard work and dedication required to be successful in the engineering field. This program also demonstrated the satisfaction one receives after finishing a project and seeing it put to use as a small, yet essential piece of the puzzle of an aerospace vehicle. In conclusion, this experience gave me a sample of engineering and strengthened my desire to pursue a career in this exciting field.

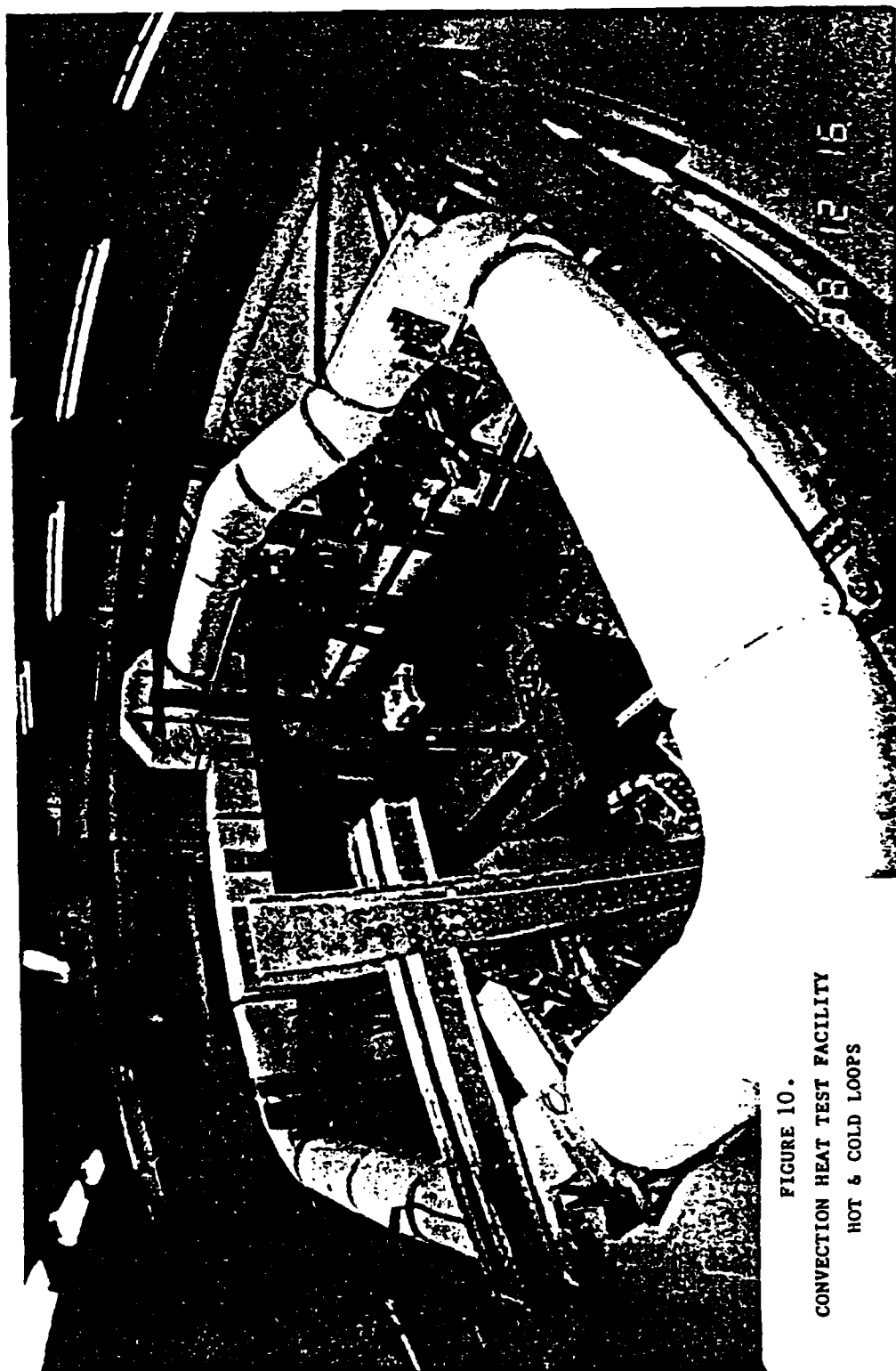


FIGURE 10.  
CONVECTION HEAT TEST FACILITY  
HOT & COLD LOOPS

## VII. REFERENCES/BIBLIOGRAPHY

1. M. O. Varner and C. A. Babish III, Status of a New Aerothermodynamic Analysis Tool for High-Temperature Resistant Transparencies, paper presented at the 14th Conference on Aerospace Transparent Materials and Enclosures, 11-14 July 1973, published by S. A. Marolo, Conference on Aerospace Transparent Materials and Enclosures, Air Force Wright Aeronautical Laboratories, Wright-Patterson Air Force Base, Ohio 45433, AFWAL-TR-83-4154, December 1983.
2. M. O. Varner, J. C. Adams, D. E. Boylan, A. F. Gwinn, Jr., R. A. LeMaster, W. R. Martindale, and V. Nopratvarakorn, Specific Thermal Analyzer Program for High-Temperature Resistant Transparencies for High-Speed Aircraft (STAPAT), Volume I Methodology, Air Force Wright Aeronautical Laboratories, Wright-Patterson Air Force Base, Ohio 45433, AFWAL-TR-84-3086, Volume I, (AD B089 497), October 1984.
3. M. O. Varner, J. C. Adams, D. F. Boylan, A. F. Gwinn, Jr., R. A. LeMaster, W. R. Martindale, and V. Nopratvarakorn, Specific Thermal Analyzer Program for High-Temperature Resistant Transparencies for High-Speed Aircraft (STAPAT), Volume II, Users Manual, Main Text, Air Force Wright Aeronautical Laboratories, Wright-Patterson Air Force Base Ohio 45433, AFWAL-TR-84-3086, Volume II, (AD B090 894L), October 1984.
4. M. O. Varner, J. C. Adams, D. E. Boylan, A. F. Gwinn, Jr., R. A. LeMaster, W. R. Martindale, and V. Nopratvarakorn, Specific Thermal Analyzer Program for High-Temperature Resistant Transparencies for High-Speed Aircraft (STAPAT), Volume III, Appendices of Sample Problems, Air Force Wright Aeronautical Laboratories, Wright-Patterson Air Force Base, Ohio 45433, AFWAL-TR-84-3086, Volume III, (AD B090 895L), October 1984.

5. C. A. Babish III and L. V. Garrett, Validation Check of STAPAT - A Specific Thermal Analyzer Program for Aircraft Transparencies - Comparison of STAPAT Predictions With Measurements Taken During Flight Tests of an F-4B Aircraft, Air Force Wright Aeronautical Laboratories, Wright-Patterson Air Force Base, Ohio 45433, AFWAL/FIER Letter Report, September 1985.
6. M. J. Rakolta and C. A. Babish III, Validation Check of STAPAT - A Specific Thermal Analyzer Program for Aircraft Transparencies - Comparison of STAPAT Predictions With Measurements From Wind Tunnel Tests on the Supersonic Tactical Missile (STM), Air Force Wright Aeronautical Laboratories, Wright Patterson Air Force Base, Ohio 45433, AFWAL/FIER Letter Report, April 1987.
7. C. A. Babish III and J. R. Hayes, Heat Transfer Rates on an Analytic Forebody in the AFWAL Mach 3 High Reynolds Number Wind Tunnel - Comparison of Test Results With Predictions from STAPAT (A Specific Thermal ANalyzer Program for Aircraft Transparencies), Air Force Wright Aeronautical Laboratories, Wright-Patterson Air Force Base, Ohio 45433, AFWAL-TR-87-3091, April 1988.
8. B. L. Boman and C. A. Babish III, Hypersonic Thermal Analysis for Aircraft Transparencies, paper presented at the Fifteenth Conference on Aerospace Transparent Materials and Enclosures, 16-20 January 1989, published by S. A. Marolo, Conference on Aerospace Transparent Materials and Enclosures, Volumes I and II, Air Force Wright Research and Development Center, Wright-Patterson Air Force Base, Ohio 45433, WRDC-TR-89-4044, April 1989.
9. Ames Research Staff, Equations, Tables, and Charts for Compressible Flow, National Advisory Committee for Aeronautics, Report 1135, 1953.
10. V. Dahlem, and M. L. Buck, Experimental and Analytical Investigation of Vehicle Design for High Lift-Drag Ratios in Hypersonic Flight, Air Force Flight Dynamics Laboratory, Wright-Patterson Air Force Base, Ohio 45433, AFFDL-TR-67-138, June 1967.

11. J. E. Gregoire and R. J. Krieger, Aerodynamic Prediction Rationale for Advanced Arbitrarily Shaped Missile Concepts, AIAA paper 80-0256 presented at the 18th Aerospace Sciences Meeting, Pasadena, California, 14-16 January 1980.
12. B. L. Boman, Hypersonic Thermal Analysis of Aircraft Transparencies - STAPAT II Requirements, McDonnell Douglas Corporation report MDC-B0911, 17 March 1988.
13. J. C. Townsend, et al., Surface Pressure Data on a Series of Analytic Forebodies at Mach Numbers from 1.70 to 4.50 and Combined Angles of Attack and Sideslip, National Aeronautics and Space Administration, Langley Research Center, Hampton, Virginia 23365, NASA Technical Memorandum 80062, (N79-29145), June 1979.
14. K. Y. Lau and R. R. Cosner, NASP Generic Technology Option No. 2 Final Report - Volume IV Blended Wing - Body Aerothermal Model and Test Results, McDonnell Douglas Corporation report, MDC Report Q0927, 1 September 1988.

1989 Air Force Office of Scientific Research

High School Apprenticeship Program

Mark Boeke, Apprentice

Mike Stringer, Mentor

Flight Dynamics Laboratory

August 14, 1989

## Part I : Acknowledgements

During my eight weeks working for the Flight Dynamics Laboratory, I have met many new and fascinating people. Invaluable knowledge that I received from my experience will be a great tool in helping me plan a career. There are many people who have made these eight weeks a success, and I would now like to thank them for their help. My family, for giving me support when I was unsure about applying for work at WPAFB. Mr. J.B. Scroeder, for informing me about this program and providing me transportation to and from the base. Mr. Milton Danishek, who coordinated this program and helped the apprentices with any concerns. Mr. Mike Stringer, for giving me assistance in getting started at work and making sure that everything ran smoothly despite the fact that I did not work for him directly. Lt. John Cannon, who I worked for on agility research and for helping me understand what aircraft parameters are and how they apply to agility. I would also like to thank all of the other members of the High Speed Aero Performance Branch, headed by Mr. Val Dahlem, and the members of my group, led by Mr. Dave Johnson. Mr. Mike Stringer, Lt. Col. Jun Mizusaki, Mr. Kevin Langan, Mr. Harry Karasopoulos, Mrs. Rhonda Duvall, and Lt. John Cannon. My thanks also goes to Mr. Dick Smith and James Wilkinson, the other mentor and apprentice I worked with. Finally, my thanks goes out to everyone at Universal Energy Systems and WPAFB who made this program work, including Mr. Adolph Harris and Mr. Rodney Darrah, program directors, Mrs. Sue Espy, program coordinator, and Mrs. Missy Tomlin. There are more than likely other people who deserve to be on this page, and I also thank these people who I have not mentioned above.



## Part II : An Introduction to Agility Research

Agility is an elusive, deceptive quality, or metric, of an aircraft that has not been given a definition as to exactly what it is. Agility is the ability to change maneuvers rapidly with precision and control. Many different metrics from various researchers have been proposed as to how agility should be measured. In the agility study being done by Lt. Cannon that I have assisted with over the past two months the metrics proposed by the Air Force Flight Test Center (AFFTC), Eidetics, General Dynamics (GD), Northrop, and Herbst, along with their corresponding maneuvers to compare agility, have been taken from the point of raw data and theory to the point of scaled plots with actual data from test flights. At times this process became tedious when little seemed to result from our efforts because, having done this for the first time, we had nothing to base our research on. The results achieved over the past few weeks have been rewarding due to the fact that our long hours of reducing data and re-reducing it again because of changes in initial conditions have finally produced scaled plots for four of the five metrics, excluding only the Herbst metric.

My place in the broader spectrum of this agility study is, basically, the recording of specific parameters pertaining to four of the metrics from test flights and reducing this data into the two parameters needed for the axes of each plot. This involved many calculations to simplify data and take out variables that would complicate matters when it came to plotting. It also involved a process of screening the data to make sure a certain maneuver was done by the pilot well enough to be considered for use in our reasearch. This screening was done by checking if a maneuver

met certain conditions, or, "capture tolerances". To put it in a numerical sense, I reduced 26 flights with a total of 294 maneuvers to a form that was corrected for variables and was screened for pilot error. Some of the maneuvers were even used for more than one metric. From the maneuvers that met our capture tolerances a total of 48 plots pertaining to the four completed metrics were done. More often than not, something would be wrong with our plots and a correction would be made. After the completion of the plotting, the plots will be put into a report, which is being done by Lt. Cannon. As this is but a brief introduction of our agility research, these steps will be more fully expained in later parts of my final report.

### Part III : Methods of Measuring Agility

As explained briefly in Part II, my part in this study of aircraft agility is the compiling of plots that, instead of showing the theoretical curves of a certain metric without a scale, show the actual curve on a scaled plot using actual test flight data. In the following parts of my final report, I am going to go through the steps leading from raw data to a scaled plot. The construction of a scaled plot is a more accurate measure of aircraft agility because it helps prove or disprove the proposed metric by the use of actual test flight data.

To show how this process works, I am going to go through the steps to each of the four proposed metrics of measuring agility from the Air Force Flight Test Center, Eidetics, General Dynamics, and Northrop. A series of calculations for the reduction of the data from each metric will be shown step by step. Some of the reduction involves only basic algebra, while others touch upon some trigonometry. As new equations are needed, they will be provided in, for the most part, the form of the equation solved for the variable desired. Lt. Cannon has shown me how many of these equations work, and how they affect the way an airplane flies by increasing a variable, etc., and I will do as well as I can to go into explanation on the calculations I am performing, so please bear with me and my incomplete understanding of aerodynamics.

\*\*\*NOTE\*\*\* If it happens that a variable, parameter, abbreviation, etc., is unclear to you, simply refer to Appendix I : Parameters, or Appendix II : metrics in the back of this report. I will attempt to provide a list of

all of the parameters and metrics that I use in my explanations in these appendixes.

#### Part IV : AFFTC

\*\*\*NOTE\*\*\* All numbers used in calculations are strictly for the purpose of demonstration. These numbers in no way represent any actual flight test data from my research.

In this section, I will attempt to explain in detail the steps required in going from a list of aircraft parameters taken at several intervals per second to the point of having a  $\Delta t$  (time required to fly the maneuver) and airspeed in Knots Equivalent (KEAS) for that maneuver. For each of the 294 maneuvers, made up of rolls, pitches, Nz captures, and DT turns (level turn to point), I went through this process of looking up these numbers in the time histories of the maneuvers. The  $\Delta t$  value was taken when the maneuver was completed, so as to see how long it took to perform a certain maneuver. KEAS values indicated the dynamic pressure (the blast force of the wind) at which the maneuver was flown. For this example, I am going to go through the process of determining the  $\Delta t$  and KEAS value for a standard  $90^\circ$  roll.

All of the data from the AFFTC is recorded in the form of printouts organized by flight # and then within the flight, the specific maneuver. Within the maneuver, there are listings of parameters taken at 20 intervals per second starting from a brief time before the maneuver began to when the maneuver had been completed for a short time. This was so the start and finish of a maneuver could be determined. For a roll-type maneuver, I determined the start from when the pilot started pushing the control stick sideways (lateral stick input), which is what a pilot

does when he wants his plane to roll. Besides the latstk input, there were other conditions which had to be individually considered to determine if the maneuver was properly executed. The most important of these is, in the case of a roll-type maneuver is the bank angle, or  $\phi$ . For a roll to be good, the initial  $\phi$  had to be  $\pm 5^\circ$  of 90, or on its side. The end of the maneuver was determined by whether  $\phi$  came within  $\pm 10^\circ$  of 0, or level, along with the other conditions that had to be met. The time it took from when the pilot pushed the latstk until the aircraft came within its  $\pm 10^\circ$  "bandwidth" is the  $\Delta t$ . Along with recording these in a flight log, I also had to record what, if anything, went wrong with the maneuver and also, the airspeed in Knots Calibrated (KCAS) value at the start of the maneuver. The time histories had no KEAS values, only KCAS, so a conversion had to be made from KCAS to KEAS by looking up the KEAS value, given a certain KCAS value, M, and an alt. The conversion from KCAS to KEAS takes out the effects of the air being compressed by the airplane.

After each of these values had been discovered, I recorded them in a flight log. The flight log listed maneuvers like this:

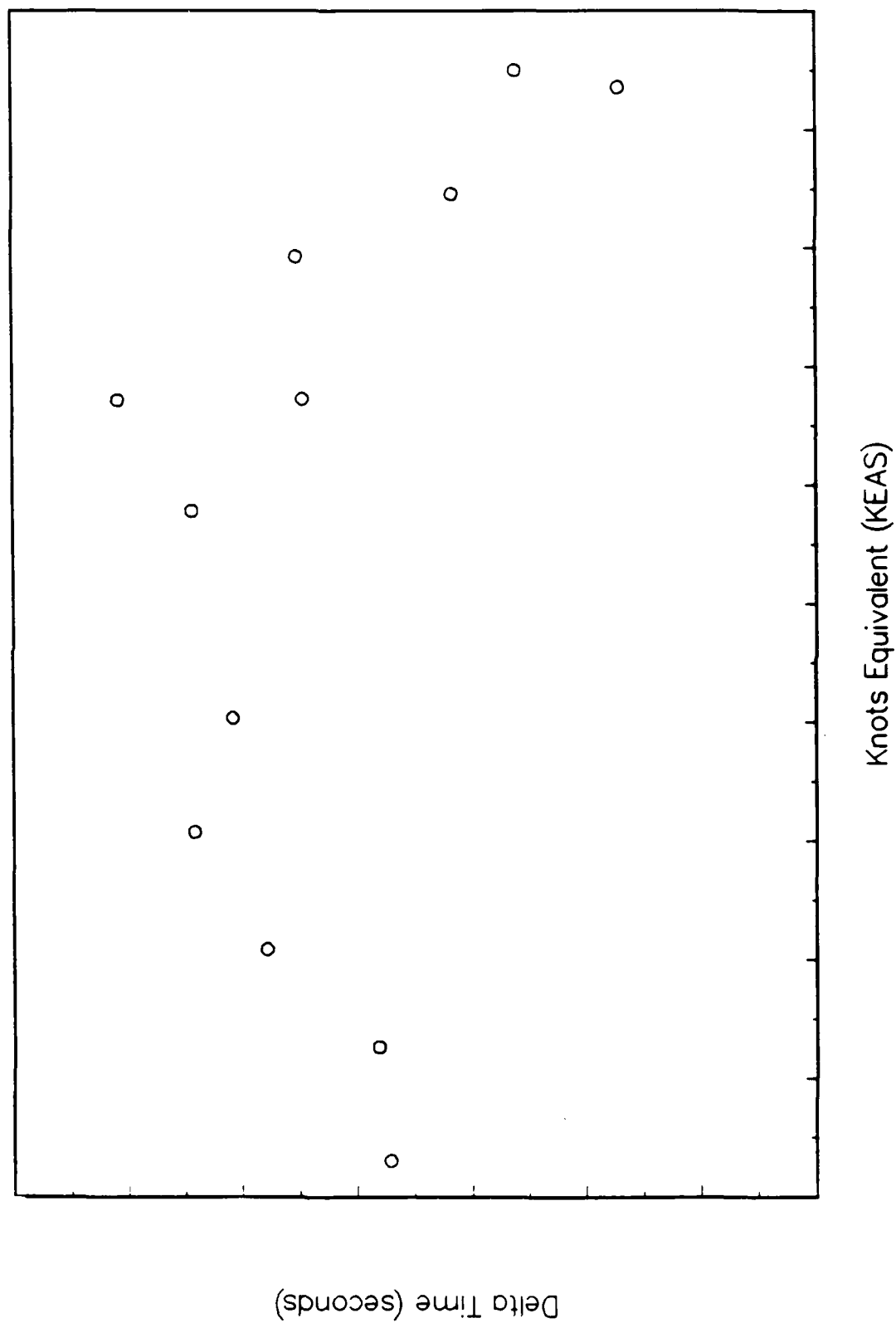
|                       |             |           |
|-----------------------|-------------|-----------|
| Flight # / maneuver # | constraints | M # / alt |
|-----------------------|-------------|-----------|

These entries were in vertical columns, with the lowest numbered flight at the top of the page. The information I looked up was recorded in the right margin across from the flight from which the information came, along with any bad conditions.

These maneuvers were plotted with KEAS along the x-axis and  $\Delta t$  along the y-axis. Because of the numbers of variables encountered for all of

one type of maneuver, I had to differentiate between these points. This was done by giving different shapes, shading or not shading, and "flagging" them. On the example plot that falls immediately after this part, the points represent fictitious data. Consequently, this plot only serves to give a visual representation of my simplifying of AFFTC data. I have left out the different symbols, shading, and flagging for simplicity.

Air Force Flight Test Center – Sample 90 deg Roll





## Part V : Eidetics

This part of my final report shows in detail the steps to take a list of parameters through numerous calculations and solve for the Specific Excess Power (Ps) and Torsional Agility (Tor) values for the sample maneuver. A total of 14 steps that varied in length and difficulty were done for 35 maneuvers. I would like to point out that I did all of these calculations with only the benefit of a calculator. The first few steps were simple in that they only involved the looking up of parameters. This is very similar, in that regard, to what I did to reduce the AFFTC data.

The Ps value showed the aircraft's rate of change of total energy, or the potential energy change. Tor implies that if two aircraft have the same Tor, they have the same agility. There are two fighters, A and B. Fighter A can roll slowly and turn quickly and fighter B can roll quickly and turn slowly. They have equal Tor, yet, turn rate is better in one combat situation while a small  $\Delta t$  is better in another. This example shows that the Torsional Agility metric should perhaps be more carefully examined. Getting back to the sample calculation, I will now go through all of the steps from starting conditions to the final Ps and Tor values.

For the initial values given, there are M, alt, and Nz. For demonstration purposes, I will assign values to these initial conditions.  $M=1.0$ ,  $alt=10000$ , and  $Nz=1.0$ . These, in conjunction with the values I recorded in the AFFTC metric, will be used to solve for Ps and Tor.

First, thrust is found by looking it up on a thrust table, given M and alt. From the table,  $thrust \approx 20000$ . Next, a (the speed of sound) is looked up on an a table, given alt. From the table,  $a \approx 1000$ .

The  $\sigma$  value comes from the same table.  $\sigma \approx .75$ . Now, the first calculation is done to find U.

$$U = (a) (M) \quad V:I$$

$$U = (1000) (1)$$

$$U = 1000 \text{ ft/sec}$$

Now that I have U, I solve for L.  $W=25000$ .

$$L = (Nz) (W) \quad V:II$$

$$L = (1) (25000)$$

$$L = 25000 \text{ lbs}$$

After L is computed, I solve for  $\rho$ , given a constant and  $\sigma$ .

$$\rho = (.00237) (\sigma) \quad V:III$$

$$\rho = (.00237) (.75)$$

$$\rho \approx .00178 \text{ slug/cubic ft}$$

Now, I solve for  $C_l$ .  $S=250$ .

$$C_l = \frac{2L}{(\rho) (U^2) (S)} \quad V:IV$$

$$C_l = \frac{(2) (25000)}{(.00178) (1000^2) (250)}$$

$$C_l \approx .112$$

From a table of  $C_l$  and  $C_d$  values, a  $C_d$  is looked up, given a M.  $C_d \approx .025$ .

Drag can then be computed by this equation.

$$D = (.5) (\rho) (U^2) (S) (Cd)$$

V:V

$$D = (.5) (.00375) (1000^2) (250) (.025)$$

$$D = 11718.75 \text{ lbs}$$

Now I have all of the information to compute  $P_s$ . For the sake of simplicity, I am making a small  $\alpha$  assumption, which lets the thrust act along the flight path.

$$P_s \approx (T - D) (U)$$

V:VI

---

W

$$P_s \approx (20000 - 11718.75) (1000)$$

---

25000

$$P_s \approx 331.25 \text{ ft/sec}$$

From this  $P_s$  value, the aircraft would be able to accelerate since  $P_s$  is positive. Now,  $Tor$  is more simply found than  $P_s$ . The  $TR$ , from the lists of parameters I discussed in Part IV : AFFTC, is recorded. This value is then divided by the  $\Delta t$  to roll  $90^\circ$  ( $\Delta t_{,0}$ ) that I recorded, as also described in Part IV : AFFTC.  $\Delta t_{,0} \approx 1.5$ .

$$Tor = TR / \Delta t_{,0}$$

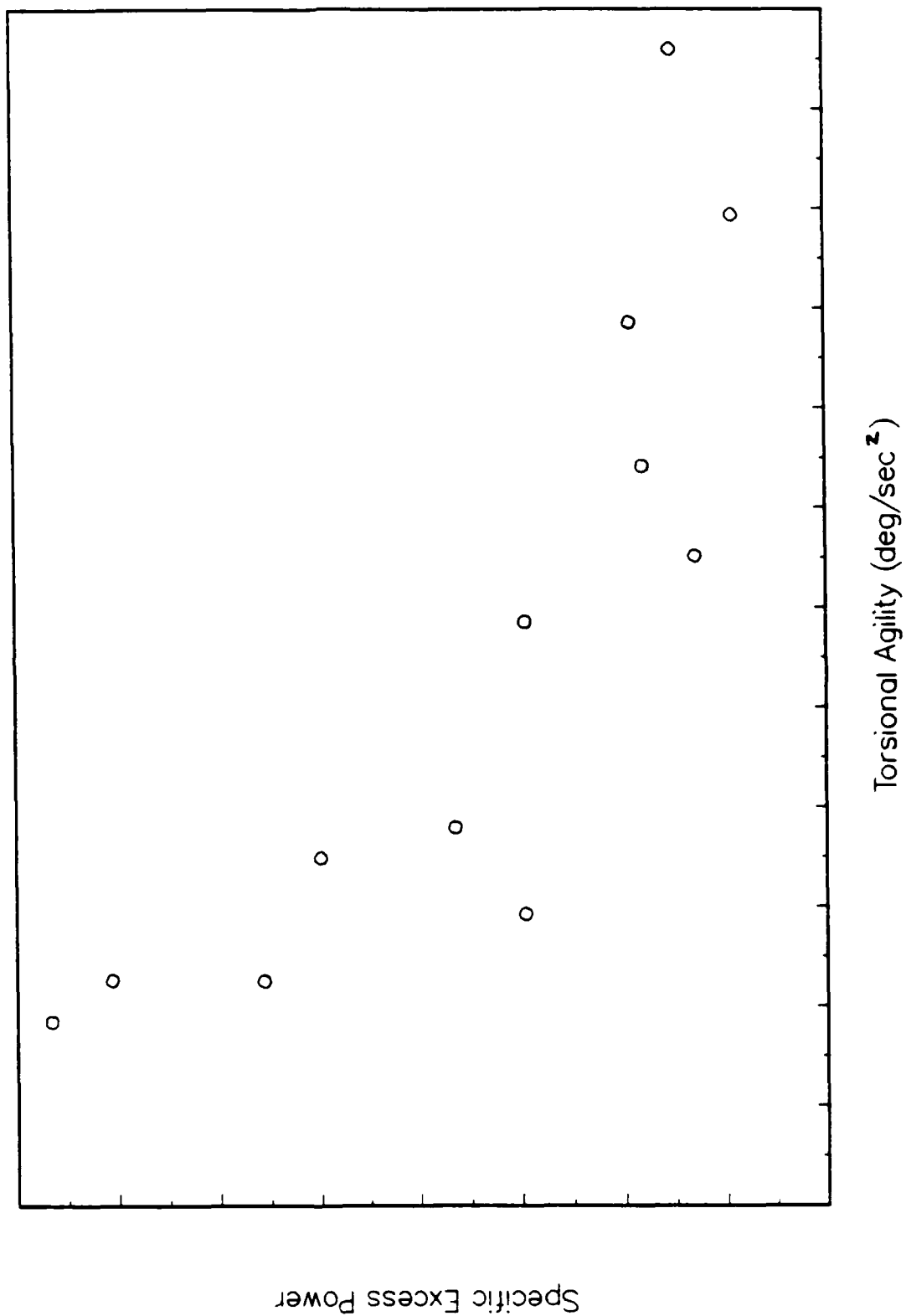
V:VII

$$Tor = 10.0 / 1.5$$

$$Tor \approx 6.7 \text{ deg/sec squared}$$

It is now possible to construct a plot with Tor along the x-axis and Ps along the y-axis. A sample plot of what an imaginary Tor -vs- Ps trend might look like immediately follows this section. Very much like the AFFTC data, many points had to be shaded and flagged so as to differentiate between changes in initial conditions. Again, the shading and flags have been left out for simplicity.

Eidetics – Sample Torsional Agility



## Part VI : GD

For this part of my final report, I will go through the steps to show how, given an airspeed (KEAS) and an angle of attack ( $\alpha$ ), Turn Rate (TR), and airspeed Bleed Rate (BR) values are calculated for a sample maneuver. The first few steps were conversions, while later steps involved calculations. I went through this process of calculations 39 times, by hand. This number of repetitions was required to satisfy the bulk of information needed to get enough points on a plot. This process can be done anywhere from 2 up to an  $\infty$  number of times to make a trend on a plot. On certain occasions, I had to "iterate" to get a result that was satisfactory. To iterate basically means that once a run is made through these calculations and a corresponding set of numbers is arrived at, another run is made using one of the numbers from the first run to get a new and more precise set of numbers. This can be done as many times as needed, until the set of numbers is precise enough for the job.

I have briefly touched on the meaning of TR in previous parts of my final report. For the GD metric, TR refers to how quickly the aircraft can turn at the airspeed TR was calculated. BR shows how quickly the aircraft slows at a certain airspeed. When TR and BR are plotted against each other, the trend the points make is one of a "banana" shaped curve, with the end of the banana as the corner speed. Corner Speed is the point in the flight envelope where maximum  $N_z$  and  $\alpha$  can be pulled simultaneously. From this point I will start with the calculations. I will assign an initial value to KEAS for the purpose of a hypothetical demonstration. KEAS=250. From KEAS I can calculate  $V_t$ .

$$V_t = (2.31) \text{ (KEAS)}$$

VI:I

$$V_t = (2.31) (250.0)$$

$$V_t = 577.5 \text{ ft/sec}$$

Next, from a  $V_t$  value,  $M$  can be computed.  $a=1037.0$  at an alt of 20000.

$$M = V_t$$

VI:II

—

$a$

$$M = 577.5$$

—

1037

$$M \approx .6$$

For simplicity, this is an  $\alpha$  limited maneuver, so  $\alpha=30.0$ . Now,  $C_l$  is found by looking on a chart of  $C_l$  -vs-  $\alpha$ . From the chart,  $C_l \approx 1.5$ . Once a  $C_l$  value is determined, it can be used to find  $L$ .  $\rho=.00127$  and  $S=250$ .

$$L = (.5) (\rho) (U^2) (S) (C_l)$$

VI:III

$$L = (.5) (.00127) (577.5^2) (250) (1.5)$$

$$L \approx 79416.0 \text{ lbs}$$

$N_z$  can be computed from a  $L$  value.  $W=25000$ .

$$N_z = L / W$$

VI:IV

$$N_z = 79416.0 / 25000$$

$$N_z \approx 3.2$$

From a chart of  $C_l$  -vs-  $C_d$ ,  $C_d=.5$ . With a  $C_d$  value,  $D$  can now be computed.

$$D = (.5) (\rho) (U^2) (S) (.5) \quad \text{VI:V}$$

$$D = (.5) (.00127) (577.2^2) (250) (.5)$$

$$D \approx 26472.0 \text{ lbs}$$

BR can be computed now that all the variables are calculated.  $T=15000$ ,  
from the thrust table, given M and alt.

$$BR \approx (g/2.31W) [T (\cosine \alpha) - D] \quad \text{VI:VI}$$

$$BR \approx (.00127) [15000 (.866) - 26472]$$

$$BR \approx -17.12 \text{ knots/sec}$$

This BR shows that the aircraft would be slowing down at this  $V_t$  and  $\alpha$ .

There is only one calculation to solve for TR.

$$TR = (1844 / V_t) [\text{square root } (N_z^2 - 1)] \quad \text{VI:VII}$$

$$TR = (1844 / 577.5) [\text{sq. rt. } (3.2^2 - 1)]$$

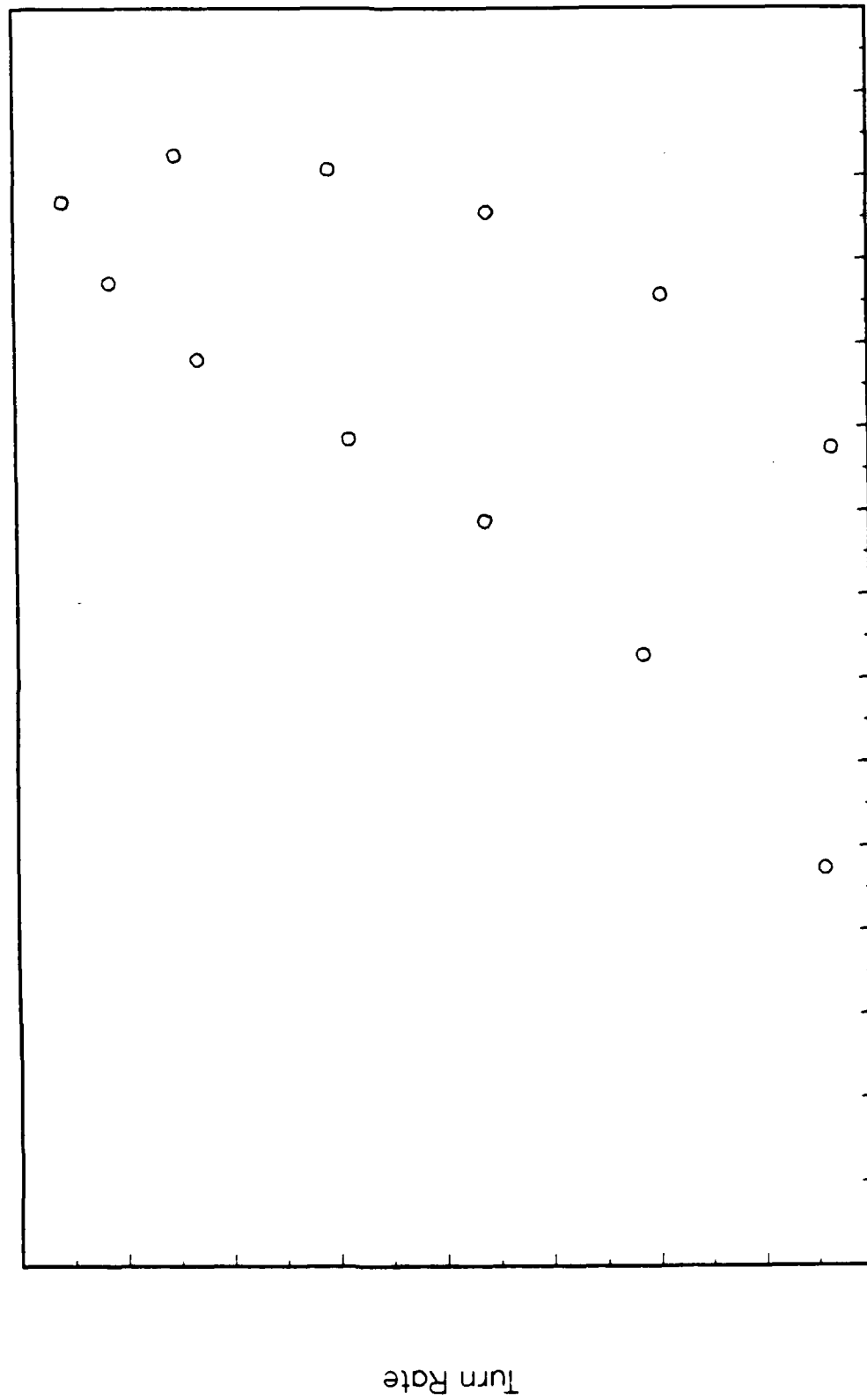
$$TR \approx 9.71 \text{ deg/sec}$$

This TR shows the aircraft had the ability to turn over  $9^\circ$  per second.

The plot constructed using these values has BR along the x-axis and TR along the y-axis. An example of a "banana" curve follows this part of my final report. Same as the last two parts, points are not shaded or flagged to make the plot simpler.



General Dynamics - Sample "Banana" Curve



## Part VII : Northrop

During this final description of how a metric, specifically the DT metric, was reduced, I will go through the steps to show how the lists of parameters were reduced and I will also give a brief description of what Lt. Cannon has done with the point and shoot DT metric. The reduction of this metric is almost exactly the one I described in Part IV : AFFTC. The only difference is that instead of plotting  $\Delta t$  -vs- KEAS I plotted DT -vs- KEAS. DT is, in my opinion, an excellent metric to be used to define agility. My basis for this is a simple scenario. There are two fighters, A and B, who pass very close to each other going opposite directions. When they pass, they both fire their guns at each other, and both miss. Obviously, they wish to turn around so as to get another shot. The fighter who can turn around more quickly and in a shorter Crossrange (CRNG) can "point and shoot" more quickly than the other. It follows that if  $\Delta t$  is multiplied by CRNG, whoever has the smallest product is going to get off the first shot. This product is DT. The DT metric hasn't yet been completely verified, but at this point it seems to predict fairly well the ability of a fighter to point and shoot in certain scenarios.

Since I have given a basic rundown on what the DT metric means, I will go through the steps to reduce the lists of parameters to a DT value. From the flight log where I recorded KEAS and  $\Delta t$  values, (see Part IV :AFFTC) I can get the  $\Delta t$  to plug into the DT equation.

$$DT = (CRNG) (\Delta t) \qquad \text{VII:I}$$

Plugging in an imaginary  $\Delta t$  for a DT maneuver into equation VIII:I, I get

$$DT = (CRNG) (10.0)$$

Now, I need CRNG to complete the equation. This can be looked up at the point in time (in the lists of parameters) when the pilot has flown through  $180^\circ \psi$  so he is pointing in the other direction. For this example, I will set CRNG=5000. Plugging CRNG into equation VII:I, I get

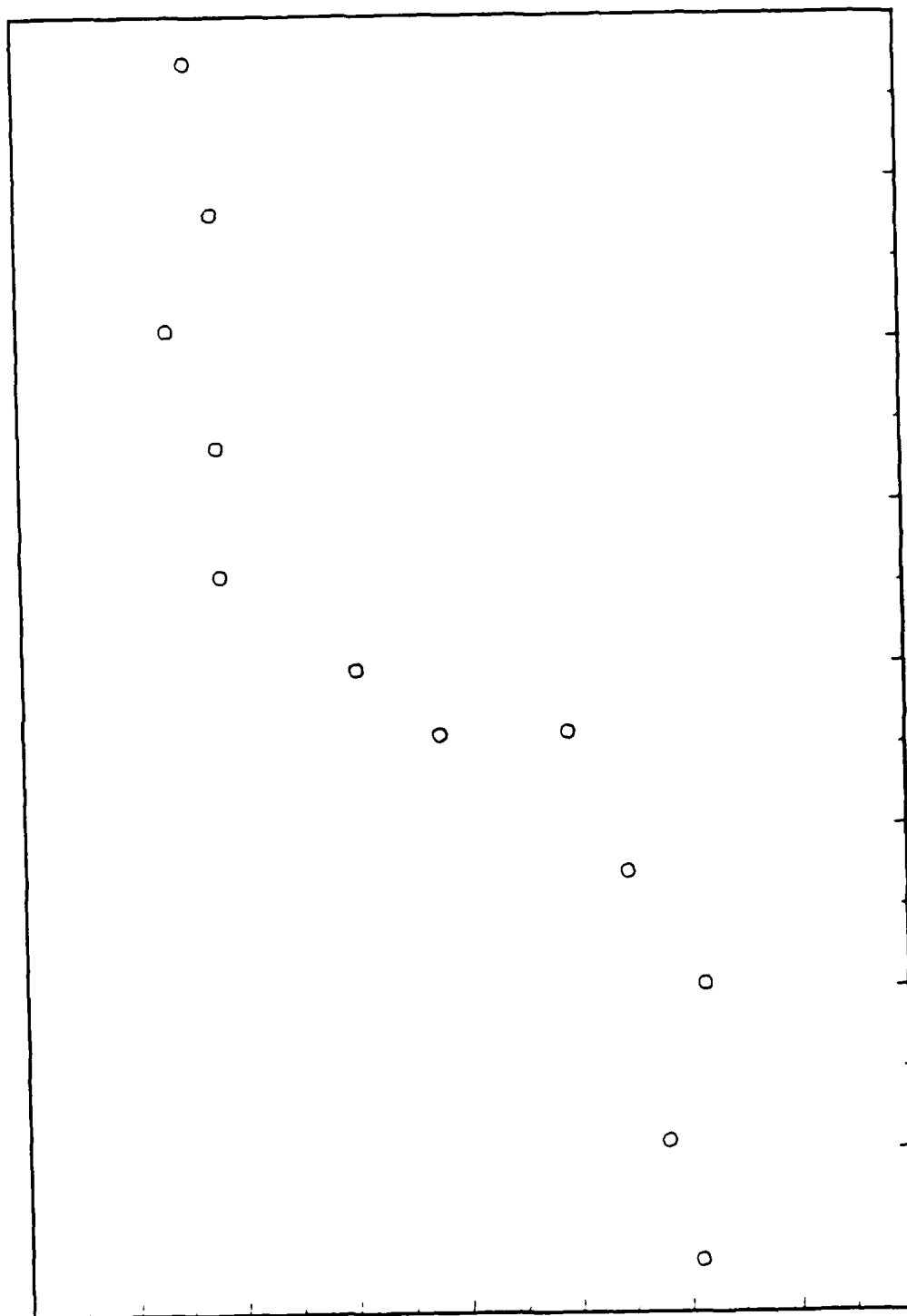
$$DT = (5000) (10.0)$$

$$DT = 50000 \text{ nautical mile seconds}$$

The work I have done with DT is just a part of the Northrop DT metric. Lt. Cannon has been running trajectories on the computers to find the most efficient method of flying a DT maneuver under a great variety of conditions. The DT maneuver can be optimized for a number of qualities such as minimum time and/or minimum fuel consumption at a given CRNG.

The plotting I have done for the DT maneuver/metric has KEAS along the x-axis and DT along the y-axis. My final sample plot shows what a DT -vs- KEAS trend might look like. As with the other plots, the shading and flagging has been excluded for the sake of simplicity.

Northrop - Sample DT Turn



(Distance)(Time) (nautical mile seconds)

Knots Equivalent (KEAS)

## Part VIII : Results and Conclusions

Because of the sensitive nature of the actual test flight data that I used to measure agility, I can only write in generalities when I draw conclusions on this research Lt. Cannon and I have conducted. From my relatively complete analysis of the four metrics, I can determine that these metrics are all "pieces in the puzzle" of agility. I believe at this point in the agility research, the conclusions that we have drawn are correct yet still incomplete, as there are still missing "pieces", such as the Herbst metric. My four examples of the reduction of metrics are only four of the more common reductions out of all of the different types. All of the other types of maneuvers previously mentioned could have been used as additional examples. Some of the metrics have a sort of "sub-metric" that could be separate reports in themselves. My point is, I believe I have presented enough examples to give a picture of what agility is. Hopefully, this report has shed a little light on a previously unknown quality, agony (uh, I mean agility).

## Appendix I : Parameters

| Parameter  | Symbol         |
|--|----------------|
| -----  |                |
| <u>Alpha</u> (degrees)<br>Angle of attack  | $\alpha$       |
| <u>Altitude</u> (ft)   | alt            |
| <u>Beta</u> (degrees)<br>Angle of sideslip   | $\beta$        |
| <u>Coefficient of Lift</u> (dimensionless)<br>This "normalizes" the lift. Related directly<br>to alpha | C <sub>L</sub> |
| <u>Coefficient of Drag</u> (dimensionless)<br>This "normalizes" the drag.                              | C <sub>D</sub> |
| <u>Gross Range</u> (ft)<br>How far the aircraft has traveled "across".                                 | CRNG           |
| <u>Down Range</u> (ft)<br>How far the aircraft has traveled "down".                                    | DRNG           |
| <u>Drag</u> (lbs)<br>Acts tangent to flight path   | D              |

Knots Indicated

KIAS

This is what is shown on the aircraft dial.

It is only corrected for instrument error.

Knots Calibrated

KCAS

This is KIAS also corrected for the error in the placement of the static pressure port.

Knots Equivalent

KEAS

This is KCAS also corrected for compressibility effects.

Lateral Stick Displacement (inches)

latstk

Lift

L

Acts normal to flight path.

Load Factor (dimensionless)

Nz

Equal to L/W.

Longitudinal Stick Displacement (inches)

lonstk

Mach (True air speed/Ambient speed of sound)

M

Phi

$\phi$

Body axis roll angle.

Phi dot

$\dot{\phi}$

This is the body axis roll rate.

Psi

$\psi$

Body axis heading angle.

Rho (slug/ft<sup>2</sup>)

$\rho$

Air density.

Rudder Pedal Displacement (inches)

rudped

Sigma ( $\rho/\rho_{sl}$ )

$\sigma$

Density ratio at altitude.

Speed of Sound (ft/sec)

a

Theta

theta

Body axis pitch angle.

Thrust

T

Function of Mach, altitude, and throttle setting.

True Airspeed (ft/sec)

U, V, Vt

Turn Rate (deg/sec)

TR

Measures turn rate of the velocity vector.



Weight (of aircraft) (lbs)

W

Wing Area (ft<sup>2</sup>)

S

## Appendix II : Metrics

| Metric   | Symbol     |
|--|------------|
| -----  |            |
| <u>Acceleration</u> (kts/sec)                              | accel      |
| (g/W) [ T ( cosine $\alpha$ ) - D ]                        |            |
| For constant altitude flight.                              |            |
| <u>Airspeed</u> (KEAS)                                     | KEAS       |
| <u>Bleed Rate</u> (kts/sec)                                | BR         |
| (g/W) [ T ( cosine $\alpha$ ) - D ]                        |            |
| <u>Delta Time</u> (sec)                                    | $\Delta t$ |
| This is the time to complete a maneuver.                   |            |
| (Also, just time)  |            |
| ( <u>Distance</u> )( <u>Time</u> ) (nautical mile seconds) | DT         |
| <u>Knots Equivalent</u>                                    | KEAS       |
| <u>Load Factor</u> - <u>Mean Nz</u>                        | MNz        |
| <u>Load Factor</u> - <u>Standard Deviation of Nz</u>       | SDNz       |
| This is the square root of the  variance .                 |            |
| <u>Specific Excess Power</u> (ft/sec)                      | Ps         |

This describes the aircraft's ability to  
accelerate or decelerate.

Torsional Agility (deg/sec<sup>2</sup>)

Tor

$TR/\Delta t_{,0}$

Turn Rate (deg/sec)

TR

$( 1844/U ) [ \text{sq. rt. } ( n^2 - 1 ) ]$

## References

Dorn, M. Aircraft Agility : The Science and the Opportunities. American Institute of Aeronautics and Astronautics. Paper presented July 31-2 August 1989, Seattle WA, AIAA-89-2015. pp. 1-11

Kalviste, J. Spherical Mapping and Analysis of Aircraft Angles for Maneuvering Flight. American Institute of Aeronautics and Astronautics. Paper presented August 18-20 1986, Williamsburg VA, AIAA-86-2283. pp 1-10.

Lan, Chuan-Tau Edward and Roskam, Jan. Airplane Aerodynamics and Performance. Roskam Aviation and Engineering Corporation. Ottawa, Kansas. 1981. pp xi-xxiii and 15-53.

INSTRUMENTATION OF  
AEROSPACE STRUCTURAL  
INTEGRITY TESTS

By: Wendy Choate

Mentor: Joe Pokorski

August 21, 1989

## ACKNOWLEDGMENTS

I would like to give my thanks to Joe Pokorski, Ann Driscoll, Cliff Hichcock, Norman Wildenhaus, Jim Wieher, Ron Ditmer, Larry Kretz, John Pappas, Steve Litke, Ray Fisher, Jack Smith, Fred Hussong, everybody in the TM room and anybody else who I've met during my time at the base. I owe them all a lot of thanks and I'm glad to have met everyone of them.

The research done at the Structures Test Branch is mostly composed of actual fatigue testing with instrumentation being done in the building. These fatigue tests are done with tension or compression (the use of hydraulic weights) and/or temperature (mainly heat) devices to stress the material. The tension and compression test are currently being done on a F-15's wings and different materials for students working on their thesis. The temperature test is currently being done on a panel from the National Aerospace Plane and on a portion of a Boeing airplane. These fatigue tests help determine the limits of certain materials and designs. Most of the information is passed on to another laboratory for redesign or further testing. But the material is not sent to the lab ready to test. First it has to be instrumented with different types of measurement devices.

Most of these devices are strain gages and thermocouples. Thermocouples are used to measure temperature of a certain material by creating an electrical impulse between two different type wires which is measured and converted into a temperature. Strain gages are used to measure stress on a material and are fairly easy to install. First the area in which the gage is to be attached is sanded and cleaned with chloroethene. The surface is then cleaned again with a conditioner and then wiped off with a neutralizer. Then pencil marks are measured as to where the gage is to be placed. The gage is then attached (bond side down) to a piece of cellophane tape. Then the gage is aligned on the pencil marks. After alignment, the tape is lifted off one end while the other stays intact with the material. The tape is pulled back so

that the gage is no longer touching the material and is lying flat with bonded side up. The surface is then cleaned again with chlorothene to erase pencil marks. The exposed part of the gage is then wiped with the catalyst and the glue applied to the surface of the material in the place where the gage is to be placed. Immediately take the tape and pull it over the glue but not touching the glue. Then take a piece of teflon and slide it along the tape till it covers the gage. Keep pressure on the gage for approximately one minute. After one minute, remove finger and let the gage sit for several minutes, then remove tape by sliding it back over itself. The gage is bonded to the material and is then wired with solder.

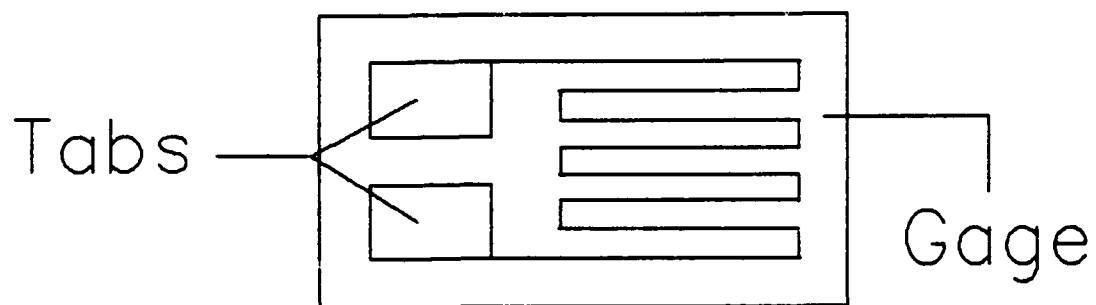
The strain gage is a device that measures stress on a material. There are many different types of gages for different materials and different stress tests. The two most popular are rosettes and axials. A rosette measures stress at three different angles (0, 90, and 45) while an axial measures only one angle. The gages measure stress by the use of Ohm's law which states that  $E=IR$  ( $E$ =current in volts,  $I$ =amperes, and  $R$ =resistance in ohms). When the sample is put under stress the gage is also put under stress and is either stretched or compressed. The amount is so small, it sometimes cannot be seen by the unaided eye. This is where Ohm's law takes over. The current is kept constant through the gage. The stress on the gage causes a change in the resistance. Stretching increases resistance while compression reduces it. These two known variables are put into Ohm's equation and fed into a computer. The computer converts



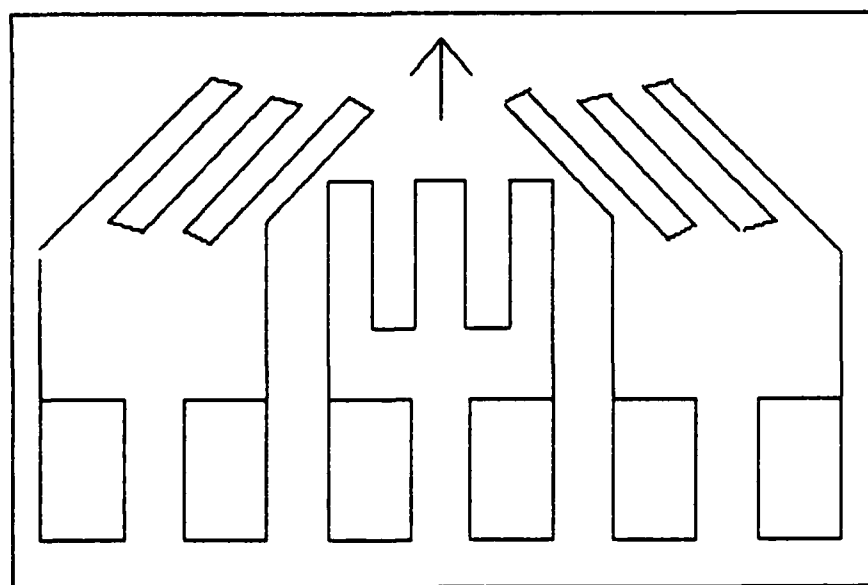
the amperes into a percentage of strain on the sample. The computer also converts the data into the number of pounds applied to the sample. The test is run several times with the same or duplicate samples.

Most of the strain gage application done this summer was done for graduate students working on their thesis. The installation of the gages is the same but the size, composition of the material, and the types of tests done varied from what was being done on the test floor. The students projects ranged from aluminum to composite samples, in sizes from half inch by two inches to panels that were eight inches by 13 inches. Each student required different gages in different locations. Some of the samples were to be heated beyond the point at which the usual adhesive worked. The alternative adhesive is 610, but is a time consuming process because of the curing time required to enable to the bond to last beyond the temperature at which the test is to be run at. Approximately 1000 gages were installed over the summer for the students and other project within the building.

# Types of Gages



Axial Gage



Rosette Gage

## BIBLIOGRAPHY

Strain Gage Installations with M-Bond 200 Adhesive. Micro-  
Measurements Divisions. Measurements Group, Inc.  
Everybody at the Structures Test Branch.

William Davenport  
Final Report Number 63  
No Report Submitted

Andrea Dean

Final Report Number 64

No Report Submitted

WORKING ON THE Z-248  
14 INCH COLOR MONITOR

by Cedric McGhee

## INTRODUCTION

The 248 Zenith Computer will be discussed in the report. Databasing, programming, wordprocessing, and graphing are the priorities. Databasing and programming are done on the DBASE III PLUS System; wordprocessing is done on the Word Perfect Version 5 System; and graphing is done on the Harvard Graphics System.

The first step that you learn in the Z-248 14-inch color monitor is databasing. Use the assist menu for databasing; open "Set Up" menu to set up your database in a disk drive, and open "create" menu to create your database. Once you have created the database, you can edit, add, or remove any information in the "Update" menu. Otherwise, you can create sorted, index, and query files to gather your information faster; also, you can create formats, lists, and reports. Use the "Retrieve Menu" and select (execute the command) to display your information; type "Y" to print the information or "N" not to print. The status bar at the bottom of the screen usually tells you what to do. Now you should be ready for programming.

Before programming, you leave the Assist Menu by pressing the escape button (ESP). Now you are in Dot Prompt. At the prompt, you type in certain commands such as set, do, help, etc. To write and edit programs, you simply type: modify command and enter the name of your program. You can make four type of programs. They are as follows: Do-Enddo, Input-Output, If-Endif, and Do Case-Endcase. Do-Enddo commands means do something and then end it; Input-Output commands means putting in information and then give out information; If-Endif commands mean do something if given required information or end it if not given required information. Do Case-Endcase commands mean do two or more things and then end them. There are many, many more commands in programming.

In wordprocessing, you write and revise documents. You block any characteristics that you want to change. You can insert and delete whatever you want by using the "Ins" and "Del" keys. The keys F1-F12 should be labeled with wordprocessing codes; for example, Shift F8 is the format page. You should always proofread your document by pressing Alt-F3. You



can even do your math in "word perfect" wordprocessing by using Alt-F7 codes. Use F1 for more help on knowing the codes.

In graphing, you make charts. In Harvard Graphics, there are several types of charts; the main charts are pie area, text, multi, and hi-lo closed charts. Pie area and hi-lo closed charts are usually made to show percentages, rates and amounts. Text charts are usually made to display titles, bulletins, lists, etc. Multi charts are charts that contain two or more other charts. Select "creative new charts" to create charts and "edit" to revise the charts. Select "draw/annotate" to add in your symbols, words, or drawings. Select "set up" to adjust your chart. Press "ESP" to escape submenus. Remember to save your charts by selecting "get/save/remove"; select save charts and enter the chart's name.

If you have a printer hooked up to the Z-248, make sure that the printer is ready to print. You can print your databases, programs, documents and graphs.

## ACKNOWLEDGEMENT PAGE

You should have learned four steps in working on the Z-248 14-inch color monitor. They are databasing, programming, wordprocessing, and graphing. In databasing, you should have learned to create and process databases. Most importantly, you should have learned to gather information. In programming, you should have understood certain commands and how they are used. In wordprocessing, you should have learned about writing documents and revising the documents by using typing codes, F1-F12 buttons, etc. In graphing, you should have learned to create your own charts and drawings. You should have learned to print in all four of these steps.

Aircraft Transparency Durability:  
Analysis of the F-111 and a  
Study of the Application of  
Combat Missions to Durability  
Testing

By: Mr. David Merritt  
Approved By: Mr. Russ Urzi  
August 8, 1989

### Acknowledgements

I would like to express thanks to my mentor Russ Urzi, and to Lt. Paul Kolodziejewski, Malcolm Kelley, Lt. "TJ" Choe, Ralph Speelman, Mike Grannan, Lt. Duncan Dversdall, and Jim Terry for their support, enthusiasm, and friendship during my eight weeks at the Aircraft Windshield Systems Program Office.

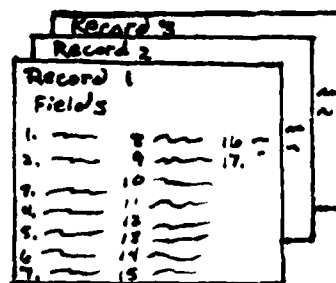
#### 1.0 Understanding the current durability of the F-111

The task of finding the current service life of F-111 windshields and canopies can be determined by investigating data from different transparencies that are and have been in service on the aircraft. This data can be sorted and used more efficiently through a computer database program. The data must be gathered from the transparencies themselves. This was done by Malcolm Kelley and Russ Urzi. They traveled to the active F-111 airbases and depots to obtain crucial information from each transparency's decal. Also by viewing the part, they could get a good look at it and provide information on its physical characteristics. The data was then entered into the database.

The value of this information is immense because by using this database, the current service life of the F-111 transparency can be found. Knowing the current durability can assist in the creation of a new, more durable transparency that is stronger and able to withstand environmental and operational stresses. The use of the database is a convenient way to store that information. The information can now be accessed quicker. It enables someone to find the average service life, dates of installments, etc. Parts can be found and their file dated to make sure it is current and most efficient. Other databases can be assembled for other aircraft transparencies.

There were several steps taken in the construction of the computer database. First, the information needs to be sorted in order to come up with the information that will be helpful in finding the current durability and make the database useful. Each of the different items is entered into the database through its own field. For instance, the serial number was put into its own field. For each transparency a different record was established with its own fields (See figure 1). By using the serial number, a specific part can

figure 1



be called up without searching through stacks of paper. After finding the needed information, it is useful to place all other information into a comment field. The comment field will then separate each transparency by its own characteristics. The F-111 database ended up with 17 fields (See table 1). Having this many fields gives the user several fields to use in searching for a specific part or querying the database for a specific question.

The equipment used in the research of current F-111 durability is as important as the information itself. DBase III Plus was the program used to store and analyze the data. The computer was a Zenith-248. It stores the DBase III Plus on its hard drive. As each transparency was entered, it too

Table 1  
Descriptions of F-111 Database Fields

| Field Name   | Description   |
|--------------|---|
| SerialNo.    | Serial number of part. Used mostly for identification.                |
| Base         | Air Force Base where the part is located. Identifies climate.         |
| Aircraft     | Tail number of aircraft on which the part is installed.               |
| Manufacturer | Identifies the company that made the part.                            |
| DOM          | Date of manufacture. Indicates when the part was made.                |
| ManuPartNo   | Manufacture Part Number, used to help identify the part.              |
| ManuContNo   | Manufacture Control Number, helps keep track of the part.             |
| DateInstll   | Date the part was installed. The first step in finding service life   |
| DateRemove   | Date of Removal. Also helps in figuring service life.                 |
| Servcelife   | Service life is the amount of time the part was installed and in use. |
| Weight       | Helps determine Birt or Adbirt and part identifier.                   |
| WghtInstll   | Weight installed is the amount of the part as in W&B records.         |
| DateInspec   | Date the part was looked at, usually tells which trip from.           |
| BirtorAdbi   | Birt or Adbirt tells whether the part is birdstrike resistant-Adbir   |
| TypePart     | Tells what position the part was on. RHWS, LHWS, LHCAN, RHCAN.        |
| ClrOrGold    | Identifies part as clear or gold.                                     |
| Comments     | This space is available for any extra information that is likely      |
|              | to be helpful in identifying the part.                                |

was stored on the hard drive. Floppy disk copies of the file were kept as backup to the hard drive. The only other equipment used was that in the collecting of the data. The transparencies themselves were obviously used. Since the data was obtained through visual inspection, it was written down in a notebook. Information was entered into the program directly from the notebook. Copies of Weight and Balance records were also helpful.

#### 1.1 Data Analysis

As the file began to grow, even though not complete, some information began to be evident. Dealing with the durability of the transparency, the database produced the average service life, in months, of the transparencies that had been entered thus far into the program. Using the database, an average of 28.3 months was calculated for the service life of F-111 aircraft transparencies. The average was taken after approximately 1550 transparency entries into the database. The 28.3 month service life is however for all of the transparencies. The database can also be used to find the durability of certain parts. For instance, the service life of left windshields at Mt. Home AFB, Idaho is 25.8 months. The service life for the same part at Cannon AFB, New Mexico is 30.6 months. The difference in the two averages may be coincidental but considering the environmental differences of the two bases, it can be assumed that nature had an effect on the service life. Averages similar to these can be found for all of the different transparency parts at the different bases



around the country. Another example would be 30.8 months for right canopies for Mt. Home, Cannon, Plattsburgh, and Pease AFB's (See table 2). Also, averages on Adbirt and Birt parts were done for Mt. Home AFB. The data is a little shakey but it shows that the birts had an longer average service life (See table 3). Almost any information variables can be calculated through the database program. These averages show the current durability for the F-111 transparencies. They can be used as a baseline to compare improved transparencies to see if they actually are more durable.

Items other than service life of F-111 transparencies were also observed. For instance, crazing is evident in many of the transparencies. When a part is crazed it has fine cracks on its outer acrylic plies. If the part remains under stress, the crazing will grow into cracks. Cleaning detergents and other chemicals can cause crazing as well as continued stress. Delamination is also fairly common. Delamination is when the adhesive holding the various plies of plastic together doesn't stick any more and an air bubble forms. Delamination usually occurs along the edge of a part. Tool scratches are a major cause for removal. Whether by accident or intentional, a tool scratch can be fatal to a transparency. Helmet scratches on the inside of canopies are also a problem. They are not usually as severe as a tool scratch but a helmet scratch can get in the way of visibility. Distortion is another cause for failure in aircraft transparencies. It was also evident in the F-111 data.

Table 2

F-111 Transparency Data Sheet

\* Number in lower right hand corner is the number of parts averaged.

\*\* Number in the center is the average service life in months.

|                       | Mt. Home   | Cannon      | Pease       | Plattsburgh | Avg. for<br>part type |
|-----------------------|------------|-------------|-------------|-------------|-----------------------|
| LHWS                  | 25.8<br>25 | 30.6<br>97  | 21.1<br>38  | 22.9<br>48  | 26.3<br>210           |
| RHWS                  | 26.2<br>26 | 27.1<br>115 | 22.8<br>48  | 24.4<br>49  | 25.6<br>238           |
| LHCAN                 | 26.8<br>23 | 35.8<br>76  | 26.2<br>24  | 27.5<br>42  | 31.0<br>165           |
| RHCAN                 | 35.6<br>21 | 35.2<br>73  | 23.1<br>27  | 30.8<br>35  | 32.1<br>157           |
| All trans.<br>at base | 28.3<br>95 | 31.5<br>361 | 23.0<br>137 | 26.0<br>174 | 28.3<br>770           |

Table 3

Mt. Home F-111 Transparency Data Sheet

Comparison: Adbirt vs. Birt

\* Number in lower right hand corner is the number of parts averaged.

\*\* Number in the center is the average service life in months.

|                               | Adbirt     | Birt       |
|-------------------------------|------------|------------|
| LHWS                          | 25.4<br>24 | 35.0<br>1  |
| RHWS                          | 25.8<br>25 | 35.0<br>1  |
| LHCAN                         | 20.0<br>18 | 46.3<br>4  |
| RHCAN                         | 29.4<br>15 | 43.6<br>5  |
| All Trans.<br>of each<br>type | 25.1<br>82 | 43.0<br>11 |

Usually distortion is due to manufacturing errors. Distortion is when the view out of the transparency is altered by a magnification or demagnification in the center of the transparency. Double vision in the F-111 transparency data can also be found. Two images of an object are seen by the pilot or WSO. This usually occurs at night.

This data is analyzed in order to know more about the current durability of the F-111 transparency. The data from the F-111 database is used by inner functions in the DBase III Plus system. Using the 'average' selection in the Retrieve sub-menu of the assistant menu, the different figures were compiled. Data can also be counted, added up, and indexed. The information in the database can be used in just about any way needed.

### 1.2 Conclusions

The writer of this report concludes that the current durability of the F-111 transparency is satisfactory but can be improved. The average service life of 29 months was less than expected. Two years and five months of use is a fairly long time. However, there are cases in which parts have been installed up to five years. Considering the cost of each transparency, if a part can be installed twice as long as another then you're getting double your moneys worth with the five year part.

### 2.0 Combat aircraft mission analysis

A study of several United States Air Force fighter

aircraft was also done. General and detailed information was gathered from books, magazines, and other literature sources. The aircraft investigated were the F-111 Aardvark, F-16 Fighting Falcon, F-15 Eagle, F-5 Aggressor, F-4 Phantom, A-10 Thunderbolt II, and the Vought A-7 Corsair II. All information gathered was condensed into this report. Some information could not be obtained due to its classification.

The reason for the investigation is to assist in creating a realistic image of what stresses an aircraft transparency experiences during flight so that information can be used in the durability facility at Wright-Patterson AFB. By placing all of this information together, it is much easier and quicker to retrieve for use in durability testing. Knowing stresses and performance in flight can be used to improve the durability of transparencies in the United States Air Force fighter fleet. The selection of these particular aircraft is due to the major roles they play in the force and in the Air Force Reserve. Having a more durable transparency will increase service life and decrease the cost to maintain all of the aircraft. It will also increase the aircraft service time and reduce aircraft down time due to maintenance.

The information was gathered from various sources dealing with each aircraft separately or having several aircraft discussed. Each was studied and information was withdrawn that would fit the need of this report. Information dealing with the aircraft missions was the subject of the search, however data on the aircraft themselves was also extracted so

that the reader becomes acquainted with the subject. Data on thrust, weight, armament, special individual features, ceilings, maximum airspeed, mission altitude, mission airspeed, historical facts and other information was all combined to familiarize the reader on the type of aircraft performing the various mission.

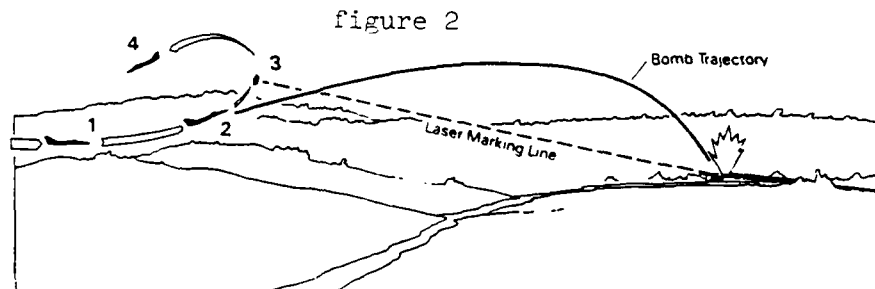
The information was taken from books, magazines, and outside reports. The WRDC Technical Library was the main source for these items. A literature search was done, however due to the writers security clearance level, none of that information was able to be reviewed. The books were the most used sources. Books dealing independently with separate aircraft provided some indepth detail on its subject. These books are listed in the reference section of this report. Magazines were viewed, but little information was withdrawn. Reports on the A-7 were viewed due to the small amount of information available on that aircraft.

## 2.1 F-111 Aardvark

The first aircraft to be discussed is the F-111. The F-111 is a high precision, low altitude, supersonic, strategic, bomber. Designed by General Dynamics in 1962, the F-111 is one of the few variable geometric aircraft in the world today. It was basically designed as a temporary replacement for the aging B-52. However, after several technological changes and improvements occurred, the aircraft became irreplaceable. It is an all-weather, all-terrain bomber thanks in part to its Terrain Following Radar System (TFR). It is used by Strategic

Air Command (SAC) as a medium range variable armament bomber. It is capable of delivering up to 6 nuclear warheads. It can also carry 4 AGM-69A SRAM air to surface missiles on its external pylons plus and additional 2 in the weapons bay. It has a ceiling of up to 66,000 ft. Its maximum airspeed is Mach 2.5. Its empty weight varies from 45,200 lbs to 55,600 lbs. Its ferry range is from 3,500 to 4,000 miles. It has two turbofan afterburning engines which produce 25,100 lbs of thrust each. The only other country that flies the F-111 is Australia.

The F-111 through its many different models has several different mission profiles. However, the most basic and widely used mission is that of the delivery of laser guided conventional bombs. Missions of this kind were performed in Vietnam and more recently against Libya. Typically the F-111 will approach the target undetected because of the low flight altitude. Traveling at 400 ft. or less above the ground, the TFR is used until the bombing run is ready to be started. The pilot then pulls into a 4 'g' vertical climb and the bombs are released at a predesignated time. The aircraft then banks 90 degrees and continues flying tangentially to the target. During this time the Weapons System Officer guides the bombs into the target with a laser tracking system. The bombs home in on the target marked with the laser. After the bombs impact, the pilot completes the turn and descends to resume low altitude toward home (See figure 2). This mission is safe for the aircraft and its crew because they are only exposed



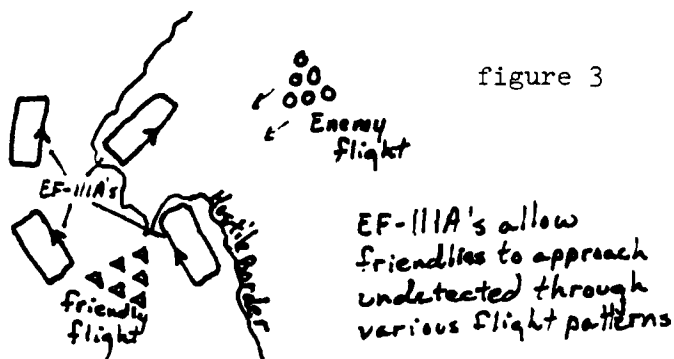
to the enemy radar for the time that the bombs are gliding to target. The same tactic can be used for the deliverance of conventional glide bombs. The MK 82 is the most common, the F-111 can carry 24 to the target area. Observers have said that its performance in both glide and laser guided bombs accuracy is exceptional.

The FB-111 a SAC bomber used to deliver the AGM-68 SRAM or 6 free falling nuclear weapons. The FB-111 cannot deliver the payload that the larger bombers are designed to but they can deliver it faster. The FB-111 is much faster than the B-52. It also does not appear on radar as well and outstanding as the B-52. However, the method of delivery is unavailable due to the security classification. It is known that with the use of external tanks the range of the FB-111 is over 4,000 miles, far enough to enter deep into any enemy territory.

The EF-111A is the electronic jammer model of the F-111. With a radius of more than 2,000 miles it is able to accompany a strike force deep into enemy territory. Once established, the EF-111A will fly an oval shaped pattern to protect other bombers or fighters from SAM's or enemy fighter attack. It carries the AN/ALQ-99E ECM System, the AN/ALZ 137 Self Protection system and the AN/ALR-62 Terminal Threat Warning



System. The EF-111A carries no armament so the entire aircraft is free to be stuffed with enough electronic equipment to make it the heaviest F-111 at 53,600 lbs. empty weight. On its missions the EF-111A flies high or low enough to avoid enemy detection. Usually there is more than one EF-111A helping jam a mission. Several will fly at different



altitudes and different patterns in order to provide a large area of cover (See figure 3). Depending on the mission, the EF-111A will fly into hostile airspace with the strike force through the entire mission.

## 2.2 F-16 Fighting Falcon

The F-16 Fighting Falcon is the worlds most maneuverable, multi-mission aircraft. With the ability to accelerate into and out of a 9 'g' turn the F-16 can fly circles around its competitors. Designed in the early 1970's, the F-16 was brought about to replace the F-4 Phantom as the United States Air Force most versatile attack aircraft. Fighters were no longer considered missile racks in the sky. Performance was mandatory. The F-16 fills that need. Not only used in air-to-air superiority but as a close air support aircraft it is capable of delivering 16 laser guided bombs to targets 500

miles away. As a fighter, it has a range of over 2,000 miles. The F-16's F-110-GE-100 turbofan afterburning engine is capable of taking the craft to speeds in excess of Mach 2. Dealing with transparencies, the new one piece 'bubble' canopy is one of the major reasons for its maneuverability. It is equipped with AIM-7 Sparrow and AIM-9 Sidewinder missiles. There are three major types of missions that the F-16 perform. They are escort, close air support, and air-to-air superiority. The F-16 has excelled at these so much that it is a major part of NATO forces.

Escort missions usually are comprised of several F-16's flying with larger bomber or refueling aircraft. In such a case the F-16's job is to protect the larger aircraft from hostile enemy fighters. The escort is flown at the same height and airspeed as the bomber. There is not really much technical detail to the escort mission.

The F-16 has recently been tested and shown effective as a close support aircraft. When equipped with the 16 laser guided bombs, the F-16 will begin a pass at approximately 500 kts over the target. Unlike the F-111, the Falcon's bombs are guided in from another tracking aircraft circling over the target area. The F-16 can deliver the bombs in either a low angle attack dive or in the manner of the F-111, a high 'g' pull up and release. In testing, the F-16 has shown great accuracy to the target. The F-16 has enough loiter ability that it can make several passes over the target.

The final type of mission, and what it was designed for,

is air-to-air superiority. Its top speed of Mach 2 and the turn capability combined with its service ceiling of 50,000 ft and its small size, the F-16 is second to none in the air. Since the Fighting Falcon is more agile than most threat aircraft, if it becomes involved in maneuvering for firing position, the hostile aircraft is in for some trouble. There are hundreds of different maneuvers in air combat but for this report, an example will be shown of when an energy fighter, speed and agility, takes on a slower less maneuverable bogey, or hostile aircraft. The key to fighter success is who sees who first. This scenario has the enemy fighter gain the advantage of first sighting. However, the F-16 also takes sight. The aircraft engage head-on. Today's aircraft missile armament is very advanced so the F-16 must not let the enemy attain a missile lock from behind. In this case the F-16 accelerates to Mach 1.5 and goes into a high angle vertical climb, 80 degrees. The enemy cannot follow. Now the F-16 will begin a slow roll around to the left, the enemy fighter is in a circle of his own coming back toward the F-16. Using gravity to gain airspeed, the F-16 accelerates to a 6 o'clock position on the enemy (See figure 4). The bogey begins a turn to escape, he turns left. The F-16 climbs, inverts and pulls positive 'g's as it comes down the inside of the loop. The bogey trying to complete its turn is now on missile lock. The AIM-9 jumps from the left wing of the F-16 leaving the bogey to become a burn mark in the desert. By using its shear capabilities, the F-16 outclasses any enemy aircraft. This

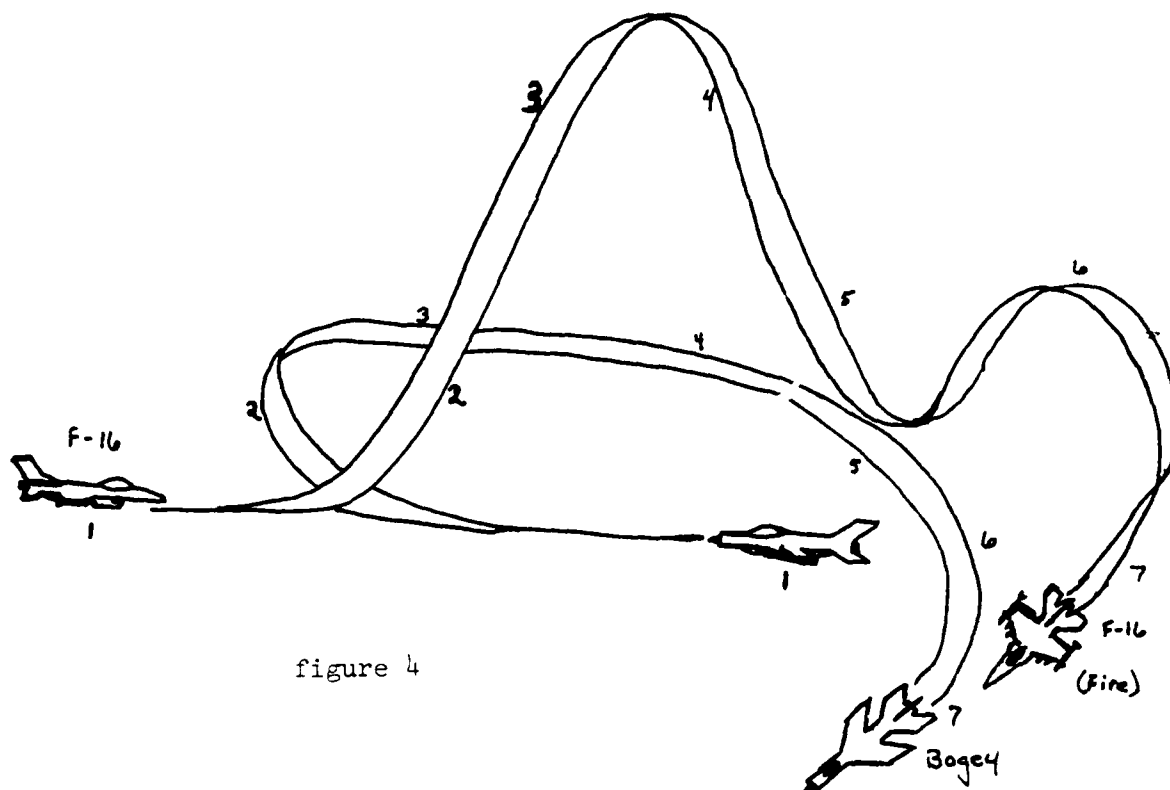


figure 4

was proved when the Israelis and the Egyptians fought in the early 70's. The Israelis using the F-16 and F-15 lost no aircraft. The Egyptians flying Mig-21's and 17's lost 94 aircraft.

### 2.3 F-15 Eagle

The F-15 Eagle is the United States Air Force main air superiority fighter. Although large for a fighter, it like the F-16 is very fast and agile. Mach 2+ maximum airspeed and twin vertical stabilizers have made the F-15 a strong fighter in several air forces throughout the world. Some technical data involves its 60,000 ft. ceiling, its two afterburning turbofan engines which provide 23,000 lbs. of thrust each. Its maximum cruise radius is 200 nm. It is designed for one crew member. It was developed in 1973 to help replace the F-4. The Eagle can hold 24,500 lbs. of ordinance which consist

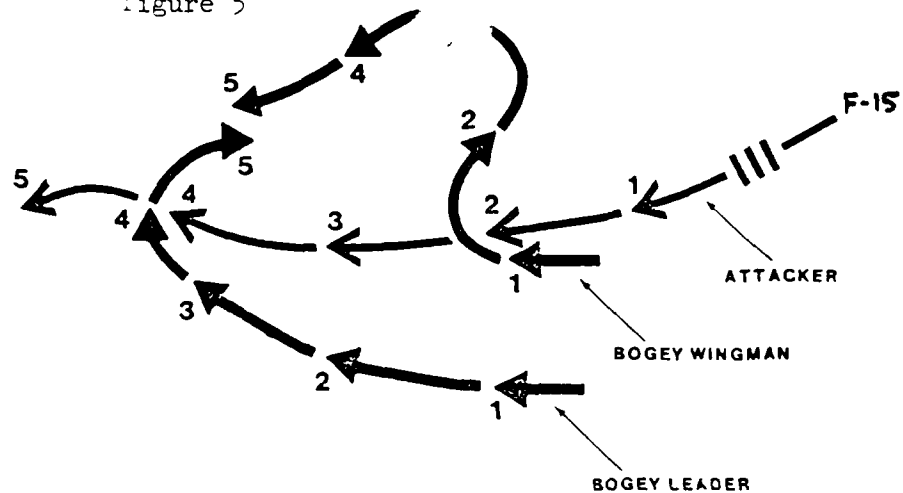
of AIM-7 Sparrows, AIM-9 Sidewinders, 8 AMRAAM's for minimum ground support, AGM-65 Maverick; GBU laser guided bombs, and GBU-15 glide bombs. Its main functions are counter air missions escorting friendly strikes into enemy airspace, making fighter sweeps ahead of escorts, and combat air patrol of friendly borders.

Again escorting missions are not specific, perhaps it would accompany a strike of F-111's to a target area. On these missions, the F-15 is basically there to protect the F-111 from hostile aircraft. The Eagle would not go with the F-111 into the target area unless enemy aircraft had been sighted.

The mission of making fighter sweeps ahead of friendly strikes is done in order to lesson the chance of enemy contact to the strike force. The F-15 almost entices a fight in order to try and destroy some enemy aircraft in the area. Using its great speed and agility, it too can become involved in a maneuvering dog-fight with great success. In this example the F-15 takes on two enemy fighters at once. The F-15 will attempt to break up the enemy formation and destroy one or both of the aircraft. The Eagle approaches from the 5 o'clock position to the bogeys. In an Israeli Tactics Manual it says that "speed is life". Well for the F-15 life is worth living. The 15 will pass the bogey wingman going right to left, crossing in front of him at high speed, Mach 2. The bogey wingman will then has made a sharp right turn and the bogey leader is in a gradual turn right (See figure 5). The

wingman now attempts to turn back toward the F-15. The F-15 is flying toward the leader. With no attempt to fire, the

Figure 5



Eagle driver takes his craft right on by the bogey leader who begins a sharp right turn. Now the bogey leader and wingman are going in opposite directions. They are separated and ready to be engaged by the F-15. All of this maneuvering is high speed and takes just a few seconds to occur. However the confusion of the enemy will take longer than that to be fixed. The F-15 like the F-16 has proven itself in battle.

The final type of F-15 mission is the protection of friendly international borders. Regular patrols in Alaska keep Soviet Bear bombers from getting too close to American airspace. In the Netherlands and other Scandinavian countries, the F-15 watches to make sure the Eastern Bloc countries don't get too friendly. There isn't much maneuvering involved, just flying along side of the bomber to make sure that it doesn't get too close.

#### 2.4 F-5 Tiger II

The F-5 Tiger II is the next fighter to be discussed.

Developed in the early 70's the F-5 saw some action in Vietnam but the aircraft was new and still under development when the U.S. Air Force decided that did not wish to purchase the F-5 as a fighter. The F-15 and F-16 were accomplishing that role. The same size as an F-16, the F-5 was opened up to foreign markets where it did extremely well. The fighters still used in the U.S. are for practice and training purposes only. The service ceiling of 36,500 ft. and the max airspeed of Mach 1.64 were considered excellent compared to what most countries had at the time. It is a very low cost low maintenance aircraft. It can carry 7,000 lbs. of ordinance on its four underwing attachments along with 2 Sidewinder missiles on the wingtips. It has two J85-GE-21B afterburning turbojets that provide over 5,000 lbs. of thrust each. It was designed for maneuverability rather than speed. Its basic roles are escort and ground support. It can however be an interceptor but would do poorly against any high energy fighter.

Escorting once again involves little maneuverability or speed but in taking the attention away from the bombers or refuelers or troop transport it performs well. An average speed of 470 kts is required and it has an escort radius of 305 miles. If it would have to break to a hostile aircraft the F-5 will also perform well. With a combat airspeed of 840 kts and a combat ceiling of 51,000 ft. it can interrupt the attackers plans. Similar to a Mig-17 or 21 it is a threat to the enemy aircraft. A slow energy fighter like the F-5 would need to use maneuverability to beat a modernized high energy

fighter (See figure 6). However, it can be done depending on the quality of the pilots of each aircraft. The F-5 pilot must never get into a speed game with a high energy

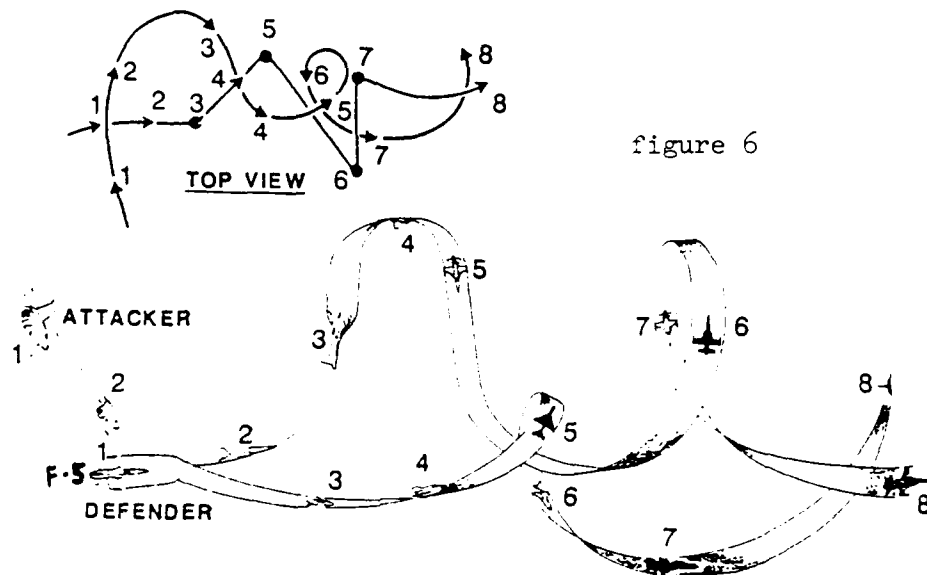


figure 6

fighter, he must use his agility to make to other fighter be agile too. Usually the one that is familiar with this type of combat will prevail, and this is undoubtedly the F-5. In a combat situation similar to this, the F-5 would perform many high 'g', tight turns in hopes of gaining a firing position on the other fighter. Combat altitude for the F-5 is usually around 35,000 ft. The maneuver in Fig. 6 is called the rolling scissors.

The F-5 is also a close support bomber. On a typical bombing mission the F-5 will have an altitude close to the ground, anywhere from 1,000 to 300 ft. above the ground. Again high angle bombing or low angle bombing are used. The significance of high angle bombing is that it is more accurate. However, the aircraft is exposed to enemy fire.

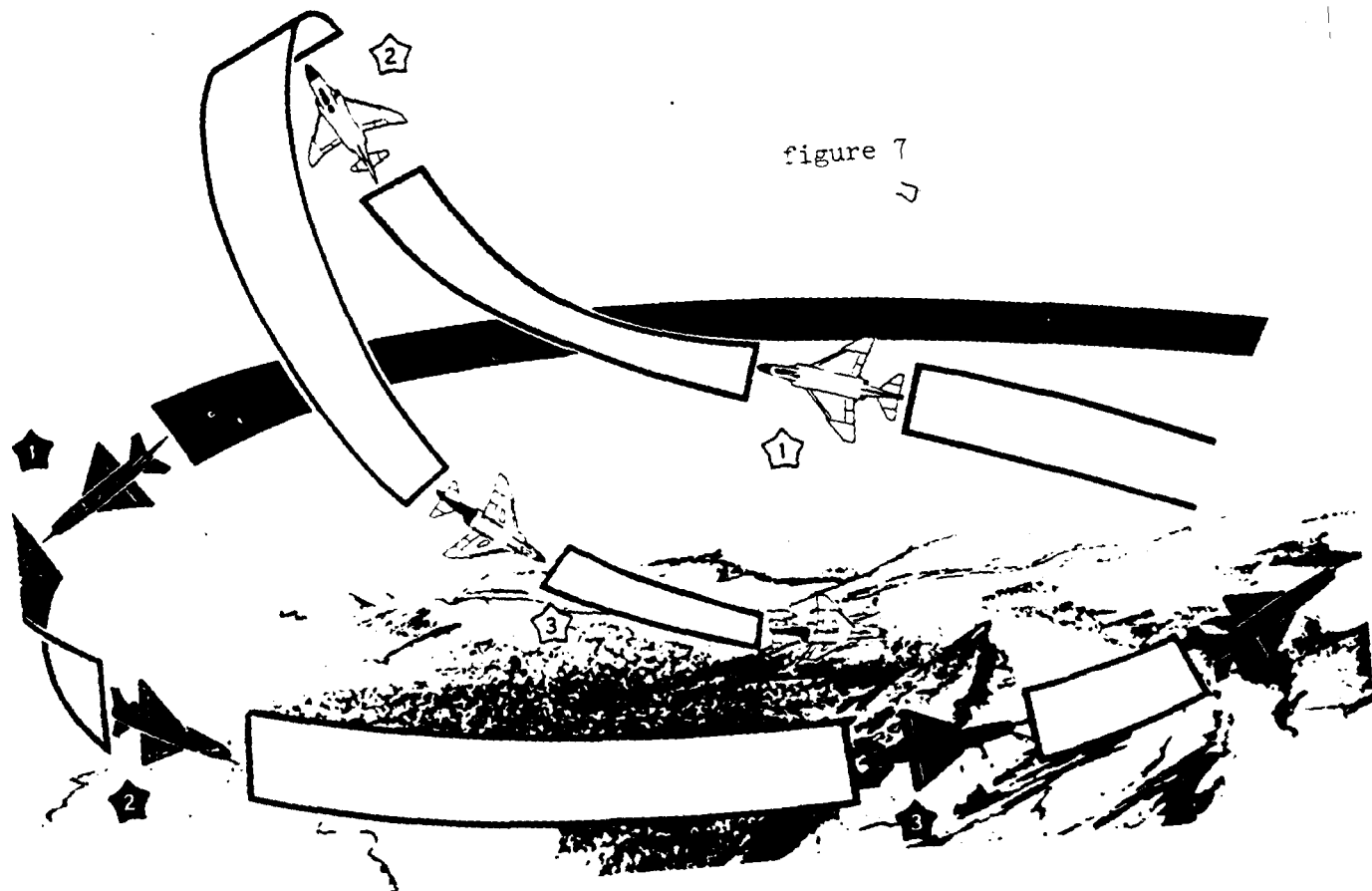


On low angle bombing, the aircraft is safer from enemy attack but is less likely to hit the target. The airspeed during weapons delivery is 654 kts. The F-5 bomber radius is 140 n mi. The bombs it delivers are glide bombs or laser guided bombs like the Maverick AGM-65. One problem in the F-5 is that it is a day/night VFR fighter, which means bad weather can force canceled missions or reduced flight time.

#### 2.5 F-4 Phantom

Since the beginning of the jet age to the early 1970's, no aircraft, fighter or bomber, has performed as well or as long as the F-4 Phantom. The workhorse of the Vietnam war it survived scrutiny and technical problems to become the greatest historical aircraft. Almost phased out of active duty in the U.S. Air Force it has served for 30 years as the number one fighter. Still in use in the reserves and other countries, the F-4 is long from dead. The day/night foul weather aircraft could use just about any type of armament that could be put on it. Its two J-79-GE-15 turbojet afterburning engines produced 17,900 lbs. of thrust each to carry the 61,795 lb. aircraft into combat. A two seater, pilot and radar, weapons officer, the F-4 carries AGM-88 HARM, 4 AIM-7E Sparrows, AGM-45A Shrike, and array of free fall bombs plus napalm canisters. Also external fuel storage can be attached to increase range. Its ceiling is 40,000 ft. with maximum airspeed of Mach 2.0. Its combat roles include escort, fighter intercept, close ground support, and border patrol. The F-4's typical tactical range is around 700 nm.

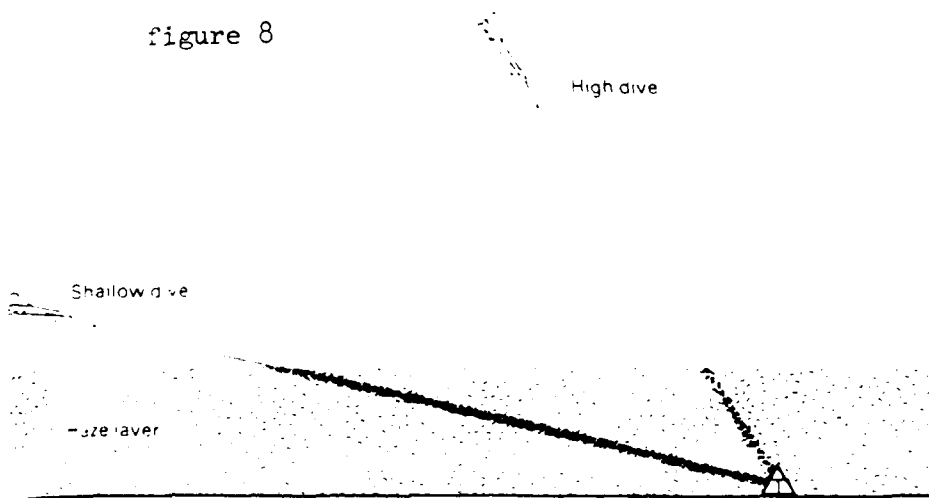
As a combat interceptor, the F-4 performed well. Not a speed demon but not slow, the F-4 had to deal with the quickness of the Mig-17 and 21. Some consider the F-4 to be a platform for the launching of missiles. In Vietnam the F-4 faced a quicker but less armed Mig-17. The F-4 statistically should have been totally dominant over the Mig. It was hard for the F-4 crew to engage because of the Migs speed and unwillingness to fight in a tricky situation. Generally the F-4 would win if there was an engagement but not because the plane was better, because of the tactics used. F-4's would engage the Migs in situations where it was to the F-4's advantage. One maneuver used by the F-4 is the High YO-YO (See figure 7). In order to avoid an overshoot of the



quicker Mig-17, the F-4 rolls a quarter turn and pulls into the vertical plane. The nose should continue to come up and roll toward the enemy. As the enemy continues his turn, the F-4 brings his nose back around and lines up with the Mig, at a six o'clock position. Once aligned the F-4 is free to fire on the enemy.

As a combat close support bomber, the F-4 performs extremely well. As the F-4 approaches the target, the pilot is putting the aircraft through small high 'g' turns to avoid enemy tracking as he pulls into final approach on the target. If the attack is low angle, the F-4 will descend to about 200 ft. and drop part of his ordinance at the time the GIB, guy in back, signals (See figure 8). As the F-4 leaves the drop zone, it will pull into a high 'g' turn and proceed back into the bombing pattern. If the attack is a high angle, (See figure 8), the F-4 will begin a dive toward the target releasing and pulling up at the time signaled by the GIB. The high angle attack is usually more accurate.

figure 8

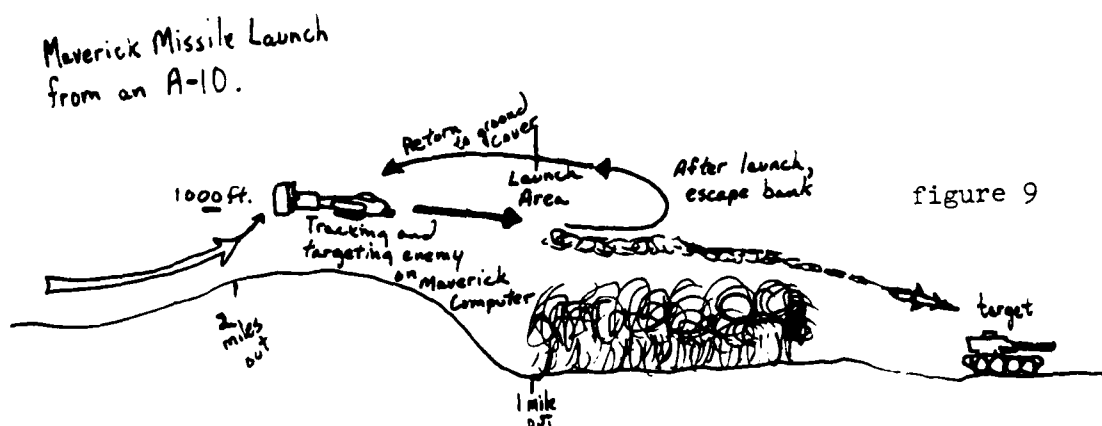


## 2.6 A-10 Thunderbolt II

In December 1974, the Fairchild Republic A-10 Thunderbolt II, better known as Warthog, made its maiden flight. Since then it has proven itself to be the U.S.A.F.'s best close support aircraft. The weapon behind, or literally in front of, the A-10's success is the GAU-8/A 30mm gun. This armor piercing cannon fires 50 rounds per second and can be fired while the aircraft is at full speed. Another of its steps to stardom is its capability to carry large loads of conventional bombs under each of its 25 ft. wings. Four pylons on each wing plus 3 under the fuselage can hold up to 16,000 lbs of ordinance. The thrust of the A-10's two huge TF34-GE-100 engines is 9,065 lbs each and can take the 50,000 lbs. maximum weight aircraft up to 400 kts. Its mission time averages short of four hours with an incredible 1.7 hour loiter time around the target. The A-10 is a single seat aircraft. The maximum ceiling is over 44,000 ft. The average combat radius is between 250-400 miles from home base. The A-10 holds various types of ordinance. The AGM-65 Maverick missile, occasionally 2 sidewinder missiles for self defense purposes, and several types of free fall and glide bombs. Through the use of its split aileron as an airbrake the A-10 can land on extremely short, unpaved, battle damaged runways. This allows the A-10 to remain close to the front line of battle. The A-10 has several missions it performs in contact. Close air support is the specialty, reconnaissance, and escort.

The A-10's close support ability is what makes this

aircraft valuable to the combat situation. The loiter range allows the A-10 to supply continuous fire to the target area. A typical Maverick missiles delivery will be explained. The A-10 which usually travel in pairs would approach the target at tree top level. Due to the low airspeed of the aircraft it can fly more precisely. When the A-10 is 2 miles from the target it will pull up to 1000 ft. (See figure 9). Here the pilot will select the target on the Maverick TV monitor. Depending on the weather, the pilot will take the A-10 in close enough that the TV monitor and computer of the missile can recognize the target. Once selected the pilot will wait



till the A-10 is one mile from the target and launch the missile. During the time the aircraft is at 1000 ft. the pilot is constantly turning the aircraft back and forth, this is called jinking. After release the A-10 will bank hard away from the target and descend to tree-top level once again and head for home. A typical pass over the target with the GAU 8/A 30mm gun will now be explained. Once again the A-10 will approach at tree-top level toward the target. When one mile out the A-10 is pulled to 700 ft. All the time jinking to

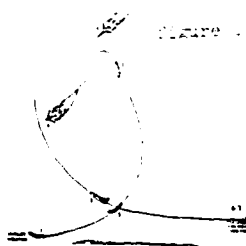
avoid ground fire. The target is sighted by aiming the nose of the aircraft at the target. Once sighted, the pilot will squeeze the trigger for one second, sending 50 rounds toward the target. After the pass, the A-10 once again breaks off on a hard turn. If there are two A-10's, they can set up a circle pattern and place continuous heat on the target area. The A-10's biggest threat is the Soviet Hind helicopter. Because of the low maximum airspeed of the A-10, helicopters pose a serious threat. The only good way to confront a helicopter by a fixed wing aircraft is head on. Fortunately, the gun of the A-10 works very well on helicopters. It works well on fixed wing aircraft also. The technic in dealing with a hostile fighter threat is to aim the nose at the bogey and spray it with the 30mm.

## 2.7 A-7 Corsair II

The final aircraft to be discussed is the Vought A-7 Corsair II. Delivered from production in 1968, the A-7 is a single seat, close support aircraft. It is an all weather bomber that saw time in Vietnam and in action over Libya. Although not its main mission, the A-7 can also be an interceptor and performed this mission in Vietnam. During action it had an extremely high kill ratio. This was due in part to the navigation and weapon system delivery system. Its Allison TF41-A-1 afterburning turbofan provides 14,250 lbs. of thrust. Its weaponry includes the AGM-65 Maverick and the AIM-9 Sidewinder. Its other arsenal includes gator mines, rockets, and gun pods. All of this hangs under its 6

underwing racks and 2 under the fuselage. It can also be equipped with the KB-18A Panoramic 70mm camera which is automatically turned on when weapons are released. All in all the A-7 can carry 15,000 lbs of ordinance. The A-7's top airspeed is 698 mph and it has a range of 2871 miles.

The A-7 bombing mission is basically ground support for combat troops. It is similar in tactics as the F-4. High angle dive attacks or low angle dive attacks, usually depending on cloud cover. Differences would be that the A-7 has an on the deck airspeed of 480 kts. Using the Pave Penny laser target tracking system, the A-7 drops its laser guided bombs from about 400 ft. Jinking is also used as a tactic for ground fire avoidance. In dealing with fighter interceptance, the A-7 is considered an energy fighter and uses its speed to deal with opponents. Vertical climbs were often used in the Vietnam war by A-7 pilots to gain airspeed on the way down to catch the Mig. On a wings level sustained 'g' pull up it is important to keep the bogey in sight so that when the descent is started the aircraft can be aimed toward the enemy (See figure 10). During the descent to the enemy the pilot should sustain zero or slight positive 'g's in order to keep maximum efficiency during the "zoom". The A-7 is currently used by the Navy and Air Force Reserves.



### 3.0 Conclusions

The main reason for this research project was so that there is data compiled on current U.S.A.F. fighter aircraft when the durability facility at Wright-Patterson AFB is completed (See figure 11). The durability facility is designed to test transparencies by simulating a flight environment. This is done by a combination of hot and cool air being passed over the transparency. The transparency is pressurized from the inside. The information compiled will be used in the testing procedure to help in the simulation process. It is helpful in the test planning to know a little bit about the aircraft and the different stresses and missions that each goes through in combat. Data on maximum airspeeds and combat ceilings can be figured into the testing procedure. The durability facility is designed to test aircraft transparencies by putting it through the conditions it would go through on the actual aircraft without putting it on the actual aircraft. The F-111 transparency is scheduled to be tested first.

The experience of working in at Wright-Patterson AFB in the Aircraft Windshield Systems Program Office has been both rewarding and fun. Rewarding is the knowledge I gained on how the United States Air Force works. Since I am planning to be commissioned in 4 years into the Air Force, this knowledge is invaluable. Also the experience of working in an office environment was rewarding. The research I participated in and observed dealt with the area of interest I have in Air Force





# DURABILITY FACILITY

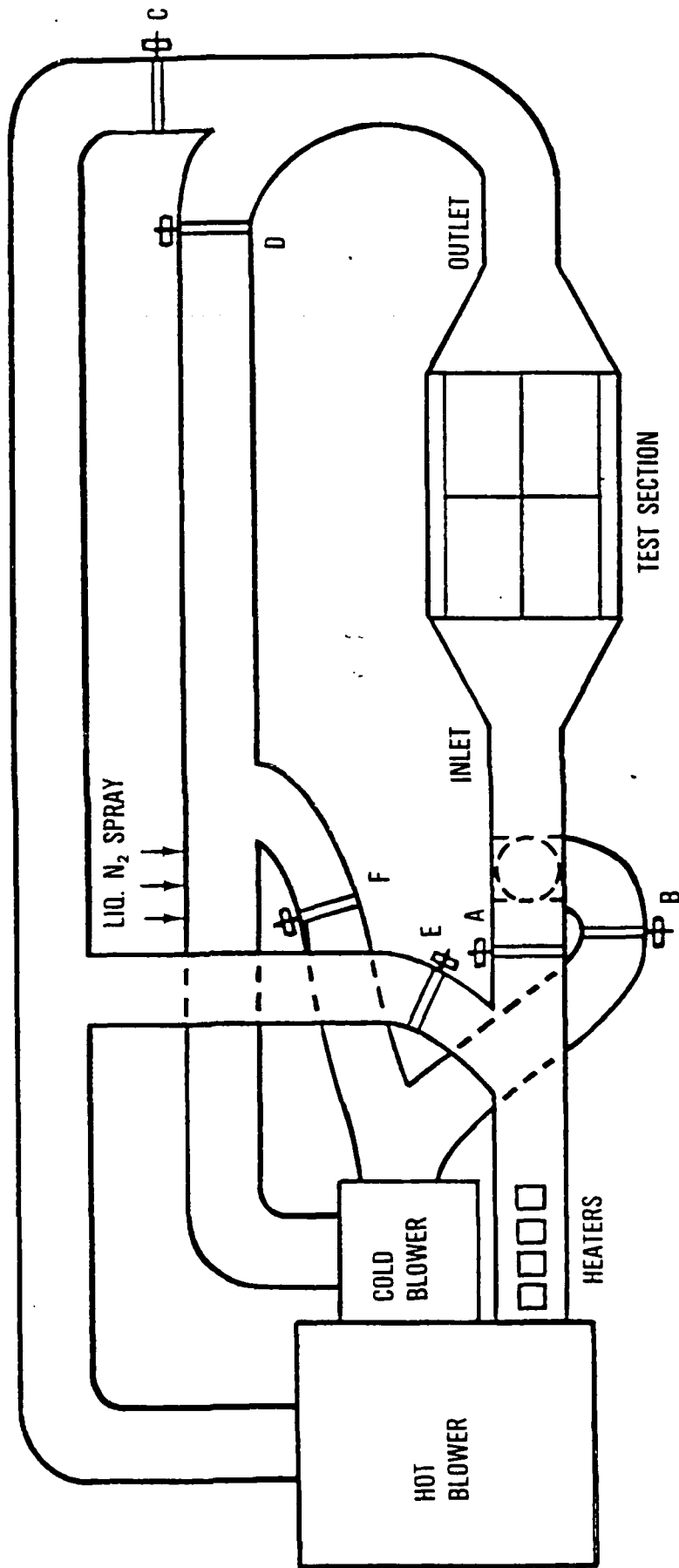


figure 11

A - HOT LOOP    C - HOT LOOP STOP    E - HOT LOOP BYPASS  
B - COLD LOOP    D - COLD LOOP STOP    F - COLD LOOP BYPASS

aircraft. I am very interested in fighter aircraft and the research I did helped me learn more about each different aircraft and influenced me on which aircraft I would like to fly. However, the most important experience is that of friendship and fun I had with the personnel in the office. Both through comedy and teaching they made my 8 weeks most enjoyable. Someday I hope to return the favor to someone else as interested as I am in the aviation field.

### References

- Nicholas, Ted G. U.S. Military Aircraft Data Book, 1988. Tenth Edition. Data Research Associates. 1987.
- Kinzey, Bert. The F-111 Aardvark. In detail and scale. Aero Publishers, Inc. Arms and Armor Press. 1982.
- Kinzey, Bert. The F-4 Phantom II. In detail and scale. Aero Publishers, Inc. Arms and Armor Press. 1982.
- Kinzey, Bert. The F-5 Tiger II. In detail and scale. Aero Publishers, Inc. Arms and Armor Press. 1982.
- Kinzey, Bert. The F-16 Fighting Falcon. In detail and scale. Aero Publishers, Inc. Arms and Armor Press. 1982.
- Kinzey, Bert. The A-10 Warthog. In detail and scale. Aero Publishers, Inc. Arms and Armor Press. 1982.
- Kinzey, Bert. The F-15 Eagle. In detail and scale. Aero Publishers, Inc. Arms and Armor Press. 1982.
- O'Brien, Frank J. The Hungry Tigers. The fighter pilots role in modern warfare. Tab Books. 1986.
- Boyne, Walter J. Phantom in Combat. Smithsonian Institution Press, Washington D.C. 1985.
- Skinner, Michael. Red Flag. Presidio Press. 1984.
- Siuru, Col. William D. and Holder, William G. General Dynamics F-16 Fighting Falcon. Aero Publishers, Inc. 1983.
- Stevenson, James Perry. MacDonald Douglas F-15 Eagle. Aero Publishers, Inc. 1978.
- Miller, Jay. F-111 Aardvark. Aero Publishers, Inc. 1982.

TESTING THE ENVIRONMENT'S EFFECTS ON  
EQUIPMENT

Written by: Valerie Petry

Mentor: Amar Bhungalia

WRDC/FIVEC

Flight Dynamics Laboratory

Vehicle Subsystems Division

Environmental Reliability Group

Date: 16 Aug 89

## 1.0 ACKNOWLEDGEMENTS

I would like to extend my appreciation to everyone in Building 45, Area B, Wright-Patterson Air Force Base, especially the people in Environmental Reliability Group, Advanced Thermal Management Group and the contractors who helped me: Ron Gould and Bob Edwards.

## 2.0

## SUMMARY

From 19 Jun to 16 Aug, I have worked with Avionics Environmental Reliability and Advanced Environmental Control Systems. I tested the software created by WRDC/FIVE and helped with refinement (see attachment 1). I also became familiar with VAX/VMS operating system.

### 3.0 Avionics Environmental Reliability (AER)

3.1 I was working on a program that tests Line Replaceable Units (LRU). LRUs are the so called black boxes of aircraft. This program uses vibration and thermal stresses to find the life of a Printed Circuit Board (PCB) in a LRU. These results will be compared with experimental results. This program will be useful to the people who design LRUs.

3.2 The main objective of the program was to make it user friendly and to automate the process. For one week, while the VAX/VMS System was down. I had to run this program in the manual mode. There are several steps to this manual version.

3.3 I used a DIGITAL VT240 model for all of my data entry. On this terminal, I logged into VAX/VMS on .FDLENG (Flight Dynamics Laboratory ENgineering).

3.4 I was assigned the task to analyze commonly used electronic components: Dual In-line Package (DIP), Hybrid, Pin Array, Flat Pack, Leadless Ceramic Chip Carrier (LCCC) while they are mounted on a PCB. These PCBs were installed in a LRU. The vibration levels are transferred from Avionics Bay to LRU and PCB to electronic components. For given

vibration levels, the life will be directly proportional to location of component on PCB. The structural finite element model of a LRU, PCB, and electronic component is shown in Figures 1 through 3. The results of this task are summarized in Figures 4 through 8.

3.5 The AER Executive gives me commands choices (see the appendix). I typed ANALYZE and started typing in the data for a test case. The program would ask me for the dimensions of the LRU and PCB and specific information about the electronic component. It would ask me for the stand off height, if the leads were bent or side brazed, if the leads were notched, the thickness of the leads, and for other pertinent information.

#### 4.0 ADVANCED ENVIRONMENTAL CONTROL SYSTEMS (AECS)

4.1 I also tested vapor cycle refrigeration systems and air cycle systems. I was comparing these results with previous results from the AECS program on the CYBER or CDC. I was running these tests, so that the engineers could tell if the program on the CDC and the VAX computed the same results.

4.2 I was testing a variety of test case systems. I also tested heating, refrigeration, and thermodynamic power cycle systems and their individual components. The test cases which I duplicated were a compressor, an expander, a refrigerator pump, a condenser, an evaporator, a refrigerant line, a vapor cycle system, a simple power cycle, a refrigeration cycle with two parallel evaporators, a NBC Carbon test and a combined refrigeration and power cycle.

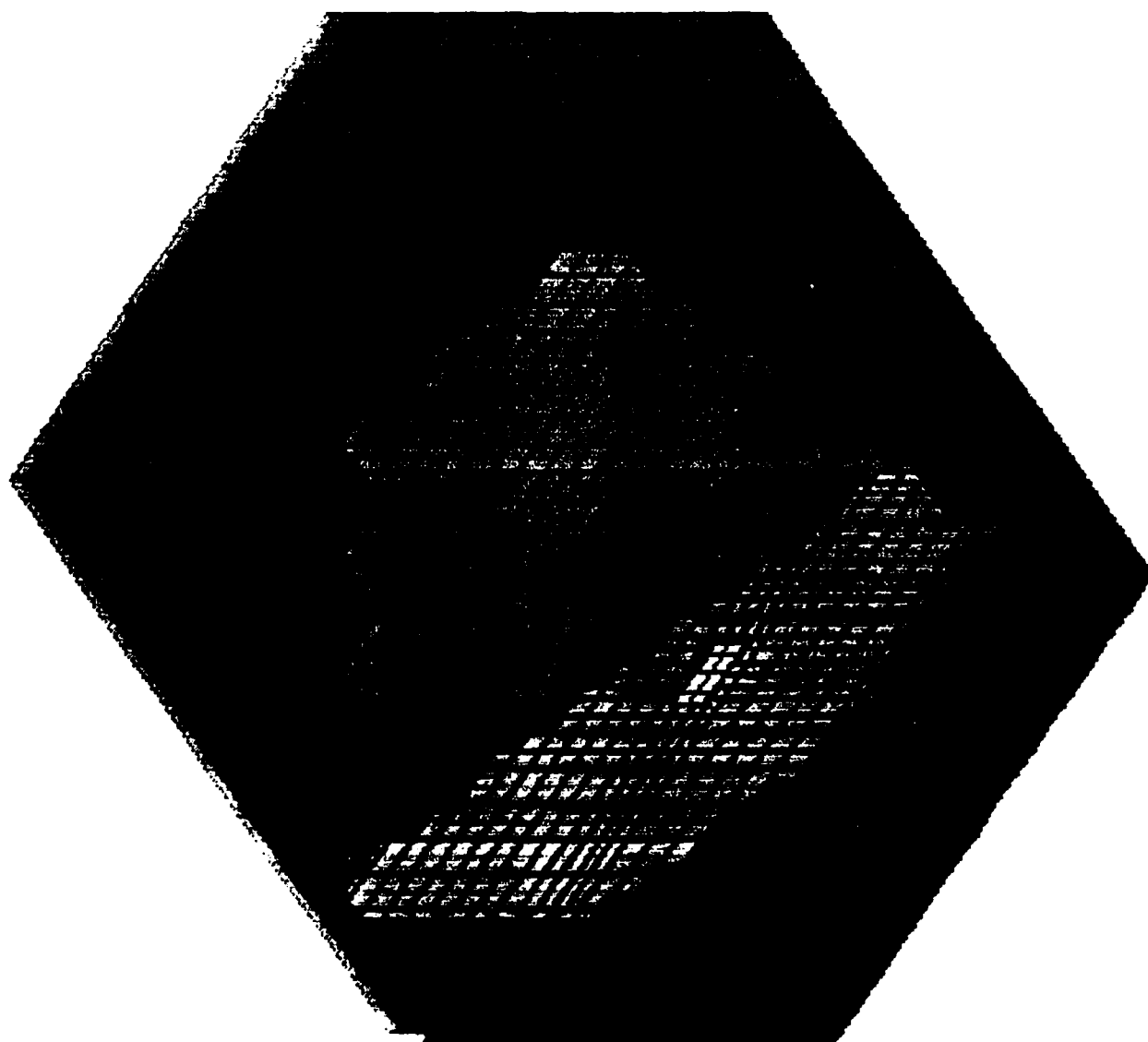


Figure 1: LRU Finite Element Model



1 ROTATE

2 ZOOM

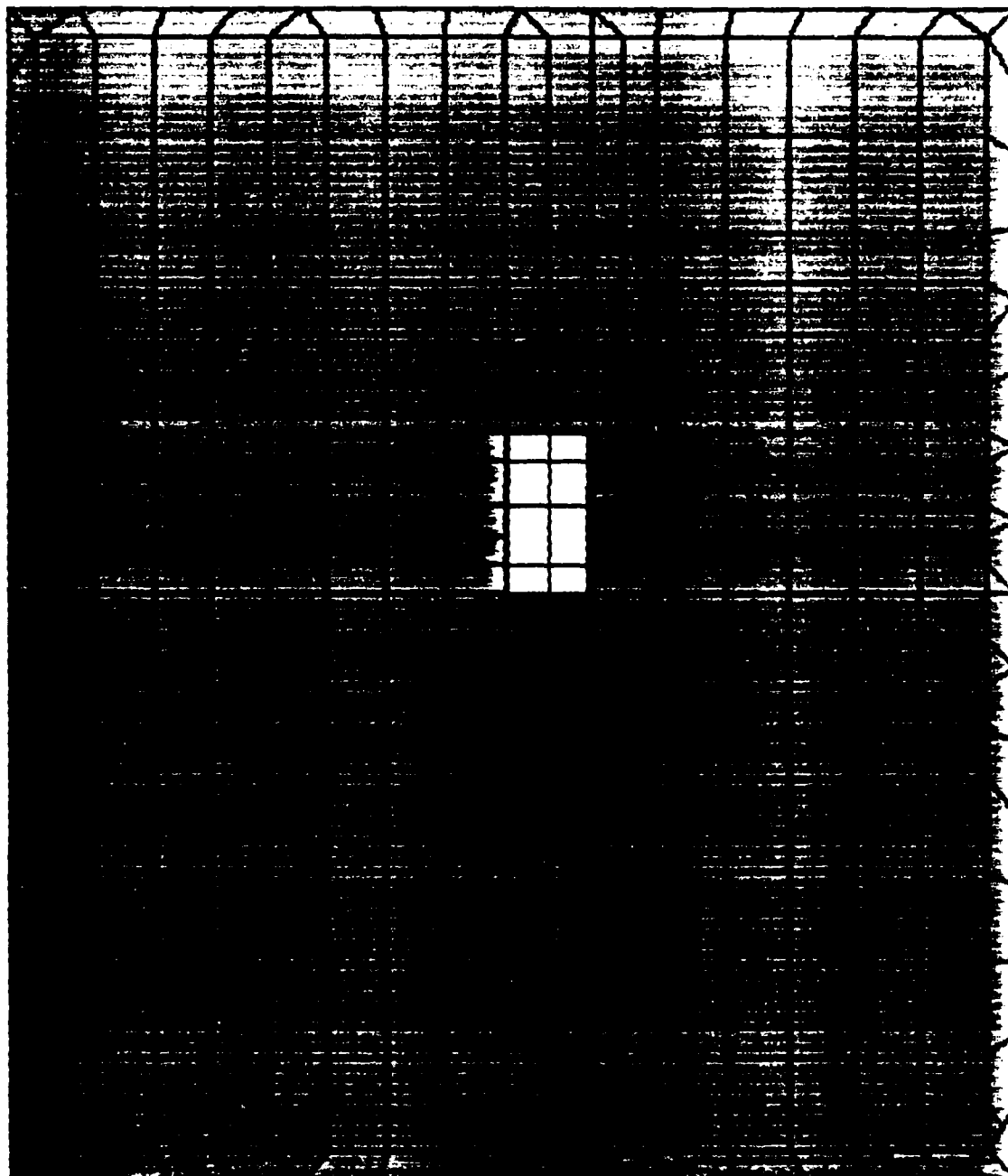
3 RESET COLORS

4 HOD-ELITE HOD

5 MAIN MENU

Type 1 2 3 4 5

RX= 0  
RY= 0  
PZ= 0



MESH for PCB # 1

Figure 2: PCB Finite Element Model

1 WHOLE PLOT

2 ZOOM AGAIN

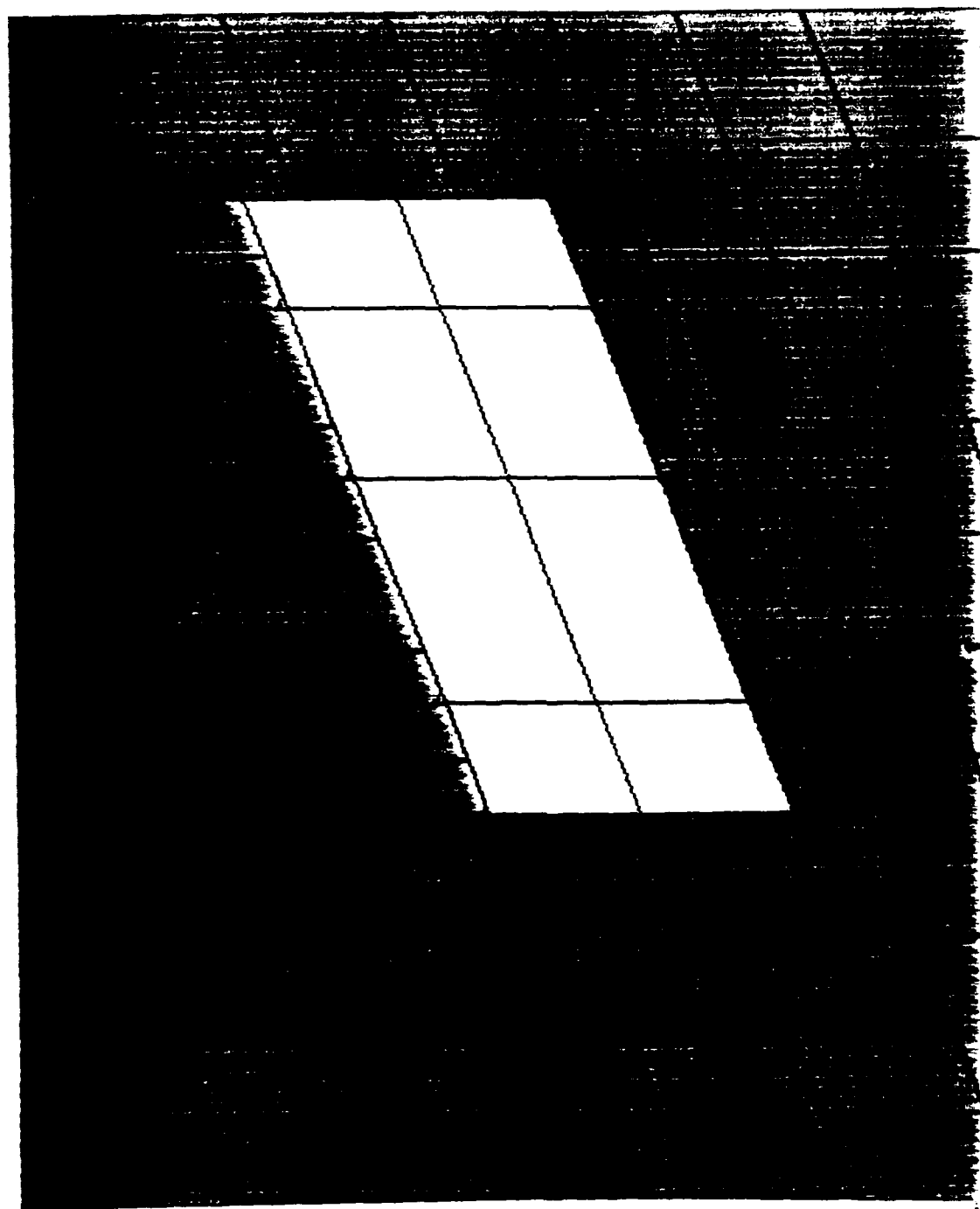
3 HOD-ELMT NUM

4 MAIN MENU

Type 1 2 3 4

RX = -35  
RY = -35  
PZ = 0

Y  
Z



MESH for PCB # 1

Figure 3: Detailed Model of Electronic Component

E.M.R.C.- DISPLAY II POST-PROCESSOR VERSION 88.0 Aug/ 4/89

MODE SHAPE PLOT  
MX. DEF - 1.22E+02  
NODE NUMBER = 397  
SCALE = 4.0  
(MAPPED SCALING)

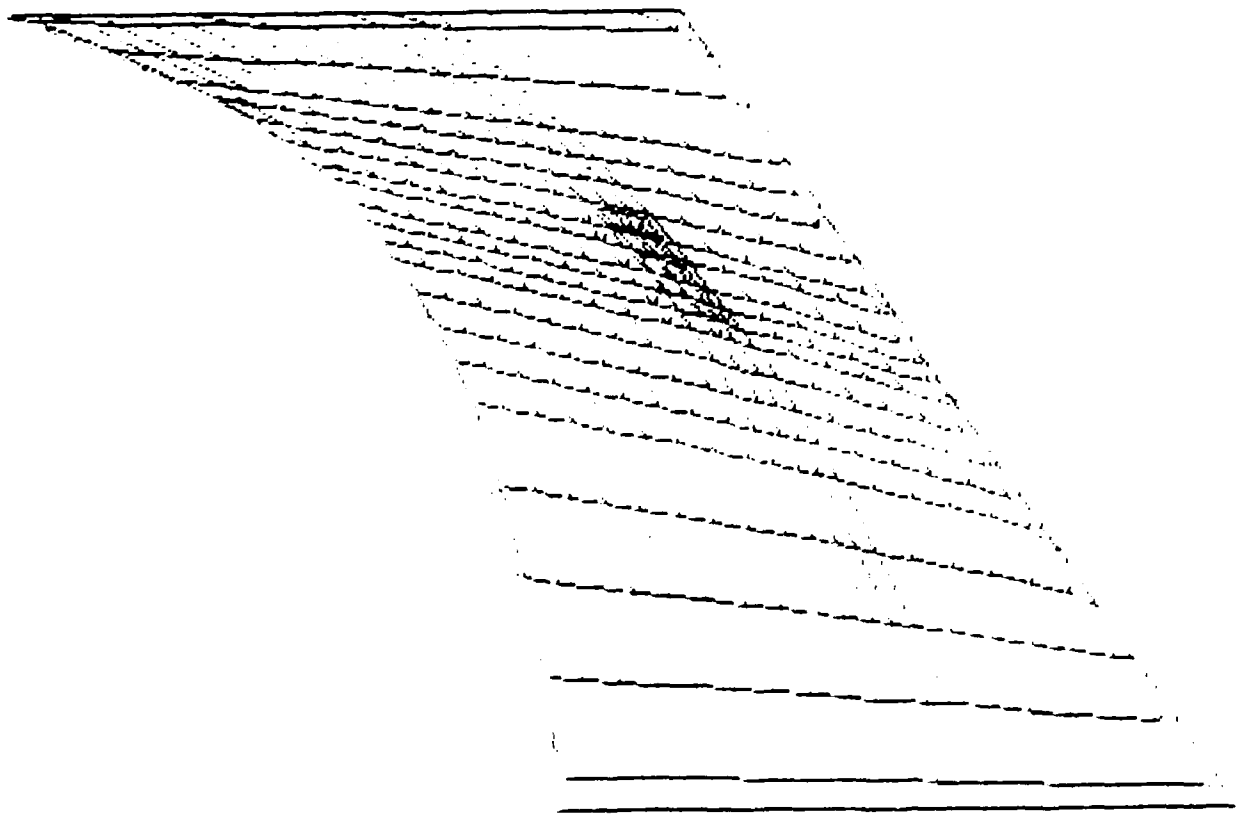
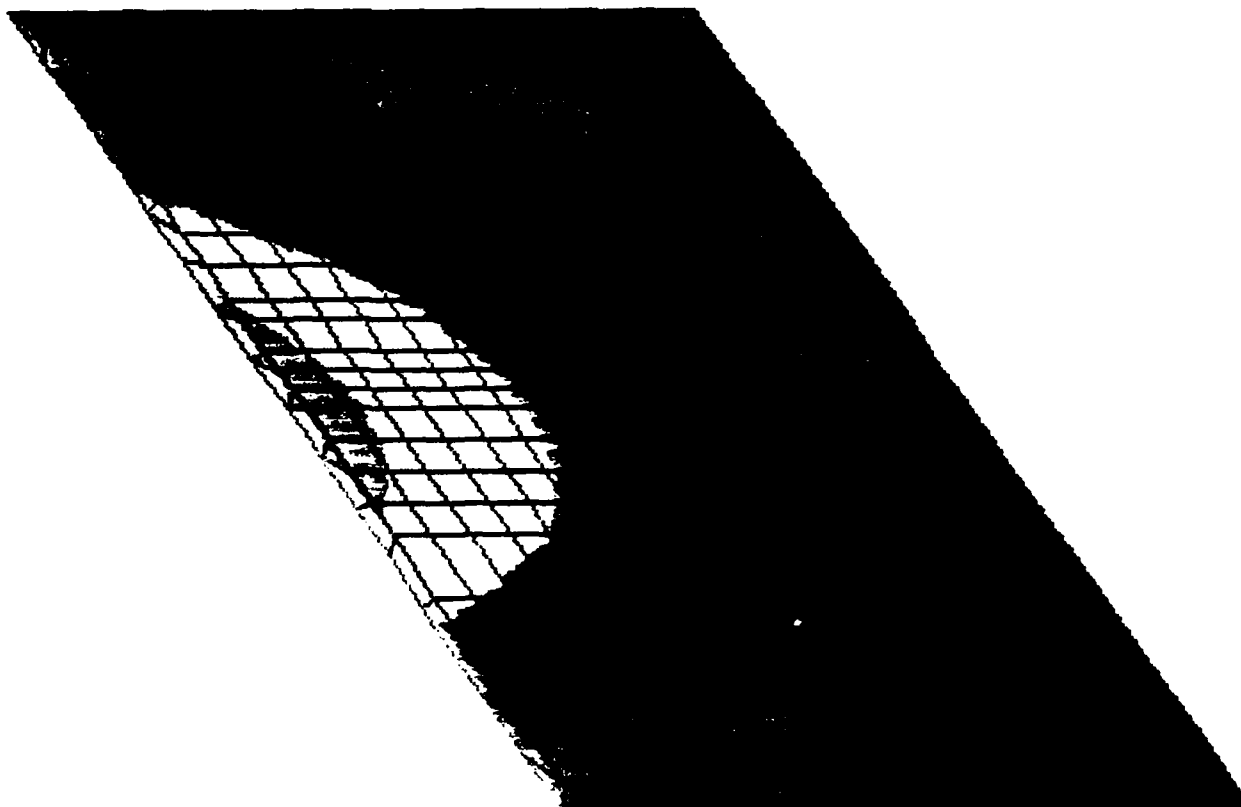


Figure 4: Deformed Mode of First Dynamic Frequency

E.M.R.C. - DISPLAY II POST-PROCESSOR VERSION 88.0 Aug/ 4/89

DISPL. CONTOURS  
Z - DISPLACEMENTS  
VIEW : 0.00E+00  
RANGE : 1.22E+02



122.0

108.4

94.89

81.35

67.78

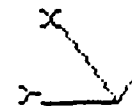
54.22

40.67

27.11

13.56

0.0



RX= 45

RY= 45

MODE NO. = 1 FREQUENCY = 1.000000000000

MESH FOR PCB # 1

Figure 6: Deformed Contours of First Dynamic Frequency

E.M.R.C.- DISPLAY II POST-PROCESSOR VERSION 88.0 Aug/ 4/89

MODE SHAPE PLOT  
MX. DEF= 1.40E+02  
MODE NUMBER= 397  
SCALE = 4.0  
(MAPPED SCALING)

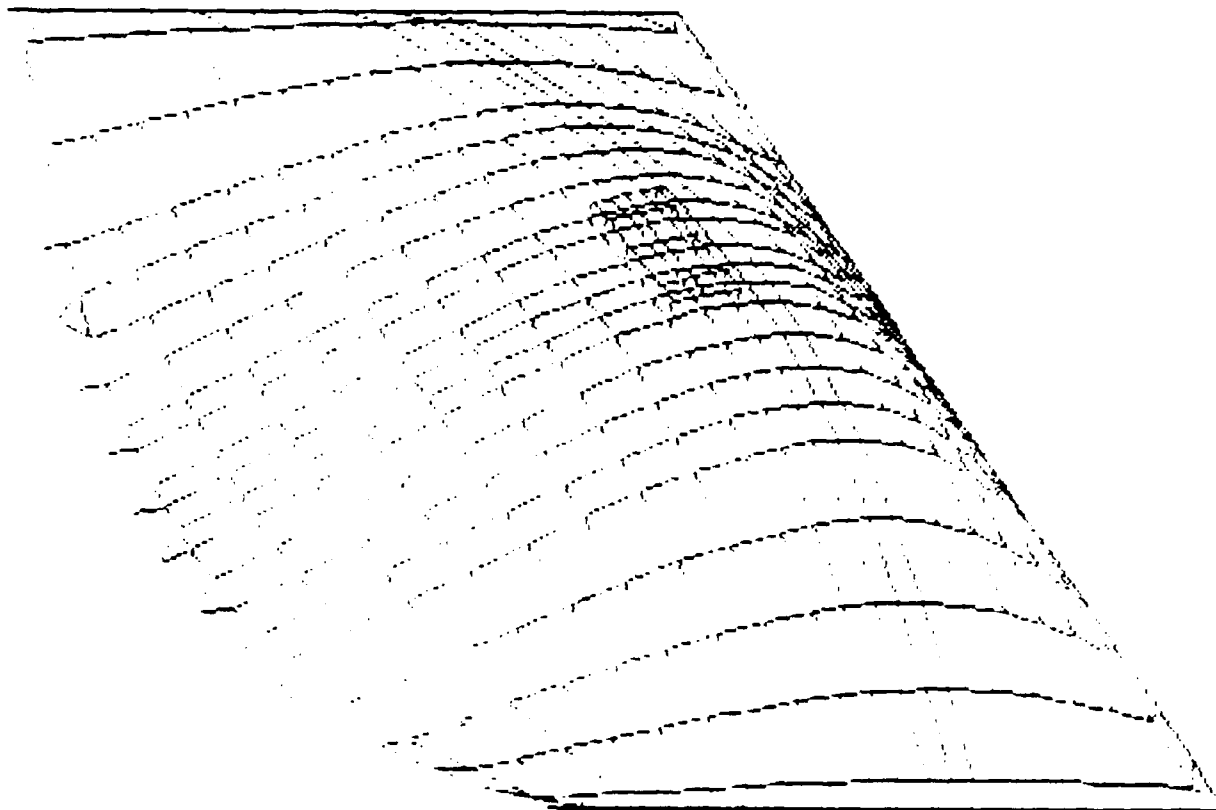


Figure 6: Deformed Mode of Second Frequency

STRESS CONTOURS

VON-MISES STRESS

VIEW : 8.32E+01

RANGE : 2.43E+04

(Equiv. 1.0E2)

243.4

216.4

189.5

162.5

135.6

108.6

81.68

54.73

27.78

0.8317

RX= -45  
RY= -45  
RZ= 0

SOLID LEAD MODEL RECTANGULAR CROSS-SECTION

LOAD CASE NO. 1

Figure 7: Dynamic Fatigue Stresses  
in a Component Lead Wire

# STAND OFF HEIGHT/NUMBER OF CYCLES

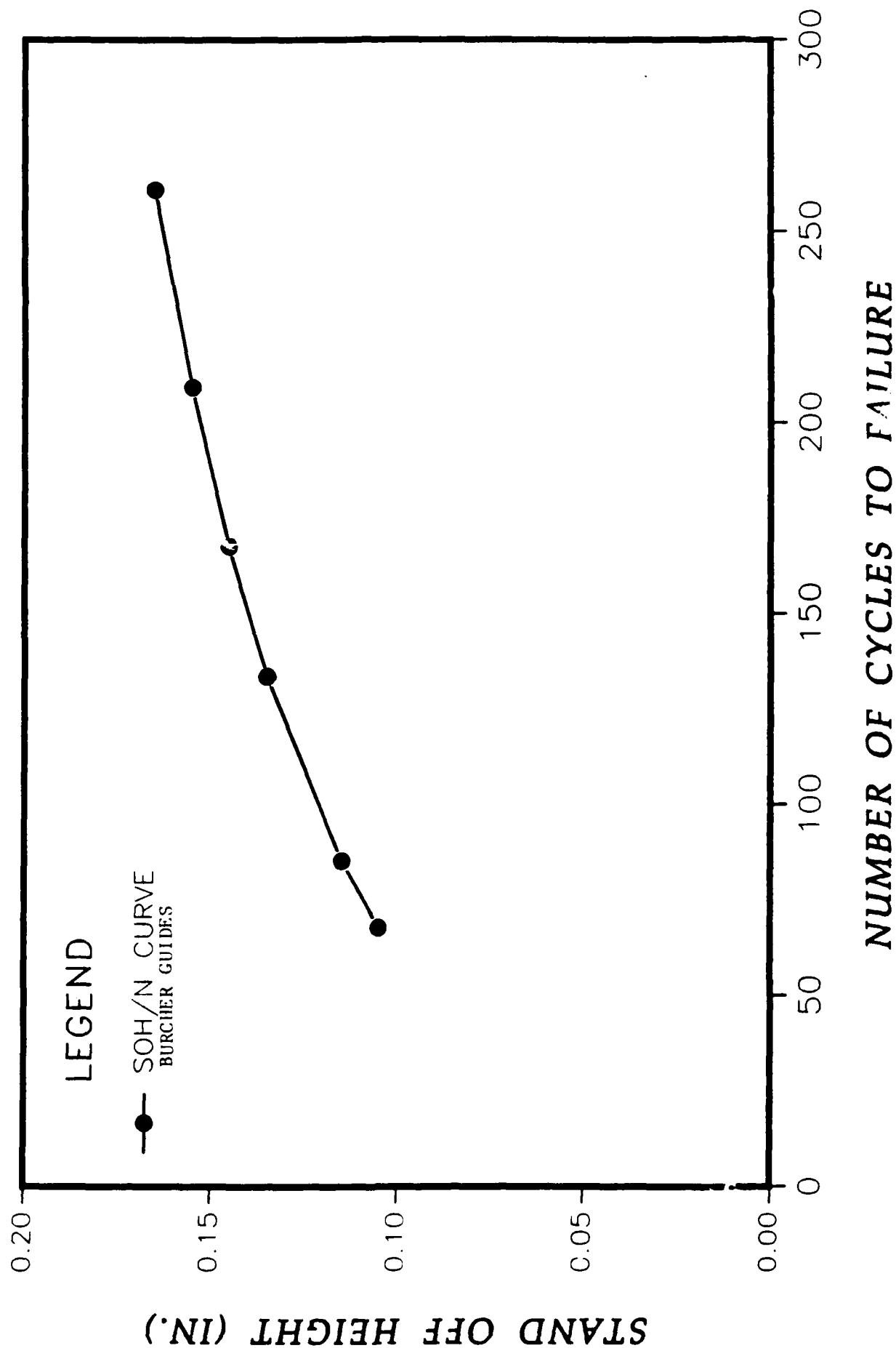


Figure 8: Plot of Predicted Life vs. Stand-Off Height

ATCH 1

MEMO: For the record

28 Jun 89

SUBJECT: NISA Input

THERMAL AUTOMATIC RUN

GENERAL COMMENTS

Suggestions are underlined throughout this attachment.

1. The computer asks if the user wants to redefine values or maintain current values. When it does, the user are not able to change all of the values in that section. It only asks for values in the table which is presented before the question, and it requires that you reenter all of the values in the table.

The program should be modified such that the user can change single values of that interactive section enabling the RETURN to default values unchanged.

2. The system asks for the user to enter the material properties which compose the PCBs.

The system should automatically feed in all required properties for the commonly used PCB material from a graphic station terminal.

SPECIFIC COMMENTS

PHASE 1

3. NISA can be used in two ways

y --Define a new problem(PCBs etc)

n --Restart for previosly defined PCBs and their components.



## PHASE 2

4. Same as Phase 1 problem of defining new problem or res.
5. The RESTART process can be executed to:  
y --Generate finite element meshes(PCBs or pins)  
n --Display previously generated meshes process heat transfer results or predict life.
6. The post-processing can be executed to:  
y --Write heat transfer results into static files  
n --Plot finite element meshes or predict life.

## PHASE 3

7. Same as Phase 1 problem of defining new problem or restart.
8. Same as Phase 2, RESTART process.
9. Finite Element Meshes can be created for:  
y --A set of PCBs(restart process)  
n --Solid model of end pins of a component  
Do you wish to generate PCB meshes? (y/n)
10. Enter the No. of the PCB you wish to analyze (0 to stop)  
Modify NISA so that if there is only one PCB, NISA will ask if the user wishes to proceed.
11. Enter the No. of the critical component the user wishes to analyze. (0 to exit)  
Modify NISA so that if there is only one critical component NISA will ask if the user wants to continue.
12. Does the user wish to analyze another component within

the same PCB? (y/n)

If a PCB only has one component which was just analyzed,  
the computer can not analyze another component on that  
PCB.

13. Do you wish to analyze another PCB? (y/n)

If only one PCB composes the LRU, there are not any more  
PCBs in that LRU to analyze.

#### PHASE 5

14. Same as Phase 1 problem of defining a new problem or  
restart.

15. Same as Phase 2 problem, RESTART process.

16. Same as Phase 2 problem, post-processing.

17. In order to make NISA more user friendly, NISA should be  
modified to ask what process the user would like to  
engage:

1) Mesh Generation

2) Heat Transfer Results

3) Predict life

4) Read input from a file

5) Define a new problem

18. Is this a SURFACE MOUNTED component? (y/n)

This question has been previously answered in Phase 4 and  
was stated with the stress values at the beginning of  
Phase 5.

19. Enter the stress concentration factor Kt (est)  
(default=1.0)

NISA asks this question twice. This option does not  
default to 1.0 when the user presses RETURN.

## APPENDIX

### AER EXECUTIVE

#### ANALYZE

ANALYZE sets up a directory for each test case. It also is used to create and submit the job created by different phases.

#### BREAK

BREAK is a routine written for coffee breaks, it allows the user to leave and the characters will not burn onto the screen.

#### EMRC1

This is the older version of AER that requires interaction between the user and the computer.

#### PLOT

PLOT allows the user to look at the data files containing values to plot a mesh.

#### QUIT

QUIT returns the user to the root directory.

#### REMOVE

It deletes all files and the subdirectory of a specific case.

#### SHOW

SHOW calls up the subdirectory of each case. It lists all of the files on the screen.

#### STATUS

STATUS shows the user the phases that have been completed or are in the process of being completed.

## APPENDIX (continued)

### TRANSFER

This command lets the user be placed in the subdirectory of a specified test case.

### VMS

VMS allows the user to enter most VAX/VMS commands and return to the AER Executive.

## REFERENCES

1. Advanced Environmental Control System  
Final Report AFFDL-TR-76-68, Volume II  
For Period August 1976 - May 1977  
Published In February 1978
2. Rough Draft of Avionics Environmental Reliability User's  
Manual
3. Meeting with Amar Bhungalia on August 4, 1989
4. Thermal Cycling Reliability Life Model For Avionics  
AFWAL-TR-88-3075  
Final Report for Period February 1986 - May 1988  
Published In June 1989
5. Vibration Reliability Life Model For Avionics  
AFWAL-TR-87-3048  
Final Report for Period September 1985 - July 1987  
Published In September 1987
6. Vibration Stress Analysis of Avionics  
AFWAL-TR-87-3023  
Final Report for Period September 1985 - November 1986  
Published In April 1987

Apprentice: Kimberly A. Schock

Mentor: William C. Lindsay

Summer Experiences

August 16, 1989

Acknowledgements: I like to thank my mentor, William Lindsay, for showing me around W.P.A.F.B. and for always trying to kept me busy. You did a great job. My thanks go to Doug Rouch for coming up with new and exciting stuff to do like the Air Show and the flight orientation. This summer would not have been as exciting without you. I also thank Antonio Ayala and Dieter Multhopp for giving me actual work that was very interesting and for helping me when I needed it. Special thanks to everyone I worked with for making this summer one I will never forget.



During the summer I have accomplished and experienced many things. Not only have I become well adjusted to the work environment but I have met several new and interesting people. I have been bombarded with several kinds of engineers that have given me the chance to ask questions and get all the answers to everything I have ever wanted to know about engineering. I am planning on being an engineer and being here this summer has help make that decision a final one. This summer has helped me and I hope that I have helped my fellow employees with the work I have done.

My eight weeks this summer were split into two parts with two different jobs. Both jobs really did not go into detailed engineering work because I did not have enough time and experience to accomplish them. Instead I have spent most of the summer listening, watching, and learning from engineers at work.

The first job I had was down in KT, the Cockpit Directorate. They work on designing the ultimate cockpit to fulfill every pilot's needs. They are trying to make a futuristic cockpit that has no gauges just three television screens with the most desirable information on them. The three screens have been put into the new F-15 Eagle but they are still revising them and hoping to turn the three screens into one screen that even has 3-D. A lot of people that work here are either human factors engineers or electrical engineers. The human factors engineers run tests on pilots to see what they like best in a cockpit, then the electrical engineers make a cockpit to satisfy their needs.

I worked with Antonio Ayala back in a laboratory where they have a demo simulation of one of the futuristic cockpits they are presently working on. The demo has four screens with old displays on them that the pilots do not like. Tony and I worked on revising these screens. We started with drawings of what the pilots wanted the displays to look like and then we plotted them out on paper so we could transferred them over to the computer. We then programed the computer to draw the displays. Some of the displays we worked on were the engine display, the bombs display, and the performance impaired display. All of these displays required some computer programing so when a button was pushed certain objects on the display would change in color and form. Like if a bomb was selected it would turn green displaying that it was ready to be fired, or if the engine failed the computer would put a red boarder around the engine and the flame would disappearing displaying that the engine was out. We had just finished the displays when it was time for me to go, but after I am gone they are planning to put the displays in their new demo.

For the last part of the summer my second job was up in FIGC, Fight Control Analysis. They mainly work on aerodynamic design and computational fluid dynamics. They are in to designing the body of the plane for the best maneuverability. Most of the people who work there are aeronautical engineers. They solve many equations and compute a lot of formulas for the perfect plane. Many times they solve their problems on paper with their own knowledge, and other times they have books of equations and computers to help them.

I worked on rewriting some programs to help them solve simple mathematical problems. I started with a copy of a basic program that did not work on the computer they had, so I had to change it around and fix it up. With my basic programing background I was able to rewrite four programs and save them for other people to use. After I had fixed the four programs I checked the data with the theoretical data to make sure it was doing what they wanted. Then I ran several tests with data and recorded the output for a record. Three of the programs solved aerodynamic problems and the other one solved a matrix problem. The programs would ask for input and then run those numbers through several equations to get the quick answer they needed. It is going to save them a lot of time using this program instead of doing it all out on paper. Even though the programs can only solve simple aerodynamic and matrix problems, they will sure save a lot of valuable time.

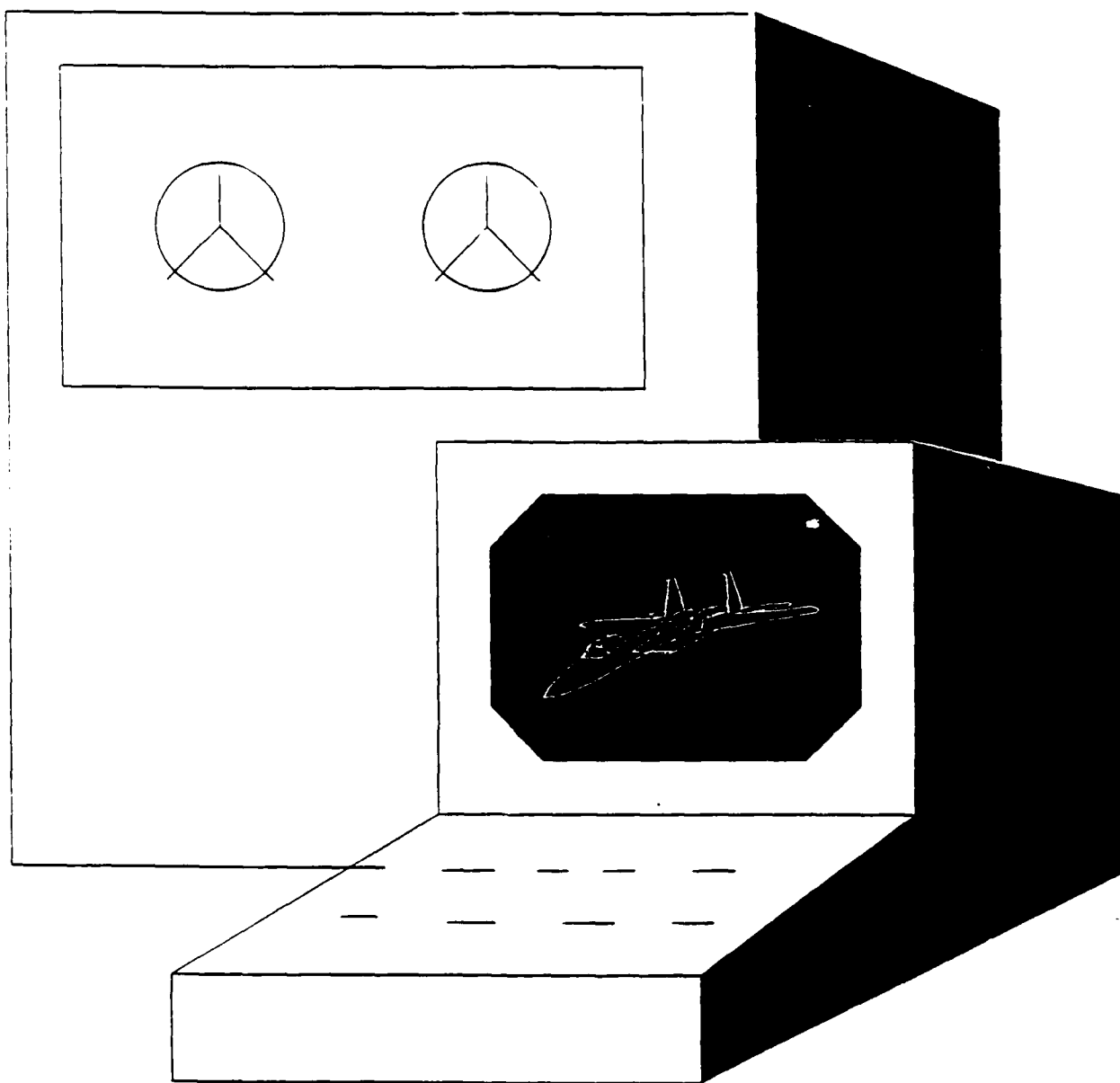
During my eight weeks here I have been able to observe and participate in many interesting activities. I saw two interesting demos this summer, one on Cat's Eyes, glasses that enable you to see in the dark, and the other one on a futuristic cockpit that was in 3-D. I was also able to go with my fellow employees to witness the test flight of the URV, Unmanned Research Vehicle, at Jefferson Proving Grounds in Indiana. Doug Rouch gave me the chance to ride in a C-135 for a flight orientation that flew to Niagara Falls and back. That was one exciting trip. Also I was able to work with my fellow employees at the Dayton International Air Show.

All these experiences I will never forget. This has been a educational summer for me. Even though I did not have a specific project to work on, just from sitting and watching other people I have learned a lot. I hope this program that I was able to get this job from will continue in the years to come because it is a great opportunity for all high school students interested in engineering. I am just glad I got a chance to be a part of it.

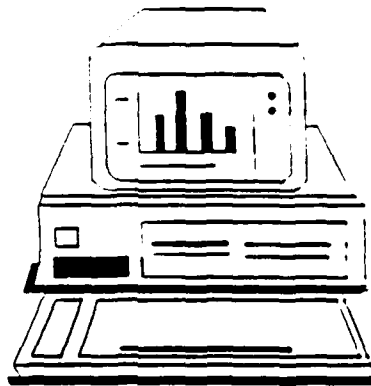
Mark Screven

Final Report Number 69

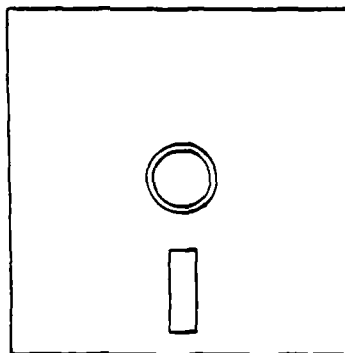
No Report Submitted



JAMES WILKINSON  
HIGH SPEED PERFORMANCE  
COMPUTER RESOURCES TEAM



Name: James L. Wilkinson  
Mentor: Richard Smith  
Lab: High Speed Aero Performance  
Computer Resources Team  
Date: August 10, 1989



The main mission of the Computer Resources Team is to plan, purchase, install, and provide maintenance for all computer equipment for all organizations within the Aeromechanics Division (FIM). The Computer Resources Team is considered the "Jack of all Trades", who's work includes everything from making computer cables to installing and operating computer systems. The most complex aspect of the job is learning different hardware, software, and operating systems that are continuously updated. Training on the different computing systems is mandatory to keep abreast of the most current technology, in this discipline.

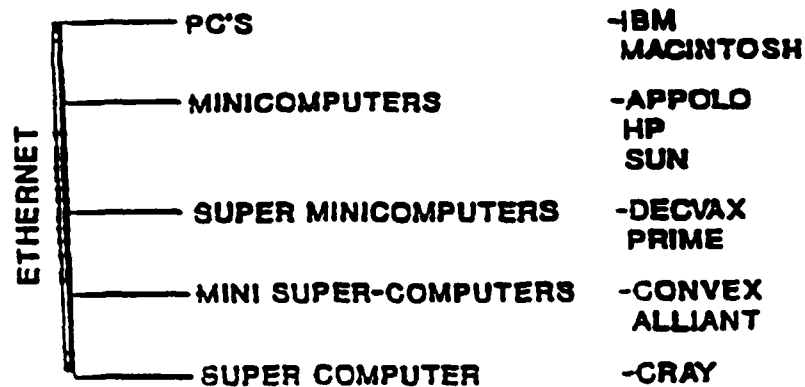
The Computer Resources Team is the office of primary responsibility for the Ethernet system of FIM. The Ethernet Local Area Network (LAN) is a communication network for highspeed computer interconnect, which allows many varieties of information processing equipment to be easily connected. Ethernet provides rapid access to data at a high transfer rate that makes information and resource sharing practical. It has two protocols Telnet and File Transfer Protocol(FTP):

Telnet - used for interactive communications.



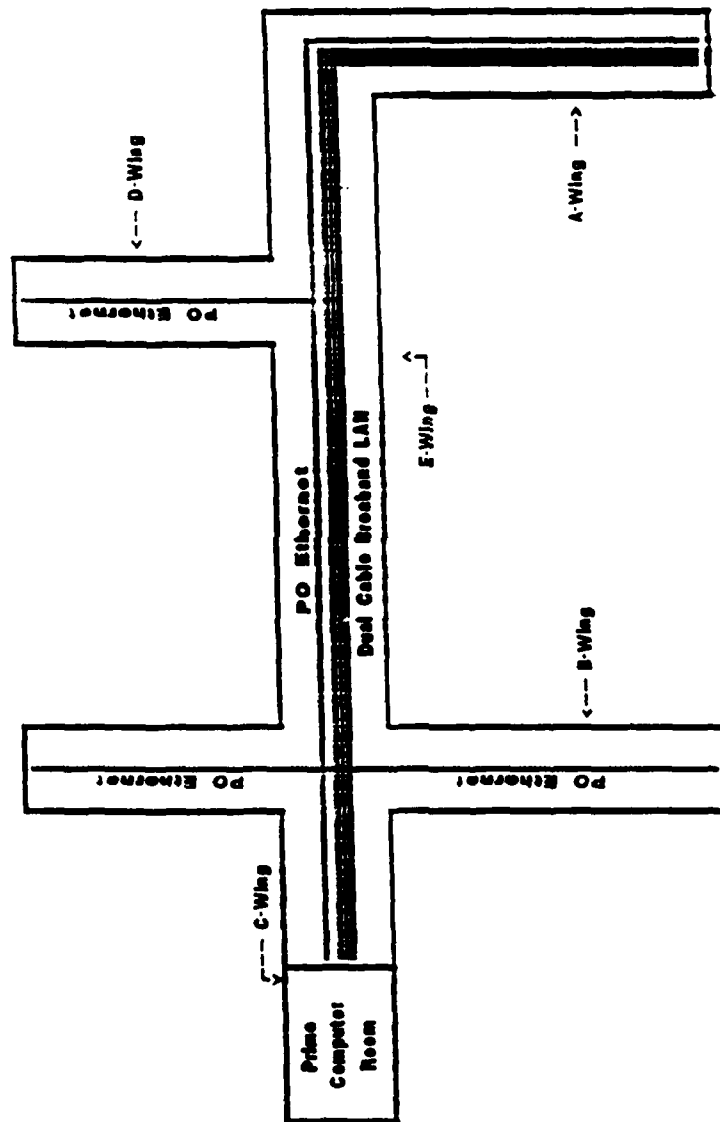
FTP - used for file transfer at high data rates.

The Ethernet is a network within itself which many operators use to communicate with other networks and computers. FIM uses Ethernet via another network called Broadband (Fig. 1). The Broadband is the primary FIM network for terminal activity and many ports are connected and used at the same time. For example, Broadband is similiar to Cable TV, in that many different channels are available, with one channel is assigned to the Ethernet. Broadband is a connector system that allows many users to log onto (logon) the FIM Prime, Vax, IRIS, or the Central ASD Computers simultaneously, without disturbing any of the other channels (Fig. 2). The Ethernet between networks and computers runs on one of the available channels simultaneously with the terminal traffic. For instance, a user on one of our PC's or terminals can communicate with a Super Computer, at Kirtland Air Force Base, in New Mexico. The Ethernet system:



This has been my most promising and rewarding summer as an Engineering Apprentice. This summer has increased my knowledge about computer systems and their work stations. I have had the experience of putting computers (Zenith Z-248) together from installing the hard drive to loading the software. I have become familiar with various operating systems, such as the Unix (VAX) and the PRIMOS (PRIME). I also learned how to make computer cables for various offices within the Division. In addition to the work, this job has helped me to become more articulate, confident, and self sufficient.

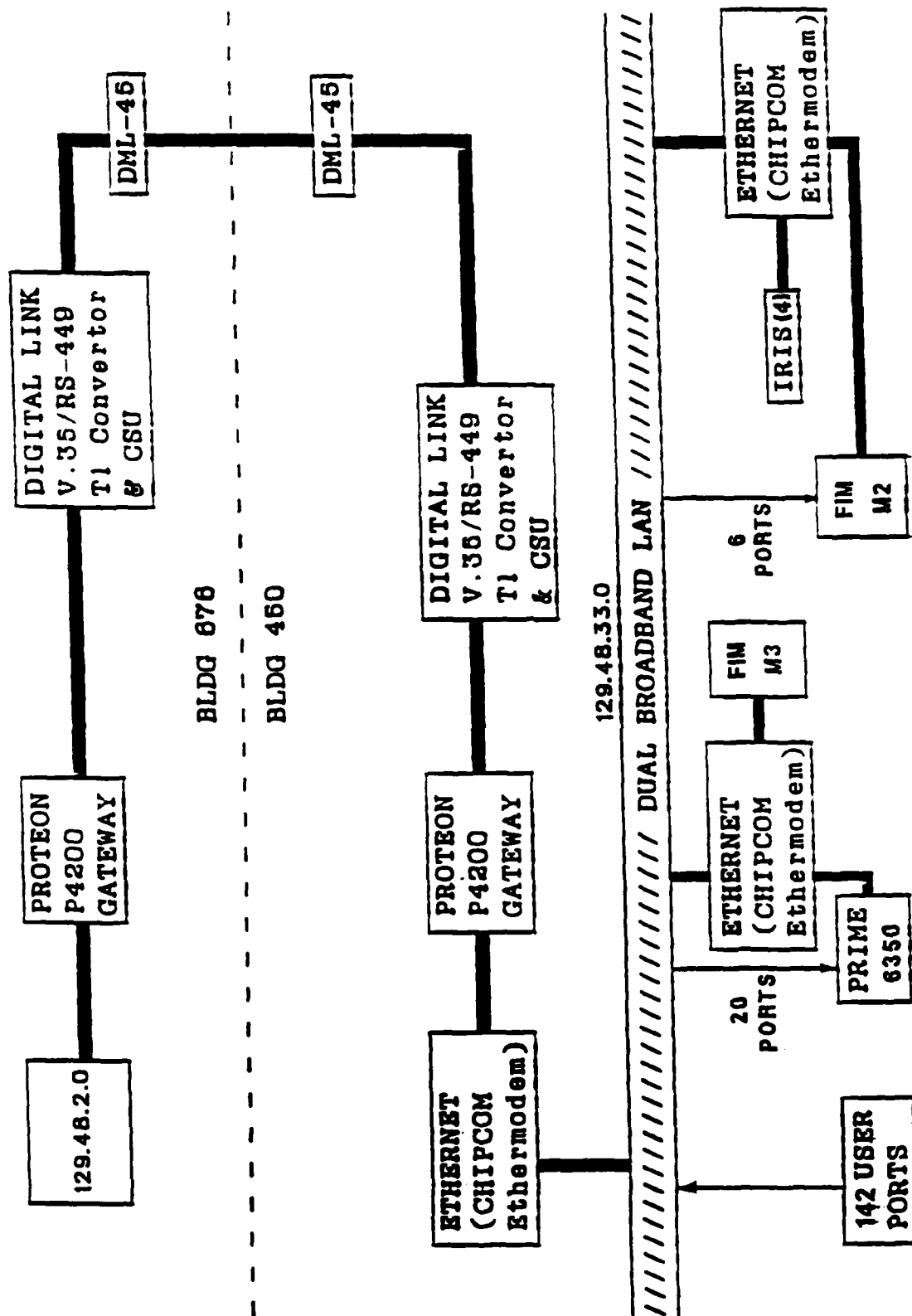
I would like to thank the program coordinators; Laboratory Director, Col. R. A. Borowski ; Laboratory Chief Scientist, Dr. J. Olsen; Program coordinator, A. Harris; High Speed Performance Branch Chief, V. Dahlem; Mentor R. Smith and C. DeMarsh. Their help has been invaluable during my employment and I am grateful for the experience.

22 MARCH 1980  
ABG**BUILDING 450 BROADBAND & ETHERNET LAYOUT**

- FIM BROADBAND UTILIZES TRW ICU INTERFACES
- FIM ETHERNET UTILIZES BROADBAND VIA CHIPCOM ETHERMODEMS
- PO ETHERNET IS THICKWIRE
- TX ETHERNET IS THICKWIRE (B-WING & PART E-WING)
- NO CURRENT CONNECTIVITY OUTSIDE TX ORGNIZATION

Fig. 2.

12 MAR 1984 1000  
RAB



Bldg 450 to Bldg 876 Ethernet Connectivity